BUREAU OF MINERAL RESOURCES,
GEOLOGY AND GEOPHYSICS

Report 188
BMR Microform MF 12

Distribution and major-element chemistry of late Cainozoic volcanoes at the southern margin of the Bismarck Sea,PNG

by R.W. Johnson

DEPARTMENT OF NATIONAL RESOURCES 1977

DEPARTMENT OF NATIONAL RESOURCES

Minister: The Rt Hon. J.D. Anthony, M.P.

Secretary: J. Scully

BUREAU OF MINERAL RESOURCES, GEOLOGY AND GEOPHYSICS

Director: L.C. Noakes

Assistant Director, Geological Branch: J.N. Casey

Published for the Bureau of Mineral Resources, Geology and Geophysics by the Australian Government Publishing Service

Manuscript Received: September 1976

Revised Manuscript Received: November 1976

Issued: May 1977

CONTENTS

FIGURES

TABLES

SUMMARY

Late Cainozoic volcanoes at the southern margin of the Bismarck Sea can be grouped into western and eastern arcs. The volcanoes of the western arc form a narrow zone which is associated with a broad zone of seismicity that marks the boundary between the South Bismarck and Indo-Australian plates. The western arc is considered to overlie a near-vertical downgoing slab which, throughout the late Cainozoic, may have been characterized by generally higher rates of subduction nearer its eastern end. The eastern arc consists of volcanoes arranged on three principal lines: (1) an east-west line formed by the Witu Islands (excluding Unea), (2) a north-south chain of volcanoes forming Willaumez Peninsula, and (3) a broad, northeast-southwest belt along the north central coast of New Britain between the southern end of Willaumez Peninsula and Likuruanga. At the present day, the volcanoes of the eastern arc overlie the northward dipping New Britain Benioff zone, which is thought to represent subduction of the Solomon Sea plate beneath the South Bismarck plate. To account for the distribution of these eastern volcanoes, an imbricate thrust slice (the Vitiaz slice) in the northwestern corner of the Solomon Sea is believed to have exerted an important influence on the geodynamics of the region throughout the late Cainozoic.

The volcanic rocks of both arcs are hypersthene-normative and highly porphyritic, especially in plagioclase. Other phenocrysts are olivine, clinopyroxene, pleochroic orthopyroxene, amphibole, iron-titanium oxides, quartz, and minor apatite and biotite. Basalts (<53 percent SiO_2) and low-silica andesites ($53 \leqslant SiO_2 < 57$ percent) are common in the western arc, high-silica andesites ($57 \leqslant SiO_2 < 62$ percent) are less common, dacites ($62 \leqslant SiO_2 < 70$ percent) are rare, and rhyolites ($\geqslant 70$ percent SiO_2) have not been found. The volcanoes of the Schouten Islands, at the western end of the western arc, are unusual because basalts appear to be absent. The range of rock types in the eastern arc

is wider: andesites are common, basalts and dacites are less common, and rhyolites are rare. Basalts in both arcs are either quartz-normative or olivine-normative. Rocks having high $Mg/(Mg + Fe^{2+})$ values are also present in both arcs, and may represent approximations to primary magmas that were in equilibrium with the olivine of upper mantle peridotite.

In comparing the compositions of rocks containing the same amounts of silica, pronounced changes can be demonstrated (1) along the western arc - in a direction parallel to the plate boundary, and (2) across the eastern arc - in a direction more or less at right-angles to the plate boundary. The compositional changes in the eastern arc appear to be related to depth to the present-day Benioff zone. A favoured model for petrogenesis in both arcs is the partial melting of upper mantle peridotite (not necessarily of uniform composition) under hydrous conditions to generate mafic primary magmas which rise and fractionate to form magmas of lower magnesia and higher silica contents.

In parts of the eastern arc, and where the downgoing slab is at a shallow depth (less than about 100 km), water may have been released from hydrated oceanic crust in the upper part of the Solomon Sea slab by subsolidus dehydration of amphibole, and may have risen into the overlying mantle and generated primary magmas by partial melting of peridotite. It is suggested that these primary magmas gave rise to the volcanic rocks between the southern end of Willaumez Peninsula and Likuruanga. At depths slightly greater than about 100 km, a hydrous eclogite part of the slab may have melted; derived water-rich siliceous melts may have risen into and partially melted the mantle to generate the primary magmas. Conditions of magma genesis over the deepest parts of the New Britain Benioff zone are as yet uncertain, although as the depth increases the magma compositions are thought to be governed increasingly by inhomogeneities in the source peridotite rather than by the influence of slab-derived melts.

Beneath Willaumez Peninsula, the descending Solomon Sea plate may move past the descending Vitiaz slice; reductions in total pressure, and possible heating by shear strain, in the drag zone between them may have enhanced dehydration or melting of subducted oceanic crust (hydrous eclogite). Water-rich fluids rose into the overlying mantle (which was not necessarily homogeneous), and generated and mixed with primary magmas that subsequently fractionated and erupted from the volcanoes of the peninsula.

The changes in rock compositions along the western arc are considered to be related to differences in the rates of subduction between different parts of the arc. Comparisons between the compositions of rocks from the eastern and western arcs suggest that primary magmas in the western arc (excluding those beneath Viai and Vokeo) may have been formed by partial melting of mantle peridotite under conditions similar to those that existed over the deeper parts of the New Britain Benioff zone. Owing to a predominance of basalts and andesites in the western arc, the primary magmas may have risen more rapidly there than in the eastern arc, where slower rates of magma ascent may have enhanced fractionation resulting in a greater proportion of acid rocks among the eastern volcanoes. Alternatively, the abundance of basalt in the western arc, and in some of the Witu Islands in the eastern arc, may be due to upwelling of hot mantle peridotite which partially melted at relatively shallow depths (possibly in a dilational environment), so that little time was available for the magmas to fractionate during their relatively short ascent to the surface. Anatexis of young crustal rocks in the South Bismarck plate cannot yet be ruled out as a possible process for the derivation of at least some acid rocks.

INTRODUCTION

Papua New Guinea, at the southwestern margin of the Pacific plate, contains about 110 principal late Cainozoic volcanoes (Fig. 1), of which 30 have been classified as 'active' (Fisher, 1957) and 14 have erupted this century (Cooke, McKee, Dent, & Wallace, 1976). The volcanoes are in a variety of tectonic environments; many of them are associated with active island arcs.

This Report details the distribution and petrology of the volcanoes bordering the southern margin of the Bismarck Sea (Fig. 1). The purpose of the Report is to describe regional variations in major-element chemistry, to show how these relate to tectonic setting, and to discuss petrogenesis in the light of plate theory and the published results of experimental petrology. 348 whole-rock chemical analyses (major oxides) are available, of which 260 are unpublished analyses of rocks collected by Bureau of Mineral Resources (BMR) field parties; about 1200 BMR rocks have been examined in thin section. Trace-element studies are underway and will be presented elsewhere. Detailed descriptions of the geology and petrography of individual volcanoes were presented by Ball & Johnson (1976), Blake & Bleeker (1970), Blake & Ewart (1974), Johnson (1970a, b, 1971), Johnson & Blake (1973), Johnson, Davies, & Palfreyman (1971), Johnson, Davies, & White (1972), and Johnson, Taylor, & Davies (1972).

The Report is divided roughly into three parts. In the first part, the distribution of the volcanoes and the nature of the associated plate boundaries are described, and the framework of a plate model is established. The geology, petrography, and major-element chemistry of the volcanoes are described in the second part of the Report. In the last part, the relation between the composition of the volcanoes and the nature of the plate boundaries is discussed and a model for petrogenesis is presented; using the chemical relations, attempts are made to refine a late Cainozoic plate model for the south Bismarck Sea.

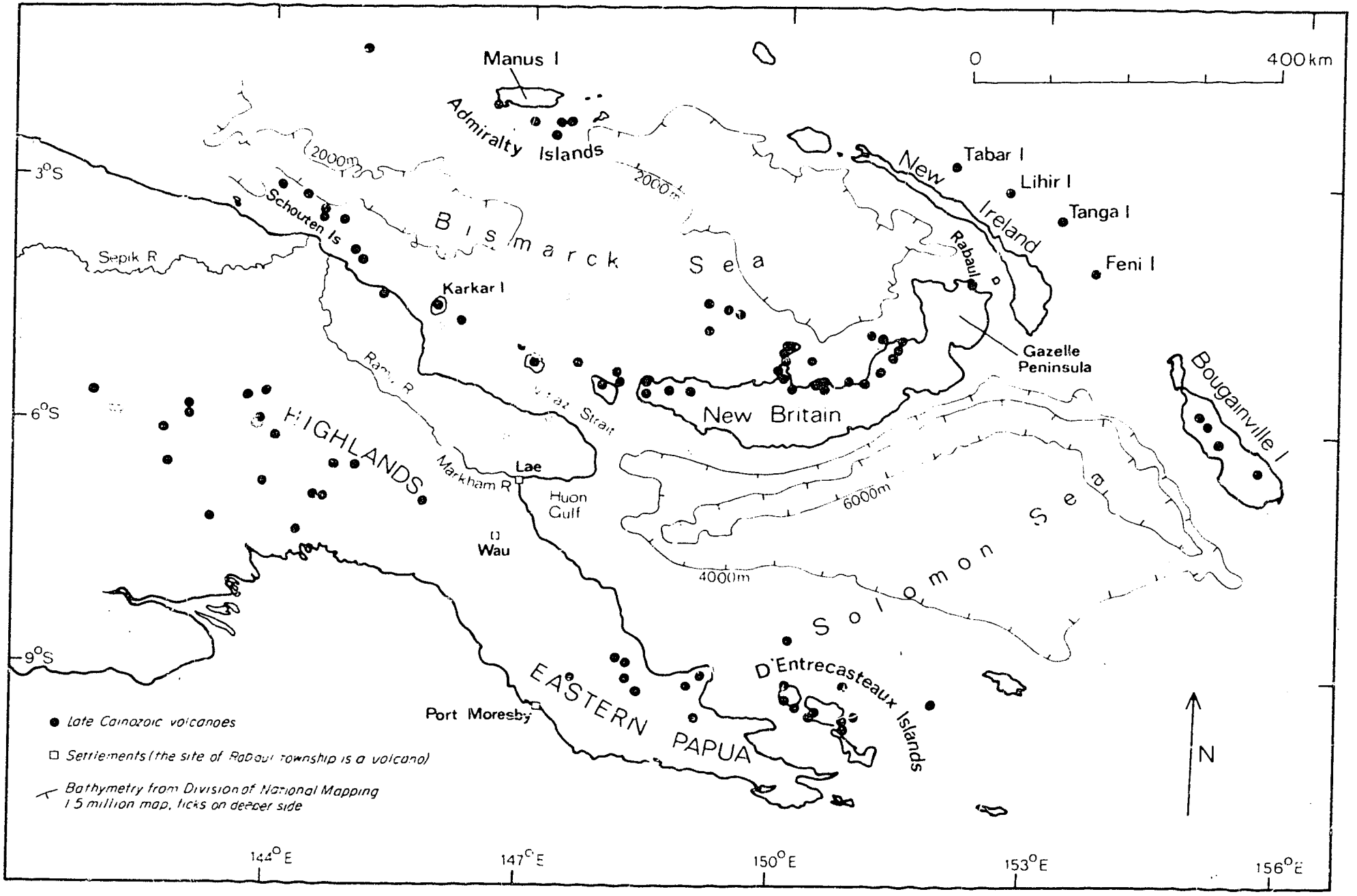

Fig. 1. Principal late Cainozoic volcanoes of Papua New Guinea.

Acknowledgements

R.P. Macnab and R.J. Ryburn participated in two field trips in 1969; R.A. Davies took part in a third field season in 1970; and the late G.A.M. Taylor collected samples from Karkar Island in 1962 and 1965. The valuable contributions made in the field by these BMR geologists, and by field assistants P. Diambari and M.A. Gillfillan, are gratefully acknowledged. Discussions on the geology and geophysics of Papua New Guinea with many colleagues in the Bureau of Mineral Resources and Geological Survey of Papua New Guinea, and with J.S. Milson, have contributed greatly towards the sections dealing with plate tectonics.

A first draft of this Report was written in 1973 at Imperial College, London, during the tenure of an Australian Government Public Service Board Overseas Scholarship. This scholarship and the hospitality of Professor J.S. Sutton and his staff at Imperial College are gratefully acknowledged. I.A. Nicholls, W.B. Dallwitz, and G.M. Bladon provided many useful criticisms of the first draft of the Report.

VOLCANOES OF PAPUA NEW GUINEA

Apart from the south Bismarck Sea volcanoes, most of the late Cainozoic volcanoes in Papua New Guinea (Fig. 1) may, owing to their tectonic setting and chemistry, be classified broadly into six groups. The wide ranges of volcanic rock compositions and tectonic styles in these six groups demonstrate that exceptionally complex geodynamic events have governed magma genesis in Papua New Guinea.

1. Volcanoes between the southwestern coast and central ranges of mainland Papua New Guinea constitute a 'Highlands group. The rocks are mainly basalts and andesites which have been classified into calcalkaline and shoshonitic associations (Jakeš & White, 1969; Mackenzie & Chappell, 1972; Johnson, Mackenzie, Smith, & Taylor, 1973; Mackenzie, 1976). Chemically, these rocks are broadly of island-arc type, although there is little seismic evidence that they are directly related to a downgoing lithospheric slab (Johnson, Mackenzie, & Smith, 1971).

2. Late Cainozoic volcanoes of eastern Papua consist of rocks also identified as calcalkaline and shoshonitic (Ruxton, 1966; Morgan, 1966; Jakeš & Smith, 1970), and again - as in the Highlands - there is little suggestion from seismic evidence that they are directly related to subducted lithosphere (Johnson, Mackenzie, & Smith, 1971). These volcanoes include Mount Lamington, whose eruption in 1951 is widely recognized as a classic example of Peléan-type activity (Taylor, 1958).

3. The volcanic islands in the southwestern part of the Solomon Sea (off the coast of eastern Papua) are made up of rocks whose compositions are in striking contrast to those of the mainland volcanoes. In the D'Entrecasteaux Islands, comendites are the voluminous end-members of a transitional-basalt/hawaiite/trachyte lineage (Morgan, 1966; Smith, 1976). This association of rocks is consistent with the presence of these volcanoes within a zone of extension (cf. Milsom, 1970; Luyendyk, MacDonald, & Br[illegible]n, 1973).

4. Volcanoes in the Admiralty Islands southeast of Manus Island consist mainly of acid rocks (Johnson & Smith, 1974), which - unlike the D'Entrecasteaux comendites - are not peralkaline. They are associated with transitional basalts, quartz tholeiites, and dacites. Adequate petrological data are not yet available for the other volcanoes in the Admiralty Islands.

5. Despite their small size and number, the Tabar, Lihir, Tanga, and Feni Islands - off the northeast coast of New Ireland - have an exceptionally wide range of volcanic rock compositions (Johnson, Wallace, & Ellis, 1976). Most of the rocks are undersaturated, and they include strongly undersaturated and fractionated types such as tephritic phonolites and phonolitic trachytes. Quartz trachytes are present on some islands, but tholeiitic basalts, andesites, and dacites appear to be absent.

6. The late Cainozoic volcanoes of Bougainville Island appear to have erupted mainly calcalkaline andesites (Baker, 1949; Blake & Miezitis, 1967; Blake, 1968; Taylor, Capp, Graham, & Blake, 1969; Bultitude, 1976), although petrological data are either incomplete or non-existent for many volcanoes. Picritic basalts of the type found in the Solomon Islands (e.g., Stanton & Bell, 1969; Cox & Bell, 1972) have not been reported from Bougainville Island.

The volcanoes of the south Bismarck Sea, which are described in this Report, have been referred to as the 'Bismarck volcanic arc' (Johnson et al., 1973), and could be considered as a seventh group. However, although this name is geographically convenient (cf. Cooke, McKee, Dent, & Wallace, 1976), it overlooks the geodynamic complexities of this region and the important differences in tectonic setting between different parts of the 'arc'. In this Report, two distinct volcanic arcs are recognized within the 'Bismarck volcanic arc', and it is further suggested that the volcanoes of the Rabaul area, in the extreme east, be considered as a province separate from those to the west.

PLATE BOUNDARIES AND GEODYNAMICS

Seismic zones and minor plates

The volcanoes of the south Bismarck Sea and of Bougainville Island coincide with a major zone of seismicity (Denham, 1969, 1973).

This zone continues westwards into Indonesia, and southeastwards through the Solomon Islands and New Hebrides, where it defines part of the boundary between the Pacific and Indo-Australian plates (Le Pichon, 1968, 1970).

In Papua New Guinea, the pattern of earthquake zones is complex, and two, or possibly three, minor plates trapped between the Pacific and Indo-Australian plates have been proposed to explain present-day tectonic activity in the region (Fig. 2). Johnson & Molnar (1972), Curtis (1973b), and Krause (1973) differed in their locations of many of the plate boundaries in this region, but they all agreed that one minor plate underlies the Solomon Sea, and that another underlies the southern half of the Bismarck Sea. These minor plates will be referred to as the Solomon Sea and South Bismarck plates (Johnson & Molnar, 1972; Figs. 2 and 3).

The late Cainozoic volcanoes described in this Report coincide with the major zone of seismicity associated with the southern margin of the South Bismarck plate (Fig. 3). The northern margin of this plate is marked by a narrow zone of shallow seismicity that crosses the Bismarck Sea from the Schouten Islands to Rabaul (Denham, 1969); focal mechanism solutions of earthquakes in this zone have been interpreted as indicating left-lateral strike-slip fault movements (Johnson & Molnar, 1972; Curtis, 1973b; Ripper, 1975, in prep. a).

The southern margin of the South Bismarck plate is adjacent to the Indo-Australian plate in the west and to the Solomon Sea plate in the east; the south Bismarck Sea volcanoes are therefore associated with two plate boundaries (Fig. 3). Because movements at these boundaries have probably had an important influence on magma genesis througnout the late Cainozoic, it is advantageous to discuss firstly the general boundary configurations that may have existed during this time. These configurations must be compatible with the present-day seismicity, but they should also be capable of accounting for the distribution pattern of the volcanoes.

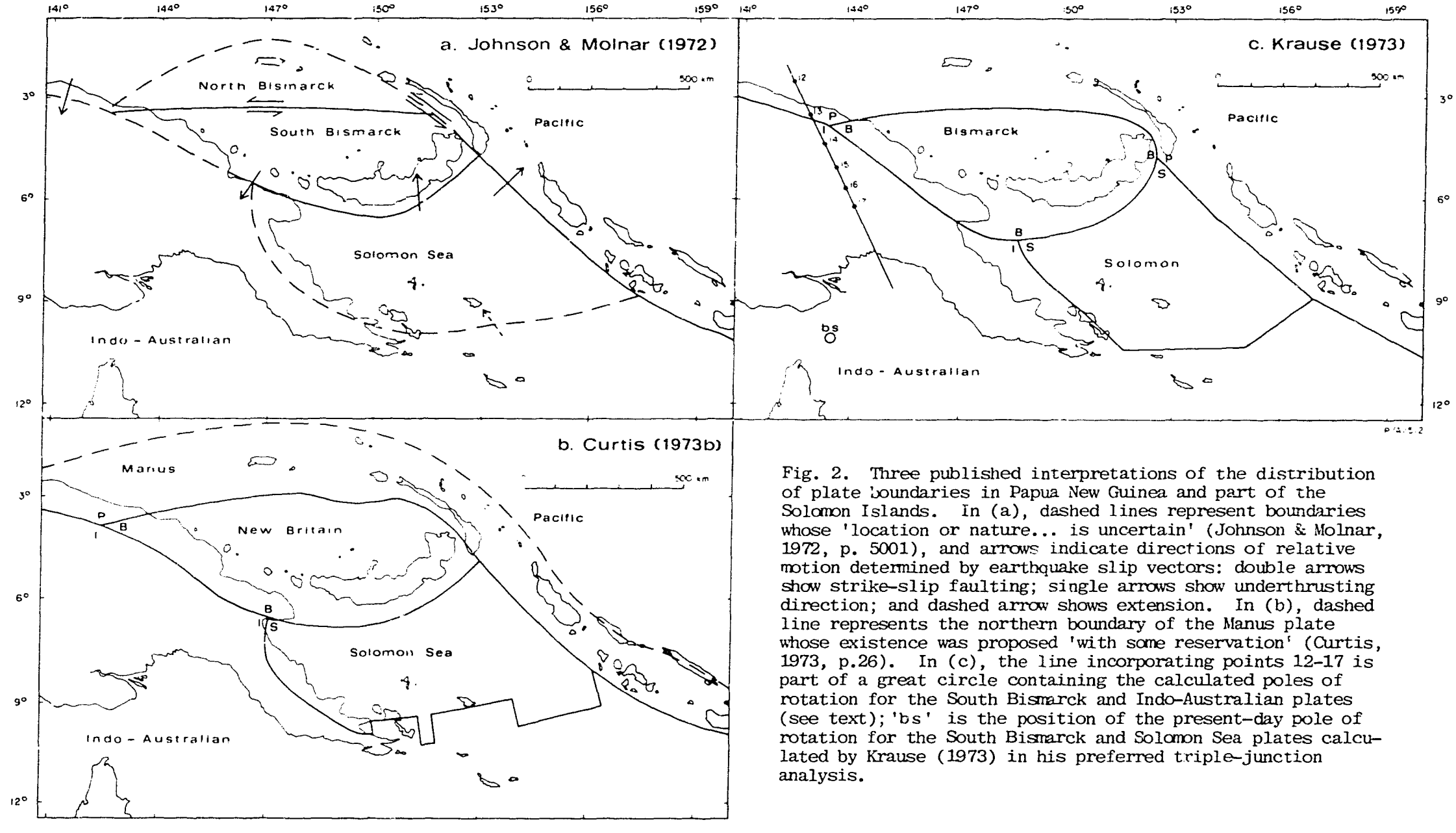

Fig. 2. Three published interpretations of the distribution of plate boundaries in Papua New Guinea and part of the Solomon Islands. In (a), dashed lines represent boundaries whose 'location or nature... is uncertain' (Johnson & Molnar, 1972, p. 5001), and arrows indicate directions of relative motion determined by earthquake slip vectors: double arrows show strike-slip faulting; single arrows show underthrusting direction; and dashed arrow shows extension. In (b), dashed line represents the northern boundary of the Manus plate whose existence was proposed 'with some reservation' (Curtis, 1973, p.26). In (c), the line incorporating points 12-17 is part of a great circle containing the calculated poles of rotation for the South Bismarck and Indo-Australian plates (see text); 'bs' is the position of the present-day pole of rotation for the South Bismarck and Solomon Sea plates calculated by Krause (1973) in his preferred triple-junction analysis.

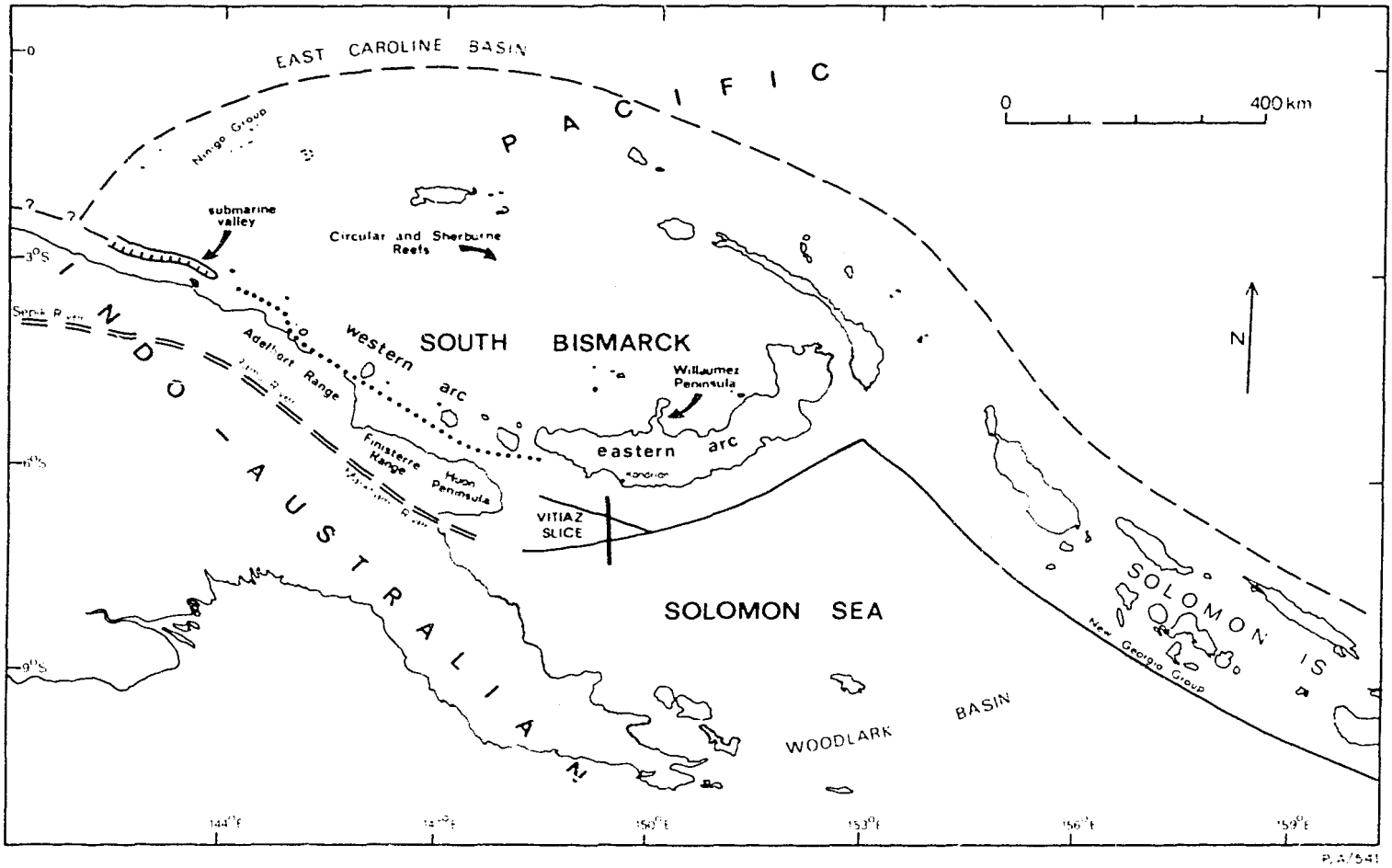

Fig. 3. Preferred locations of plate boundaries and some related tectonic features in Papua New Guinea and part of the Solomon Islands, in part adapted from Johnson & Molnar (1972), Curtis (1973b), Krause (1973), and Luyendyk et al. (1973). Solid lines are axes of submarine trenches. Stippling indicates currently active plate boundaries which are zones of seismicity that cannot be accurately portrayed by single lines. Single-dash line represents a boundary (or boundaries) which may have been more active during the earlier part of the late Cainozoic than at the present day; Johnson & Molnar (1972) and Curtis (1973) considered that this line, or part of it, represents the northern margin of a third minor plate - cf. Fig. 2. Double-dash line represents an old plate boundary that was destroyed by collision of the Australian continent (part of the Indo-Australian plate) with an Adelbert-Huon island arc (see text and Fig. 9 for details). Dotted line is a strike-line for the upper surface of the proposed lithospheric slab which dips steeply northwards beneath the western arc (see text and Fig. 39 for details). Thick line running southwards from near Kandrian is the ship's track of the seismic reflection profile given in Figure 8.

The distribution of earthquakes in the Papua New Guinea region during the last ten or twenty years is known in reasonable detail, and earthquake cross-sections such as those presented by Denham (1969), Johnson, Mackenzie, & Smith (1971), and Curtis (1973a), and in Appendix 1, indicate the plate boundary configurations at the present day. These configurations serve as a starting point for extrapolating possible configurations of plate boundaries in the early part of the late Cainozoic - that is, in the Pleistocene and late Pliocene.

South Bismarck Sea plate boundaries

At the South Bismarck/Solomon Sea plate boundary, a Benioff zone dips northwards at about 70° beneath New Britain (Denham, 1969; Johnson, Mackenzie, & Smith, 1971; Curtis, 1973a; Fig. 4). Focal mechanism solutions indicate northward underthrusting of the Solomon Sea plate beneath the South Bismarck plate (Ripper, 1970, 1975, in prep. a; Johnson & Molnar, 1972; Curtis, 1973b). In this Report, a northward-dipping Benioff zone is considered to have been in existence throughout the late Cainozoic.

West of New Britain, the nature of the South Bismarck/Indo-Australian plate boundary is uncertain, because the seismic evidence is more obscure. Johnson & Molnar (1972), among others, claimed that a Benioff zone dips southwestwards at a low angle beneath the coastal ranges of mainland Papua New Guinea (see also: Jakeš & White, 1969; Dewey & Bird, 1970; Karig, 1972). However, this interpretation is questionable, as the significance of the earthquake cross-sections and focal mechanism solutions for this area is far from certain (cf. Johnson, Mackenzie, & Smith, 1971; Curtis, 1973b). Moreover, if a Benioff zone dipped southwestwards beneath the coastal ranges, a submarine trench - not a volcanic arc - would be expected north of the ranges.

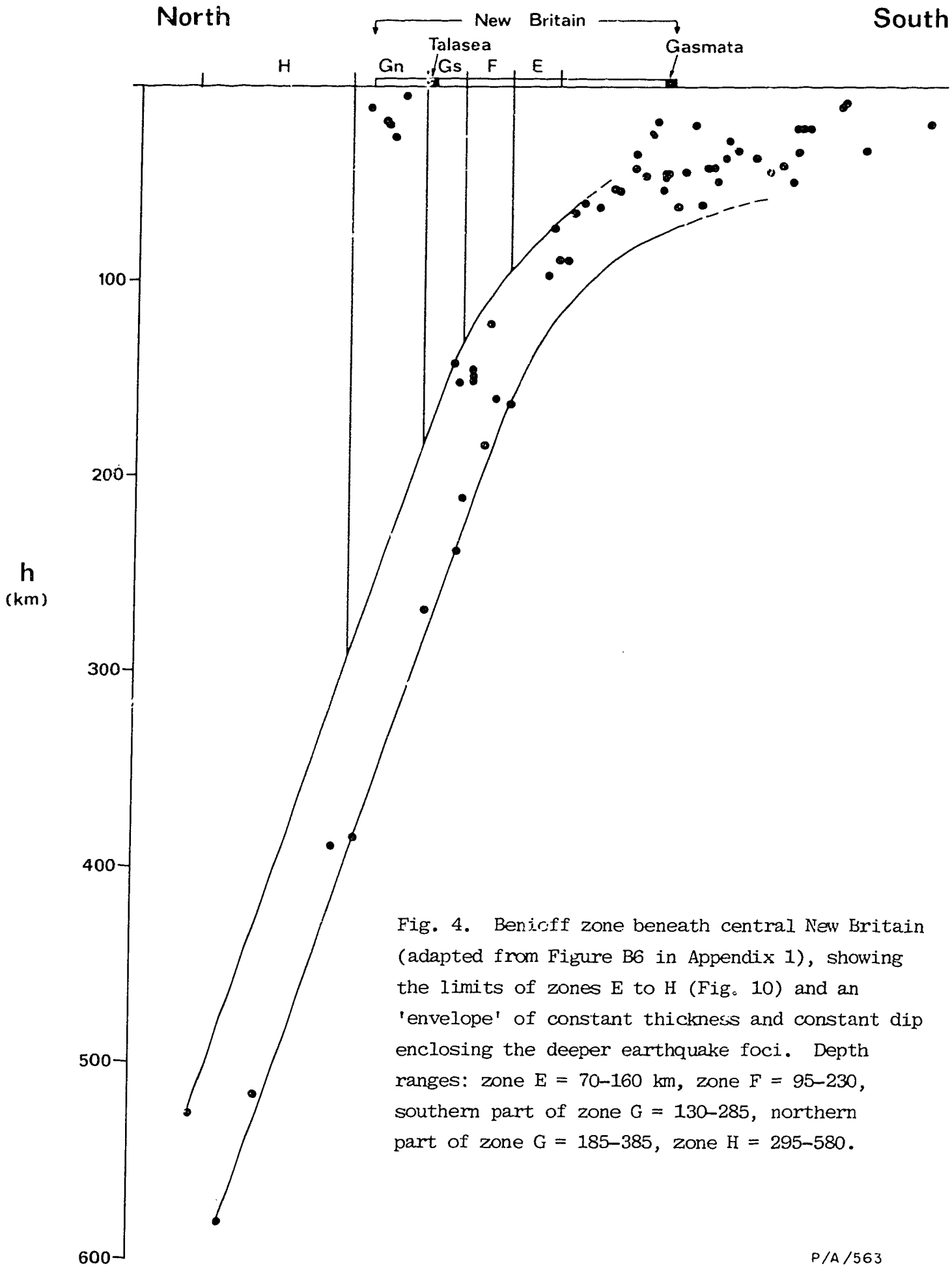

Fig. 4. Benioff zone beneath central New Britain (adapted from Figure B6 in Appendix 1), showing the limits of zones E to H (Fig. 10) and an 'envelope' of constant thickness and constant dip enclosing the deeper earthquake foci. Depth ranges: zone E = 70–160 km, zone F = 95–230, southern part of zone G = 130–285, northern part of zone G = 185–385, zone H = 295–580.

P/A/563

The interpretation adopted here is that throughout the late Cainozoic the narrow zone of volcanoes off the north coast of mainland Papua New Guinea has been associated with a continuous, near-vertical lithospheric slab immediately south of the volcanic arc (Fig. 3). Present-day seismicity is consistent with this interpretation. Intermediate-depth earthquakes recorded up to 1974 have been focussed in a narrow zone parallel to, but up to a few tens of kilometres south of, the volcanoes between Karkar Island and the west end of New Britain (Fig. 1); these earthquakes are especially common a few kilometres south of Long Island, but appear to be absent west of Karkar Island (Fig. A, Appendix 1). The earthquakes are concentrated in a zone which dips steeply northwards from depths of about 120 km down to more than 200 km, increasing in dip downwards to more than 80^{o} beneath the arc (Figs. B2 and B3, Appendix 1). Focal mechanism solutions for a few of these intermediate earthquakes give steep dip-slip underthrust senses of motion (Isacks & Molnar, 1971; Ripper, 1975, in prep. a). In this account a similarly steep northward dip is assumed to have existed throughout the late Cainozoic.

Two south Bismarck Sea volcanic arcs

Because the south Bismarck Sea volcanoes are thought to be associated with two plate boundaries, two volcanic arcs are recognized in this Report.

1. A 'western' arc consists of the volcanic centres between the Schouten Islands and the Cape Gloucester area of west New Britain (Fig. 5), and is associated with the South Bismarck/Indo-Australian plate boundary (Fig. 3).

2. An 'eastern' arc of volcanoes along the north central coast of New Britain, and including the Witu Islands (Fig. 6), is associated with the South Bismarck/Solomon Sea plate boundary (Fig. 3), but, as discussed below, this apparently simple correlation is shown to be complicated by the proposed thrust slice in the northwestern corner of the Solomon Sea.

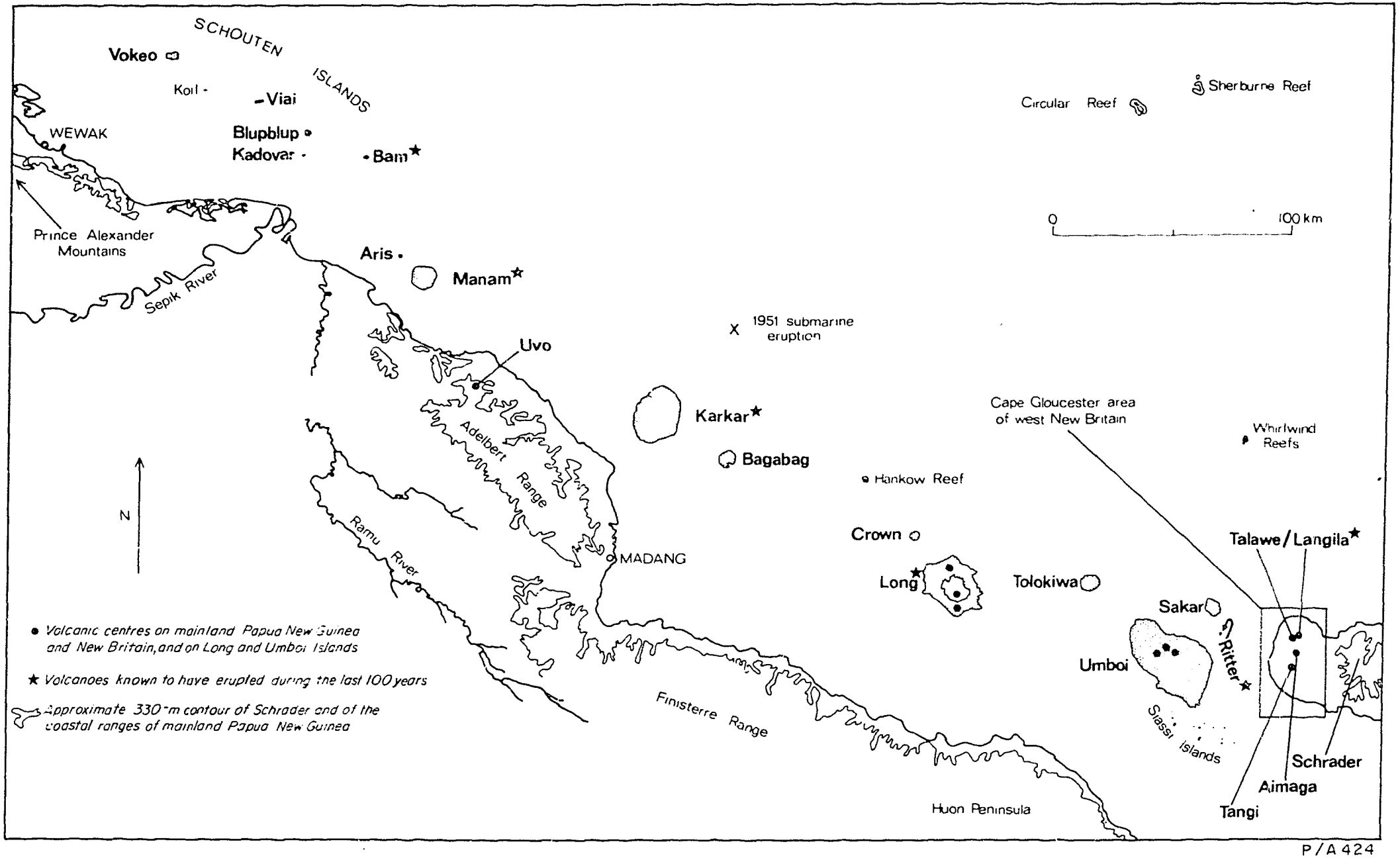

Fig. 5. Main volcanic centres of the western arc. Islands are shown stippled or solid, and volcanic islands are indicated by bold lettering. Langila is a cluster of satellite craters on the eastern flank of Talawe.

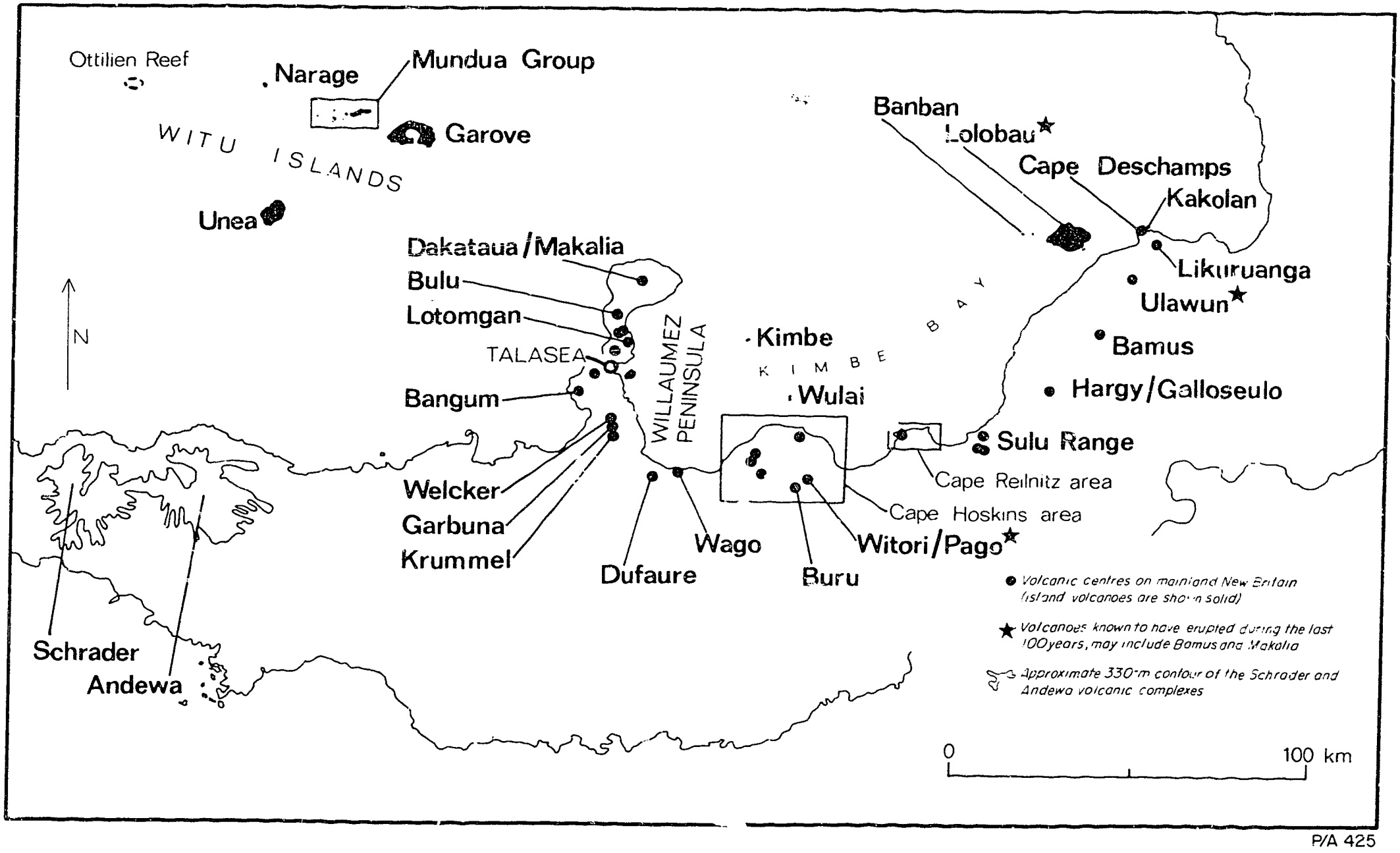

Fig. 6. Main volcanic centres of the eastern arc. Makalia, Pago, and Galloseulo are post-caldera volcanoes which respectively lie inside the older volcanoes of Dakataua, Witori, and Hargy.

One of the main purposes of this Report is to draw attention to the differences in rock chemistry between the volcanoes of each arc, and to discuss how the relative motions between the associated plates may have influenced petrogenesis.

The Rabaul volcanoes, in the extreme east (Fig. 1), are also associated with the boundary between the South Bismarck and Solomon Sea plates (Fig. 3). However, because they are separated from the volcanoes in the eastern arc by the complexly faulted Gazelle Peninsula (Davies, 1973; Fig. 1), these volcanoes are considered to occupy a structural environment distinct from those of the other south Bismarck Sea volcanoes. Consequently, the chemistry of their rocks is not discussed here in detail, but - using the chemical analyses published by Heming & Carmichael (1973), Heming (1974), and Matsumoto (1976) - is compared with the rock chemistry of the other south Bismarck Sea volcanoes (pp. 78-80).

The chemistry of rocks from Uvo (Fig. 5) and Andewa and Schrader (Fig. 6) is not discussed in this account. These volcanic centres have not been adequately studied by ground surveys, but their degrees of dissection indicate that they are older, at least in part, than the other south Bismarck Sea volcanoes. It is important to note, however, that the results of future studies of Andewa and Schrader may necessitate some amendments to the general plate model proposed in the final sections of this Report, as these two volcanic centres occupy critical positions between the eastern and western volcanic arcs as defined above.

Tectonic features of the Solomon Sea area

The submarine trench south of New Britain is more than 8000 m deep in the east, but it shallows in the west, where it branches into a southern part that extends towards Huon Gulf, and a northern part that extends into Vitiaz Strait. This branching of

the trench is shown in Figure 7 (see also Fig. 1), and also by the results of a BMR seismic traverse south of Kandrian, New Britain (Figs. 3 and 8; see also Krause, White, Piper, & Heezen, 1970). The sedimentary sequence in the southern branch is much thicker than that in the northern branch, which by implication is younger - assuming that sedimentation rates have not been much greater in the south than in the north. This splitting of the New Britain trench suggests that the northwest corner of the Solomon Sea plate has not underthrust the South Bismarck plate along a single line, but rather may carry an imbricate slice (termed the 'Vitiaz slice' in Fig. 3) beneath west New Britain (see below).

The structure of the western and southern margins of the Solomon Sea plate are complex, and their nature is much more obscure than either the eastern or northern margins, which are clearly defined by the axis of the New Britain-Bougainville submarine trench (Figs. 1 and 7). The seismicity of the western and southern margins appears to be much more diffuse and of a lower order of intensity than that of the eastern and northern margins (e.g., Denham, 1973). The southern margin (the Woodlark Basin, Fig. 3) was interpreted by Milsom (1970), and others, to be a zone of rifting (the 'Louisiade Sphenochasm' of Carey, 1958), but because the western margin has a different orientation the sense of relative motion there is believed to be more strongly transcurrent (cf. Krause, 1973). However, the western margin cannot be satisfactorily located using tectonic features on land, or the distribution of earthquakes, or bathymetric features, and the position of the zone representing the margin in Figure 3 should therefore be regarded as speculative. This zone is drawn passing northwards through Cape Ward Hunt, and corresponding with the major offset between the Adelbert-Huon coastal ranges and New Britain; it is considered to mark the present-day western extremity of the New Britain trench system, and to define the present-day junction between the western and eastern arcs (Fig. 3).

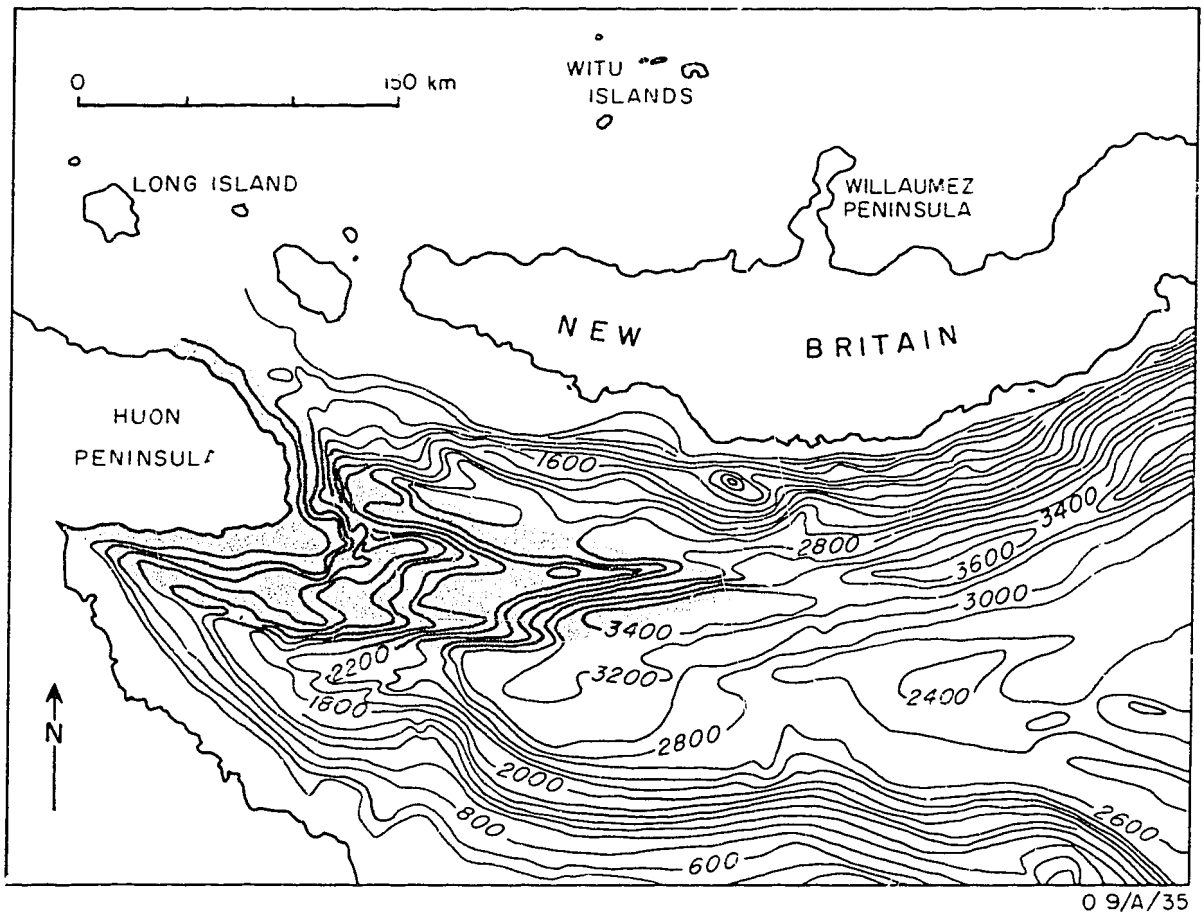

Fig. 7. Bathymetry of the northwestern corner of the Solomon Sea, showing 200-fathom isobaths (after Mammerickx et al., 1971). Submarine ridge (stippled) lies between the two branches of the western end of the New Britain trench.

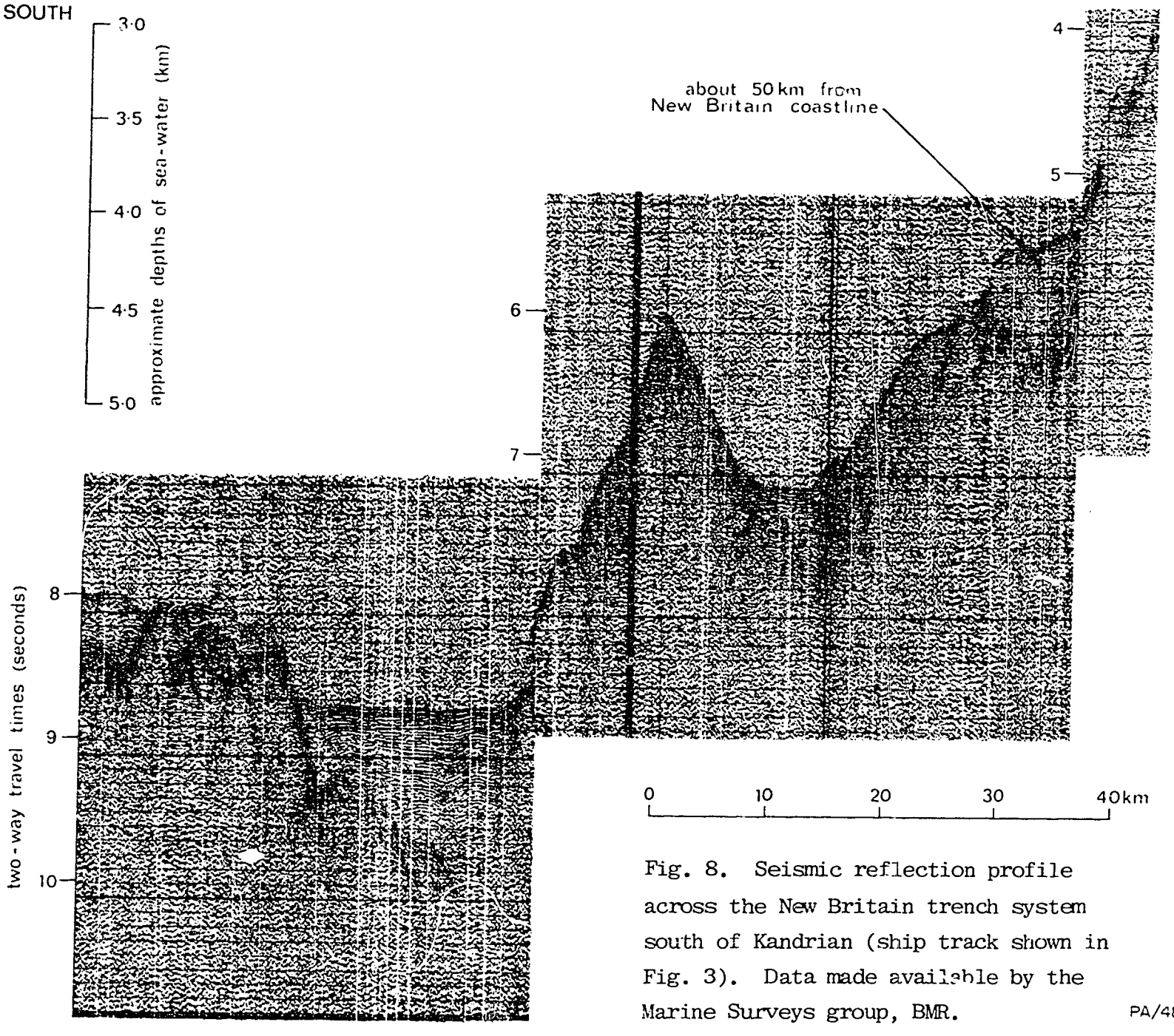

Fig. 8. Seismic reflection profile across the New Britain trench system south of Kandrian (ship track shown in Fig. 3). Data made available by the Marine Surveys group, BMR.

PA/480

Continent/island-arc collision and development of the western arc

The mainland of Papua New Guinea south of the western arc may be divided into three broad physiographic units: (1) the coastal ranges, consisting of the Adelbert and Finisterre Ranges and Huon Peninsula (Fig. 3); (2) the broad valleys of the Ramu and Markham Rivers (Figs. 1 and 3); and (3) the Highlands region (Fig. 1). Interpretations of the geological evolution of mainland Papua New Guinea are still at a speculative stage, but there appears to be general agreement that the coastal ranges are a Tertiary island arc (cf. Thompson & Fisher, 1965), and that the Highlands represent an old continental margin which collided with the arc in mid-Tertiary times producing a suture represented by the Ramu and Markham valleys (see: Dewey & Bird, 1970; Karig, 1972; Johnson & Molnar, 1972). Jaques & Robinson (in prep.) envisaged the collision taking place in late Oligocene to early Miocene time, after a period of plate convergence during which island-arc volcanism (see Jaques, 1976) prevailed between late Eocene and early Miocene time in the region now represented by the coastal ranges. This collision hypothesis forms the basis for the evolutionary interpretation illustrated in Figure 9. However, two further opinions held by several adherents of the hypothesis are not accepted in this interpretation.

Dewey & Bird (1970), Karig (1972), and Johnson & Molnar (1972) believed that the collision caused the 'flipping' (McKenzie, 1969) of a Benioff zone - that is, that a zone dipped northwards beneath the Tertiary island arc, but that after the collison the arc polarity reversed, and a zone dips southwards beneath the coastal ranges and the Highlands at the present day. As discussed above, there is little evidence for a simple southward-dipping Benioff zone, and the distribution of earthquakes suggests that the present-day tectonics of the area are more complicated than previously envisaged (for further details see Figs. 3 and 9).

Previous studies of plate tectonics in Papua New Guinea concluded that the present-day boundary between the South Bismarck and Indo-Australian plates could be represented by a single line

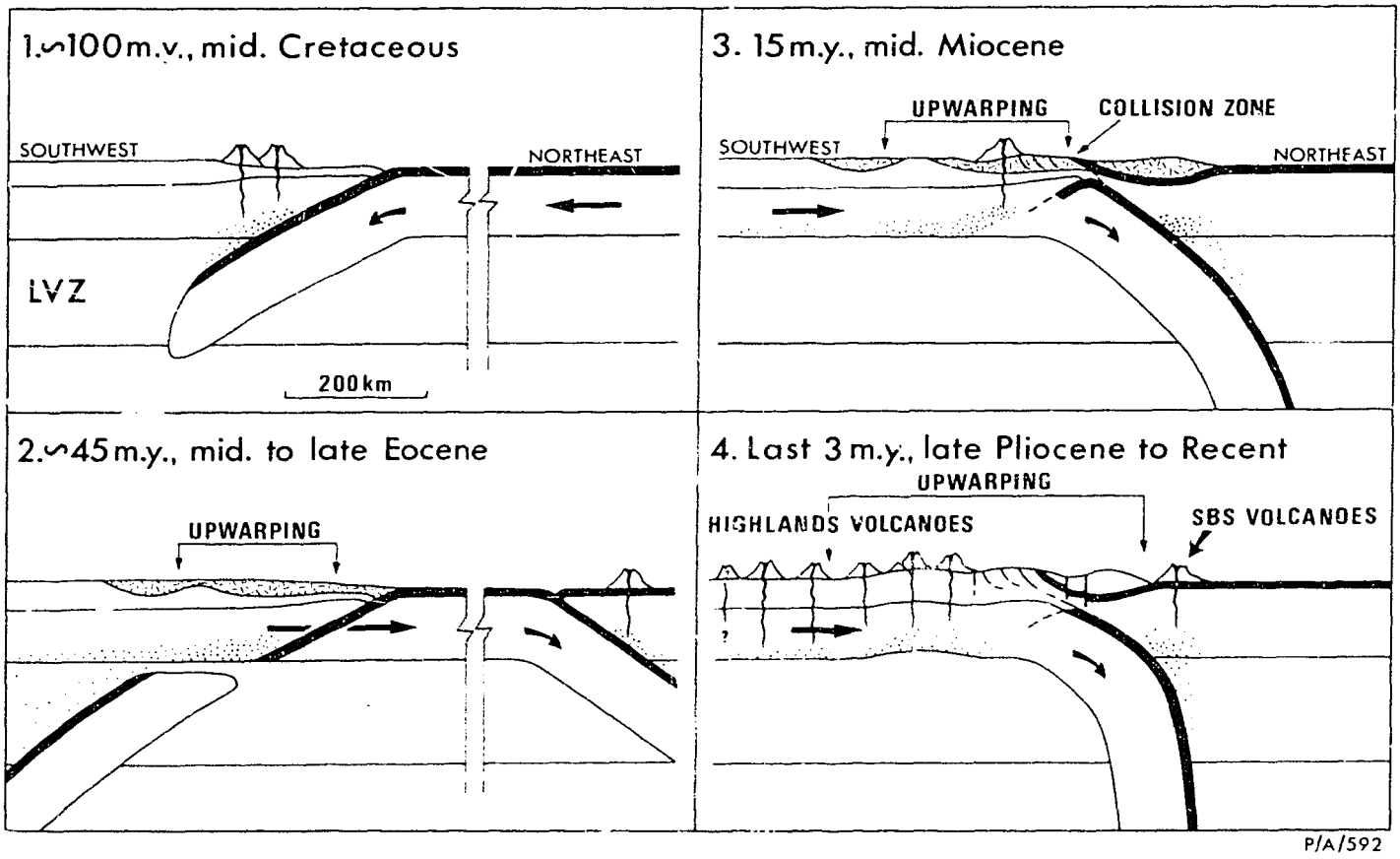

Fig. 9. Schematic representation of the tectonic evolution of mainland Papua New Guinea in a northeast-southwest section through the western arc, coastal ranges, and Highlands (see Figs. 1-3). Johnson, Mackenzie, & Smith (in prep. b) used these diagrams to illustrate the evolution of late Cainozoic volcanism in both the western arc and Highlands province (Fig. 1), but in the following description emphasis is given to those aspects of the interpretation that apply particularly to the development of the western arc. Black bands represent oceanic crust. Stippling represents chemical modification of mantle by slab-derived fluids. Short-line pattern in diagrams 2 and 3 represents post-Jurassic thickening of crust. The true thicknesses of the lithosphere and low-velocity zone (LVZ) throughout this region are unknown, and the assumed values are those determined by Brooks (1969) for the southern part of mainland Papua New Guinea.

1. Southward-dipping subduction in the mid-Cretaceous resulted in arc-trench-type volcanism, and chemically modified the mantle underlying the northern edge of the Australian continent.

2. In the Eocene the southward-dipping slab may have become detached. In the late Eocene, volcanism started in an island arc several hundreds of kilometres to the north as a result of northward subduction of the Indo-Australian plate, which carried the Australian continent northwards from Antarctica.

3. By the late Oligocene or early Miocene the continent had reached the island arc and, because it was too buoyant to descend into the subduction zone, began to collide with the arc. Subduction was arrested and island-arc volcanism ceased, but plate convergence continued, and the continental margin and arc were warped and raised. Middle Miocene magmatism south of the collision zone was initiated by partial melting of mantle which had been chemically modified during the Cretaceous subduction.

4. By the late Pliocene the slab beneath the Tertiary island arc had become steepened, and continuing subduction gave rise to the volcanoes of the western arc in the south Bismarck Sea (SBS volcanoes). Uplift and warping in the Highlands region led to partial melting in the chemically modified mantle.

passing along the axis of the Ramu and Markham valleys (Curtis, 1973b; Krause, 1973; Luyendyk et al., 1973), or along the Ramu valley and north of the Finisterre Range and Huon Peninsula (Johnson & Molnar, 1972), as shown in Figure 2. However, there is no linear concentration of earthquakes beneath the valleys; rather, the epicentres are spread more or less evenly over a wide zone covering the coastal ranges, the Ramu and Markham valleys, and the northern foothills of the Highlands region (Fig. A in Appendix 1). In addition, extensive Holocene faulting has not been reported from the Ramu and Markham valleys, and there is no evidence that Holocene faults are more common in these valleys than they are in other parts of the wide zone of present-day earthquake activity (Bain et al., 1972). Furthermore, studies in which the Ramu and Markham valleys are identified as a present-day plate boundary offer no convincing explanation for the existence of the active island-arc volcanoes of the western arc north of the coastal ranges. In this Report, the Ramu and Markham valleys are considered to represent a <u>former</u> plate boundary destroyed by the continent/island-arc collision - not a <u>present-day</u> plate boundary.

The interpretation adopted in this Report for the tectonic evolution of this area is given in Figure 9. The most important points to note are: (1) that the continent/island-arc collision destroyed the plate boundary which had existed south of the Tertiary island-arc although its eastern extension may be represented by the southern trough of the Vitiaz imbricate slice (Fig. 3); and (2) that post-Miocene plate convergence and foreshortening caused (i) the uplift of the Highlands and the coastal ranges, and (ii) the steepening of the subducted slab beneath the island/arc, which was followed by Quaternary volcanism in the western arc (see below for further details). Note also that no single line at the Earth's surface is identified as the present-day plate boundary in this region; rather, the contact between the Indo-Australian and South Bismarck plates is visualized as a broad zone of foreshortening characterized by earthquakes which show compressional focal mechanism solutions, but which beneath mainland Papua New Guinea are not concentrated along a single well defined inclined seismic zone.

Another outcome of the continent/island-arc collision may have been the formation of the Vitiaz imbricate slice (Fig. 3). Because of its relatively thin accumulation of sediment, the trough along the northern edge of the slice may be younger than that along the southern edge, and may have formed about the same time as the collision to the west.

One other notable feature (Fig. 3) is a well defined submarine valley parallel to the coastline of mainland Papua New Guinea west of Wewak (cf. Krause, 1965). The floor of this valley is about 2500 m below sea level, and slopes westwards for about 175 km from an area east of Vokeo Island and north of Wewak (Fig. 5). The southern side of the valley is steeper and much more prominent than the northern side, which is simply the southwest-dipping floor of the Bismarck Sea. Erlandson et al. (1976) called the valley the 'New Guinea trench', and regarded it as a subduction zone formed during a period of crustal spreading in the East Caroline Basin (Fig. 3) in pre-Miocene time. However, they offered no explanation for the limited extent and specific features of the valley; nor did they explain why it has not been filled by sediments during at least the last 20 million years. The valley appears to be a much younger feature, and may have originated through differences in tectonic elevation between the regions on either side of it. The present-day seismicity west of Wewak is also of uncertain significance, although Ripper (in prep. b) suggests that it marks the eastern corner of an Irian Jaya 'buffer' plate that accomodates movements between the converging Indo-Australian and Pacific plates. The nature of late Cainozoic tectonics west of Wewak is therefore unclear, although it is obviously in marked contrast to that east of Wewak, where island-arc volcanism has prevailed.

Rates of convergence and poles of rotation

Johnson & Molnar (1972) and Curtis (1973b) independently calculated the magnitude and direction of the present-day relative velocity vectors between the South Bismarck and Indo-Australian plates

(equivalent to the boundary at the western arc in this account) and between the South Bismarck and Solomon Sea plates (the boundary associated with the eastern arc). They assumed that the relative poles of rotation for the plates were a long way from the Papua New Guinea region, and showed that the rate of convergence of the South Bismarck and Solomon Sea plates is between 2 and 5 times as great as that of the South Bismarck and Indo-Australian plates (Table 1). These faster rates correlate with the shallower dip (70^{o}) of the New Britain Benioff zone (compared with the near-vertical attitude of the seismic zone beneath the western arc, where rates of convergence are slower), and are therefore consistent with the general relation between dip and rate of convergence proposed by Luyendyk (1970).

The series of calculations by Curtis (1973b, see Table 1) showed that, at the South Bismarck/Indo-Australian plate boundary, the rate of convergence was twice as great at the eastern end than at the western end, suggesting the proximity of a pole of rotation. This phenomenon was described in greater detail by Krause (1973), who calculated a series of possible motions between the South Bismarck plate and the Indo-Australian and Pacific plates. Using different positions for the pole of rotation between the South Bismarck and Pacific plates, and using different rates of left-lateral transcurrent motion along the northern margin of the South Bismarck plate, Krause calculated corresponding positions for the South Bismarck/Indo-Australian pole of rotation. He concluded that a point at latitude 14^{o}S and longitude 148^{o} or 147^{o}E was probably the most satisfactory position for the South Bismarck/Pacific pole, and that values between 12 and 17 cm/year were the most likely rates of transcurrent motion at the South Bismarck/Pacific plate boundary. The calculated positions of these poles of rotation are shown in Figure 2c, where they form a line which is part of a pole great circle containing the South Bismarck/Pacific pole (at 14^{o}S, 148^{o}E) and the Indo-Australian/Pacific pole at 58^{o}S, 169^{o}W (the 'model I' pole of Christoffel, 1971).

TABLE 1. RATES AND AZIMUTHS OF CONVERGENCE OF THE INDO-AUSTRALIAN AND SOLOMON SEA PLATES WITH THE SOUTH BISMARCK PLATE

Reference	I		S	
	Rate (cm/yr)	Azimuth (^{o}E of N)	Rate (cm/yr)	Azimuth (^{o}E of N)
Johnson & Molnar (1972)	3.3	23	9.2	343
Curtis (1973)	2.60 at IBP 5.22 at IBS	18 7.5	12.02	352
Krause (1973)*	0 at IBP 6.2 at IBS	- 31	6.2 at IBS 12.4 at BPS	5 or 327 327
Taylor (1975, unpublished)	8.04 at IBP 9.3 at IBS	29 29	11.65 at IBS 12.5 at BPS	11 8

*values calculated for a 'preferred' model in which BI pole is at IBP triple junction, and left-lateral slip rate between B and P is 13.5 cm per year (see text).

I = Indo-Australian plate

B = South Bismarck plate

S = Solomon Sea plate

P = Pacific plate

Krause (1973) also proposed that the present-day pole of rotation for the Solomon Sea and South Bismarck plates lies within the Papua New Guinea region. In his preferred triple-junction analysis of the region, he calculated a position for this pole at $10^{o}S$, $143.5^{o}E$ ('bs' in Fig. 2c). Other positions, however, are possible, and, for the purposes of this account, the instantaneous poles of rotation throughout the late Cainozoic are assumed to have lain somewhere within a few hundred kilometres of the position calculated by Krause for present-day plate motions. Rotation of the Solomon Sea plate about these pole positions during the late Cainozoic will have caused greater rates of convergence at the eastern part of the South Bismarck/Solomon Sea plate boundary than beneath the western part (cf. Table 1).

Johnson & Molnar (1972), Curtis (1973b), and Krause (1973) all regarded the seismic zone crossing the Bismarck Sea as that of a pure left-lateral transcurrent fault. However, Connelly (1976) and Taylor (1975) both provided evidence from magnetic recording surveys that movement across at least two sectors of the seismic zone was divergent, and that the Bismarck Sea floor is a marginal basin The implications of this conclusion are discussed in a later section (p. 113).

VOLCANO DISTRIBUTION AND GEOLOGICAL SETTING

Coral reefs and submarine peaks

All the principal and some of the minor late Cainozoic volcanic centres along the southern margin of the Bismarck Sea are shown in Figures 5 and 6, together with the principal coral islands and isolated coral reefs associated with the western and eastern arcs. Because most, if not all, of the principal reefs and coral islands may have volcanic foundations, their locations are taken into account in the following descriptions of volcano distribution.

The main coral islands and reefs are, from west to east: (1) Koil Island, one of the Schouten Islands, (2) Hankow Reef, northwest of Crown Island, (3) the Siassi Islands, southeast of Umboi Island, and (4) Ottilien Reef, west of the Witu Islands. Numerous areas of reef and a few coral-sand islands are also present in Kimbe Bay, east of Willaumez Peninsula.

Other prominent areas of coral in the Bismarck Sea are: Whirlwind Reefs, about 400 km west of the Witu Islands (Fig. 5); Circular and Sherburne Reefs, which appear to straddle the boundary between the South Bismarck and Pacific plates (Figs. 3 and 5); and the Purdy Islands and Alim Island, about 75 km south of Manus Island. All these islands and reefs, and the Witu Islands and Ottilien Reef, surmount a broad submarine rise that crosses the Bismarck Sea from the Admiralty Islands to the central north coast of New Britain (Connelly, 1974; Fig. 1). Although volcanism may have played a prominent role in the formation of the rise, this topic is beyond the scope of the present account.

The distribution patterns in Figures 5 and 6 are defined solely by subaerial volcanic centres and areas of coral, and the contribution made by submarine volcanoes is largely unknown. A submarine volcano is thought to be present 35 km north-northeast of Karkar Island, where marine disturbances were observed in 1951 (Taylor, 1956; Fig. 3). Moreover, the results (largely unpublished) of a BMR marine geophysical survey of the Bismarck Sea in 1970 (see Connelly, 1974), and the bathymetric map of Krause (1965), identify peaks which may be submarine volcanoes. However, more bathymetric data are needed before submarine peaks associated with the western and eastern arcs can be confidently recognized as late Cainozoic volcanoes, and before the significance of their distribution can be evaluated.

Eastern arc

New Britain has the familiar features of an active island arc: a submarine trench, over 8000 m deep and showing negative free-air gravity anomalies; an inclined Benioff zone (Fig. 4) underlying an arcuate geanticlinal island ridge which shows positive free-air and Bouguer anomalies (Finlayson & Cull, 1973; Wiebenga, 1973); and active volcanoes on the concave side of the arcuate ridge. In the vicinity of the Witu Islands, crustal thicknesses are about 20 km, but they increase to a maximum of about 45 km beneath the south central coast of New Britain (Finlayson & Cull, 1973; Wiebenga, 1973). In the Solomon Sea area, the base of the crust is 11.5 to 14 km below sea level (Furumoto et al., 1970).

Unusual features of the New Britain island arc are, firstly, the splitting of the submarine trench at its western end (see above), and, secondly, the distribution pattern of the volcanoes (Fig. 6). In the south, a prominent belt of volcanoes runs westwards along the north coast of New Britain, from Likuruanga and Lolobau Island in the east, as far as Willaumez Peninsula, where the belt terminates abruptly. The peninsula itself is an impressive north-south chain of volcanoes, 60 km long, which trends perpendicular to the central axis of New Britain. As shown in Figure 3, the line of the peninsula, when extrapolated southwards, passes more or less through the area where the New Britain trench divides into two branches. Kimbe Island is associated with neither the Willaumez Peninsula chain, nor with the north coast volcanic zone (Fig. 6), although, as demonstrated below, its rocks are chemically analogous to the volcanoes of the northern part of the peninsula.

The most northerly of the volcanoes of the eastern arc are those of the Witu Islands. They lie opposite a section of New Britain where late Cainozoic volcanoes are conspicuously absent (between Andewa and Willaumez Peninsula), and opposite the two western branches of the New Britain trench. Apart from Unea, the Witu Islands

(and Ottilien Reef) form a zone which extrapolated 170 km south-southeastwards coincides - presumably by chance - with the volcanic line of Banban, Lolobau, and Likuruanga on the north coast of New Britain (Fig. 4). The eastern volcanoes are therefore not arranged randomly; rather, they mostly lie on three well defined zones.

Western arc

In contrast to the eastern arc, the volcanoes of the western arc occupy a much narrower zone (Fig. 3). This is consistent with the interpretation presented above of a steeply dipping (almost vertical) slab of downgoing lithosphere beneath the western volcanoes, because magmas generated at or above the upper surface of the steeply inclined slab will presumably all tend to rise vertically, and have little opportunity to move away from the slab and erupt from centres over a wide volcanic zone.

Like the volcanoes of the eastern arc, the western volcanoes are arranged in a series of lines, not all of which are parallel to the general trend of the arc. Talawe, Aimaga, and Tangi form a north-south line in the Cape Gloucester area of west New Britain (Fig. 5). In addition, two parallel lines of islands trend north-westwards and intersect the general trend of the western arc at an angle of about 30° (cf. Carey, 1938); these are (1) the Siassi Islands (coral)-Umboi-Tolokiwa line, and (2) the Long-Crown-Hankow Reef (coral) line (Fig. 3). Both lines appear to be related to the fault pattern on Huon Peninsula to the south, suggesting they represent the surface traces of underlying fractures (cf. Bain et al., 1972; Robinson, 1973).

Bagabag, Karkar, Manam, and Aris Islands form a fourth line that more or less coincides with the main trend of the western arc and is parallel to the north coast of mainland Papua New Guinea. Between Karkar and Manam is a gap 100 km long where subaerial volcanoes are conspicuously absent, where submarine volcanoes have not been reported, and where the mainland coastline extends closer to the western arc than at any other point.

The Schouten Islands make up a fifth line of volcanoes. This line is parallel to the Bagabag-Aris line, but is about 25 km northeast of its western extension; it lies opposite the gap between the Prince Alexander Mountains and the Adelbert Range (Fig. 5). Bam, about 625 m above sea level, is the highest of the Schouten Islands; as the bases of most of the volcanoes in the western arc are at a constant depth of about 1000 m below sea level, and many of the volcanoes elsewhere in the western arc are higher than 1000 m above sea level, the volumes of magma produced by each of the Schouten Islands volcanoes are apparently considerably less than those produced by most of the other western volcanoes.

The distribution of the volcanoes in the western arc suggests that the underlying lithospheric slab may have two features additional to those mentioned above. Firstly, the northward offset of the Schouten Islands from the Bagabag-Aris line indicates that the western end of the slab may be bent, or offset by a hinge fault (Fig. 3). Secondly, the eastern end of the slab may dip northwards at a slightly lower angle than the western end, as the volcanic arc appears to be wider in the east, possibly because (as discussed above) rates of plate convergence are greater there.

Available bathymetric data do not indicate the presence of a submarine trench associated with the volcanoes of the western arc. Broad sedimentary troughs parallel to, and to the north and south of, the eastern part of the arc have been reported (Connelly, 1974), but they appear to be Tertiary features, and are not considered to be submarine trenches in the generally accepted sense.

VOLCANIC ACTIVITY, STRUCTURE, AND MORPHOLOGY

The south Bismarck Sea volcanoes are made up of lava flows, coulées, cumulodomes, and air-fall, pyroclastic-flow, outwash, and talus deposits. The air-fall deposits consist of dust, lapilli,

bombs, pumice, scoria, and angular accessory blocks. Because of high rainfall, most of the air-fall deposits have probably been reworked, at least to some extent. The pyroclastic-flow deposits are of nuées ardentes (including some of basaltic composition), possible lahars, 'ash-hurricane' (or ground-surge) deposits, and scoria avalanches. Welding has been observed in pyroclastic-flow deposits on Witori/Pago (Blake & Bleeker, 1970) and on Hargy/Galloseulo.

The principal volcanoes of both the western and eastern arcs are central-type stratovolcanoes. Their summits do not exceed about 2500 m above sea level, and their flanks show an upward increase in slope to a maximum of about 35^{o}. Most of the volcanoes have craters or calderas. Dykes and sills are exposed in the crater (or caldera) walls of a few volcanoes, notably in Likuruanga, Garove, and Ritter. Many of the large stratovolcanoes have satellite cones. There are, however, several minor cones, coulées, and cumulodomes, which do not appear to be related to any of the major centres. Many of these smaller volcanoes consist of silica-rich rocks (dacites and rhyolites). Examples are Banban Island, Kakolan Island, Cape Deschamps, Cape Reilnitz, centres around Talasea harbour, and the satellite cone on the northwest coast of Umboi Island (Figs. 5 and 6).

All the volcanoes, both principal and minor, were probably active in the Quaternary; some, however, may have commenced activity in the Pliocene (e.g., Andewa and Schrader), although this has not yet been confirmed by isotopic dating or fossil evidence. K-Ar dating of ten rocks from the Cape Hoskins area shows ages of less than one million years (Blake & McDougall, 1973).

Literate observers have recorded and dated subaerial eruptions from six western and three eastern volcanic centres during the last one hundred years (see Figs. 5 and 6).* Two other eastern volcanoes probably erupted during this time, and one submarine

---

*In the western arc, the period 1972-75 was unprecedented during the last 100 years for the number of volcanoes in eruption: Manam, Karkar, Long, Ritter, and Langila were all active. Ulawun, in the eastern arc, also erupted in 1973. See Cooke et al. (1976).

volcano is also known to have erupted in the western arc (Fig. 5). Pyroclastic materials were erupted at all the active subaerial centres, and lava flows issued from all but two of them (Bam and Ritter). The explosive eruptions, and the large proportions of clastic deposits air-fall, pyroclastic-flow, and reworked - testify to the important role of volatiles in determining the geology of these volcanoes. Thermal areas are widespread, and at some volcanoes rocks are severely altered. The most extensive thermal area (and one of the largest single areas in the whole of Papua New Guinea) is on Garbuna, in the southern part of Willaumez Peninsula (Fig. 6).

The volcanoes show a range in degrees of dissection, but constructional slopes or 'planezes' (Cotton, 1944) are preserved on most of them. Contrasting degrees of dissection between the volcanoes in each of three lines of volcanoes suggest a linear, unidirectional migration of volcanism. The three lines of volcanoes are:

(1) The Schouten Islands (Fig. 5). Vokeo, and probably Viai, are the remnants of dissected cones, and appear to be older than Blupblup and Kadovar farther east, both of which show well preserved constructional volcanic landforms. Bam, at the eastern end of the line, is an active volcano which has erupted several times this century (Fisher, 1957). Volcanism therefore appears to have migrated eastwards along the Schouten Islands line. Another geological feature of the Schouten Islands is that Vokeo and Koil, in the west, have been raised. Vokeo has a peripheral coral reef raised 1-5 m above sea level, and Koil is an elevated coral island a few tens of metres high. Viai, Blupblup, Kadovar, and Bam show no signs of having been raised.

(2) The Cape Gloucester area (Fig. 5). Langila is an active volcano on the northeastern flank of the extinct stratovolcano, Talawe, which is much less dissected than the volcanoes of the Aimaga volcanic complex and of Tangi to the south. In these volcanoes, therefore, activity may have migrated northwards, and then north-eastwards.

(3) Willaumez Peninsula (Fig. 6). The large stratovolcanoes at the southern end of the peninsula are more dissected than cones farther north. Makalia, at the northern tip of the peninsula, is believed to have erupted in the late nineteenth century (Branch, 1967). Volcanism, therefore, seems to have been active later in the more northerly parts of the chain. Makalia and Dakataua constitute a large volcanic centre which appears to have had a long and complex history (Lowder & Carmichael, 1970). Available bathymetric data do not indicate the presence of submarine volcanoes north of Dakataua/Makalia, and it therefore seems reasonable to conclude that the northward migration of volcanism along Willaumez Peninsula has terminated at Dakataua/Makalia, or at least that volcanism shows no signs of proceeding beyond it.

PRELIMINARY PETROLOGY

The rocks of the south Bismarck Sea volcanoes constitute a hypersthene-normative association of basalts, andesites, dacites, and rhyolites. No nepheline-normative rocks have been found. Rocks of the same silica content show a wide range of alkali contents, and, according to the alkali:silica-based classifications of other writers, the rocks cover the compositional fields of 'tholeiitic', 'calc-alkaline', 'calcic', 'high-alumina basalt', 'high-K calcalkaline', and 'shoshonitic' associations. The rocks range between rare aphyric types and more common highly porphyritic types (containing up to about 50 percent by volume of total phenocrysts) in which plagiocalse, clinopyroxene, pleochroic orthopyroxene, olivine, and amphibole are the most abundant phenocrysts.

The greatest absolute variation of all the major oxides is shown by silica (Table 2). It is therefore used here as the principal means of defining the following five rock types:

<53 percent by weight silica	:	basalt
$\geqslant 53, <57$	:	low-silica andesite
$\geqslant 57, <62$	:	high-silica andesite
$\geqslant 62, <70$	:	dacite
$\geqslant 70$	:	rhyolite

Similar schemes of rock classification were used by Taylor et al. (1969), Bryan, Stice, & Ewart (1972), Oversby & Ewart (1972), and others.

MgO values for rocks containing less than 53 percent silica range from less than 5 percent to more than 15 percent (see Fig. 23). In oceanic and continental regions, rocks with MgO values as low as 4-5 percent are generally not called basalts (see, for example, Thompson, 1973, who suggested that only rocks containing more than 6 percent MgO are true basalts). To draw attention to the wide range in MgO values, the basalts of the south Bismarck Sea are therefore subdivided as follows:

<7 percent by weight MgO	:	low-magnesia basalt
>7 percent by weight MgO	:	high-magnesia basalt

The low-magnesia variety is by far the most common basalt type in the south Bismarck Sea volcanoes (see Fig. 23). Many of the basalts are olivine-normative (in particular, the high-magnesia varieties), but most are silica over-saturated - that is, they are olivine tholeiites and quartz tholeiites respectively (Yoder & Tilley, 1962).

Of the 348 available chemical analyses, 143 are of western rocks and 205 are of eastern rocks. The chemical analyses are listed in Appendix 2, and some general statistics are given in Table 2. Chemical and modal analyses, CIPW norms, and locality descriptions of 20 selected rocks, are set out in Tables 3 and 4. Eighty-eight of the analyses were published previously by Morgan (1966), Lowder & Carmichael (1970), Johnson, Davies, & White (1972), and Blake & Ewart (1974). Most of the 260 unpublished analyses were supplied by

TABLE 2. SOME STATISTICS OF THE 348 CHEMICAL ANALYSES OF ROCKS FROM THE WESTERN AND EASTERN ARCS

Arc	Number of analyses	Oxide	Mean	Standard deviation	Minimum value	Maximum value
Western	143	SiO_2	54.93	3.92	47.47	66.76
		TiO_2	0.52	0.15	0.24	0.89
		Al_2O_3	16.40	1.69	11.69	21.56
		Fe_2O_3	2.02	0.18	1.09	2.41
		FeO	6.90	1.61	1.92	10.38
		MnO	0.17	0.03	0.06	0.26
		MgO	5.72	2.50	1.51	15.22
		CaO	9.55	1.75	4.37	13.65
		Na_2O	2.44	0.53	0.94	3.82
		K_2O	1.14	0.51	0.13	3.14
		P_2O_5	0.20	0.08	0.08	0.63
Eastern	205	SiO_2	58.60	6.29	48.24	76.19
		TiO_2	0.66	0.28	0.24	1.93
		Al_2O_3	16.60	1.65	12.57	20.44
		Fe_2O_3	2.02	0.38	0.33	3.28
		FeO	5.81	1.82	0.85	9.05
		MnO	0.15	0.03	0.05	0.24
		MgO	4.07	2.21	0.24	11.35
		CaO	8.13	2.58	1.23	13.10
		Na_2O	2.98	0.80	1.52	5.74
		K_2O	0.85	0.67	0.16	3.88
		P_2O_5	0.12	0.07	0.02	0.41

All analyses have been recalculated to 100 percent without volatiles using the Irvine & Baragar (1971) transform. See Appendix 2 for full list of chemical analyses.

TABLE 3. CHEMICAL AND MODAL ANALYSES AND CIPW NORMS OF 10 ROCKS SELECTED FROM 143 ANALYSED ROCKS FROM THE WESTERN ARC

	1	2	3	4	5	6	7	8	9	10
SiO_2	60.5	54.9	60.2	51.80	55.1	48.1	51.2	64.3	52.40	55.1
TiO_2	0.36	0.38	0.29	0.33	0.59	0.66	0.76	0.69	0.52	0.53
Al_2O_3	16.7	16.50	17.40	14.19	17.3	17.9	16.60	15.00	14.30	16.8
Fe_2O_3	1.38	4.80	3.90	6.18	2.55	4.75	4.05	1.08	4.00	3.35
FeO	3.40	4.25	2.40	4.02	5.90	6.65	4.90	5.35	5.50	5.65
MnO	0.09	0.16	0.14	0.15	0.17	0.20	0.17	0.09	0.15	0.18
MgO	4.95	5.40	3.45	8.73	4.90	6.85	6.80	1.50	8.35	4.10
CaO	8.00	9.40	7.55	10.58	9.05	11.50	10.80	4.35	11.30	8.8
Na_2O	2.80	2.25	3.05	2.50	2.45	1.99	2.35	3.80	1.97	2.75
K_2O	0.59	1.36	1.16	0.83	0.65	0.72	1.34	3.00	0.83	1.58
P_2O_5	0.13	0.19	0.16	0.19	0.15	0.15	0.27	0.37	0.18	0.18
H_2O+	0.66	0.36	0.07	0.13	0.49	0.40	0.24	0.19	0.20	0.70
H_2O-	0.36	0.10	0.09	0.08	0.47	0.09	0.16	0.07	0.06	0.01
CO_2	<0.05	0.04	0.08	-	0.05	<0.05	<0.05	0.10	<0.05	0.05
Total	99.97	100.09	99.94	99.71	99.82	99.96	99.64	99.89	99.76	99.78
CIPW norms[a]:										
Q	17.26	7.22	15.69	-	10.12	-	0.32	17.57	2.45	6.92
or	3.55	8.09	6.91	4.96	3.90	4.31	7.98	17.78	4.96	9.45
ab	24.36	19.20	25.96	21.32	20.97	17.00	20.05	32.31	16.75	23.51
an	31.37	31.11	30.49	25.29	34.73	38.05	31.11	15.09	27.93	29.61
di (wo	3.28	6.10	2.55	11.04	4.06	7.71	8.85	1.74	11.42	5.77
di (en	2.20	3.28	1.42	6.59	2.23	4.10	5.42	0.57	7.01	2.82
di (fs	0.84	2.62	1.03	3.88	1.68	3.36	2.93	1.22	3.75	2.85
hy (en	10.25	10.26	7.21	12.56	10.12	6.69	11.66	3.19	13.93	7.52
hy (fs	3.90	8.21	5.20	7.39	7.63	5.48	6.30	6.78	7.45	7.61
ol (fo	-	-	-	1.95	-	4.48	-	-	-	-
ol (fa	-	-	-	1.27	-	4.05	-	-	-	-
il	0.68	0.72	0.55	0.63	1.14	1.27	1.46	1.31	0.99	1.03
mt	2.02	2.74	2.61	2.68	3.07	3.16	3.31	1.58	2.94	2.97
ap	0.31	0.45	0.38	0.45	0.36	0.36	0.64	0.88	0.43	0.43
Volume percent phenocrysts										
Plagioclase	26	27	28		28	27	23	3	25	26
Olivine	<1	-	<1		1	3	3	<1	<1	<1
Orthopyroxene	4	3	1		8	-	-	-	4	3
Clinopyroxene	4	9	2		6	<1	21	1	21	9
Fe/Ti oxides	<1	1	2		1	<1	1	<1	-	2
Amphibole	-	-	1		-	-	-	-	-	-
Total	34	40	34		44	30	48	4	50	40

1. High-silica andesite[b], Vokeo (18NG1037)[c].
2. Low-silica andesite, Bam (18NG1010).
3. High-silica andesite, Aris (19NG0965).
4. High-magnesia olivine-tholeiite basalt, Manam (Morgan, 1966; his sample 12). This sample is quartz-normative when Fe_2O_3/FeO value of the original analysis is used in the norm calculation. No modal analysis available.
5. Low-silica andesite, Bababag (26NG0792).
6. Low-magnesia olivine-tholeiite basalt, Long (32NG0754).
7. Low-magnesia quartz-tholeiite basalt, Tolokiwa (32NG0719).
8. Dacite, Umboi (32NG0110B).
9. High-magnesia quartz-tholeiite basalt, Ritter (32NG0004A).
10. Low-silica andesite, Langila (32NG0024B).

a. Calculated without volatiles using the Fe_2O_3/FeO transform of Irvine & Baragar (1971).

b. Rock names based on classification shown on page 25, using the silica value obtained after re-calculating to 100 percent without volatiles using the Irvine & Baragar (1971) transform.

c. BMR sample numbers shown in parentheses for samples 1-3, and 5-10.

TABLE 4. CHEMICAL AND MODAL ANALYSES AND CIPW NORMS OF 10 ROCKS SELECTED FROM 205 ANALYSED ROCKS FROM THE EASTERN ARC

	1	2	3	4	5	6	7	8	9	10
SiO_2	72.4	52.43	53.9	53.85	58.30	63.9	59.0	51.57	53.7	49.2
TiO_2	0.31	0.77	0.67	0.52	0.46	0.80	0.51	0.80	1.54	1.14
Al_2O_3	13.4	17.80	18.5	17.30	15.9	14.50	16.9	15.91	15.10	15.0
Fe_2O_3	0.88	3.32	2.95	3.68	3.65	1.81	3.15	2.74	3.95	3.45
FeO	1.48	6.55	5.70	5.53	3.75	5.55	3.90	7.04	7.95	6.05
MnO	0.07	0.18	0.15	0.15	0.13	0.15	0.13	0.17	0.24	0.18
MgO	0.81	5.17	3.90	4.82	4.70	1.95	3.40	6.73	4.15	11.3
CaO	2.75	10.61	9.70	9.45	8.15	5.70	6.70	11.74	7.90	10.8
Na_2O	4.05	2.35	2.50	2.55	2.85	3.60	2.90	2.41	3.60	2.2
K_2O	1.64	0.36	0.36	0.56	0.88	0.99	1.34	0.44	0.45	0.25
P_2O_5	0.03	0.08	0.07	0.12	0.13	0.18	0.14	0.11	0.19	0.11
H_2O+	1.98	0.19	0.86	)	0.45	0.54	1.07	0.35	0.43	<0.01
H_2O-	0.11	0.07	0.48	) 0.72	0.47	0.09	0.59	0.10	0.55	0.27
CO_2	0.04	0.05	<0.05	)	0.04	<0.05	0.05	-	<0.05	0.05
Total	99.95	99.93	99.74	99.25	99.86	99.76	99.78	100.11	99.75	100.00
CIPW norms[a]:										
Q	35.60	5.51	9.63	7.66	13.51	22.71	15.91	1.79	6.37	-
or	9.93	2.13	2.19	3.37	5.26	5.95	8.09	2.60	2.72	1.48
ab	35.01	19.96	21.48	21.91	24.44	30.70	25.04	20.47	30.87	18.69
an	13.74	37.16	38.86	34.69	28.33	20.69	29.74	31.42	24.01	30.44
C	0.04	-	-	-	-	-	-	-	-	-
di (wo	-	6.34	4.02	5.09	4.90	2.78	1.37	10.98	6.04	9.44
di (en	-	3.32	2.03	2.62	2.84	1.10	0.73	6.37	2.83	6.60
di (fs	-	2.84	1.90	2.33	1.83	1.72	0.59	4.09	3.15	2.05
hy (en	2.07	9.60	7.86	9.57	9.01	3.81	7.91	10.45	7.68	12.65
hy (fs	1.63	8.19	7.38	8.51	5.80	5.99	6.34	6.71	8.50	3.93
ol (fo	-	-	-	-	-	-	-	-	-	6.31
ol (fa	-	-	-	-	-	-	-	-	-	2.16
il	0.61	1.46	1.29	1.01	0.89	1.54	0.99	1.52	2.96	2.17
mt	1.30	3.31	3.20	2.97	2.89	2.65	2.97	3.35	4.47	3.84
ap	0.07	0.19	0.17	0.28	0.31	0.43	0.33	0.26	0.45	0.26
Volume percent phenocrysts										
Plagioclase	20	26	27	29	23	14	26	3	<1	-
Olivine	-	2	<1	1	-	-	-	-	-	10
Orthopyroxene	<1	1	1	5	3	1	2	-	-	-
Clinopyroxene	<1	<1	-	4	11	2	10	3	<1	-
Fe/Ti oxides	1	-	-	1	1	1	2	-	-	-
Amphibole	2	-	-	-	-	-	-	-	-	-
Quartz	13	-	-	-	-	-	-	-	-	-
Total	36	29	28	40	38	18	40	6	ca.1	10

1. Rhyolite[b], Sulu Range (51NG3032A)[c].
2. Low-magnesia quartz-tholeiite basalt, Ulawun (Johnson, Davies, & White, 1972; 51NG0156).
3. Low-silica andesite, Likuruanga (53NG0852A).
4. Low-silica andesite, Mataleloch, Cape Hoskins area (Blake & Ewart, 1974; their sample 77).
5. High-silica andesite, Dufaure (51NG2685B).
6. Dacite, Lolobau (52NG1049).
7. High-silica andesite, Bangum (51NG2708).
8. Low-magnesia quartz-tholeiite basalt, Dakataua (Lowder & Carmichael, 1970; their sample 311).
9. Low-silica andesite, Garove (48NG0537).
10. High-magnesia olivine-tholeiite basalt, Mundua Group (48NG0582).

a,b. See footnotes for Table 3.

c. BMR sample numbers shown in parentheses for samples 1-3, 5-7, 9, and 10.

the Australian Mineral Development Laboratories (AMDL, Adelaide), who used mainly 'wet chemical' analytical methods (MgO, CaO, Na_2O, K_2O were determined by atomic absorption). Four unpublished analyses (using mainly X-ray fluorescence methods) were kindly provided by Professor A.J.R. White (Latrobe University, Melbourne). Chemical data for Manam Island are incomplete*; the only analyses of Manam rocks used in this Report are those given by Morgan (1966), but these are almost entirely of rocks erupted in 1957-62. One of the 25 analyses given by Morgan (op. cit., his sample number 23, from Karkar) is not used here as it is known to contain secondary silica (G.A.M. Taylor, pers. comm., 1972). The groundmass analysis of an andesite given by Lowder & Carmichael (1970) is also excluded.

One of the principal purposes of this Report is to draw attention to regional differences in chemical composition between different groups of volcanoes in both the western and eastern arcs, and between the volcanoes of each arc. To facilitate a description of these differences, the volcanoes have been grouped into eight zones, as shown in Figure 10: the western volcanoes are grouped into zones A, B, C, and D; the eastern volcanoes are grouped into zones E, F, G, and H.

Zones A, B, C, and D are sectors of the western arc. The line of volcanoes making up the Schouten Islands defines zone A, but note that zones B, C, and D do not correspond to the lines of volcanic centres described earlier, on page 20 , for the other western volcanoes: Long and Tolokiwa, which belong to different structural lines, are grouped in the same zone, C; Crown is included in zone B with Aris, Manam, Karkar, and Bagabag; Umboi, Sakar, Ritter, and the volcanoes of the Cape Gloucester area are grouped together in zone D.

---

*This volcano was being studied independently by G.A.M. Taylor, whose sudden death on the island in August 1972 prevented his contribution to this Report.

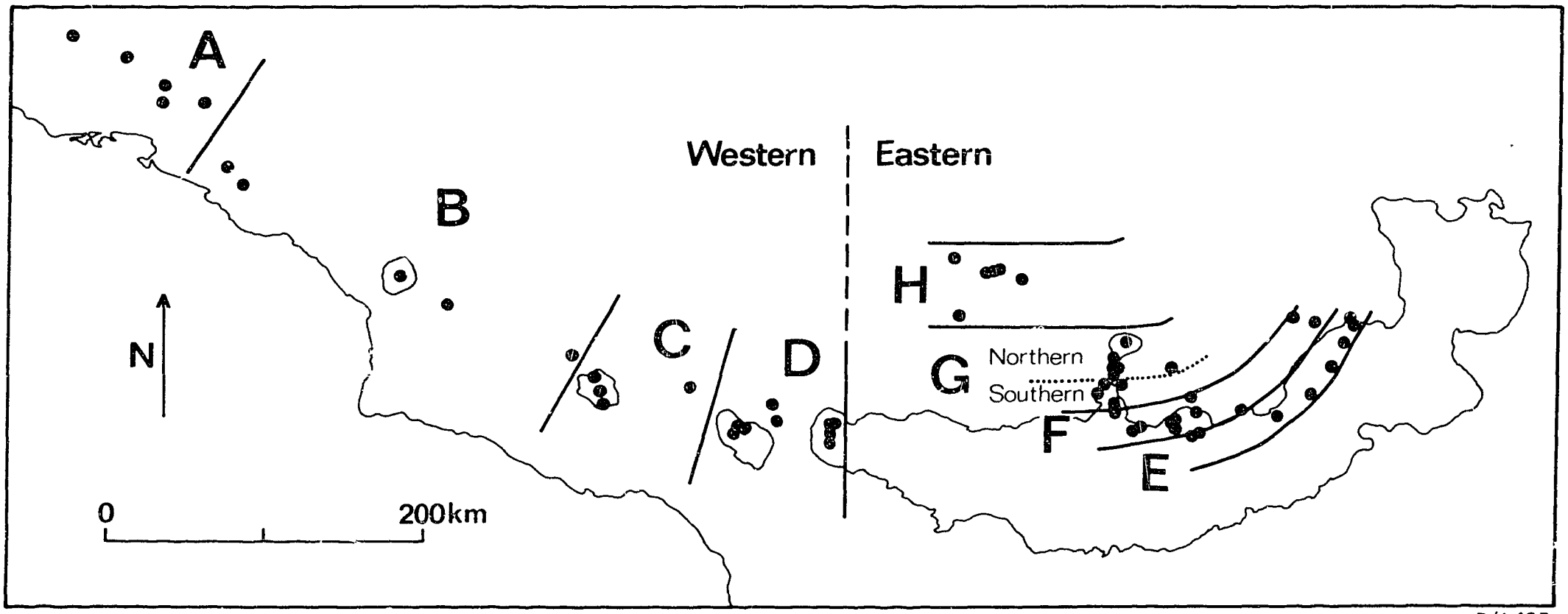

Fig. 10. South Bismarck Sea volcanoes (solid circles) grouped into western zones - A, B, C, D - and eastern zones - E, F, G, H. Zone A - Schouten Islands. Zone B - Aris to Crown. Zone C - Long and Tolokiwa. Zone D - Umboi to Cape Gloucester area. Zone E - Kakolan Island, Cape Deschamps, Likuruanga, Ulawun, Bamus, Hargy/Galloseulo, Sulu, Witori/Pago, and Buru. Zone F - Lolobau Island, Banban Island, Cape Reilnitz area, Cape Hoskins area (excluding Witori/Pago and Buru), Wulai Island, Dufaure, Wago, and Krummel. Zone G - Willaumez Peninsula (excluding Krummel) and Kimbe Island; the 'southern' volcanoes of zone G are Garbuna, Welcker, Bangum, and all those south of Lotomgan near Talasea Harbour. Zone H - the Witu Islands.

The volcanoes of the eastern zones, in the order E, F, G, and H, overlie progressively deeper parts of the present-day New Britain Benioff zone (Fig. 4), and in Figure 10 the boundaries between these zones are taken to be more or less parallel to the strike of the Benioff zone. The volcanoes of the Witu Islands are grouped as zone H. Except for Krummel, all the volcanoes of Willaumez Peninsula, and Kimbe Island, are grouped together in zone G. The remaining eastern volcanoes are divided into zones E and F. Note, however, that whereas zones E, F, and H contain belts of volcanoes which are more or less parallel to the strike of the New Britain Benioff zone, zone G consists of a chain of volcanoes at right-angles to the strike. Therefore, the use of the term 'zone' for the volcanoes of Willaumez Peninsula and Kimbe Island has a different connotation from that used for zones E, F, and H. Within zone G there are some striking differences in chemistry between volcanoes in northern Willaumez Peninsula (including Kimbe Island) and those in the south; a subdivision of zone G is therefore made into 'northern' and 'southern' parts (Fig. 10).

RELATIVE ABUNDANCES OF ROCK TYPES

An attempt has been made to calculate the relative abundances of rock types among the south Bismarck Sea volcanoes. As in other volcanic provinces, this attempt is greatly hindered by the problem of selecting a statistically representative suite of samples, and the calculations given here are therefore considered to be no more than rough estimates.

Several factors prevent the collection of a truly representative suite of rocks. The most important of these factors are probably (1) poor rock exposure (tropical rainforest covers much of the country), (2) juvenile dissection (which is inadequate to expose the cores of many volcanoes), (3) the inaccessibility of the submarine

parts of island volcanoes, and (4) in the search for unweathered rocks, lava flows were sampled more often than pyroclastic deposits. Nevertheless, because a large number (1200) of rocks has been examined in thin section, and because a large number (348) of chemical analyses is available, the estimates given here are considered to be not wholly unrealistic.

The analyses have been culled so that (1) the number of analysed rocks from any one volcano is roughly proportional to the volume of the subaerial part of the volcano, and (2) in any one volcano, the analysed rocks represent as uniform a range of compositions as possible. Applying these constraints, 316 rocks are used in the following frequency diagrams. The analyses of Lowder & Carmichael (1970) and of Blake & Ewart (1974) are all included, but all those of Morgan (1966) and a few of those of Johnson, Davies, & White (1972) are omitted, because they are biased towards recently erupted rocks. No rocks from Manam, Uvo, Andewa, and Schrader are represented.

Cumulative frequency curves - I and II for 124 western and 192 eastern rocks respectively - are shown in Figure 11. These curves show that (1) basalts are more common in the west than in the east, (2) low-silica andesite is the most common rock type in both arcs (compare the median values in Fig. 11; see also Table 2), (3) almost 15 percent of the eastern rocks have silica contents greater than the highest silica content of all the western rocks, and (4) in the western arc, dacites are uncommon and rhyolites are absent. A distinctive feature of the zone A volcanoes (Fig. 10) is the absence of basalts. When the zone A analyses are eliminated from the western suite, the corresponding frequency curve - III (Fig. 11) - is displaced to the left of curve I, emphasizing further the pronounced difference in the relative abundances of rock types between the western and eastern arcs.

Another striking feature of Figure 11 is the difference in shape between curve I (or III), which shows a positively skewed distribution, and curve II, which shows a bimodal distribution. Curve

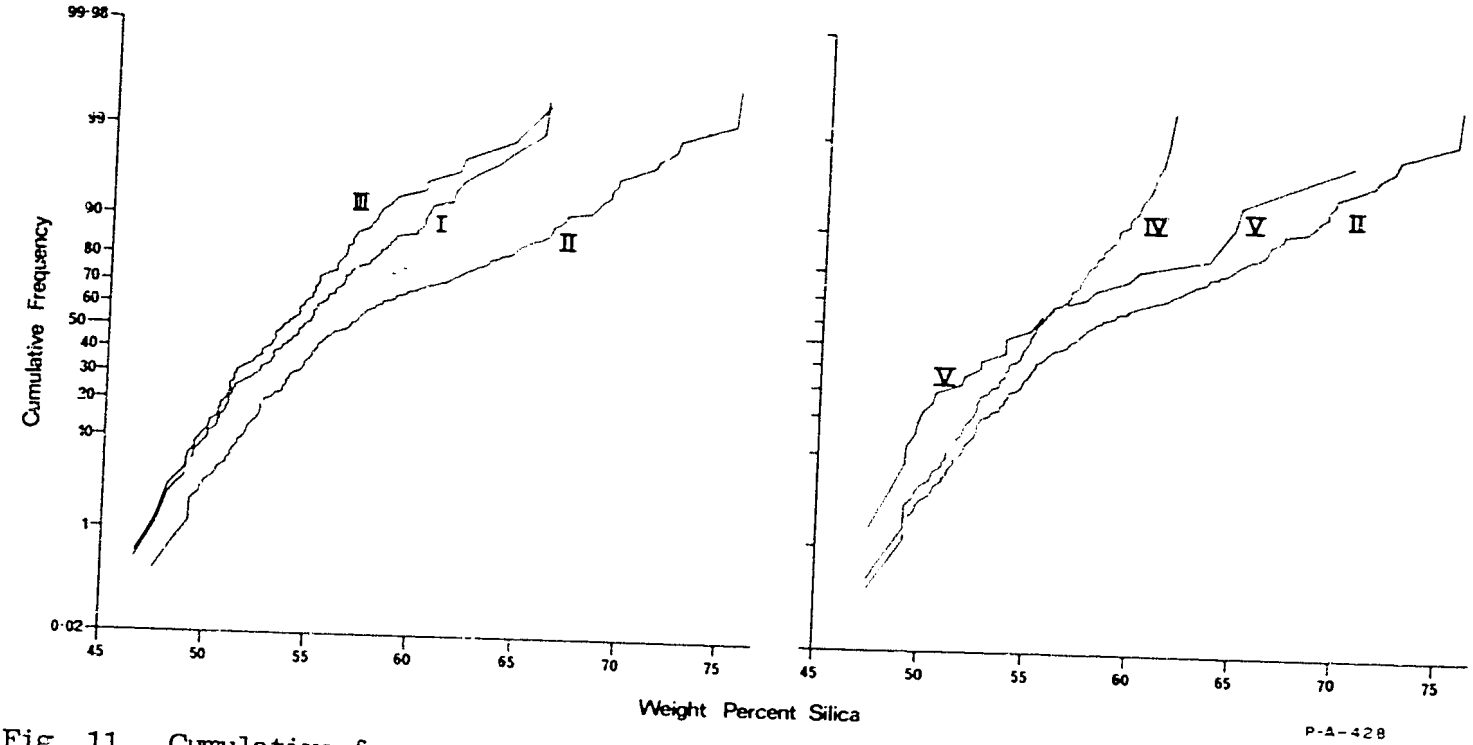

Fig. 11. Cumulative frequency curves for five suites of rocks from the south Bismarck Sea volcanoes. Silica values (% by weight) taken from original analyses. I = western rocks. II = eastern rocks. III = western rocks excluding those of zone A. IV = eastern rocks containing 61.5 percent by weight silica, or less. V = rocks of zone H.

Curve	Number of samples	Silica range	Median silica value
I	124	46.6 - 65.9	54.3
II	192	47.5 - 75.33	56.6
III	102	46.6 - 65.9	53.35
IV	138	47.5 - 61.5	54.7
V	29	47.5 - 70.3	53.7

II has an inflexion between about 61 and 62 percent silica, which corresponds roughly to the andesite/dacite boundary (see p. 25); this indicates that (1) rocks of this composition are relatively uncommon among the eastern rocks, and (2) dacites and rhyolites of the eastern volcanoes seem to constitute a population separate from that of the basalts and andesites. When analyses of rocks containing more than 61.5 percent silica are eliminated from the eastern suite, the corresponding frequency curve - IV (Fig. 11) - of the remaining 138 analyses is remarkably close to being a straight line, indicating (because of the vertical probability scale) that this suite of rocks shows - for all practical purposes - 'normal' or Gaussian distribution. (See p.127 for discussion on acid rocks.)

Among the eastern volcanoes, three other aspects of rock-type distribution are noteworthy. The first is that although dacites and rhyolites appear to be distributed throughout the eastern arc, a large proportion of them appears to be present in the volcanoes of the southern part of zone G (Fig. 10): of the 17 analysed rocks from these volcanoes, only two contain less than 60 percent silica, and one of these is a gabbroic inclusion. Secondly, the only dacites and rhyolites which have been found in the volcanoes of zone H are from Garove Island. Thirdly, as shown by curve V in Figure 11, basalts appear to be more common in the volcanoes of zone H than they are in the other eastern zones. Many of these zone H basalts are high-magnesia types (Fig. 23). However, Unea, the most southerly zone H volcano, appears to have few basalts, and, furthermore, in contrast to the other zone H volcanoes, to have the fullest development of andesites.

STRATIGRAPHIC CHANGES IN ROCK TYPE

Marked differences in rock type have been noted at different stratigraphic levels in each of five western and five eastern volcanoes; each of the zones, except G, contains at least one of these volcanoes. The stratigraphic changes are listed in simplified

form in Table 5, which shows that in seven of the ten volcanoes the younger rocks are consistently richer in silica than the older rocks. The three exceptions are Long, in the western arc, and Garove and Lolobau, in the eastern arc. On Garove, the sequence appears to be reversed, as dacites and rhyolites are the oldest exposed rocks, and basalts seem to be the youngest. The older parts of Long show a basalt-to-andesite sequence, but basalts were again erupted in 1968 and 1973-74 (Cooke et al., 1976). On Lolobau the sequence is andesite-basalt-dacite; it is the only example found in the south Bismarck Sea of a 'divergent-type' of volcano (McBirney, 1968), in which one group of younger rocks is more siliceous and another group is less siliceous than the oldest rocks of the same eruptive sequence.

A comparatively large number of samples from different parts of Ulawun and Umboi have established no large-scale stratigraphic differences in rock type in either volcano. Both, therefore, appear to be equivalent to McBirney's 'coherent-type' of volcano. Witori/Pago (Blake & Bleeker, 1970; Blake & Ewart, 1974) and Dakataua/Makalia (Lowder & Carmichael, 1970) may be other examples of coherent-type volcanoes. The stratigraphies of the other south Bismarck Sea volcanoes are unknown because exposure is insufficient, or because additional field studies are required to establish them.

PETROGRAPHY

The rocks of the south Bismarck Sea volcanoes are petrographically similar to those of many other island arcs. In this section, therefore, a summary of petrography is presented rather than a detailed account; differences between the rocks of the western and eastern arcs and between those of zones A to H are emphasized, as well as the more unusual aspects of petrography shown by the rocks of individual volcanoes. Petrographic details are presented in the reports listed on page 4 . A comprehensive mineralogical study of these rocks has yet to be undertaken, but electron microprobe analyses are available for the minerals of some rocks (Lowder, 1970; McKee, Cooke, & Wallace, 1976; R.N. England, unpublished data).

TABLE 5. SIMPLIFIED STRATIGRAPHIES OF TEN VOLCANOES

Volcano	Sequence
Kadovar* (Zone A)	low-silica andesites → crater formation → high-silica andesite (only slightly richer in silica).
Aris* (Zone B)	low-silica andesites → crater formation → high-silica andesites.
Long+ (Zone C)	basalts, type 1 → basalts, type 2 (richer in silica), and andesites associated with cauldron subsidence → basalts, type 2.
Sakar* (Zone D)	basalts → crater formation → high-silica andesites.
Talawe/ Langila* (Zone D)	Talawe basalts and low-silica andesites → Langila low-silica andesites (richer in silica). Langila is a satellite volcano on the northeastern flank of Talawe.
Hargy/ Galloseulo* (Zone E)	andesites → cauldron subsidence → andesites (mainly richer in silica) → Galloseulo dacites.
Bamus* (Zone E)	andesites (mainly low-silica) → collapse event → high-silica andesites.
Lolobau (Zone F)	andesites and (?)dacites → basalt → cauldron subsidence → basalt (poorer in Fe) dacites and rhyolites. Several samples of uncertain relative age.
Unea* (Zone H)	basalts and andesites → cauldron subsidence → andesites (mainly richer in silica).
Garove (Zone H)	dacites and rhyolites → low-silica andesites → cauldron subsidence → basalts. Several samples of uncertain relative age, including the basalts, which are only assumed to be post-caldera in age.

The prefixes 'low-silica' and 'high-silica' are omitted where both varieties of andesite are represented. Comments in parentheses describe rocks in relation to those of the same name in an earlier part of the same eruptive sequence. Zones A-H are shown in Figure 10.

*Volcanoes in which younger rocks are consistently more siliceous than older ones.

+Long should be considered as three volcanoes because two older basalt (type 1) cones flank a mainly younger central caldera complex (basalts type 2 and andesites).

Probably the most striking petrographic feature of the south Bismarck Sea rocks is their wide range in total phenocryst contents. Some rocks contain only a few percent phenocrysts (a few are virtually aphyric), whereas others contain more than 50 percent*. The phenocryst minerals are, in order of decreasing abundance, plagioclase, augite (sensu lato), pleochroic orthopyroxene, olivine, amphibole, iron-titanium oxides, low-2V clinopyroxene, quartz, apatite, and biotite. These minerals are present as individual phenocrysts, but phenocrysts of one or more of these minerals mostly form aggregates - the glomeroporphyritic texture commonly found in island-arc rocks.

In general, the rocks of the eastern arc contain fewer phenocrysts (mainly 20-40%) than those of the western arc (mainly 30-50%, Fig. 12). Most of the rocks containing less than 15 percent phenocrysts are from the eastern arc, and most of these are from zone H and Dakataua volcano: in Figure 12, 18 out of 27 rocks from zone H, and 5 out of 7 rocks from Dakataua, are shown to contain less than 15 percent phenocrysts. In the eastern arc, therefore, the least porphyritic rocks overlie the deepest part of the New Britain Benioff zone. Western rocks containing less than 15 percent phenocrysts are mainly from clastic deposits on Long Island.

In both the western and eastern arcs, high-silica rocks contain fewer phenocrysts than low-silica rocks (Fig. 12). Among the eastern rocks, lower phenocryst contents are characteristic of rocks

---

*Modal analyses for the BMR rocks were made by counting 2000-2500 points for each sample (excluding vesicles) using a 1/3 mm grid. These values are probably reasonably accurate estimates for most rocks, but some samples - particularly those from the western arc - contain phenocrysts or phenocryst aggregates of clinopyroxene several millimetres wide, and in these the area used for point-counting is not necessarily representative of the entire rock. (Using the visual estimation charts of Terry & Chilingar, 1955, estimation of hand specimens shows that the clinopyroxene contents are probably accurate to within about 5 percent absolute.) Moreover, in some samples there is no well defined limit between 'phenocryst' and 'groundmass' grains, and a more or less arbitrary limit was chosen between the two in each sample.

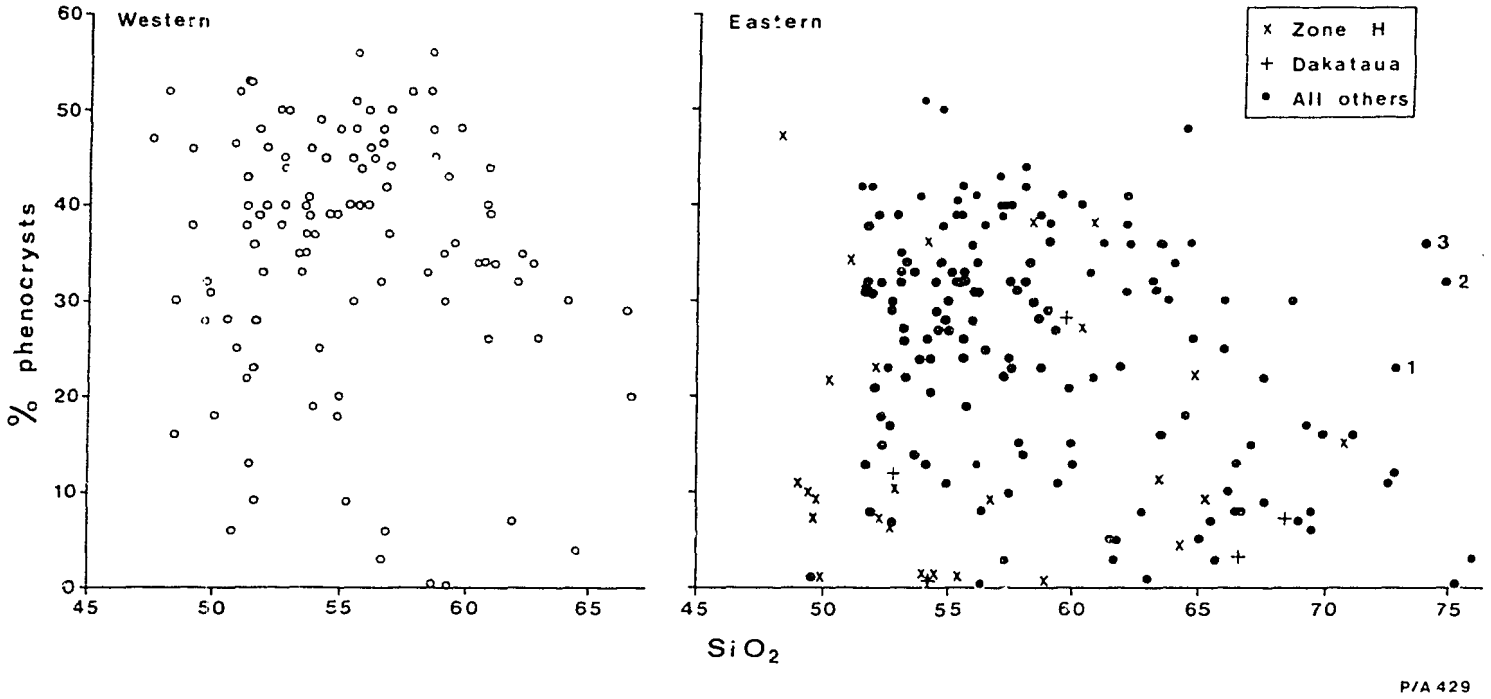

Fig. 12. Volume percent total phenocryst contents v. weight percent SiO_2 for 162 eastern and 106 western rocks (including data of Lowder & Carmichael, 1970, and Blake & Ewart, 1974). Samples 1, 2, and 3 are quartz-rich rhyolites from Sulu Range containing 4, 9, and 13 percent quartz phenocrysts respectively.

containing more than about 64 percent silica, whereas in the western arc phenocrysts are less abundant in rocks containing more than about 59 percent silica. Rhyolites in the eastern arc contain less than 20 percent phenocrysts, except for three unusually quartz-rich samples from the Sulu Range (Fig. 12).

Plagioclase is by far the most common phenocryst, and shows the characteristic features of plagioclase in other island-arc rocks: normal and complex oscillatory zoning is common; 'dust'-like inclusions are concentrated in bands parallel to the zoning; and the cores of many crystals contain abundant irregular areas of groundmass material (mostly glass which in many examples is laden with opaque minerals), suggesting that the phenocrysts have grown rapidly. The compositions of plagioclase phenocrysts from many basalts and andesites - determined optically by the Carlsbad-Albite twin method - are predominantly bytownite-labradorite; plagioclase compositions are less calcic in the more acid rocks. In common with other island-arc andesites, therefore, the south Bismarck Sea andesites are characterized by plagioclase phenocrysts of high anorthite content.

Augite phenocrysts are also common. The term 'augite' is used here in a broad sense for all calcium-rich and iron-poor clinopyroxenes that have moderate 2V (25-60°) and cover the compositional fields of augite (sensu stricto), diopside, endiopside, and salite (Deer, Howie, & Zussman, 1966). The augite phenocrysts are pale brown or pale green, and some show oscillatory zoning. They commonly form aggregates (with or without other minerals), and in many rocks they have cores of pleochroic orthopyroxene. Some western rocks contain augite aggregates 0.5-1 cm in diameter; these rocks, which are well developed on Aris, Long, Sakar, and Ritter, are distinctive in the field, and in hand specimen appear to be identical with rocks described by Stanton & Bell (1969) from the New Georgia group in the Solomon Islands (Fig. 3), where - like the western volcanoes - they overlie a near-vertical Benioff zone (cf. Cox & Bell, 1972), and where - unlike the western volcanoes - they are associated with picrite basalts.

Probably the most striking petrographic difference between the rocks of the western and eastern arcs is the generally higher proportion of augite phenocrysts in the western rocks. Most eastern rocks contain less than 5 percent clinopyroxene phenocrysts, whereas western rocks containing more than 5 percent are common, and some contain more than 15 percent (Fig. 13). The amount of clinopyroxene phenocrysts also shows a pronounced decrease as the silica content of the rocks increases, and the rocks of the Schouten Islands, zone A (Fig. 10), are richer in clinopyroxene phenocrysts than are those of the same silica content from other parts of the western arc (Fig. 13).

Low-2V (0-25°) clinopyroxene microphenocrysts are present in several basalts and low-silica andesites, particularly from zones E and F (cf. Johnson, Davies, & White, 1972; Blake & Ewart, 1974). These pyroxenes are probably pigeonite or subcalcic augite. They rarely constitute more than 1 percent of a rock, and they are included in the clinopyroxene abundances given in Figure 13.

Phenocrysts of pleochroic orthopyroxene (probably mainly hypersthene) are common, particularly in the andesites and dacites. They are, however, comparatively rare, or absent, in the rocks of zones C and H. With a few exceptions, orthopyroxene phenocrysts are less abundant than augite phenocrysts in the same rock. In many samples, orthopyroxene phenocrysts are jacketed by augite which in some rocks, is restricted to the prism faces of the orthopyroxene crystals; in a few samples, the augite and the orthopyroxene jackets are intergrown. Aggregates of orthopyroxene phenocrysts are common, and in some rocks they enclose phenocrysts of iron-titanium oxides.

Relative abundances of olivine phenocrysts are inversely proportional to those of orthopyroxene. Olivine phenocrysts are common in the basalts, and are present in lesser amounts in the andesites. The petrographic character of the olivine phenocrysts appears to depend on two main factors: (1) the degree of silica saturation of the rock containing them, and (2) the degree of crystallinity of the groundmass. Olivine phenocrysts are most abundant (up to 18%) in the olivine tholeiites, in which many of them are euhedral

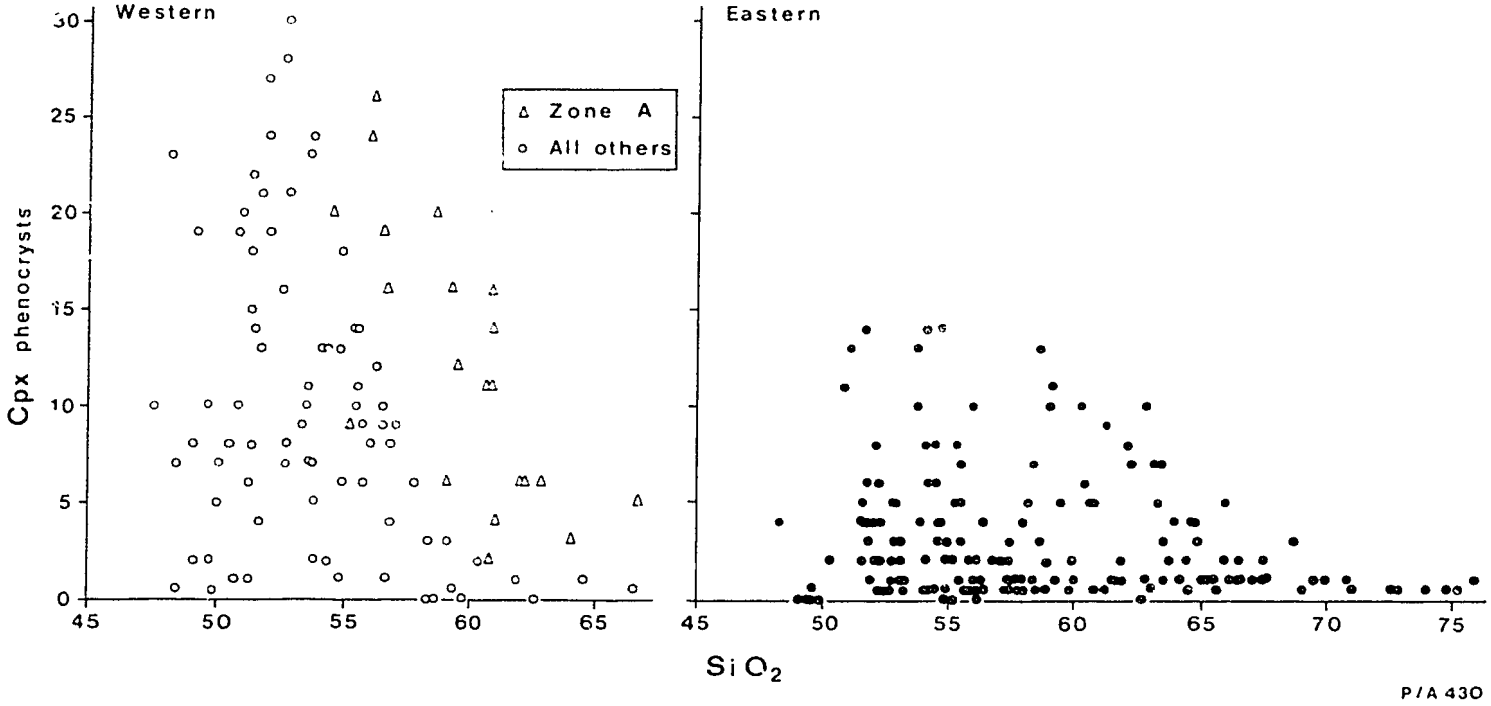

Fig. 13. Volume percent clinopyroxene (Cpx) phenocryst contents v. weight percent SiO_2 for rocks from the western and eastern arcs. Rare (about 2 percent, or less) low-2V clinopyroxene phenocrysts are present in a few rocks, and their abundances are included in the Cpx values.

and show no evidence of resorption; olivine is also present in the groundmass, indicating that it continued to crystallize throughout most of the cooling history of the rocks. In contrast, olivine phenocrysts are, as would be expected, less common in the quartz tholeiites and andesites, in which they show clear evidence of resorption particularly in coarsegrained lavas which have apparently cooled more slowly than those of finer grainsize. Reaction coronas of low-calcium pyroxene are abundant in these rocks, especially in those from zones E and F, and they have almost certainly originated by the familiar tholeiitic relation in which olivine reacts with silica-rich liquid (e.g., MacDonald & Katsura, 1964):

$$(Mg, Fe)_2SiO_4 + SiO_2 = 2(Mg, Fe)SiO_3 \qquad (1)$$

In some rocks, zones of iron-titanium oxides are commonly present between the pyroxene coronas and olivine cores. Both the pyroxene and the oxides may be the result of oxidation of olivine, as expressed by the following equation (Muir, Tilley, & Scoon, 1957):

$$3Fe_2SiO_4 + 3Mg_2SiO_4 + O_2 = 2Fe_3O_4 + 6MgSiO_3 \qquad (2)$$

Kuno (1950) and Presnall (1966), however, suggested that the iron-titanium oxides surrounding olivine phenocrysts are also the product of a crystal/liquid-reaction relation, analogous to equation (1) above. In some south Bismarck Sea rocks, olivine phenocrysts are rimmed, or appear to be completely pseudomorphed by, iron-titanium oxides alone. These relations are found in both fine-grained and coarse-grained rocks, which suggests they are not due to slow rates of cooling and did not result from crystal/liquid equilibria. It is assumed, therefore, that the iron-titanium oxide rims and pseudomorphs originated by oxidation of olivine, as shown by equation (2), and that the pyroxene components of the reaction are present but not visible between the oxide grains, or are concentrated in the surrounding groundmass.

The pyroxene of the olivine reaction coronas is orthopyroxene, or [illegible] in many zone E rocks - low-2V clinopyroxene (pro-

bably pigeonite or subcalcic augite). In some rocks, the grainsize is too small to identify the pyroxene species by optical means alone. The olivine phenocrysts in a few rocks, particularly from the western arc, have rims of augite; these phenocrysts may have acted as nucleation sites for the growth of augite grains, or they may indicate a second type of olivine/liquid-reaction relation observed in experiments on synthetic systems (O'Hara, 1968):

Olivine + quartz-normative liquid $\longrightarrow$ diopside (3)

'Iddingsite' partly or completely pseudomorphs olivine phenocrysts in some rocks. In many of these, the absence of a pyroxene corona around the pseudomorphs suggests the olivine was replaced at a higher temperature than the reaction of equation (1), as the olivine phenocrysts of other rocks of similar composition from the same volcano have pyroxene coronas but are not replaced by 'iddingsite'.

Amphibole phenocrysts are present in some rocks from both the western and eastern arcs. Their green/brown pleochroism differs in hue and intensity from one rock to another, but most, it not all, are probably hornblende (cf. Lowder, 1970). In many of these rocks, the amphibole is rimmed, or pseudomorphed, by iron-titanium oxides - accompanied in some samples by pyroxene, or pyroxene and feldspar; these are the familiar breakdown products of amphibole in a low-pressure volcanic environment (e.g., Lambert & Wyllie, 1970; Stewart, 1975). Rocks containing amphibole (or its pseudomorphs) are found in all the zones, A to H (Fig. 10), but they appear to be extremely rare in zones C and H.

Amphibole phenocrysts appear to be more common in the western arc than in the eastern arc. They are found in post-crater rocks on Aris and Sakar (Table 5); in several samples from Vokeo (mainly as pseudomorphs) and Crown; as uncommon constituents in rocks from Blupblup and Kadovar; and in one rock from Tolokiwa.

These rocks are either high-silica andesites or dacites. In contrast, phenocrysts of primary amphibole have not been found in any andesites from the eastern arc; they appear to be restricted to the rhyolites and, possibly to a lesser extent, to the dacites. They are, for example, present in quartz-phyric rhyolites from the Sulu Range; in pumices from Witori/Pago (Blake & Ewart, 1974); in rhyolites from northern Willaumez Peninsula (Lowder & Carmichael, 1970); and in some dacites from Dufaure, Welcker, and Garbuna.

A few rocks from both the western and eastern arcs contain polymineralic clusters that show prismatic habit. These have a wide range of composition and texture, but several examples consist of a pyroxene host (augite or orthopyroxene) containing laths of another pyroxene (orthopyroxene or augite) or plagioclase, or both, and grains of iron-titanium oxides. These are probably coarse-grained pseudomorphs of amphibole (cf. Stewart, 1975).

Iron-titanium oxide phenocrysts are present in most rocks, but in amounts that rarely exceed 1 to 2 percent. They are present in most high-silica andesites, dacites, and rhyolites, but they are absent, rare, or present only as microphenocrysts, in many basalts and low-silica andesites. In general, therefore, iron-titanium oxide phenocrysts are best developed in rocks containing orthopyroxene, rather than olivine, phenocrysts. In many of these rocks, orthopyroxene and iron-titanium oxides form conspicuous bimineralic aggregates. On the other hand, the basalts from some volcanoes contain prominent oxide phenocrysts - notably those from Long and Tolokiwa (the volcanoes of zone C), most of which are characterized by the absence of orthopyroxene. Except for those of Vokeo, the rocks of zone A (the Schouten Islands) contain relatively high abundances of iron-titanium oxide phenocrysts: Blupblup rocks contain 1 to 3 percent; and those of Kadovar contain 2 to 4 percent, which is higher than for any other rocks in both the western and eastern arcs.

Apatite phenocrysts are conspicuous in some rocks, particularly in silica-rich ones. They are less easily identified in basalts and low-silica andesites, because apatite grains, especially where small, may be easily mistaken for pyroxene. Apatite phenocrysts are, for example, expecially prominent in the rocks of zone H, and in the amphibole-bearing lavas of Sakar.

Quartz phenocrysts are present in several rhyolites, in some dacites, and in a few andesites. Amounts rarely exceed 1 to 2 percent, except in the rocks of the Sulu Range, some of which contain several percent (up to 13% in one sample, see Fig. 12). Rare biotite phenocrysts are also restricted to rocks of high-silica content. Blake & Ewart (1974) identified them in the matrix of an agglomerate from the Cape Hoskins area, and Lowder & Carmichael (1970) described them from rhyolites in the Talasea area.

The groundmasses of the south Bismarck Sea rocks show a wide range in texture and mineralogy. In most rocks, the common constituents are plagioclase, augite, orthopyroxene, iron-titanium oxides, and interstitial glass. In many of the basalts (especially in those of zone E) the calcium-poor pyroxene is low-2V clinopyroxene (pigeonite or subcalcic augite), rather than orthopyroxene. Olivine is present in the groundmass of the olivine tholeiites. In rocks richer in silica, high-temperature polymorphs of silica (tridymite and cristobalite) are present in the groundmass, or in small vesicles, and alkali feldspar is present interstitially. Apatite is probably ubiquitous, although it is difficult to recognize optically because of its small grainsize. A distinctive groundmass texture is found in many acid rocks: colourless, more or less circular areas up to about 0.1 mm in diameter and consisting mainly of salic minerals are enclosed by a darker, more glassy matrix; grains of iron-titanium oxides are scattered throughout the rocks, but in some the oxides are concentrated at the edges of the colourless areas. Spherulitic structures are preserved in some glassy rocks. True obsidians are found only in the Talasea area.

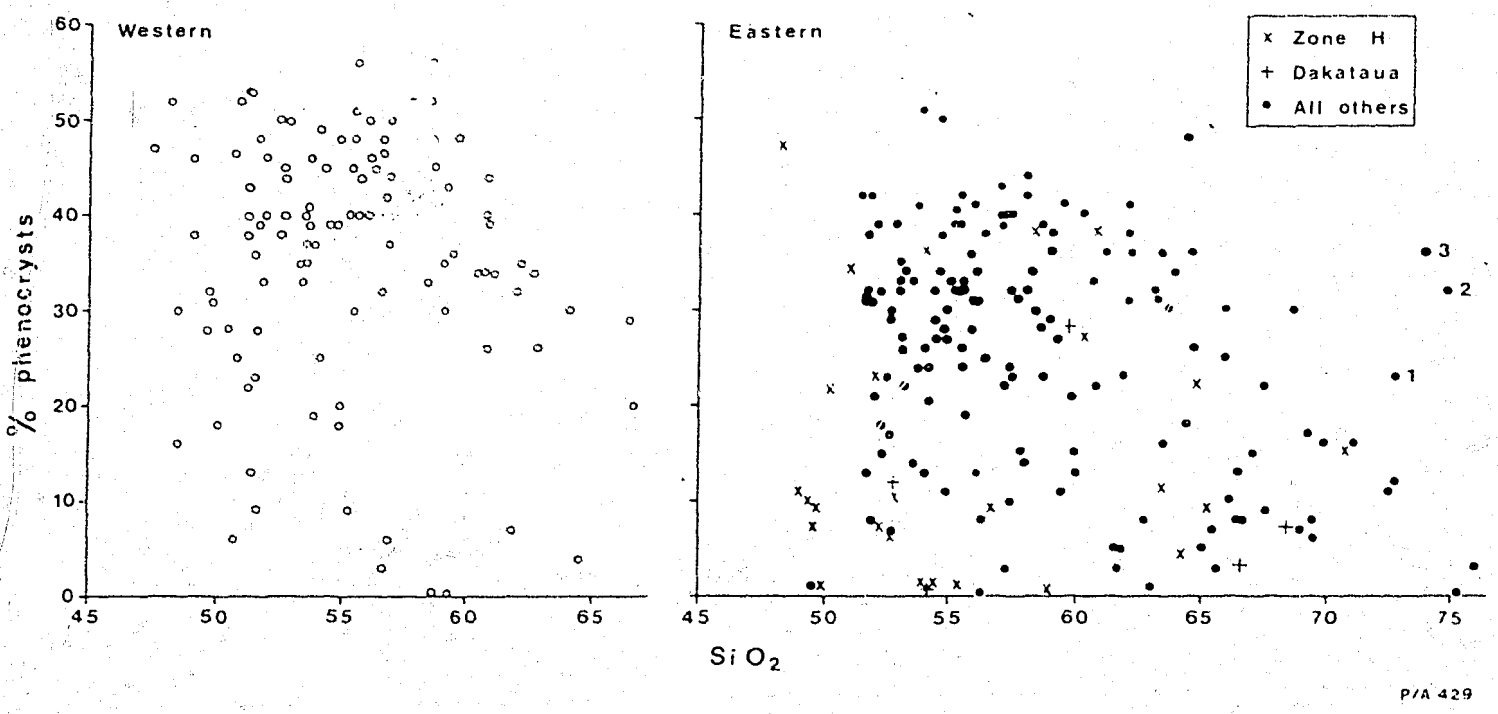

Fig. 12. Volume percent total phenocryst contents v. weight percent SiO_2 for 162 eastern and 106 western rocks (including data of Lowder & Carmichael, 1970, and Blake & Ewart, 1974). Samples 1, 2, and 3 are quartz-rich rhyolites from Sulu Range containing 4, 9, and 13 percent quartz phenocrysts respectively.

Some silica-rich lava flows contain inclusions of material coarser in grainsize than the lavas containing them. Similarly coarse-grained rocks are found as fragments in pyroclastic-flow and air-fall deposits. These inclusions are thought to be fragments torn from the conduits of the volcanoes. The grainsize of some samples suggests the rocks are probably from dykes and sills, or from the centres of slowly cooled lava flows, but others have a coarser grain suggesting derivation from larger intrusive bodies, or from slowly cooled material constituting the conduit walls.

Chemical analyses are available for three sets of host-lava/inclusion pairs: (1) amphibole-bearing gabbroic inclusions (49.46-51.62 % SiO_2) in an amphibole-bearing high-silica andesite cumulodome on Aris, (2) a gabbroic inclusion (51.97 % SiO_2) in a dacite on Bangum, and (3) an andesitic inclusion in a dacite lava flow at Cape Deschamps. In each of these samples the host lava contains more silica than the inclusions. The Aris inclusions are especially striking; they consist of zoned plagioclase, augite, brown amphibole in grains up to 3 cm long, rare pleochroic orthopyroxene, olivine, iron-titanium oxides, and interstitial cristobalite. At least one inclusion from Aris is olivine-normative; it contains about 1 percent alkalis, which is the lowest value of all the analysed rocks from both the western and eastern arcs (Fig. 18).

VARIATION DIAGRAMS

Types of diagrams

Many studies of island arcs have demonstrated that in rocks of the same silica content, total alkalis ($Na_2O + K_2O$) and K_2O show systematic changes as depth to the Benioff zone increases. In this study, variations in all the major oxides (excluding water and

carbon dioxide) relative to silica are described. Total alkalis and K_2O are shown to change systematically throughout both the western and eastern arcs, and it is also demonstrated that Na_2O, K_2O/Na_2O, TiO_2, P_2O_5, CaO, Al_2O_3, MgO, and MnO show systematic variations.

Unless stated otherwise, the oxide and normative values used in the variation diagrams are those obtained after the analyses have been recalculated to 100 percent without volatiles, and after the oxidation state of iron has been standardized by the procedure recommended by Irvine & Baragar (1971) - that is, if $Fe_2O_3 > TiO_2 + 1.5$, sufficient Fe_2O_3 is converted to FeO for Fe_2O_3 to equal $TiO_2 + 1.5$. Statistics of these transformed oxide values are given in Table 2. To avoid unnecessary congestion, a few rocks are not plotted on many of the variation diagrams, and natural logarithmic scales are used in some diagrams to disperse points in areas of high density.

Limitations of the method of data presentation

In all the variation diagrams, each rock-point symbol is identified with either one or more volcanoes or one or more of the zones A to H (Fig. 10). To identify the rocks of every volcano in each variation diagram is impracticable, and therefore the only volcanoes distinguished are those whose rocks appear to be chemically distinct from those of all the other volcanoes in the same arc. This, however, is a biased procedure, because the rocks of each volcano are 'distinct' from the other rocks to the extent that all depart, in different degrees, from an 'average' set of compositions for an entire arc. To define these departures statistically is beyond the purpose of this study, but note that in each of the variation diagrams a single rock-point symbol identified with more than one volcano in one or more zones does not imply that the rocks of each volcano cannot be statistically distinguished in the variation diagrams.

Another limitation of the method of data presentation is in the grouping of the volcanoes into zones, A to H (Fig. 10). This grouping was found by trial and error to be the most useful for describing overall chemical differences, but it is not necessarily

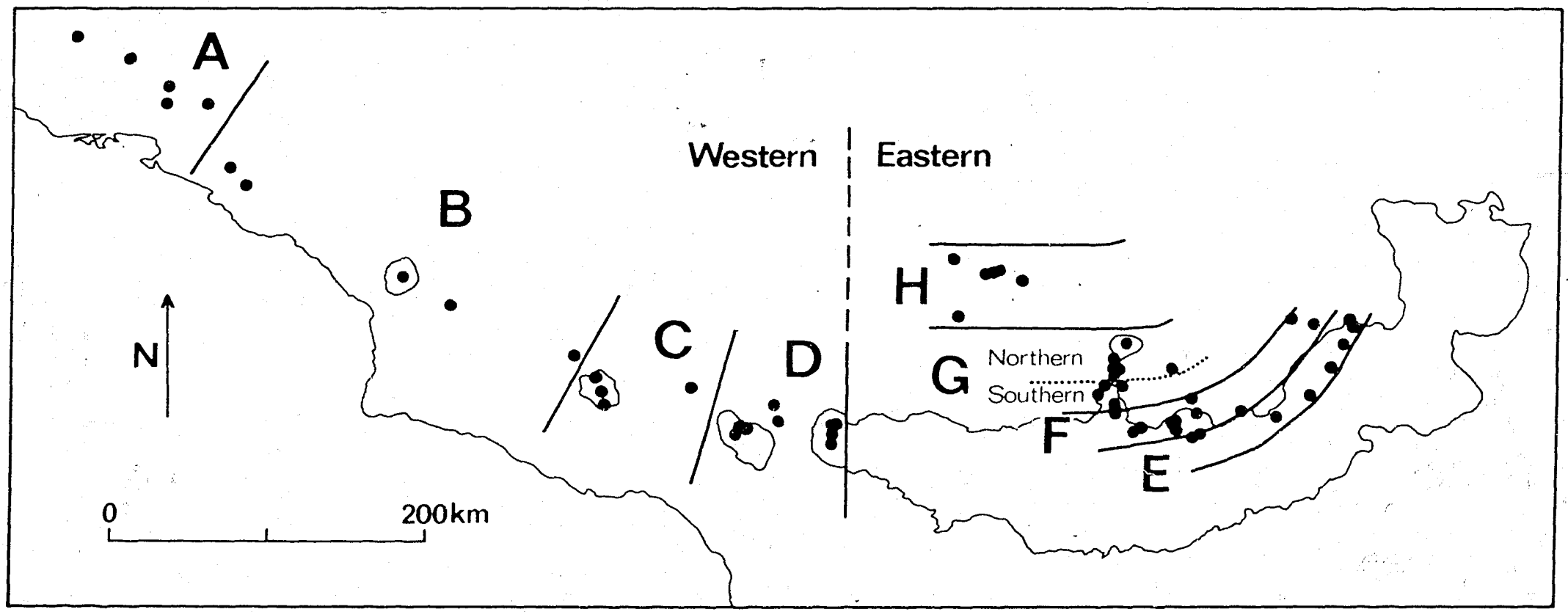

Fig. 10. South Bismarck Sea volcanoes (solid circles) grouped into western zones - A, B, C, D - and eastern zones - E, F, G, H. Zone A - Schouten Islands. Zone B - Aris to Crown. Zone C - Long and Tolokiwa. Zone D - Umboi to Cape Gloucester area. Zone E - Kakolan Island, Cape Deschamps, Likuruanga, Ulawun, Bamus, Hargy/Galloseulo, Sulu, Witori/Pago, and Buru. Zone F - Lolobau Island, Banban Island, Cape Reilnitz area, Cape Hoskins area (excluding Witori/Pago and Buru), Wulai Island, Dufaure, Wago, and Krummel. Zone G - Willaumez Peninsula (excluding Krummel) and Kimbe Island; the 'southern' volcanoes of zone G are Garbuna, Welcker, Bangum, and all those south of Lotomgan near Talasea Harbour. Zone H - the Witu Islands.

TABLE 2. SOME STATISTICS OF THE 348 CHEMICAL ANALYSES OF ROCKS FROM THE WESTERN AND EASTERN ARCS

Arc	Number of analyses	Oxide	Mean	Standard deviation	Minimum value	Maximum value
Western	143	SiO_2	54.93	3.92	47.47	66.76
		TiO_2	0.52	0.15	0.24	0.89
		Al_2O_3	16.40	1.69	11.69	21.56
		Fe_2O_3	2.02	0.18	1.09	2.41
		FeO	6.90	1.61	1.92	10.38
		MnO	0.17	0.03	0.06	0.26
		MgO	5.72	2.50	1.51	15.22
		CaO	9.55	1.75	4.37	13.65
		Na_2O	2.44	0.53	0.94	3.82
		K_2O	1.14	0.51	0.13	3.14
		P_2O_5	0.20	0.08	0.08	0.63
Eastern	205	SiO_2	58.60	6.29	48.24	76.19
		TiO_2	0.66	0.28	0.24	1.93
		Al_2O_3	16.60	1.65	12.57	20.44
		Fe_2O_3	2.02	0.38	0.33	3.28
		FeO	5.81	1.82	0.85	9.05
		MnO	0.15	0.03	0.05	0.24
		MgO	4.07	2.21	0.24	11.35
		CaO	8.13	2.58	1.23	13.10
		Na_2O	2.98	0.80	1.52	5.74
		K_2O	0.85	0.67	0.16	3.88
		P_2O_5	0.12	0.07	0.02	0.41

All analyses have been recalculated to 100 percent without volatiles using the Irvine & Baragar (1971) transform. See Appendix 2 for full list of chemical analyses.

a satisfactory one for each of the diagrams. In some diagrams, the rocks of one volcano may show the chemical features of rocks from one zone, but in other diagrams they may show features more in common with those of other zones. For example, the rocks of Unea are chemically similar to most other zone H rocks, but as shown in Figure 16 their Na_2O contents are more similar to those of rocks from the northern part of zone G. The rocks of Kimbe Island (Fig. 6) also have an ambivalent status, and, although Kimbe is considered in all the diagrams to belong to the northern part of zone G, in some diagrams its rocks have closer chemical affinities with those from the southern part of zone G. In spite of these problems, and instead of defining new sets of zones for each of the diagrams, it has been found easier to retain the grouping A to H in all the diagrams, and to make reference in the text or figure captions to anomalous aspects of the grouping.

Regression lines

Least-squares lines of best fit for the rocks of most zones are shown on the two-axis variation diagrams, and in the following sections are used to describe differences between the 'average' compositions of rocks from different zones. These regression lines were computed using program BMD05R (Dixon, 1971) with modifications by Mayo & Long (1976). Silica (weight percent) is plotted along the horizontal axis of all but one of the two-axis diagrams, and in the regression calculations is treated as the independent variable; in Figure 25, a plot of MgO versus $FeO + Fe_2O_3$, MgO is the independent variable.

For any data set, program BMD05R calculates a series of lines of best fit, starting with a simple linear regression, and successively increasing the degree of the polynomial - through two-degree (quadratic), three-degree (cubic), and so on - to some predetermined limit - in this study, to the fifth degree. F values are calculated for each regression line, and are compared with one another. If each of two successive term additions to the polynomial

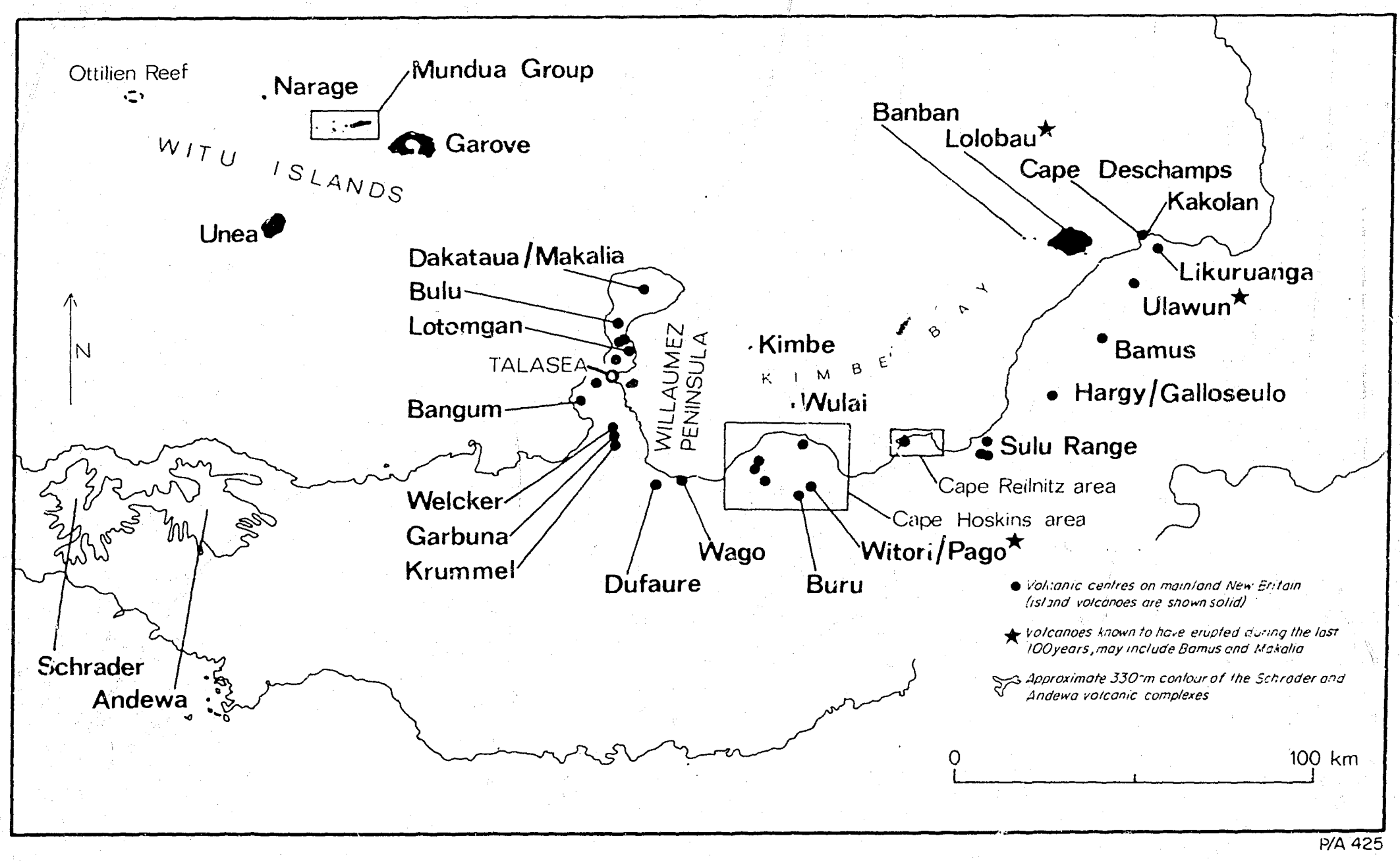

Fig. 6. Main volcanic centres of the eastern arc. Makalia, Pago, and Galloseulo are post-caldera volcanoes which respectively lie inside the older volcanoes of Dakataua, Witori, and Hargy.

does not remove significantly more of the remaining sum of squares produced by the data points about the regression line, the polynomial obtained before the addition of the two terms is assumed to give the best fit through the data points. The significance of the difference between the sum of squares of two successive regression lines is measured by dividing the difference by the mean-square value about the regression. This calculation gives an F value which can be compared with the critical F value corresponding to the appropriate number of degrees of freedom (i.e., the number of samples in the data set, less one, less the degree of the higher-degree polynomial) at the 95 percent confidence level. If the calculated F value is greater than the critical F value, the higher-degree regression is judged to be a significantly better fit of the data points. In some data sets the calculated F value for linear (one-degree) regressions is less than the corresponding critical F value at the 95 percent confidence level, and, when the quadratic regression does not give a significantly better fit, no regression line is obtained.

A measure of the closeness of fit about each regression line is given by the ratio, RSS, of the sum of squares due to the fit of the polynomial and the total sum of squares. RSS values multiplied by 10^3 are given in Table 6 for the rocks of each of the zones, A to H. The values are low for a poor fit; they increase as the fit improves, and would be 1000 for a perfect fit. The separation between and the shapes of the regression lines, and the RSS values, are used below to generalize the descriptions of regional chemical variations in the western and eastern arcs.

Other statistical tests

The above multiple-regression program tests the relations between only two variables at any one time. To enable differences in the major-element chemical compositions of the whole rock to be statistically evaluated, two other programs have been used in this study: one involves Q-mode factor analysis (Klovan & Imbrie, 1971); the other uses nonlinear mapping (Howarth, 1973), for which techniques and results are discussed in Appendix 3.

TABLE 6. RSS VALUES X 10^3 OF REGRESSION LINES FOR ROCKS OF ZONES A TO H SHOWN IN VARIATION DIAGRAMS

Figure Number	15	16	17	18	19	20	21	22	23	24	25	26	27
Variation diagram	K_2O v. SiO_2	Na_2O v. SiO_2	K_2O/Na_2O v. SiO_2	Na_2O+K_2O v. SiO_2	TiO_2 v. SiO_2	P_2O_5 v. SiO_2	CaO v. SiO_2	Al_2O_3 v. SiO_2	MgO v. SiO_2	$FeO+Fe_2O_3$ v. SiO_2	MgO v. $FeO+Fe_2O_3$	FeO/Fe_2O_3 v. SiO_2	MnO v. SiO_2
Zone A n* = 24		473 (1)		396 (2)			913 (1)		584 (1)	749 (3)	392 (1)		757 (3)
Zone B n = 52	690 (2)	672 (2)	123 (1)	791 (3)	155 (5)		891 (2)	274 (2)	767 (3)	579 (2)		281 (2)	118 (1)
Zone C n = 23	817 (1)	886 (1)	644 (1)	883 (1)		563 (1)	917 (1)	177 (1)	621 (1)	188 (1)			182 (2)
Zone D n = 44	744 (1)	707 (1)	367 (1)	811 (1)		447 (3)	872 (1)	320 (2)	629 (2)	772 (3)	615 (5)	227 (2)	426 (1)
Zone E n = 83	859 (1)	819 (3)	646 (1)	894 (3)	457 (3)	370 (3)	957 (1)	545 (5)	643 (2)	884 (5)	814 (3)		736 (5)
Zone F n = 58	894 (1)	847 (2)	691 (4)	931 (2)		318 (2)	973 (1)	519 (1)	847 (1)	841 (1)	728 (2)		549 (3)
Zone Gs n = 17	978 (1)	933 (2)	886 (1)	986 (1)	892 (5)	682 (2)	990 (2)	769 (4)	850 (1)	964 (1)	939 (4)	538 (1)	927 (1)
Zone Gn n = 18	827 (1)	970 (2)	639 (1)	946 (2)	400 (2)	452 (2)	977 (2)	387 (1)	909 (2)	912 (2)	939 (5)		582 (2)
Zone H n = 29	788 (4)	918 (1)	527 (4)	975 (4)		751 (5)	944 (2)	314 (1)	769 (2)	671 (2)	592 (3)	459 (4)	

*n = number of samples

Numbers in parentheses indicate degrees of regression

Silica saturation

The degree of silica saturation in the rocks of the south Bismarck Sea is illustrated in Figure 14 with reference to the normative pseudoternary system Ol-Ne-Q (the base of the 'basalt tetrahedron', Ol-Ne-Q-Di, of Yoder & Tilley, 1962; see inset in Fig. 14). By plotting molecular percentages, and by using the joins Ab-Ol and Ab-Hy as field boundaries, the three principal types of basalt - alkali, olivine tholeiite, and quartz tholeiite - can be distinguished. The normative proportions of the south Bismarck Sea rocks have been calculated using the oxidation adjustment discussed on page 39 (Irvine & Baragar, 1971). Because the effect of this adjustment is to reduce the Fe_2O_3/FeO values of some rocks, the degree of silica saturation shown by the CIPW norm is lowered: 31 of the rocks shown in Figure 14 are olivine tholeiites (ol-normative and hy-normative), but 12 of them are Q-normative (quartz tholeiites) when the Fe_2O_3/FeO values of the original analyses are used in the CIPW calculation.

Figure 14 is a ternary variation diagram, and no regression lines have been calculated for the rocks of zones A to H. However, to facilitate description, generalized field boundaries have been drawn to the diagram. These boundaries have no precise statistical significance, and to different extents all are drawn somewhat arbitrarily. The lower-case letters a to h in Figure 14 indicate that the appropriate compositional field is characterized by a relative abundance of rocks from the respective zones A to H. The field boundaries define a series of compositional fields for the rocks of both the western and eastern arcs, and show that the rocks of each zone differ in their degrees of silica saturation. The fields trend away from the Ol apex, and away from the Ab-Ol join.

Most of the rocks from zone A fall in field a (Fig. 14), which represents the most silica-saturated compositions of all the western rocks; no basalts have been found on the volcanoes of zone A. The rocks of zones B and D define a joint field b-d; these rocks are less silica-saturated than those of zone A, and include many basalts,

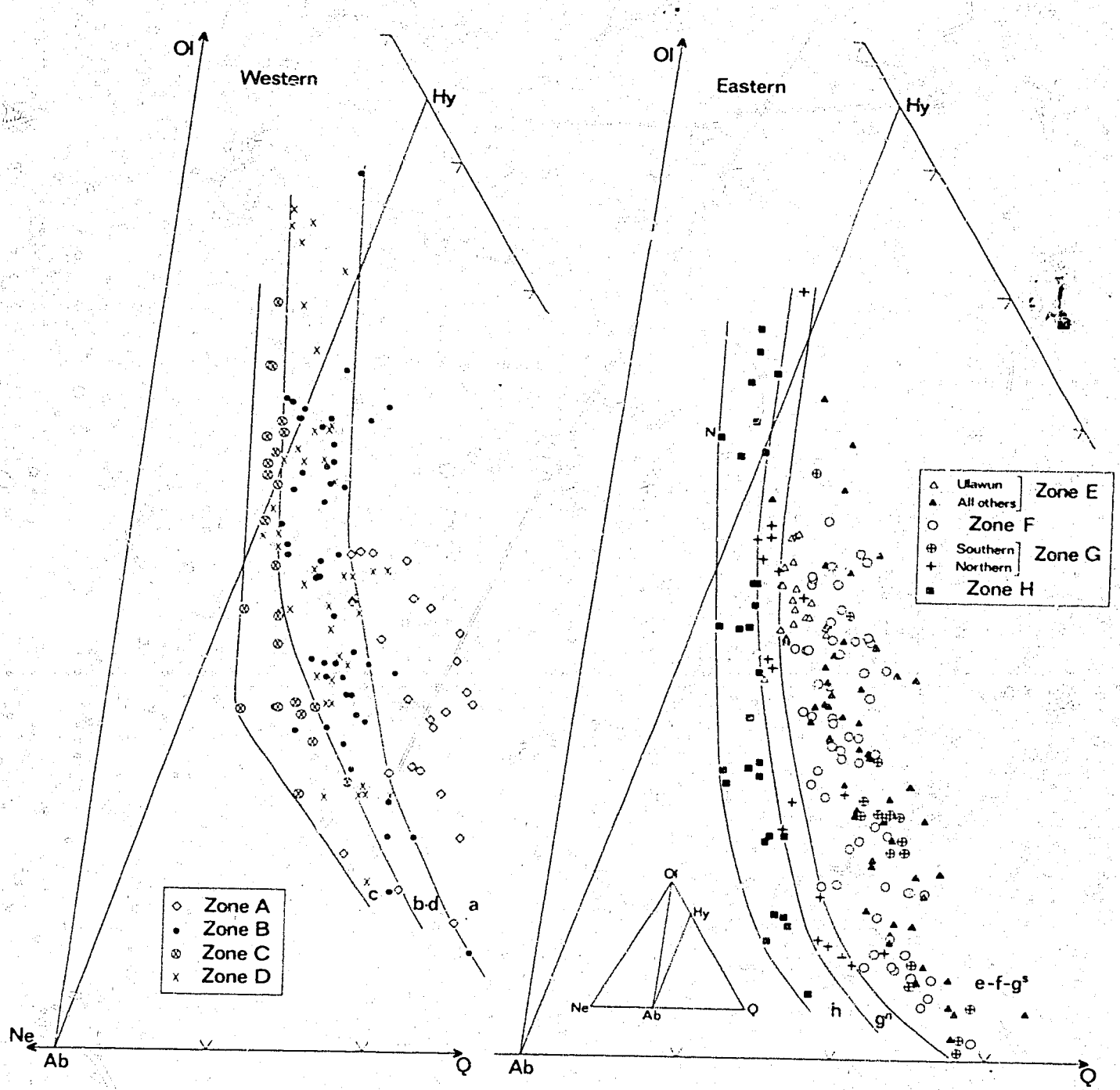

P/A 431

Fig. 14. Molecular percentages of rocks from the western and eastern arcs plotted in part of the normative pseudo-ternary system Ol–Ne–Q (see inset of right-hand diagram). 21 of 24 zone A rocks define field a. 83 of 96 rocks from zones B and D define field b–d. 22 of 23 zone C rocks define field c. 156 of 158 rocks from zones E and F, and from the southern part of zone G, define field e–f–g^s. 15 of 18 rocks from the northern part of zone G define field g^n. All 29 zone H rocks define field h. N is the one sample from Narage.

of which 14 are olivine tholeiites. Field c contains most of the rocks from the two volcanoes in zone C; these rocks are the least silica-saturated of the western rocks, and 9 of them (out of a total of 21) are olivine tholeiites. Consistent changes in the degree of silica saturation are therefore observed throughout the length of the western arc.

A similar pattern of chemical variation is shown by the rocks of the eastern arc. Rocks from zones E and F, and from the southern part of zone G, are combined in a single field e-f-g^s, within which the rocks of the southern part of zone G and of zone E - except those of Ulawun - fall mainly in the Q-rich part whereas many of those from zone F plot closer to the Ab-Ol join; these rocks are the most silica-saturated of all the eastern rocks, and, although many basalts are represented, none of them is olivine-normative. Field g^n contains points representing rocks from the northern part of zone G; these rocks are less silica-saturated than those of field e-f-g^s, and they include one olivine tholeiite - from Kimbe Island. All the rocks of zone H fall in field h; they are the least silica-saturated of all the eastern rocks, and they include seven olivine tholeiites, of which five are from the Mundua Group. The one sample from Narage Island, which is the most northern volcano in the eastern arc, is the closest of all the olivine-normative basalts to the Ab-Ol join, and appears, therefore, to be the least silica-saturated; however, this rock has a high original Fe_2O_3/FeO value, and it is slightly Q-normative when this value is used in the CIPW norm calculation.

In the eastern arc, therefore, pronounced decreases in the degree of silica saturation are observed as depth to the New Britain Benioff zone increases. Exceptions to this general conclusion are the rocks of Ulawun and those of volcanoes in the southern part of zone G, which plot in inappropriate parts of field e-f-g^s.

Whether or not many of the olivine tholeiites mentioned above represent the compositions of true magmas cannot be ascertained for two reasons. Firstly, because of post-emplacement oxidation effects, the Fe_2O_3/FeO values of the rocks may not represent those

of the magmas at the time of generation or eruption. Oxidation adjustments - such as those used in the scheme of Irvine & Baragar (1971) - standardize the rocks for petrological comparison, but there is no certain way of knowing if the adjusted Fe_2O_3/FeO values are accurate estimates of the original ratios in the magmas. Because Fe_2O_3/FeO governs the appearance of olivine in the CIPW norm, the recognition of true olivine tholeiite magmas is hindered by the difficulties of choosing the most representative Fe_2O_3/FeO values.

Secondly, olivine phenocrysts may or may not have accumulated in the rocks. Of the 19 south Bismarck Sea rocks which are olivine-normative using the Fe_2O_3/FeO value of the original analyses, all but two contain olivine phenocrysts. If these olivine crystals are cumulates, the compositions of the rocks plotted in Figure 14 will have been displaced towards the Ol apex from the true liquid compositions, which for some rocks may have been Q-normative. The proporportion (if any) of olivine phenocrysts that represents a cumulus fraction cannot be estimated, so some of the rocks may owe their olivine-normative character to the accumulation of olivine. However, two of the 19 olivine-normative rocks contain less than 1 percent total phenocrysts, and almost certainly represent liquids of true olivine tholeiite composition.

In spite of these difficulties, there is little doubt that real differences in the degree of silica saturation exist between the most basic rocks in each of the zones, A to H. In the western arc, no basalts have been found in zone A; quartz tholeiites are common, and olivine tholeiites much less common, in zones B and D; and both olivine tholeiites and quartz tholeiites are common in zone C. In the eastern arc, quartz tholeiites are common in zones E, F, and the southern part of G, but olivine tholeiites appear to be absent; quartz tholeiites and rare olivine tholeiites are present in the northern part of zone G; and olivine tholeiites and quartz tholeiites are common in zone H.

K_2O:SiO_2

Because potassium is believed to be the most sensitive of the major elements to differences in the tectonic setting of island-arc volcanoes, many studies have given considerable attention to potash:silica relations. Correlations between increasing potassium content (for rocks containing the same amounts of silica) and increasing depth to the underlying Benioff zone are now recognized as common features of island-arc geology (e.g., Dickinson & Hatherton, 1967), and some authors have used potassium as a principal chemical parameter in classifying island-arc rock associations (e.g., Taylor et al., 1969; Jakeš & Gill, 1970; Mackenzie & Chappell, 1972; Ninkovich & Hays, 1972).

Variations in K_2O in the rocks of the south Bismarck Sea volcanoes are illustrated in Figure 15 with reference to the zones defined in Figure 10. The regression lines for the rocks of the western zones B, C, and D show that zone C rocks have the highest K_2O contents (comparing rocks of the same silica content), and that the rocks of zone D are more potassic than those of zone B. The K_2O contents of rocks from zone A show a comparatively wide range: two samples from Kadovar plot above the zone C regression line, but all the others plot below the zone D regression line; and nine samples from Vokeo and Viai Islands, in the west, have the lowest K_2O values of all the western rocks containing the same amount of silica. This scatter of points is so broad that the calculated F value was too low to allow a regression line to be calculated for these zone A rocks. Nevertheless, in spite of the scatter, and except for the two anomalous samples from Kadovar, Figure 15 shows that, for rocks of the same silica content, K_2O contents generally increase between zone A and zone C, and decrease in zone D.

Most eastern rocks contain less than half as much K_2O as western rocks with the same silica content, but there is considerable compositional overlap. Except for those of Ulawun, the rocks from

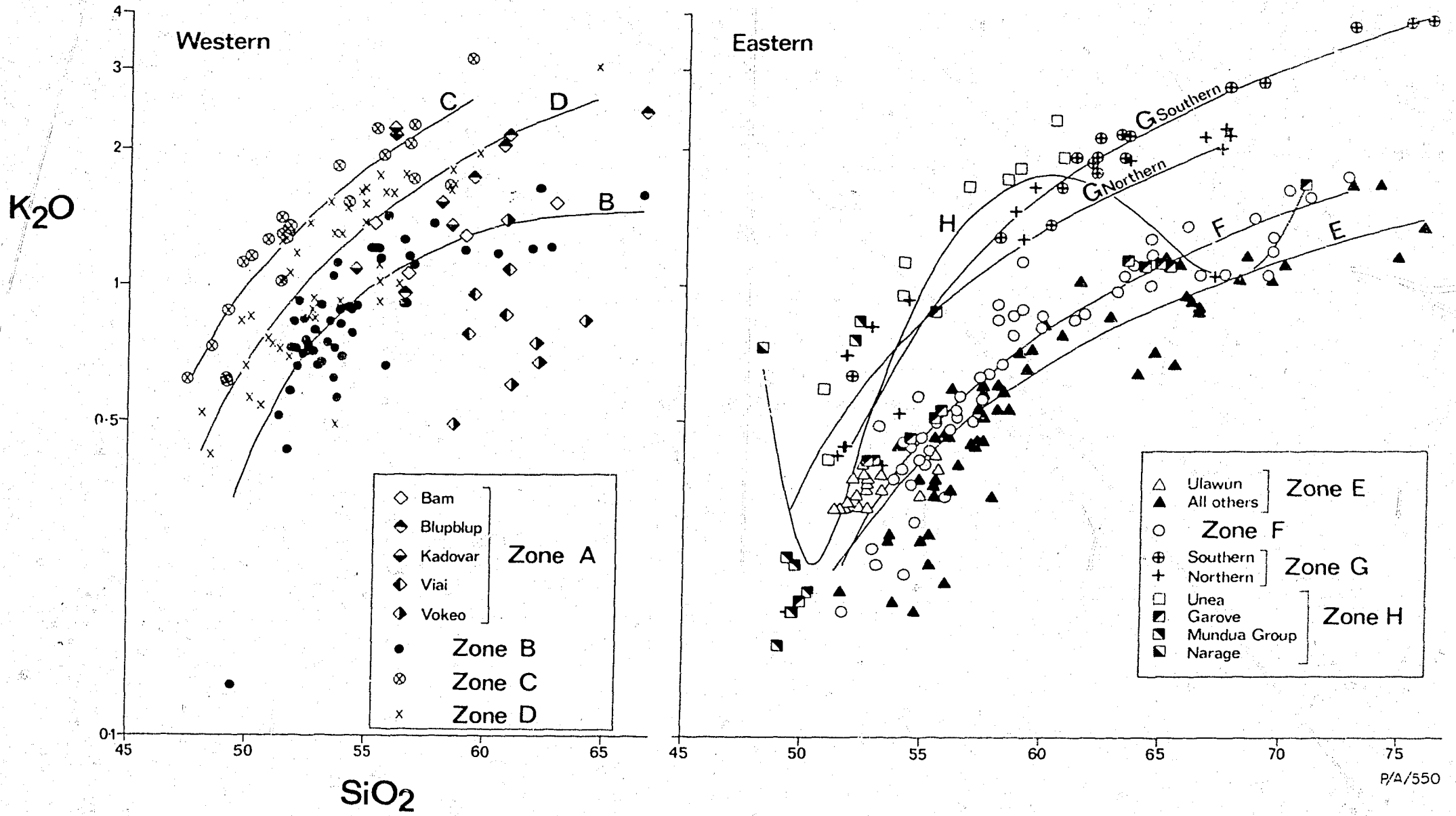

Fig. 15. Weight percent K_2O ($\log_{10}$ scale) v. SiO_2 for rocks from the western and eastern arcs. RSS values (x 10^3) for regression lines: B = 690, C = 817, D = 744, E = 859, F = 894, G southern = 978, G northern = 827, H = 788.

volcanoes in zone E contain the least K_2O of all the eastern rocks, as shown by regression line E, and the rocks of zone F are generally more potassic; the rocks of Ulawun, a zone E volcano, also have generally higher K_2O contents. This general increase in K_2O content northwards (Ulawun excluded) is consistent with the generally accepted view that rocks richer in K_2O overlie the deeper parts of the underlying Benioff zone. However, many of the rocks from the southern part of zone G seem to contain more K_2O than rocks of the same silica content from the northern part of zone G. Within zone G, therefore, lower K_2O values correlate with the deeper parts of the Benioff zone. In the north, where the Benioff zone is deepest, the rocks of zone H show a wide range of K_2O values at any given silica level; only 11 of 29 samples (mainly from Unea) plot above the two zone G regression lines, and the four-degree regression line of zone H cuts across both of them. The dacites and rhyolite of zone H (all from Garove Island) have K_2O contents similar to those of zone F, and the zone H regression line therefore has a pronounced minimum at the silica-rich end.

In common with the rocks in other island arcs, therefore, rocks of the same silica content in the south Bismarck Sea generally increase in K_2O content as the depth to the Benioff zone increases. However, Ulawun, the volcanoes in the southern part of zone G, and some volcanoes of zone H, all have rocks whose K_2O values are inconsistent with a regular pattern of continuously increasing K_2O as depth to the Benioff zone increases. These rocks demonstrate that, in this island arc, the correlation of K_2O values with depth to the Benioff zone is not a clear one, and that the rocks of volcanoes overlying one part of the Benioff zone cannot be expected to plot consistently in a predicted part of the K_2O:SiO_2 diagram (see p. 72 for further discussion).

A striking feature of Figure 15 is the wide range in K_2O contents for most silica values in rocks from both the western and eastern arcs. Some rocks have low K_2O values - for example, some of those from zones A, E, and F - and could, therefore, be con-

sidered as members of a 'tholeiitic' association (cf. Jakeš & Gill, 1970). At the other extreme are rocks which are rich in K_2O - for example, the andesites of zone C. Some of these K_2O-rich rocks are shown to be 'shoshonitic' when plotted on the K_2O:SiO_2 grid of Mackenzie & Chappell (1972), but only two of them - both from Kadovar - are found to be 'shoshonites' sensu stricto when Mackenzie & Chappell's K_2O/Na_2O limits are applied (greater than 0.6 at 50% SiO_2, greater than 1.0 at 60% SiO_2). Between the two extremes are rocks which can be termed 'calcalkaline' and 'high-K calcalkaline', depending on which scheme of classification is used (cf. Taylor, et al., 1969; Jakeš & Gill, 1970; Mackenzie & Chappell, 1972).

In Figure 15, points representing the rocks of the eastern arc are not spread evenly across the variation diagram: a gap between the F and northern G regression lines contains relatively few points. A similar gap identified by Jakeš & Gill (1970) was used to discriminate between tholeiitic and calcalkaline rocks. However, as discussed below (p. 65), none of the previously published classifications based on K_2O:SiO_2 relations is suitable for discriminating between the rocks of the south Bismarck Sea volcanoes. These classifications divide the spectra of points in Figure 15, for both the western and eastern arcs, into arbitrary fields which are of no practical significance. Moreover, in these classifications different association names, or more than one name, are assigned to rock groups from individual volcanoes in each of the zones, A to H - and in particular to those of zones A and H. For example, in zone A, Vokeo and Viai are 'tholeiitic' (cf. Jakeš & Gill, 1970), but Kadovar is partly 'shoshonitic' and partly 'calcalkaline' (cf. Mackenzie & Chappell, 1972).

Throughout the following pages, attention is drawn to other variation diagrams which have been used in the literature to discriminate between 'tholeiitic' and 'calcalkaline' rock associations. The validity of these associations is discussed on page 65.

$Na_2O:SiO_2$

The pattern of $Na_2O:SiO_2$ variations in the rocks of the south Bismarck Sea shows some similarities to that for $K_2O:SiO_2$. There are, however, important differences which suggest that, to a large extent, Na_2O and K_2O behave independently. $Na_2O:SiO_2$ variations are closely similar to the patterns discussed earlier for Ol-Ne-Q relations (Fig. 14).

As shown in Figure 16, the rocks of zone C, which are the richest in K_2O (Fig. 15), have the highest Na_2O values of all the rocks from the western arc. The lowest values are in the rocks of zone A, and the values in rocks from zones B and D are intermediate. For practical purposes, the rocks of zones B and D are not distinguishable by their $Na_2O:SiO_2$ relations, although the basic rocks of zone B tend to be less sodic than those of zone D. The Na_2O values for both zones are exceptionally low (mostly less than 2 percent) for island-arc rocks. Compared with rocks of the same silica content from the eastern zones, zone A rocks have low Na_2O contents, and, unlike their K_2O contents, their points in Figure 16 are sufficiently well clustered to allow a regression line to be calculated, although the RSS value of 473 is comparatively low.

Consistent patterns of variation in Na_2O across inclined Benioff zones (in rocks containing the same amount of silica) are thought to be either less clear than those using $K_2O:SiO_2$ relations (e.g., Ninkovich & Hays, 1972), or even non-existent (e.g., Hatherton, 1969). As shown in Figure 16, the zones E, F, northern G, and H regression lines demonstrate progressively increasing Na_2O values northwards across the New Britain Benioff zone. Rocks from the southern part of zone G are an important exception in this sequence, as they have anomalously low Na_2O values that cluster about a regression line below the one for the rocks of zone E. Rocks from Ulawun have high Na_2O values compared with other zone E rocks having the same silica content, and this accounts for the basic end of the zone E regression line crossing over the zone F line (see also Fig.

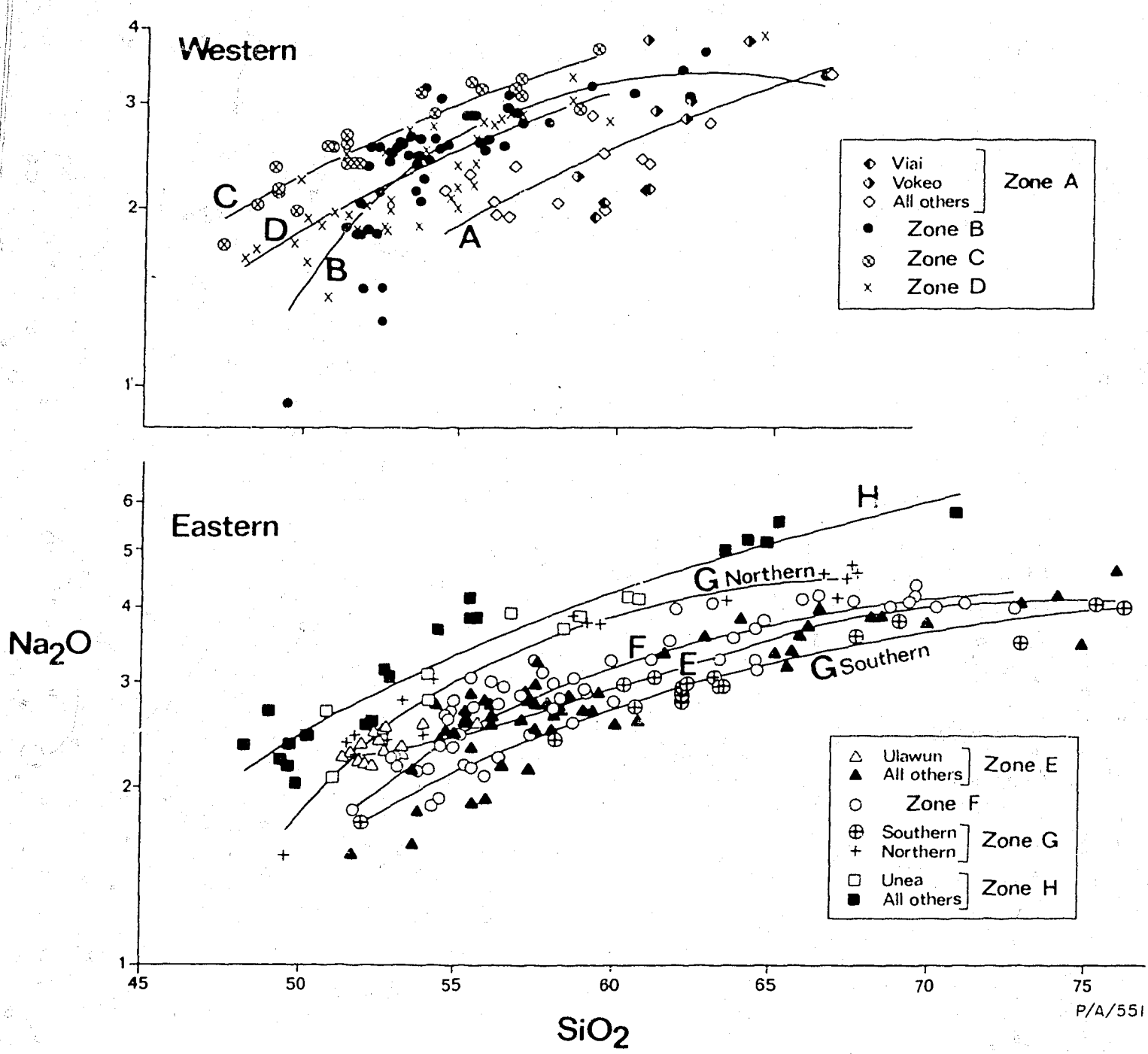

Fig. 16. Weight percent Na_2O (log_{10} scale) v. SiO_2 for rocks from the western and eastern arcs. RSS values ($\times 10^3$) for regression lines: A = 473, B = 672, C = 886, D = 707, E = 819, F = 847, G southern = 933, G northern = 970, H = 918.

15). Another feature of these $Na_2O:SiO_2$ relations is that the rocks of Unea, the southernmost volcano of zone H, have Na_2O values which are closer to those of rocks from the northern part of zone G than to those of other zone H rocks. Excluding the basalts, the rocks of zone H and the northern part of zone G contain more Na_2O than almost all the rocks of the same silica content from the western arc.

Therefore, in rocks of the same silica content from the eastern arc, Na_2O generally increases as the depth to the Benioff zone increases. However, note that these increases are shown more clearly by the rocks in the northern part of the arc than by those in the southern part. This is the reverse of the pattern for the $K_2O:SiO_2$ relations illustrated in Figure 15, where the rocks from the southern volcanoes are distinguished from one another much more clearly than are those from the northern zones. Another feature shown by a comparison of Figures 15 and 16 is that in rocks containing the same amount of silica from different volcanoes - especially those from zones A and H - relative differences in K_2O are not necessarily commensurate with similar relative differences in Na_2O. Thus, in zone A, Vokeo rocks are less potassic than those of Viai (Fig. 15), but they contain more Na_2O than do the Viai rocks (Fig. 16); and, in zone H, Unea rocks contain more K_2O but less Na_2O than those of Garove (Figs. 15 and 16). A more complete evaluation of variations in the ratio of K_2O to Na_2O is given in the following section.

$K_2O/Na_2O:SiO_2$

A plot of alkali ratios against silica for the rocks from the south Bismarck Sea is given in Figure 17.

The pattern of regression lines for the zones of the western arc is rather similar to that for $K_2O:SiO_2$ relations in Figure 15: the lines for zones C, D, and B show progressively lower K_2O/Na_2O values (comparing rocks with the same silica contents), and no regression line has been obtained for zone A because of the exceptionally wide spread of points. Within zone C, note that most

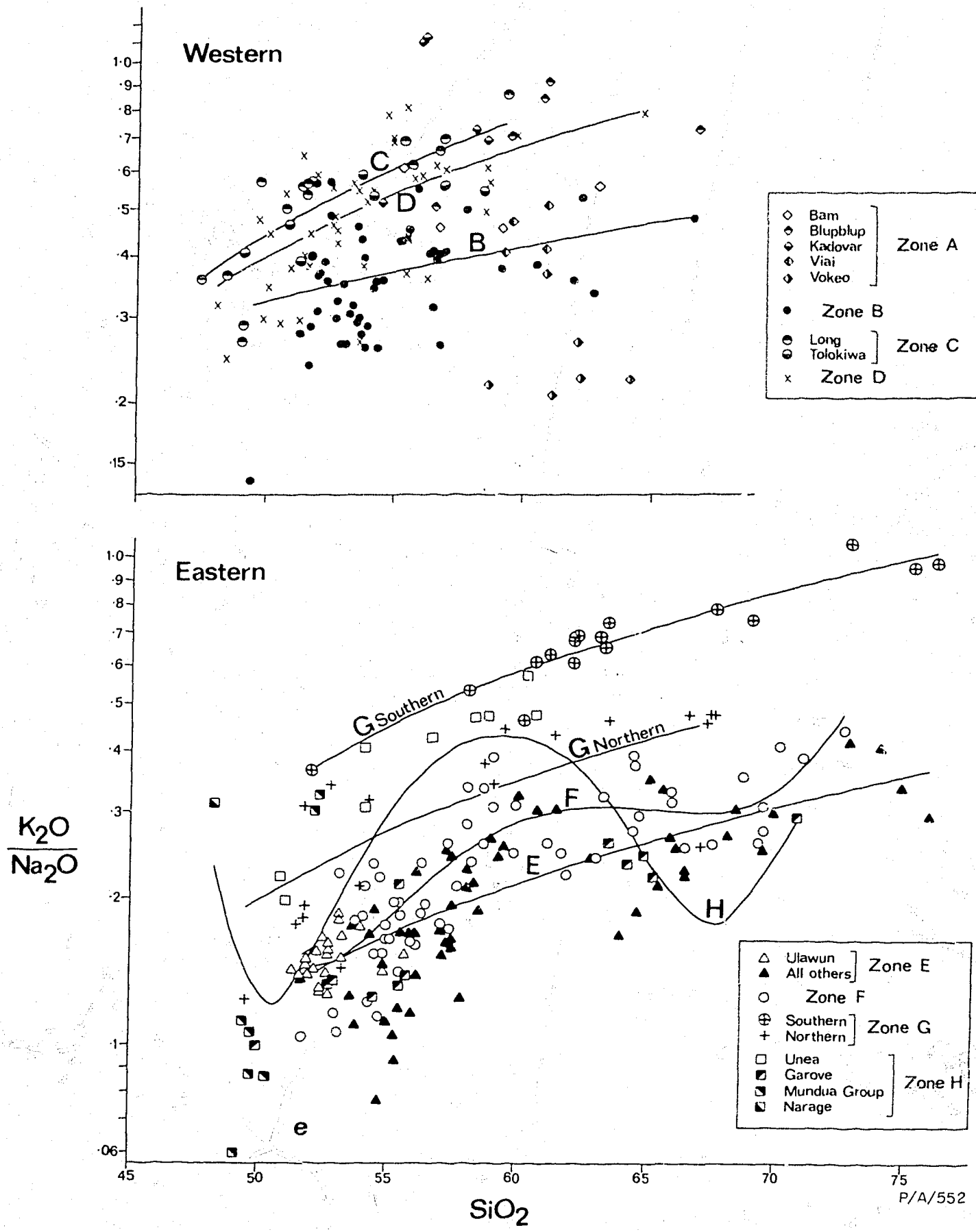

Fig. 17. Weight percent K_2O/Na_2O ($\log_{10}$ scale) v. SiO_2 for rocks from the western and eastern arcs. RSS values ($\times 10^3$) for regression lines: B = 123, C = 644, D = 367, E = 646, F = 691, G southern = 886, G northern = 639, H = 527.

K_2O/Na_2O values for the rocks of Tolokiwa are lower than those for Long Island rocks, and are generally similar to those for zone D rocks. The only two samples having K_2O/Na_2O values greater than 1 are from Kadovar (zone A), whereas notably low values are shown by five rocks from Vokeo.

Because K_2O is thought to show proportionally greater increases than Na_2O, the ratio K_2O/Na_2O is generally believed to increase systematically across island arcs (in rocks containing the same amounts of silica) in a similar manner to K_2O (e.g., Jakeš & White, 1972). This generalization is true only in part for the rocks of the eastern arc. As shown in Figure 17, K_2O/Na_2O increases slightly between zones E and F in rocks with the same silica contents, but it then increases sharply in rocks from the southern part of zone G. K_2O/Na_2O values of rocks from the northern part of zone G are lower than those of rocks from the southern part of zone G. The rocks of volcanoes in zone H show a wide range in K_2O/Na_2O for any given silica value. The four-degree regression line for zone H cuts across the lines for zones E, F, and northern G, and the K_2O/Na_2O value for the only sample from Narage (the northernmost volcano of zone H) falls above the extrapolation of the regression line for the southern part of zone G. Thus, in the eastern arc, K_2O/Na_2O in rocks with the same silica content generally increases northward from zone E to zone F, to the southern part of zone G, to Narage. However, the other rocks do not accord with this progression, and the overall pattern in the eastern arc is that of K_2O/Na_2O increasing northwards to a maximum in the southern part of zone G, and decreasing in the rocks of zone H and the northern part of zone G.

$Na_2O + K_2O$:SiO_2

In early studies, such as those of Tomkieff (1949), Rittman (1953), Kuno (1959, 1966), and Sugimura (1960), total alkalis:silica relations were used as the principal means of illustrating changes in the chemical composition of volcanic rocks across island arcs and

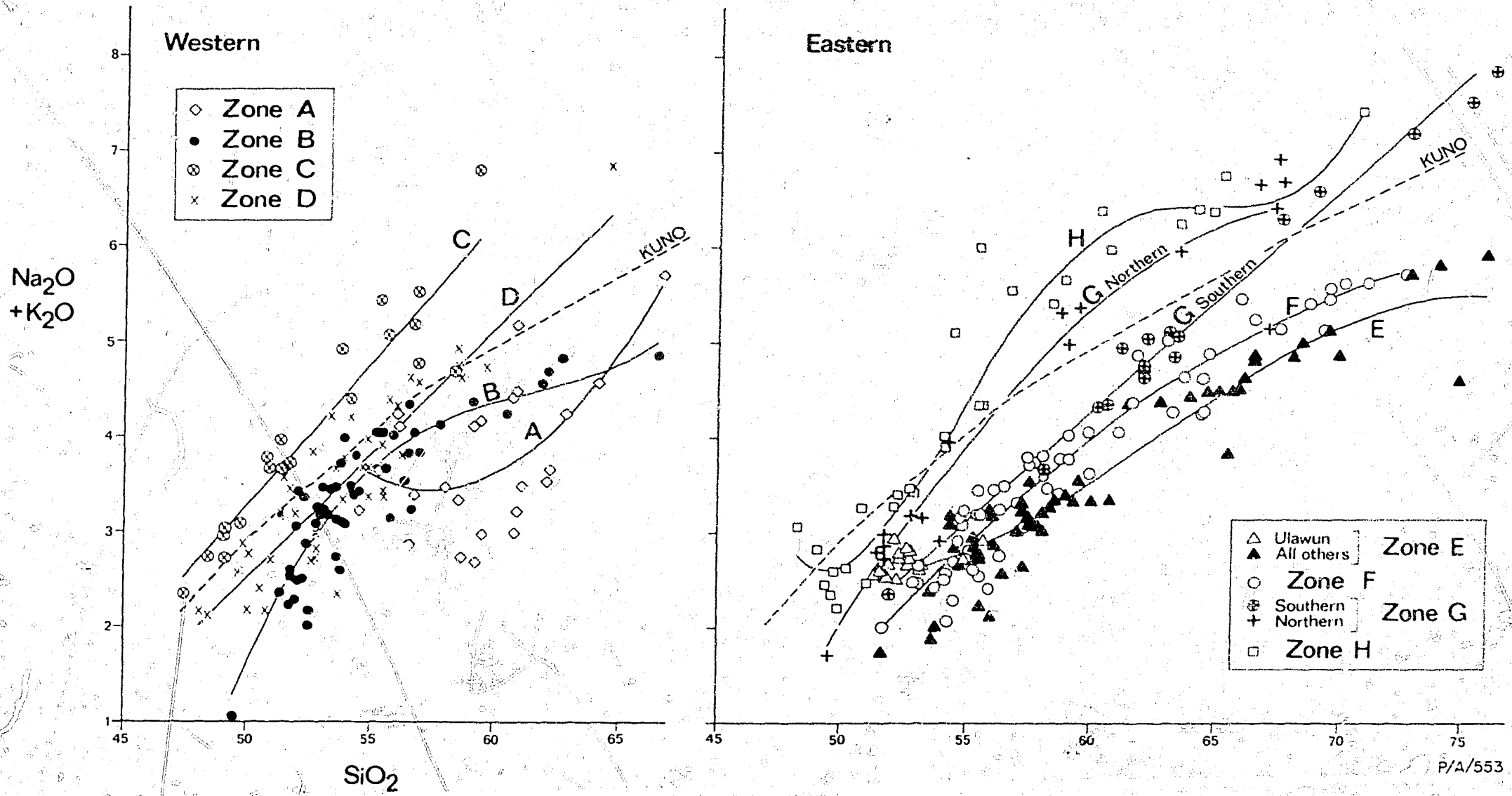

Fig. 18. Weight percent $Na_2O + K_2O$ v. SiO_2 for rocks from the western and eastern arcs. The dashed line separates Kuno's (1959) 'high-alumina basalt' (upper) and 'tholeiitic' fields. RSS values ($\times 10^3$) for regression lines: A = 396, B = 791, C = 883, D = 811, E = 894, F = 931, G southern = 986, G northern = 946, H = 975.

According to Kuno's (1959) boundary line (Fig. 18), most rocks in both the western and eastern arcs are 'tholeiitic', and the remainder belong to the 'high-alumina basalt series'. This division, however, is inappropriate for these rocks, because the boundary line separates silica-rich rocks from silica-poor rocks of the same volcano or volcanic zone, and assigns a different association name to each group. Similarly, when the 'serial index' grid of Rittman (1958) is superimposed on Figure 18, the same relation emerges - the more basic rocks of some volcanoes or zones have serial indices different from those of rocks richer in silica. Therefore, neither of these classifications is successful in producing a meaningful subdivision of the broad fields of points in Figure 18.

TiO_2:SiO_2

Regional variations in titania contents are not normally described for the rocks of island-arc volcanoes, but pronounced differences are observed among the volcanoes of the south Bismarck Sea. These variations are illustrated in Figure 19.

In the western zones A, C, and D, the ranges of TiO_2 values at most silica levels are wide, and corresponding regression lines have not been calculated. The TiO_2:SiO_2 relations are different for the rocks of these three zones: the rocks of zones C and A generally contain the highest and lowest TiO_2 values respectively, and the rocks of zone D have intermediate values (comparing rocks with the same silica content). The regression line for zone B shows that low-silica andesites in zone B have TiO_2 values similar to those of zone D, whereas rocks with higher silica contents have TiO_2 contents closer to those of the zone A rocks; zone B basalts (mainly from Manam) have the lowest TiO_2 contents of all basalts from the western arc.

For the eastern arc, regression lines have been calculated only for the rocks of zones E and G (Fig. 19). These regression lines, in conjunction with sample points for the other eastern zones

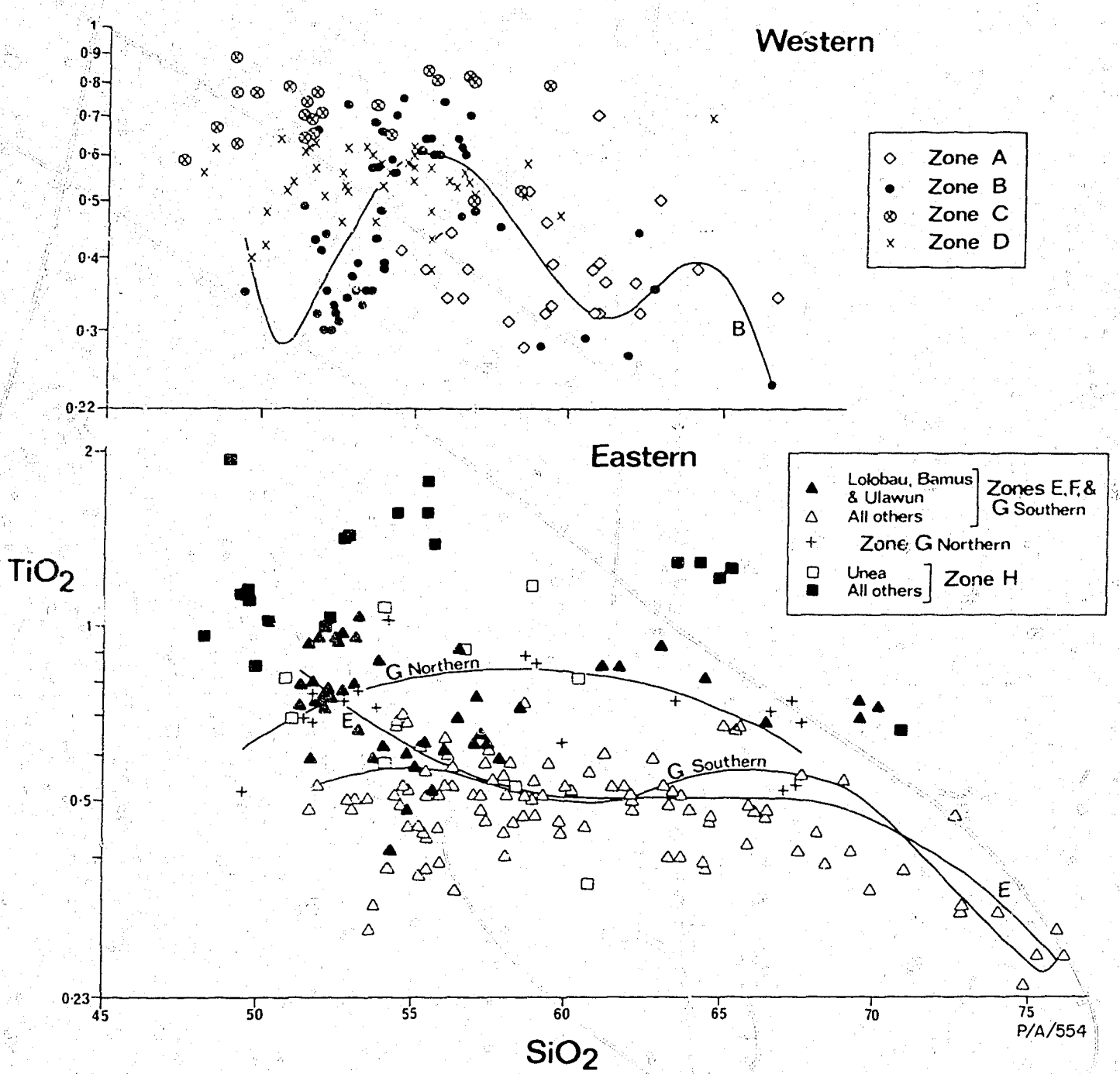

Fig. 19. Weight percent TiO_2 v. SiO_2 for rocks from the western and eastern arcs. RSS values (x 10^3) for regression lines: B = 455, E = 457, G southern = 892, G northern = 400.

plotted in Figure 19, indicate some progressive changes in TiO_2 contents across the New Britain Benioff zone. Rocks with the same silica content from zones E, F, and southern G show generally similar TiO_2 values. However, within these zones, rocks from Lolobau (zone F) and Bamus and Ulawun (zone E) have TiO_2 values which are generally higher than those of rocks from the other volcanoes, although similar to those of rocks from the northern part of zone G. The highest TiO_2 values are in the rocks of zone H, although, like the Na_2O:SiO_2 relations (Fig. 16), the rocks of Unea have generally lower values which are similar to those of rocks from the more southerly zones. Two zone H rocks have more than 1.75 percent TiO_2, which - according to Chayes (1965) - is more typical of oceanic rocks than circumoceanic ones. Overall, therefore, the pattern of TiO_2:SiO_2 variation appears to be one of generally increasing TiO_2 values (in rocks with the same silica content) across the New Britain Benioff zone, although the increases between one zone and the next are generally not as clear as for the other chemical relations discussed above.

P_2O_5:SiO_2

Consistent regional variations in P_2O_5:SiO_2 relations are shown by the south Bismarck Sea volcanoes (Fig. 20).

In the western arc, no regression lines have been calculated for the rocks of zones A and B. The regression lines for zones C and D, however, indicate that P_2O_5 values are higher in the rocks of zone C, and that the rocks of zones D and B have rather similar levels of P_2O_5 (comparing rocks with the same silica content). These relations are closely parallel to those for Na_2O:SiO_2 (Fig. 16). The rocks of zone A have a wide range of P_2O_5 values; those from Vokeo and Viai contain the lowest amounts of P_2O_5 (compared with other western rocks with the same silica content), and they therefore show relative abundances similar to those shown by K_2O:SiO_2 relations (cf. Fig. 15). P_2O_5 is generally more abundant in rocks from the western arc than in those from the eastern arc (Fig. 20).

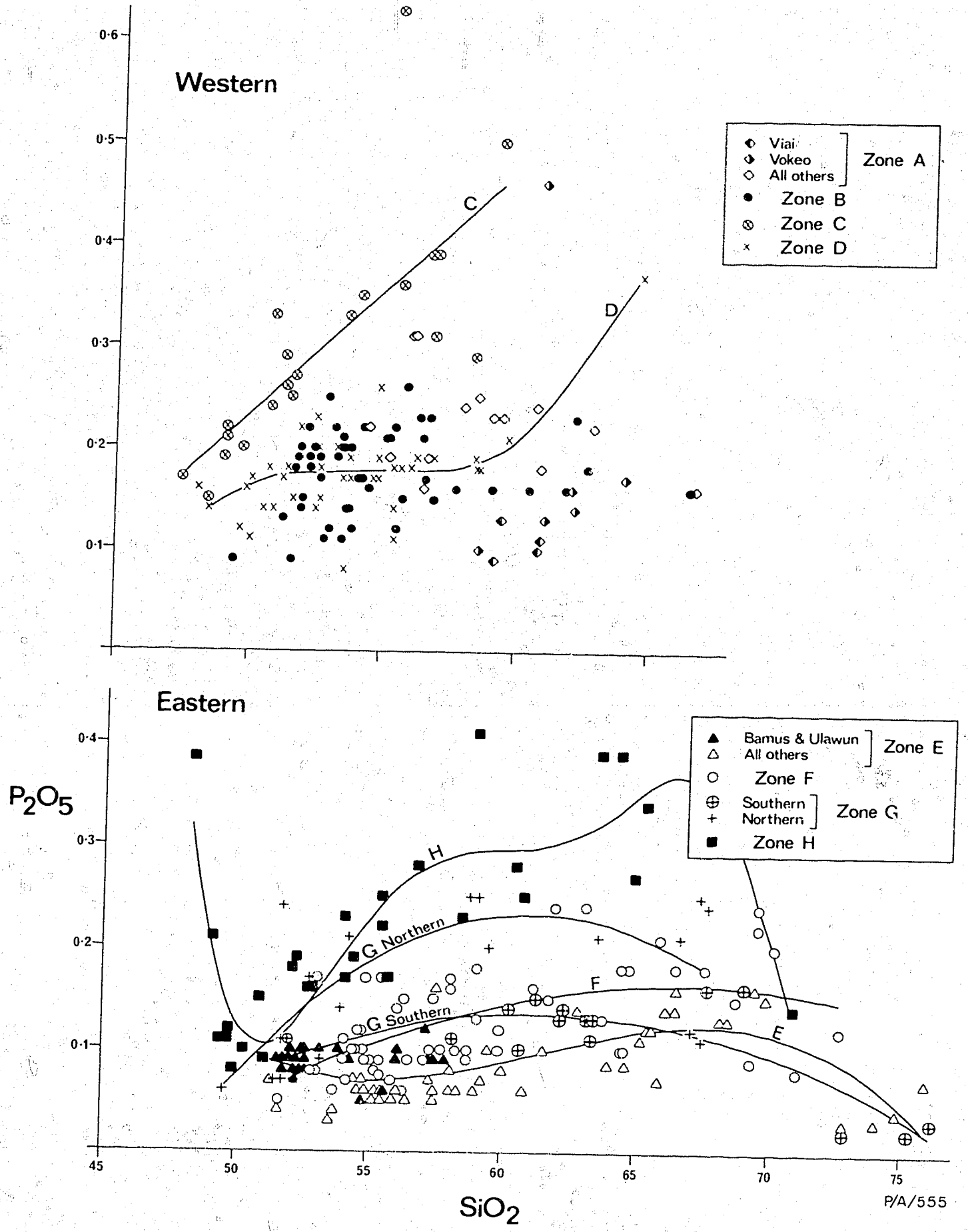

Fig. 20. Weight percent P_2O_5 v. SiO_2 for rocks from the western and eastern arcs. RSS values (x 10^3) for regression lines: C = 563, D = 447, E = 370, F = 318, G southern = 682, G northern = 452, H = 751.

continental margins. In particular, the three compositional 'series' identified by Kuno (1959) for Japanese volcanoes - 'tholeiite', 'high-alumina basalt', 'alkali', which overlie successively deeper parts of the Benioff zone - have in some studies been adopted as a standard by which rocks from other island arcs can be compared (e.g., Kuno, 1966; Brothers, 1970; Mitchell & Warden, 1971). The boundary line between Kuno's 'tholeiitic' and 'high-alumina basalt' fields is drawn in Figure 18, which shows $Na_2O + K_2O:SiO_2$ relations for the south Bismarck Sea rocks.

In Figure 18, the four regression lines for the zones of the western arc, in the order A-B-D-C, show generally increasing alkali contents for rocks of the same silica content. Thus alkali contents are shown to increase eastwards between zones A and C, and to decrease in zone D to values which are generally slightly higher than those of zone B. The separation of points representing the rocks of zones A and B is fairly clear, although both ends of the zone A regression line cross the regression line of zone B.

The regression lines for the eastern zones - E, F, G, and H - indicate that rocks from the more northerly zones are consistently richer in total alkalis. In Figures 15, 16, and 17, the regular patterns of northward increasing values for K_2O, Na_2O, and K_2O/Na_2O were interrupted by the rocks of some volcanoes, or groups of volcanoes; but when Na_2O and K_2O values are added together and plotted against silica, a much more even pattern of increasing values is evident (Fig. 18) Even the regression line for high K_2O/Na_2O rocks from the southern part of zone G falls in the appropriate part of the diagram - that is, between the zone F and northern zone G regression lines. However, once again the rocks of Ulawun (zone E) are exceptions, as their higher alkali contents cause the lower end of the zone E regression line to cross the zone F and southern zone G regression lines; this effect is eliminated when the zone E regression line is recalculated excluding the Ulawun rocks (not illustrated here).

Regression lines for rocks of all zones in the eastern arc (Fig. 20) indicate that the overall chemical pattern is very similar to that for the $Na_2O:SiO_2$ relations. Comparing rocks with the same silica content from zones E, F, northern G, and H, a progressive northwards increase in P_2O_5 is evident. Rocks from the southern part of zone G do not accord closely with this progression, but rather have values which are similar to those of both zones E and F. Moreover, the rocks of Ulawun and, to a lesser extent, Bamus have slightly higher P_2O_5 values than rocks with the same silica content from other zone E volcanoes, and this accounts for the intersection of the E and F regression lines at the basic end of the compositional spectrum. Most zone E rocks contain less than 0.1 percent P_2O_5; this contrasts with the values of the western rocks, most of which contain more than 0.1 percent P_2O_5.

$CaO:SiO_2$

Compared with the oxides considered above, CaO has a narrow range of values in rocks containing the same amounts of silica, and regression lines with high RSS values have been calculated for rocks from all the zones (Fig. 21, Table 6). In spite of the narrow range, consistent regional patterns of CaO variation are evident, though not on the same scale as those for the oxides considered above.

The rocks of zone A are richer in CaO than those with the same silica content from the remainder of the western volcanoes (Fig. 21). This is the only prominent difference between one group of western volcanoes and all the others. The low CaO values indicated by the zone C regression line are due mainly to the rocks of Long Island, whose andesites appear to form a subsidiary trend which diverges from the main trend of points. The andesites of Karkar (zone B) also appear to be poor in CaO. It is emphasized, however, that these low values are characteristic of the rocks from two distinct and geographically well separated volcanoes (Fig. 5), and are not regarded as contributing to a regular pattern of chemical variation throughout the western arc.

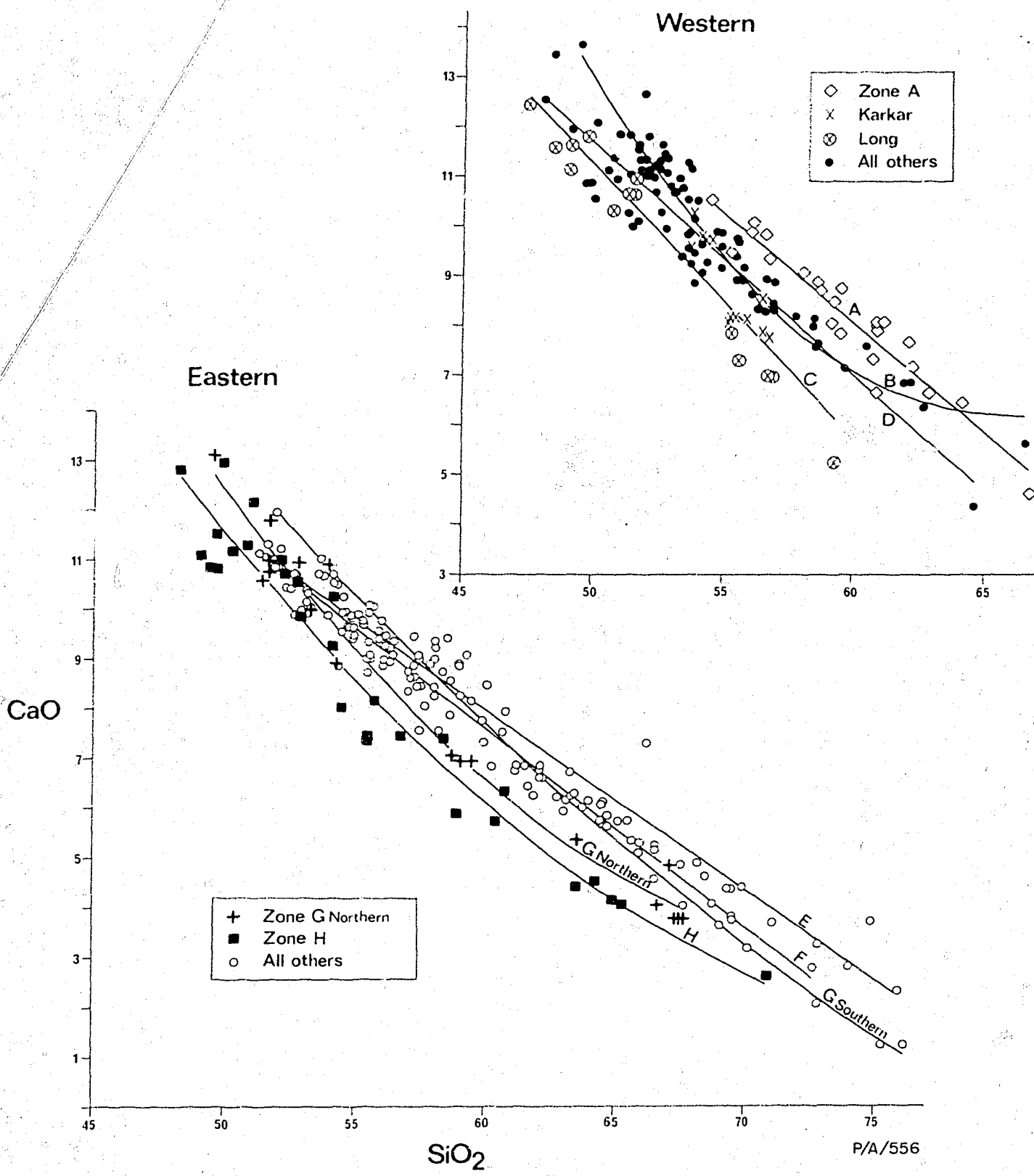

Fig. 21. Weight percent CaO v. SiO_2 for rocks from the western and eastern arcs. In order that the regression lines can be clearly seen, many low-silica rocks have not been plotted. RSS values (x 10^3) for regression lines: A = 913, B = 891, C = 917, D = 872, E = 957, F = 973, G southern = 990, G northern = 977, H = 944.

In the eastern arc, a general decrease in CaO northwards across the New Britain Benioff zone is shown by rocks containing the same amounts of silica. The rocks of zone H have the lowest CaO values. Those from the northern part of zone G have higher CaO values, and the remainder of the eastern rocks show the highest values of all. The distinctions between rocks from zones E, F, and southern G are not particularly clear, but the relations shown by the corresponding regression lines appear to be generally similar to those for Na_2O:SiO_2 (Fig. 16) and P_2O_5:SiO_2 (Fig. 20), except they are reversed: (1) the zones E and F regression lines cross over at the low-silica end, but remain separate when the rocks of Ulawun are excluded from zone E; and (2) the positions of the regression lines for zones E to H are consistent with progressive changes in CaO contents across the New Britain Benioff zone, if the regression line for the southern part of zone G is excluded. Hatherton (1969) showed that the CaO contents of circum-Pacific rocks could be correlated inversely with increasing depth to Benioff zones. The eastern volcanoes of the south Bismarck Sea demonstrate the same feature, and emphasize a correlation that tends to be overlooked in studies of island-arc petrology.

Peacock (1931) defined a rock association as 'calc-alkalic' when rocks with a silica content of between 56 and 61 percent had equal weight proportions of CaO and $Na_2O + K_2O$ - or, expressed in a different way, the 'alkali-lime index' of calcalkaline rocks is between 56 and 61. Rocks with an alkali-lime index of more than 61 were called 'calcic' by Peacock. Since 1931, the term 'calcalkaline' has been used in different senses and defined in different ways, and Peacock's definition (see also Holmes, 1921) has, to a large extent, been superseded. The term 'calcic' is also more or less outmoded, as most 'tholeiitic' rock associations have alkali-lime indices greater than 61.

A comparison of CaO:SiO_2 relations in Figure 21 with $Na_2O + K_2O$:SiO_2 relations in Figure 18 shows that the alkali-lime

indices for rocks from zone A, in the western arc, and from zones E, F, and G, in the eastern arc, are greater than 61. These rocks are therefore 'calcic' in the sense of Peacock (1931). The alkali-lime indices for rocks in zones B, C, D, and H cluster about 61, and therefore could be considered as partly 'calcalkaline' and partly 'calcic'. However, Peacock's limit of 61 seems to have been chosen arbitrarily, and its use for subdividing the rocks of any of the zones B, C, D, or H is considered unrealistic.

Al_2O_3:SiO_2

Al_2O_3 values have a wider range than CaO in rocks containing the same amounts of silica from the south Bismarck Sea volcanoes, especially in the basalts and andesites (Fig. 22). Most rocks from both the western and eastern arcs have Al_2O_3 contents of more than 15 percent; values in excess of 18 percent are not uncommon, and only a few rocks contain less than 13 percent. These relatively high values appear to be typical of most circumoceanic volcanic rocks (Chayes, 1965).

In the western arc, rocks from three zone A volcanoes - Viai, Kadovar, and Blupblup - have much lower Al_2O_3 contents than other western rocks with the same silica contents. The Long Island andesites are also characterized by relatively low Al_2O_3, but the basalts, on the other hand, have high Al_2O_3 contents. These differences in Al_2O_3, content in the Long Island rocks to a large extent control the negative slope of the regression line for zone C (Fig. 22). The rocks of zones B and D have similar Al_2O_3 contents, as shown by the close correspondence of their regression lines. Like CaO, therefore, Al_2O_3 does not increase or decrease in any clearly systematic pattern along the western arc in the same way as alkalis, TiO_2, and P_2O_5.

Excluding the rocks from the southern part of zone G, a broad subdivision can be established from Al_2O_3:SiO_2 relations among the eastern volcanoes (Fig. 22). Regression lines show that Al_2O_3

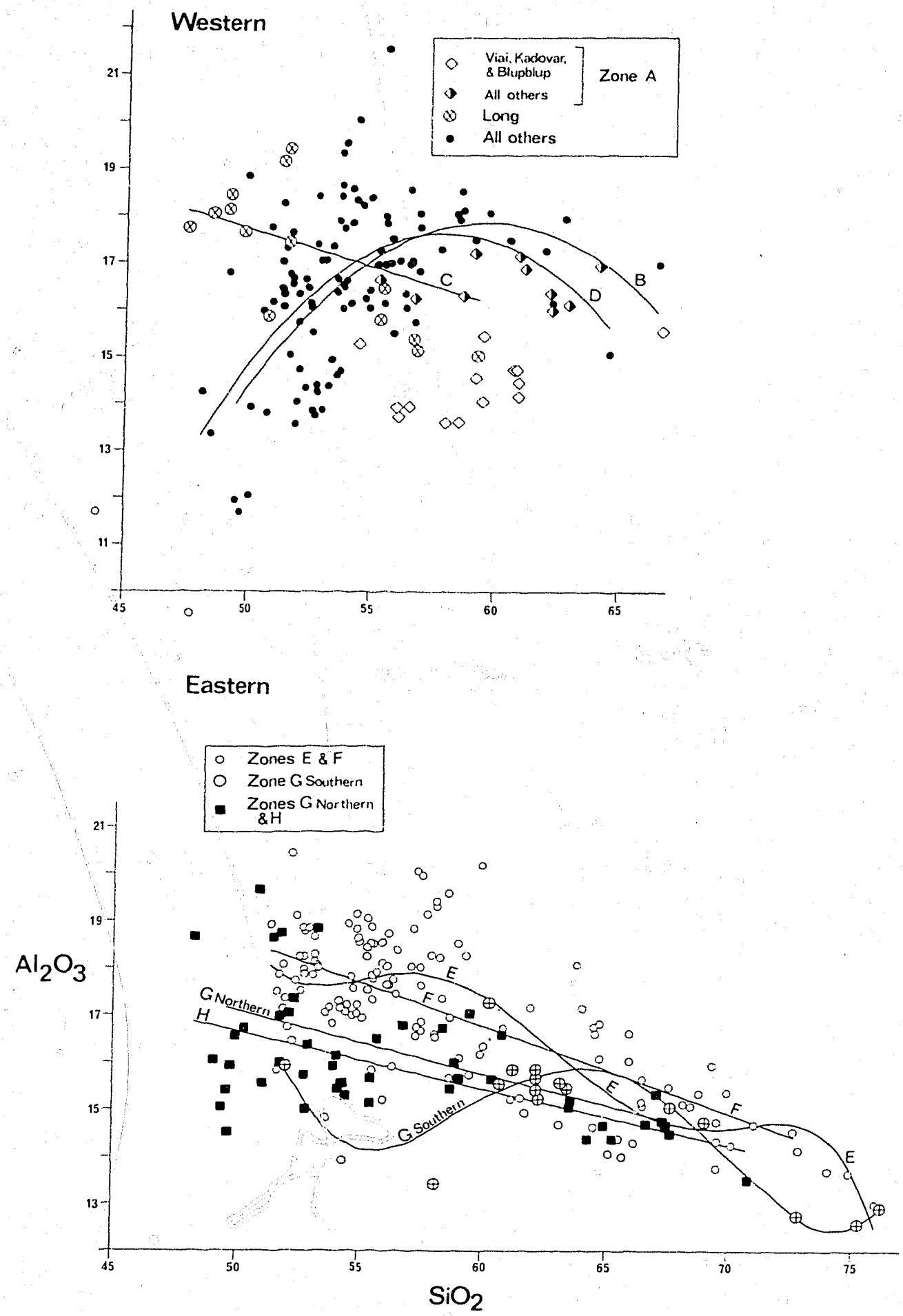

Fig. 22. Weight percent Al_2O_3 v. SiO_2 for rocks from the western and eastern arcs. RSS values (x 10^3) for regression lines: B = 274, C = 177, D = 320, E = 545, F = 519, G southern = 769, G northern = 387, H = 314.

values are lower in most rocks from zones H and northern G than in those from zones E and F, farther south. Therefore, lower Al_2O_3 values in rocks containing the same amount of silica correlate with the deeper part of the Benioff zone. However, this inverse correlation is more poorly defined than correlations described earlier for other oxides, and the regression line for the rocks of the southern part of zone G cuts across all those for the rocks of the other eastern zones.

MgO:SiO_2

MgO:SiO_2 relations for rocks from the western and eastern arcs are illustrated in Figure 23. The basalts of each arc show a wide range of MgO values, but the range is much less for the non-basaltic rocks. High-magnesia basalts are more common in the west than in the east, and in the east they appear to be most common in the volcanoes of zone H.

Among the western volcanoes, variations in MgO are similar to the variations shown by CaO (cf. Fig. 21). Except those of Bam, the rocks of zone A are richer in MgO than other western rocks with the same silica content. On the other hand, rocks from Karkar and Long volcanoes (in zones B and C, respectively) are comparatively low in MgO. The only regional difference, therefore, between one group of geographically related western volcanoes and any other is the higher MgO contents of rocks from the western end of the arc - that is, from west of Bam volcano.

Hatherton (1969) demonstrated that MgO, like CaO, decreases in rocks of the same silica content as the depth of the Benioff zone increases. This, however, is only partly true for the rocks of the eastern arc: most andesites and dacites from zones E and F contain less MgO than those with the same silica content from the southern part of zone G (Fig. 23); moreover, a greater proportion of zone E rocks - particularly the andesites - apparently have lower MgO values than those of zone F. In these rocks, therefore, MgO appears to

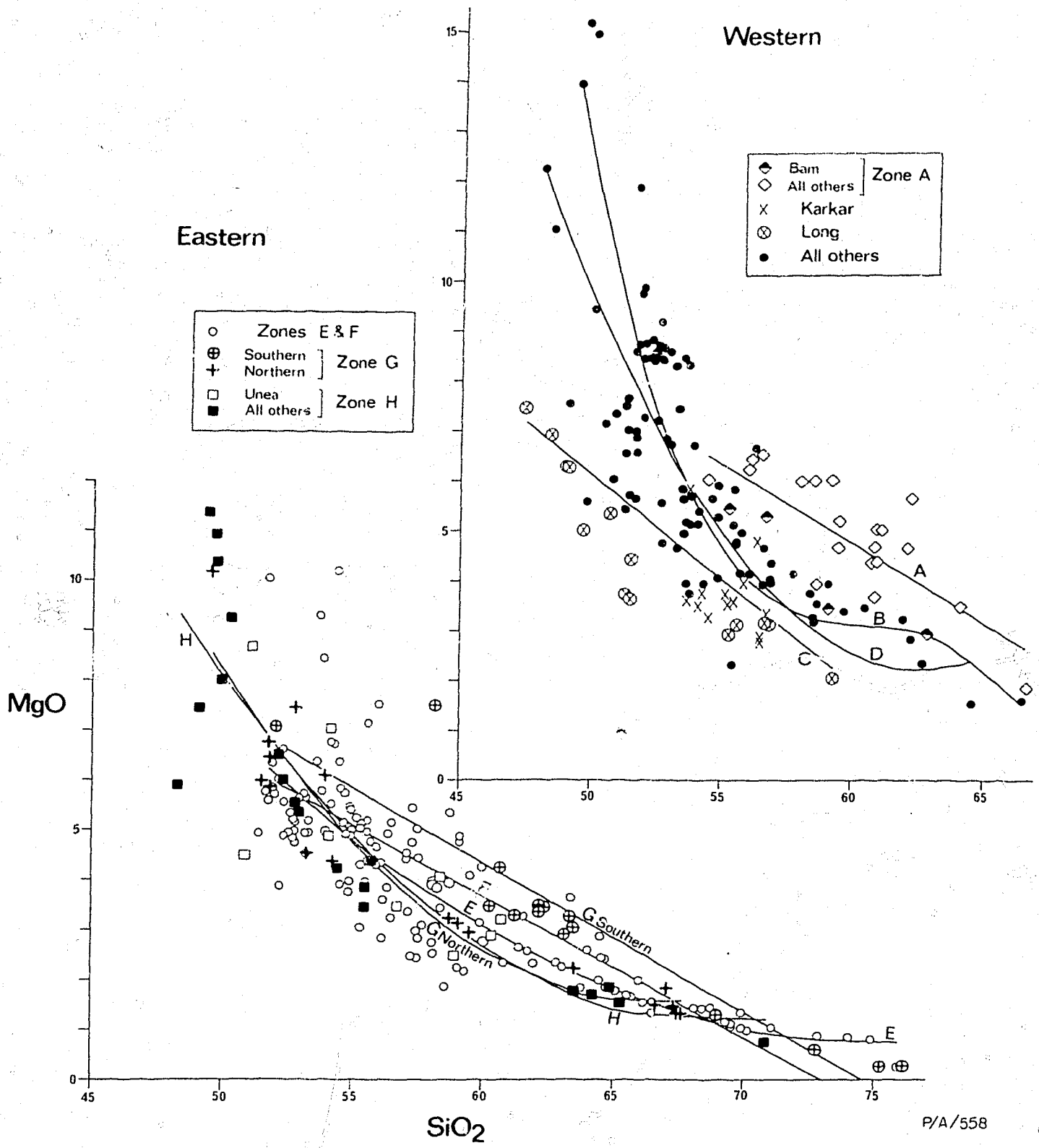

Fig. 23. Weight percent MgO v. SiO_2 for rocks from the western and eastern arcs. RSS values ($\times 10^3$) for regression lines: A = 584, B = 767, C = 621, D = 629, E = 643, F = 847, G southern = 850 G northern = 909, H = 769.

increase in rocks with the same silica content as the depth to the New Britain Benioff zone increases. However, rocks from the northern part of zone G contain less MgO than those with the same silica content from the southern part; and zone H rocks contain less MgO than those of zone G, especially when the rocks of Unea are excluded. In these rocks, therefore, MgO decreases as the depth to the Benioff zone increases (cf. Hatherton, 1969).

$FeO + Fe_2O_3$:SiO_2

The total iron oxide contents of rocks from the western and eastern arcs are plotted against silica in Figure 24, where they form broad bands with negative slopes. Within each of the bands, no regional patterns of chemical variation are evident: rocks from any one of the zones A to D, or E to H, do not appear to be consistently more, or less, iron-rich than those with the same silica content from other zones in the same arc. Possible exceptions are the volcanoes of zone A, of which three have rocks whose total iron oxide contents are higher than those of other western rocks containing the same amount of silica (Fig. 24). However, because Bam rocks are not especially iron-rich, and because those of Vokeo are definitely iron-poor, consistently higher iron contents do not appear to be characteristic of all rocks from zone A. Other notable western rocks are those of Karkar (zone B) and Long (zone C), which have higher total iron oxide contents than other rocks of similar silica content (Fig. 24).

The bundle of regression lines for the rocks of the eastern zones indicates no obvious regional differences in Fe_2O_3 + FeO:SiO_2 relations, although there is a suggestion that some andesites from zones H and northern G may be significantly, but slightly, more iron-rich.

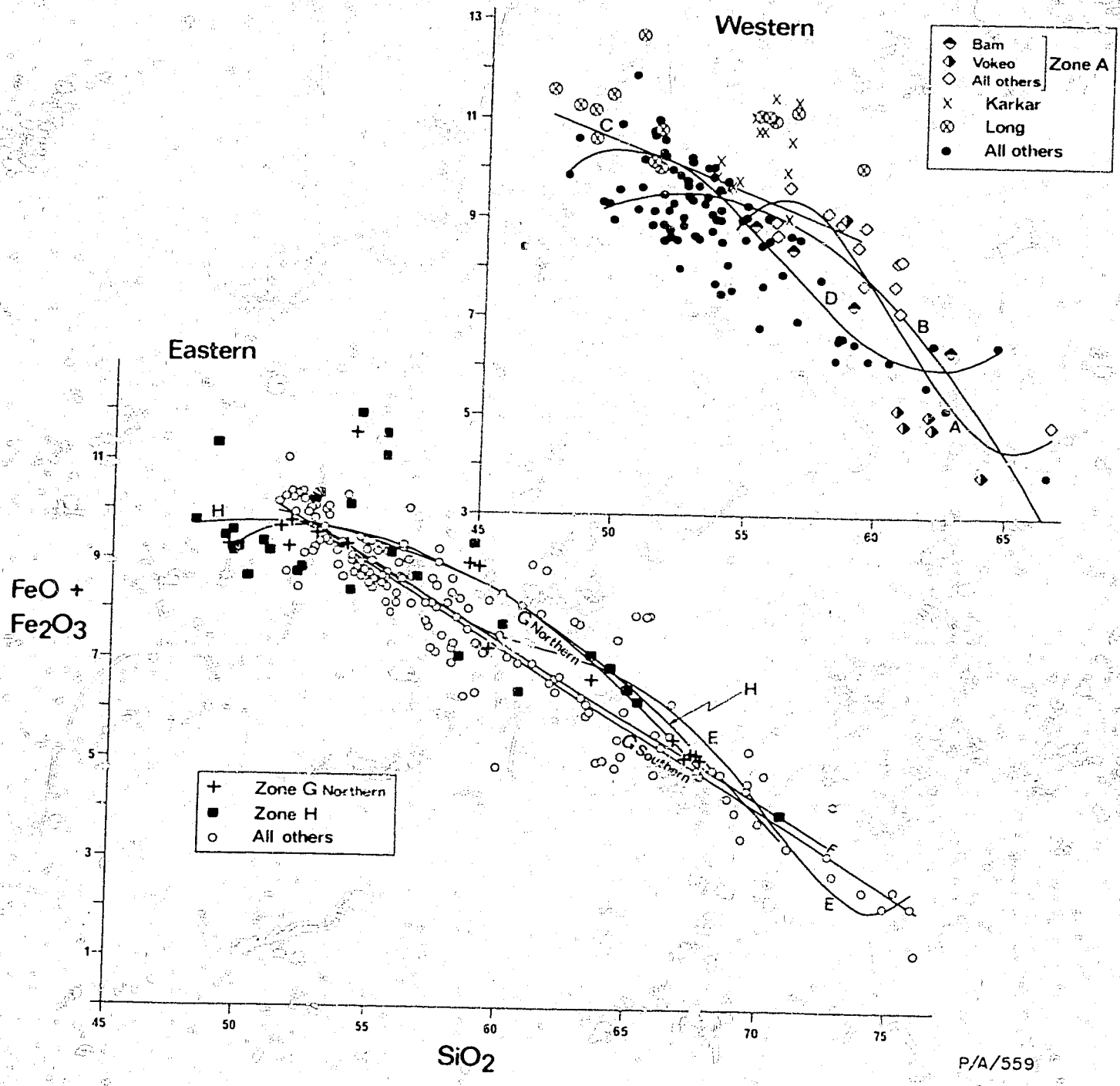

Fig. 24. Weight percent FeO + Fe_2O_3 v. SiO_2 for rocks from the western and eastern arcs. FeO and Fe_2O_3 proportions computed by the method of Irvine & Baragar (1971), and whole-rock analyses recalculated to 100 percent without volatiles. RSS values ($\times 10^3$) for regression lines: A = 749, B = 579, C = 188, D = 772, E = 884, F = 841, G southern = 964, G northern = 912, H = 671.

Traditionally, variations in the total iron oxide (F) contents of island-arc rocks are illustrated relative to magnesia (M) in MF diagrams, or to magnesia and total-alkalis (A) in FMA diagrams. Other variations in total iron oxide contents for the south Bismarck Sea rocks are therefore discussed in the following section with reference to both Figure 24 and to the MF diagram, Figure 25.

MgO:FeO + Fe_2O_3

In MF and FMA diagrams, the intermediate members of tholeiitic rock associations are said to be richer in iron than those of calcalkaline associations (e.g., Tilley, 1950; Kuno, 1968; Irvine & Baragar, 1971). However, in both types of diagram, there appear to be different opinions on where the boundary between the two associations should be drawn.

As shown in Figures 24 and 25, the FeO + Fe_2O_3 contents of most rocks from the western and eastern arcs are low, so the rocks could be termed calcalkaline. Nevertheless, in rocks with MgO contents within the range 2 to 7 percent, there is a considerable range in total iron oxide values, and some rocks have sufficiently high values to warrant the term tholeiitic (Fig. 25). For example, Jakeš & White (1969) considered the rocks of the south Bismarck Sea (whose analyses were presented by Morgan, 1966) to be tholeiitic. In addition, in FMA diagrams, these and other rocks fall in the tholeiitic fields of Kuno (1968) and Irvine & Baragar (1971). Note that in Figure 25 the points of rocks of both the western and eastern arcs do not concentrate in iron-poor and iron-rich fields; rather, they form a continuum of compositions which cannot be divided into meaningful groups by means of a single boundary line.

Because alkali contents are lower in tholeiitic rocks than in calcalkaline rocks, and iron contents are lower in calcalkaline rocks than in tholeiitic ones, high iron contents shown in MF and FMA diagrams are commonly regarded as a function of de-

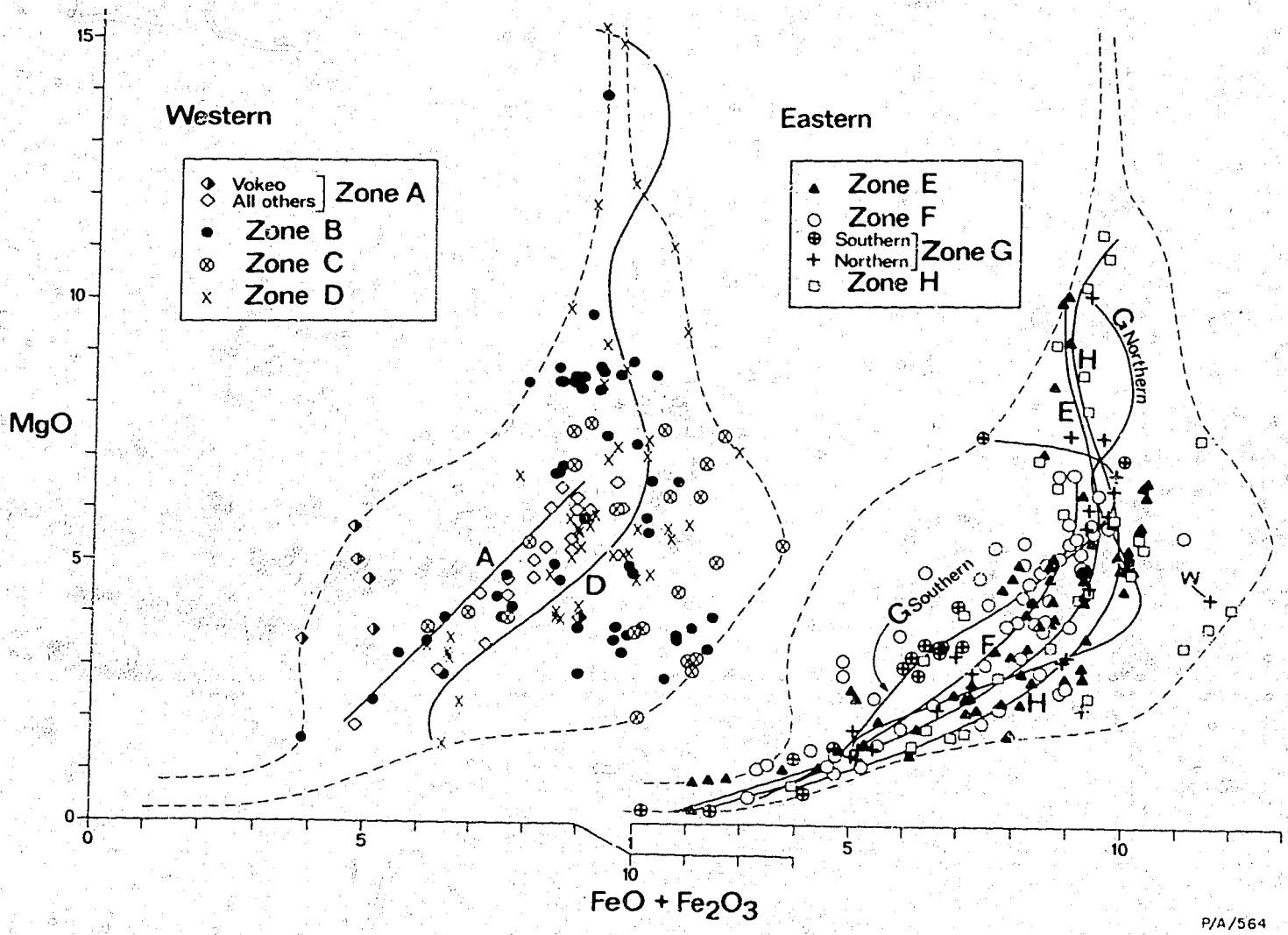

Fig. 25. Weight percent MgO v. FeO + Fe_2O_3 for rocks from the western and eastern arcs. FeO and Fe_2O_3 proportions computed by the method of Irvine & Baragar (1971), and whole-rock analyses recalculated to 100 percent without volatiles. The pairs of dashed lines in both diagrams define the compositional field covered by rocks from all the zones. W is sample 339 of Lowder & Carmichael (1970). RSS values ($\times 10^3$) for regression lines: A = 392, D = 615, E = 814, F = 728, G southern = 939, G northern = 939, H = 592.

creasing alkali content ($Na_2O + K_2O$, or K_2O) in rocks containing the same amount of silica. Jakeš and Gill (1970) and Jakeš & White (1972), for example, held this view, and claimed that rocks showing greater enrichments in iron overlie the shallower parts of Benioff zones. A comparison of Figure 25 with Figures 15 and 18 shows that neither correlation seems to hold for the south Bismarck Sea rocks.

Firstly, rocks from the alkali-poor zones are not more iron-enriched than those from the alkali-rich zones. On the contrary, Figure 25 shows that to some extent the opposite may be true because, in the range 3 to 8 percent MgO, no rocks from the low-alkali volcanoes of zones A and E contain more than 10.5 percent total iron oxides, whereas high-iron rocks are present in high-alkali volcanoes such as Long (zone C) and those of zones G and H (Figs. 24 and 25). However, this is not a clear correlation, and it is considered more accurate to simply conclude that iron-rich compositions are not characteristic of low-alkali volcanoes.

Secondly, in the eastern arc, the rocks from volcanoes overlying the shallower parts of the New Britain Benioff zone are not more iron-rich than those of volcanoes overlying the deeper parts in the north. Again, to some extent the reverse seems to be true, because a few rocks from volcanoes in zones G and H have the highest total iron oxide contents of all the eastern rocks. Nevertheless, because these iron-rich samples are comparatively rare, and because many more rocks from zones G and H have iron-oxide values which are indistinguishable from those of rocks from zones E and F, a correlation between higher iron contents and the deeper parts of the Benioff zone cannot be recognized with a high degree of confidence.

Lowder & Carmichael (1970) analysed eleven rocks from five volcanic centres at, and north of, Talasea in the northern part of Willaumez Peninsula (Fig. 6), and drew a line of 'moderate iron-enrichment' through points plotted in a MF diagram. Part of this 'Talasea trend' is defined by an andesite (W in Fig. 25) which is much more iron-rich than most other rocks with similar MgO contents

plotted in Figure 25. The 'Talasea trend' is therefore unrepresentative of most rocks from the eastern arc. Moreover, Jakeš & White (1969, fig. 2) used FMA relations to show that the rocks discussed by Morgan (1966) from volcanoes in the western arc, and those discussed by Miyake & Sugiura (1953) from the Rabaul volcanoes, formed a tholeiitic rock association which was iron-enriched relative to calcalkaline rocks from other parts of Melanesia. However, the iron-rich part of this tholeiitic trend is defined mainly by Morgan's analyses of Karkar rocks, which - as shown in Figure 24 - have unusually high total iron oxide values compared with those for rocks from other parts of the western and eastern arcs. Therefore, the 'New Guinea-New Britain arc' trend of Jakeš & White - like the 'Talasea trend' of Lowder & Carmichael - cannot be regarded as representative of all the rocks from either the western ('New Guinea') or eastern ('New Britain') volcanic arcs.

$Fe_2O_3/FeO:SiO_2$

The cooling of many south Bismarck Sea rocks after their eruption is likely to have been accompanied by different degrees of oxidation of FeO to Fe_2O_3. Therefore, the Fe_2O_3/FeO values of the rocks would be expected to be higher than those of the magmas before eruption, so regional patterns of variations in magmatic Fe_2O_3/FeO values might be obscured by atmospheric oxidation.

Some south Bismarck Sea rocks contain more Fe_2O_3 than FeO and are therefore highly oxidized. (Such rocks at some volcanoes were selected for analysis because less altered ones could not be collected.) However, when rocks having Fe_2O_3/FeO values of less than 1.1 are plotted against silica, as in Figure 26, a systematic pattern of regional variation emerges. Twenty-four eastern rocks, and twenty-seven western rocks, having Fe_2O_3/FeO values of greater than 1.1 are excluded from Figure 26; twelve of these are analyses of Manam rocks given by Morgan (1966), six are Cape Hoskins rocks analysed by Blake & Ewart (1974), and three are analyses of rocks from northern Willaumez Peninsula given by Lowder & Carmichael (1970). Thirteen other excluded rocks are amphibole-bearing types from Aris, Crown, Tolokiwa, Sakar, and Dufaure.

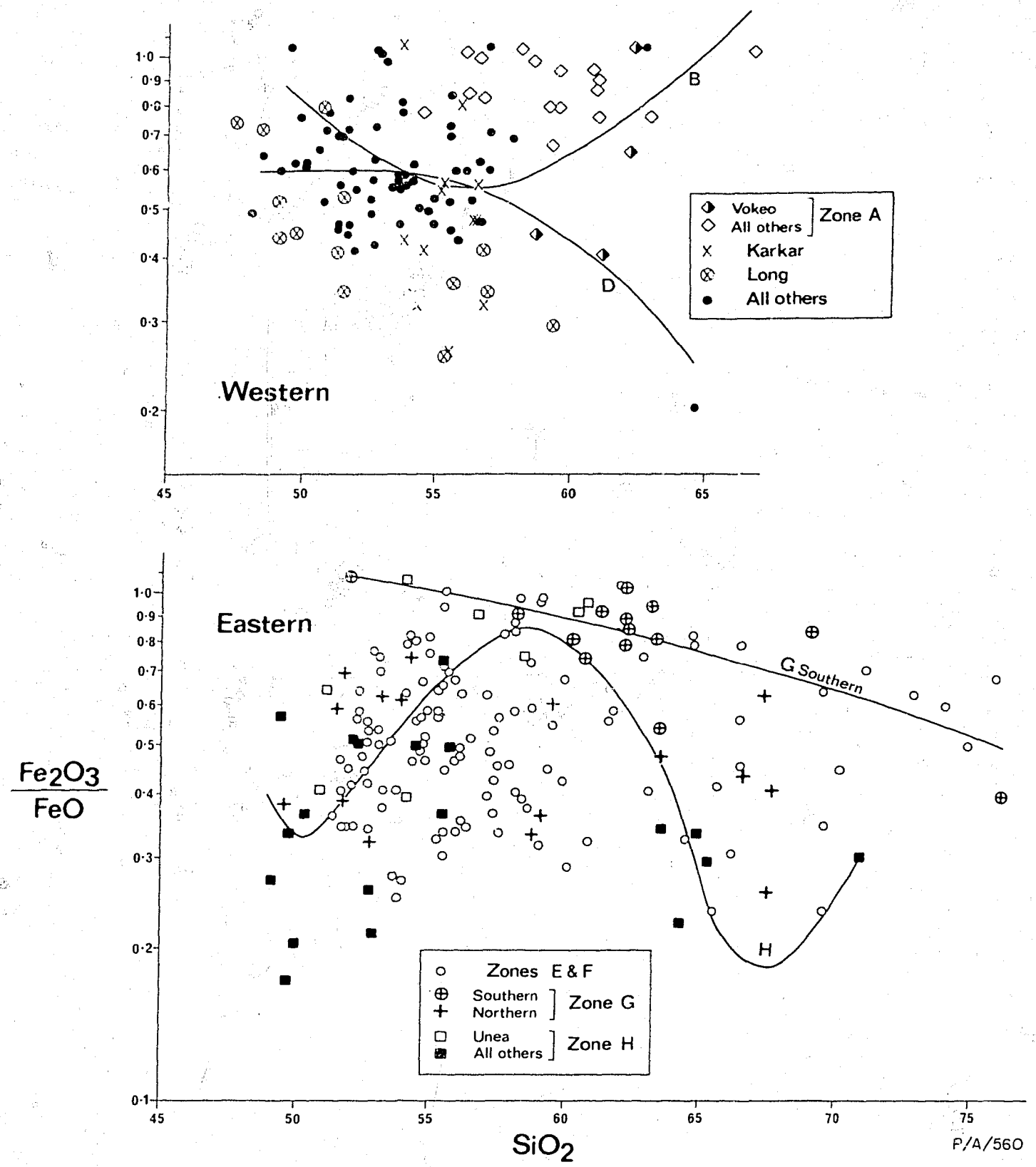

Fig. 26. Weight percent Fe_2O_3/FeO (log_{10} scale) v. SiO_2 for rocks from the western and eastern arcs. 27 western rocks and 24 eastern rocks showing Fe_2O_3/FeO values greater than 1.1 are excluded (see text). Fe_2O_3 and FeO values taken from original analyses. SiO_2 values are those used in Figures 11 to 27. RSS values (x 10^3) for regression lines: B = 281, D = 227, G southern = 538, H = 459.

In Figure 26, many rocks with a high silica content from Karkar and Long volcanoes are shown to have lower Fe_2O_3/FeO values than those with the same silica content from other western volcanoes. Except for three Vokeo rocks, samples from zone A are characterized by Fe_2O_3/FeO values consistently higher than those of other rocks containing the same amount of silica. These relative differences are similar to those shown by the $MgO:SiO_2$ relations illustrated in Figure 23.

The pattern of variation for the eastern rocks in Figure 26 is also analogous to that for $MgO:SiO_2$ relations: rocks from the southern part of zone G have higher Fe_2O_3/FeO values than those with a similar silica content from zones E and F; more zone E rocks than zone F rocks contain low Fe_2O_3/FeO values (to avoid confusion, this feature is not illustrated in Fig. 26, in which the similarities between Ulawun rocks and rocks of zones E and F are also not defined); rocks from the northern part of zone G are lower in Fe_2O_3/FeO than those with the same silica content from the southern part; and zone H rocks, excluding some from Unea, have lower Fe_2O_3/FeO values than the rocks of zone G (cf. Fig. 23).

Therefore, although the total iron oxide contents of the south Bismarck Sea rocks are not related to the regional tectonic setting of the volcanoes (see p. 58), the oxidation state of iron - and therefore FeO and Fe_2O_3 independently - apparently shows systematic regional patterns similar to those for $MgO:SiO_2$ variations. It follows also that M/F values must also be related to the oxidation state of iron (see below).

$MnO:SiO_2$

The range of MnO values is narrow. Most rocks have MnO contents between 0.1 and 0.2 percent, but values are commonly less than 0.1 percent in the acid rocks (Fig. 27). Despite this restriction, differences in MnO content can be detected between some volcanoes, and between a few groups of volcanoes.

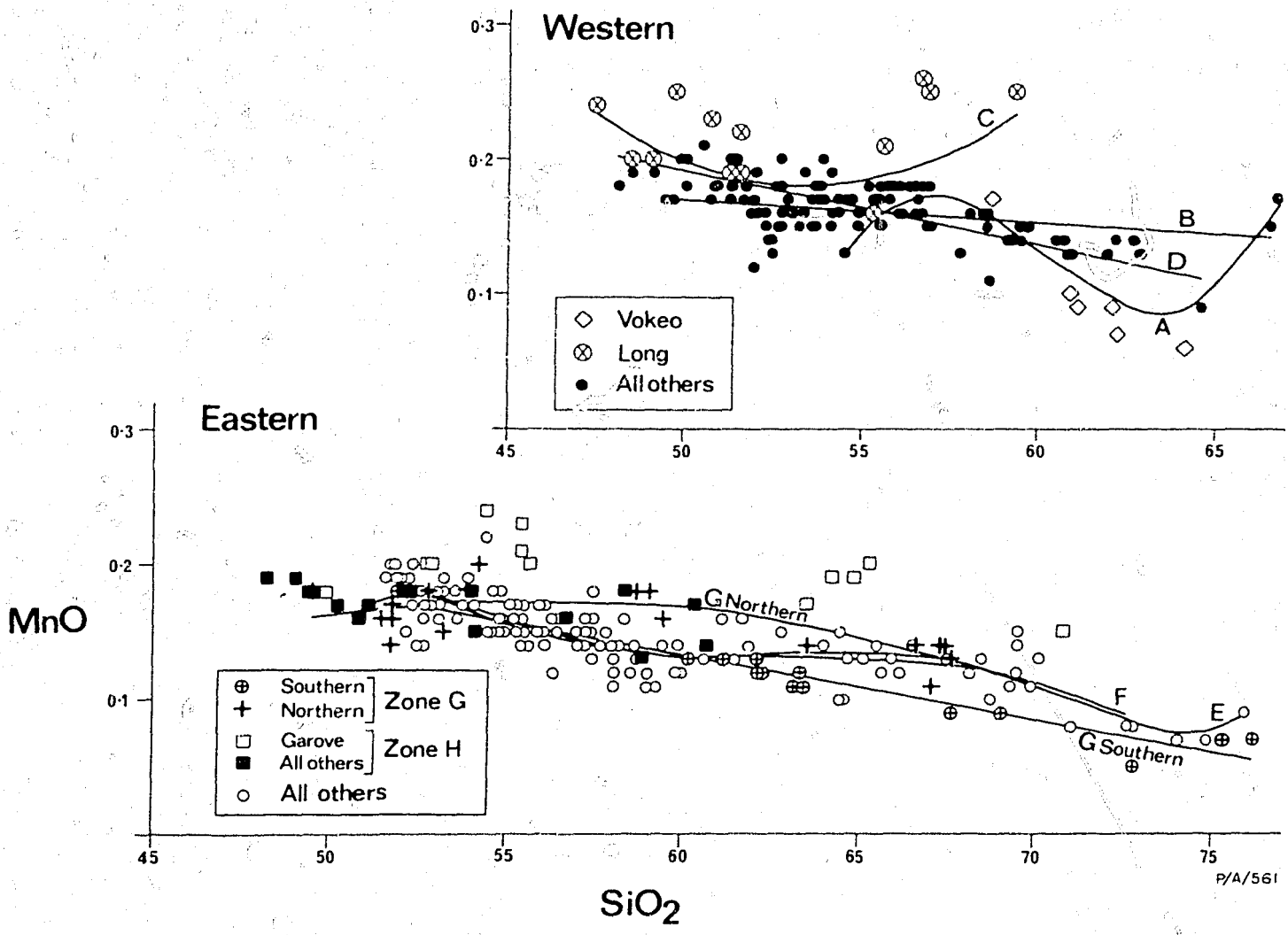

Fig. 27. Weight percent MnO v. SiO_2 for rocks from the western and eastern arcs. RSS values (x 10^3) for regression lines: A = 757, B = 118, C = 182, D = 426, E = 736, F = 549, G southern = 927, G northern = 582.

Consistent regional differences in MnO content between the rocks from one group of western volcanoes and those from any other group are not apparent. However the rocks from Long Island have much higher MnO contents (mostly greater than 0.2 percent), and those from Vokeo have lower MnO contents, than rocks with the same silica content from other western volcanoes. These relations appear to correlate with high and low total iron oxide contents respectively in Long Island and Vokeo rocks (cf. Fig. 24).

The non-basaltic rocks of the eastern volcanoes show some broad differences in MnO contents between rocks with the same silica content from different parts of the arc. The rocks of Garove Island, zone H, are the richest in MnO (Fig. 27). Those of the other eastern volcanoes form a broad zone of low MnO values, within which the rocks from the other zone H volcanoes and from the northern part of zone G appear to be slightly more MnO-rich than some of those from volcanoes farther south, and significantly more MnO-rich than those from the southern part of zone G. The high MnO contents of the Garove rocks may correlate with correspondingly high FeO values because, as shown in Figure 26, Fe_2O_3/FeO values are low in zone H rocks (except those of Unea). Similarly, the low MnO contents of rocks from the southern part of zone G seem to correlate with high Fe_2O_3/FeO, and correspondingly low FeO (Fig. 26; see below for further discussion).

Q-mode factor analysis

In the previous sections, chemical variations within the western and eastern arcs were described in terms of changes in the content of one or two oxides relative to silica (or to total iron oxides in Fig. 25). In this section, the variations of all 11 major oxides (volatiles excluded) are considered together using Q-mode factor analysis with an orthogonal VARIMAX rotation (Klovan & Imbrie, 1971).

Briefly the procedure in Q-mode analysis is to calculate a series of sets of decreasing numbers of 'factors' which express in decreasing degree the total variation among all 11 oxides; as the number of factors decreases so does the amount of variation accounted for by the factors. Three major factors are usually interpreted, as they can be plotted in triangular diagrams. Ideally the three factors should correspond to recognizable petrological parameters. Varimax factor scores indicate the relative dominance of each oxide in each composite factor.

Oxide percentages were first normalized by a percentage range conversion, so as to avoid overweighting by the most abundant oxides. Loadings computed for three factors for the rocks of the western and eastern arcs are plotted in Figures 28 and 29; scaled varimax factor scores for the oxides in each factor are listed in Tables 7 and 9; and oxides with the highest absolute scores ($>|1|$) are listed in Tables 8 and 10. 96.93 percent of the variation in all 11 oxides is accounted for by the three factors for each of the western and eastern arcs.

Factors 1 and 2 for the rocks of both arcs are respectively dominated by the oxides which make up the common rock-forming mafic and salic minerals (Tables 7-10). In Figures 28 and 29, therefore, the distance from factor 1 along the factor 1-2 join is a measure of magmatic differentiation and is largely equivalent to increasing silica content.

The composition of factor 3 is different for the rocks of the western and eastern arcs. In the western arc, TiO_2 is by far the highest-scoring oxide in factor 3 (Table 7), and the overall pattern shown in Figure 28 is rather similar to that in the TiO_2:SiO_2 plot (Fig. 19): the rocks of zones A and C contain the lowest and highest TiO_2 values respectively, and those of zones B and D contain similar intermediate TiO_2 values. In the eastern arc, points representing rocks from zones northern G and H plot progressively

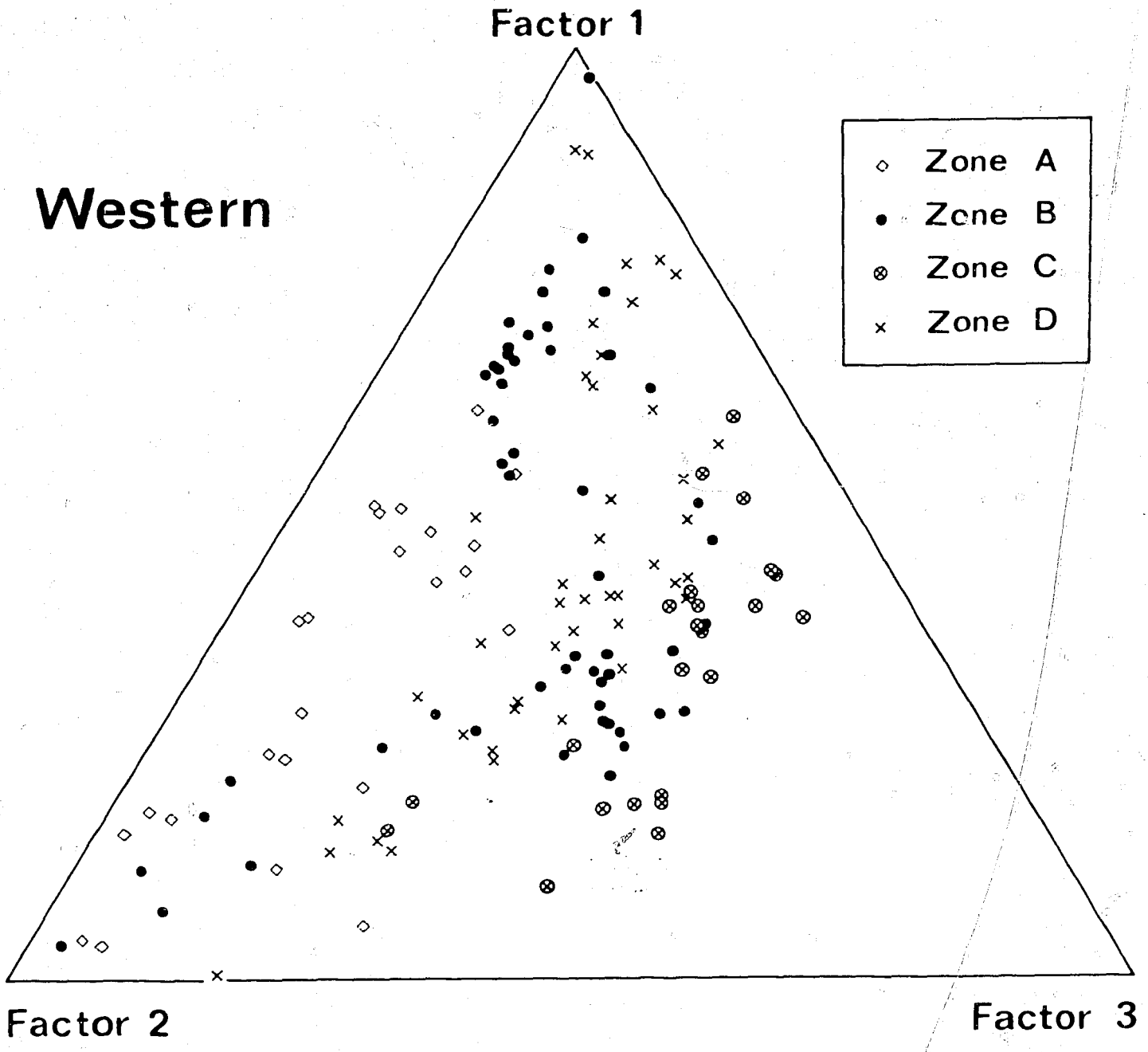

Fig. 28. Loadings for three Q-mode factors accounting for 96.93 percent of the variation among eleven oxides in analysed rocks from the western arc.

TABLE 7. SCALED VARIMAX FACTOR SCORES FOR Q-MODE FACTOR ANALYSIS OF ROCKS FROM WESTERN ARC (cf. Fig. 28)

Oxides	Factors		
	1	2	3
SiO_2	0.034	2.234	0.959
TiO_2	-0.292	-0.246	-2.347
Al_2O_3	-0.021	0.907	-0.966
Fe_2O_3	0.857	0.720	-1.003
FeO	1.441	-0.137	-0.767
MnO	0.911	0.129	-0.862
MgO	1.789	-0.073	-0.882
CaO	2.005	-0.045	0.146
Na_2O	-0.139	1.797	-0.274
K_2O	-0.143	1.094	-0.308
P_2O_5	-0.103	0.369	-0.576

TABLE 8. OXIDES SHOWING ABSOLUTE VARIMAX FACTOR SCORES OF GREATER THAN UNITY FOR EACH OF THE FACTORS IN TABLE 7 AND FIGURE 28, AND LISTED FROM TOP TO BOTTOM IN ORDER OF DECREASING SCORE

Factors	1	2	3
Oxides	CaO	SiO_2	TiO_2
	MgO	Na_2O	Fe_2O_3
	FeO	K_2O	-

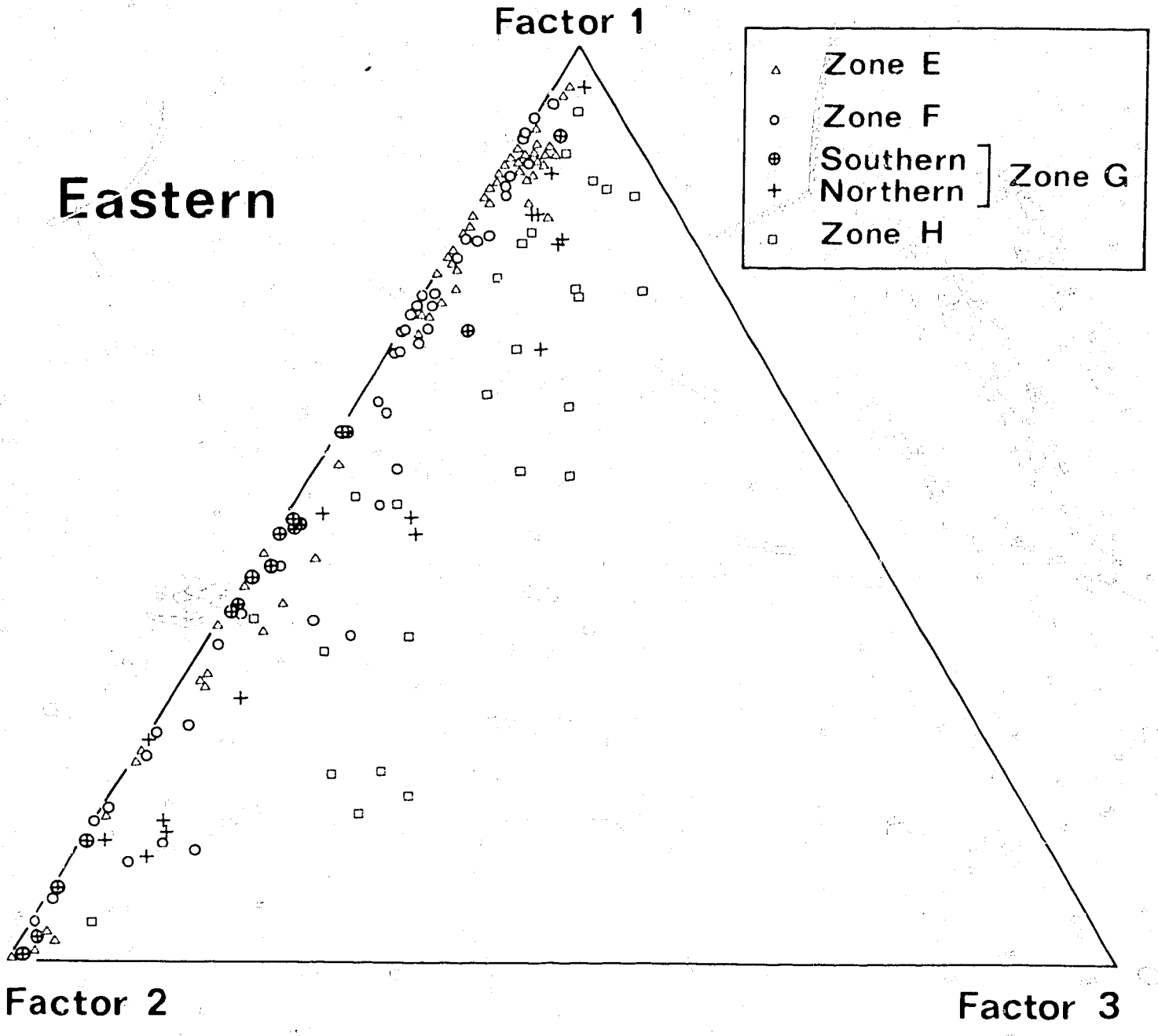

Fig. 29. Loadings for three Q-mode factors accounting for 96.93 percent of the variation among eleven oxides in analysed rocks from the eastern arc.

TABLE 9. SCALED VARIMAX FACTOR SCORES FOR Q-MODE FACTOR ANALYSIS OF ROCKS FROM EASTERN ARC (cf. Fig. 29)

Oxides	Factors		
	1	2	3
SiO_2	-0.325	2.208	-0.856
TiO_2	0.312	0.167	1.499
Al_2O_3	1.444	0.402	1.760
Fe_2O_3	1.059	0.790	0.063
FeO	1.544	0.032	0.716
MnO	1.027	0.380	1.063
MgO	1.077	-0.268	0.368
CaO	1.672	0.021	-0.408
Na_2O	-0.266	1.699	0.434
K_2O	-0.353	1.276	-0.023
P_2O_5	-0.044	0.760	1.668

TABLE 10. OXIDES SHOWING ABSOLUTE VARIMAX FACTOR SCORES OF GREATER THAN UNITY FOR EACH OF THE FACTORS IN TABLE 9 AND FIGURE 29, AND LISTED FROM TOP TO BOTTOM IN ORDER OF DECREASING SCORE

Factors	1	2	3
Oxides	CaO	SiO_2	Al_2O_3
	FeO	Na_2O	P_2O_5
	Al_2O_3	K_2O	TiO_2
	MgO	-	MnO
	Fe_2O_3	-	-
	MnO	-	-

closer to the factor 3 apex (Fig. 29). Al_2O_3, P_2O_5, and TiO_2 dominate factor 3 (Table 10), and the pattern of points in Figure 29 is rather similar to that in Figures 19, 20, and 22, in which the rocks from zones northern G and H can in general be readily distinguished from one another and from rocks of the other zones. The combination Al_2O_3-P_2O_5-TiO_2 does not correspond to any familiar petrological parameter, but note that (1) P_2O_5 and TiO_2 are the oxides of incompatible major elements, and (2) as in factor 3 for the rocks of the western arc, TiO_2 has a significantly high varimax factor score (see below for further discussion).

For the rocks of both arcs, factor 3 is dominated by oxides which have wide ranges relative to their average abundances at any given silica level. This is illustrated clearly in Table 6, where - because of the wide ranges - regression lines were not determined for TiO_2:SiO_2 relations in five of the nine zones, and where RSS values for the regression lines for Al_2O_3:SiO_2 and P_2O_5:SiO_2 relations are relatively low.

Results from the Q-mode factor analysis are similar to those from the nonlinear mapping (NLM) program (Appendix 3). However, the relative importance of components in the two composite parameters which determine the NLM patterns cannot be identified directly, and, therefore, for the purposes of this Report, Q-mode factor analysis is the more useful technique.

ROCK CLASSIFICATION

Since 1950 (Tilley, 1950; Kuno, 1950), two hypersthene-normative associations - calcalkaline and tholeiitic - have commonly been distinguished in studies of island-arc volcanic rocks. Calcalkaline rocks are said to overlie deeper parts of Benioff zones than tholeiitic ones (e.g., Ringwood, 1974). The chemical differences between these associations have never been rigorously

defined; but recently Jakeš & Gill (1970) and Jakeš & White (1972) proposed an empirical classification, in which the two associations represent end members 'between which there is considerable overlap', and in which some of the chemical features 'may vary independently thereby blurring the distinction'. According to Jakeš, Gill, and White, the differences between calkalkaline rocks and rocks of an 'island arc tholeiitic series' are as follows.

(1) Tholeiitic rocks contain less K_2O and $Na_2O + K_2O$ than calcalkaline rocks with the same silica content, and K_2O is relatively less enriched in tholeiitic rocks with a higher silica content. Jakeš & Gill (1970, fig. 2) presented a K_2O:SiO_2 diagram which shows one field of calcalkaline rocks and another of tholeiitic rocks joined at their basic ends but divergent at higher silica values (Fig. 30).

(2) K_2O/Na_2O values in the tholeiitic rocks are mostly less than 0.35, whereas the range for calcalkaline rocks is 0.35-0.75.

(3) Rocks of the tholeiitic series have a lower 'silica mode': the most common rock type contains about 53 percent silica, whereas in calcalkaline associations the 'mode' is about 59 percent.

(4) Tholeiitic rocks show greater degrees of iron-enrichment in MF and FMA diagrams. Jakeš, Gill, and White did not propose a precise boundary for dividing tholeiitic rocks from calcalkaline ones, but in an FMA diagram they illustrated the general chemical features of each association by using examples from Melanesian island arcs (cf. Jakeš & White, 1972, fig. 2).

Using these principal criteria, Jakeš & Gill (1970) drew attention to differences in trace-element contents between the two associations, and especially to differences in rare-earth-element concentrations. Jakeš & White (1972) outlined a few of the general chemical characteristics of rocks from shoshonitic associations (higher K_2O and higher K_2O/Na_2O values than calcalkaline rocks with the same silica content).

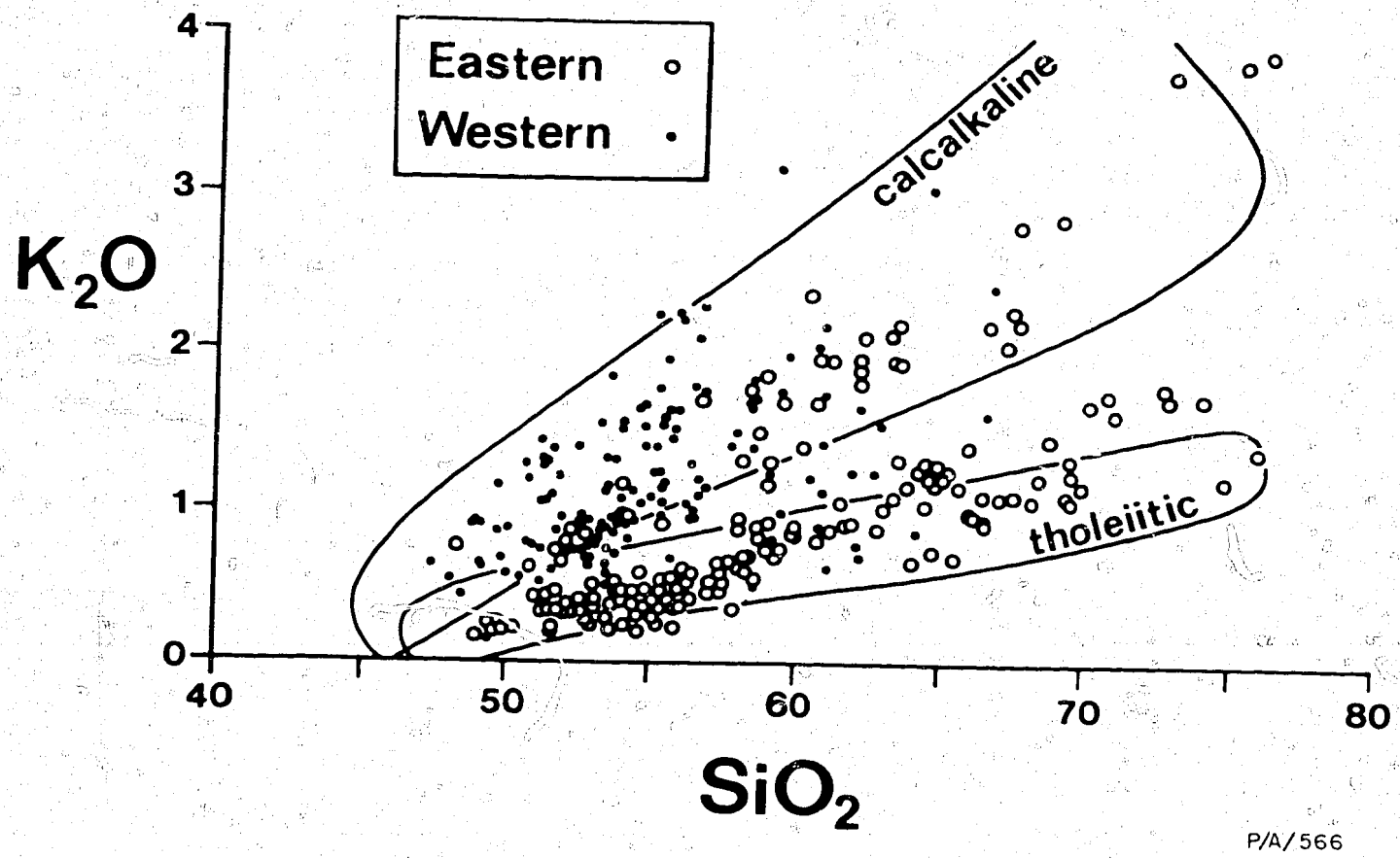

Fig. 30. K_2O:SiO_2 for rocks from the south Bismarck Sea volcanoes in relation to the generalized calcalkaline and tholeiitic field boundaries of Jakeš & Gill (1970).

The hypersthene-normative rocks of the south Bismarck Sea volcanoes show a wide range of chemical compositions, and provide an ideal opportunity for testing the significance of the commonly recognized subdivision into calcalkaline and tholeiitic associations. Apart from two rocks from Kadovar, none of the south Bismarck Sea rocks is shoshonitic (in the sense used by Mackenzie & Chappell, 1972, for rocks from the Papua New Guinea Highlands), and this association is therefore excluded from the following discussion. Using commonly accepted criteria, including those summarized by Jakeš, Gill, and White, the rocks of the south Bismarck Sea cannot be effectively divided into calcalkaline and tholeiitic associations, for the reasons outlined below.

Firstly, boundaries used in K_2O:SiO_2 diagrams by other authors to discriminate between different associations divide the rocks of the south Bismarck Sea into artificial fields which have no geological significance. For example, in Figure 30 the rocks of the south Bismarck Sea are plotted in relation to the gap between the generalized calcalkaline and tholeiitic fields of Jakeš & Gill (1970). This gap is partly filled by points representing rocks which cannot be assigned to either association, and the gap does not correspond with the zone of low point-density for the rocks from the eastern arc (see p.47 , Fig. 15). Similarly as discussed above (p. 52) the field boundaries of Kuno (1959) and of Rittmann (1958) - using Na_2O+K_2O:SiO_2 relations - have no relevance to the south Bismarck Sea rocks, as they separate rocks of different silica contents from the same volcano or volcanic zone.

Secondly, most of the western rocks have K_2O/Na_2O values greater than 0.35 (calcalkaline), and most of the eastern rocks have values of less than 0.35 (tholeiitic, Fig. 17). Therefore, according to the classification of Jakeš, Gill, and White, the most common rock type in the eastern arc should have a silica content less than that of the most common rock type in the western arc. But the reverse appears to be true, because the median silica value of the

eastern rocks is 56.6 and that for the western rocks is 54.3 (Fig. 11). Moreover, within each of the western and eastern arcs, the high total alkali zones (calcalkaline) contain greater proportions of rocks poorer in silica (see Fig. 18). In the eastern arc, therefore, basic rocks appear to be more common over the deeper parts of the New Britain Benioff zone. These correlations are also the reverse of those suggested by Jakeš, Gill, and White.

Thirdly, as discussed on page 59, a continuum between iron-poor and iron-rich compositions is shown in the MF diagram (Fig. 25). Any subdivisions into calcalkaline and tholeiitic parts is arbitrary and little significance can be attached to any line of separation between iron-poor and iron-rich fields. For the same reason, in FMA diagrams, the field boundaries identified - for example, by Kuno (1968), Jakeš & White (1972), and Irvine & Baragar (1971) - have no relevance to the rocks of the south Bismarck Sea (see Fig. 37).

Fourthly, as discussed on page 60 with reference to Figures 15, 18, and 25, no relation can be established between increasing total alkali content and lower degrees of iron-enrichment in the rocks of either arc. Although the opposite may be true to a slight extent, for all practical purposes the degree of iron-enrichment is considered to be independent of $Na_2O + K_2O:SiO_2$ and $K_2O:SiO_2$ relations.

Fifthly, the rocks of many volcanoes from both the western and eastern arcs are tholeiitic by one set of criteria, but calcalkaline by another set. For example, because the rocks of Dufaure (zone F) and Vokeo (zone A) are poor in alkalis and K_2O, they are tholeiitic in character; however, their iron-contents are low, which is a calcalkaline feature. Johnson, Davies, & White (1972) showed that the total alkali and the K_2O contents of Ulawun rocks (zone E) were also of tholeiitic type, and that their iron contents were of calcalkaline type. Long Island rocks (zone C) have high K_2O, $Na_2O + K_2O$, and K_2O/Na_2O values - a calcalkaline feature - but are iron-rich - a tholeiitic feature. The silica contents of the most common rocks from each of these volcanoes indicate that the rocks of Dufaure and Vokeo are calcalkaline, and those of Long Island and Ulawun are tholeiitic.

For all these reasons, it is concluded that an effective calcalkaline/tholeiitic subdivision cannot be recognized in the rocks of the south Bismarck Sea. Instead, the rocks of both the western and eastern arcs should be recognized as a single, hypersthene-normative rock association characterized by wide, and essentially continuous, ranges in oxide contents (in rocks containing the same amount of silica), and by different relative abundances of rock types in each arc. The association can be termed 'subalkaline' (to distinguish it from nepheline-normative 'alkaline' rocks), but attempts to subdivide the association into calcalkaline and tholeiitic types using current schemes of classification lead to arbitrary and artificially defined categories which have no practical significance for these rocks.

PATTERNS OF CHEMICAL VARIATION

Variations in major-element chemistry in both the western and eastern volcanic arcs can be considered at three levels:

(1) Interzonal variations: that is, differences between the rocks of zones A to D in the western arc, and of zones E to H in the eastern arc;

(2) Intervolcano variations: that is, differences between the rocks of one volcano and those of other volcanoes in the same zone, or in the same volcanic arc;

(3) Intravolcano variations: that is, differences within individual volcanoes.

Variations at levels (1) and (2) are discussed in this section; those at level (3) are dealt with briefly on page 125 . In this section particular attention is given to K_2O:SiO_2 relations in the eastern arc because of the widespread interest in these parameters relative to depths to underlying Benioff zones.

Interzonal variations

The chemical changes between zones are the most important type of variation as they depend upon first-order differences in conditions of magma genesis. In order that these interzonal changes in the contents of individual oxides can be compared with one another, an attempt has been made in Figures 31 and 32 to summarize the chemical variations using 'average' values for each oxide (or oxide combination) in rocks from each zone. The procedure for the construction of Figures 31 and 32 was as follows.

1. Silica values of 50, 55, and 59 percent were selected as representative of basalts, low-silica andesites, and high-silica andesites, respectively, in the western arc; and values of 52.5, 55, 60, and 65 percent silica were selected as representative of basalts, low-silica andesites, high-silica andesites, and dacites, respectively, in the eastern arc.

2. Using the above silica values, and the regression lines in Figures 15-24, 26, and 27, corresponding oxide values were read off each diagram and plotted in Figures 31 and 32.

3. In diagrams where no regression lines were computed for some zones, an arithmetic mean was calculated for the oxide values lying within the appropriate silica range given on page 25 . These mean values are represented by solid dots in Figures 31 and 32.

With regard to the interpretation of the variations shown in Figures 31 and 32, note that no measure is given of the significance of changes in average oxide contents between one zone and another. For example, there is little doubt that at 55 percent silica the K_2O/Na_2O values of rocks from the southern part of zone G are significantly higher than those for zone F, but there is much more doubt that, for example, at 52.5 percent silica the MnO values in zone F are significantly higher than those for zone E. Considerable care must therefore be taken so that interpretations of the apparent changes in average oxide contents are not exaggerated.

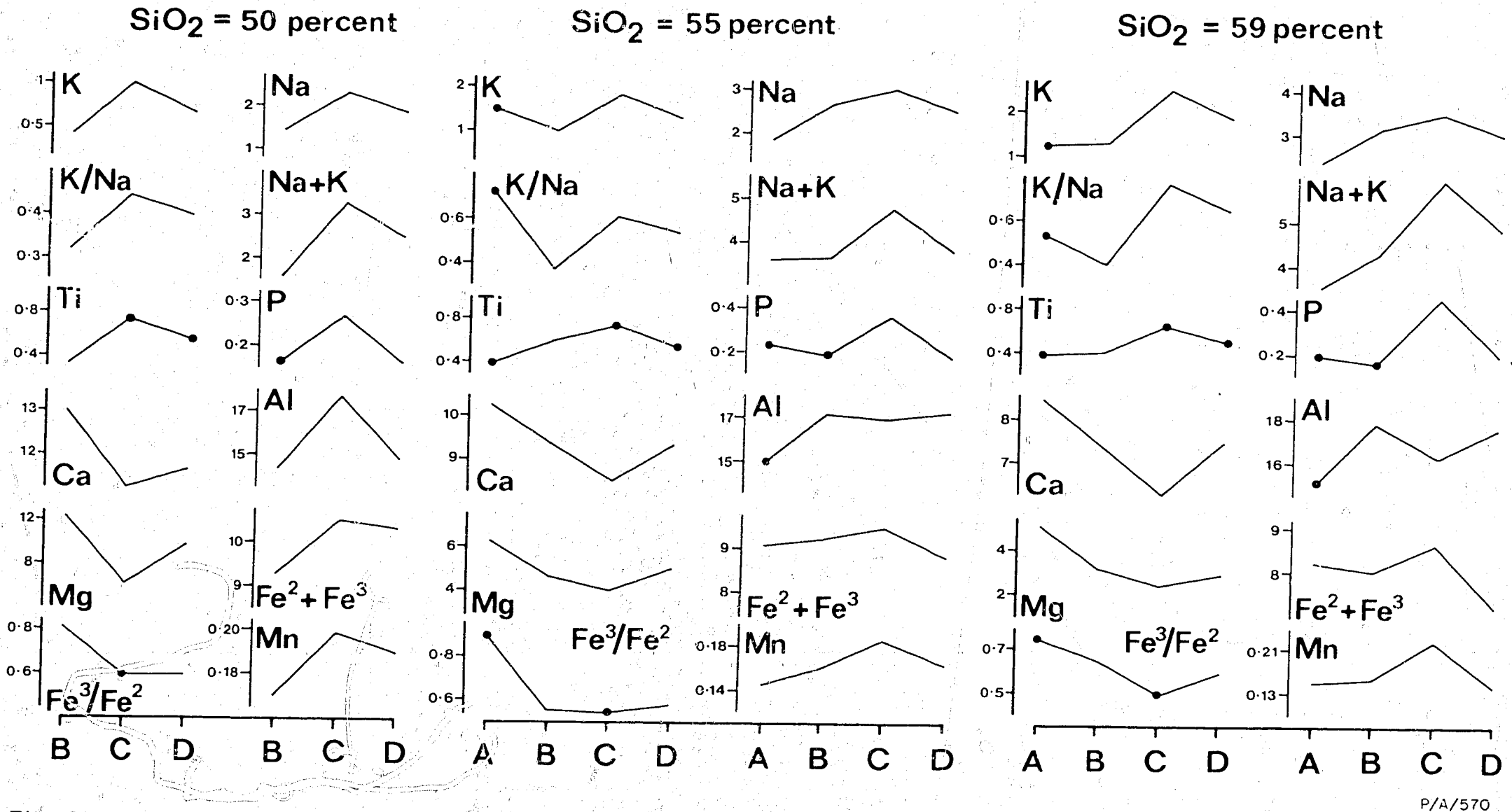

Fig. 31. Generalized oxide variations with different silica contents in rocks from the western arc. Individual oxide values for each zone are arithmetic means (dots) or were determined from the regression lines in Figures 15–24, 26, and 27 (see text for details).

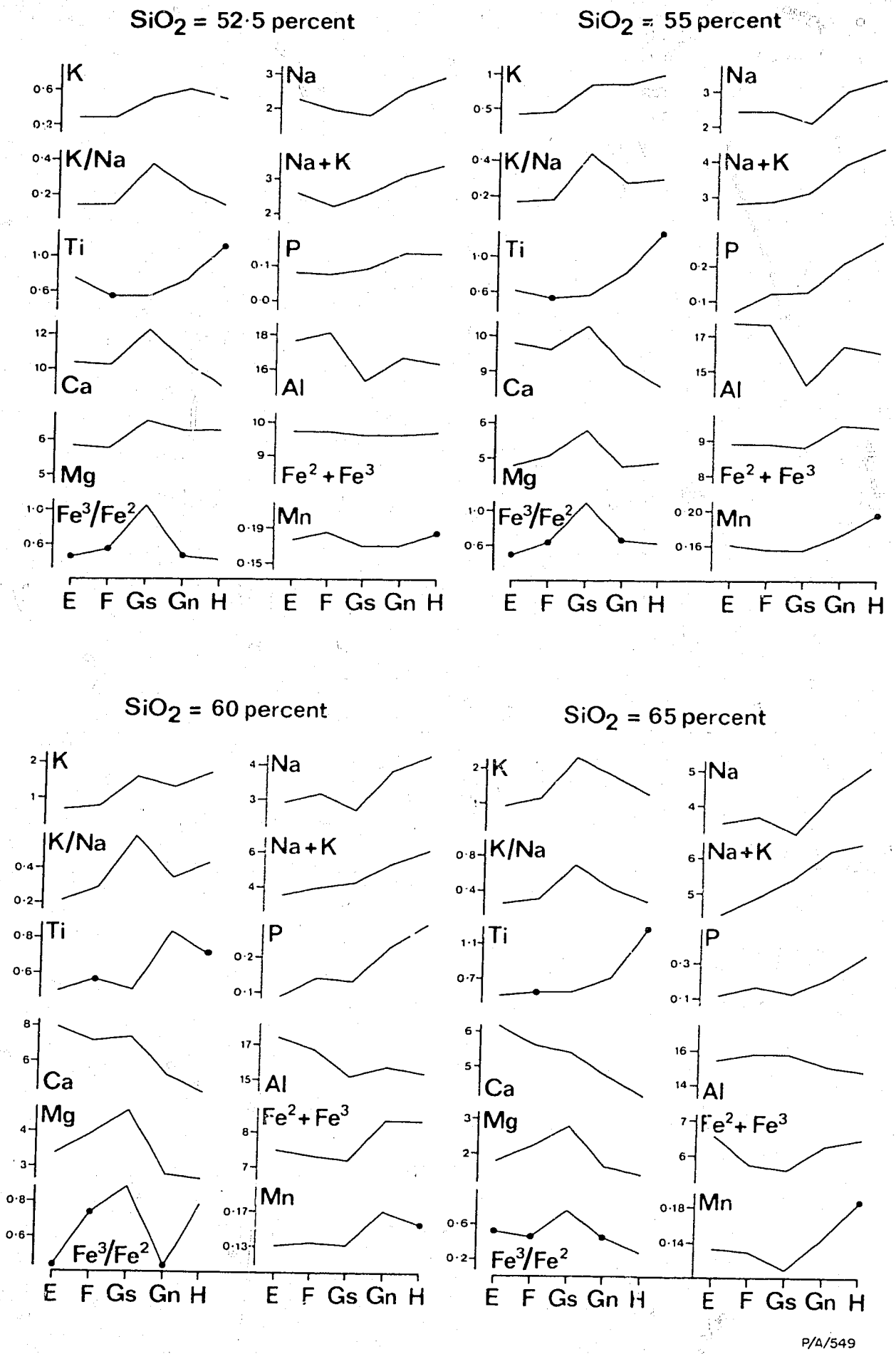

Fig. 32. Generalized oxide variations with different silica contents in rocks from the eastern arc. Individual oxide values for each zone are arithmetic means (dots) or were determined from the regression lines in Figures 15-24, 26, and 27 (see text for details).

Oxides having similar patterns of variation in Figures 31 and 32 have been grouped together in Table 11, in which two main groups - 1 and 2 - and four subgroups are identified. The most noteworthy aspect of this classification is that oxides of elements which generally concentrate in residual liquids during fractionation, or enter first-formed anatectic liquids, appear together in group 1A.

In the eastern arc, the oxides (and oxide combinations) of group 1 have generally higher values in the more northerly zones. Notable exceptions are: (1) K_2O, which decreases northwards in rocks from zones G and H containing more than about 60 percent SiO_2 (see next section for a detailed discussion); (2) Na_2O, which has minimum values in rocks from the southern part of zone G; and consequently (3) K_2O/Na_2O, which shows maximum values in the southern part of zone G, and decreasing values farther north in rocks from zones G and H with more than 60 percent silica. Northward increases are also shown by the group 1B oxides, but are much less clear than those shown by the group 1A oxides. In contrast to group 1, the group 2 oxides (and oxide combinations) generally have lower values in rocks from the more northerly zones, or else values are more or less constant from south to north. Exceptions are rocks from the southern part of zone G in which the group 2A oxides show maximum values. Lower percentages of total phenocrysts and amphibole phenocrysts are also contained in rocks from the more northerly zones (see p. 31 and 35).

In the western arc, the group 1 oxides generally have maximum values in zone C and to a lesser extent (P_2O_5 and K_2O/Na_2O are notable exceptions) minimum values in zone A. These relations are more clearly shown by the oxides of group 1A than by those of group 1B. The group 2A oxides generally have minimum values in zone C and maximum values in zone A. The group 2B oxide (Al_2O_3) shows erratic behaviour between the western zones. Minimum percentages of amphibole phenocrysts are also contained in zone C rocks, and minimum percentages of total phenocrysts are contained in some rocks from Long Island, in zone C (see pp. 31 and 35).

TABLE 11. MAJOR OXIDES (INDIVIDUAL, RATIOS, AND SUMS) CLASSIFIED ON BASIS OF GENERALLY SIMILAR BEHAVIOUR IN ROCKS WITH THE SAME SILICA CONTENT BETWEEN ZONES A TO H OF THE EASTERN AND WESTERN ARCS

Group	Subgroup	Oxides
1	A	K_2O, Na_2O, TiO_2, P_2O_5 K_2O/Na_2O, Na_2O+K_2O
	B	$FeO+Fe_2O_3$, MnO
2	A	CaO, MgO, $MgO/FeO+Fe_2O_3$, Fe_2O_3/FeO
	B	Al_2O_3

K-h relations in the eastern arc

During recent years, considerable attention has been given to the relations between the K_2O and SiO_2 contents of circumoceanic rocks and the depth, h, to Benioff zones underlying the arc-trench systems. Since 1967, 'K-h' relations (Dickinson & Hatherton, 1967) have been reported from many circumoceanic regions (e.g., Dickinson, 1968; Hatherton & Dickinson, 1969; Ninkovich & Hays, 1972; Nielson & Stoiber, 1973; Hutchison, 1975; Whitford & Nicholls, 1976), and it is now widely accepted that K_2O increases in rocks with the same silica content as h increases; on this assumption, K_2O:SiO_2 relations have been used to identify the existence, polarity, and inclination of palaeoseismic zones (e.g., Lipman, Prostka, & Christiansen, 1971).

Because of this interest, K-h relations for the rocks of the eastern arc, which overlies the inclined Benioff zone beneath New Britain, are considered here in greater detail. 'Average' K_2O values at the four silica levels in Figure 32 ($K_{52.5}$, K_{55}, K_{60}, K_{65}), and depth ranges (h) of the New Britain Benioff zone beneath each of the zones in the volcanic arcs (Fig. 4), are plotted in Figure 33.

K52.5. For two reasons, little significance can be attributed to the relative differences in K_2O between each of the zones E to H at the 52.5 percent SiO_2 level shown in Figure 33: firstly, among the analysed rocks of the eastern arc, basalts are well represented only in zone H; and secondly all the regression lines in Figure 15 indicate K_2O contents of less than 0.6 percent by weight, and at these low levels routine analysis of K_2O is not especially accurate. Nevertheless, Figure 15 shows that K_2O is lower in the basalts of zones E and F than in many of those from zones G and H.

K55. The low-silica andesites show a general but irregular increase in K_2O northwards across the New Britain Benioff zone. There is no effective distinction between the low-silica andesites of the northern and southern parts of zone G, and the apparently

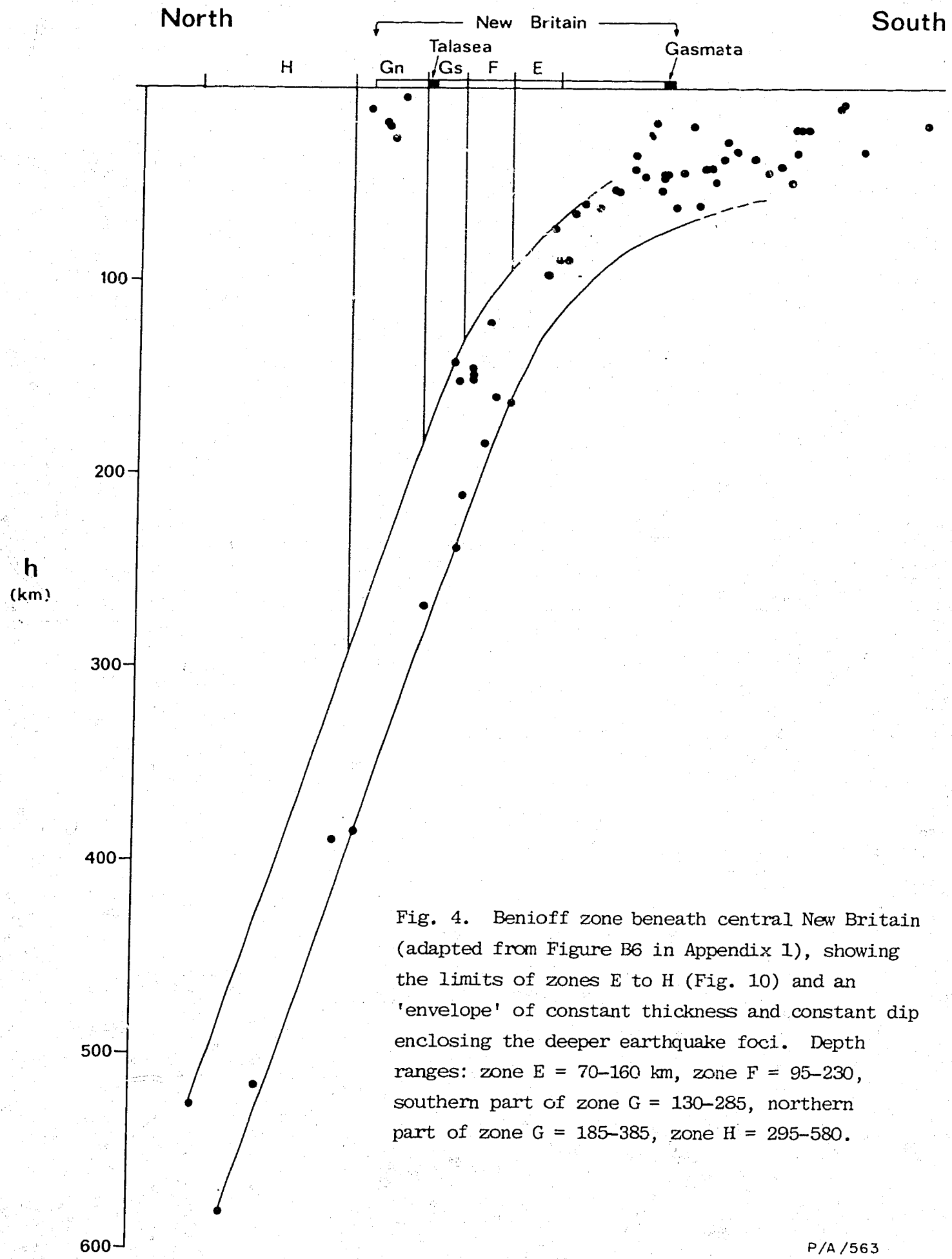

Fig. 4. Benioff zone beneath central New Britain (adapted from Figure B6 in Appendix 1), showing the limits of zones E to H (Fig. 10) and an 'envelope' of constant thickness and constant dip enclosing the deeper earthquake foci. Depth ranges: zone E = 70–160 km, zone F = 95–230, southern part of zone G = 130–285, northern part of zone G = 185–385, zone H = 295–580.

P/A/563

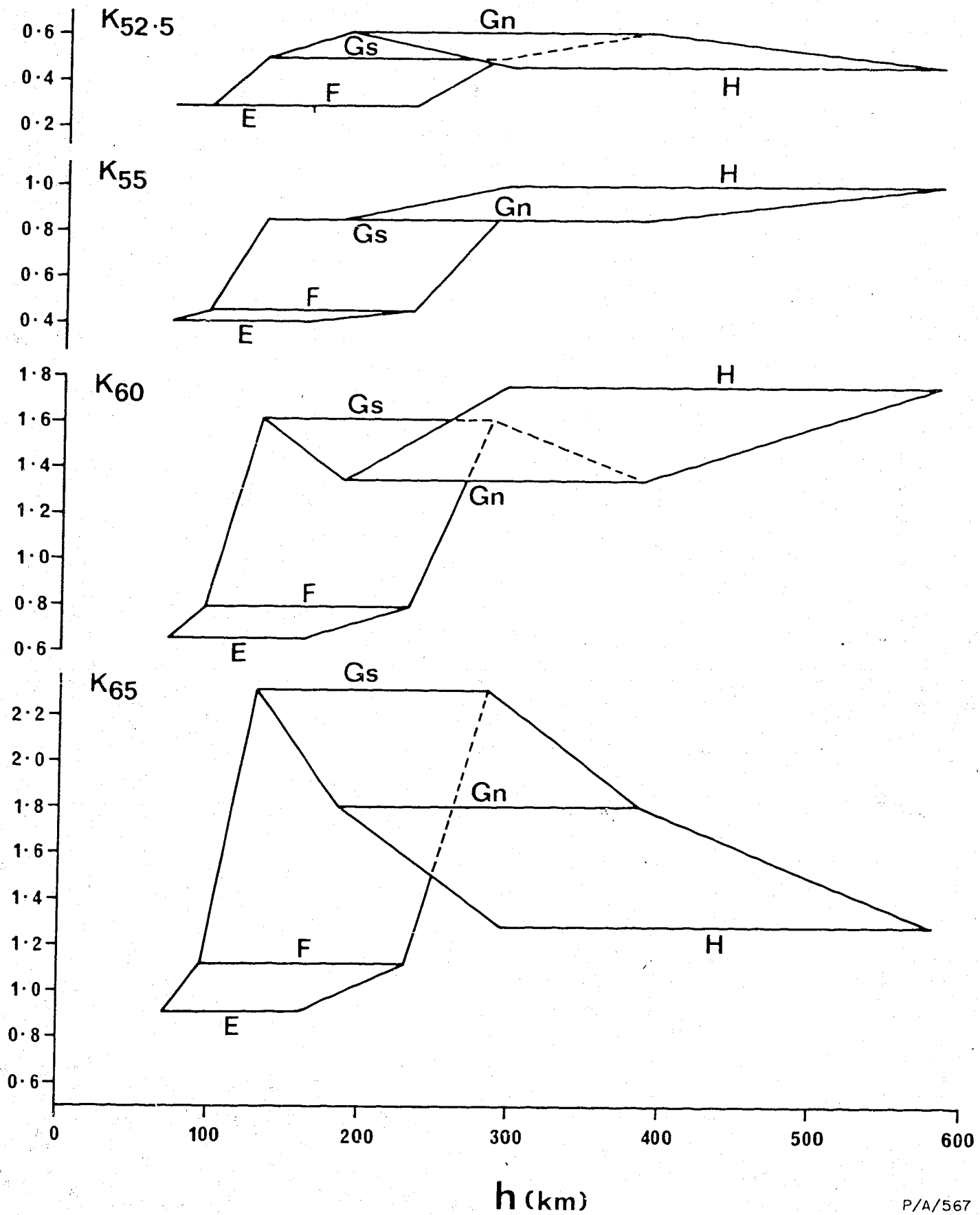

Fig. 33. K_2O contents - determined from the regression lines in Figure 15 at 52.5, 55, 60, and 65 percent silica levels - plotted against depth-ranges to the New Britain Benioff zone - determined from Figure 4, and for zone E also from Figure B7 in Appendix A. Letters corresponding to each zone are drawn opposite the midpoint of the lines representing each depth range.

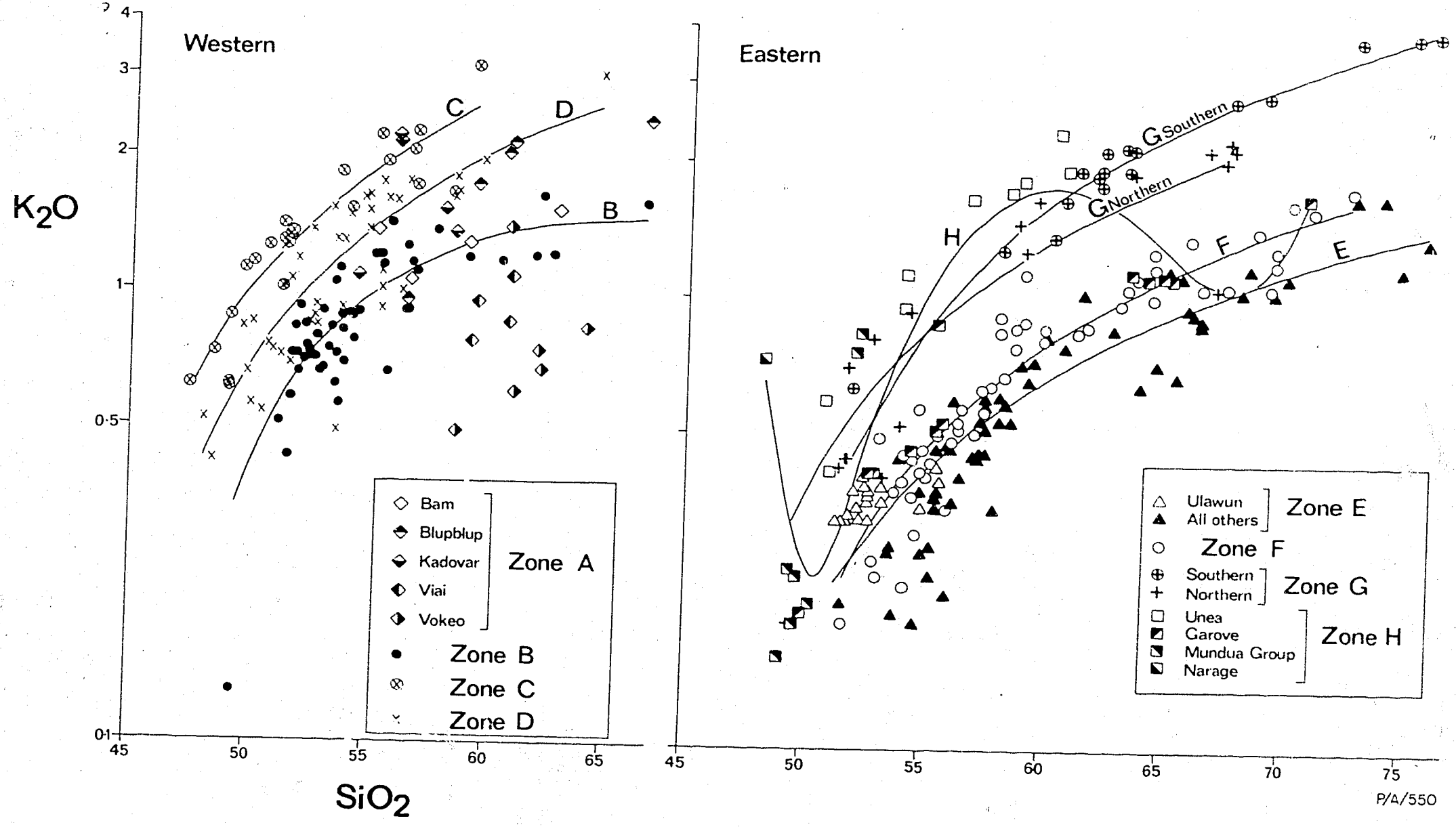

Fig. 15. Weight percent K_2O ($\log_{10}$ scale) v. SiO_2 for rocks from the western and eastern arcs. RSS values (x 10^3) for regression lines: B = 690, C = 817, D = 744, E = 859, F = 894, G southern = 978, G northern = 827, H = 788.

higher K_2O value for zone F compared with that for zone E is so slight as to be of no practical significance. However, the absence of any significant separation between the regression lines for zones E and F at K55 - and at K52.5 (see above) - is largely due to the effect of rocks from Ulawun (a zone E volcano), whose K_2O contents are closer to those of zone F rocks than to zone E rocks (Fig. 15). If the Ulawun rocks are excluded from the data set, there is a much clearer separation of the two regression lines at low SiO_2 values (not illustrated here).

K60. At 60 percent SiO_2, K_2O increases from zone E to zone F and abruptly to the southern part of zone G. But this trend of increasing K_2O does not continue into the northern part of zone G, which - rather - apparently has a lower K_2O content. However, this reversal in trend may not be a real feature, for Figure 15 shows that the high-silica andesites of the southern and northern parts of zone G are indistinguishable. A further increase in K_2O is indicated by the zone H regression line, whose position at K60 is controlled by the high-silica andesites from one volcano - Unea.

K65. The K_2O variation is more clearly defined for the dacites than for the other rock types. The K-h plot for K65 is similar to that for K60, but, in contrast, indicates a diminishing K_2O content from the southern part of zone G through the northern part of zone G to zone H. The low K_2O value in zone H is due to the dacitic and rhyolitic rocks of Garove Island, whose K_2O contents are similar to those in the dacites and rhyolites of zone F (Fig. 15). Thus, in the progression northwards from zone E to zone H, the K_2O contents of the dacites reach a maximum halfway across the Benioff zone, and decrease as the depth to the Benioff zone increases further.

A comparison of all four K-h plots in Figure 33 shows that, although the overall trend is towards higher K_2O contents in rocks (with the same SiO_2 content) overlying deeper parts of the Benioff zone, there are notable exceptions, and the trend is not

necessarily the same at each SiO_2 level. The four plots also emphasize the conclusion reached above - that, in the south, K_2O increases progressively between zones E, F, and southern G, and that, in the north, K_2O variations between both parts of zone G and zone H appear to be unsystematic. K_2O does not necessarily increase as h increases; in fact, in rocks from the northern zones containing more than 60 percent silica, K_2O decreases as depth to the Benioff zone increases.

Integration of K-h relations for many island arcs (especially Pacific ones) into a worldwide correlation has been attempted by several investigators. For example, in a recent study Ninkovich & Hays (1972) plotted K_2O versus SiO_2 for many rocks from several arcs in the circum-Pacific region, and drew contours dividing the points roughly into fields corresponding to the depths to the Benioff zone above which the volcanic rocks were sampled. Three of these contours are shown in Figure 34. The five regression lines for the New Britain volcanic arc (Fig. 15) are also shown in Figure 34; they all fall below the 'h = 150 km' contour of Ninkovich & Hays (1972), despite the fact that the depth of the New Britain Benioff zone ranges between 70 and 580 km.

Dickinson (1975) also recently examined K57.5-h relations for 64 selected volcanoes and volcano clusters in 14 different arc-trench systems overlying Benioff zones down to depths of 280 km. The data for the New Britain zones E, F, and southern G plot in the general field of Dickinson's 'intra-oceanic arcs', and those for the northern part of zone G and zone H fall outside this field and its extension. The southerly zones of the eastern arc, therefore, accord reasonably well with the worldwide K-h correlations of both Ninkovich & Hays (1972) and Dickinson (1975), but the northerly ones show pronounced departures.

Intervolcano variations

Superimposed on the interzonal variations are the compositional traits of rocks from different volcanoes in the same zone.

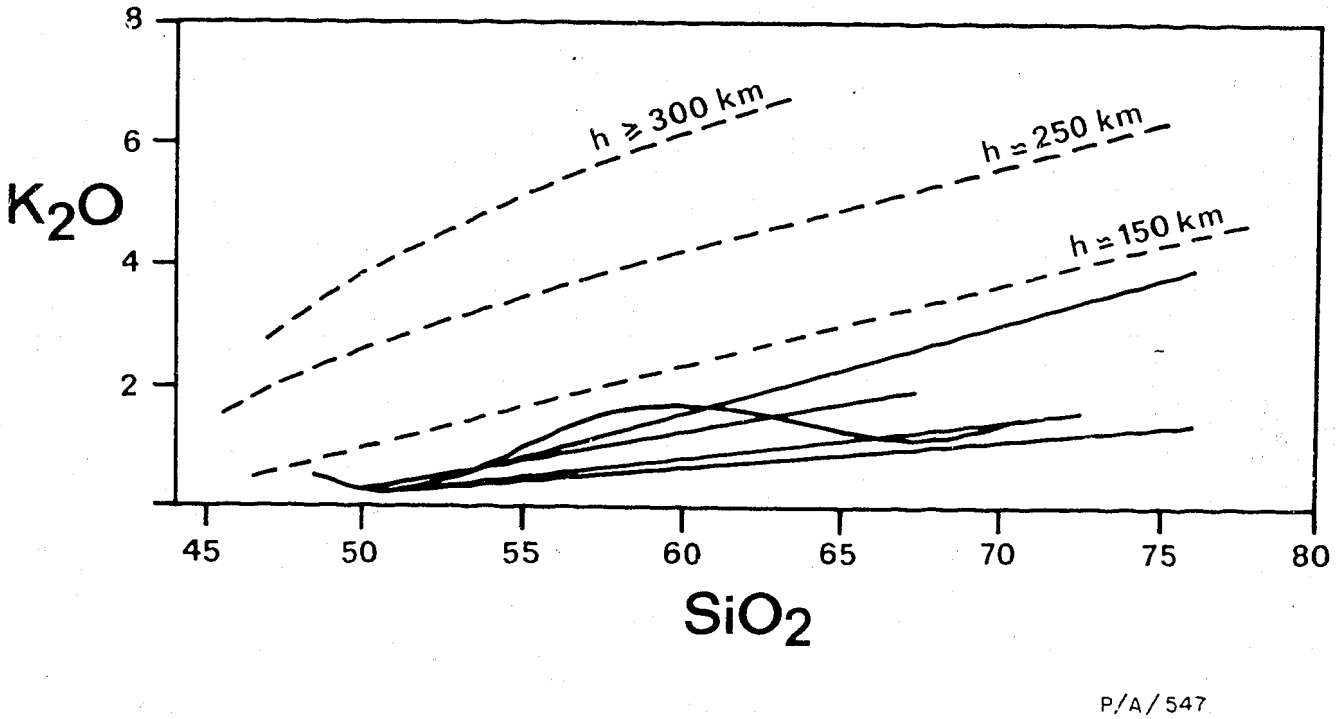

Fig. 34. Regression lines of Figure 15 plotted on the K-h grid of Ninkovich & Hays (1972); h values represent depths to Benioff zones.

These traits indicate that, although the chemistry of individual volcanoes is controlled to a large extent by their tectonic setting, chemical features in some volcanoes appear to be independent of the position of the volcanic centre within the arc. Rocks of the following volcanoes are particularly conspicuous in showing distinctive bulk rock compositions.

(1) Vokeo. Compared with other western rocks of the same silica content, those of Vokeo, and of Viai, have exceptionally low K_2O and P_2O_5 contents (Figs. 15 and 20). Vokeo rocks are further distinguished by their low FeO + Fe_2O_3 and MnO contents (Figs. 24 and 27).

(2) Karkar and Long. In addition to having exceptionally high FeO + Fe_2O_3 contents (Fig. 24), rocks from Karkar (zone B) and Long (zone C) are also characterized by low CaO, MgO, and Fe_2O_3/FeO values (Figs. 21, 23, and 26). In addition, the rocks of Long have the highest MnO values of all the western rocks, and the andesites are especially low in Al_2O_3 (Figs. 27 and 22).

(3) Ulawun. In almost all the variation diagrams, the rocks of Ulawun, in zone E, show the chemical characteristics of rocks from zone F (see Table 4). The chemical individuality of the Ulawun rocks is particularly striking, especially when they are compared with those of Bamus, the neighbouring volcano to the southwest (Fig. 6). Both Ulawun and Bamus are stratovolcanoes over 2000 m high, and have erupted throughout the Quaternary. The Bamus rocks are mainly low-silica andesites whose chemistry is similar to that of andesites from other zone E volcanoes. The Ulawun rocks, on the other hand, are mainly low-magnesia basalts which show zone F chemistry. These relations imply that the courses of magmatic evolution were independent for each volcano. Note, however, that the rocks of Ulawun and Bamus, and of Lolobau, share one chemical feature: they have higher TiO_2 values than other rocks from zones E and F (see Fig. 19).

TABLE 4. CHEMICAL AND MODAL ANALYSES AND CIPW NORMS OF 10 ROCKS SELECTED FROM 205 ANALYSED ROCKS FROM THE EASTERN ARC

	1	2	3	4	5	6	7	8	9	10
SiO_2	72.4	52.43	53.9	53.85	58.30	63.9	59.0	51.57	53.7	49.2
TiO_2	0.31	0.77	0.67	0.52	0.46	0.80	0.51	0.80	1.54	1.14
Al_2O_3	13.4	17.80	18.5	17.30	15.9	14.50	16.9	15.91	15.10	15.0
Fe_2O_3	0.88	3.32	2.95	3.68	3.65	1.81	3.15	2.74	3.95	3.45
FeO	1.48	6.55	5.70	5.53	3.75	5.55	3.90	7.04	7.95	6.05
MnO	0.07	0.18	0.15	0.15	0.13	0.15	0.13	0.17	0.24	0.18
MgO	0.81	5.17	3.90	4.82	4.70	1.95	3.40	6.73	4.15	11.3
CaO	2.75	10.61	9.70	9.45	8.15	5.70	6.70	11.74	7.90	10.8
Na_2O	4.05	2.35	2.50	2.55	2.85	3.60	2.90	2.41	3.60	2.2
K_2O	1.64	0.36	0.36	0.56	0.88	0.99	1.34	0.44	0.45	0.25
P_2O_5	0.03	0.08	0.07	0.12	0.13	0.18	0.14	0.11	0.19	0.11
H_2O+	1.98	0.19	0.86	)	0.45	0.54	1.07	0.35	0.43	<0.01
H_2O-	0.11	0.07	0.48	) 0.72	0.47	0.09	0.59	0.10	0.55	0.27
CO_2	0.04	0.05	<0.05	)	0.04	<0.05	0.05	-	<0.05	0.05
Total	99.95	99.93	99.74	99.25	99.86	99.76	99.78	100.11	99.75	100.00
CIPW norms[a]:										
Q	35.60	5.51	9.63	7.66	13.51	22.71	15.91	1.79	6.37	-
or	9.93	2.13	2.19	3.37	5.26	5.95	8.09	2.60	2.72	1.48
ab	35.01	19.96	21.48	21.91	24.44	30.70	25.04	20.47	30.87	18.69
an	13.74	37.16	38.86	34.69	28.33	20.69	29.74	31.42	24.01	30.44
C	0.04	-	-	-	-	-	-	-	-	-
di (wo	-	6.34	4.02	5.09	4.90	2.78	1.37	10.98	6.04	9.44
di (en	-	3.32	2.03	2.62	2.84	1.10	0.73	6.37	2.83	6.60
di (fs	-	2.84	1.90	2.33	1.83	1.72	0.59	4.09	3.15	2.05
hy (en	2.07	9.60	7.86	9.57	9.01	3.81	7.91	10.45	7.65	12.65
hy (fs	1.63	8.19	7.38	8.51	5.80	5.99	6.34	6.71	8.50	3.93
ol (fo	-	-	-	-	-	-	-	-	-	6.31
ol (fa	-	-	-	-	-	-	-	-	-	2.16
il	0.61	1.46	1.29	1.01	0.89	1.54	0.99	1.52	2.96	2.17
mt	1.30	3.31	3.20	2.97	2.89	2.65	2.97	3.35	4.47	3.84
ap	0.07	0.19	0.17	0.28	0.31	0.43	0.33	0.26	0.45	0.26
Volume percent phenocrysts										
Plagioclase	20	26	27	29	23	14	26	3	<1	-
Olivine	-	2	<1	1	-	-	-	-	-	10
Orthopyroxene	<1	1	1	5	3	1	2	-	-	-
Clinopyroxene	<1	<1	-	4	11	2	10	3	<1	-
Fe/Ti oxides	1	-	-	1	1	1	2	-	-	-
Amphibole	2	-	-	-	-	-	-	-	-	-
Quartz	13	-	-	-	-	-	-	-	-	-
Total	36	29	28	40	38	18	40	6	ca.1	10

1. Rhyolite[b], Sulu Range (51NG3032A)[c].
2. Low-magnesia quartz-tholeiite basalt, Ulawun (Johnson, Davies, & White, 1972; 51NG0156).
3. Low-silica andesite, Likuruanga (53NG0852A).
4. Low-silica andesite, Mataleloch, Cape Hoskins area (Blake & Ewart, 1974; their sample 77).
5. High-silica andesite, Dufaure (51NG2685B).
6. Dacite, Lolobau (52NG1049).
7. High-silica andesite, Bangum (51NG2708).
8. Low-magnesia quartz-tholeiite basalt, Dakataua (Lowder & Carmichael, 1970; their sample 311).
9. Low-silica andesite Garove (48NG0537).
10. High-magnesia olivine-tholeiite basalt, Mundua Group (48NG0582).

a,b. See footnotes for Table 3.

c. BMR sample numbers shown in parentheses for samples 1-3, 5-7, 9, and 10.

(4) Garove. Compared with the other eastern rocks, those of Garove are especially high in MnO (Fig. 27). In addition, they have lower K_2O contents than other zone H rocks with the same silica content (Fig. 15), and they include dacites and rhyolites, which are absent from the other zone H volcanoes (see p. 29).

Attention is drawn to these volcanoes because they clearly illustrate chemical individuality. They are not, however, the only south Bismarck Sea volcanoes that show this feature, and the point made on page 39 is worth re-emphasizing - that the analysed rocks of each volcano are in different degrees chemically distinct from those of other volcanoes in the same zone, and in the same arc.

General theories for the origin of the rocks in both the western and eastern arcs must therefore explain, not only the regional chemical variations, but also the chemical independence of volcanoes. In addition, these theories, in both arcs, must account for (1) the distribution pattern of the volcanoes in relation to the geometry of the late Cainozoic plate boundaries (p. 17), (2) the relative abundances of rock types (p. 27), (3) stratigraphic differences in rock type (p. 29), and (4) differences in petrography (p. 30). These problems are dealt with in the last sections of the Report. In the following section the compositions of the rocks of the south Bismarck Sea are compared with those of island-arc-type rocks from other late Cainozoic volcanic provinces in Papua New Guinea.

COMPARISONS WITH OTHER VOLCANIC ROCKS FROM PAPUA NEW GUINEA

Three volcanic rock associations

Using major-element chemical analyses of 868 late Cainozoic volcanic rocks, including those discussed in this Report, Johnson, Mackenzie & Smith (in prep.a) identified seven island-arc-

type volcanic provinces in Papua New Guinea, and classified them into three magmatic associations: the rocks of the eastern and western arcs were grouped into a 'SBS' (south Bismarck Sea) association; those of mainland Papua New Guinea (Highlands and eastern Papua, excluding the D'Entrecasteaux Islands), the Rabaul area, and Bougainville Island were combined as a 'MRB' association; and rocks from the Tabar-to-Feni Islands were grouped in a 'TLTF' association (see p. 5 and Fig. 1).

From a consideration of several types of chemical variation diagrams, Johnson et al. (in prep. a) concluded that the three above associations could be effectively distinguished using the normative mineralogical parameters shown in Figure 35. The principal features of the SBS association shown in this diagram are: (1) the absence of alkaline (nepheline-normative) rocks (which are commonly found in the MRB and, especially, TLTF associations); (2) compared with hypersthene-normative rocks from the MRB association with the same DI (i.e., the same amount of salic normative minerals), the SBS rocks are much more strongly silica-oversaturated (corresponding to lower alkali contents in rocks with the same silica content).

Q-mode factor analysis was also performed on the 868 chemical analyses. Three factors were obtained whose loadings are similar to those reported above (p. 64) for the SBS rocks alone. On a triangular diagram showing factor loadings, distance from the factor 1 apex along the factor 1-2 join was shown to be equivalent to increasing content of salic normative minerals (cf. the differentiation index, DI, of Fig. 35), and factor 3 was dominated by the oxides of the three major incompatible elements P, Ti, and K. Figure 36, a plot of the oxide abundances of these three elements against differentiation index, illustrates a further important characteristic of the SBS rocks - that they have much lower incompatible-element abundances than rocks with the same DI from the MRB and TLTF associations.

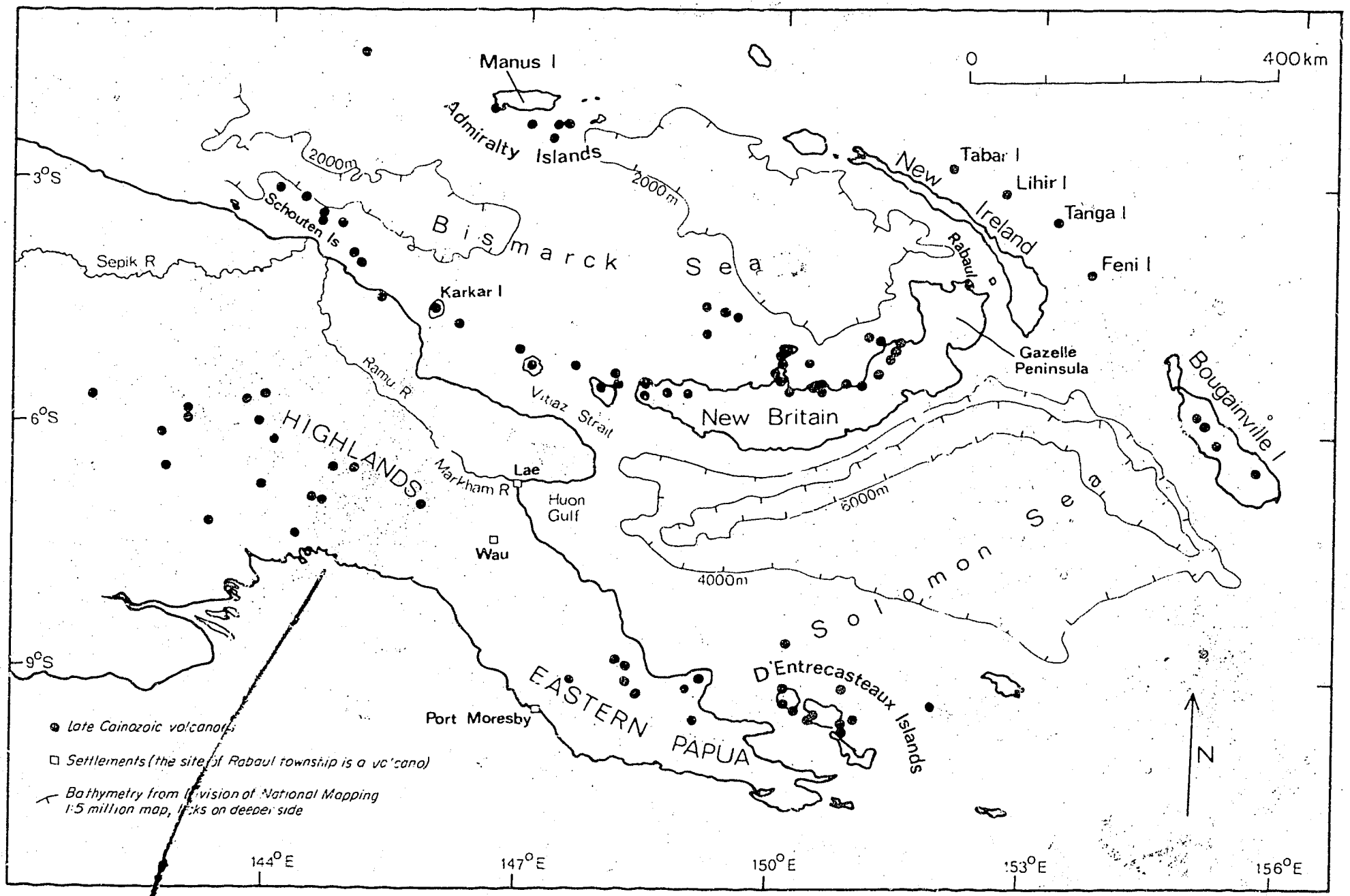

Fig. 1. Principal late Cainozoic volcanoes of Papua New Guinea.

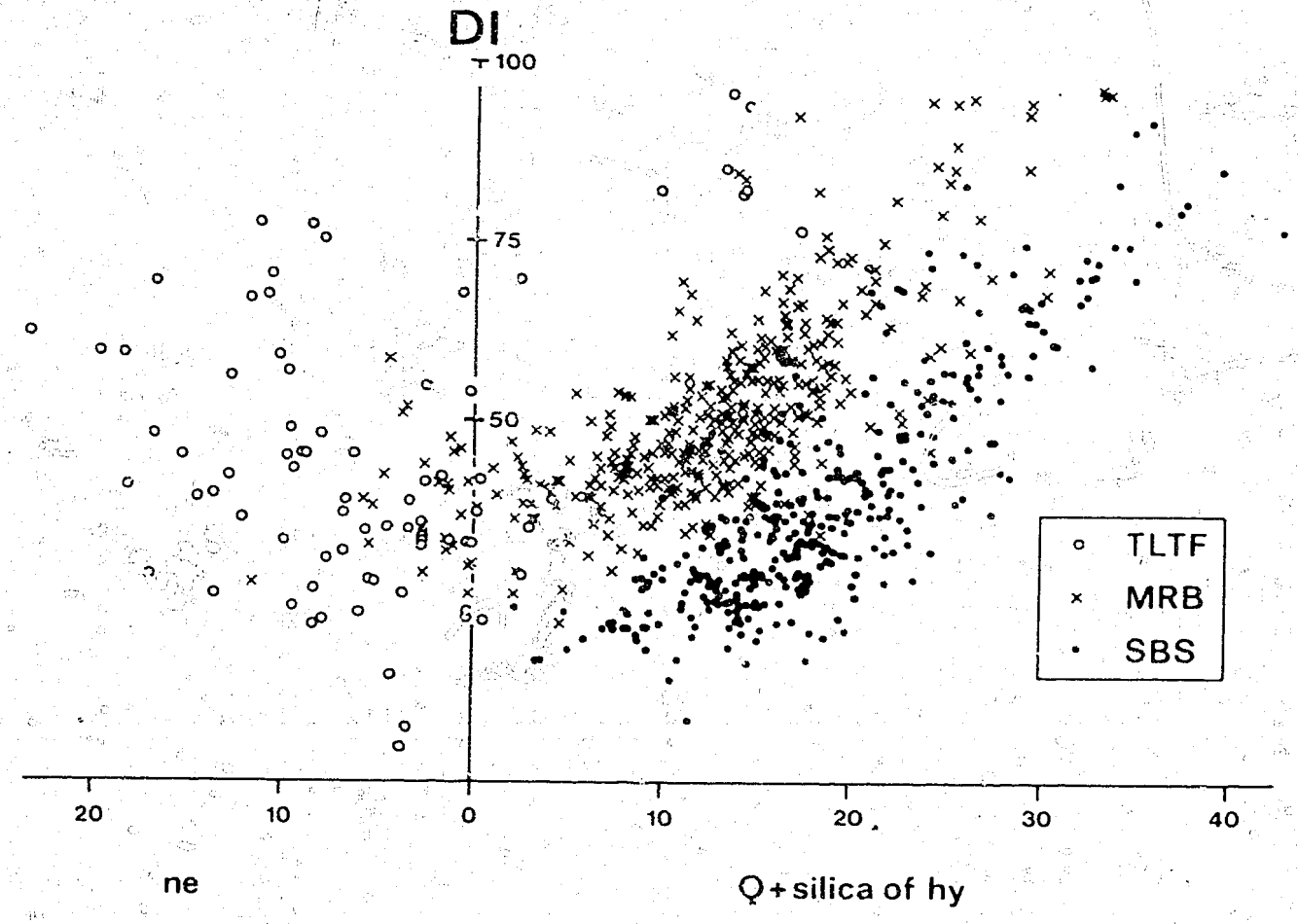

Fig. 35. Differentiation index (DI, Thornton & Tuttle, 1960) v. normative nepheline (ne) and normative quartz (Q) plus the silica of normative hypersthene (hy). See text for explanation of TLTF, MRB, and SBS rock groups. From Johnson et al. (in prep. a).

P/A/548

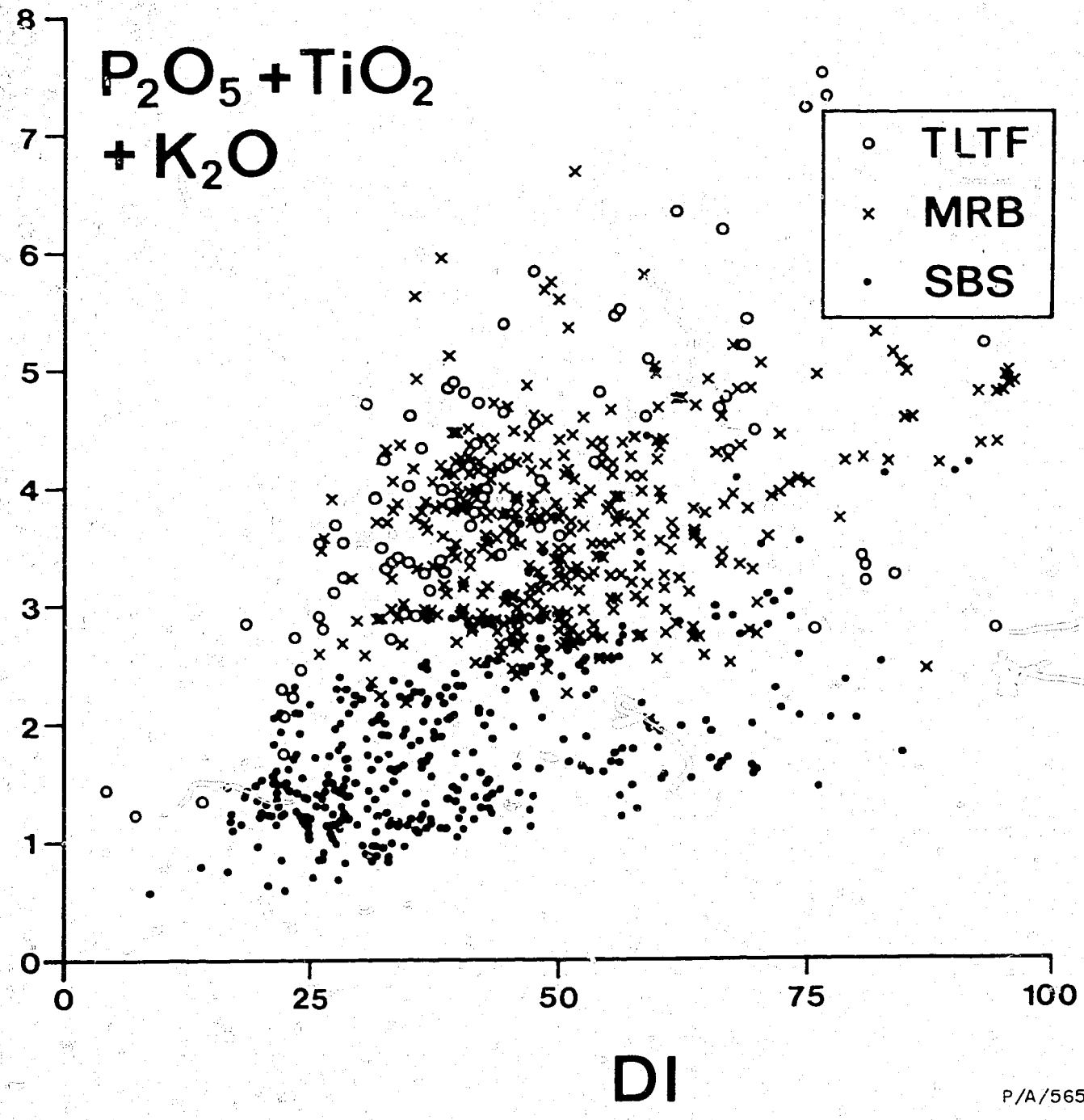

Fig. 36. $P_2O_5 + TiO_2 + K_2O$ v. differentiation index (DI). See text for explanation of TLTF, MRB, and SBS rock groups. From Johnson et al. (in prep.a).

Johnson et al. (in prep. a) also examined the chemical differences between the three associations in standard variation diagrams which have been used extensively in the literature - including the FMA diagram, shown in Figure 37. In this diagram there is considerable overlap of the SBS group with the MRB and TLTF groups, but the samples richest in iron are from the SBS group.

In the identification of the three associations, note that rocks from the Rabaul area (Fig. 1) were not included in the SBS group, even though (1) the Rabaul complex is associated with the same plate boundary as the SBS volcanoes in the eastern arc (Fig. 3), and (2) the Rabaul rocks are chemically similar to the rocks from zone H, in the eastern arc (see below). Nevertheless, the compositions of the Rabaul rocks do not reflect the systematic pattern of variation across the eastern arc as the depth to the New Britain Benioff zone increases (see below), and, as the Rabaul complex is also geographically distinct, it is regarded as a separate volcanic province. Moreover, by including the Rabaul rocks in the MRB group a greater polarization of the SBS and MRB groups is obtained.

Rabaul volcanic complex

The volcanic complex occupied by the township of Rabaul is at the northeastern tip of New Britain, and is a breached double caldera rimmed by older and younger volcanoes (Fisher, 1939; Heming, 1974). In the eastern part of the caldera is Tavurvur volcano, which last erupted in 1941-43 (Fisher, 1976). Tavurvur had previously been active in 1937, when complementary activity built up a new cone - Vulcan - in the western part of the caldera (Fisher, 1939). The caldera is seismically active (Myers, 1976).

Major-element chemical analyses of 27 volcanic rocks from Rabaul were presented by Heming & Carmichael (1973), Heming (1974), and Matsumoto (1976). Eight samples were of water-rich

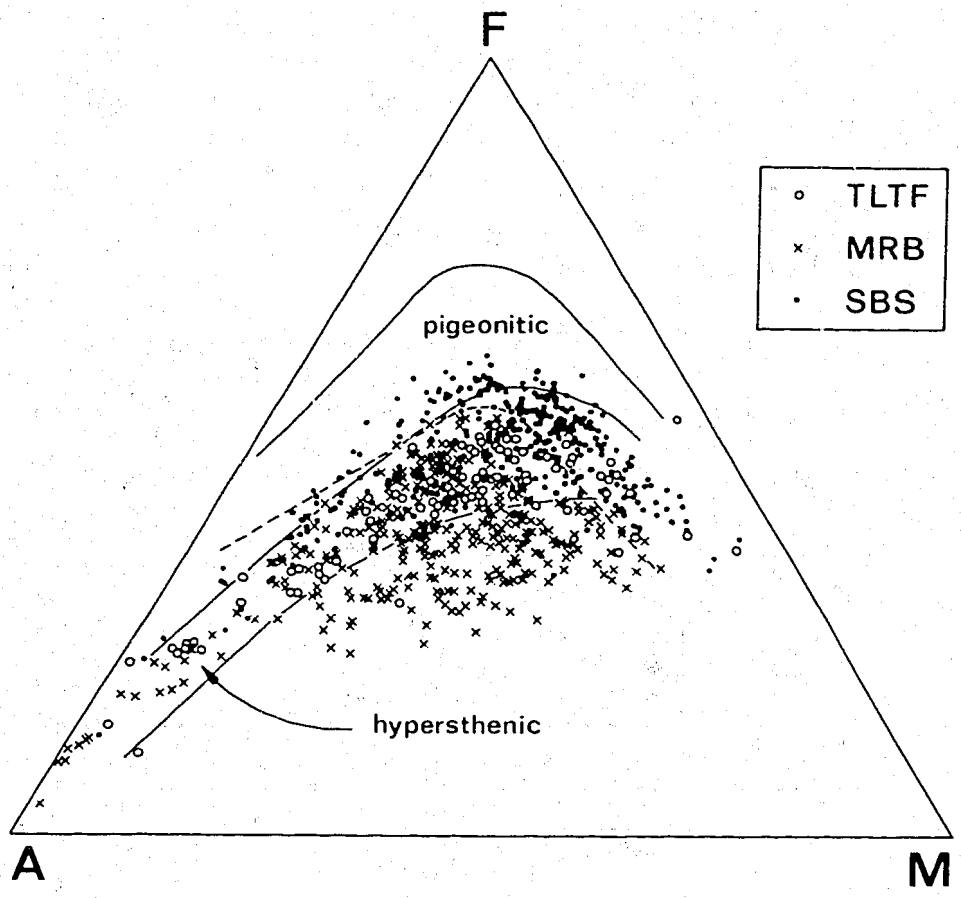

P/A/546

Fig. 37: Relations between F (FeO + Fe_2O_3), M (MgO), and A (Na_2O + K_2O), where the proportion of iron oxides is given by the formula Fe_2O_3/total Fe as Fe_2O_3 = 0.2 See text for explanation of TLTF, MRB, and SBS rock groups. From Johnson et al. (in prep.a).

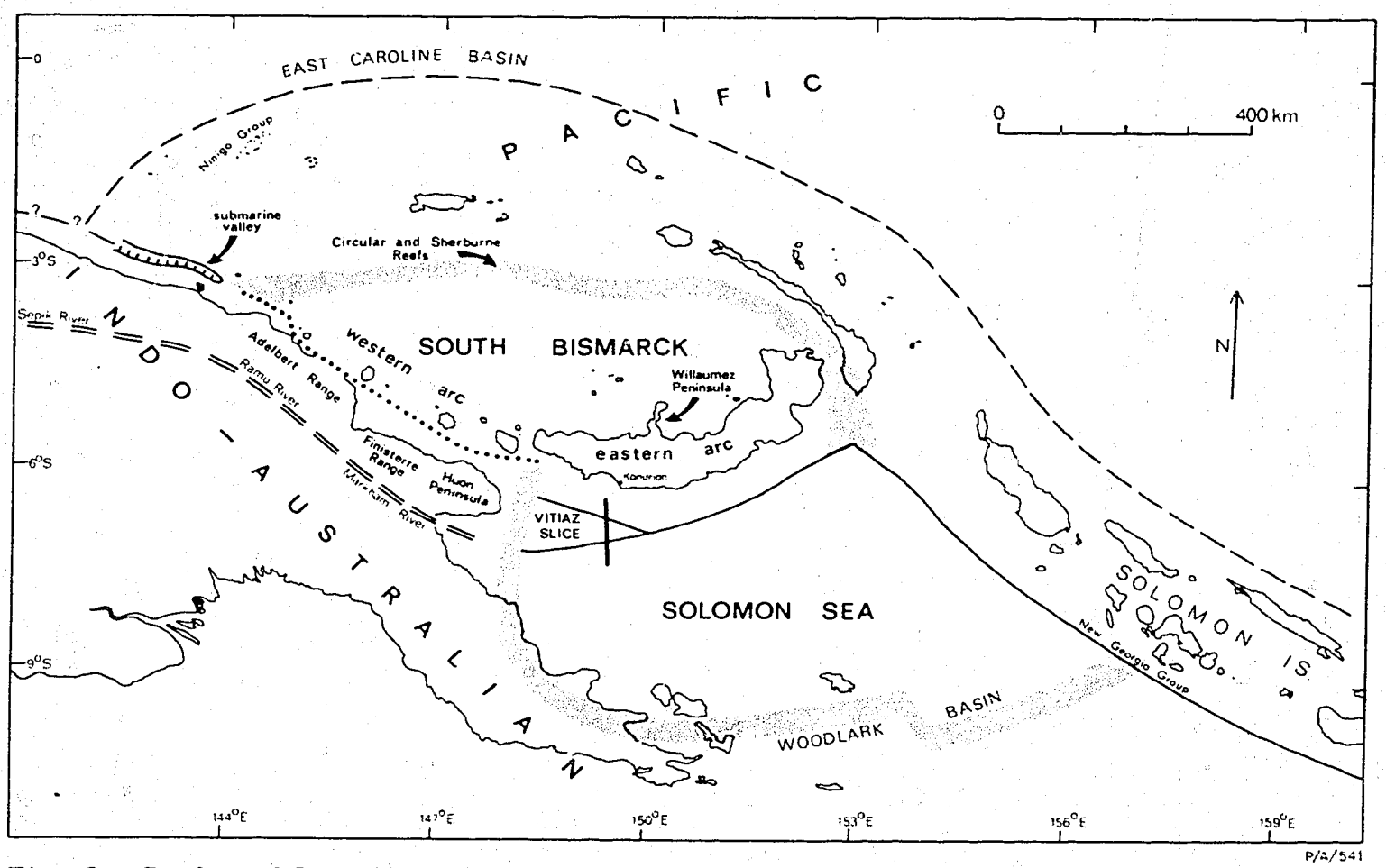

Fig. 3. Preferred locations of plate boundaries and some related tectonic features in Papua New Guinea and part of the Solomon Islands, in part adapted from Johnson & Molnar (1972), Curtis (1973b), Krause (1973), and Luyendyk et al. (1973). Solid lines are axes of submarine trenches. Stippling indicates currently active plate boundaries which are zones of seismicity that cannot be accurately portrayed by single lines. Single-dash line represents a boundary (or boundaries) which may have been more active during the earlier part of the late Cainozoic than at the present day; Johnson & Molnar (1972) and Curtis (1973) considered that this line, or part of it, represents the northern margin of a third minor plate - cf. Fig. 2. Double-dash line represents an old plate boundary that was destroyed by collision of the Australian continent (part of the Indo-Australian plate) with an Adelbert-Huon island arc (see text and Fig. 9 for details). Dotted line is a strike-line for the upper surface of the proposed lithospheric slab which dips steeply northwards beneath the western arc (see text and Fig. 39 for details). Thick line running southwards from near Kandrian is the ship's track of the seismic reflection profile given in Figure 8.

pumices which may have been chemically modified by ground-water leaching. Using the Irvine & Baragar (1971) oxidation transform (see p. 39) the 27 analyses have been recalculated without volatiles; by adopting the classification scheme on page 25 , they correspond with a range of compositions from basalt (both olivine-normative and quartz-normative) through andesite and dacite, to rhyolite (one hydrated pumice). Heming (1974) noted the absence of rocks with SiO_2 contents in the range 55.5-60 percent, and drew attention to similar compositional gaps reported from Talasea (Lowder & Carmichael, 1970) and from the Tonga-Kermadec island-arc (Brothers, 1970). This suggestion of a bimodal suite at Rabaul is consistent with the findings discussed above (p. 28) with reference to curve II in Figure 11.

The Rabaul analyses were plotted (though not illustrated in this Report) in Figures 15-24, 26, and 27 to compare them with the analyses of rocks with the same silica content from the eastern arc. The rock compositions resemble those of zone H and to a lesser extent those of the northern part of zone G.

K_2O and K_2O/Na_2O values in the Rabaul rocks are high throughout the basalt-to-rhyolite range; in the andesites they are similar to values in the zone H andesites, but in the basalts they are higher than in many basalts from the Mundua group and Garove Island (zone H), and K_2O contents in the dacites and rhyolites are higher than in those of Garove. Na_2O contents resemble those of rocks from the more northerly zones in the eastern arc; some Rabaul pumices are relatively Na_2O-poor, perhaps because of post-emplacement leaching. $Na_2O+K_2O:SiO_2$ relationships in the Rabaul rocks are the same as those for rocks from zone H, except for two alkali-deficient pumices. Rabaul TiO_2 contents are mostly in the range 0.8-1 percent, and typical of those in rocks from the northern part of zone G and

from zone H. P_2O_5 values are also similar*, but none is as high as the maximum P_2O_5 value found in a rock from zone H. CaO contents in the Rabaul rocks are low and identical with those of zone H. Al_2O_3, MgO, Fe_2O_3+FeO, and MnO values are all similar to those for rocks from the northern zones G and H, but as discussed above these oxides are poor discriminants for the rocks of all the eastern zones. Some Rabaul MnO values exceed the maximum values in the eastern arc, in rocks from Garove Island.

Despite many similarities between the compositions of rocks from zone H and Rabaul, there is no correspondence with depths to the New Britain Benioff zone: the depth range of earthquakes beneath zone H exceeds 300 km (Fig. 4), but, as shown in Figure A of Appendix 1, the Benioff zone beneath Rabaul is less than 300 km deep.

ISLAND-ARC MAGMA GENESIS

Role of water, subducted sediments, and radiogenically enriched crust

Explanations for the origin of island-arc-type magmas are numerous - Oversby & Ewart (1972), for example, listed eight different modern hypotheses. However, according to plate theory, the lithospheric slabs that move across ocean basins are subducted beneath island arcs, and the downgoing slabs carry hydrated oceanic crust, or wet sediments, to levels where water is liberated and magmas are

---

*Note that the P_2O_5 values reported by Matsumoto (1976) for six rocks are in the range 0.10-0.14 percent, whereas those given by Heming & Carmichael (1973) and Heming (1974) for 21 rocks are, with two exceptions, consisently higher (range 0.19-0.37). The range of higher values is more typical of rocks from the northern part of zone G and from zone H.

generated under hydrous conditions (e.g., McBirney, 1969; Wyllie, 1971). (These conditions contrast with those at mid-oceanic ridges where new lithosphere is created and plates separate, and where magma is generated under essentially anhydrous, or low pH_2O, conditions, e.g., Green, 1971.)

Because both the western and eastern arcs overlie regions where plates may have underthrust one another (see above), most of the magmas in both arcs are thought to have been generated under conditions controlled or influenced by significant quantities of water derived from the upper parts of the Indo-Australian and Solomon Sea plates. The explosive character of the volcanoes, and the presence of amphibole, amphibole relics, and biotite in the rocks, are consistent with this interpretation.

At present, the balance of evidence from trace-element and isotope studies on other island-arc rocks appears to be against (e.g., Taylor et al., 1969; Oversby & Ewart, 1972; Church, 1973; Gill, 1974), rather than for (e.g., Tatsumoto, 1969; Armstrong & Cooper, 1971), the incorporation of large quantities of partially melted subducted sediments in island-arc magmas. It is assumed here, therefore, that water is provided from oceanic crust consisting of '...a heterogeneous mixture of anhydrous mafic rocks, amphibolites, greenschists, and included blocks of serpentinite...' (Nicholls & Ringwood, 1972, p. 245; after Cann, 1970). The crustal rocks that have underthrust the western and eastern arcs may be similar to basaltic rocks that cap the Papuan Ultramafic Belt, an obducted slab of oceanic crust and upper mantle derived from the Solomon Sea area (Davies, 1968, 1971); the basaltic rocks are '...uralitized, chloritized, and epidotized to some extent, and some are completely altered to epidote' (Davies, 1968, p. 216).

Twenty-four rocks from the western and eastern arcs have initial Sr^{87}/Sr^{86} ratios in the range 0.7034-0.7038 (Peterman, Lowder, & Carmichael, 1970; Page & Johnson, 1974), except for an

andesite from Karkar which had a value of 0.7041. Peterman & Heming (1974) reported Sr^{87}/Sr^{86} values in the range 0.7035-0.7040 (mean = 0.7038) for eight rocks from the Rabaul area (Fig. 1). These data indicate that (1) significant quantities of old radiogenically enriched crustal material have not been incorporated into the magmas, nor have the magmas been derived from such material, and (2) the source region of the magmas is essentially isotopically homogeneous, with the exception of the region beneath Karkar.

Experimental petrology

The most important contributions to studies of island-arc petrogenesis have been from the field of experimental petrology. The results of experiments under hydrous conditions have been reported in numerous papers during recent years, and there is general agreement that these results are applicable to an understanding of the origin of magmas erupted in island arcs. Nevertheless, there has been, and still is, considerable controversy over the results of some critical experiments, as discussed briefly below. Four different laboratories have contributed relevant experimental results:

1. Australian National University (ANU), Canberra (D.H. Green, 1972, 1973a, b, 1976; T.H. Green, 1972; Green & Ringwood, 1968, 1972; Nicholls, 1974; Nicholls & Ringwood, 1972, 1973, 1974).

2. Carnegie Institution and Pennsylvania State University, Washington (Allen et al., 1972; Eggler, 1972, 1974; Eggler & Burnham, 1973; Holloway & Burnham, 1972; Kushiro, 1969, 1972, 1974; Kushiro et al., 1968, 1972; Mysen, 1973, 1975; Mysen & Kushiro, 1974; Mysen & Boettcher, 1975a, b, 1976).

3. University of Edinburgh (Cawthorn, 1976; Cawthorn et al., 1973a, b; Cawthorn & O'Hara, 1976);

4. University of Chicago (Huang & Wyllie, 1973, 1975; Lambert & Wyllie, 1968, 1970; Maaløe & Wyllie, 1975; Milhollen et al., 1974; Nehru & Wyllie, 1975; Stern, 1974; Stern & Wyllie, 1973a, b);

Results from several of these studies have been used in support of the proposal (cf. Kuno, 1959) that the volcanic magmas of island arcs are direct partial melts of the basaltic crustal portions of downgoing slabs (e.g., Green & Ringwood, 1968; Holloway & Burnham, 1972). However, several criticisms can be levelled at this proposal. At depths greater than about 100 km the hydrated basaltic crust will be converted to eclogite (e.g., Ringwood, 1974), and direct partial melts should therefore be in equilibrium with garnet, which preferentially incorporates the heavy rare-earth elements (REE); but island-arc-type magmas are not strongly depleted in heavy REE, and therefore cannot have been in equilibrium with an eclogitic source (see, for example, Gill, 1974, for these and other geochemical arguments against a direct slab origin). In addition, basaltic magmas erupted above Benioff zones at depths less than about 100 km can be generated from the downgoing basaltic crust only by complete or near-complete melting (e.g., Holloway & Burnham, 1972); however, it is doubtful (1) if the high temperatures (greater than about 1100°C) required for complete anatexis are reached at these depths (see, for example, the review of thermal regimes in island arcs by Wyllie, 1973), and (2) whether complete anatexis can ever take place without refractory phases settling out during melting (e.g., Green & Ringwood, 1967; Green, 1972). Moreover, total melting will completely destroy the subducted oceanic crust, which cannot therefore be the same source of basaltic magmas erupted over the deeper parts of Benioff zones. Finally, if the different types of basalt found at convergent plate boundaries are all derived by complete melting of oceanic crust, it is difficult to envisage a similarly wide range of basaltic or eclogitic compositions for the crust, and impossible to account for the origin of alkali basalts by complete melting of an oceanic tholeiite source (e.g., Cawthorn, 1976).

Many investigators now favour the generation of primary island-arc-type magmas not in the downgoing slabs but in the wedge of upper mantle peridotite above the slabs where melting is believed to take place by the influx of water from the underlying subducted oceanic crust. Experiments aimed at duplicating these conditions have been the cause of a controversy.

Several investigators of the Washington school (in particular Kushiro and Mysen) claimed that the liquids derived from experiments on peridotite-plus-water compositions at mantle pressures (up to 30 kb) were rich in silica (about 60% or more). These results were assumed to verify earlier speculations that the andesites and dacites of island-arcs are derived from the mantle (Poldervaart, 1955; O'Hara, 1965). Other investigators, however, have at different times posed the question: do these experimentally derived, high-silica compositions represent liquids in equilibrium with the liquidus minerals under the stated conditions of the experiment? Experimental petrologists from the three other schools have, as a result of their own experiments, stated that glasses quenched from these liquids are not in equilibrium with the liquidus minerals, as they appear to have been modified by crystallization of low-temperature minerals, or else equilibrium was never achieved because of the unsuitable grainsize of the starting materials (e.g., Nicholls & Ringwood, 1973,1974; Cawthorn et al., 1973a; Nehru & Wyllie, 1975). Loss of iron from the experimental charge into the platinum capsules during long runs, and the difficulties of analysing pools of glass with the electron microprobe, provide additional problems in the interpretation of results (e.g., Merrill & Wyllie, 1973). In spite of these problems members of the Washington school have continued to claim the validity of their experimental results (e.g., Mysen, 1975).

As a non-specialist, I am not qualified to judge this issue. However, as the Washington experiments have been critized by three independent schools, the concept that the high-silica

rocks of island arcs are derived from the mantle is not emphasized in the following sections, and the widely accepted view that these rocks are derived by crystal fractionation of primary basic magmas is favoured. Another mode of origin for the dacites and rhyolites is also discussed in a later section.

Recognition of primary magmas

Derivation of primary magmas from upper mantle peridotite requires that they must have been in equilibrium with upper mantle olivine and orthopyroxene (Green & Ringwood, 1967). Conversely, the liquids should have olivine and orthopyroxene on or close to their liquidi at upper mantle pressures or, if olivine is not a liquidus phase, it should be when only a small amount of olivine is added to the experimental charge (Nicholls, 1974; see also the discussion by Mysen & Kushiro, 1974, and Nicholls & Ringwood, 1974).

Green (1971) suggested that rocks having $100Mg/(Mg + Fe^{2+})$ values (i.e., 'Mg-numbers' in which Fe^{2+} is the atomic ferrous iron content shown in the rock analysis) in the range 63-73 could have been in equilibrium with mantle olivine of $100Mg/(Mg + Fe^{2+}) = 87-92$. Rocks with Mg-numbers much less than 63 were considered more likely to represent magmas which fractionated on their way to the surface. In rocks with Mg-numbers greater than 63, the amount of MgO (weight percent) is more or less equal to, or greater than, that of FeO (weight percent).

The criteria suggested by Green (1971) for the recognition of possible primary magmas partly depend on the results of iron/magnesium partitioning experiments performed by Roeder & Emslie (1970), who showed that at 1 atmosphere the partition coefficient

$$K_D = \frac{(X_{FeO}^{Olivine})}{(X_{FeO}^{Liquid})} \cdot \frac{(X_{MgO}^{Liquid})}{(X_{MgO}^{Olivine})}$$

is 0.3 (0.29-0.34 taking into account analytical error in the determination of olivine compositions). Green used this value of 0.3 to test for magmas that could have been in equilibrium with mantle minerals (e.g., Green, 1976). K_D values are, however, functions of parameters such as temperature, pressure, water content, oxygen fugacity, etc. Roeder & Emslie (1970), for example, reported a range of K_D values between 0.26 and 0.36 for 27 experiments under different conditions. Nicholls (1974) also reporded K_D values of 0.33-0.50 for hydrous experiments, and Mysen (1975) suggested that the ranges might be even greater, as his experiments with oxygen fugacity controlled by the magnetite-hematite buffer showed that 'equilibrium' liquids (the claim of equilibrium is disputed) were strongly depleted in magnesium. (Mysen & Kushiro (1974) used these results in support of the concept that andesites (low in MgO) are derived from the mantle; Nicholls & Ringwood (1974), however, argued that, irrespective of the correctness of the experimental method, the strongly oxidizing conditions determined by the magnetite-hematite buffer were unlikely to apply in the upper mantle, and therefore that Mysen & Kushiro's (1974) concept was unacceptable.)

It seems therefore that Mg-numbers in the range 63-73 cannot be used as precise indicators of equilibrium with mantle minerals. Although in the following discussion attention will be drawn to rocks whose Mg-numbers fall within the range 63-73, this does not necesarily imply that rocks with Mg-numbers below 63 cannot have been produced directly from the upper mantle.

It is not known if any of the erupted rocks of the south Bismarck Sea volcanoes have the exact compositions of primary magmas. Some of the primary magmas may have been picritic (cf. Stanton & Bell, 1969); others may even have been alkaline*. However, in the absence of definite evidence to the contrary, it will be assumed that the primary magmas were all hypersthene-normative, and that the most basic rocks in most of the volcanic zones are the nearest approximations to the compositions of the primary magmas.

---

*Arculus & Curran (1972) and Sigurdsson et al. (1972), for example, suggested that the parental magmas of hypersthene-normative island-arc rocks from the Lesser Antilles were strongly nepheline-normative.

Temperature distributions in the mantle

A wide range of conditions determines the extent of partial melting in the upper mantle and, therefore, the compositions of the resulting primary magmas. One of the most important conditions is the distribution of temperatures.

Recent investigations into the thermal regimes beneath island arcs have shown that many factors influence the pattern of isotherms, but the relative importance of these factors is not well known. However, there is general agreement that the downgoing slabs of island arcs are colder than the mantle material through which they descend, and that they are capable of extracting heat from the surrounding mantle (e.g., Oxburgh & Turcotte, 1970; Minear & Toksöz, 1970a, b; Griggs, 1972; Le Pichon, Francheteau, & Bonnin, 1973; Toksöz, Sleep, & Smith, 1973). Slowly descending slabs are likely to heat up more readily than quickly descending ones with the same composition and thickness. Thus, rates of slab descent will govern the thermal regimes of the slabs, and of those parts of the upper mantle above the slabs where primary magmas are believed to form. In addition, if intermediate and deep-focus earthquakes in Benioff zones are due to mechanical failure in the cold interiors of the downgoing slabs, the deeper earthquakes will take place more readily in those parts of the slabs which have remained colder to greater depths - that is, in slabs which have been subducted more rapidly (Isacks, Oliver & Sykes, 1968).

Rates of slab descent may be a primary control on the distribution of isotherms beneath island arcs, but other factors may also have an influence - for example, lateral changes in the thickness of the slab, lateral differences in thermal properties of the slab and overlying mantle, and changes in the positions of instantaneous poles of rotation throughout geological time. The possible interactions between all these variables are so complex that they cannot be elucidated satisfactorily at present, and petrological interpretations for specific island arcs, such as those given in the following sections, must therefore remain largely

speculative. However, in the following geodynamic interpretations, rates of slab descent are considered to be of primary importance, and the effect of all other unstated factors is assumed to be constant.

ANU model for island-arc petrogenesis

Despite the considerable interest in island-arc petrology by the four schools of experimental petrology listed above, only the group at the Australian National University (ANU) has attempted to integrate experimental results into general island-arc models using results from the fields of isotope and trace-element geochemistry, geophysics (especially studies of thermal regimes), and geology. The latest version of one widely publicized ANU model was described by Ringwood (1974, 1975) and Nicholls (1974), and its essential features are shown in Figure 38.

Ringwood and Nicholls believed that the hypersthene-normative rocks of island-arc volcanoes can be grouped into tholeiitic and calcalkaline associations. They also accepted the claim of Jakeš & White (1969), Jakeš & Gill (1970), and Gill (1970) that the tholeiitic magmas are produced during the early stages of island-arc development, in contrast to the calcalkaline ones which form later - during a more evolved stage.

In the tholeiitic stage (Fig. 38 upper) the amphibolite of subducted oceanic crust reaches depths of 80-100 km, where temperatures are judged to be about, or less than, 650°C. The amphibolite dehydrates (subsolidus) to form eclogite, and releases water into the overlying peridotite, parts of which rise as diapirs to depths where partial melting under hydrous conditions generates tholeiitic magmas close to silica saturation. During their ascent to the surface, these tholeiitic magmas fractionate olivine and, at lower pressures, pyroxene and amphibole, producing a spectrum of compositions from quartz tholeiite to more strongly oversaturated compositions.

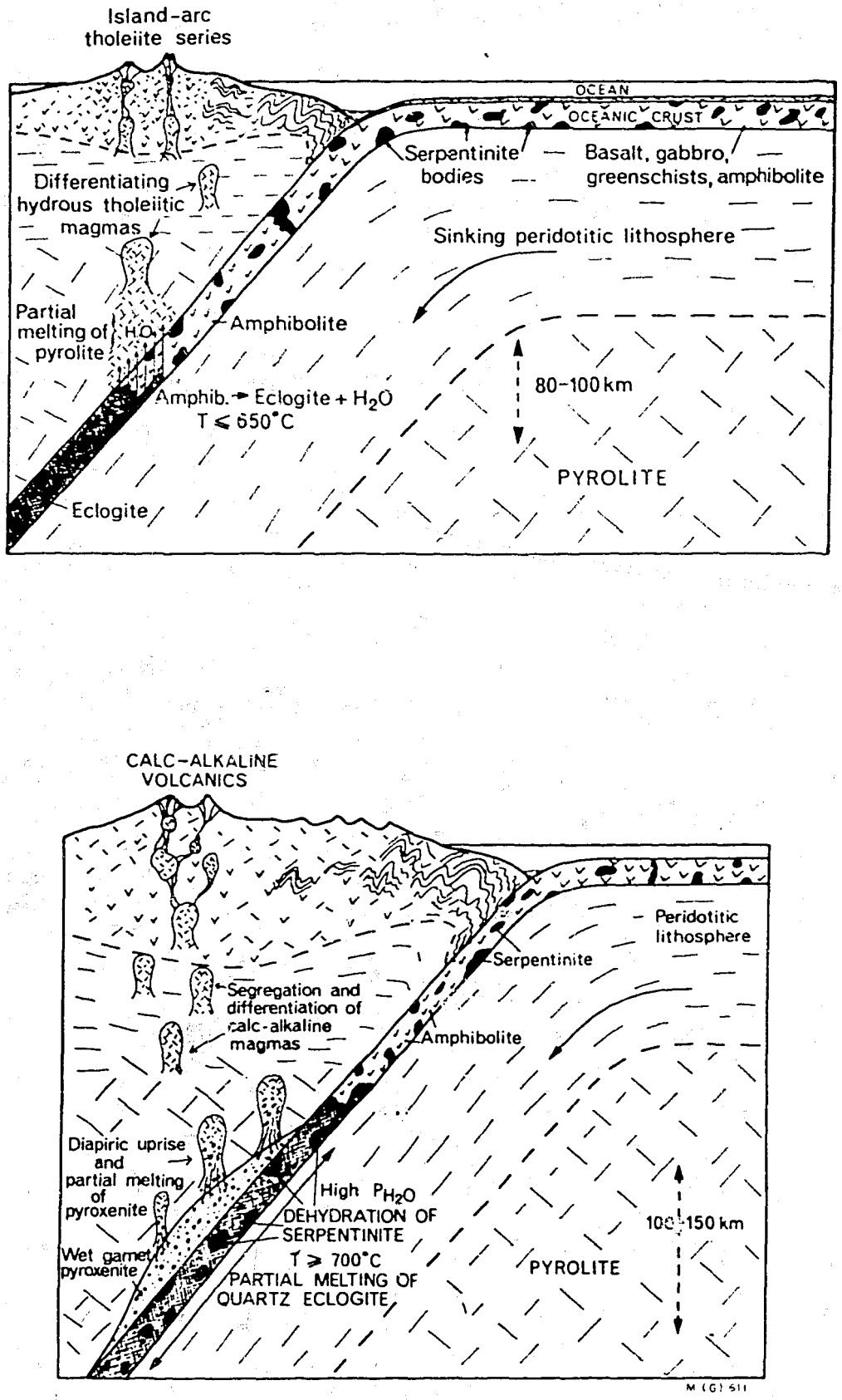

Fig. 38. Idealized cross-sections showing generation of island-arc-type magmas by the scheme of Nicholls & Ringwood (1972, 1973). From Ringwood (1974), and reproduced with the permission of the Geological Society of London. Upper: 'Early phase of development of an island arc involving dehydration of amphibolite in subducted oceanic crust, introduction of water into the overlying wedge, and generation of "island-arc tholeiite" igneous series'. Lower: 'Later phase of island-arc development involving partial melting of subducted oceanic crust, and reaction of liquids with mantle above Benioff zone, leading to diapiric uprise and formation of calcalkaline-type magmas'.

In the calcalkaline stage (Fig. 38 lower) hydrated oceanic crust descends below about 100 km, and is converted to quartz eclogite; a high water-vapour pressure is maintained in the downgoing slab by the breakdown of hydrous minerals such as serpentine, talc, micas, epidote, and, at greater depths, high-pressure hydroxylated magnesian silicates. Below 100 km, temperatures in the slab are estimated to exceed 700°C, and the quartz eclogite partially melts under hydrous conditions. These slab melts are K_2O/Na_2O-rich and silica-rich and they rise into the upper mantle, where they react with the peridotite to form rocks which have been called 'wet garnet pyroxenite' (Nicholls & Ringwood, 1973), 'peridotite-pyroxenite' (Nicholls, 1974), olivine-garnet pyroxenite (Ringwood, 1975), and 'modified pyrolite' (Ringwood, 1976). Diapirs are formed, and the 'pyroxenite' partially melts to form andesites and, with higher degrees of partial melting at shallower depths, basalts which are close to silica saturation and which may subsequently fractionate.

The broad features of this model are therefore (1) that the composition of the upper mantle giving rise to the primary magmas above downgoing slabs is essentially homogeneous before subduction, and (2) that the variations in volcanic rock compositions across island arcs - particularly in K_2O/SiO_2 - are due to chemical interactions between the mantle, and the slab-derived siliceous melts, whose compositions and volumes are functions of depth to the Benioff zone*.

The validity of this model is accepted by Green (1976), also of the ANU school. Green (1973a, 1976) has, however, proposed an alternative but much less developed hypothesis in which LIL (large-ion lithophile) element and isotope variations in island arcs

---

*Wilson (1954) was the first to speculate on the interaction between slab-derived siliceous melts and the upper mantle peridotite beneath island arcs (quoted in Ringwood, 1975).

are accounted for by differences in source peridotite compositions before subduction (see p. 97). Both ANU models are tested in the following sections, and concepts in each of them are found to be useful. However, note that the generalized time relations shown in Figure 38 have very little application to either the western or eastern arcs, in both of which the 'tholeiitic' and the 'calc-alkaline' volcanism are essentially contemporaneous (p. 22), and in which the 'tholeiitic' and 'calcalkaline' groupings are inappropriate (p. 65).

GENESIS OF PRIMARY MAGMAS IN THE EASTERN ARC

Introduction

The volcanoes of the eastern arc are associated with the more familiar type of island arc where one plate underthrusts another in a direction more or less orthogonal to the plate boundary, and where the compositions of the volcanic rocks change in the same direction. On the other hand, in the western arc, pronounced changes in chemistry (and possibly rates of convergence) along the length of the arc imply a further degree of complexity to the discussion of plate movements and the formation of primary magmas, so petrogenesis in the eastern arc is discussed first.

In New Britain, where the South Bismarck plate is believed to override the subducted Solomon Sea plate (see p. 9), the volcanoes are not arranged in a simple chain parallel to the plate boundary; instead, as described above (p.19) they are mostly distributed along three well defined belts: (1) along the north coast of New Britain between Lolobau and Likuruanga in the east and Dufaure and Wago in the west - that is, zones E and F (excluding Krummel, Fig. 10), (2) the north-south chain of volcanoes making up Willaumez Peninsula - zone G (and Krummel), and (3) the Witu

Islands - zone H. The explanation adopted here for this curious distribution is that the relative motion between the downgoing lithosphere and the overlying South Bismarck plate is different beneath each of the three structural groups of volcanoes. These differences will be described in the following sections with reference to Figures 39 and 40.

Zones E and F

Beneath the north coast volcanoes at the present day, the Solomon Sea plate probably carries hydrated oceanic crust into the upper mantle (Fig. 39 and 40B). Rates of subduction are probably of the order of 9-12 cm/year (Table 1).

Experiments have indicated that the stability of amphibole at mantle pressures and temperatures depends strongly on pressure, and that along most likely geotherms amphibole probably breaks down within the range 20-30 kilobars, equivalent to depths of about 70-100 km (e.g., Lambert & Wyllie, 1968, 1970; Hill & Boettcher, 1970; D.H. Green, 1972; Nicholls & Ringwood, 1972). In a descending slab, therefore, the amphibole of uralitized oceanic crust may break down, liberating water, over a similar depth-range. If, as in the Ringwood and Nicholls model (see above), the mean temperature of the downgoing oceanic crust at these depths is less than about 650°C, none of the slab will melt because this temperature is below the basalt-eclogite-amphibolite solidus ($pH_2O = P_{total}$).

Beneath zones E and F, therefore, it is postulated that water is released from the slab by subsolidus dehydration of amphibole (e.g., at point X in Fig. 40A). This water either initiates diapiric ascent of peridotite (as in the Ringwood and Nicholls model) or rises farther into the mantle (e.g., McBirney, 1969; Best, 1975) where, in either case, temperatures are sufficiently high (higher than in the underlying slab) to partially melt the peridotite under hydrous conditions. Thus, in Figure 40A, if sufficient water

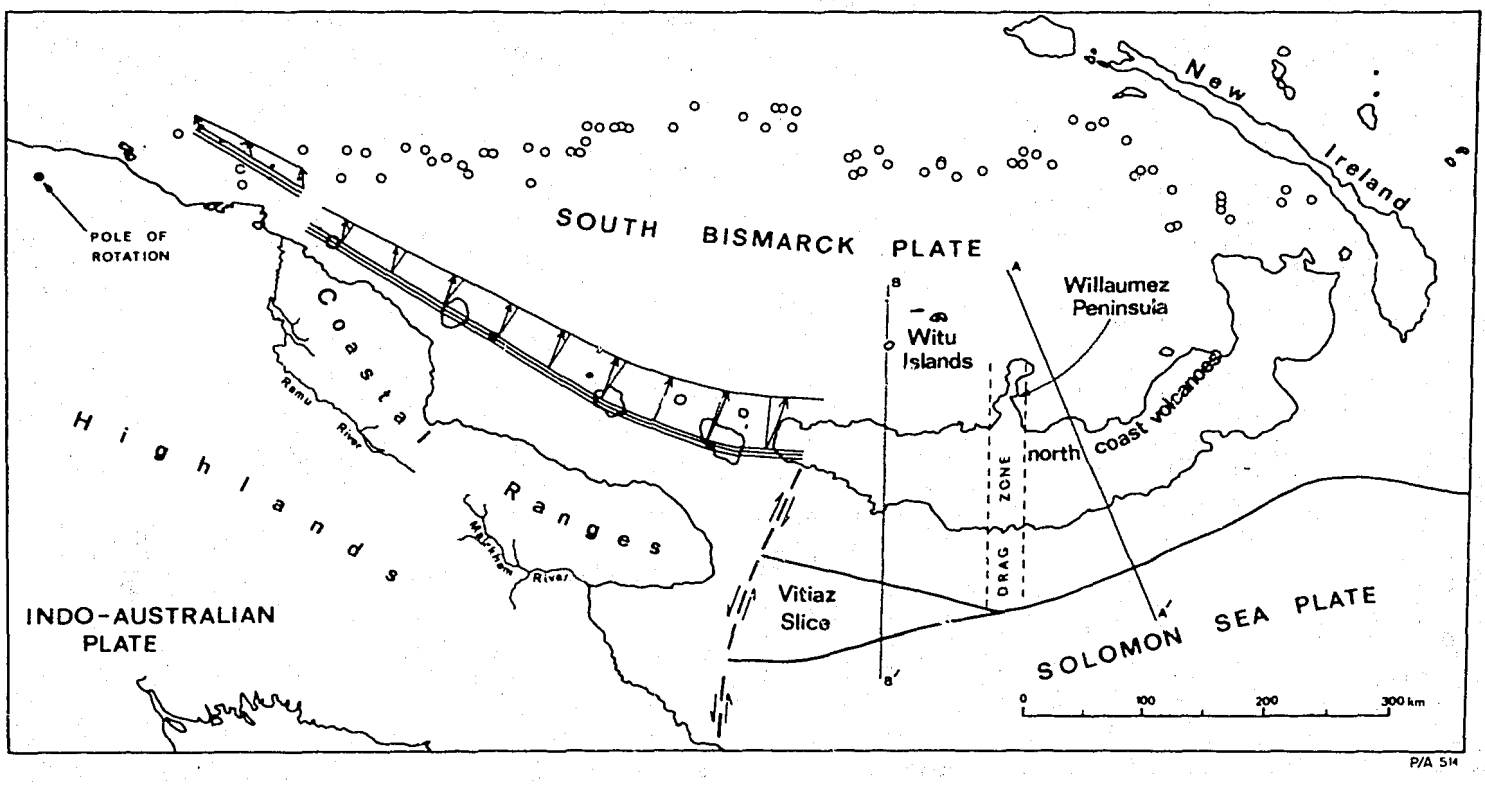

Fig. 39. Tectonic features at the southern margin of the Bismarck Sea. Open circles represent epicentres of earthquakes that define the northern margin of the South Bismarck plate (after Denham, 1973). This northern margin is thought to continue southeastwards and reach the Solomon Sea plate at a triple junction south of New Ireland (see Figs. 2 and 3). The three closely spaced lines north of the coastal ranges are hypothetical strike-lines for the upper surface of the postulated, northward-dipping slab beneath the western arc. The set of arrows illustrates the effect of plate convergence about a single position for a series of instantaneous poles of rotation (other positions in the northwest part of mainland Papua New Guinea have similar effects) - i.e., that those points at the upper surface of the downgoing slab further from the finite pole move greater distances for any rotation about the pole; in other words, rates of plate convergence increase away from the pole. The straight lines accompanying each arrow are normal to the strike-lines. Note that because of the differences in orientation of the strike-lines on either side of Long Island, the transcurrent components of movement for this particular pole position change from right-lateral west of the island to left-lateral east of it. A-A' and B-B' are lines of cross-sections in Figure 40A and B, respectively. See text for explanation of 'drag zone'.

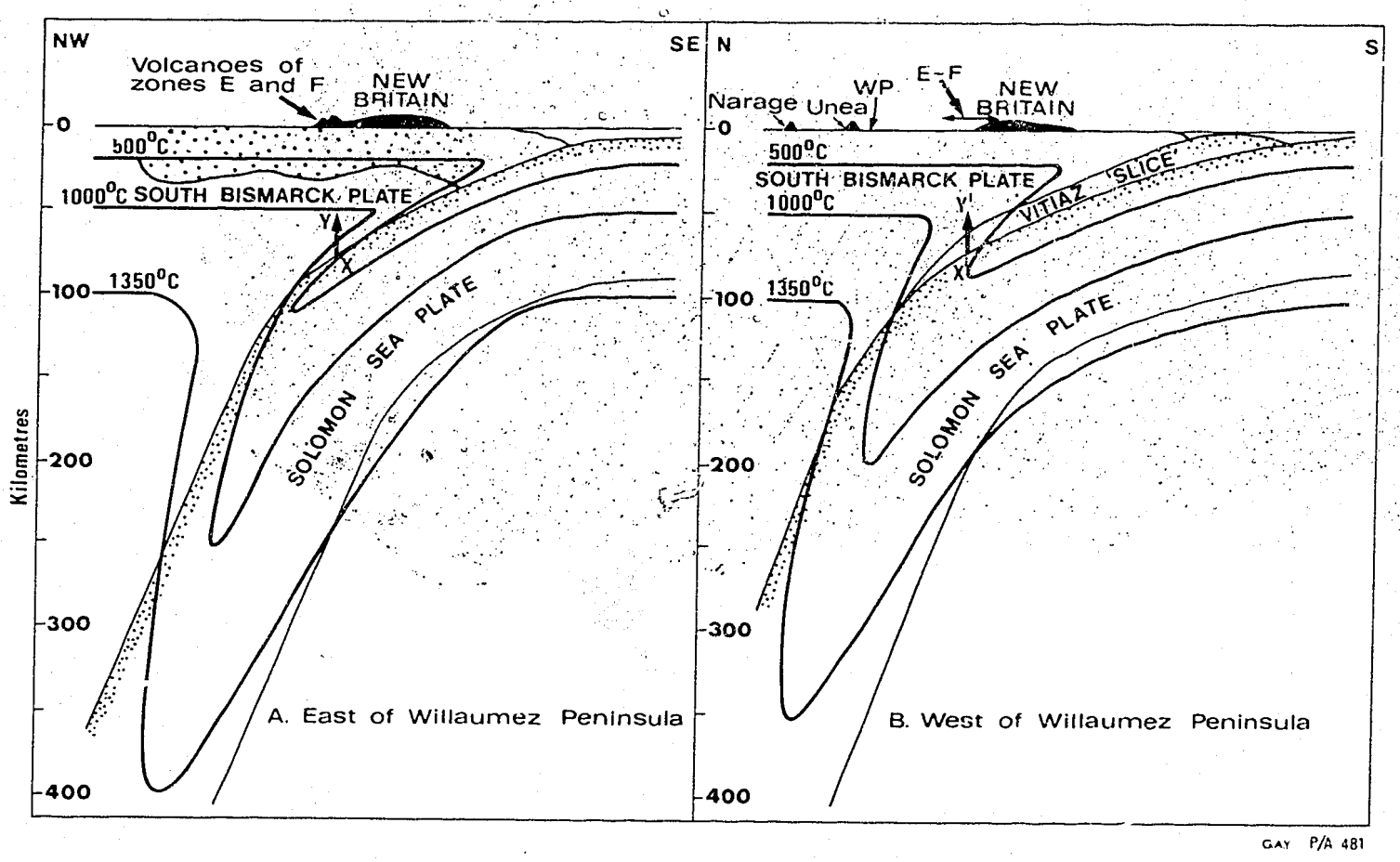

Fig. 40. Cross-sections showing schematic configurations of downgoing slabs and speculative thermal regimes east (A) and west (B) of Willaumez Peninsula. Lines of cross-sections are shown in Figure 39. Light stippling shows hydrated crustal rocks in the upper parts of the slabs. Coarse stippling indicates thickness of crust in cross-section A, which coincides with the crustal profile K-L given by Finlayson & Cull (1973, fig. 9b; crustal thicknesses beneath west New Britain are undetermined). WP and E-F represent the northern end of Willaumez Peninsula, and zones E and F (Fig. 10), respectively, projected from the east onto cross-section B. X-Y and X'-Y' are ascent paths of slab-derived water (see text for details). The flat parts of the isotherms are taken from the 'undisturbed' mantle geotherm of Griggs (1972).

TABLE 1. RATES AND AZIMUTHS OF CONVERGENCE OF THE INDO-AUSTRALIAN AND SOLOMON SEA PLATES WITH THE SOUTH BISMARCK PLATE

Reference	I		S	
	Rate (cm/yr)	Azimuth (°E of N)	Rate (cm/yr)	Azimuth (°E of N)
Johnson & Molnar (1972)	3.3	23	9.2	343
Curtis (1973)	2.60 at IBP 5.22 at IBS	18 7.5	12.02	352
Krause (1973)*	0 at IBP 6.2 at IBS	- 31	6.2 at IBS 12.4 at BPS	5 or 327 327
Taylor (1975, unpublished)	8.04 at IBP 9.3 at IBS	29 29	11.65 at IBS 12.5 at BPS	11 8

*values calculated for a 'preferred' model in which BI pole is at IBP triple junction, and left-lateral slip rate between B and P is 13.5 cm per year (see text).

I = Indo-Australian plate

B = South Bismarck plate

S = Solomon Sea plate

P = Pacific plate

rises from X to Y, the peridotite will melt at Y, where the temperature of 1000°C is above the water-saturated peridotite solidus at 15 kilobars (D.H. Green, 1972; see Fig. 41). It is postulated that partial melting of the peridotite generates batches of magma whose compositions beneath different volcanoes, and at different times, may differ but are essentially magnesia-rich and quartz-normative, or close to silica-saturation.

Experiments by Green (1973b) under water-saturated conditions at 10 kilobars (equivalent to about 35 km depth) showed that liquids of magnesia-rich, quartz-normative composition might be generated by 28-32.5 percent partial melting of peridotite (of model 'pyrolite' composition). At 1100°C (28 percent melting) the calculated equilibrium liquid had 56.1 percent silica, 9.3 percent MgO, and 100 $Mg/(Mg + Fe^{2+})$ = 74 (table 3 of Green, 1973b). At 1200°C (32.5 percent melting), the calculated composition had 54.6 percent silica, 11.9 percent MgO, and 100 $Mg/(Mg + Fe^{2+})$ = 75.5. Both liquids, therefore, are of high-magnesia, low-silica andesite composition. Green concluded that quartz-normative basalts and low-silica andesites might be generated at depths of up to 60 km under water-saturated conditions. The maximum depths at which quartz-normative magmas can be generated when pH_2O is less than P_{total} will be less than 60 km, because anhydrous or low-pH_2O (0.1 percent H_2O) experiments demonstrated that quartz-normative liquids can be generated only at pressures equivalent to depths of less than about 15 km (Green & Ringwood, 1968; Green, 1971; see also Nicholls & Ringwood, 1973). Nicholls & Ringwood (1972, 1973, see above) considered that primary magmas derived at 10 kilobars under water-saturated conditions are tholeiitic basalts close to silica saturation. However, after further experiments, Nicholls (1974) amended this conclusion to allow for the generation of magnesian andesites at depths of less than 35 km; 'andesite'-like liquids were produced at 15 kilobars, but these were olivine-normative and alkali-rich compared with natural quartz-normative andesites.

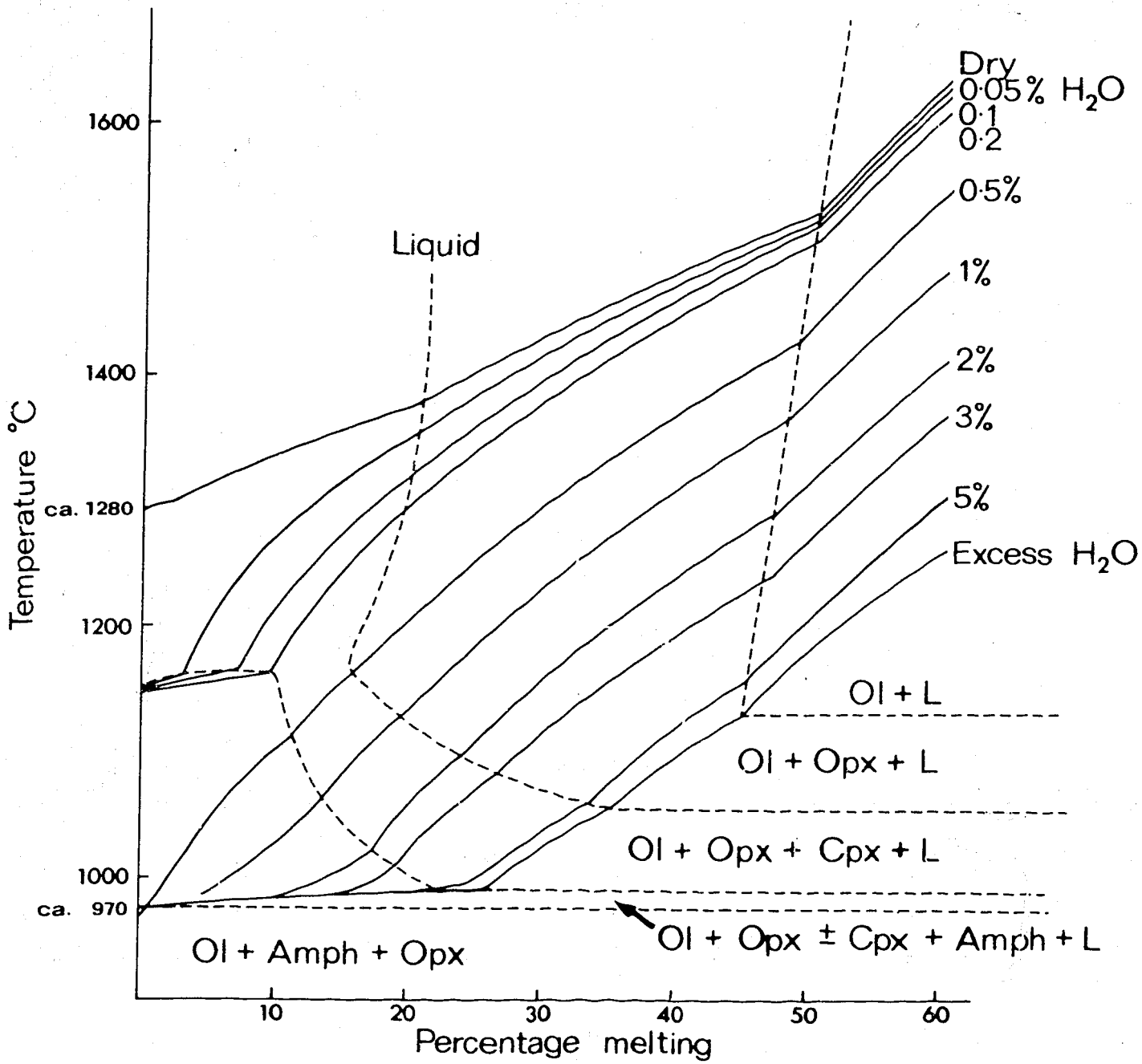

Fig. 41. Temperature v. percentage-melting diagram for a model peridotite composition at about 15 kilobars (after fig. 3 of D.H. Green, 1972). The solidus temperature of about 1280°C under water-free conditions decreases, as water content increases, to about 970°C under water-saturated conditions (excess water). For constant water contents, rises in temperature cause increasing degrees of melting along the stepped paths shown as solid curves. Different amounts of water introduced into peridotite at different temperatures will have different effects; for example, 0.5 percent water introduced into anhydrous mantle at 1200°C will cause about 20 percent melting, but at 1000°C only about 1 percent of melt will be produced. At temperatures of less than about 970°C, any amount of water will not cause melting; it will be used up in subsolidus reactions to form amphibole. (According to Green, up to about 30 percent amphibole could form from his model peridotite.) The dashed lines between the dry and excess water curves define four fields in which partial melts of different compositions are in equilibrium with different phase assemblages; Ol = olivine, Opx = orthopyroxene, Cpx = clinopyroxene, Amph = amphibole, L = liquid. Beneath the volcanoes of zones E and F (Fig. 10), water from the downgoing slab may have been introduced into the overlying upper mantle at a temperature above that of the water-saturated solidus, and so have caused melting. West of zones E and F, the mantle temperature may have been below the solidus temperature, and no melting may have taken place (see text and Fig. 40 for details).

Rare basalts and low-silica andesites with high Mg-numbers are found in the volcanoes of zones E and F along the north coast of New Britain. Because their 100 $Mg/(Mg + Fe^{2+})$ values are greater than about 63, the compositions of the rocks may be close to those of primary magmas generated by partial melting of 'wet' peridotite. These primary magmas are assumed to have originated at depths between 35 km - the depth of the crust beneath the north coast volcanoes (Finlayson & Cull, 1973; Wiebenga, 1973) - and 60 km. This conclusion, however, does not preclude fractionation of the primary magmas during their ascent to the surface. Because a reduction in total pressure decreases the solubility of water, liquidus temperatures will rise, and the primary magma will crystallize (e.g., Nicholls & Ringwood, 1973). The proportion of crystals will almost certainly change before these magmas are erupted in their highly porphyritic condition. Slower rates of magma ascent will promote more extensive fractionation and will allow the formation of low-magnesia high-silica magmas.

As shown in the variation diagrams presented above, the chemical distinction between the rocks of zones E and F - especially of the basic rocks - is not as clear as that between the rocks of other eastern zones (see Fig. 32). The differences in chemistry between the rocks of zones E and F may be due to consistent differences in fractionation trends of essentially similar primary magmas in both zones E and F, or to consistent dissimilarities in composition between the primary magmas of zones E and F. If the latter is true, the primary magmas of Ulawun volcano, in zone E, were nearer in composition to the primary magmas of zone F than they were to those of zone E. As the water derived by amphibole dehydration is unlikely to remain pure (cf. Ninkovich & Hays, 1972; Best, 1975; Fyfe & McBirney, 1975), the water which rose from the slab beneath zone E may have contained different proportions of solvent elements than that beneath zone F, so that chemical differences were imposed on the primary magmas generated beneath zones E and F. Alternatively, the differences in primary magma composition may be due to differences in source peridotite compositions (see below).

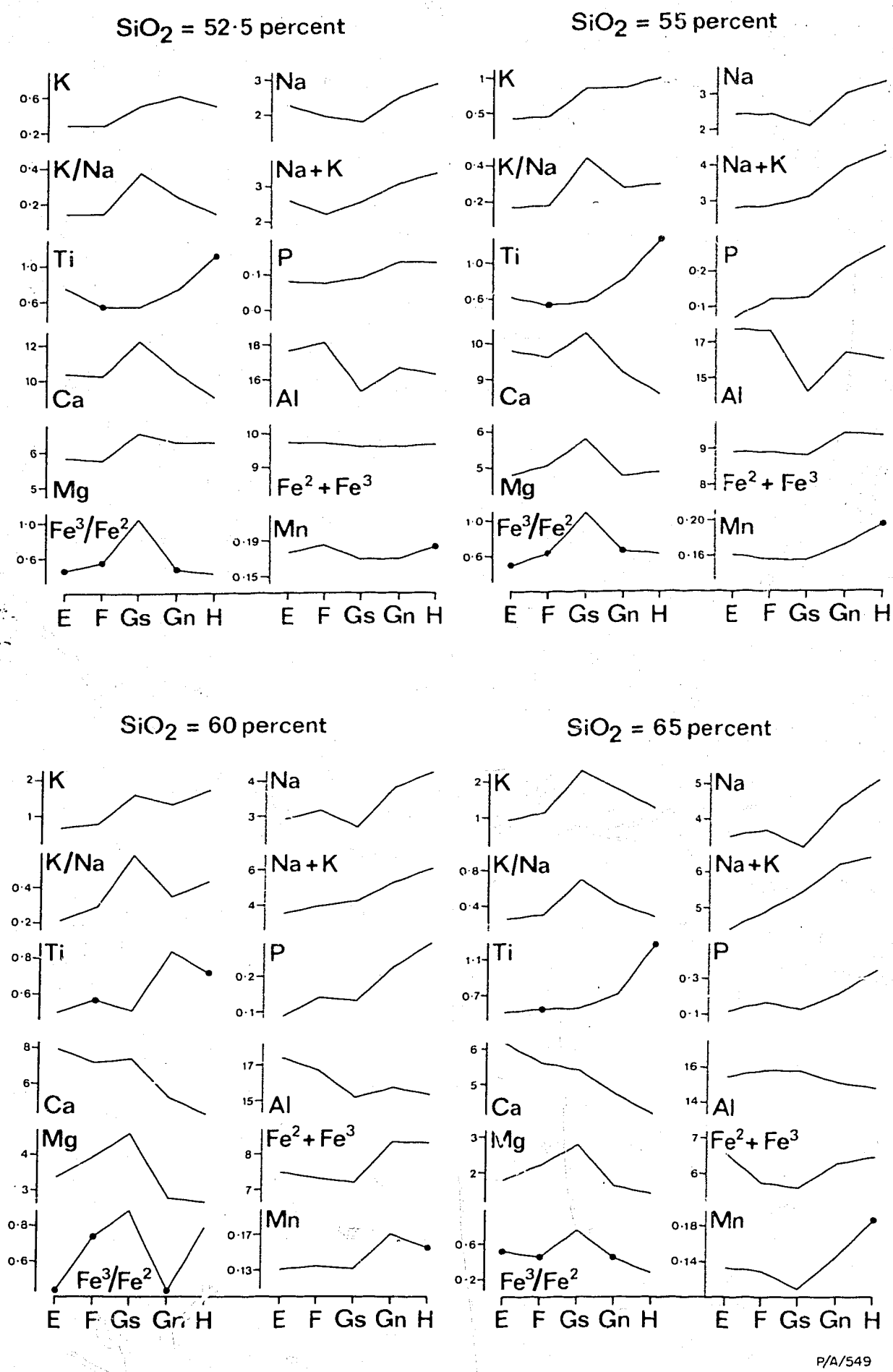

Fig. 32. Generalized oxide variations with different silica contents in rocks from the eastern arc. Individual oxide values for each zone are arithmetic means (dots) or were determined from the regression lines in Figures 15–24, 26, and 27 (see text for details).

Vitiaz slice and Willaumez Peninsula

The volcanoes of zones E and F do not continue west of the southern end of Willaumez Peninsula (Fig. 6). Because this distinct demarcation implies an abrupt change in geodynamic behaviour, the mechanism of magma genesis beneath Willaumez Peninsula and the Witu Islands is considered to be distinct from that east of the peninsula. This difference in behaviour to the east and west of the peninsula is thought to be due to the influence of the Vitiaz imbricate slice (Figs. 3 and 39).

The Vitiaz slice is visualized as a northward-dipping sliver of upper mantle and oceanic crust between the South Bismarck and Solomon Sea plates (Fig. 40F). Down-dip, the slice is considered to thin out, extending no farther than about 70 or 80 km north of the north coast of New Britain, and no deeper than about 100 km. The surface expression of the slice is thought to be the area of sea floor between the two branches of the western end of the New Britain submarine trench (Figs. 7 and 39). The length of sea floor underthrust by the northern margin of the Vitiaz slice is unknown.

It is suggested that throughout the late Cainozoic the South Bismarck plate has been underthrust along a single trench east of Willaumez Peninsula (see above) but along two trenches - that is, along the southern and northern margins of the Vitiaz slice - west of the peninsula. Thus, the rate of subduction at each of the South Bismarck/Vitiaz (BV) and Vitiaz/Solomon Sea (VS) boundaries would have been much less than that at the South Bismarck/Solomon Sea boundary (BS); for example, if at any instant of time at the junction of all three boundaries, the rate of subduction along the boundary BS were $\underline{x}$, the sum of the rates of subduction along the boundaries BV and VS would probably also be very close to $\underline{x}$, and therefore the rate of subduction along the boundary BV would be much less than that along BS.

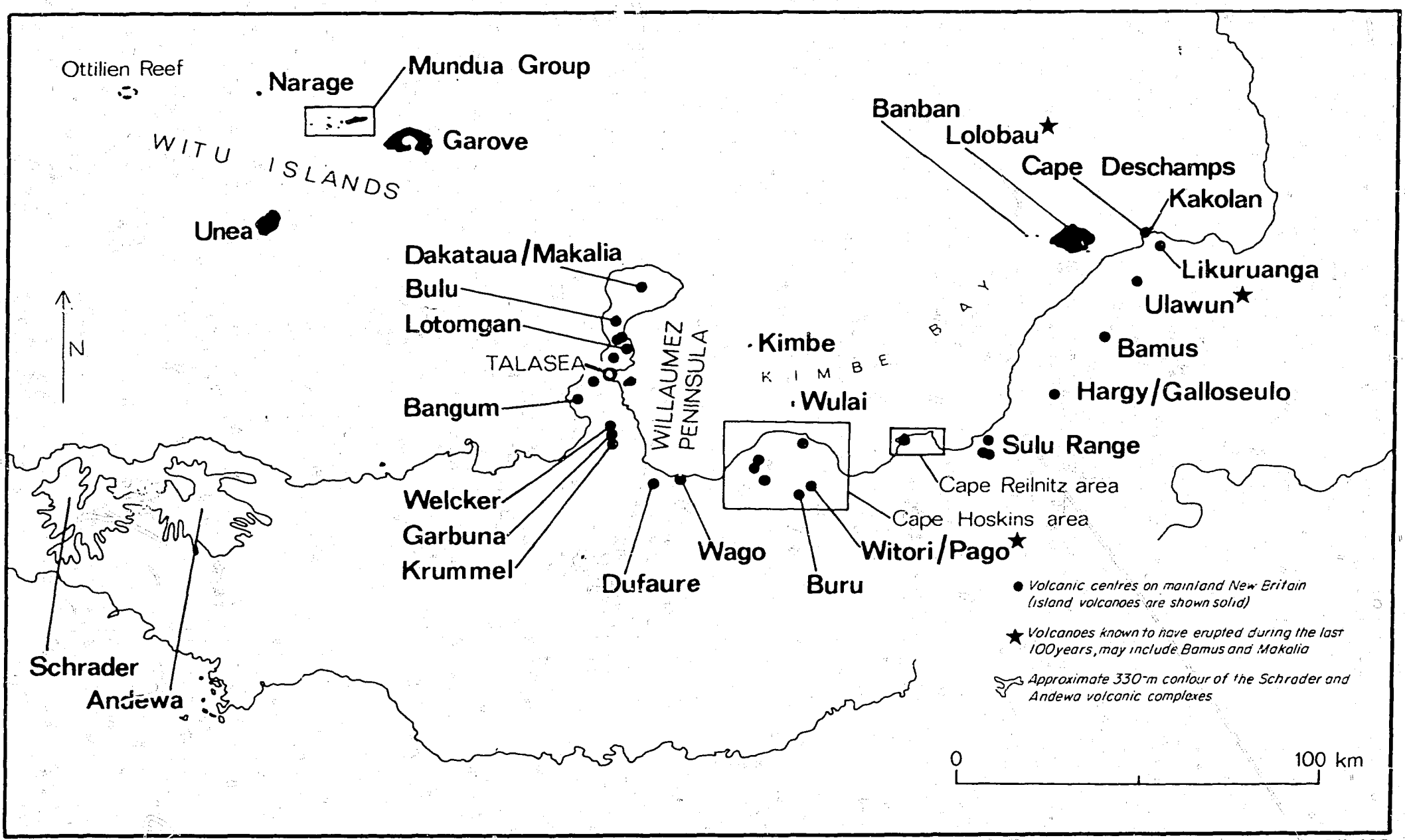

Fig. 6. Main volcanic centres of the eastern arc. Makalia, Pago, and Galloseulo are post-caldera volcanoes which respectively lie inside the older volcanoes of Dakataua, Witori, and Hargy.

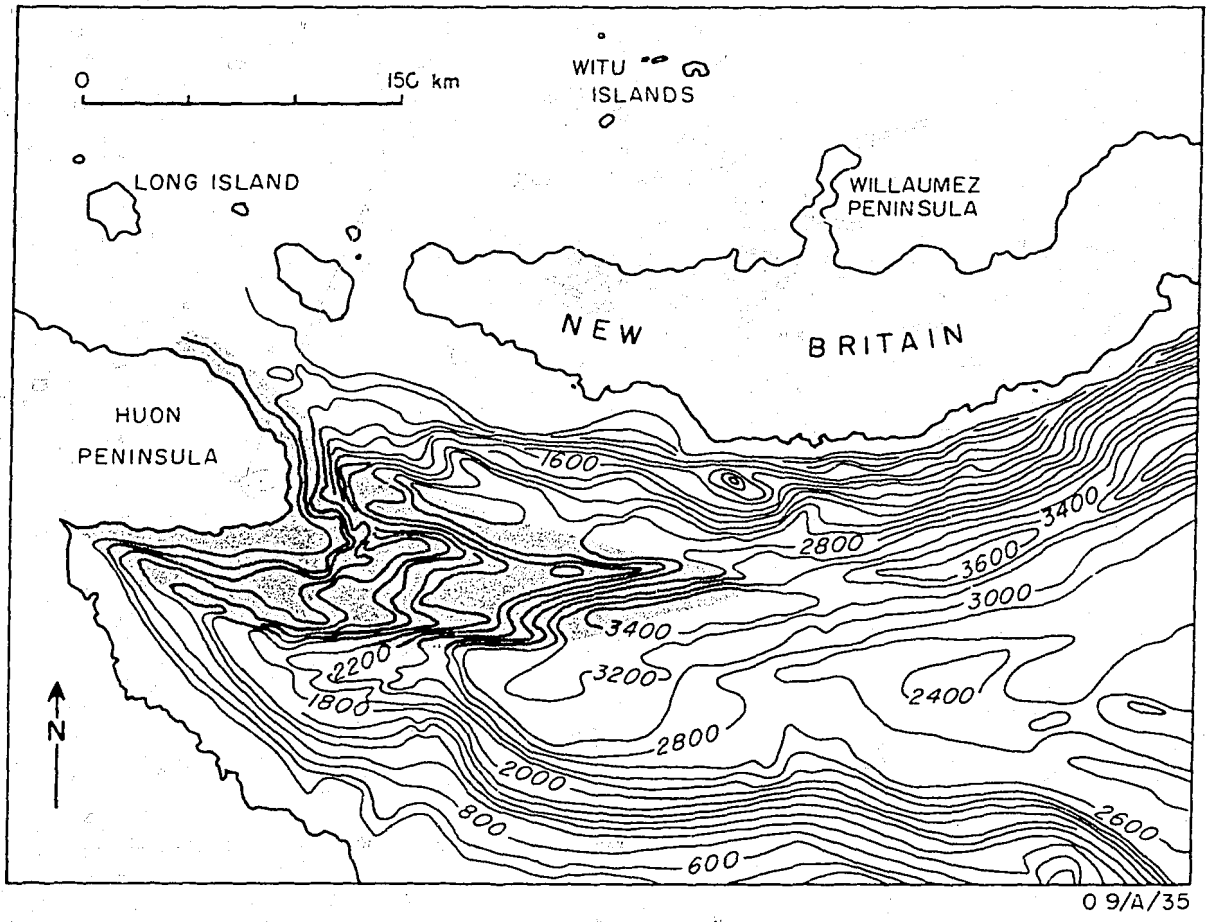

Fig. 7. Bathymetry of the northwestern corner of the Solomon Sea, showing 200-fathom isobaths (after Mammerickx et al., 1971). Submarine ridge (stippled) lies between the two branches of the western end of the New Britain trench.

If, throughout the late Cainozoic, the rates of subduction along the South Bismarck/Vitiaz boundary have been much lower than those along the South Bismarck/Solomon Sea boundary to the east, the region beneath Willaumez Peninsula and the South Bismarck plate is a zone where the downgoing Solomon Sea slab has been dragged past the Vitiaz slice. It is suggested that within this zone of shear, or drag zone (Fig. 39), P_{total} was reduced and shear-strain (frictional) heating was enhanced, and that throughout the late Cainozoic these phenomena contributed to partial melting of the slab and to the generation of primary magmas in the upper mantle (see below). The magmas rose through the South Bismarck plate, erupted, and formed Willaumez Peninsula, whose trend reflects the orientation of the drag zone at depth.

The line of Willaumez Peninsula projected southwards intersects the point where the New Britain trench splits (Fig. 39). This point is regarded as the intersection of the drag zone with the Earth's surface. The trend of the peninsula is therefore the trace of the late Cainozoic average direction of underthrusting at the South Bismarck/Solomon Sea/Vitiaz junction, which has not migrated significantly westwards or eastwards.

The volcanoes of Willaumez Peninsula are grouped into three zones (Fig. 10). From north to south, these are: (1) Krummel, a zone F volcano (see above); (2) volcanoes in the southern part of zone G; and (3) those in the northern part of zone G. The chemical distinctions between these zones are well defined for many of the major oxides (Fig. 32), but perhaps the most striking differences are shown by the rocks from the southern part of zone G.

Southern part of zone G

The rocks of this subzone generally have higher CaO, MgO, $MgO/FeO+Fe_2O_3$, and Fe_2O_3/FeO (the group 2A oxides and oxide ratios of Table 11), and K_2O/Na_2O values, and lower Na_2O and Al_2O_3 contents,

than rocks with the same silica content from other parts of the eastern arc. In addition these volcanoes appear to have a predominance of rocks containing greater than 60 percent silica (p. 29). These petrological features are especially striking when they are compared with those of zone F, and when it is recalled that the gap in the K_2O:SiO_2 variation diagram (Figs. 15 and 30) is due mainly to pronounced differences in composition between the rocks of zones E and F and zones G and H (see p. 47). These relatively abrupt compositional changes between zones F and G imply marked differences in conditions of magma genesis.

The depth of the Benioff zone beneath the southern part of zone G is within the range 130-285 km (Fig. 4). It is postulated therefore that the crust of the subducted Solomon Sea slab is deeper than about 100 km, and has been converted to quartz eclogite. Melting of the eclogite at temperatures greater than about 700°C is enhanced in the drag zone beneath the South Bismarck plate (see above), and is effected in the presence of water provided by the breakdown of serpentine (as in the Ringwood and Nicholls model) or from other hydrous minerals still contained in the eclogite.

Experiments by Green & Ringwood (1968, 1972), T.H. Green (1972), and Stern & Wyllie (1973a) indicated that the liquids produced by partial melting of hydrous quartz eclogite are rich in silica, alkalis, and water, and may be high in K_2O/Na_2O. These liquids have been called 'rhyodacite-rhyolite' (Ringwood, 1974, p. 199), although Stern & Wyllie (1973a) argued that their experimentally derived compositions were not those of natural acid lavas; the alkali-rich compositions may be closer to those of trachytes. (Smith, Johnson, Mackenzie, & Taylor, in prep., described natural trachytes from Papua New Guinea in which high La/Yb values and extreme depletions in heavy REE suggest they are derived from a garnet-bearing slab.) However, in experiments by K.L. Harris (pers. comm., 1976) liquids showing low K/Na values were obtained, corresponding to rocks of trondjhemitic compositions.

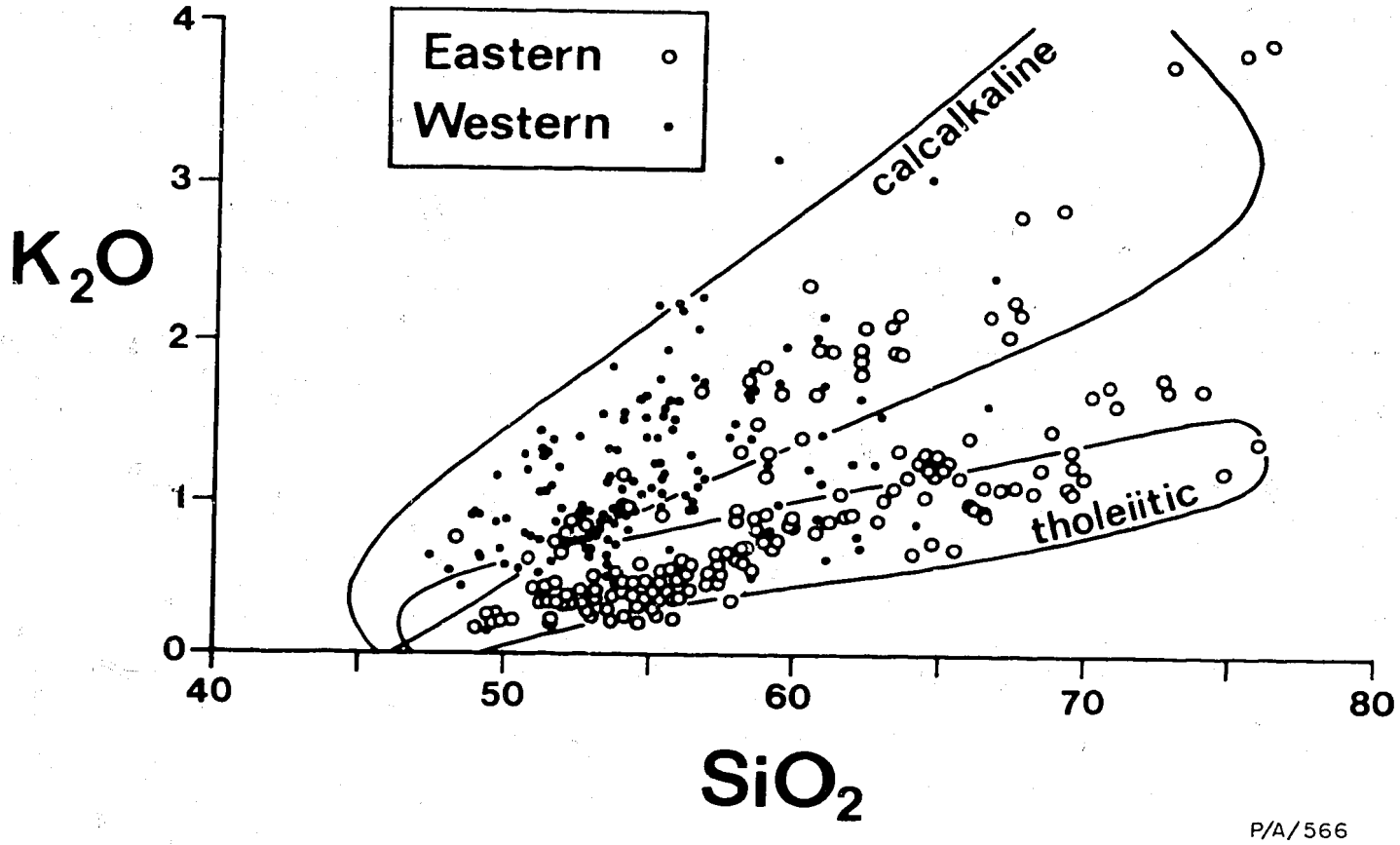

Fig. 30. K_2O:SiO_2 for rocks from the south Bismarck Sea volcanoes in relation to the generalized calcalkaline and tholeiitic field boundaries of Jakeš & Gill (1970).

To account for a few of the specific chemical features of rocks from the southern part of zone G, the melts derived from the underlying eclogitic source are considered to have been notably rich in SiO_2, K_2O (and consequently K_2O/Na_2O), and water. These melts perhaps rose into the upper mantle, where they reacted with olivine - and so became enriched in pyroxene - and formed diapirs (as in the Ringwood and Nicholls model) or, because of their fluidity, they reached levels in the upper mantle where, in either case, anatexis took place under hydrous conditions. The components of the slab melt and the original peridotite may have been mixed to different degrees to form 'primary' magmas that were silica oversaturated and generally high in SiO_2, K_2O, K_2O/Na_2O, and water*. After possible fractionation, all the lavas that finally erupted were high in K_2O/Na_2O, and most of them were silica-rich; (a notable exception is a gabbroic inclusion from Bangum). Because of the generally high water contents, oxidizing conditions prevailed, and the volcanic rocks are therefore characterized by high Fe_2O_3/FeO values. In these generally silica-rich volcanic rocks there is an apparent correlation between high oxidation states and high $MgO/FeO+Fe_2O_3$ values. This is the reverse of the relations demonstrated experimentally by Mysen (1975) in which the 'Mg/(Mg + ΣFe) [of the liquid in equilibrium with olivine] decreases strongly and nonlinearly with increasing oxygen fugacity' (Mysen, 1975, p. 71).

Mantle heterogeneity beneath island arcs

The results of experimental petrology have played an important role in discussions up to this point. However, the interpretations presented below are much more speculative, because detailed experimental results on the possible compositions of slab-derived melts are few, and because, as discussed above, the experiments are technically difficult to perform. In addition, standard experimental

*Preliminary trace-element results also indicate high La/Yb values, supporting the postulated influence of a garnet-equilibrium slab melt.

methods do not reproduce pressures of much greater than about 30 kilobars (about 100 km), and consequently the nature of liquids generated from downgoing slabs at depths greater than 100 km is unknown. Moreover, the peridotite overlying the deep parts of downgoing slabs - for example, in the low-velocity zone (LVZ) of the mantle - may not have the same composition as peridotite in the plates above the LVZ. This possibility of heterogeneity in the mantle peridotite adds further difficulties to the erection of reliable models.

If the petrological evolution of the South Bismarck plate has been similar to that of the lithosphere generated at the divergent boundaries of mid-oceanic rises, much of the ultrabasic portion of the plate can be regarded as peridotite that has already partially melted to form the overlying basaltic rocks (cf. Gast, 1968; Ringwood, 1969). This peridotite may therefore be depleted in LIL elements, and probably sodium, relative to that of 'normal' mantle. In addition, owing to the influence of rising melts enriched in LIL elements, the underlying LVZ may have become geochemically stratified. (Green, 1971; Green & Lieberman, 1976).

Beneath island arcs, a third type of peridotite may form a zone between the upper 'depleted' lithosphere and the peridotite of the LVZ. The top of the LVZ is generally regarded as marking the onset of a small degree of partial melting in the upper mantle (e.g., Lambert & Wyllie, 1968; Wyllie, 1971), and therefore represents the intersection of a peridotite solvus with the local geothermal gradient. If the plate eventually becomes located over a Benioff zone, water derived from the downgoing slab may be added to the upper mantle above the LVZ, the solvus temperature of this peridotite will be lowered, and the top of the LVZ may therefore rise. Green (1973b) postulated that the addition of more than 0.4 percent water will cause the 'roof' of the LVZ to rise abruptly from depths of 85-95 km up to 60-70 km. By this process, the originally 'depleted' peridotite may subsequently become enriched in a melt fraction derived from the

lower parts of the LVZ. A possible example of a similar process was recorded by Frey & Green (1974), who described lherzolite nodules from Victorian basanites and postulated that they consist of two components: 'A', consisting of refractory ferromagnesian minerals; and 'B', a later LIL-element-enriched melt fraction.

Thus, a simplified downward sequence of types of peridotite above the deeper parts of downgoing slabs may be: (1) depleted peridotite, (2) the upper part of the LVZ consisting of depleted peridotite plus an introduced LIL-element-enriched fraction, (3) the lower part of the LVZ, which overall may be relatively undepleted, but which may be geochemically stratified, and (4) 'normal' mantle beneath the LVZ.

Any one of these four peridotite types may generate the primary magmas for volcanoes overlying the deeper parts of the Benioff zone. However, additional factors may impose more complex relations. For example, fluids (melts or water plus solvent elements) derived from the downgoing slab may chemically modify each of the four peridotite zones in different ways. Moreover, upward movement - such as diapirism (cf. Fig. 38) - of some parts of the upper mantle may destroy any simple layered structure beneath island arcs. It has also been suggested that the young marginal basins behind island arcs originated by lithospheric spreading triggered either by heat convected upwards from the downgoing slab (e.g., Karig, 1971) or by hydrodynamic convection cells within the LVZ (Sleep & Toksöz, 1971); whatever the mechanism mantle materials may become recycled, mantle from lower levels may rise to regions where anatexis takes place, and mantle layering may become distorted.

Clearly, there is considerable scope for speculation in any discussion on the origin of magmas erupted from volcanoes above the deeper parts of the Benioff zone - for example, those of zone H and the northern part of zone G. However, an attempt is made to minimize speculations in the following section; trace-element data

are required before the wide range of possible models can be properly evaluated. Nevertheless, one general principle is adopted - that the chemical influence of fluids derived from the downgoing slab is reduced as depths to the Benioff zone increase (cf. Wyllie, 1973). As the oceanic crust descends, its components presumably must become more and more refractory (as the low-melting-point components are lost during successive melting episodes), and differences in the chemistry of volcanic rocks overlying the deeper parts of Benioff zones will therefore be governed increasingly by differences in the compositions of mantle peridotite little modified by the introduction of slab-derived melts. Thus, the Ringwood and Nicholls model of 'pyroxenite diapirs' is judged to become less applicable as the slab reaches greater depths, and the concept of a heterogeneous mantle as described above (based mainly on the views of D.H. Green) is considered to become more important.

Northern part of zone G

In the deeper part of the drag zone beneath the South Bismarck plate, eclogite of the downgoing Solomon Sea plate may have been previously depleted by partial melting. It may have undergone further melting in the drag zone in the presence of water, or else water was derived from it by subsolidus breakdown of hydrous minerals. It is postulated that one or other (or both) of these fluids rose into the overlying upper mantle and initiated partial melting.

In the northern part of zone G, the most basic rocks are high-magnesia basalts which have low normative quartz or olivine, and $100Mg/(Mg + Fe^{2+})$ values within the range 63-73. Crystallization experiments by Nicholls & Ringwood (1973) on a melt with a composition similar to that of the basic rocks from northern Willaumez Peninsula showed that the addition of water greatly increases the stability limit of liquidus olivine (up to 11, 14, 17, and 20 kilobars in runs containing 5, 10, and 15 percent water, and at

$pH_2O = P_{total}$, respectively), and that orthopyroxene was a near-liquidus phase in some of the runs. Rocks of this composition may therefore have been in equilibrium with mantle peridotite under water-saturated or water-undersaturated conditions. The basic rocks of the northern Willaumez Peninsula could, therefore, be close to the compositions of primary magmas of upper mantle peridotite.

The compositions and volumes of the postulated slab fluids are unknown. However, as the K_2O/Na_2O values are lower in rocks from the northern part of zone G than in those from the southern part, fluids may have had lower K_2O/Na_2O values than those derived from the shallower parts of the slab and may have chemically modified the primary peridotite-derived magmas. On the other hand, the lower K_2O/Na_2O values in the rocks from the northern part of zone G may be functions solely of the source peridotite composition; the compositions of the primary magmas may have been unaffected by the mixing of slab melts (if they existed), and water may have been the only significant slab-derived fluid. Similarly, the higher Na_2O, TiO_2, and P_2O_5 values of rocks from the northern part of zone G may indicate that the source peridotite is enriched in these oxides relative to the 'depleted' peridotite that gave rise to the primary magmas of zones E and F. Perhaps the source region is depleted lithospheric peridotite that is now the upper part of the LVZ and enriched in a 'component B' (Frey & Green, 1974).

The most northerly volcano on Willaumez Peninsula is Dakataua, whose rocks - like those of zone H (see below) - are less porphyritic than the rocks of volcanoes farther south (Fig. 12). These low phenocryst abundances may indicate that relatively low water contents prevailed - at least at low pressures - and that the correspondingly higher liquidus temperatures of the magmas before eruption prevented the same high degree of crystallization that characterized the volcanic magmas farther south.

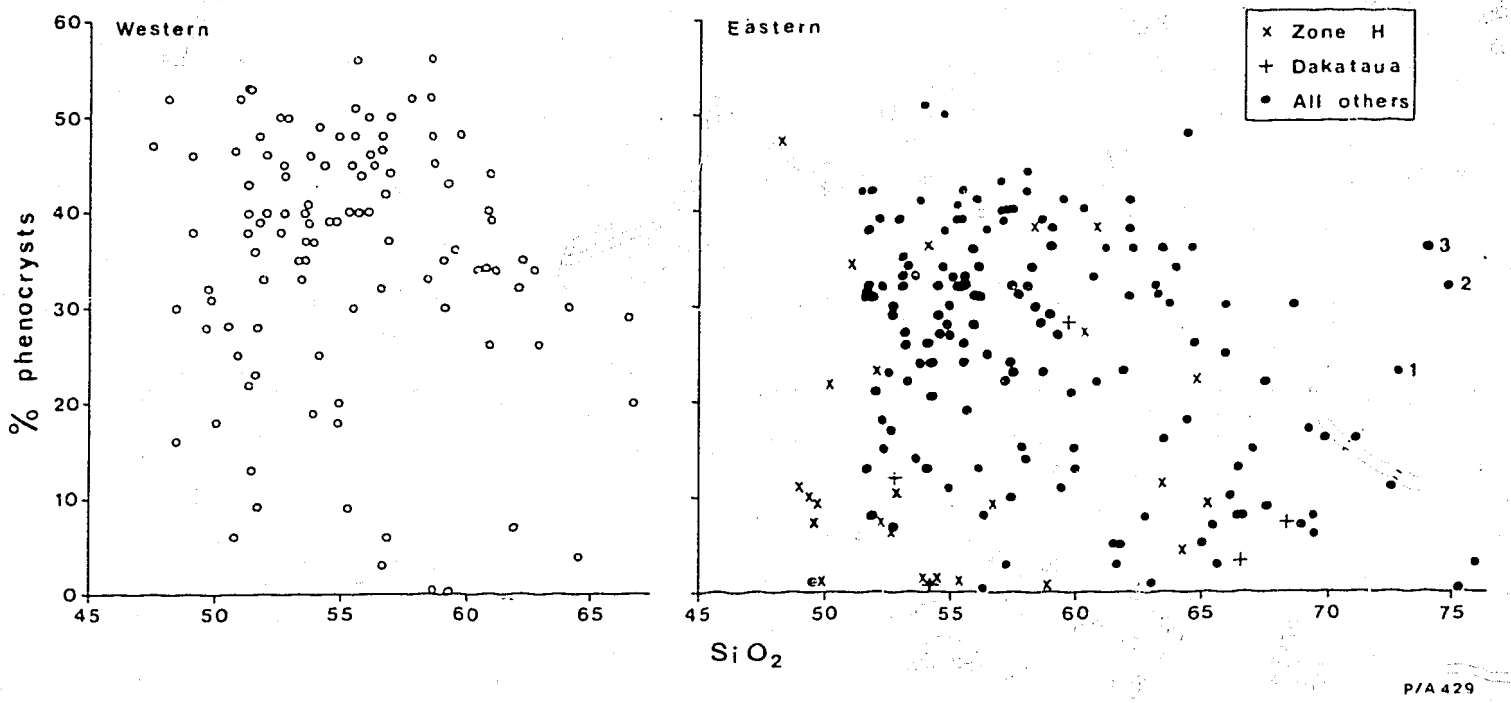

Fig. 12. Volume percent total phenocryst contents v. weight percent SiO_2 for 162 eastern and 106 western rocks (including data of Lowder & Carmichael, 1970, and Blake & Ewart, 1974). Samples 1, 2, and 3 are quartz-rich rhyolites from Sulu Range containing 4, 9, and 13 percent quartz phenocrysts respectively.

The rocks of Kimbe Island, which lies about 30 km east of Willaumez Peninsula (Fig. 6), have compositions similar to those from the northern part of the peninsula. The primary magmas of Kimbe may have been generated beneath the peninsula, and perhaps rose to the surface, fractionating on their way, in a conduit inclined to the east. Alternatively, slab fluids and primary magmas may have been generated in favourable, and apparently unique, circumstances east of the drag zone, and the primary magmas may have fractionated in vertical conduits.

Although slab descent and melting may still be current beneath the southern end of the peninsula, they are hardly reflected in the low frequency of volcanic eruptions in modern times (see p. 24). Thermal areas, however, are widespread, particularly on Garbuna, whose summit area has been greatly affected by thermal alteration. A possible explanation for these features is that large quantities of early-formed water-rich siliceous melts released from the slab have extensively melted the overlying upper mantle, so that only refractory peridotite remains there. Water-rich melts may continue to rise from the downgoing slab at the present day, but they are inadequate to cause further extensive partial melting of the upper mantle, and they crystallize before reaching the surface. Consequently, volcanism has diminished, but hydrothermal fluids still rise from the crystallizing slab melts, producing thermal areas throughout the southern Willaumez Peninsula - in particular, on Garbuna. The water-rich siliceous melts may have extensively altered the crust at depth.

The depleted eclogite formed during the earlier slab-melting beneath the southern part of zone G may now constitute the top of the slab beneath the northern part of zone G.

Zone H and the absence of volcanism to the south

The volcanoes and rocks of zone H, the Witu Islands (Fig. 10), have several features which distinguish them from other volcanoes and rocks in the eastern arc. Firstly, they overlie the deepest part of the New Britain Benioff zone, and the widest range of earthquake depths (Fig. 4). Secondly, basalts are common on all the islands except Unea, which - in contrast - has the fullest development of andesites (p. 29). Thirdly, many zone H rocks are poor in phenocrysts (Fig. 12). Fourthly, variations in the contents of many oxides are greater in the zone H rocks than in rocks with the same silica content from elsewhere in the eastern arc (see, for example, the RSS-values in Table 6). Fifthly, the results of Q-mode factor analysis (p. 63) and nonlinear mapping (Appendix 3) indicate that zone H rocks have the most distinct compositions of any of the rocks from other zones in the eastern arc.

Two other features of the volcanoes of zone H are noteworthy. Firstly, in other parts of the world, island-arc volcanoes overlying the deepest parts of inclined Benioff zones have erupted rocks which are described as either 'alkaline' (i.e., undersaturated) or, at least, strongly potassic (e.g., Kuno, 1959; Hatherton & Dickinson, 1969; Ninkovich & Hays, 1972). However, neither generalization holds for the volcanic rocks of the Witu Islands, which are all hypersthene-normative (Figs. 14 and 35), and low in potassium (see especially Fig. 34).

Secondly, no volcanoes of the same age appear to exist south of the Witu Islands, nearer to New Britain, over the shallower part of the Benioff zone (Fig. 6). In the following it is postulated that the absence of these volcanoes is due to the influence of the Vitiaz slice, and that the apparently unique position of the Witu Islands over the deepest part of the New Britain Benioff zone is due to the thermal regime, which - because this part of the arc

TABLE 6. RSS VALUES X 10^3 OF REGRESSION LINES FOR ROCKS OF ZONES A TO H SHOWN IN VARIATION DIAGRAMS

Figure Number	15	16	17	18	19	20	21	22	23	24	25	26	27
Variation diagram	K_2O v. SiO_2	Na_2O v. SiO_2	K_2O/Na_2O v. SiO_2	Na_2O+K_2O v. SiO_2	TiO_2 v. SiO_2	P_2O_5 v. SiO_2	CaO v. SiO_2	Al_2O_3 v. SiO_2	MgO v. SiO_2	FeO+ Fe_2O_3 v. SiO_2	MgO v. FeO+ Fe_2O_3	FeO/ Fe_2O_3 v. SiO_2	MnO v. SiO_2
Zone A n* = 24		473 (1)		396 (2)			913 (1)		584 (1)	749 (3)	392 (1)		757 (3)
Zone B n = 52	690 (2)	672 (2)	123 (1)	791 (3)	455 (5)		891 (2)	274 (2)	767 (3)	579 (2)		281 (2)	118 (1)
Zone C n = 23	817 (1)	886 (1)	644 (1)	883 (1)		563 (1)	917 (1)	177 (1)	621 (1)	188 (1)			182 (2)
Zone D n = 44	744 (1)	707 (1)	367 (1)	811 (1)		447 (3)	872 (1)	320 (2)	629 (2)	772 (3)	615 (5)	227 (2)	426 (1)
Zone E n = 83	859 (1)	819 (3)	646 (1)	894 (3)	457 (3)	370 (3)	957 (1)	545 (5)	643 (2)	884 (5)	814 (3)		736 (5)
Zone F n = 58	894 (1)	847 (2)	691 (4)	931 (2)		318 (2)	973 (1)	519 (1)	847 (1)	841 (1)	728 (2)		549 (3)
Zone Gs n = 17	978 (1)	933 (2)	886 (1)	986 (1)	892 (5)	682 (2)	990 (2)	769 (4)	850 (1)	964 (1)	939 (4)	538 (1)	927 (1)
Zone Gn n = 18	827 (1)	970 (2)	639 (1)	946 (2)	400 (2)	452 (2)	977 (2)	387 (1)	909 (2)	912 (2)	939 (5)		582 (2)
Zone H n = 29	788 (4)	918 (1)	527 (4)	975 (4)		751 (5)	944 (2)	314 (1)	769 (2)	671 (2)	592 (3)	459 (4)	

*n = number of samples

Numbers in parentheses indicate degrees of regression

is nearer to the postulated pole of rotation for the South Bismarck and Solomon Sea plates - is distinct from that east of Willaumez Peninsula. This proposed distinction between the thermal regimes east and west of Willaumez Peninsula is illustrated in Figure 40. The shapes of the isotherms in Figure 40 are highly speculative, although they are consistent with the concept of downgoing slabs as heat-sinks, and of fast-descending slabs being colder than slowly descending ones at the same depth (see p. 87).

At depths less than about 100 km west of Willaumez Peninsula, the combined effect of the downgoing Solomon Sea plate and the overlying Vitiaz slice is that of a thickened layer of cold crust and upper mantle which is a more effective heat-sink than the Solomon Sea plate alone east of Willaumez Peninsula (Fig. 40). Therefore at depths less than 100 km west of the peninsula, parts of the upper mantle above the Vitiaz slice may be colder than the mantle at the same depth east of the peninsula (compare equivalent points Y and Y' in Fig. 40). While the slab and slice descended in the west, water may have been driven off the Solomon Sea plate by amphibole dehydration (at points represented by X' in Fig. 40B), in the same way as suggested for beneath zones E and F (p. 91) east of Willaumez Peninsula (cf. X in Fig. 40A). This water may have risen, and have entered the overlying parts of the South Bismarck plate and Vitiaz slice. However, because temperatures there - for example, at Y' in Figure 40B (equivalent to Y in Fig. 40A) - were lower than those of the peridotite-water solidi at 15 kilobars (see Fig. 41) the peridotite would not have melted; instead, the water would have undergone subsolidus reactions with the peridotite. Thus, no volcanism evolved west of Willaumez Peninsula on the extension of zones E and F.

Unea Island represents the first visible signs of late Cainozoic volcanism north of the north coast of New Britain (Fig. 6). Compared with other zone H rocks with the same silica content, the

rocks of Unea have notably higher K_2O, lower Na_2O (and therefore higher K_2O/Na_2O), lower TiO_2, and higher Fe_2O_3/FeO values, and in some of these features resemble rocks from the northern part of zone G. On the other hand, rocks from Unea show many other chemical features that relate them to zone H. The rocks from Unea, therefore, appear to be transitional between those of zone G and those in other parts of zone H, and presumably must have developed under conditions distinctly different from those elsewhere in the arc. The Unea primary magmas are considered to have been generated from upper mantle peridotite under hydrous conditions, but - like the primary magmas postulated for the northern part of zone G - how far they reflect the composition of the source peridotite is not known: their compositions may be due to the specific chemical characteristics of the initial peridotite, yet they may have been influenced by the introduction of slab fluids. In either case, water contents in the underlying mantle may have been less than those beneath zones E, F, and G (except, perhaps, the region beneath Dakataua volcano - see above), because the underlying eclogitic slab at depths greater than 300 km is likely to have been less hydrous than it was at depths of less than 300 km. (Relatively low water contents are indicated by the low phenocryst contents of some Unea rocks.)

The rocks of the other Witu Islands north of Unea are predominantly basalts and low-silica andesites; rocks containing greater than about 61 percent silica are present only on Garove Island, where dacites and rhyolites are among the oldest exposed rocks (Table 5). These volcanoes and Ottilien Reef (Fig. 6) form an east-west zone which is far removed from the boundary between the South Bismarck plate and the Vitiaz slice, and also from the deepest part of the downgoing Solomon Sea slab.

Tholeiitic basalts containing up to about 11 percent normative olivine are present on all the Witu Islands north of Unea. Several of them are high-magnesia varieties, and several have

TABLE 5. SIMPLIFIED STRATIGRAPHIES OF TEN VOLCANOES

Volcano	Sequence
Kadovar* (Zone A)	low-silica andesites → crater formation → high-silica andesite (only slightly richer in silica).
Aris* (Zone B)	low-silica andesites → crater formation → high-silica andesites.
Long+ (Zone C)	basalts, type 1 → basalts, type 2 (richer in silica), and andesites associated with cauldron subsidence → basalts, type 2.
Sakar* (Zone D)	basalts → crater formation → high-silica andesites.
Talawe/ Langila* (Zone D)	Talawe basalts and low-silica andesites → Langila low-silica andesites (richer in silica). Langila is a satellite volcano on the northeastern flank of Talawe.
Hargy/ Galloseulo* (Zone E)	andesites → cauldron subsidence → andesites (mainly richer in silica) → Galloseulo dacites.
Bamus* (Zone E)	andesites (mainly low-silica) → collapse event → high-silica andesites.
Lolobau (Zone F)	andesites and (?)dacites → basalt → cauldron subsidence → basalt (poorer in Fe) → dacites and rhyolites. Several samples of uncertain relative age.
Unea* (Zone H)	basalts and andesites → cauldron subsidence → andesites (mainly richer in silica).
Garove (Zone H)	dacites and rhyolites → low-silica andesites → cauldron subsidence → basalts. Several samples of uncertain relative age, including the basalts, which are only assumed to be post-caldera in age.

The prefixes 'low-silica' and 'high-silica' are omitted where both varieties of andesite are represented. Comments in parentheses describe rocks in relation to those of the same name in an earlier part of the same eruptive sequence. Zones A-H are shown in Figure 10.

*Volcanoes in which younger rocks are consistently more siliceous than older ones.

+Long should be considered as three volcanoes because two older basalt (type 1) cones flank a mainly younger central caldera complex (basalts type 2 and andesites).

100 $Mg/(Mg + Fe^{2+})$ values greater than 63. Assuming that none of the olivine phenocrysts (up to 10 percent by volume) in these rocks have accumulated, the rocks could be approximations to primary olivine tholeiite magmas generated by partial melting of peridotite under water-undersaturated conditions.

Experiments under water-saturated conditions (Green, 1973b) have suggested that tholeiitic liquids low in normative olivine content could be generated from peridotite ('pyrolite') by (1) about 40 percent partial melting at 10 kb (about 35 km depth), or (2) 27-30 percent partial melting at 20 kb (about 70 km). The complete pressure/temperature range under which olivine tholeiites might be generated in a water-saturated environment is at present unknown, but probably they can be produced at depths greater than 70 km (20 kb). However, where pH_2O is less than P_{total}, the maximum pressure for olivine tholeiite generation will probably be less than that for water-saturated conditions (see, for example, Nicholls & Ringwood, 1973). The depths of partial melting for the primary magmas of zone H - and those of zone G - are at present unknown, but future attempts to estimate these depths will depend upon a critical evaluation of the relative roles of water content, total pressure, and degrees of partial melting in the mantle peridotite (cf. Green 1973a).

Some of the zone H olivine tholeiites, especially those from the Mundua Group, are extremely depleted in K_2O (Fig. 15) but relatively rich in TiO_2 (Fig. 19), and resemble the tholeiitic rocks recorded from ocean basins and from the marginal basins behind island arcs (e.g., Sclater, Hawkins, Mammerickx, & Chase, 1971; Hawkins, 1976). Similarly, some of the low-silica andesites have compositions which, except for most TiO_2 values, are not unlike those of 'oceanic andesites' or 'icelandites' (Carmichael, 1964), which are believed to have been generated under relatively high water-vapour pressures in ocean basins or at divergent plate

boundaries (e.g., Hald, Noe-Nygaard, & Pederson, 1971). These similarities suggest that any fluids derived from the downgoing Solomon Sea slab at depths greater than 300 km did not greatly modify the compositions of the primary magmas generated beneath the zone H islands north of Unea. However, some questions remain unanswered: Were small amounts of water the only slab-derived fluids? Did the slab merely provide a tectonic regime suitable for magma genesis - for example, hydrodynamic convection in the LVZ and upwelling of hot peridotite to levels where melting was induced - and contribute no materials to the overlying upper mantle? Nevertheless, it is postulated that the Solomon Sea slab did control a tectonic regime that favoured magma genesis west of Willaumez Peninsula but was not duplicated east of the peninsula.

If the instantaneous poles of rotation for the South Bismarck and Solomon Sea plates throughout the late Cainozoic lay in the southwestern part of Papua New Guinea (see bs in Fig. 2c, and page 17; after Krause, 1973), then that part of the Solomon Sea slab east of Willaumez Peninsula, and at depths greater than 100 km, descended more rapidly than the equivalent part west of the peninsula, and remained colder to greater depths. Consequently, in Figure 40A, isotherms for the eastern part of the Solomon Sea slab are shown depressed more deeply into the slab than are those for the western part, and the overlying mantle in the eastern part at depths greater than about 100 km is depicted as having had more heat extracted from it than in the west. Temperatures at the surface of the Solomon Sea slab beneath the Witu Islands may therefore have been higher than those of the equivalent parts of the slab east of Willaumez Peninsula. This temperature difference may have had either or both of two effects.

The higher temperatures of the slab in the west may have been sufficient to cause the overlying peridotite in the LVZ to rise to levels where it melted, whereas in the east the same temperatures

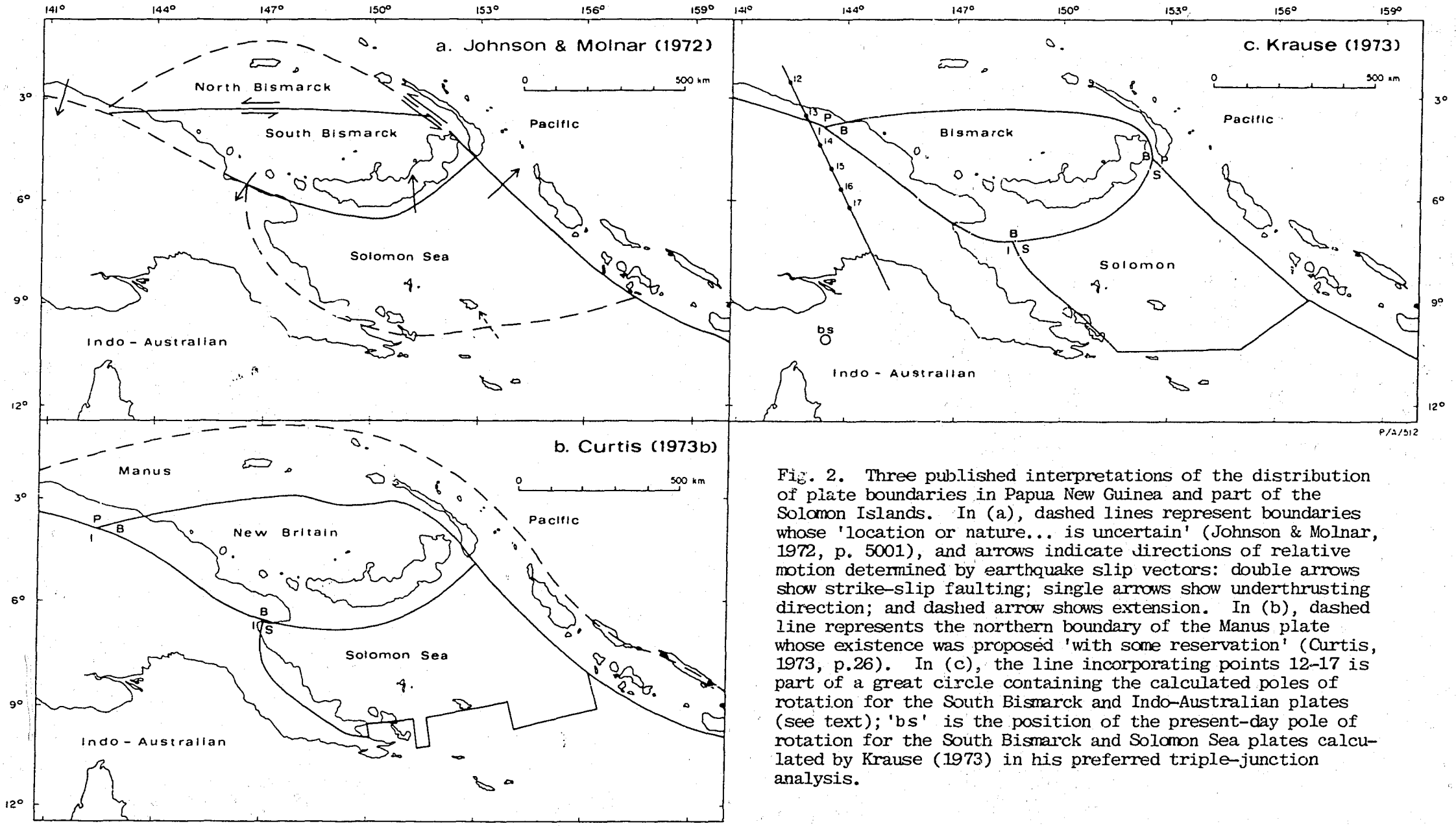

Fig. 2. Three published interpretations of the distribution of plate boundaries in Papua New Guinea and part of the Solomon Islands. In (a), dashed lines represent boundaries whose 'location or nature... is uncertain' (Johnson & Molnar, 1972, p. 5001), and arrows indicate directions of relative motion determined by earthquake slip vectors: double arrows show strike-slip faulting; single arrows show underthrusting direction; and dashed arrow shows extension. In (b), dashed line represents the northern boundary of the Manus plate whose existence was proposed 'with some reservation' (Curtis, 1973, p.26). In (c), the line incorporating points 12-17 is part of a great circle containing the calculated poles of rotation for the South Bismarck and Indo-Australian plates (see text); 'bs' is the position of the present-day pole of rotation for the South Bismarck and Solomon Sea plates calculated by Krause (1973) in his preferred triple-junction analysis.

were reached at too great a depth (perhaps even below the LVZ) to effect mantle upwelling. Alternatively, some of the eclogitic crust may have melted at depths greater than about 150 km east and west of Willaumez Peninsula, but because of the differences in temperatures the volumes of slab melts in the east were inadequate to melt and mix with the overlying peridotite; or else primary magmas were formed and did not erupt, or were erupted in insufficient quantities to be detected on the Bismarck Sea floor.

GENESIS OF PRIMARY MAGMAS IN THE WESTERN ARC

Introduction

The familiar pattern of chemical zonation in island arcs is shown by the eastern arc, whose rock compositions change in a direction perpendicular to the plate boundary. In contrast, rock compositions in the western arc change along the volcanic chain - that is, in a direction parallel to the margin of the South Bismarck plate. These lateral changes in chemistry are interpreted as functions of differences in the rates of convergence along the Indo-Australian/South Bismarck plate boundary.

Plate kinematics

During the mid-Tertiary, the northern edge of the Australian continent is thought to have collided with the Adelbert-Finisterre-Huon island arc, destroying a northward-dipping subduction system that had given rise to predominantly Oligocene island-arc-type volcanism (see pages 13-15). Hydrated oceanic crust is considered to have formed the sea floor between the island arc and the leading edge of the Australian continent, and to have been subducted northwards beneath the arc (Fig. 9).

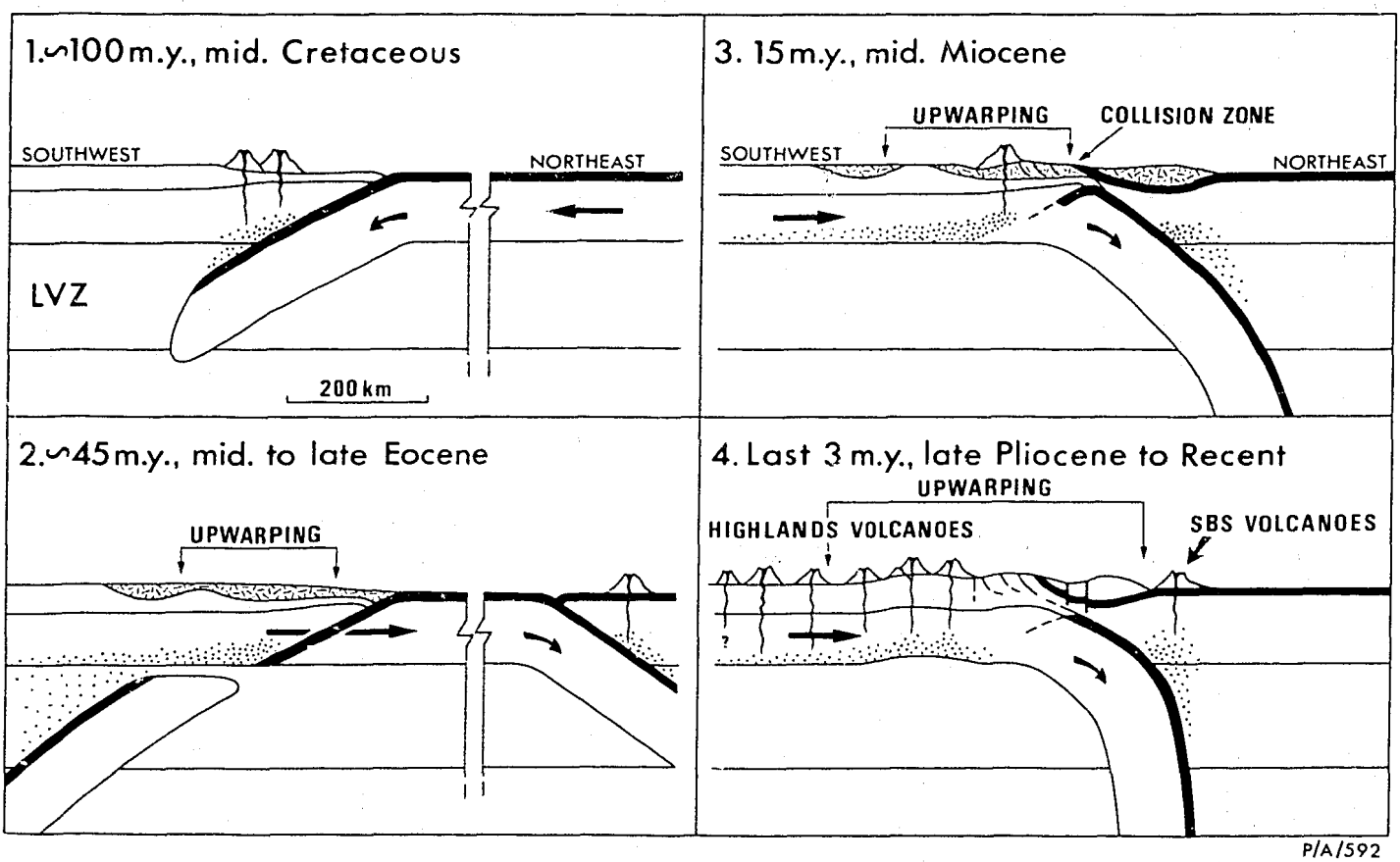

Fig. 9. Schematic representation of the tectonic evolution of mainland Papua New Guinea in a northeast-southwest section through the western arc, coastal ranges, and Highlands (see Figs. 1-3). Johnson, Mackenzie, & Smith (in prep. b) used these diagrams to illustrate the evolution of late Cainozoic volcanism in both the western arc and Highlands province (Fig. 1), but in the following description emphasis is given to those aspects of the interpretation that apply particularly to the development of the western arc. Black bands represent oceanic crust. Stippling represents chemical modification of mantle by slab-derived fluids. Short-line pattern in diagrams 2 and 3 represents post-Jurassic thickening of crust. The true thicknesses of the lithosphere and low-velocity zone (LVZ) throughout this region are unknown, and the assumed values are those determined by Brooks (1969) for the southern part of mainland Papua New Guinea.

1. Southward-dipping subduction in the mid-Cretaceous resulted in arc-trench-type volcanism, and chemically modified the mantle underlying the northern edge of the Australian continent.

2. In the Eocene the southward-dipping slab may have become detached. In the late Eocene, volcanism started in an island arc several hundreds of kilometres to the north as a result of northward subduction of the Indo-Australian plate, which carried the Australian continent northwards from Antarctica.

3. By the late Oligocene or early Miocene the continent had reached the island arc and, because it was too buoyant to descend into the subduction zone, began to collide with the arc. Subduction was arrested and island-arc volcanism ceased, but plate convergence continued, and the continental margin and arc were warped and raised. Middle Miocene magmatism south of the collision zone was initiated by partial melting of mantle which had been chemically modified during the Cretaceous subduction.

4. By the late Pliocene the slab beneath the Tertiary island arc had become steepened, and continuing subduction gave rise to the volcanoes of the western arc in the south Bismarck Sea (SBS volcanoes). Uplift and warping in the Highlands region led to partial melting in the chemically modified mantle.

A favoured interpretation is that the continent first collided with the western part of the arc in the late Oligocene to early Miocene, when island-arc volcanism stopped and arc sedimentation started (see: Jaques & Robinson, in prep.; Johnson & Jaques, in prep.). This western part of the arc may have then been raised above sea level to form the Adelbert Range, and the underlying part of the downgoing slab may have become steepened and its downward movement retarded (Fig. 9). Further collision of the arc and continent is considered to have restarted in the late Pliocene, and to have taken place progressively eastwards, so that the more easterly ranges were the last part of the arc to be raised above sea level, and the more easterly parts of the downgoing slab were the last to have their downward motion arrested. The gap between the arc and the encroaching continent is therefore visualized as closing like a pair of scissors - that is, in the late Pliocene and Quaternary, rates of plate convergence were greater in the east than in the west, and were governed by instantaneous poles of rotation near or in the northwestern part of mainland Papua New Guinea (Krause, 1973).

This interpretation is consistent with the known geology of the coastal ranges (Jaques & Robinson, in prep.). In the extreme east, recent rapid uplift is indicated by late Pliocene limestone capping Huon Peninsula, and by an extensive flight of Holocene coral terraces on the northeast coast (Chappell, 1974). In contrast, in the Adelbert Range, to the west, limestones postdating the collision are poorly developed, and the Holocene terraces are absent. There, instead, thick wedges of Neogene terrestrial clastic rocks flank the earlier island-arc volcanic rocks, indicating subaerial erosion during a period when middle Miocene to Pliocene limestones were being deposited on the more easterly, submarine parts of the arc.

The above geodynamic interpretation is also consistent with the differences in heights of the coastal ranges. The ranges are highest in the southeast on Huon Peninsula (over 4000 m), where rates of plate convergence and uplift have been greater. They are lower in the Adelbert Range (less than 2000 m) because rates of

uplift and plate convergence have been less, and because the arc has been exposed to subaerial erosion for longer.

The overall effect of the continent/arc collision is thought to have been the formation of a 'hanging' slab - that is, a near-vertical slab of lithosphere whose downward motion has been slower than it was before the collision (Fig. 9). The downward motion of slabs is widely considered to be due to gravitational forces caused by the density contrast between the colder and therefore denser slab (in part eclogitic) and the surrounding hotter and less dense mantle (e.g. McKenzie, 1969; Sleep, 1975; Sung & Burns, 1976). Thus, once subduction is initiated, the slab should continue to descend under its own weight, slab-derived fluids should continue to rise from the slab, and island-arc-type volcanism should prevail until the slab becomes detached and finally inactivated. However, this interpretation is difficult to reconcile with the geology of the coastal ranges, where island-arc volcanism ceased between the middle Miocene and late Pliocene (Jaques & Robinson, in prep.). If the slab kept sinking under its own weight, why did volcanism cease in the middle Miocene, and why did it start again in the late Pliocene or early Quaternary?

To account for this cessation in volcanism the motion of the hanging slab immediately after the collision is considered to have been governed by the movement of the plates, rather than by the gravitational effect of the slab's weight. Thus, when the continent and arc first collided the result of most of the subsequent plate convergence was crustal foreshortening and uplift, and the only significant motion of the slab was steepening; subduction effectively ceased, and so no volcanism took place. However, subduction and volcanism resumed when the plates began to converge again in the late Pliocene.

This interpretation is consistent with the known distribution of earthquakes in the slab beneath the western arc (Appendix 1). Intermediate and deep-focus earthquakes have not

been recorded west of Karkar Island, perhaps because rates of subduction since the collision have been so slow that the slab there has had greater opportunity to thermally equilibrate with the surrounding mantle. In contrast, intermediate-focus earthquakes are common east of Karkar. There, the slab may have been subducted at greater rates for a longer time, and accordingly there has been less opportunity for thermal equilibration with the mantle, and the slab has remained colder to greater depths than in the west.

Present-day form and motion of the hanging slab

The present-day three-dimensional form of the hanging slab beneath the entire western arc cannot be deduced directly because of the apparent absence of intermediate and deep earthquakes west of Karkar Island. However, the distribution pattern of the volcanoes may be taken as circumstantial evidence for establishing the general shape of the slab throughout the late Cainozoic. The three closely spaced parallel lines in Figure 39 are hypothetical strike-lines for the upper surface of the hanging slab. They are drawn parallel to the general trend of the western arc, and may correspond to depths between about 150 and 250 km. Two features are noteworthy. Firstly, because the Schouten Islands line is offset, the underlying slab may be similarly displaced. Secondly, the lines are straight between the Schouten Islands and Long Island, but east of Long Island they curve towards the east (Fig. 30). The concentration of earthquakes south of Long Island (Fig. A, Appendix 1) coincides with the change in orientation of the strike-lines, and may be due to high stresses set up where the slab is strongly bent.

Using this slab configuration, and (1) accepting the proposal of Krause (1973) that the instantaneous poles of rotation for the Indo-Australian and South Bismarck plates could be in the northwestern part of mainland Papua New Guinea, and (2) assuming that all the downward motion of the slab is due to pushing in the

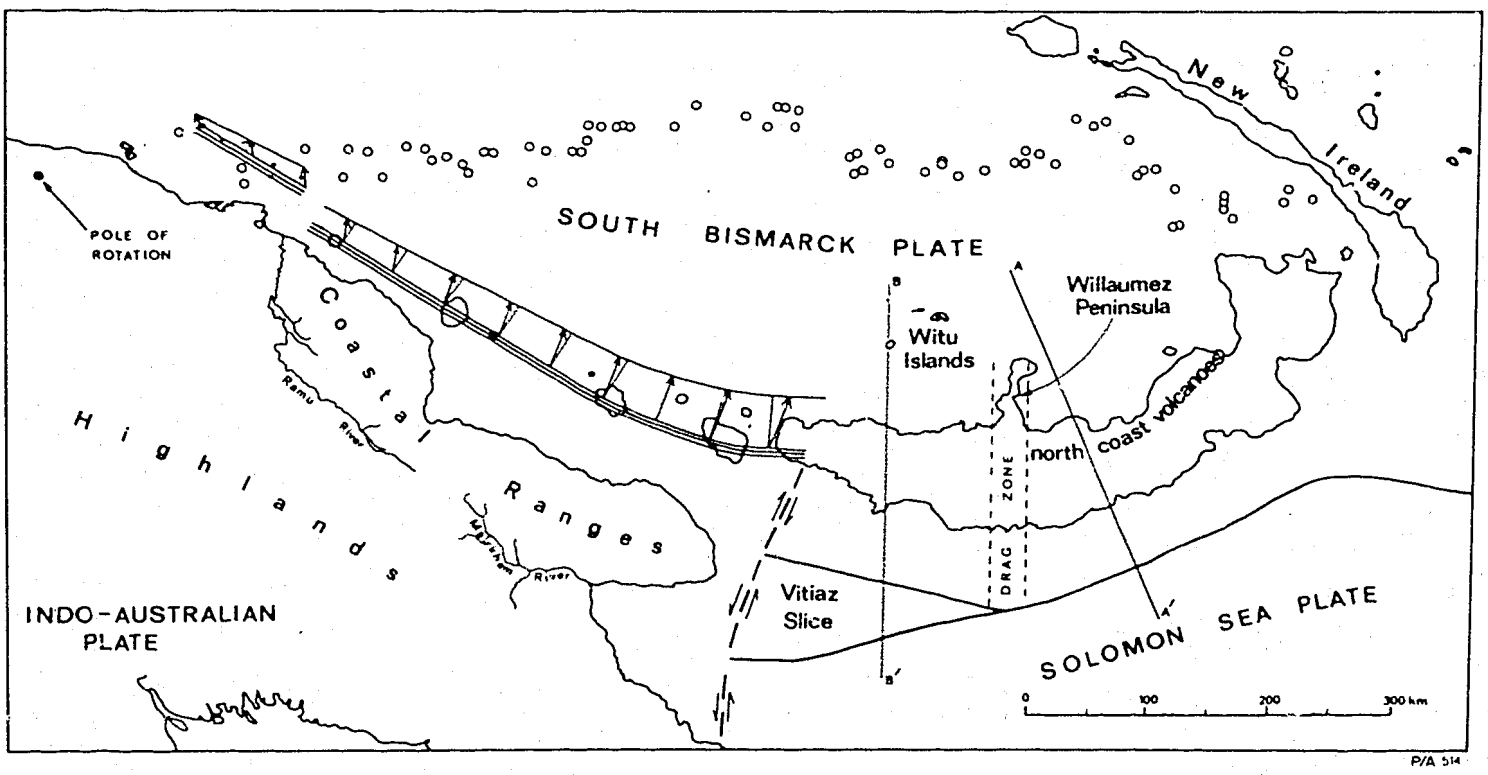

Fig. 39. Tectonic features at the southern margin of the Bismarck Sea. Open circles represent epicentres of earthquakes that define the northern margin of the South Bismarck plate (after Denham, 1973). This northern margin is thought to continue southeastwards and reach the Solomon Sea plate at a triple junction south of New Ireland (see Figs. 2 and 3). The three closely spaced lines north of the coastal ranges are hypothetical strike-lines for the upper surface of the postulated, northward-dipping slab beneath the western arc. The set of arrows illustrates the effect of plate convergence about a single position for a series of instantaneous poles of rotation (other positions in the northwest part of mainland Papua New Guinea have similar effects) - i.e., that those points at the upper surface of the downgoing slab further from the finite pole move greater distances for any rotation about the pole; in other words, rates of plate convergence increase away from the pole. The straight lines accompanying each arrow are normal to the strike-lines. Note that because of the differences in orientation of the strike-lines on either side of Long Island, the transcurrent components of movement for this particular pole position change from right-lateral west of the island to left-lateral east of it. A-A' and B-B' are lines of cross-sections in Figure 40A and B, respectively. See text for explanation of 'drag zone'.

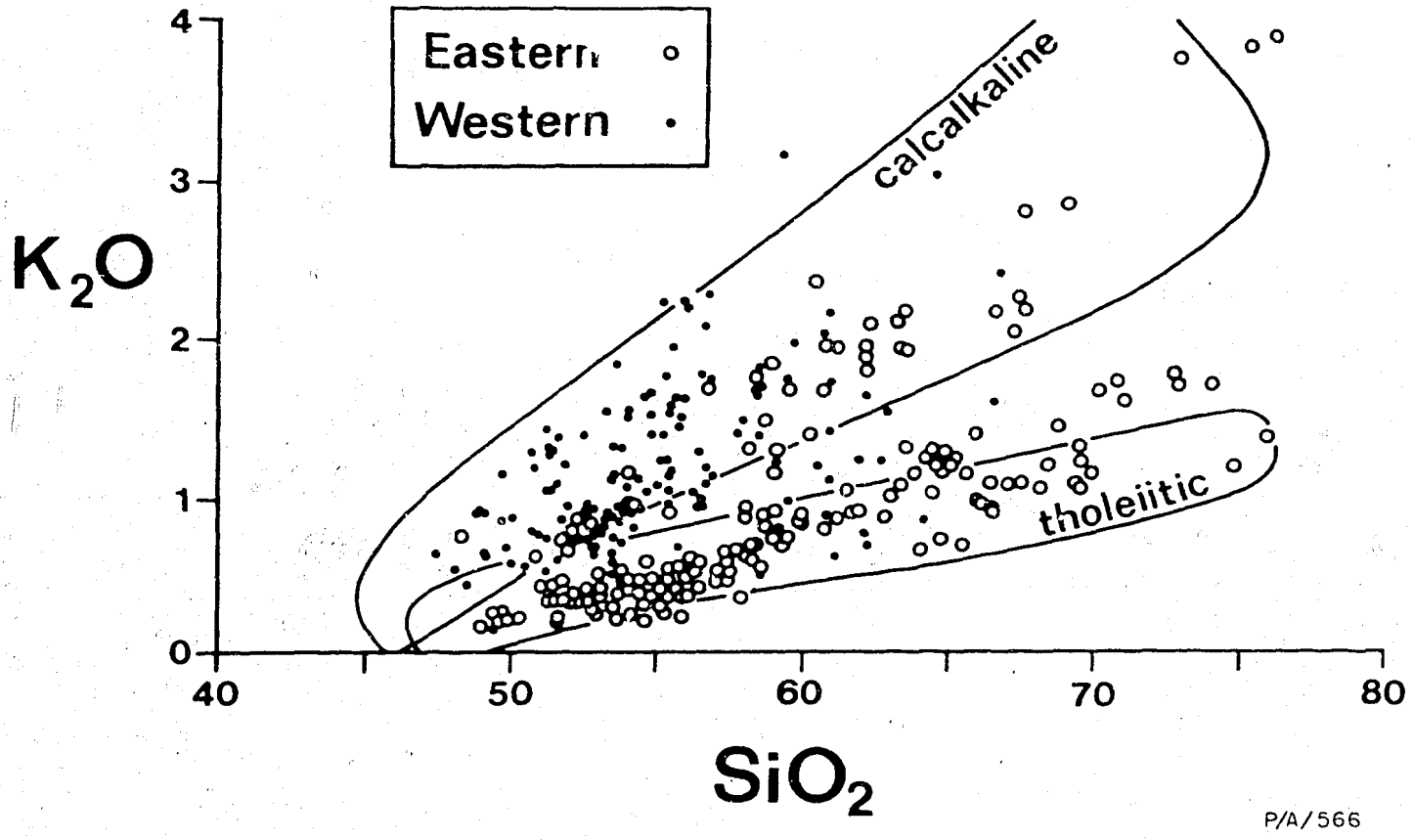

Fig. 30. K_2O:SiO_2 for rocks from the south Bismarck Sea volcanoes in relation to the generalized calcalkaline and tholeiitic field boundaries of Jakeš & Gill (1970).

same direction from the Indo-Australian plate (see above), it can be shown that for any finite period of time the magnitudes and directions of the relative velocity vectors change progressively along the contact of the two plates at depth. For example, using the pole position in Figure 39, rates of plate convergence increase proportionally between the Schouten Islands and the Cape Gloucester area because of the increasing distance from the pole. The direction of plate convergence will not, however, be at right-angles to the strike-lines in Figure 39, but will contain transcurrent components of motion. West of Long Island this transcurrent component will be right-lateral, but east of Long Island it will change to left-lateral, as distance from the pole of rotation increases, because of the change in orientation of the strike-lines. Similar changes in the rate of plate convergence (and the sense of transcurrent motion) can be proposed using many other pole positions in the northwestern part of mainland Papua New Guinea.

The above reasoning is partly invalidated if the present-day downward motion of the slab is due entirely to the gravitational effect of the slab's weight (see above). Even if this is so, rates of subduction will still be greater towards the east because the slab is colder there (and the mantle/slab density contrast accordingly greater), but the motion will not contain transcurrent components of motion; subduction will be normal to the postulated strike-lines throughout the length of the slab.

The above interpretation is based initially on the pole positions suggested by Krause (1973), who regarded the South Bismarck/Pacific plate boundary as a pure, left-lateral, transcurrent fault whose curvature defines the pole of rotation. However, not only does Krause (1973) seem to have overestimated the degree of curvature of the seismic zone across the Bismarck Sea, but the concept of left-lateral transcurrent motion has also been refuted - by Connelly (1976), and also by Taylor (1975) in an independent unpublished report.

Connelly and Taylor both argued that the Bismarck Sea floor is a marginal basin, and that the seismic zone crossing it is essentially a divergent boundary where spreading is accommodated in two, northwest-trending, left-lateral, transcurrent segments. Taylor regarded both transcurrent segments as straight linear features (although, in fact, they may be zones of deformation and slightly curved), and accordingly located the South Bismarck/Pacific plate boundary a long way from Papua New Guinea. In his triple-junction analysis, Taylor calculated that the rates of convergence between the South Bismarck and Indo-Australian plates were between 8.04 (in the west) and 9.3 (in the east) cm/year (see Table 1). These values are much higher than those (Table 1) estimated by Johnson & Molnar (1972), Curtis (1973), and Krause (1973), all of whom, however, regarded the Bismarck Sea seismic zone as a pure, left-lateral transcurrent boundary. Taylor's values also allow for very little difference in rates of plate convergence along the South Bismarck/Indo-Australian plate boundary. However, Connelly (1976) postulated that the rates of spreading at the Bismarck Sea seismic zone are demonstrably greater in the east than in the west, and that the present-day pole of rotation lies 'somewhere in the New Guinea mainland'. If so, the great circle containing the poles representing the plate boundaries at triple junction IBP (Fig. 2, Table 1) would pass through mainland Papua New Guinea, and the South Bismarck/Indo-Australian pole position would lie on it, possibly in or near the northwestern part of mainland Papua New Guinea (depending on the sense and rate of motion at the western end of the Bismarck Sea seismic zone - see below). Thus, although the reasons for Krause's (1973) location of the South Bismarck/Pacific pole of rotation may have been unfounded, the outcome for rates of convergence along the South Bismarck/Indo-Australian boundary may be more or less correct.

Implications for magma genesis

If rates of plate convergence and subduction are a primary influence on the thermal regimes of the slab and the over-

TABLE 1. RATES AND AZIMUTHS OF CONVERGENCE OF THE INDO-AUSTRALIAN AND SOLOMON SEA PLATES WITH THE SOUTH BISMARCK PLATE

Reference	I		S	
	Rate (cm/yr)	Azimuth (°E of N)	Rate (cm/yr)	Azimuth (°E of N)
Johnson & Molnar (1972)	3.3	23	9.2	343
Curtis (1973)	2.60 at IBP 5.22 at IBS	18 7.5	12.02	352
Krause (1973)*	0 at IBP 6.2 at IBS	- 31	6.2 at IBS 12.4 at BPS	5 or 327 327
Taylor (1975, unpublished)	8.04 at IBP 9.3 at IBS	29 29	11.65 at IBS 12.5 at BPS	11 8

*values calculated for a 'preferred' model in which BI pole is at IBP triple junction, and left-lateral slip rate between B and P is 13.5 cm per year (see text).

I = Indo-Australian plate

B = South Bismarck plate

S = Solomon Sea plate

P = Pacific plate

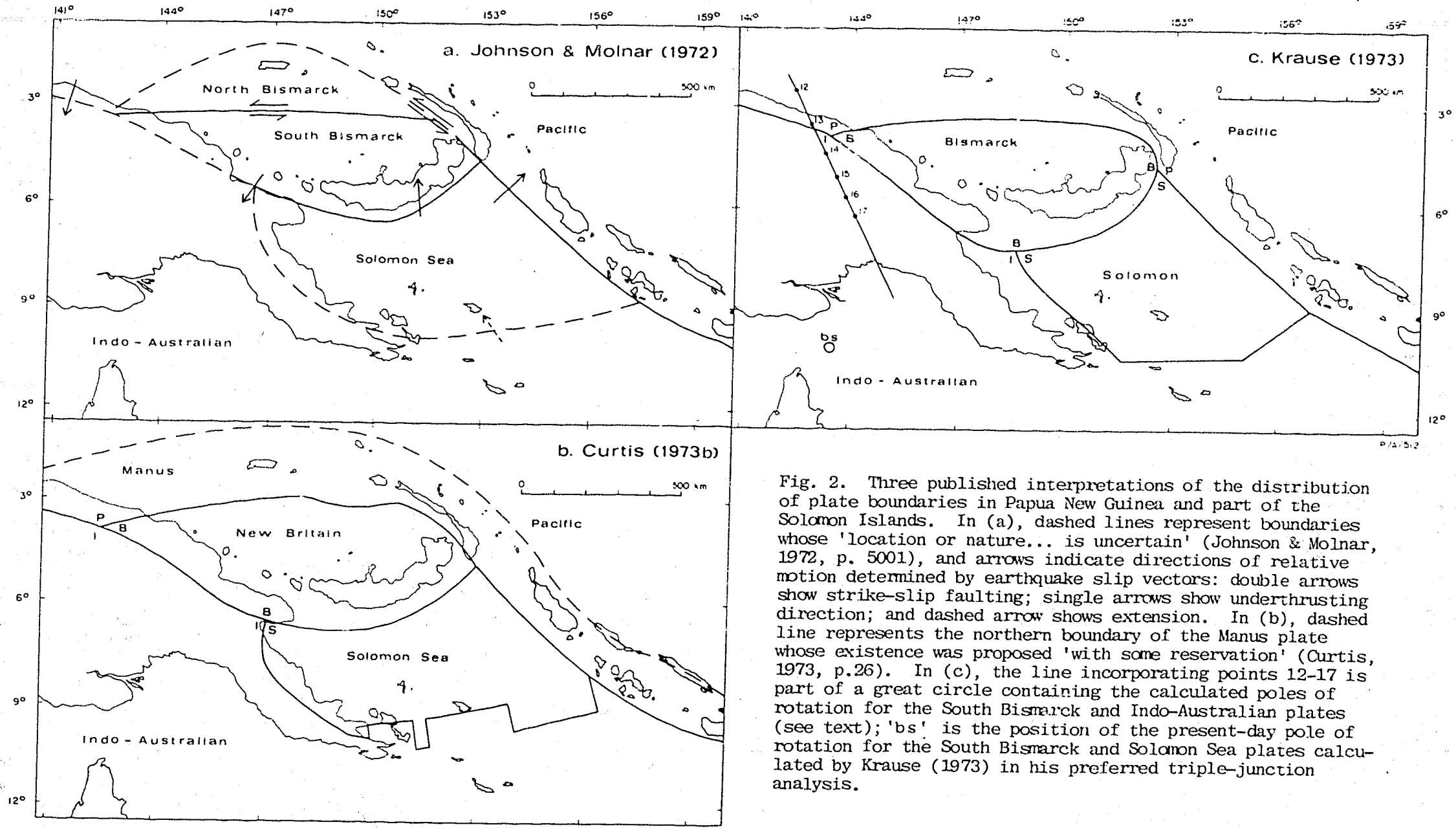

Fig. 2. Three published interpretations of the distribution of plate boundaries in Papua New Guinea and part of the Solomon Islands. In (a), dashed lines represent boundaries whose 'location or nature... is uncertain' (Johnson & Molnar, 1972, p. 5001), and arrows indicate directions of relative motion determined by earthquake slip vectors: double arrows show strike-slip faulting; single arrows show underthrusting direction; and dashed arrow shows extension. In (b), dashed line represents the northern boundary of the Manus plate whose existence was proposed 'with some reservation' (Curtis, 1973, p.26). In (c), the line incorporating points 12-17 is part of a great circle containing the calculated poles of rotation for the South Bismarck and Indo-Australian plates (see text); 'bs' is the position of the present-day pole of rotation for the South Bismarck and Solomon Sea plates calculated by Krause (1973) in his preferred triple-junction analysis.

lying upper mantle (see p. 87), the conclusion that rates of present-day subduction, and rates of plate convergence since the late Pliocene, increase progressively eastwards along the South Bismarck/Indo-Australian boundary has important consequences for theories of magma genesis. Because of these lateral changes, the relative disposition of isotherms may differ in all sections drawn perpendicular to the western arc. Slab-derived water and melts may therefore rise from the downgoing slab at different depths in each section, and may cause partial melting at different depths in the overlying mantle peridotite, which may be chemically stratified. Magmas beneath each part of the arc may therefore be generated under unique sets of conditions of pressure, temperature, contents of volatiles, and composition and volume of the slab melts (which may mix with the mantle-derived magmas). The possible interactions between these variables (and others listed on p. 87) are, of course, so complex that they cannot be defined satisfactorily at present. However it is suggested that the changes in rock compositions along the western arc are functions of differences in the thermal regimes beneath each part of the arc, and that these, in turn, depend upon differences in rates of plate convergence and subduction.

These interpretations are consistent with the apparent increase in the volume of subaerial volcanic rocks from west to east along the western arc. The volumes of slab-derived water and melts may be greater in the east than in the west, because a greater supply of subducted, water-rich crustal rocks will be available for dehydration or fusion. These larger volumes in the east are likely to induce more extensive partial melting of mantle peridotite than in the west, and possibly, therefore, lead to the eruption of a proportionally greater volume of magma.

The above interpretation provides conditions for magma genesis broadly analogous to those in the eastern arc. However, unlike the eastern arc, where volcanoes can be related to present-day depths to the New Britain Benioff zone, there is great uncertainity

in the western arc about how the distribution of the volcanoes and the compositions of their rocks are related to depths to an underlying lithospheric slab. This is because, firstly, the model of a near-vertical slab is largely inferred, and present-day seismicity gives only a limited indication of the slab's true form; and secondly, because in the model of a near-vertical plate boundary, volcanoes cannot be related to a limited depth range to the slab as easily as they can where the slab is inclined at a much lower angle. However, some tentative explanations are offered for the compositional variations along the western arc; these are based on the relation described above and on comparisons with the compositions of the eastern volcanoes.

In earlier parts of the Report, the chemistry (e.g., Fig. 31), distribution (p.21), and rock type relative abundances (p. 28) of the Schouten Islands' volcanoes (zone A) were shown to be different from those of the other volcanoes in the western arc. In the following, therefore, generation of primary magmas beneath zones B, C, and D, is discussed separately from that beneath zone A.

Zones B, C, and D

Rocks with $Mg/(Mg + Fe^{2+})$ values greater than about 63 are present in each of the zones B, C, and D. These rocks contain low percentages of normative olivine or normative quartz, except in four samples whose normative olivine contents exceed 14 percent and percentages of olivine phenocrysts exceed 9 percent. Apart from these four rocks (in which the olivine phenocrysts may have accumulated to form the high normative olivine values), the low-ol (less than 9 percent) and low-Q (less than 8 percent) rocks are suggested to be near-equivalents to primary magmas generated by hydrous partial melting in the upper mantle. In zone B, these rocks have been found on Aris, Manam, and Bagabag, but not on Karkar; in zone C, on Tolokiwa, but not commonly on Long (whose rocks have unusually low MgO contents and unusually high iron contents - see Figs. 23 and 24); and in zone D, on Sakar and Ritter and in the Cape Gloucester area.

In each of the zones B, C, and D, the low-ol and low-Q rocks are similar in their degrees of silica saturation, for they plot at similar distances from the Hy-Ab plane (Fig. 14). However, they show marked differences in composition when rocks of the same silica content are compared with one another. In particular, the zone C rocks are generally higher in K_2O, Na_2O, K_2O/Na_2O, P_2O_5, $FeO + Fe_2O_3$, and MnO, and lower in CaO and MgO, than those of zones B and D; and zone D rocks are higher in K_2O than those of zone B (Fig. 31).

Another important comparison is that the basic rocks from any one of the western zones B, C, and D are generally higher in K_2O, K_2O/Na_2O, P_2O_5, and TiO_2 than those with the same silica content from the eastern zones E and F. They are, however, closer in chemical composition to the rocks of the eastern zones G and H, although they have generally higher K_2O/Na_2O values, and zone C rocks are notably higher in K_2O. If similarities in composition of island-arc rocks can justifiably be equated with similarities in petrological processes, then the rocks of zones B, C, and D may have formed under conditions which were different from those of the eastern zones E and F but were similar to those of zones G and H; that is, beneath zones B, C, and D, water (perhaps containing solvent elements) or water-bearing siliceous melts (or both) were generated from subducted eclogitic crust at the surface of the steeply inclined downgoing slab, and rose, melting the upper mantle peridotite at different levels (possibly corresponding to different initial peridotite compositons), with possible mixing of slab-derived fluids. In part, the downgoing slab may have also provided geodynamic conditions favourable to the upwelling of hot mantle in the manner postulated for the development of basalts in marginal basins (see below). Because rocks equivalent in composition to those of zones E and F appear to be absent from zones B, C, and D, subsolidus breakdown of amphibole in the downgoing slab is inferred not to have played an important part in the genesis of primary mafic magmas beneath zones B, C, and D.

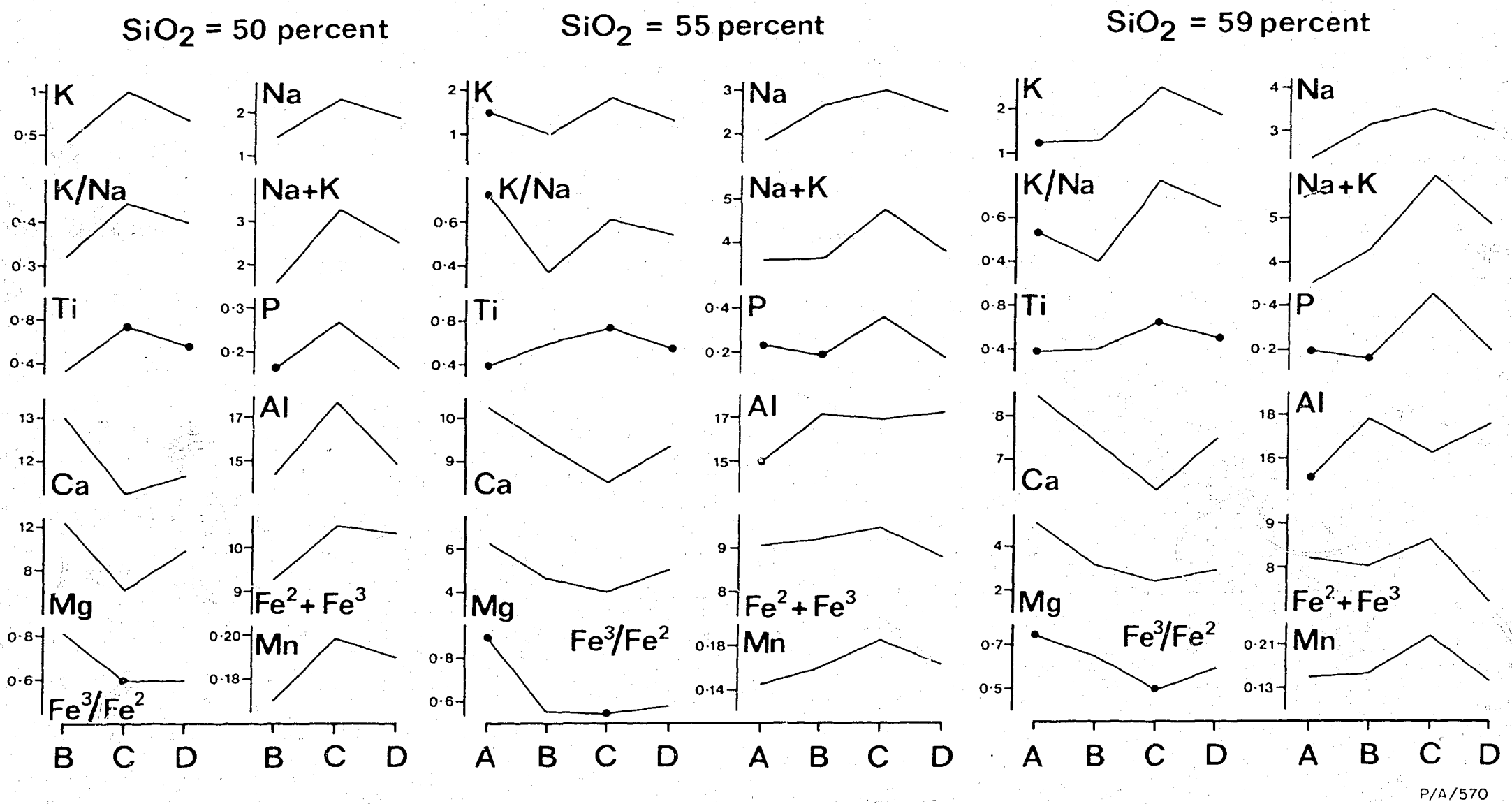

Fig. 31. Generalized oxide variations with different silica contents in rocks from the western arc. Individual oxide values for each zone are arithmetic means (dots) or were determined from the regression lines in Figures 15-24, 26, and 27 (see text for details).

In addition to the chemical differences mentioned above, there are two other prominent differences between the rocks of zones B, C, and D, and those of zones G and H. The first difference is that the western rocks are highly porphyritic, whereas those of zone H and of the northernmost volcano of zone G, Dakataua, have low phenocryst contents (Fig. 12). If high phenocryst contents are a function of high water contents (see above), the rocks of zones B, C, and D may have been generated under higher partial pressures of water than those of the eastern zones G and H.

The second difference is that basalts are relatively more common in zones B, C, and D than they are in the eastern zones G and H, and that dacites and rhyolites, which are common in the eastern arc, are extremely rare in zones B, C, and D (see p. 28). The differences in relative abundances of basalt may be due to differences in rates of magma ascent. In the western zones, primary magmas may have risen rapidly through fractures in the upper parts of the South Bismarck plate, as suggested by the lines formed by the volcanoes in zones B, C, and D (see p. 20 and Fig. 5). Thus, rapid rates of ascent may have given little opportunity for the primary magmas to fractionate much beyond high-silica andesite compositions. In contrast, primary magmas in the eastern arc may have risen through the overlying wedge of upper mantle and crust above the inclined Solomon Sea slab without the benefit of major zones of weakness, or fractures, to aid their ascent. Ascent rates may therefore have been much slower in the eastern arc, allowing the primary magmas more time to fractionate to liquids which were much richer in silica so that fewer basic magmas reached the surface.

Alternatively, the high proportion of basic rocks in the western arc may be due to the upwelling of hot mantle beneath the Bismarck Sea marginal basin to relatively shallow levels where the primary basalts were generated (cf. some zone H basalts - see above). Some marginal basins are believed to develop over the deeper parts of inclined downgoing slabs (Karig, 1971), and mantle upwelling

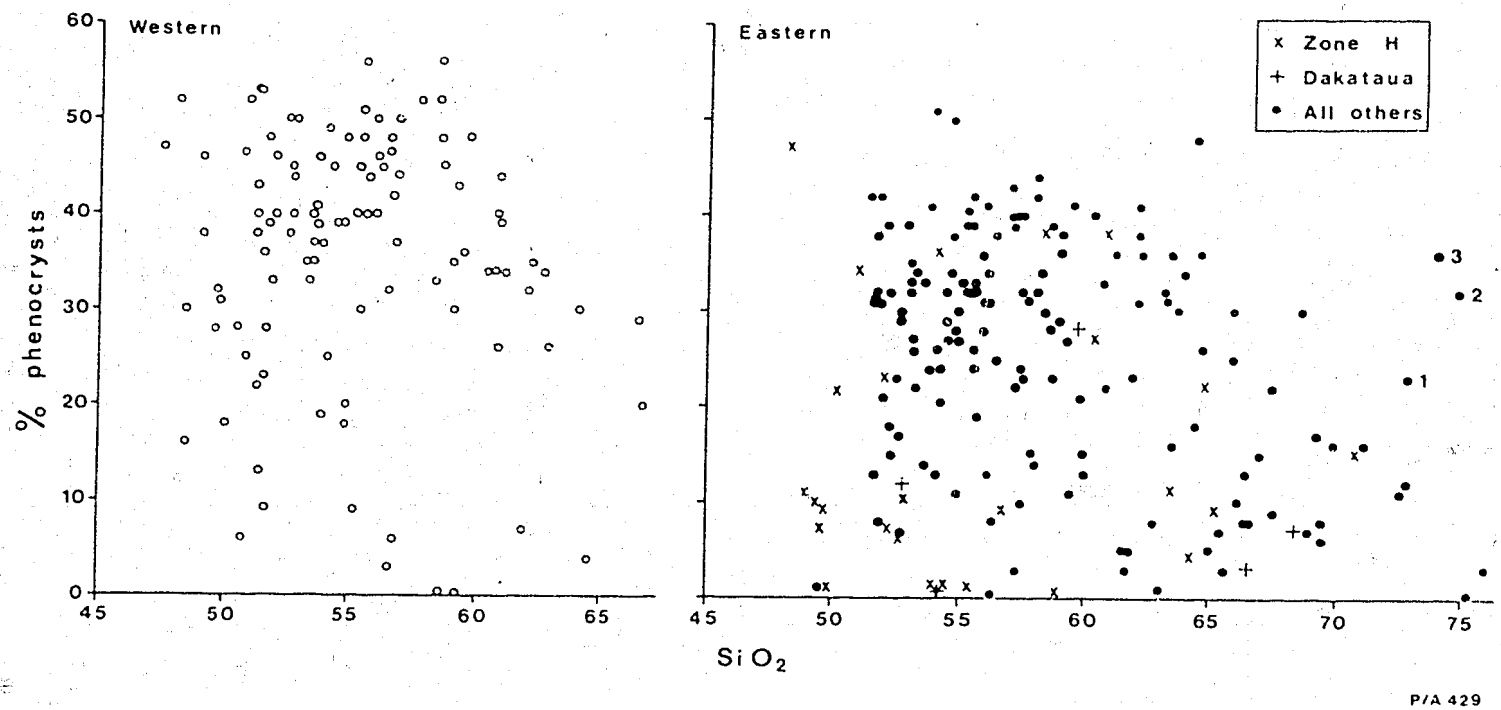

Fig. 12. Volume percent total phenocryst contents v. weight percent SiO_2 for 162 eastern and 106 western rocks (including data of Lowder & Carmichael, 1970, and Blake & Ewart, 1974). Samples 1, 2, and 3 are quartz-rich rhyolites from Sulu Range containing 4, 9, and 13 percent quartz phenocrysts respectively.

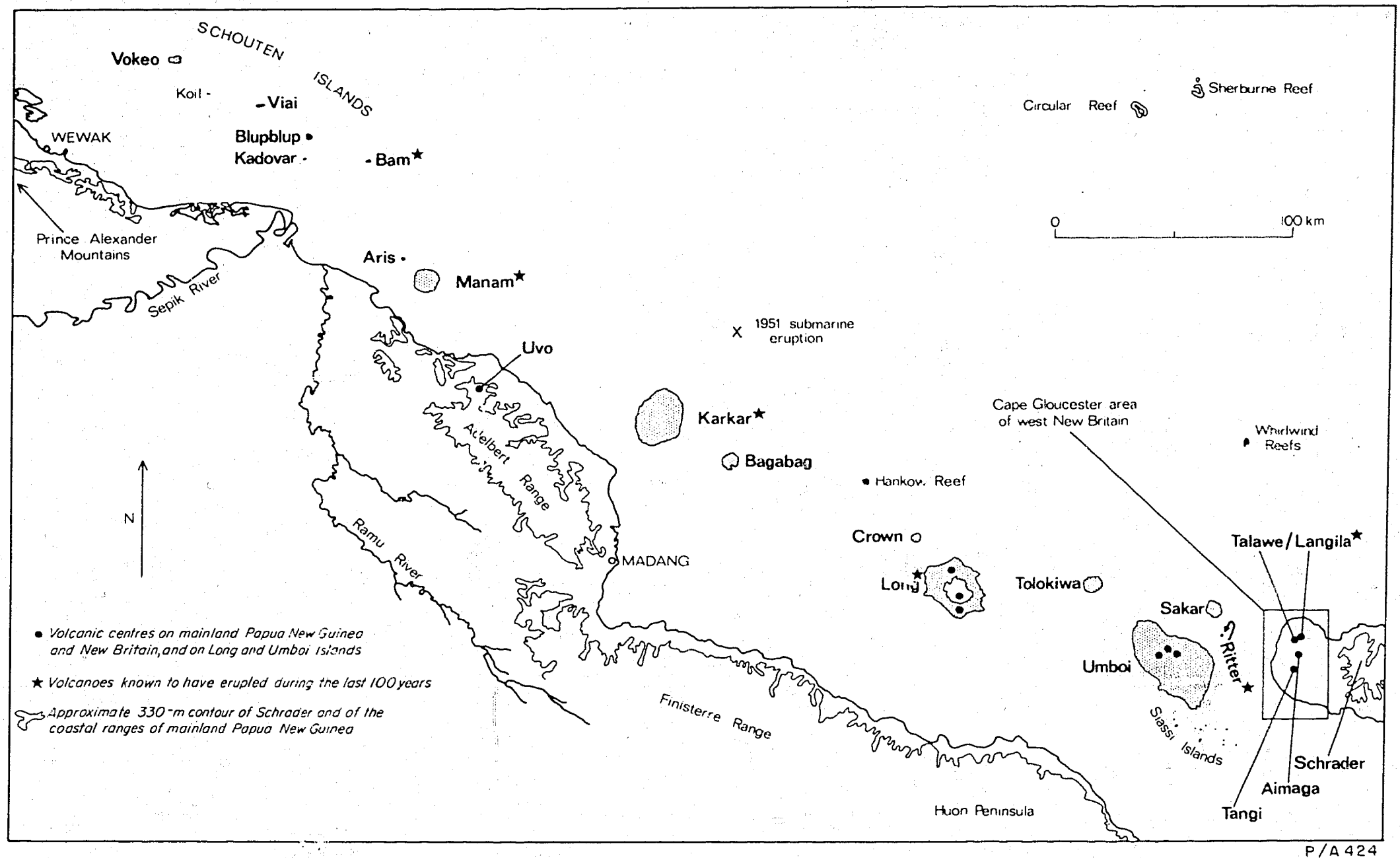

Fig. 5. Main volcanic centres of the western arc. Islands are shown stippled or solid, and volcanic islands are indicated by bold lettering. Langila is a cluster of satellite craters on the eastern flank of Talawe.

and basalt extrusion take place up to a few hundred kilometres from the submarine trench. However, where a slab is essentially vertical - as beneath the western arc - upwelling and extrusion may take place much closer to the shallowest parts of the downgoing slab. If mantle upwelling also enhances lithospheric dilatation, some rising basaltic magmas may have had little opportunity to fractionate before they erupted. A correlation between near-vertical downgoing slabs and basaltic volcanism was also pointed out by Cox & Bell (1972) for the Solomon Islands region.

In summary, therefore, the model favoured for petrogenesis in zones B, C, and D, is as follows. Throughout the late Cainozoic, the near-vertical downgoing slab beneath the South Bismarck plate moved at rates which were higher towards the east. These differences in subduction rates produced differences in the thermal regimes beneath each zone, and may therefore have controlled the depths of origin, composition, and relative volumes of the water and water-bearing siliceous melts generated from the downgoing slab beneath each zone. Movement of these slab melts or water (or both) into different parts of the overlying, or adjacent, upper mantle resulted in different degrees of chemical modification of peridotite, which may have welled up towards the surface. Partial melting generated primary magmas of different compositions, and fractionation of the primary magmas during their relatively rapid rise to the surface resulted in rocks mainly of basaltic and andesitic composition. Thus, the composition of the rocks depend on the original compositions of the primary magmas which, ultimately, were functions of different rates of subduction along the western arc.

Zone A - the Schouten Islands

Compared with the volcanoes of zones B, C, and D, those of the Schouten Islands show several distinctive features. Firstly they constitute a volcanic line which is offset about 25 km from the remainder of the western arc (Figs. 1, 3, and 39). Secondly,

volcanism appears to have migrated eastwards along the line (see p. 23). Thirdly, basalts have not been found on any of the islands; only andesites and dacites seem to be present (p. 28). Fourthly, the distinctive petrological features of zone A rocks, compared with those with the same silica content from the other zones in the western arc, are higher percentages of clinopyroxene phenocrysts (Fig. 13), higher degrees of silica oversaturation (Fig. 14), lower Na_2O, $Na_2O + K_2O$, TiO_2, and higher CaO, MgO, and Fe_2O_3/FeO values (Fig. 31). Thus, in many respects the zone A rocks represent extreme compositions for the western arc. This is consistent with the view that the Schouten Islands correspond with the lowest rates of convergence between the South Bismarck and Indo-Australian plates, and with the slowest descending portion of the underlying slab. Nevertheless, considerable ranges in K_2O, K_2O/Na_2O, and P_2O_5 values in the zone A rocks (Figs. 15, 17, and 20) imply different conditions of magma genesis beneath each volcano in zone A.

No high-magnesia rocks have been found in the Schouten Islands, although five samples from Vokeo have sufficiently high $100Mg/(Mg + Fe^{2+})$ values to have been in equilibrium with upper mantle peridotite; these samples contain 60 percent SiO_2 and less than 5.5 percent MgO, and are unusually low in iron (Figs. 23 and 24). With the possible exception of these samples, the analysed rocks from the Schouten Islands may be products of crystal fractionation of originally high-magnesia primary magmas generated in the upper mantle. Perhaps the region beneath the Schouten Islands is characterized by the absence of mantle upwelling; primary magmas may have formed in a non-dilatational region, such that they were able to rise more slowly and fractionate more extensively than those in zones B, C, and D.

Vokeo and Viai, at the western end of the Schouten Islands, show two distinctive features: (1) their rocks have the lowest K_2O, K_2O/Na_2O, and P_2O_5 values of all the western rocks (Figs. 15, 17, and 20); and (2) they are the most dissected of the volcanoes in the Schouten Islands (p. 23). These differences may be related to an eastward migration of the western end of the South Bismarck/Pacific plate boundary (Fig. 42).

Taylor (1975) suggested that the western end of the boundary had a definite divergent component of motion. However, east-west strike-slip motion is indicated by earthquake focal mechanism solutions (Johnson & Molnar, 1972; Curtis, 1973; Ripper 1970, 1975, in prep.a), and Connelly (1976) found no evidence from magnetics for a significant component of spreading. When subaerial volcanism first commenced in zone A, the South Bismarck/Pacific boundary may have been west of Vokeo, near the head of the submarine valley described on page 15 (Fig. 42). The rocks erupted at this time are thought to be represented on Vokeo and Viai; they are low in K_2O, K_2O/Na_2O, Na_2O, P_2O_5, and TiO_2, and are therefore of similar composition to those of zones E and F in the eastern arc. By analogy, the compositions of these rocks may have developed by fractionation of primary magmas derived by the process described above, in which water - released by sub-solidus dehydration of amphibole in the downgoing slab - enters the overlying upper mantle and causes partial melting of peridotite.

After this first phase of volcanism, the South Bismarck/Pacific boundary may have migrated eastwards to a position between Viai and Blupblup, as shown in Figure 42. At the present day, therefore, Vokeo and Viai are on the Pacific plate, and, because they are no longer associated with the active Indo-Australian/South Bismarck plate boundary, they have become volcanically inactive. On the other hand, Blupblup, Kadovar, and Bam lie on the South Bismarck plate, which - up to modern times - has overridden the Indo-Australian plate. As described on page 23, Bam volcano is still active; and Blupblup and Kadovar retain youthful volcanic landforms, so cannot yet be regarded as extinct.

A possible variation on the above mechanism of plate boundary migration is that, throughout the late Cainozoic, the South Bismarck/Pacific plate boundary was a zone of strike-slip faults - not a single fault as shown schematically in Figure 42. In this alternative model, the two PB boundary positions (Fig. 42)

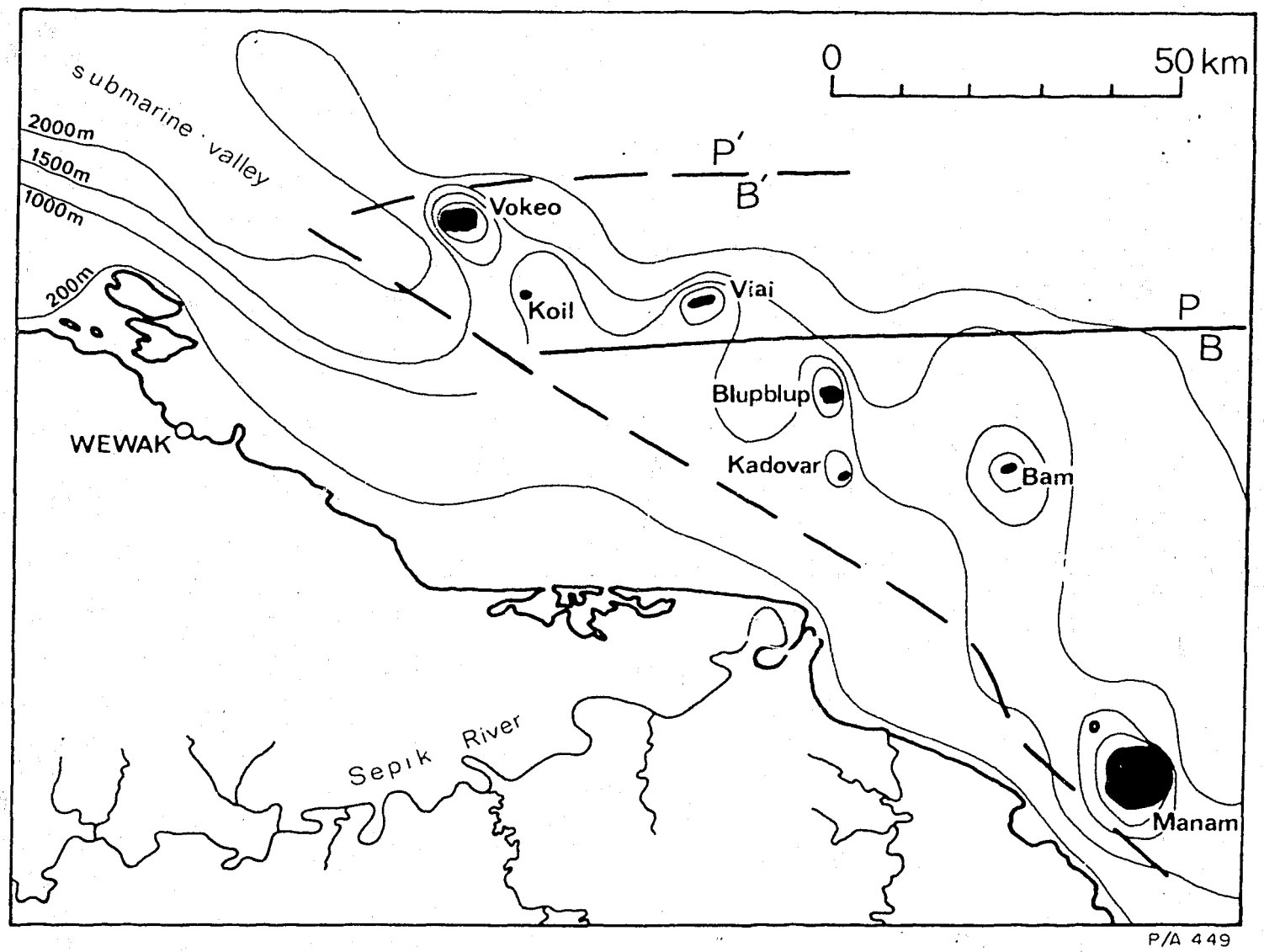

Fig. 12. Postulated relations between late Cainozoic plate boundaries at the western end of the western arc. Bathymetry adapted from 1:1 million geological map of Papua New Guinea (Rogerson et al., 1972). Assuming the Pacific(P)/South Bismarck(B) plate boundary (PB) is a single fault, the present-day position of PB is shown as a solid line between Viai and Blupblup: Vokeo and Viai are on the Pacific plate (Koil is a coral island), and Blupblup, Kadovar, and Bam are on the South Bismarck plate. A possible older position for the Pacific/South Bismarck plate boundary is shown by P'B', in which case all the volcanoes are on the South Bismarck plate (see text for an alternative interpretation). Longer dashed line represents speculative strike-lines for the upper surface of the downgoing slab.

represent parts of the same plate boundary which were active at different times. In the earlier part of the late Cainozoic, much of the strike-slip movements may have been taken up along faults north of Vokeo. Later movements may have been mainly along faults between Viai and Blupblup when the northern strike-slip faults were inactive.

The rocks of Blupblup, Kadovar, and Bam have higher K_2O, K_2O/Na_2O, and P_2O_5 values than those with the same silica content from Vokeo and Viai. These differences in composition imply pronounced differences in courses of differentiation, or changes in the conditions of partial melting in the upper mantle, or both. Because the rocks of Blupblup, Kadovar, and Bam have K_2O, K_2O/Na_2O, and P_2O_5 values similar to those of the eastern zones G and H and of the western zones B, C, and D, they may have originated by a similar process - that is, by fractionation of primary magmas generated when water or water-rich siliceous melts derived from the downgoing slab entered the upper mantle and caused partial melting of peridotite.

COMMENTS ON COURSES OF CRYSTAL FRACTIONATION

Basalt fractionation

In the previous sections, possible causes were discussed for the chemical variations of magmas generated at peridotitic source regions beneath the eastern and western arcs. However, few, if any, of the volcanic rocks are likely to have the exact composition of the primary magmas at the time they left the source region; rather, many of the magmas probably fractionated.

Crystallization of island-arc primary magmas probably commences soon after they begin to rise from their source in the upper mantle (e.g., Nicholls & Ringwood, 1973), and the courses of crystallization for the magmas probably involve exceedingly complex phase equilibria. Jamieson (1970), for example, drew particular attention to the complications of polythermal, polybaric crystallization in the anhydrous system diopside-forsterite-silica, and emphasized the important role of different rates of magma ascent. In natural basalt systems, phase relations will be even more complex, and possibly will be most complex in island-arc basalts in which fugacities (especially of H_2O, O_2, H_2, and CO_2) may differ, not only during the ascent of a single magma body, but at different sites of magma generation. The purpose of this section, however, is not to consider complexities; rather, it is to draw attention to some general features of fractionation in the south Bismarck Sea rocks which will serve as a broad basis for more detailed future studies.

Rates of ascent

On page 117, differences in rates of magma ascent were proposed to account for the differences in rock-type relative abundances in the western and eastern arcs. Ascent rates beneath zones B, C, and D were suggested to have been relatively fast, with the result that the magmas did not have the opportunity to fractionate much beyond that of basaltic or andesitic compositions. Rocks of more silica-rich compositions are, however, more common in zone A, and zones E to H, where magmas may have risen more slowly (see above). Other lines of evidence support these interpretations.

Firstly, as shown in Table 5 and discussed on page 29, in seven of ten volcanoes the younger rocks are consistently richer in silica than the older rocks; this suggests that faster-rising and less fractionated magmas were erupted first, and were followed

TABLE 5. SIMPLIFIED STRATIGRAPHIES OF TEN VOLCANOES

Volcano	Sequence
Kadovar* (Zone A)	low-silica andesites → crater formation → high-silica andesite (only slightly richer in silica).
Aris* (Zone B)	low-silica andesites → crater formation → high-silica andesites.
Long+ (Zone C)	basalts, type 1 → basalts, type 2 (richer in silica), and andesites associated with cauldron subsidence → basalts, type 2.
Sakar* (Zone D)	basalts → crater formation → high-silica andesites.
Talawe/ Langila* (Zone D)	Talawe basalts and low-silica andesites → Langila low-silica andesites (richer in silica). Langila is a satellite volcano on the northeastern flank of Talawe.
Hargy/ Galloseulo* (Zone E)	andesites → cauldron subsidence → andesites (mainly richer in silica) → Galloseulo dacites.
Bamus* (Zone E)	andesites (mainly low-silica) → collapse event → high-silica andesites.
Lolobau (Zone F)	andesites and (?)dacites → basalt → cauldron subsidence → basalt (poorer in Fe) → dacites and rhyolites. Several samples of uncertain relative age.
Unea* (Zone H)	basalts and andesites → cauldron subsidence → andesites (mainly richer in silica).
Garove (Zone H)	dacites and rhyolites → low-silica andesites → cauldron subsidence → basalts. Several samples of uncertain relative age, including the basalts, which are only assumed to be post-caldera in age.

The prefixes 'low-silica' and 'high-silica' are omitted where both varieties of andesite are represented. Comments in parentheses describe rocks in relation to those of the same name in an earlier part of the same eruptive sequence. Zones A-H are shown in Figure 10.

*Volcanoes in which younger rocks are consistently more siliceous than older ones.

+Long should be considered as three volcanoes because two older basalt (type 1) cones flank a mainly younger central caldera complex (basalts type 2 and andesites).

by slower-rising ones which had greater opportunity to fractionate. Secondly, in three examples of analysed inclusion/host-rock pairs, the inclusions are more basic than the rock containing them (see p. 38); this suggests that slower-rising, silica-rich magmas plucked rock inclusions from the walls of conduits which had previously been used by fast-rising, more basic magmas. Thirdly, the presence of amphibole in andesites from zones B, C, and D, and its apparent absence from andesites in the eastern arc, suggest that in the east the comparatively slow upward movement of magmas favoured the breakdown of amphibole as they approached the surface, whereas in zones B, C, and D the amphibole-bearing andesites rose more quickly, and were erupted before the amphibole could dehydrate.

If these interpretations are correct, and, assuming that primary magmas in the western arc were not generated at depths much greater than those in the eastern arc, it follows that higher-pressure crystal-liquid equilibria may have had a greater influence on fractionation in the eastern arc than in the western arc. However, zone A may be an exception: the compositions of its rocks - among which basalts appear to be absent - are consistently different from those with the same silica content from the western arc, and more closely resemble those of the eastern arc; therefore, the primary magmas of zone A may have risen more slowly, and fractionated for a longer time under higher pressures than those of the other western zones. In the eastern arc, basalts (including olivine tholeiites) are common in the volcanoes north of Unea in zone H. These too, therefore, may be exceptions to the general case of slow rates of ascent for magmas in the eastern arc; like the basalts of zones B, C, and D, they may have risen to the surface comparatively rapidly, perhaps because of mantle upwelling and crustal dilatation (see above).

Fractionating minerals

Primary magmas generated under hydrous conditions by partial melting of peridotite at pressures greater than about 20 kb are

likely to crystallize garnet and clinopyroxene during the early part of their ascent to the surface (cf. Green & Ringwood, 1968; T.H. Green, 1972; Nicholls & Ringwood, 1973). At lower pressures, these magmas, and those hydrous primary magmas generated in the upper mantle at pressures of less than about 20 kb, will subsequently undergo more complex fractionation trends mainly involving olivine, clinopyroxene, orthopyroxene, amphibole, plagioclase, and iron-titanium oxides.

The fractionation of subsilicic amphibole from basalts offers a particularly effective means of producing voluminous silica-rich derivatives, and has been suggested as an important process by several investigators (e.g., Green & Ringwood, 1968; Nicholls, 1971; Allen et al. 1972; Cawthorn et al. 1973a; Boettcher, 1973). The amphibole-bearing basalt inclusions of Aris (see p.38) are striking evidence for the crystallization of amphibole in the early stages of fractionation. Whereas olivine and clinopyroxene separation will lead to iron-enriched residues, early separation of iron-bearing amphibole will prevent iron-enrichment, and will produce the iron-poor compositions which are characteristic of many island-arc rocks, including those of the south Bismarck Sea (cf. Green & Ringwood, 1968).

According to Osborn (1959, 1969), low iron:magnesium ratios result when 'constant pO_2' (in effect, high oxygen fugacity) is maintained in a fractionating magma. In this controversial theory he suggested that, if high oxygen fugacites are maintained, magnetite crystallization is favoured, thus precluding strong iron-enrichment. In the south Bismarck Sea rocks, high Fe_2O_3/FeO values appear to correlate with high MgO/Fe_2O_3 + FeO values (see Table 11), but this correlation has not been proved to be due to enhanced separation of magnetite under oxidizing conditions. (For debates on Osborn's model, see, for example, Smith & Carmichael, 1968; Taylor et al., 1969; Lowder & Carmichael, 1970; Eggler & Burnham, 1973; Boettcher, 1973.)

Liquid lines of descent

Each of the minerals listed above may have played a significant role in the fractionation of many batches of primary magma between the time of their generation in the upper mantle and their eruption at the surface. The compositions of these magmas are believed to have followed complex evolutionary courses, and the composition of each rock at the surface probably represents the end-product of a single liquid line of descent formed by subtractions, and modified by additions, of crystals.

The rocks of any one volcano are not necessarily members of the same liquid line of descent. They may represent the results of courses of fractionation which were similar to one another, but, more probably, each of them represents the termination of different liquid lines of descent (including their modifications by crystal accumulation). The characteristics of each of these lines will have depended primarily on differences in the original compositions of the primary magmas, and on differences in the rates of magma ascent. The courses of fractionation for the rocks of any one volcano therefore define a 'bundle' of individual liquid lines of descent, rather than a single line of chemical evolution. The 'bundle' of each volcano has given rise to intravolcano compositional variations (see p. 69).

This concept has implications for attempts to relate rock types by mass-balance calculations involving phenocryst phases. Lowder & Carmichael (1970) and Lowder (1970), for example, suggested that the compositions of 10 rocks, and of the groundmass glass of an eleventh rock, from Willaumez Peninsula may represent a liquid line of descent; they calculated the percentages of phenocrysts of given compositions that would have to be extracted from each one of their 10 whole-rock samples to leave a residue of composition

similar to that of another of their rock samples - its neighbour farther down the supposed liquid line of descent; the groundmass glass of their eleventh sample - with a composition similar to that of rhyolites on Willaumez Peninsula - was at the base of their supposed liquid line of descent. However, the eleven compositions are unlikely to define a liquid line of descent, for two reasons.

Firstly, the 11 rocks are from six different volcanoes: six rocks were collected from Dakataua at the northern end of Willaumez Peninsula, and the others were taken from separate centres as far south as Garbuna (Fig. 6). As individual volcanoes erupt rocks with distinctive compositional traits (see p.74), which implies independent trends of evolution for the rocks of different volcanoes (see also Lowder & Carmichael, 1970, p. 30), 11 rocks from six volcanoes that are spatially independent of one another are unlikely to be related to a single liquid line of descent.

Secondly, three of the six volcanoes are in the northern part of zone G, and the other three are in the southern part (Figs. 6 and 10). On page 101 it was concluded that the compositions of the primary magmas generated beneath zone G differed in the northern and southern parts - in particular, the primary magmas in the south had higher K_2O/Na_2O values than those in the north. If true, then the 11 rocks analysed by Lowder and Carmichael were derived from primary magmas of at least two different compositions, so they cannot lie on the same liquid line of descent.

Lowder and Carmichael calculated that crystal fractionation of a basaltic parent at high levels in the Earth's crust might have controlled the generation of the magmas of northern Willaumez Peninsula, but they emphasized that their model did not account for the dominance of andesite in the area. Low-pressure fractionation of crystals in the proportions commonly found as phenocrysts in these rocks is unlikely to have yielded large volumes of silica-rich magma,

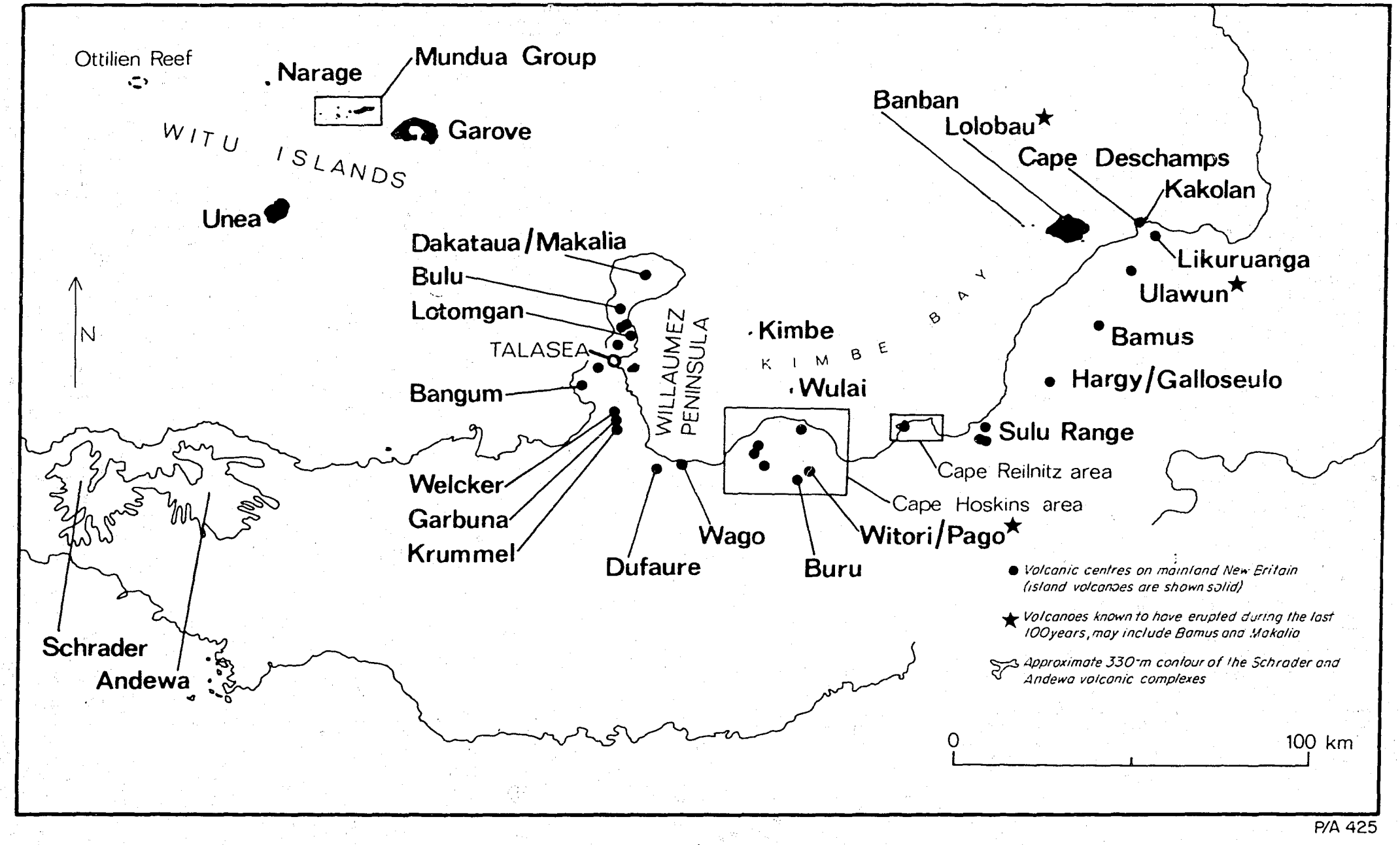

Fig. 6. Main volcanic centres of the eastern arc. Makalia, Pago, and Galloseulo are post-caldera volcanoes which respectively lie inside the older volcanoes of Dakataua, Witori, and Hargy.

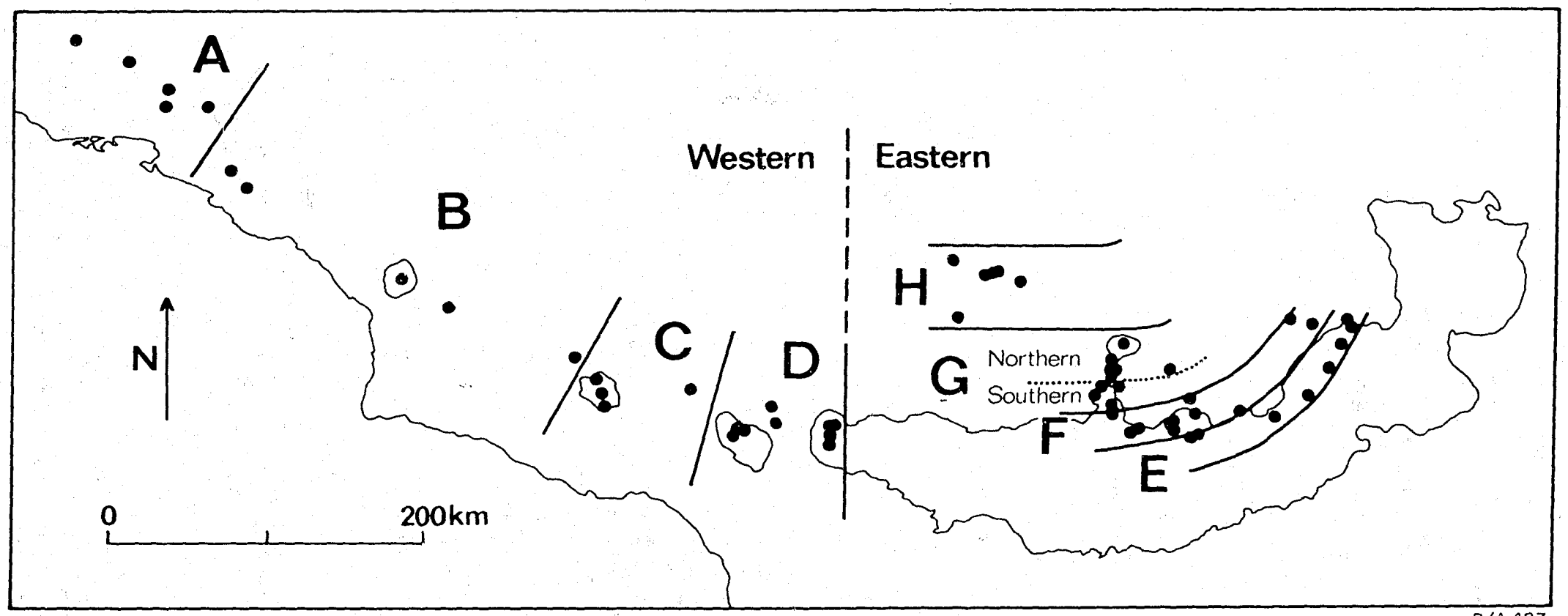

Fig. 10. South Bismarck Sea volcanoes (solid circles) grouped into western zones - A, B, C, D - and eastern zones - E, F, G, H. Zone A - Schouten Islands. Zone B - Aris to Crown. Zone C - Long and Tolokiwa. Zone D - Umboi to Cape Gloucester area. Zone E - Kakolan Island, Cape Deschamps, Likuruanga, Ulawun, Bamus, Hargy/Galloseulo, Sulu, Witori/Pago, and Buru. Zone F - Lolobau Island, Banban Island, Cape Reilnitz area, Cape Hoskins area (excluding Witori/Pago and Buru), Wulai Island, Dufaure, Wago, and Krummel. Zone G - Willaumez Peninsula (excluding Krummel) and Kimbe Island; the 'southern' volcanoes of zone G are Garbuna, Welcker, Bangum, and all those south of Lotomgan near Talasea Harbour. Zone H - the Witu Islands.

so, in terms of the model for petrogenesis presented earlier, mass-balance calculations must take into account the minerals likely to have formed at higher pressures (P_{total}, pH_2O) - for example, amphibole. However, a major problem with calculations of this kind is that more than one combination of mineral compositions and mineral proportions may account for the differences in composition between two rocks, and that none of them can prove that the rocks represent magmas that lie on the same liquid line of descent. On the contrary, the viewpoint described at the beginning of this section takes an opposite stand - that the rocks, even from the same volcano, have compositions which may have evolved, at least to some extent, along independent lines which may, or may not, have been modified by crystal accumulation.

Problems of the acid rocks

In each of the variation diagrams presented earlier, most rocks from each of the zones, except zone C, form a more or less continuous band of composition from andesite to dacite, and to rhyolite in the eastern zones (E to H). The most obvious explanation for this feature is that the acid rocks are the products of crystal fractionation from andesitic parents. But there are five problems.

Firstly, as discussed on page 28 with reference to curves II and IV in Figure 11, the eastern rocks appear to show bimodal distribution; and when the acid rocks are excluded the remaining basalts and andesites are extremely close to showing normal or Gaussian distribution, suggesting that they constitute a natural population distinct from that of the acid rocks.

Secondly, Page & Johnson (1974) showed that acid rocks and rocks containing less than 62 percent silica have slight but apparently real differences in Sr^{87}/Sr^{86} ratios. Five dacites and rhyolites from the eastern arc have ratios of 0.7037-0.7038 ($\pm$ 0.0001 standard

deviation), whereas seven basalts and andesites from both arcs have values of 0.7034-0.7036. If the acid rocks are the products of crystal fractionation of andesite, why are their Sr^{87}/Sr^{86} values higher than those of the andesites?

Thirdly, many of the dacites and rhyolites form minor cones, coulées, and cumulodomes, which are apparently unrelated to the major stratovolcanoes that produced the basaltic and andesitic rocks. If the acid rocks were produced by crystal fractionation of andesite, why were they not all erupted from the same vents as the andesites?

Fourthly, of the ten volcanoes whose stratigraphies are shown in Table 5, only three have acid rocks, and the time relations between the acid rocks and the associated basalts and andesites are different in each of them: on Garove, dacites and rhyolites are older than the andesites; on Hargy/Galloseulo, dacites are younger than the andesites; and in the Lolobau sequence, older andesites and younger dacites and rhyolites are separated from one another by basalts of intermediate age. Therefore, the eruptions of dacites and rhyolites appear to have been random events relative to those of the basalts and andesites.

Finally, not all the acid rocks appear to be comagmatic with the basalts and andesites of the same zone. For example: one of the five rocks from Kimbe Island, a zone G volcano, is a dacite, but in several variation diagrams it shows the chemical characteristics of dacites from other zones; and, in Figure 20, points representing rocks containing more than 67 percent silica from some of the zones in the eastern arc fall well below the P_2O_5:SiO_2 trends shown by rocks with less silica from the same zone.

The explanations for each of these features may be independent of one another. For example: perhaps the acid centres of volcanism are separated from the major centres of basaltic and andesitic volcanism, because the rheology of, or energy deficiencies

in, the acid magmas prevented their rise through the central conduits of the large stratovolcanoes, but nevertheless allowed them to find other independent courses to the surface; and, perhaps the slight differences in Sr^{87}/Sr^{86} values are due to as yet unknown differences in the behaviour of Sr^{87} and Sr^{86} during differentiation (cf. Boettcher, 1973; Gill & Compston, 1973). On the other hand, all the above difficulties may point to an alternative mode of origin for at least some of the acid rocks.

At present, anatexis of young, non-radiogenically enriched crustal rocks cannot be discounted. Crustal thicknesses beneath the volcanoes of zones E and F, for example, are about 35 km (e.g., Finlayson & Cull, 1973), and the depth of origin of the primary magmas for these volcanoes has been interpreted to lie between 35 and 60 km (see p. 93). Water rising from the downgoing Solomon Sea slab may have partially melted the upper mantle to form the primary mafic magmas, and at present there seems to be no reason why water-induced melting could not also have taken place at the base of the crust to form magmas. These acid magmas would therefore be able to rise and erupt independently of the basaltic and andesitic magmas.

Throughout the late Cainozoic the crust at the southern margin of the Bismarck Sea may have been thickened by island-arc-type magmas intruding its base. Accordingly, it will be low in radiogenic strontium (Sr^{87}) relative to older continental crust. Moreover, if the differences in composition between the intruding magmas were analogous to those shown by the late Cainozoic volcanic rocks, the base of the crust would show a lateral compositional zonation. Anatexis of this crust may therefore be a source of acid rocks which are only slightly higher in Sr^{87}/Sr^{86} than the mantle-derived basalts and andesites, and whose bulk-rock compositions depend on which part of the crust from which they were derived.

Anatexis of young crust is proposed as an alternative to crystal fractionation, until such time as more detailed work is able to clarify the significance of the problems outlined above.

CONCLUSION

It is concluded that plate theory, the results of experimental petrology, and crystal fractionation offer explanations for the distribution and composition of the volcanoes at the southern margin of the Bismarck Sea. However, in the preceding sections these explanations are presented only as a broad framework which might prove useful for future work; additional studies are needed before the framework can be regarded as secure. For example, more detailed seismological data are required to confirm, and refine, concepts of the form of the present-day plate boundaries, and to determine more accurately the style of relative movements between the plates. In addition, petrological conclusions may have to be revised in the light of data provided by trace-element and isotope geochemistry, by mineral analysis, and by further high-pressure experiments. Additional geophysical studies on crustal thickness, heat flow, sea-floor topography and structure, and heat distribution in downgoing slabs may also demand revisions to the interpretations presented in this Report. Nevertheless, it is thought that the concepts of lithospheric subduction, and of partial fusion of upper mantle (and possibly crust) under hydrous conditions, followed by crystal fractionation, should form the basis for further studies in this region in the immediate future.

REFERENCES

ALLEN, J.C., MODRESKI, P.J., HAYGOOD, C., & BOETTCHER, A.L., 1972 - The role of water in the mantle of the Earth: the stability of amphiboles and micas. Proc. 24th int. geol. Cong.,.Sec. 2, 231-40.

ARCULUS, R.J., & CURRAN, E.B., 1972 - The genesis of the calc-alkaline rock suite. Earth planet. Sci. Lett., 15, 255-62.

ARMSTRONG, R.L., & COOPER, J.A., 1971 - Lead isotopes in island arcs. Bull. Volc., 35, 27-63.

BAIN, J.H.C., 1973 - A summary of the main structural elements of Papua New Guinea; in COLEMAN, P.J., (ed.) - THE WESTERN PACIFIC: ISLAND ARCS, MARGINAL SEAS, GEOCHEMISTRY. Perth, Univ. W. Aust. Press, 147-61.

BAIN, J.H.C., DAVIES, H.L., HOHNEN, P.D., RYBURN, R.J., SMITH, I.E., GRAINGER, R., TINGEY, R.J., & MOFFAT, M.R., 1972 - Geology of Papua New Guinea. Canberra, Bur. Miner. Resour. Aust. 1:1 000 000 map.

BAKER, G., 1949 - Note on volcanic rocks, with special reference to plagioclase feldspars, from Mt. Bagana, Bougainville Island, Solomon Islands. Trans. Am. geophys. Un., 30, 250-62.

BALL, E.E., & JOHNSON, R.W., 1976 - Volcanic history of Long Island, Papua New Guinea; in JOHNSON, R.W., (ed.) - VOLCANISM IN AUSTRALASIA. Amsterdam, Elsevier, 133-47.

BEST, M.G., 1975 - Migration of hydrous fluids in the upper mantle and potassium variation in calc-alkalic rocks. Geology, 3, 429-32.

BLAKE, D.H., 1968 - Post Miocene volcanoes on Bougainville Island, Territory of Papua New Guinea. Bull. Volc., 32, 121-38.

BLAKE, D.H., & BLEEKER, P., 1970 - Volcanoes of the Cape Hoskins area, New Britain, Territory of Papua and New Guinea. Bull Volc., 34, 385-405.

BLAKE, D.H., & EWART, A., 1974 - Petrography and geochemistry of the Cape Hoskins volcanoes, New Britain, Papua New Guinea. J. geol. Soc. Aust., 21, 319-31.

BLAKE, D.H., & McDOUGALL, I., 1973 - Ages of the Cape Hoskins volcanoes, New Britain, Papua New Guinea. J. geol. Soc. Aust., 20, 199-204.

BLAKE, D.H., & MIEZITIS, Y., 1967 - Geology of Bougainville and Buka Islands, New Guinea. Bur. Miner. Resour. Aust. Bull. 93.

BOETTCHER, A.L., 1973 - Volcanism and orogenic belts - the origin of andesites. Tectonophysics, 17, 223-40.

BRANCH, C.D., 1967 - Short papers from the volcanological observatory, Rabaul, New Britain. Bur. Miner. Resour. Aust. Rep. 107.

BROOKS, J.A., 1969 - Rayleigh waves in southern New Guinea: II. A shear velocity profile. Bull. seismol. Soc. Am., 59, 2017-38.

BROTHERS, R.N., 1970 - Petrochemical affinities of volcanic rocks from the Tonga-Kermadec island arc, southwest Pacific. Bull. Volc., 34, 308-29.

BRYAN, W.B., STICE, G.D., & EWART, A., 1972 - Geology, petrography, and geochemistry of the volcanic islands of Tonga. J. geophys. Res., 77, 1566-85.

BULTITUDE, R.J., 1976 - Eruptive history of Bagana volcano, Papua New Guinea, between 1882 and 1975; in JOHNSON, R.W., (ed.) - VOLCANISM IN AUSTRALASIA. Amsterdam, Elsevier, 317-36.

CANN, J.R., 1970 - A new model for the structure of the oceanic crust. Nature, 222, 928.

CAREY, S.W., 1938 - The morphology of New Guinea. Aust. Geogr., 3, 3-31.

CAREY, S.W., 1958 - A tectonic approach to continental drift; in Continental drift: a symposium. Hobart, Univ. Tasmania, 177-355.

CARMICHAEL, I.S.E., 1964 - The petrology of Thingmuli, a Tertiary volcano in eastern Iceland. J. Pet., 5, 435-60.

CAWTHORN, R.G., 1976 - Melting relations in part of the system $CaO-MgO-Al_2O_3-SiO_2-Na_2O-H_2O$ under 5 kb pressure. J. Pet., 17, 44-72.

CAWTHORN, R.C., CURRAN, E.B., & ARCULUS, R.J., 1973a - A petrogenetic model for the origin of the calc-alkaline suite of Grenada, Lesser Antilles. J. Pet., 14, 327-37.

CAWTHORN, R.G., FORD, C.E., BIGGAR, G.M., BRAVO, M.S., & CLARKE, D.B., 1973b - Determination of the liquid composition in experimental samples: discrepancies between microprobe analysis and other methods. Earth planet. Sci. Lett., 21, 1-5.

CAWTHORN, R.G., & O'HARA, M.J., 1976 - Amphibole fractionation in calc-alkaline magma genesis. Am. J. Sci., 276, 309-29.

CHAPPELL, J., 1974 - Geology of coral terraces, Huon Peninsula, New Guinea: a study of Quaternary tectonic movements and sea-level changes. Bull. geol. Soc. Am., 81, 17-38.

CHAYES, F., 1965 - Titania and alumina content of oceanic and circum-oceanic basalt. Miner. Mag., 34, 126-31.

CHRISTOFFEL, D.A., 1971 - Motion of the New Zealand Alpine fault deduced from the pattern of sea-floor spreading. Bull. R. Soc. NZ. Upper Mantle Project scient. Rep., 33, 25-30.

CHURCH, S.E., 1973 - Limits of sediment involvement in the genesis of orogenic volcanic rocks. Contr. Miner. Pet., 39, 17-32.

CONNELLY, J.B., 1974 - A structural interpretation of magnetometer and seismic profiler records in the Bismarck Sea, Melanesian Archipelago. J. geol. Soc. Aust., 21, 459-69.

CONNELLY, J.B., 1975 - Magnetic and gravity modelling in the Bismarck Sea. Bull. Aust. Soc. Expl. Geophys., 6, 52.

CONNELLY, J.B., 1976 - Tectonic development of the Bismarck Sea based on gravity and magnetic modelling. Geophys. J. R. astr. Soc., 45, 23-40.

COOKE, R.J.S., McKEE, C.O., DENT, V.F., & WALLACE, D.A., 1976 - Striking sequence of volcanic eruptions in the Bismarck volcanic arc, Papua New Guinea, in 1972-75; in JOHNSON, R.W., (ed.) - VOLCANISM IN AUSTRALASIA. Amsterdam, Elsevier, 149-72.

COTTON, C.A., 1944 - VOLCANOES AS LANDSCAPE FORMS. Christchurch, Whitcombe and Tombs.

COX, K.G., & BELL, J.D., 1972 - A crystal fractionation model for the basaltic rocks of the New Georgia Group, British Solomon Islands. Contr. Miner. Pet., 37, 1-14.

CURTIS, J.W., 1973 - The spatial seismicity of Papua New Guinea and the Solomon Islands. J. geol. Soc. Aus., 20, 1-19.

CURTIS, J.W., 1973b - Plate tectonics and the Papua-New Guinea-Solomon Islands region. J. geol. Soc. Aust., 20, 21-36.

DAVIES, H.L., 1968 - Papuan Ultramafic Belt. Proc. 23rd int. geol. Cong., Sec. 1, 209-20.

DAVIES, H.L., 1971 - Peridotite-gabbro-basalt complex in eastern Papua: an overthrust plate of oceanic mantle and crust. Bur. Miner. Resour. Aust. Bull. 128.

DAVIES, H.L., 1973 - Gazelle Peninsula, New Britain - 1:250 000 Geological Series. Bur. Miner. Resour. Aust. explan. Notes SB/56-2.

DEER, W.A., HOWIE, R.A., & ZUSSMAN, J., 1966 - AN INTRODUCTION TO THE ROCK-FORMING MINERALS. New York, John Wiley & Sons.

DENHAM, D., 1969 - Distribution of earthquakes in the New Guinea-Solomon Islands region. J. geophys. Res., 74, 4290-9.

DENHAM, D., 1973 - Seismicity, focal mechanisms, and the boundaries of the Indian-Australian plate; in COLEMAN, P.J., (ed.) - THE WESTERN PACIFIC: ISLAND ARCS, MARGINAL SEAS, GEOCHEMISTRY. Perth, Univ. W.Aust. Press.

DEWEY, J.F., & BIRD, J.M., 1970 - Mountain belts and the new global tectonics. J. geophys. Res., 75, 2625-47.

DICKINSON, W.R., 1968 - Circum-Pacific andesite types. J. geophys. Res. 73, 2261-9.

DICKINSON, W.R., 1975 - Potash-depth (K-h) relations in continental margin and intra-oceanic magmatic arcs. Geology, 3, 53-6.

DICKINSON, W.R., & HATHERTON, T., 1967 - Andesitic volcanism and seismicity around the Pacific. Science, 157, 801-3.

DIXON, W.J., 1971 - Biomedical computer programs. Univ. Calif. Publs. Automatic Computation 2.

EGGLER, D.H., 1972 - Water-saturated and undersaturated melting relations in a Paricutin andesite and an estimate of water content in the natural magma. Contr. Miner. Pet., 34, 261-71.

EGGLER, D.H., 1974 - Application of a portion of the system $CaAl_2Si_2O_8$-$NaAlSi_3O_8$-SiO_2-MgO-Fe-O_2-H_2O-CO_2 to genesis of the calc-alkaline suite. Am. J. Sci., 274, 297-315.

EGGLER, D.H., & BURNHAM, C.W., 1973 - Crystallisation and fractionation trends in the system andesite-H_2O-CO_2-O_2 at pressures to 10 kb. Bull. geol. Soc. Am., 84, 2517-32.

ERLANDSON, D.L., ORWIG, T.L., KILSGAARD, G., MUSSELLS, J.H., & KROENKE, L.W., 1976 - Tectonic interpretations of the East Caroline and Lyra Basins from reflection-profiling investigations. Bull. geol. Soc. Am., 87, 453-62.

FINLAYSON, D.M., & CULL, J.P., 1973 - Structural profiles in the New Britain-New Ireland region. J. geol. Soc. Aust., 20, 37-47.

FISHER, N.H., 1939 - Geology and vulcanology of Blanche Bay and the surrounding area, New Britain. Terr. New Guinea Geol. Bull. 1.

FISHER, N.H., 1957 - CATALOGUE OF THE ACTIVE VOLCANOES OF THE WORLD INCLUDING SOLFATARA FIELDS - PART V, MELANESIA. Naples, int. volc. Ass.

FISHER, N.H., 1976 - 1941-42 eruption of Tavurvur volcano, Rabaul, Papua New Guinea; in JOHNSON, R.W., (ed.)- VOLCANISM IN AUSTRALASIA. Amsterdam, Elsevier, 201-10.

FREY, F.W., & GREEN, D.H., 1974 - The mineralogy, geochemistry and origin of lherzolite inclusions in Victorian basanites. Geochim. cosmochim. Acta, 38, 1023-59.

FURUMOTO, A.S., HUSSONG, D.M., CAMPBELL, J.F., SUTTON, G.H., MALAHOFF, A., ROSE, J.C., & WOOLLARD, G.P., 1970 - Crustal and upper mantle structure of the Solomon Islands as revealed by seismic refraction survey of November-December 1966. Pac. Sci., 24, 315-32.

FYFE, W.S., & McBIRNEY, A.R., 1975 - Subduction and the structure of andesitic volcanic belts. Am. J. Sci., 275A, 285-97.

GAST, P.W., 1968 - Trace element fractionation and the origin of tholeiitic and alkaline magma types. Geochim. cosmochim. Acta, 32, 1057-86.

GILL, J.B., 1970 - Geochemistry of Viti Levu, Fiji, and its evolution as an island arc. Contr. Miner. Pet. 27, 179-203.

GILL, J.B., 1974 - Role of underthrust oceanic crust in the genesis of a Fijian calc-alkaline suite. Contr. Miner. Pet., 43, 29-46.

GILL, J. & COMPSTON, W., 1973 - Strontium isotopes in island arc volcanic rocks; in COLEMAN, P.J., (ed.) - THE WESTERN PACIFIC: ISLAND ARCS, MARGINAL SEAS, GEOCHEMISTRY. Perth, Univ. W.Aust. Press, 493-6.

GREEN, D.H., 1971 - Composition of basaltic magmas as indicators of conditions of origin: application to oceanic volcanism. Phil. Trans. R. Soc. Lond., A, 268, 707-25.

GREEN, D.H., 1972 - Magmatic activity as the major process in the chemical evolution of the Earth's crust and mantle. Tectonophysics, 13, 47-71.

GREEN, D.H., 1973a - Contrasting melting relations in a pyrolite upper mantle under mid-oceanic ridge, stable crust, and island arc environments. Tectonophysics, 17, 285-97.

GREEN, D.H., 1973b - Experimental melting studies on a model upper mantle composition at high pressure under water-saturated and water-undersaturated conditions. Earth. planet. Sci. Lett., 19, 37-53.

GREEN, D.H., 1976 - Experimental testing of 'equilibrium' partial melting of peridotite under water-saturated, high pressure conditions. Canad. Mineralogist, 14, 255-68.

GREEN, D.H., & LIEBERMANN, R.C., 1976 - Phase equilibria and elastic properties of a pyrolite model for the oceanic upper mantle. Tectonophysics, 32, 61-92.

GREEN, D.H., & RINGWOOD, A.E., 1967 - The genesis of basalt magmas. Contr. Miner. Pet., 15, 103-90.

GREEN, T.H., 1972 - Crystallisation of calc-alkaline andesite under controlled high-pressure hydrous conditions. Contr. Miner. Pet., 34, 150-66.

GREEN, T.H., & RINGWOOD, A.E., 1968 - Genesis of the calc-alkaline igneous rock suite. Contr. Miner. Pet., 18, 105-62.

GREEN, T.H., & RINGWOOD, A.E., 1972 - Crystallisation of garnet-bearing rhyodacite under high pressure hydrous conditions. J. geol. Soc. Aust., 19, 203-12.

GRIGGS, D.T., 1972 - The sinking lithosphere and the focal mechanism of deep earthquakes; in ROBERTSON, E.C., (ed.) - THE NATURE OF THE SOLID EARTH. New York, McGraw-Hill, 361-84.

HALD, N., NOE-NYGAARD, A., & PEDERSON, A.K., 1971 - The Kroksfjordur central volcano in northwest Iceland. Acta Naturalia Islandica, 2, 1-27.

HATHERTON, T., 1969 - The geophysical significance of calc-alkaline andesites in New Zealand. NZ J. Geol. Geophys., 12, 436-59.

HATHERTON, T., & DICKINSON, W.R., 1969 - The relationship between andesitic volcanism and seismicity in Indonesia, the Lesser Antilles, and other island arcs. J. geophys. Res. 74, 5301-10.

HAWKINS, J.W., Jr, 1976 - Petrology and geochemistry of basaltic rocks of the Lau Basin. Earth planet. Sci. Lett., 28, 283-97.

HEMING, R.F., 1974 - Geology and petrology of Rabaul caldera, Papua New Guinea. Bull. geol. Soc. Am., 85, 1253-64.

HEMING, R.F., & CARMICHAEL, I.S.E., 1973 - High-temperature pumice flows from the Rabaul caldera, Papua New Guinea. Contr. Miner. Pet., 38, 1-20.

HILL, R.E.T., & BOETTCHER, A.L., 1970 - Water in the Earth's mantle: melting curves of basalt-water and basalt-water-carbon dioxide. Science, 167, 980-1.

HOLLOWAY, J.R., & BURNHAM, W.C., 1972 - Melting relations of basalt with equilibrium water pressure less than total pressure. J. Pet. 13, 1-29.

HOLMES, A., 1921 - PETROGRAPHIC METHODS AND CALCULATION WITH SOME EXAMPLES OF RESULTS ACHIEVED. London, Murby.

HOWARTH, R.J., 1973 - Preliminary assessment of a non-linear mapping algorithm in a geological context. Math. Geol., 5, 39-57.

HUANG, W.L., & WYLLIE, P.J., 1973 - Melting relations of muscovite-granite to 35 kbar as a model for fusion of metamorphosed subducted oceanic sediments. Contr. Miner. Pet., 42, 1-14.

HUANG, W.L., & WYLLIE, P.J., 1975 - Melting reactions in the system $NaAlSi_3O_8$-$KAlSi_3O_8$-SiO_2 to 35 kilobars, dry and with excess water. J. Geol., 83, 737-48.

HUTCHISON, C.S., 1975 - Correlation of Indonesian active volcanic geochemistry with Benioff zone depth. Geol. Mijnbouw, 54, 157-68.

IRVINE, T.N., & BARAGAR, W.R.A., 1971 - A guide to the chemical classification of the common volcanic rocks. Canad. J. Earth Sci., 8, 523-48.

ISACKS, B., & MOLNAR, P., 1971 - Distribution of stresses in the descending lithosphere from a global survey of focal-mechanism solutions of mantle earthquakes. Rev. Geophys. Space Phys. 9, 103-74.

ISACKS, B., OLIVER, J., & SYKES, L.R., 1968 - Seismology and the new global tectonics. J. geophys. Res., 73, 5855-99.

JAKEŠ, P., & GILL, J.B., 1970 - Rare earth elements and the island arc tholeiitic series. Earth planet. Sci. Lett., 9, 17-33.

JAKEŠ, P., & SMITH, I.E., 1970 - High potassium calc-alkaline rocks from Cape Nelson, eastern Papua. Contr. Miner. Pet., 28, 259-71.

JAKEŠ, P., & WHITE, A.J.R., 1969 - Structure of the Melanesian arcs and correlation with distribution of magma types. Tectonophysics, 8, 223-36.

JAKEŠ, P., & WHITE, A.J.R., 1972 - Major and trace element abundances in volcanic rocks of orogenic areas. Bull. geol. Soc. Am., 83, 29-40.

JAQUES, A.L., 1976 - High-K_2O island-arc volcanic rocks from the Finisterre and Adelbert Ranges, northern Papua New Guinea. Bull. geol. Soc. Am., 87, 861-7.

JAQUES, A.L., & ROBINSON, G.P., in prep. - Geology of a continent/island-arc collision, northern Papua New Guinea.

JAMIESON, B.G., 1970 - Differentiation of ascending basic magma. Geol. J., 2, 165-76.

JOHNSON, R.W., 1970a - Ulawun volcano, New Britain: geology, petrology, and eruptive history between 1915 and 1967. Bur. Miner. Resour. Aust. Rec. 1970/21 (unpubl.).

JOHNSON, R.W., 1970b - Likuruanga volcano, Lolobau Island, and associated volcanic centres, New Britain: geology and petrology. Bur. Miner. Resour. Aust. Rec. 1970/42 (unpubl.).

JOHNSON, R.W., 1971 - Bamus volcano, Lake Hargy area, and Sulu Range, New Britain: volcanic geology and petrology. Bur. Miner. Resour. Aust. Rec. 1971/55 (unpubl.).

JOHNSON, R.W., & BLAKE, D.H., 1973 - The Cape Hoskins area, southern Willaumez Peninsula, the Witu Islands, and associated volcanic centres, New Britain: volcanic geology and petrology. Bur. Miner. Resour. Aust. Rec. 1972/133 (unpubl.).

JOHNSON, R.W., DAVIES, R.A., & PALFREYMAN, W.D., 1971 - Cape Gloucester area, New Britain: volcanic geology, petrology, and eruptive history of Langila craters up to 1970. Bur. Miner. Resour. Aust. Rec. 1971/14 (unpubl.).

JOHNSON, R.W., DAVIES, R.A., & WHITE, A.J.R., 1972 - Ulawun volcano, New Britain. Bur. Miner. Resour. Aust. Bull. 142.

JOHNSON, R.W., & JAQUES, A.L., in prep. - Continent-arc collision and reversal of arc polarity: new interpretations from a critical area. Submitted to Geology.

JOHNSON, R.W., MACKENZIE, D.E., & SMITH, I.E., 1971 - Seismicity and late Cenozoic volcanism in parts of Papua-New Guinea. Tectonophysics, 12, 15-22.

JOHNSON, R.W., MACKENZIE, D.E., & SMITH, I.E.M., in prep.a - Volcanic rock associations at convergent plate boundaries: re-appraisal of the concept using case histories from Papua New Guinea. Bull. geol. Soc. Am.

JOHNSON, R.W., MACKENZIE, D.E., & SMITH, I.E.M., in prep. b - Late Cainozoic volcanic magmas associated with past and present arc-trench systems in Papua New Guinea. Submitted to J. Volc. Geothermal Res.

JOHNSON, R.W., MACKENZIE, D.E., SMITH, I.E., & TAYLOR, G.A.M., 1973 - Distribution and petrology of Late Cainozoic volcanoes in Papua New Guinea; in COLEMAN, P.J., (ed.) - THE WESTERN PACIFIC: ISLAND ARCS, MARGINAL SEAS, GEOCHEMISTRY. Perth, Univ. W. Aust. Press, 523-33.

JOHNSON, R.W., & SMITH, I.E., 1974 - Volcanoes and rocks of St Andrew Strait, Papua New Guinea. J. geol. Soc. Aust., 21, 333-49.

JOHNSON, R.W., TAYLOR, G.A.M., & DAVIES, R.A., 1972 - Geology and petrology of the Quaternary volcanic islands off the north coast of New Guinea. Bur. Miner. Resour. Aust. Rec. 1972/21 (unpubl.).

JOHNSON, R.W., WALLACE, D.A., & ELLIS, D.J., 1976 - Feldspathoid-bearing potassic rocks and associated types from volcanic islands off the coast of New Ireland, Papua New Guinea: a preliminary account of geology and petrology; in JOHNSON, R.W., (ed.)- VOLCANISM IN AUSTRALASIA. Amsterdam, Elsevier, 297-316.

JOHNSON, T., & MOLNAR, P., 1972 - Focal mechanisms and plate tectonics of the southwest Pacific. J. geophys. Res., 77, 5000-32.

KARIG, D.E., 1971 - Origin and development of marginal basins in the western Pacific. J. geophys. Res., 76, 2542-61.

KARIG, D.E., 1972 Remnant arcs. Bull. geol. Soc. Am., 83, 1057-68.

KLOVAN, J.E., & IMBRIE, J., 1971 - An algorithm and FORTRAN-IV program for large-scale Q-mode factor analysis and calculation of factor scores. Math. Geol., 3, 61-7.

KRAUSE, D.C., 1965 - Submarine geology north of New Guinea. Bull. geol. Soc. Am., 76, 27-42.

KRAUSE, D.C., 1973 - Crustal plates of the Bismarck and Solomon Seas; in FRASER, R., (ed.) - OCEANOGRAPHY OF THE SOUTH PACIFIC 1972. Wellington, NZ nat. Comm. UNESCO, 271-80.

KRAUSE, D.C., WHITE, W.C., PIPER, D.J.W., & HEEZEN, B.C., 1970 - Turbidity currents and cable breaks in the western New Britain trench. Bull. geol. Soc. Am., 81, 2153-60.

KUNO, H., 1950 - Petrology of Hakone volcano and the adjacent areas, Japan. Bull. geol. Soc. Am., 61, 957-1020.

KUNO, H., 1959 - Origin of Cenozoic petrographic provinces of Japan and surrounding areas. Bull. Volc., 20, 37-76.

KUNO, H., 1966 - Lateral variation of basalt magma type across continental margins and island arcs. Bull. Volc., 29, 195-222.

KUNO, H., 1968 - Differentiation of basalt magmas; in HESS, H.H., & POLDERVAART, A., (eds.) - BASALTS : THE POLDERVAART TREATISE ON ROCKS OF BASALTIC COMPOSITION, Vol. 2. New York, John Wiley & Sons.

KUSHIRO, I., 1969 - The system forsterite-diopside-silica with and without water at high pressures. Am. J. Sci., 267A, 269-94.

KUSHIRO, I., 1972 - Effect of water on the composition of magmas formed at high pressures. J. Pet., 13, 311-34.

KUSHIRO, I., 1974 - Melting of hydrous upper mantle and possible generation of andesitic magma: an approach from synthetic systems. Earth planet. Sci. Lett., 22, 294-9.

KUSHIRO, I., SHIMIZU, N., NAKAMURA, Y., & AKIMOTO, S., 1972 - Compositions of co-existing liquid and solid phases formed upon melting of natural garnet and spinel lherzolites at high pressures: a preliminary report. Earth planet. Sci. Lett., 14, 19-25.

KUSHIRO, I., SYONO, Y., & AKIMOTO, S., 1968 - Melting of peridotite nodule at high pressures and high water pressures. J. geophys. Res. 73, 6023-9.

LAMBERT, I.B., & WYLLIE, P.J., 1968 - Stability of hornblende and a model for the low velocity zone. Nature, 219, 1240-1.

LAMBERT, I.B., & WYLLIE, P.J., 1970 - Low velocity zone of the Earth's mantle: incipient melting caused by water. Science, 169, 764-6.

LE PICHON, X., 1968 - Sea-floor spreading and continental drift. J. geophys. Res. 73, 3661-97.

LE PICHON, X., 1970 - Correction to paper by Xavier Le Pichon 'Sea-floor spreading and continental drift'. J. geophys. Res. 75, 2793.

LE PICHON, X., FRANCHETEAU, J., & BONNIN, J., 1973 - PLATE TECTONICS. Amsterdam, Elsevier.

LIPMAN, P.W., PROSTKA, H.J., & CHRISTIANSEN, R.L., 1971 - Evolving subduction zones in the western United States, as interpreted from igneous rocks. Science, 174, 821-5.

LOWDER, G.G., 1970 - The volcanoes and caldera of Talasea, New Britain: mineralogy. Contr. Miner. Pet., 26, 324-40.

LOWDER, G.G., & CARMICHAEL, I.S.E., 1970 - The volcanoes and caldera of Talasea, New Britain: geology and petrology. Bull. geol. Soc. Am., 81, 17-38.

LUYENDYK, B.P., 1970 - Dips of downgoing lithospheric plates beneath island arcs. Bull. geol. Soc. Am., 81, 3411-6.

LUYENDYK, B.P., MACDONALD, K.C., & BRYAN, W.B., 1973 - Rifting history of the Woodlark Basin in the southwest Pacific. Bull. geol. Soc. Am., 84, 1125-34.

MAALØE, S., & WYLLIE, P.J., 1975 - Water content of a granite magma deduced from the sequence of crystallisation determined experimentally with water-undersaturated conditions. Contr. Miner. Pet., 52, 175-91.

McBIRNEY, A.R., 1968 - Petrochemistry of the Cascade andesitic volcanoes. State Oreg. Dept. Geol. Miner. Ind. Bull. 62, 16-27.

McBIRNEY, A.R., 1969 - Compositional variations in Cenozoic calc-alkaline suites of Central America. State Oreg. Dept. Geol. Miner. Ind. Bull. 65, 185-9.

MACDONALD, G.A., & KATSURA, T., 1964 - Chemical composition of Hawaiian lavas. J. Pet., 5, 82-133.

McKEE, C.O., COOKE, R.J.S., & WALLACE, D.A., 1976 - 1974-75 eruptions of Karkar volcano, Papua New Guinea; in JOHNSON, R.W., (ed.) - VOLCANISM IN AUSTRALASIA. Amsterdam, Elsevier, 173-90.

MACKENZIE, D.E., 1976 - Nature and origin of late Cainozoic volcanoes in western Papua New Guinea; in JOHNSON, R.W., (ed.) - VOLCANISM IN AUSTRALASIA. Amsterdam, Elsevier, 221-38.

MACKENZIE, D.E., & CHAPPELL, B.W., 1972 - Shoshonitic and calc-alkaline lavas from the Highlands of Papua New Guinea. Contr. Miner. Pet., 35, 50-62.

McKENZIE, D.P., 1969 - Speculations on the consequences and causes of plate motions. Geophys. J. R. astr. Soc., 18, 1-32.

MAMMERICKX, J., CHASE, T.E., SMITH, S.M., & TAYLOR, I.L., 1971 - Bathymetry of the south Pacific, chart 11. Scripps Inst. Oceanog. and Inst. Marine Resour.

MATSUMOTO, H., 1976 - Petrological study on some rocks from Rabaul volcano. Kumamoto J. Sci. (Geology), 10, 19-26.

MAYO, W., & LONG, K.A., 1976 - Documentation of BMR Geological Branch computer programs. Bur. Miner. Resour. Aust. Rec. 1976/82 (unpubl.).

MERRILL, R.B., & WYLLIE, P.J., 1973 - Absorption of iron by platinum capsules in high-pressure rock melting experiments. Am. Mineralogist., 58, 16-20.

MILHOLLEN, G.L., IRVING, A.J., & WYLLIE, P.J., 1974 - Melting interval of peridotite with 5-7 percent water to 30 kilobars. J. Geol., 82, 575-87.

MILSOM, J.S., 1970 - Woodlark Basin, a minor centre of sea-floor spreading in Melanesia. J. geophys. Res., 75, 7335-9.

MINEAR, J.W., & TOKSÖZ, M.N., 1970a - Thermal regime of a downgoing slab and new global tectonics. J. geophys. Res., 75, 1397-419.

MINEAR, J.W., & TOKSÖZ, M.N., 1970b - Thermal regime of a downgoing slab. Tectonophysics, 10, 367-90.

MITCHELL, A.H.G., & WARDEN, A.T., 1971 - Geological evolution of the New Hebrides island arc. J. geol. Soc. Lond., 127, 501-29.

MIYAKE, Y., & SUGIURA, Y., 1953 - On the chemical composition of the volcanic eruptives in New Britain islands, Pacific Ocean. Proc. 7th Pac. Sci. Cong., Wellington, 2, 361-3.

MORGAN, W.R., 1966 - A note on the petrology of some lava types from east New Guinea. J. geol. Soc Aust., 13, 583-91.

MUIR, I.D., TILLEY, C.E., & SCOON, J.H., 1957 - Petrology of Hawaiian basalts: I. The picrite-basalts of Kilauea. Am. J. Sci., 255, 241-53.

MYERS, N.O., 1976 - Seismic surveillance of volcanoes in Papua New Guinea; in JOHNSON, R.W., (ed.) - VOLCANISM IN AUSTRALASIA. Amsterdam, Elsevier, 91-9.

MYSEN, B.O., 1973 - Melting in a hydrous mantle: phase relations of mantle peridotite with controlled water and oxygen fugacities. Carnegie Inst. Wash. Yearbk, 72, 467-78.

MYSEN, B.O., 1975 - Partitioning of iron and magnesium between crystals and partial melts in peridotitic upper mantle. Contr. Miner. Pet., 52, 69-76.

MYSEN, B.O., & BOETTCHER, A.L., 1975a - Melting of a hydrous mantle: I. Phase relations of natural peridotite at high pressures and temperatures with controlled activities of water, carbon dioxide, and hydrogen. J. Pet., 16, 520-48.

MYSEN, B.O., & BOETTCHER, A.L., 1975b - Melting of a hydrous mantle: II. Geochemistry of crystals and liquids formed by anatexis of mantle peridotite at high pressures and high temperatures as a function of controlled activities of water, hydrogen, and carbon dioxide. J. Pet., 16, 549-93.

MYSEN, B.O., & BOETTCHER, A.L., 1976 - Melting of a hydrous mantle: III. Phase relations of garnet websterite + H_2O at high pressures and temperatures. J. Pet., 17, 1-14.

MYSEN, B.O., & KUSHIRO, I., 1974 - A possible mantle origin for andesitic magmas: discussion of a paper by Nicholls and Ringwood. 1 - Opening discussion; 3 - Comments on the reply of Nicholls and Ringwood. Earth planet. Sci. Lett., 21, 221-9.

NEHRU, C.E., & WYLLIE, P.J., 1975 - Compositions of glasses from St Paul's peridotite partially melted at 20 kilobars. J. Geol., 83, 455-71.

NICHOLLS, I.A., 1971 - Petrology of Santorini volcano, Cyclades, Greece. J. Pet., 12, 609-47.

NICHOLLS, I.A., 1974 - Liquids in equilibrium with peridotitic mineral assemblages at high water pressures. Contr. Miner. Pet., 45, 289-316.

NICHOLLS, I.A., & RINGWOOD, A.E., 1972 - Production of silica-saturated tholeiitic magmas in island arcs. Earth planet. Sci. Lett., 17, 243-6.

NICHOLLS, I.A., & RINGWOOD, A.E., 1973 - Effect of water on olivine stability in tholeiites and the production of silica saturated magmas in the island-arc environment. J. Geol., 81, 285-300.

NICHOLLS, I.A., & RINGWOOD, A.E., 1974 - A possible mantle origin for andesitic magmas: discussion of a paper by Nicholls and Ringwood. 2 - Reply to opening discussion; 4 - Final reply. Earth planet. Sci. Lett., 21, 221-9.

NIELSON, D.R., & STOIBER, R.E., 1973 - Relationship of potassium content in andesitic lavas and depth to the seismic zone. J. geophys. Res., 78, 6887-92.

NINKOVICH, D., & HAYS, J.D., 1972 - Mediterranean island arcs and origin of high potash volcanics. Earth planet. Sci. Lett., 16, 331-45.

O'HARA, M.J., 1965 - Primary magmas and the origin of basalts. Scott. J. Geol., 1, 19-40.

O'HARA, M.J., 1968 - The bearing of phase equilibria studies on synthetic and natural systems on the origin and evolution of basic and ultrabasic rocks. Earth-Sci. Rev. 4, 69-133.

OSBORN, E.F., 1959 - Role of oxygen pressure in the crystallisation and differentiation of basaltic magma. Am. J. Sci., 257, 609-47.

OSBORN, E.F., 1969 - The complimentariness of orogenic andesites and alpine peridotite. Geochim. cosmochim. Acta, 33, 307-24.

OVERSBY, V.M., & EWART, A., 1972 - Lead isotopic compositions of Tonga-Kermadec volcanics and tneir petrogenetic significance. Contr. Miner. Pet., 37, 181-210.

OXBURGH, E.R., & TURCOTTE, D.L., 1970 - Thermal structure of island arcs. Bull. geol. Soc. Am., 81, 1665-88.

PAGE, R.W., & JOHNSON, R.W., 1974 - Strontium isotope ratios of Quaternary volcanic rocks from Papua New Guinea. Lithos, 7, 91-100.

PAGE, R.W., & McDOUGALL, I., 1970 - Potassium-argon dating from the Tertiary f_{1-2} stage in New Guinea and its bearing on the geological time scale. Am. J. Sci., 269, 321-42.

PEACOCK, M.A., 1931 - Classification of igneous rocks. J. Geol., 39, 54-67.

PETERMAN, Z.E., & HEMING, R.F., 1974 - Sr^{87}/Sr^{86} ratios from the Rabaul caldera, Papua New Guinea. Bull. geol. Soc. Am., 85, 1265-8.

PETERMAN, Z.E., LOWDER, G.G., & CARMICHAEL, I.S.E., 1970 - Sr^{87}/Sr^{86} ratios of the Talasea Series, New Britain, Territory of New Guinea. Bull. geol. Soc. Am., 81, 39-40.

POLDERVAART, A., 1955 - Chemistry of the earth's crust; in POLDERVAART, A., (ed.) - Crust of the earth. Geol. Soc. Am. spec. Pap. 62, 119-44.

PRESNALL, D.C., 1966 - The join Forsterite-Diopside-Iron-Oxide and its bearing on the crystallisation of basaltic and ultramafic magmas. Am. J. Sci., 264, 753-809.

RINGWOOD, A.E., 1969 - Composition and evolution of the upper mantle. Am. geophys. Un. Monogr., 13, 1-17.

RINGWOOD, A.E., 1974 - Petrological evolution of island arc systems. J. geol. Soc. Lond., 130, 183-204.

RINGWOOD, A.E., 1975 - COMPOSITION AND PETROLOGY OF THE EARTH'S MANTLE. New York, McGraw-Hill.

RINGWOOD, A.E., 1976 - Petrogenesis of island arc systems (abstract); in The Ewing Symposium: Problems in the evolution of island arcs, deep sea trenches, and back-arc basins. New York, Lamont-Doherty Geological Observatory of Columbia University, G. Unger Vetlesen Foundation, National Science Foundation, and Office of Naval Research, 18-9.

RIPPER, I.D., 1970 - Global tectonics and the New Guinea-Solomon Islands region. Search, 1, 226-32.

RIPPER, I.D., 1975 - Some earthquake focal mechanisms in the New Guinea/Solomon Islands region, 1963-1968. Bur. Miner. Resour. Aust. Rep. 178.

RIPPER, I.D., in prep.a - Some earthquake focal mechanisms in the New Guinea/Solomon Islands region, 1969-1971. Bur. Miner. Resour. Aust. Rep. 192.

RIPPER, I.D., in prep. b - Earthquake focal mechanisms and tectonics of the New Guinea/Solomon Islands region. Bur. Miner. Resour. Aust. Rep.

RITTMANN, A., 1953 - Magmatic character and tectonic position of the Indonesian volcanoes. Bull. Volc., 14, 45-58.

RITTMANN, A., 1958 - Determination of a serial index of volcanic rocks. Bull. Volc., 19, 41-2.

ROBINSON, G.P., 1973 - Stratigraphy and structure of the Huon Peninsula, New Guinea, within the framework of the Outer Melanesian arc; in FRASER, R., (ed.) - OCEANOGRAPHY OF THE SOUTH PACIFIC 1972. Wellington, NZ Nat. Comm. UNESCO, 291-7.

ROBINSON, G.P., JAQUES, A.L., & BROWN, C.M., 1976 - Madang, Papua New Guinea - 1:250 000 Geological Series. Bur. Miner. Resour. Aust. explan. Notes SB/55-6.

ROEDER, P.L., & EMSLIE, R.F., 1970 - Olivine-liquid equilibrium. Contr. Miner. Pet., 29, 275-89.

RUXTON, B.P., 1966 - A late Pleistocene to Recent rhyodacite-trachybasalt-basaltic latite volcanic association in northeast Papua. Bull. Volc., 29, 347-74.

SCLATER, J.G., HAWKINS, J.W., MAMMERICKX, J., & CHASE, C.G., 1971 - Crustal extension between the Tonga and Lau Ridges: petrologic and geophysical evidence. Bull. geol. Soc. Am., 83, 505-18.

SIGURDSSON, H., TOMBLIN, J.F., BROWN, G.M., HOLLAND, J.G., & ARCULUS, R.J., 1973 - Strongly undersaturated magmas in the Lesser Antilles island arc. Earth planet. Sci. Lett., 18, 285-95.

SLEEP, N.H., 1975 - Stress and flow beneath island arcs. Geophys. J. R. astr. Soc., 48, 827-57.

SLEEP, N., & TOKSÖZ, M.N., 1971 - Evolution of marginal basins. Nature, 233, 548-50.

SMITH, A.L., & CARMICHAEL, I.S.E., 1968 - Quaternary lavas from the southern Cascades, western USA. Contr. Miner. Pet., 19, 212-38.

SMITH, I.E.M., 1976 - Peralkaline rhyolites from the D'Entrecasteaux Islands, Papua New Guinea; in JOHNSON, R.W., (ed.) - VOLCANISM IN AUSTRALASIA. Amsterdam, Elsevier, 275-85.

SMITH, I.E.M., JOHNSON, R.W., MACKENZIE, D.E., & TAYLOR, S.R., in prep. - Garnet-equilibrium trachytes from Papua New Guinea.

STANTON, R.L., & BELL, J.D., 1969 - Volcanic and associated rocks of the New Georgia group, British Solomon Islands Protectorate. Overseas Geol. Miner. Resour., 10, 113-45.

STERN, C.R., 1974 - Melting products of olivine tholeiite basalt in subduction zones. Geology, 2, 227-30.

STERN, C.R., & WYLLIE, P.J., 1973a - Melting relations of basalt-andesite-rhyolite-H_2O and pelagic red clay at 30 kb. Contr. Miner. Pet. 42, 313-23.

STERN, C.R., & WYLLIE, P.J., 1973b - Water-saturated and under-saturated melting relations of a granite to 35 kilobars. Earth planet. Sci. Lett., 18, 163-7.

STEWART, D.C., 1975 - Crystal clots in calc-alkaline andesites as breakdown products of high-Al amphiboles. Contr. Miner. Pet., 53, 195-204.

SUGIMURA, A., 1960 - Zonal arrangement of some geophysical and petrological features in Japan and its environs. Univ. Tokyo J. Fac. Sci., 12, 133-53.

SUNG, C.M., & BURNS, R.G., 1976 - Kinetics in high pressure phase transformations: implications to the evolution of the olivine spinel transition in the downgoing lithosphere and its consequences on the dynamics of the mantle. Tectonophysics 31, 1-32.

TATSUMOTO, M., 1969 - Lead isotopes in volcanic rocks and possible ocean-floor thrusting beneath island arcs. Earth planet. Sci. Lett., 6, 369-76.

TAYLOR, B., 1975 - Tectonics of the Bismarck Sea. BSc honours thesis, Univ. Sydney. (unpubl.).

TAYLOR, G.A., 1956 - Review of volcanic activity in the Territory of Papua New Guinea, the Solomon and New Hebrides Islands, 1951-53. Bull. Volc., 18, 25-37.

TAYLOR, G.A., 1958 - The 1951 eruption of Mount Lamington, Papua. Bur. Miner. Resour. Aust. Bull. 38.

TAYLOR, S.R., CAPP, A.C., GRAHAM, A.L., & BLAKE, D.H., 1969 - Trace element abundances in andesites: II. Saipan, Bougainville and Fiji. Contr. Miner. Pet., 23, 1-26.

TERRY, R.D. & CHILINGAR, G.V., 1955 - Summary of 'Concerning some additional aids in studying sedimentary formations' by M.S. Shvetsov. J. sed. Pet., 25, 229-34.

THOMPSON, J.E., & FISHER, N.H., 1965 - Mineral deposits of New Guinea and Papua; and their tectonic setting. Proc. 8th Comm. Min. Metall. Cong., 6, 115-48.

THOMPSON, R.N., 1973 - One-atmosphere melting behaviour and nomenclature of terrestrial lavas. Contr. Miner. Pet., 41, 197-204.

THORNTON, C.P., & TUTTLE, O.F., 1960 - Chemistry of igneous rocks: I. Differentiation index. Am. J. Sci., 258, 664-84.

TILLEY, C.E., 1950 - Some aspects of magmatic evolution. J. geol. Soc. Lond., 106, 37-61.

TOKSÖZ, M.N., SLEEP, N.H., & SMITH, T.A., 1973 - Evolution of the downgoing lithosphere and mechanisms of deep focus earthquakes. Geophys. J.R. astr. Soc., 35, 285-310.

TOMKEIEFF, S.I., 1949 - The volcanoes of Kamchatka. Bull. Volc., 8, 87-114.

WHITFORD, D.J., & NICHOLLS, I.A., 1976 - Potassium variation in lavas across the Sunda arc in Java and Bali; in JOHNSON, R.W., (ed.) - VOLCANISM IN AUSTRALASIA. Amsterdam, Elsevier, 63-75.

WIEBENGA, W.A., 1973 - Crustal structure of the New Britain-New Ireland region; in COLEMAN , P.J., (ed.) - THE WESTERN PACIFIC: ISLAND ARCS, MARGINAL SEAS, GEOCHEMISTRY. Perth, Univ. W. Aust. Press, 163-77.

WILSON, J.T., 1954 - The development and structure of the crust; in KUIPER, G.P., (ed.) - THE EARTH AS A PLANET. Univ. Chicago Press, 138-214.

WYLLIE, P.J., 1971 - Role of water in magma generation and initiation of diapiric uprise in the mantle. J. geophys. Res., 76, 1328-38.

WYLLIE, P.J., 1973 - Experimental petrology and global tectonics - a preview; in Experimental petrology and global tectonics. Tectonophysics, 17, 189-209.

YODER, H.S., & TILLEY, C.E., 1962 - Origin of basalt magmas: an experimental study of natural and synthetic rock systems. J. Pet., 3, 342-532.

APPENDIX 1

EARTHQUAKE DISTRIBUTION AT THE SOUTHERN MARGIN OF THE BISMARCK SEA

by

V.F. DENT AND R.W. JOHNSON

Epicentres of well located earthquakes between January 1969 and June 1974 are shown in Figure A. The data sources and selection criteria for these earthquakes are as follows.

Events in 1969 and 1970, and between July and December 1971: data source - Regional Catalogue of Earthquakes, v. 6, nos. 1 and 2, v. 7, nos. 1 and 2, and v. 8, no. 2 (published by The International Seismological Centre, Scotland); selection criteria - only those events recorded by 10 or more stations, and with co-ordinates given to two decimal places. Events between January and June 1971 and between January 1972 and June 1974: data source - earthquake data file of the Bureau of Mineral Resources; selection criterion - only those events recorded by 10 or more stations.

Cross-sections showing the distribution of the earthquakes beneath four sectors of the western arc and three of the eastern arc are presented in Figures B1 to B7. The surface traces of the cross-section planes are shown as solid lines in Figure A. The two dashed lines on either side of each solid line indicate the boundaries of the area within which the epicentres were projected normally onto each central plane.

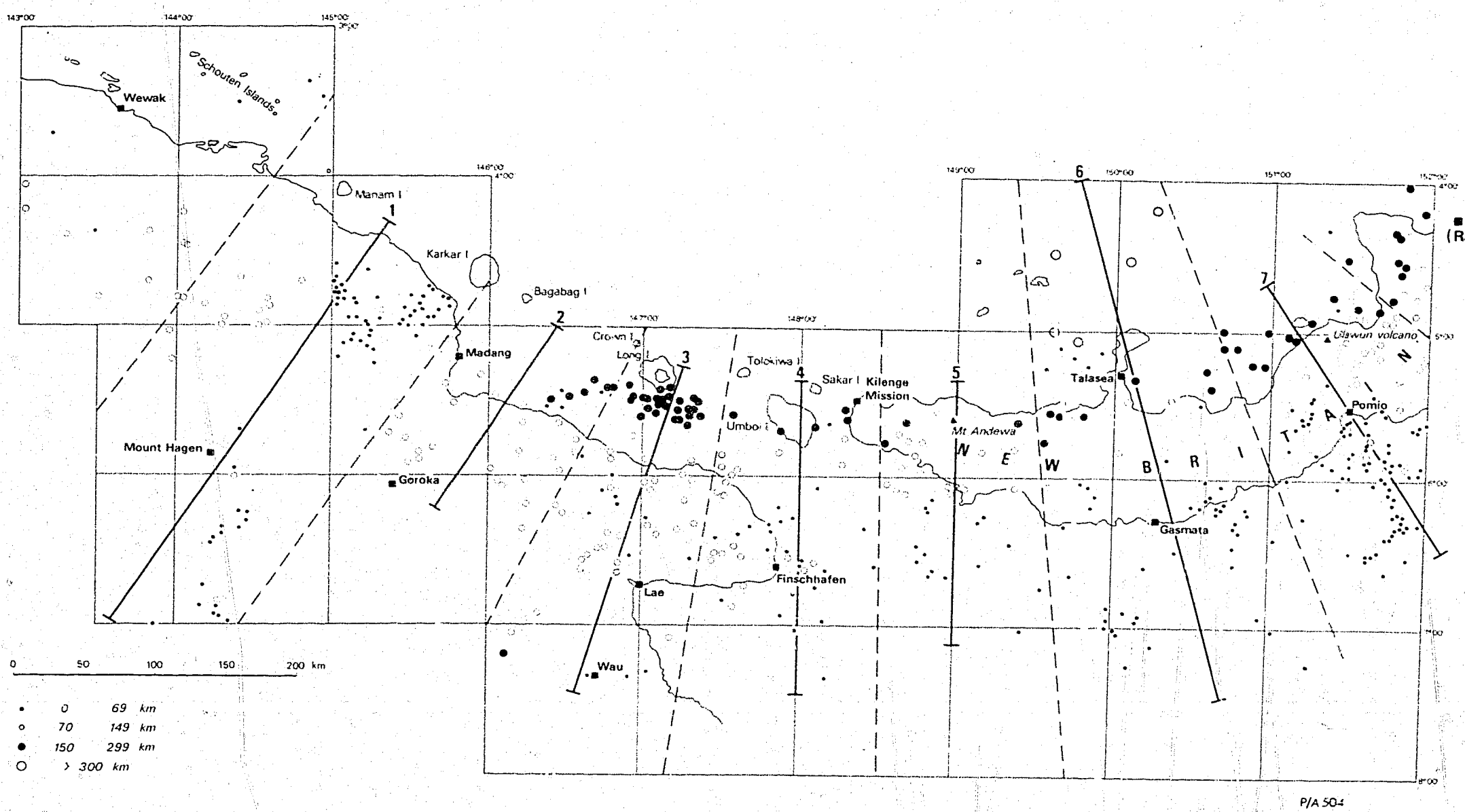

Fig. A. Distribution of epicentres.

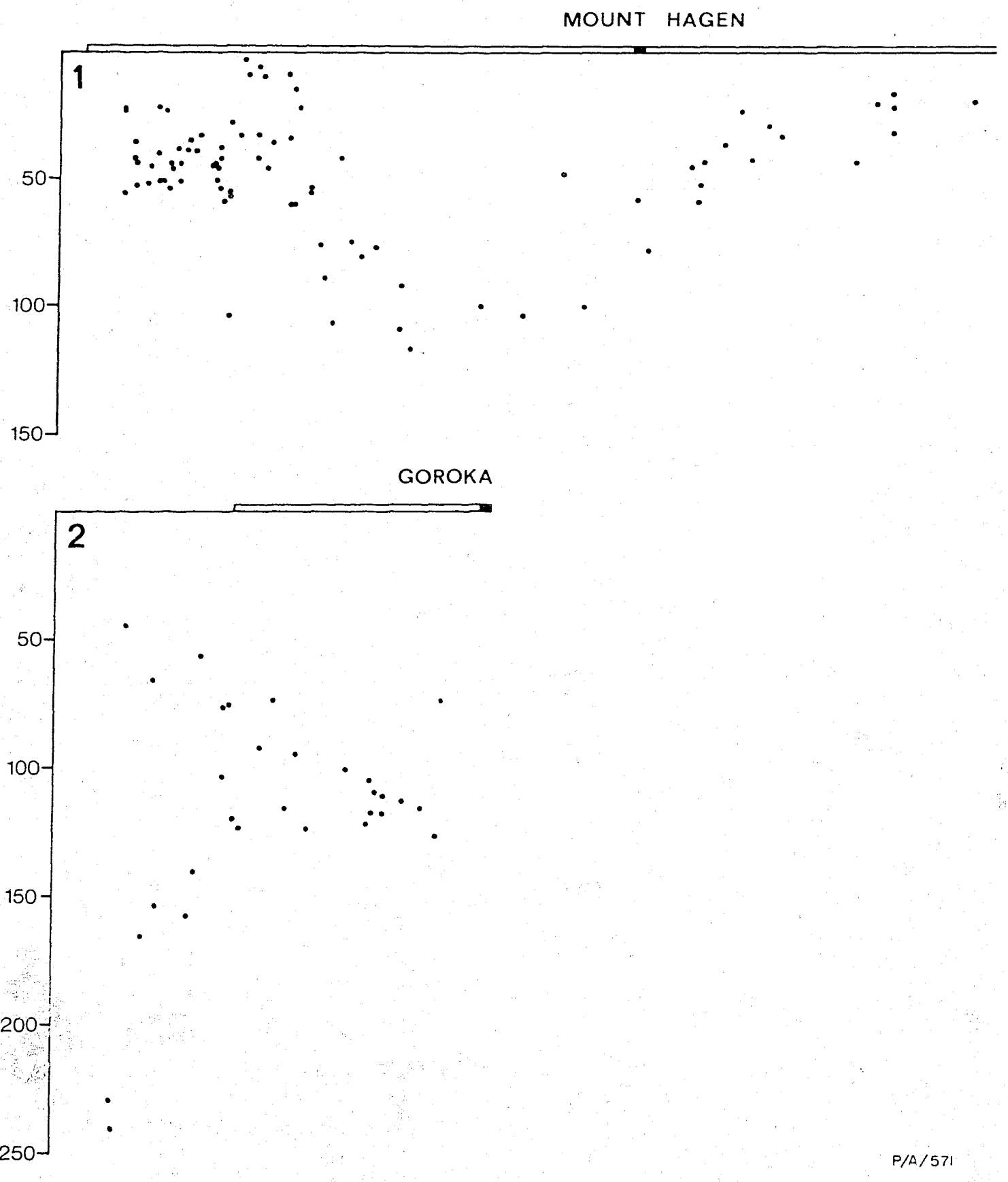

Fig. B, 1 to 7 (see also next four pages). Cross-sections through the western and eastern arcs (cf. Fig. A). Northern ends of the sections are on the left-hand side, and vertical and horizontal scales are equal.

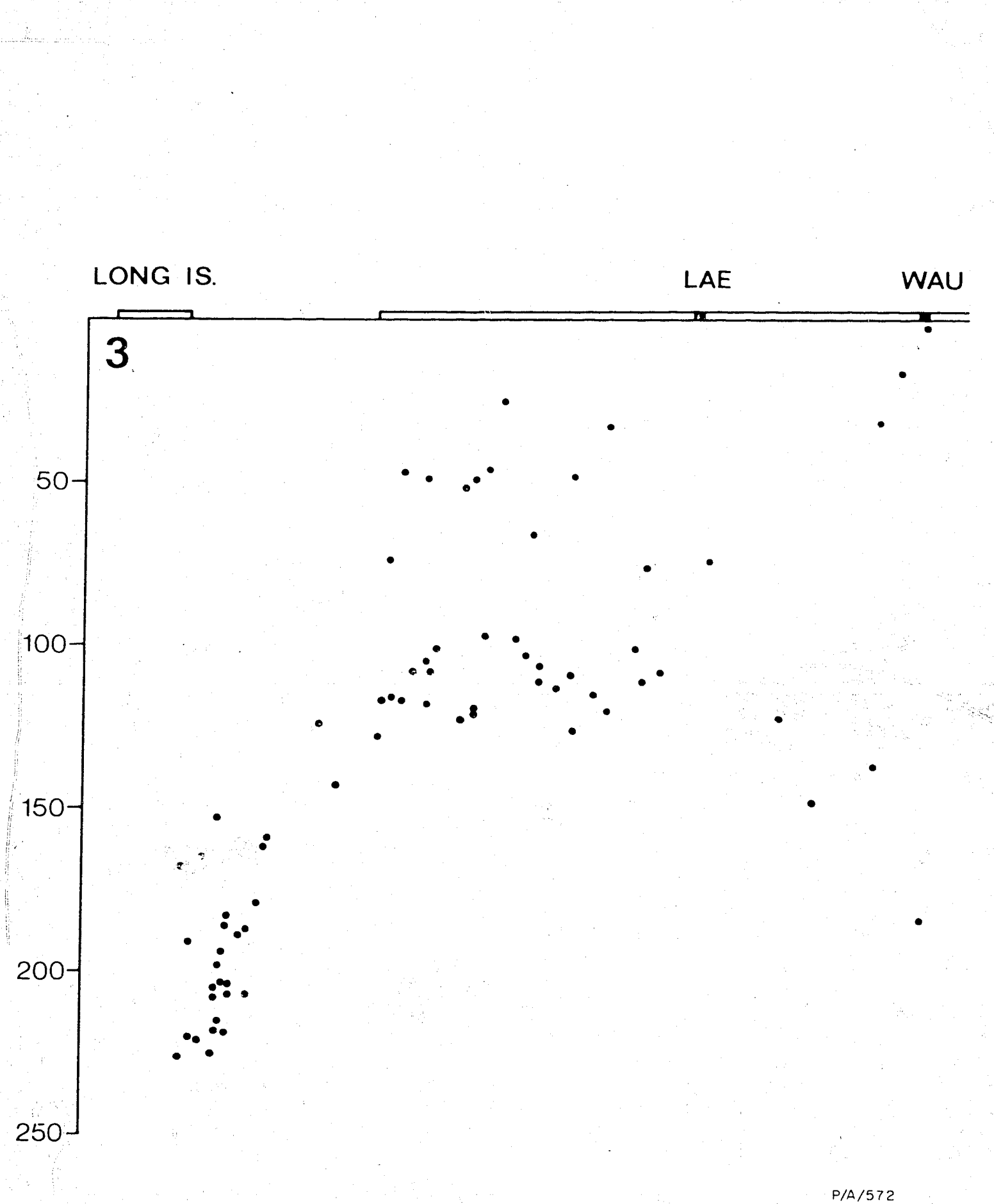
LONG IS.
LAE
WAU
3
50
100
150
200
250
P/A/572

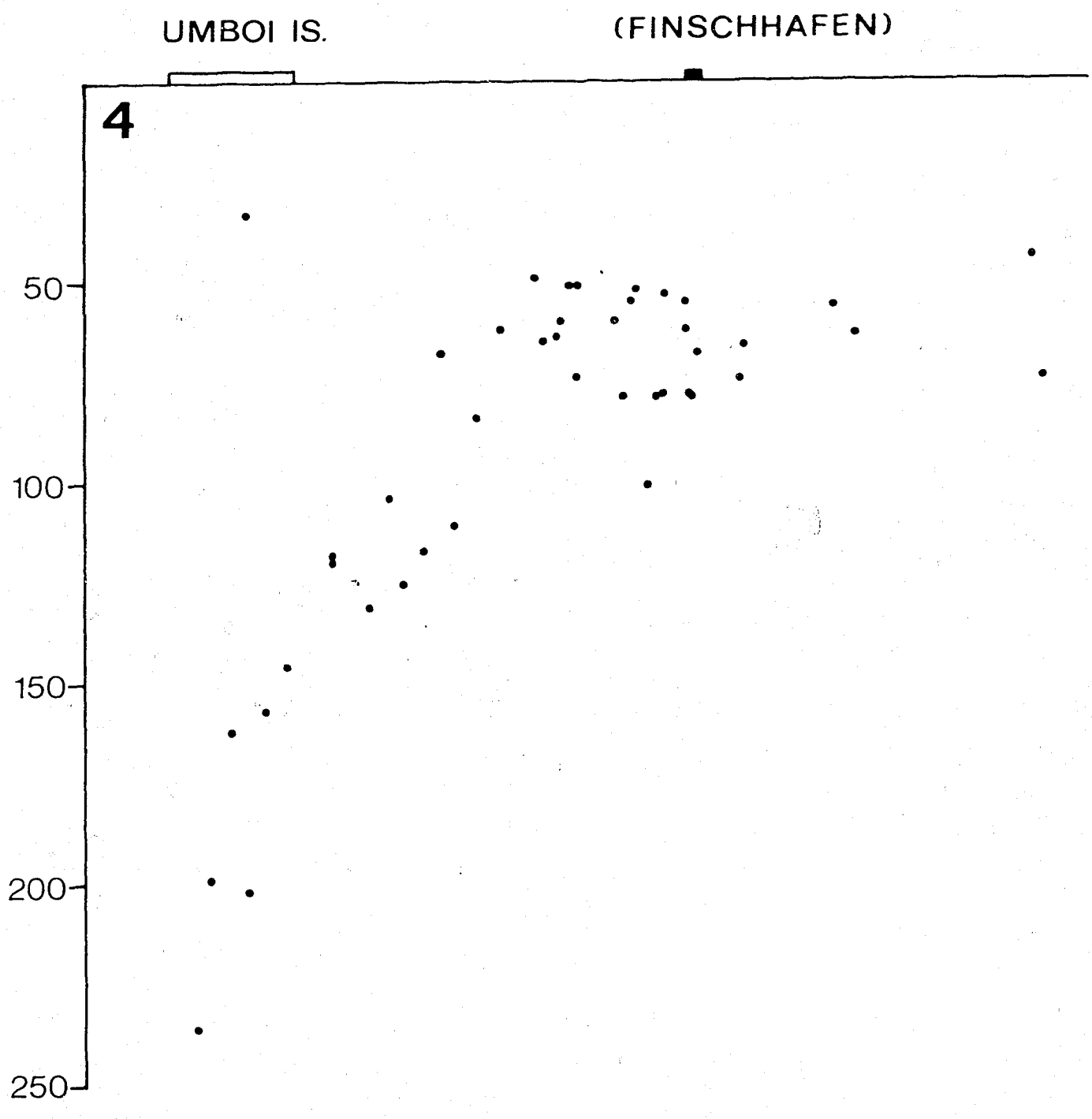

P/A/573

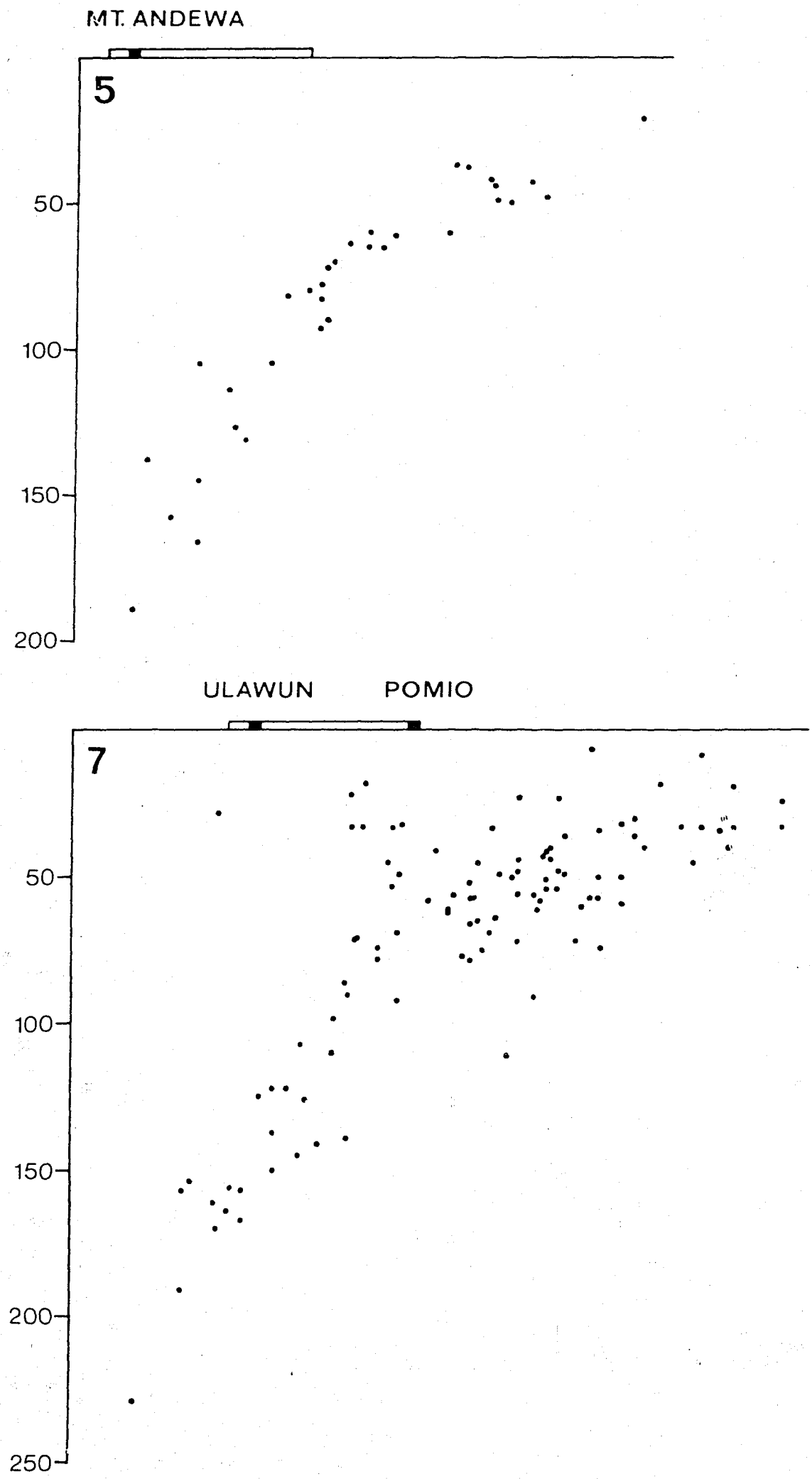

P/A/574

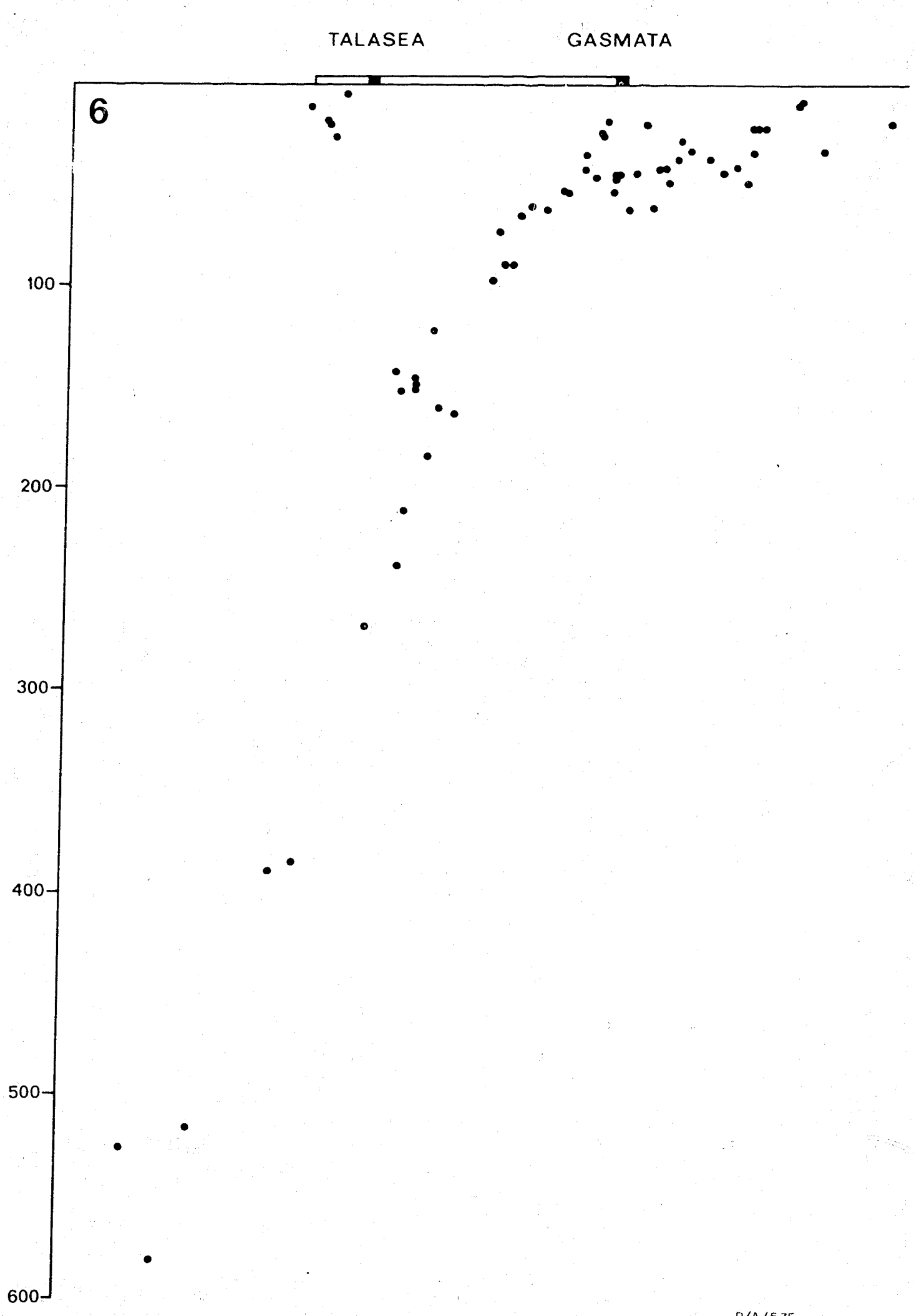
TALASEA
GASMATA
6
100
200
300
400
500
600
P/A/575

APPENDIX 2 LIST OF 348 CHEMICAL ANALYSES

	SiO_2	TiO_2	Al_2O_3	Fe_2O_3	FeO	MnO	MgO	CaO	Na_2O	K_2O	P_2O_5	H_2O^+	H_2O^-	CO_2
ZONE A														
18NG1010	54.90	.38	16.50	4.80	4.25	.16	5.40	9.40	2.25	1.36	.19	.36	.10	.04
18NG1013	62.50	.50	16.00	2.75	3.65	.13	2.90	6.60	2.70	1.50	.22	.13	.09	.05
18NG1019	56.30	.38	16.10	3.85	4.65	.16	5.25	9.25	2.30	1.05	.19	.32	.06	0.00
18NG1023	58.80	.46	17.10	3.25	4.10	.14	3.40	8.00	2.80	1.27	.25	.08	.02	0.00
18NG0989	55.60	.44	13.60	4.00	4.75	.16	6.35	10.00	1.91	2.15	.31	.11	.19	.08
18NG0992	58.10	.28	13.50	4.50	4.30	.16	5.95	8.80	1.95	1.35	.25	.29	.04	.05
18NG0997	53.90	.41	15.10	4.30	5.55	.13	5.95	10.40	2.10	1.08	.22	.37	.10	.05
18NG1001	55.50	.34	13.80	4.60	4.50	.16	6.15	9.80	2.00	2.20	.31	.13	.19	.08
18NG0966	65.70	.33	15.30	2.45	2.40	.17	1.62	4.55	3.25	2.35	.16	.77	.32	.10
18NG0973	55.60	.33	15.70	4.65	4.90	.17	6.40	9.65	1.88	.94	.16	.59	.30	.10
18NG0980	59.80	.36	14.20	3.25	4.35	.13	4.30	7.75	2.30	2.10	.16	1.37	.09	.05
18NG0982	59.80	.37	14.50	3.75	4.00	.14	4.30	7.20	2.35	1.98	.24	.45	.44	.05
18NG1018	58.60	.32	14.40	3.40	5.10	.14	5.95	8.40	1.89	.77	.09	.78	.26	.10
18NG1028	60.30	.32	14.60	3.80	4.45	.13	4.65	8.00	2.10	.85	.10	.34	.38	.07
18NG1031	58.40	.36	13.80	4.30	4.60	.14	5.10	8.60	1.98	.93	.15	.83	.36	.13
18NG1034	60.20	.32	14.00	3.90	4.35	.13	4.95	7.85	2.10	1.07	.11	.47	.65	.12
18NG1036	60.40	.69	17.00	3.30	1.95	.10	3.65	6.60	3.75	1.38	.46	.27	.21	0.00
18NG1037	60.50	.36	16.70	1.30	3.40	.09	4.95	8.00	2.85	.59	.13	.66	.36	0.00
18NG1038	63.50	.38	16.80	1.99	1.80	.06	3.45	6.40	3.70	.82	.17	.42	.56	0.00
18NG1038	61.50	.32	15.60	2.45	2.35	.07	5.55	7.10	2.95	.66	.14	.51	.71	.08
18NG1039	61.50	.36	16.20	1.95	3.05	.09	4.60	7.60	2.75	.73	.16	.65	.23	0.00
18NG1043	57.60	.51	16.00	2.75	6.15	.17	3.85	8.54	2.20	.48	.10	1.21	.32	.04
GTR15614	57.60	.31	13.50	4.75	4.60	.16	5.95	9.00	2.00	1.45	.24	.33	.16	.02
GTR15617	58.50	.32	15.20	3.40	4.30	.15	4.60	7.70	2.40	1.69	.23	1.48	.38	.01
ZONE B														
27NG0763	53.90	.69	19.90	2.50	5.00	.16	3.90	9.20	3.00	.77	.22	.37	.33	.06
27NG0764	65.90	.24	16.80	1.92	1.92	.15	1.50	5.55	3.25	1.55	.16	.76	.12	.06
27NG0764	61.90	.35	17.70	2.65	2.55	.14	2.30	6.30	3.55	1.19	.16	.78	.28	.12
27NG0764	52.80	.65	19.20	8.80	.66	.20	3.65	8.70	3.10	.80	.24	.69	.19	.06
27NG0767	56.40	.46	17.60	3.10	4.40	.15	4.30	8.80	2.70	1.10	.15	.25	.23	.16
27NG0769	54.80	.59	17.60	2.35	5.20	.15	4.70	9.55	2.50	1.12	.12	.71	.39	.04
26NG0083	50.40	.40	13.20	3.35	5.65	.16	9.45	12.30	1.42	.81	.16	.87	1.33	.20
26NG0780	53.20	.56	16.50	3.30	5.80	.17	5.75	10.40	2.35	1.08	.21	.19	.33	.11
26NG0787	52.10	.72	17.20	3.95	6.30	.18	5.50	9.85	2.35	.70	.19	.27	.25	.14
26NG0788	51.20	.65	16.40	3.25	7.00	.18	6.50	11.20	2.00	.57	.16	.48	.34	.10
26NG0790	56.80	.44	17.00	3.15	4.60	.15	4.05	8.05	2.70	1.35	.16	.80	.40	.06
26NG0792	55.10	.59	17.30	2.55	5.90	.17	4.90	9.05	2.45	.65	.15	.49	.47	.05
26NG0793	51.60	.44	15.60	3.55	6.50	.19	7.20	11.70	1.82	.65	.14	.22	.28	.11
26NG0796	55.90	.59	16.80	2.75	5.85	.17	4.60	8.80	2.30	.90	.17	.48	.60	.17
26NG0801	53.80	.49	16.30	3.35	7.40	.19	6.50	11.70	1.83	.51	.15	.23	.14	.05
26NG0811	55.90	.63	15.90	3.20	6.75	.18	4.75	8.40	2.50	1.00	.25	.60	.18	.03
65400056	55.10	.73	15.30	5.15	6.40	.18	3.90	8.00	2.55	1.40	.20	.78	.18	.04
65400057	55.90	.61	16.80	3.80	6.80	.18	2.75	7.80	3.05	1.25	.21	.45	.28	.06
65400065	56.30	.47	18.40	2.90	6.10	.16	2.85	8.45	2.90	.90	.16	.63	.26	.02
65400066	54.90	.63	16.80	2.20	8.45	.17	3.55	8.10	2.80	1.20	.22	.67	.20	0.00
65400071	52.90	.56	18.40	5.15	4.35	.15	3.55	9.45	2.55	1.10	.20	.72	.26	.07
65400074	54.70	.60	16.80	3.90	7.20	.18	3.70	8.00	2.80	1.20	.21	.37	.37	.07
65400074	53.40	.48	15.90	3.10	7.10	.18	5.80	10.20	2.20	.87	.14	.28	.24	.03
65400074	54.80	.63	17.10	3.90	6.95	.17	3.50	8.10	2.80	1.20	.21	.34	.22	.03
19NG0952	58.80	.28	17.40	4.75	2.00	.14	3.90	8.00	3.15	1.18	.16	.28	.08	.05
19NG0953	53.00	.42	14.50	3.95	5.10	.17	8.20	11.00	2.00	.55	.14	.79	.11	.04
19NG0954	51.10	.43	14.90	6.00	4.60	.17	8.50	11.40	1.78	.43	.09	.41	.03	.12
19NG0955	48.90	.35	11.80	4.85	4.65	.17	13.80	13.50	.93	.13	.09	.28	.18	.09
19NG0959	61.70	.27	17.20	3.30	2.45	.13	3.20	6.80	3.35	1.20	.16	.15	.05	.09
19NG0961	53.20	.35	14.50	5.30	3.70	.15	8.40	11.20	2.10	.62	.11	.21	.07	.13
19NG0965	60.20	.29	17.40	3.90	2.40	.14	3.45	7.55	3.05	1.16	.16	.07	.09	.08
GTR15618	56.30	.69	15.60	2.75	8.55	.18	3.30	7.70	2.85	1.15	.23	.59	.20	.01
GTR15628	54.20	.57	18.30	2.35	7.30	.17	3.75	9.70	2.50	.88	.17	.26	.15	.02
GTR15635	54.20	.75	18.10	2.85	6.90	.17	3.25	9.65	2.50	.89	.16	.12	.11	.04
GTR15479	54.20	.59	18.60	2.45	7.20	.16	3.50	9.80	2.60	.89	.17	.15	.07	.05
GTR15639	62.00	.44	16.10	3.35	3.25	.14	2.80	6.85	3.05	1.61	.23	.07	.13	.01
GTR15636	53.90	.38	16.60	4.90	3.90	.17	6.70	10.50	2.40	.69	.12	.06	.07	.05
GAMTMD21	53.20	.33	14.39	6.11	3.60	.15	8.30	10.93	2.44	.74	.22	0.00	.03	0.00
GAMTMD23	53.08	.35	14.84	5.96	3.81	.16	7.37	10.70	2.61	.83	.19	.07	.03	0.00
GAMTMD25	53.05	.35	13.90	6.07	3.99	.16	8.60	10.68	2.57	.90	.25	0.00	0.00	0.00
GAMTMD31	52.79	.30	14.28	4.90	4.75	.16	8.66	11.08	2.46	.79	.17	0.00	.02	0.00
GAMTMD56	52.16	.30	16.62	6.23	2.73	.16	8.45	10.96	1.80	.70	.22	0.00	0.00	0.00
GAMTMD58	51.80	.33	14.19	6.18	4.02	.15	8.73	10.58	2.50	.83	.19	.13	.08	0.00
GAMTMD59	51.76	.31	16.01	5.87	3.25	.14	8.45	11.00	1.44	.70	.20	0.00	0.00	0.00
GAMTMD60	51.76	.32	16.29	5.20	3.32	.14	8.31	11.10	2.10	.74	.18	0.00	0.00	0.00
GAMTMD61	51.74	.32	16.68	5.20	3.65	.18	8.71	11.10	1.80	.72	.18	0.00	0.00	0.00
GAMTMD62	51.74	.31	15.84	6.33	2.99	.13	8.42	11.15	1.26	.72	.20	0.00	0.00	0.00
GAMTMD63	51.52	.30	16.18	5.75	3.16	.12	8.37	10.90	2.32	.71	.20	0.00	0.00	0.00
GAMTMD64	51.45	.35	14.56	5.01	4.49	.16	8.64	10.99	2.48	.91	.15	0.00	.02	0.00
GTR15649	52.70	.37	17.00	4.45	4.40	.17	6.80	10.75	2.50	.66	.11	.08	0.00	.02
GTR15651	52.90	.39	17.00	4.35	4.45	.16	6.70	10.65	2.55	.67	.12	.15	.03	.02
GTR15612	53.30	.68	17.80	3.50	6.40	.17	4.90	9.50	2.40	.72	.20	.31	.46	.02

For more precise locality descriptions, see references listed in the introduction P/A 576

'NG' sample numbers refer mainly to hitherto unpublished BMR analyses.

ZONE	C	SiO_2	TiO_2	Al_2O_3	Fe_2O_3	FeO	MnO	MgO	CaO	Na_2O	K_2O	P_2O_5	H_2O^+	H_2O^-	CO_2
	32NG0702	57.60	.51	17.80	5.85	.62	.16	3.70	7.65	3.00	1.63	.29	.42	.16	0.00
	32NG0702	53.70	.64	17.70	3.05	5.00	.15	5.35	9.20	2.85	1.51	.35	.16	.18	.05
	32NG0704	56.70	.50	18.00	3.60	3.45	.15	4.00	8.40	3.05	1.71	.31	.09	.19	.05
	32NG0709	50.90	.69	16.90	3.65	5.25	.17	7.45	10.50	2.60	1.01	.29	.19	.11	.12
	32NG0719	51.20	.76	16.60	4.05	4.90	.17	6.80	10.80	2.35	1.34	.27	.24	.16	0.00
	32NG0721	50.90	.73	16.20	2.90	6.20	.18	7.60	10.60	2.35	1.26	.26	.39	.17	.07
	32NG0722	53.00	.72	19.10	3.45	4.25	.15	3.90	9.10	3.05	1.88	.33	.64	.18	0.00
	32NG0726	48.90	.63	16.70	3.95	6.65	.19	7.50	11.90	2.15	.88	.22	.16	.12	.08
	32NG0728	50.70	.71	17.70	4.05	5.70	.16	6.00	10.90	2.50	1.16	.35	.17	.13	0.00
	GTR15285	55.60	.81	16.50	2.90	8.20	.21	3.10	7.30	3.13	1.93	.36	.13	.23	.02
	32NG0120	48.50	.88	17.90	3.80	7.35	.20	6.20	11.00	2.30	.61	.19	.45	.61	.05
	32NG0124	56.70	.80	15.10	2.80	8.20	.25	3.10	6.95	3.25	2.25	.39	.07	.05	.10
	32NG0127	58.50	.76	14.80	2.25	7.65	.25	1.99	5.20	3.60	3.10	.44	1.22	.18	0.00
	32NG0131	49.00	.77	18.40	3.25	7.40	.19	6.25	11.60	2.10	.61	.21	.05	.31	0.00
	32NG0140	55.30	.84	15.70	2.25	8.75	.16	2.90	7.60	3.20	2.20	.63	.40	.02	.11
	32NG0142	49.30	.76	17.50	3.55	7.95	.25	4.95	11.70	1.95	1.11	.20	.30	0.00	.11
	32NG0143	51.40	.65	17.40	2.75	8.05	.22	4.40	10.90	2.35	1.33	.25	.17	.01	.13
	32NG0730	50.30	.78	15.70	5.70	7.20	.23	5.30	10.20	2.50	1.25	.24	.19	.09	.10
	32NG0739	50.90	.68	19.20	3.45	6.55	.19	3.60	10.50	2.35	1.25	.25	.33	.33	.05
	32NG0739	56.40	.82	15.30	3.25	7.90	.26	3.15	6.95	3.10	2.05	.39	.19	.01	0.00
	32NG0744	51.10	.64	19.10	2.95	7.20	.19	3.70	10.60	2.55	1.40	.26	.46	.08	0.00
	32NG0754	48.10	.66	17.90	4.75	6.65	.20	6.85	11.50	1.99	.72	.15	.40	.09	0.00
	32NG0759	46.60	.58	17.40	4.95	6.70	.24	7.30	12.20	1.70	.61	.17	.40	.86	0.00
ZONE D															
	32NG0001	55.60	.54	16.90	3.35	5.65	.18	4.10	8.55	2.70	1.56	.18	.35	.03	.15
	32NG0002	50.50	.61	17.00	4.50	6.50	.20	5.60	9.80	2.50	1.00	.16	.86	.50	.05
	32NG0003	53.70	.56	16.10	3.55	6.25	.19	5.10	9.55	2.70	1.47	.22	.23	.04	.15
	32NG0013	54.90	.43	17.80	3.90	4.65	.18	4.70	8.80	2.55	1.10	.12	.73	.27	.05
	32NG0020	56.40	.56	17.00	3.35	5.40	.17	3.90	8.25	2.85	1.74	.19	.06	.06	.05
	32NG0021	56.90	.51	16.80	3.25	5.45	.16	3.95	8.30	2.85	1.71	.19	.15	.02	.05
	32NG0024	55.10	.53	16.80	3.35	5.65	.18	4.10	8.80	2.75	1.58	.18	.70	.01	.05
	32NG0026	47.90	.61	13.20	4.15	6.50	.19	10.90	13.30	1.68	.41	.14	.69	.35	.05
	32NG0026	50.40	.53	16.00	4.50	5.80	.18	7.25	11.70	1.94	.73	.14	.50	.20	.05
	32NG0028	50.50	.60	18.00	3.65	6.95	.20	5.35	10.10	2.40	.71	.17	.69	.31	.05
	32NG0030	54.40	.37	15.80	3.70	5.10	.18	5.70	9.55	2.30	1.00	.11	1.27	.21	.05
	32NG0031	49.70	.48	13.80	4.20	6.80	.20	9.35	12.00	1.90	.84	.17	.32	.06	.05
	32NG0036	52.60	.61	17.10	3.55	6.45	.19	4.60	9.25	2.65	1.50	.20	.86	.12	.05
	32NG0037	50.90	.56	17.40	4.45	6.20	.19	5.55	9.95	2.35	1.04	.15	.80	.13	.05
	32NG0040	52.90	.52	16.20	3.25	5.85	.17	5.60	9.95	2.45	1.27	.17	.99	.30	.05
	32NG0043	53.00	.59	16.20	3.70	6.35	.17	5.55	9.70	2.35	1.29	.17	.36	.18	.09
	32NG0047	52.20	.56	15.40	3.30	6.35	.18	7.15	10.20	2.45	1.36	.23	.62	.14	0.00
	32NG0051	49.30	.40	11.60	3.55	5.80	.17	15.10	10.80	1.73	.82	.12	.35	.10	.05
	32NG0086	56.20	.53	16.30	2.70	5.20	.07	6.65	8.30	2.80	1.00	.19	.12	.06	0.00
	32NG0091	51.80	.51	14.00	2.55	6.20	.17	9.85	11.30	2.00	1.18	.22	.20	.08	0.00
	32NG0094	52.40	.52	14.30	4.00	5.50	.15	8.35	11.30	1.97	.83	.16	.20	.06	0.00
	32NG0094	52.40	.53	13.70	3.45	6.05	.15	9.15	11.40	1.82	.88	.20	.15	.05	0.00
	32NG0067	57.90	.57	17.90	3.90	2.80	.11	3.50	7.55	2.90	1.65	.16	.85	.26	.05
	32NG0067	57.50	.50	18.20	4.30	2.40	.15	3.10	7.45	2.90	1.76	.16	1.21	.25	.10
	32NG0067	58.10	.46	17.60	6.20	.22	.15	3.30	6.95	2.70	1.90	.20	1.73	.33	0.00
	32NG0070	57.80	.44	17.70	3.50	3.10	.16	3.20	8.05	3.25	1.60	.19	.41	.25	0.00
	32NG0079	47.60	.55	14.10	3.25	6.60	.18	12.10	12.40	1.62	.51	.16	.17	.21	.20
	32NG0082	52.00	.46	13.70	3.20	6.55	.18	8.60	11.50	1.82	.84	.14	.67	.16	0.00
	32NG0085	51.10	.62	16.60	2.90	6.55	.17	6.90	11.50	1.80	.68	.18	.41	.17	.05
	32NG0629	50.00	.51	13.60	3.10	6.05	.17	11.70	11.20	1.39	.75	.18	1.10	.09	.05
	32NG0072	50.80	.63	15.90	3.65	6.55	.19	6.95	10.50	1.92	1.24	.27	.33	.23	.05
	32NG0075	54.00	.56	18.10	4.65	4.05	.15	4.00	8.00	2.30	1.60	.26	.36	.66	.15
	32NG0096	54.50	.54	16.30	3.10	5.95	.16	5.25	9.80	2.15	1.49	.19	.09	.11	0.00
	32NG0100	52.40	.62	16.30	3.05	7.20	.20	4.70	9.90	2.05	.92	.15	.21	.15	.05
	32NG0106	55.30	.48	21.50	2.80	4.05	.15	2.30	9.65	2.50	.92	.14	.27	.07	0.00
	32NG0107	53.30	.46	18.30	3.15	6.75	.18	5.15	9.80	1.84	.49	.08	0.00	.32	0.00
	32NG0110	64.30	.69	15.00	1.08	5.35	.09	1.50	4.35	3.80	3.00	.37	.19	.07	.10
	32NG0111	49.90	.42	12.00	3.65	6.05	.18	14.90	10.50	1.62	.56	.11	.25	.07	0.00
	32NG0662	54.40	.61	15.90	2.95	6.30	.16	5.85	9.50	1.97	1.36	.17	.37	.33	0.00
	32NG0667	54.20	.57	16.10	2.95	6.00	.17	5.60	9.80	2.05	1.60	.17	.65	.15	0.00
	32NG0674	54.90	.56	16.30	3.00	5.85	.16	5.05	9.30	2.15	1.72	.18	.29	.13	0.00
	32NG0675	53.40	.58	17.60	3.55	6.10	.18	5.10	9.40	2.40	.91	.19	.30	.18	0.00
	32NG0679	49.50	.60	18.70	4.80	6.35	.20	5.55	10.80	2.20	.66	.16	.24	.08	.10
	32NG0682	50.00	.63	15.80	4.75	7.25	.21	7.05	11.00	1.84	.53	.14	.30	.20	0.00
ZONE E															
	53NG0850	55.30	.50	17.90	3.35	5.00	.15	4.25	9.30	2.75	.46	.07	.43	.37	0.00
	53NG0850	53.80	.67	18.70	3.10	5.55	.15	3.85	10.10	2.35	.44	.07	.66	.29	0.00
	53NG0852	53.90	.67	18.50	2.95	5.70	.15	3.90	9.70	2.50	.36	.07	.86	.48	0.00
	53NG0857	64.70	.48	15.70	3.65	1.95	.13	1.95	5.20	3.50	.93	.07	.76	.88	0.00

ZONE	C	SiO_2	TiO_2	Al_2O_3	Fe_2O_3	FeO	MnO	MgO	CaO	Na_2O	K_2O	P_2O_5	H_2O^+	H_2O^-	CO_2
	32NG0702	57.60	.51	17.80	5.85	.62	.16	3.70	7.65	3.00	1.63	.29	.42	.16	0.00
	32NG0702	53.70	.64	17.70	3.05	5.00	.15	5.35	9.20	2.85	1.51	.35	.16	.18	.05
	32NG0704	56.70	.50	18.00	3.60	3.45	.15	4.00	8.40	3.05	1.71	.31	.09	.19	.05
	32NG0709	50.90	.69	16.90	3.65	5.25	.17	7.45	10.50	2.60	1.01	.29	.19	.11	.12
	32NG0719	51.20	.76	16.60	4.05	4.90	.17	6.80	10.80	2.35	1.34	.27	.24	.16	0.00
	32NG0721	50.90	.73	16.20	2.90	6.20	.18	7.60	10.60	2.35	1.26	.26	.39	.17	.07
	32NG0722	53.00	.72	19.10	3.45	4.25	.15	3.90	9.10	3.05	1.88	.33	.64	.18	0.00
	32NG0726	48.90	.63	16.70	3.95	6.65	.19	7.50	11.90	2.15	.88	.22	.16	.12	.08
	32NG0728	50.70	.71	17.70	4.05	5.70	.16	6.00	10.90	2.50	1.16	.35	.17	.13	0.00
	GTR15285	55.60	.81	16.50	2.90	8.20	.21	3.10	7.30	3.13	1.93	.36	.13	.23	.02
	32NG0120	48.50	.88	17.90	3.80	7.35	.20	6.20	11.00	2.30	.61	.19	.45	.61	.05
	32NG0124	56.70	.80	15.10	2.80	8.20	.25	3.10	6.95	3.25	2.25	.39	.07	.05	.10
	32NG0127	58.50	.76	14.80	2.25	7.65	.25	1.99	5.20	3.60	3.10	.44	1.22	.18	0.00
	32NG0131	49.00	.77	18.40	3.25	7.40	.19	6.25	11.60	2.10	.61	.21	.05	.31	0.00
	32NG0140	55.30	.84	15.70	2.25	8.75	.16	2.90	7.60	3.20	2.20	.63	.40	.02	.11
	32NG0142	49.30	.76	17.50	3.55	7.95	.25	4.95	11.70	1.95	1.11	.20	.30	0.00	.11
	32NG0143	51.40	.65	17.40	2.75	8.05	.22	4.40	10.90	2.35	1.33	.25	.17	.01	.13
	32NG0730	50.30	.78	15.70	5.70	7.20	.23	5.30	10.20	2.50	1.25	.24	.19	.09	.10
	32NG0739	50.90	.68	19.20	3.45	6.55	.19	3.60	10.50	2.35	1.25	.25	.33	.33	.05
	32NG0739	56.40	.82	15.30	3.25	7.90	.26	3.15	6.95	3.10	2.05	.39	.19	.01	0.00
	32NG0744	51.10	.64	19.10	2.95	7.20	.19	3.70	10.60	2.55	1.40	.26	.46	.08	0.00
	32NG0754	48.10	.66	17.90	4.75	6.65	.20	6.85	11.50	1.99	.72	.15	.40	.09	0.00
	32NG0759	46.60	.58	17.40	4.95	6.70	.24	7.30	12.20	1.70	.61	.17	.40	.86	0.00
ZONE D															
	32NG0001	55.60	.54	16.90	3.35	5.65	.18	4.10	8.55	2.70	1.56	.18	.35	.03	.15
	32NG0002	50.50	.61	17.00	4.50	6.50	.20	5.60	9.80	2.50	1.00	.16	.86	.50	.05
	32NG0003	53.70	.56	16.10	3.55	6.25	.19	5.10	9.55	2.70	1.47	.22	.23	.04	.15
	32NG0013	54.90	.43	17.80	3.90	4.65	.18	4.70	8.80	2.55	1.10	.12	.73	.27	.05
	32NG0020	56.40	.56	17.00	3.35	5.40	.17	3.90	8.25	2.85	1.74	.19	.06	.06	.05
	32NG0021	56.90	.51	16.80	3.25	5.45	.16	3.95	8.30	2.85	1.71	.19	.15	.02	.05
	32NG0024	55.10	.53	16.80	3.35	5.65	.18	4.10	8.80	2.75	1.58	.18	.70	.01	.05
	32NG0026	47.90	.61	13.20	4.15	6.50	.19	10.90	13.30	1.68	.41	.14	.69	.35	.05
	32NG0026	50.40	.53	16.00	4.50	5.80	.18	7.25	11.70	1.94	.73	.14	.50	.20	.05
	32NG0028	50.50	.60	18.00	3.65	6.95	.20	5.35	10.10	2.40	.71	.17	.69	.31	.05
	32NG0030	54.40	.37	15.80	3.70	5.10	.18	5.70	9.55	2.30	1.00	.11	1.27	.21	.05
	32NG0031	49.70	.48	13.80	4.20	6.80	.20	9.35	12.00	1.90	.84	.17	.32	.06	.05
	32NG0036	52.60	.61	17.10	3.55	6.45	.19	4.60	9.25	2.65	1.50	.20	.86	.12	.05
	32NG0037	50.90	.56	17.40	4.45	6.20	.19	5.55	9.95	2.35	1.04	.15	.80	.13	.05
	32NG0040	52.90	.52	16.20	3.25	5.85	.17	5.60	9.95	2.45	1.27	.17	.99	.30	.05
	32NG0043	53.00	.59	16.20	3.70	6.35	.17	5.55	9.70	2.35	1.29	.17	.36	.18	.09
	32NG0047	52.20	.56	15.40	3.30	6.35	.18	7.15	10.20	2.45	1.36	.23	.62	.14	0.00
	32NG0051	49.30	.40	11.60	3.55	5.80	.17	15.10	10.80	1.73	.82	.12	.35	.10	.05
	32NG0086	56.20	.53	16.30	2.70	5.20	.07	6.65	8.30	2.80	1.00	.19	.12	.06	0.00
	32NG0091	51.80	.51	14.00	2.55	6.20	.17	9.85	11.30	2.00	1.18	.22	.20	.08	0.00
	32NG0094	52.40	.52	14.30	4.00	5.50	.15	8.35	11.30	1.97	.83	.16	.20	.06	0.00
	32NG0094	52.40	.53	13.70	3.45	6.05	.15	9.15	11.40	1.82	.88	.20	.15	.05	0.00
	32NG0067	57.90	.57	17.90	3.90	2.80	.11	3.50	7.55	2.90	1.65	.16	.85	.26	.05
	32NG0067	57.50	.50	18.20	4.30	2.40	.15	3.10	7.45	2.90	1.76	.16	1.21	.25	.10
	32NG0067	58.10	.46	17.60	6.20	.22	.15	3.30	6.95	2.70	1.90	.20	1.73	.33	0.00
	32NG0070	57.80	.44	17.70	3.50	3.10	.16	3.20	8.05	3.25	1.60	.19	.41	.25	0.00
	32NG0079	47.60	.55	14.10	3.25	6.60	.18	12.10	12.40	1.62	.51	.16	.17	.21	.20
	32NG0082	52.00	.46	13.70	3.20	6.55	.18	8.60	11.50	1.82	.84	.14	.67	.16	0.00
	32NG0085	51.10	.62	16.60	2.90	6.55	.17	6.90	11.50	1.80	.68	.18	.41	.17	.05
	32NG0629	50.00	.51	13.60	3.10	6.05	.17	11.70	11.20	1.39	.75	.18	1.10	.09	.05
	32NG0072	50.80	.63	15.90	3.65	6.55	.19	6.95	10.50	1.92	1.24	.27	.33	.23	.05
	32NG0075	54.00	.56	18.10	4.65	4.05	.15	4.00	8.00	2.30	1.60	.26	.36	.66	.15
	32NG0096	54.50	.54	16.30	3.10	5.95	.16	5.25	9.80	2.15	1.49	.19	.09	.11	0.00
	32NG0100	52.40	.62	16.30	3.05	7.20	.20	4.70	9.90	2.05	.92	.15	.21	.15	.05
	32NG0106	55.30	.48	21.50	2.80	4.05	.15	2.30	9.65	2.50	.92	.14	.27	.07	0.00
	32NG0107	53.30	.46	18.30	3.15	6.75	.18	5.15	9.80	1.84	.49	.08	0.00	.32	0.00
	32NG0110	64.30	.69	15.00	1.08	5.35	.09	1.50	4.35	3.80	3.00	.37	.19	.07	.10
	32NG0111	49.90	.42	12.00	3.65	6.05	.18	14.90	10.50	1.62	.56	.11	.25	.07	0.00
	32NG0662	54.40	.61	15.90	2.95	6.30	.16	5.85	9.50	1.97	1.36	.17	.37	.33	0.00
	32NG0667	54.20	.57	16.10	2.95	6.00	.17	5.60	9.80	2.05	1.60	.17	.65	.15	0.00
	32NG0674	54.90	.56	16.30	3.00	5.85	.16	5.05	9.30	2.15	1.72	.18	.29	.13	0.00
	32NG0675	53.40	.58	17.60	3.55	6.10	.18	5.10	9.40	2.40	.91	.19	.30	.18	0.00
	32NG0679	49.50	.60	18.70	4.80	6.35	.20	5.55	10.80	2.20	.66	.16	.24	.08	.10
	32NG0682	50.00	.63	15.80	4.75	7.25	.21	7.05	11.00	1.84	.53	.14	.30	.20	0.00
ZONE E															
	53NG0850	55.30	.50	17.90	3.35	5.00	.15	4.25	9.30	2.75	.46	.07	.43	.37	0.00
	53NG0850	53.80	.67	18.70	3.10	5.55	.15	3.85	10.10	2.35	.44	.07	.66	.29	0.00
	53NG0852	53.90	.67	18.50	2.95	5.70	.15	3.90	9.70	2.50	.36	.07	.86	.48	0.00
	53NG0857	64.70	.48	15.70	3.65	1.95	.13	1.95	5.20	3.50	.93	.07	.76	.88	0.00

ZONE F	SiO_2	TiO_2	Al_2O_3	Fe_2O_3	FeO	MnO	MgO	CaO	Na_2O	K_2O	P_2O_5	H_2O^+	H_2O^-	CO_2
53NG2814	54.70	.57	16.80	6.15	3.35	.17	5.20	9.80	2.40	.4[illegible]	.09	.34	.08	0.00
53NG0814	68.50	.76	13.90	1.45	3.20	.13	.96	3.10	3.90	1.60	.20	1.72	.35	.04
53NG0819	65.90	.67	15.50	1.96	3.50	.14	1.55	4.55	4.15	1.05	.16	.40	.26	0.00
53NG0827	53.50	.59	17.10	2.70	6.65	.17	5.75	10.60	2.05	.37	.06	.35	.14	0.00
53NG0832	54.40	.60	19.00	2.72	5.80	.16	3.70	9.80	2.65	.41	.16	.43	.29	0.00
53NG0835	55.90	.66	18.20	2.75	5.35	.15	3.20	9.25	2.90	.56	.09	.56	.17	0.00
53NG0839	50.90	.58	17.60	2.62	8.15	.20	5.50	10.60	1.79	.19	.05	.64	.69	0.00
53NG0846	59.90	.83	14.50	3.20	5.45	.16	2.50	6.25	3.40	.84	.15	1.86	.66	0.00
53NG1047	68.70	.84	15.10	7.46	1.97	.16	2.65	6.70	3.20	.83	.16	.14	.29	0.00
53NG1049	63.90	.80	14.50	1.81	5.55	.15	1.95	5.70	3.60	.99	.16	.54	.09	0.00
53NG1051	69.20	.74	13.70	.99	4.20	.14	1.16	3.80	4.15	1.26	.24	.46	.04	0.00
53NG1054	62.20	.91	14.50	2.20	5.45	.16	2.20	5.85	4.00	.97	.24	.95	.15	0.00
53NG1056	68.80	.41	15.50	2.57	1.01	.11	1.14	4.35	4.05	1.05	.09	.42	.17	0.00
53NG2523	53.60	.61	15.90	3.50	5.55	.17	6.70	10.60	2.10	.39	.09	.43	.06	0.00
53NG2526	69.40	.69	14.30	1.16	3.40	.15	1.15	3.75	4.35	1.20	.22	.56	.05	0.00
51NG0218	55.60	.56	15.70	2.55	7.40	.16	4.85	9.10	2.20	.52	.06	.62	.34	.03
51NG0220	71.40	.46	14.30	2.55	.61	.08	.50	2.75	3.90	1.72	.12	.83	.69	.06
51NG3052	56.50	.47	16.50	2.40	5.55	.15	5.35	8.50	2.40	.6[illegible]	.1[illegible]	.94	0.00	.06
66490203	54.56	.49	17.74	2.91	5.90	.15	5.12	9.94	2.62	.30	.12	0.00	0.00	0.00
66490213	57.15	.56	17.92	2.66	5.85	.15	2.97	8.40	3.21	.56	.15	0.00	0.00	0.00
66490247	55.48	.52	17.46	2.58	5.76	.15	4.31	8.87	2.96	.47	.14	0.00	0.00	0.00
66490277	53.85	.52	17.30	3.66	5.53	.15	4.82	9.45	2.55	.56	.12	0.00	0.00	0.00
66490292	65.26	.42	16.44	2.61	1.97	.13	1.54	5.05	4.07	1.35	.21	0.00	0.00	0.00
66490102	55.00	.52	17.26	3.37	5.75	.16	5.42	9.41	2.78	.46	.17	0.00	0.00	0.00
66490106	51.24	.52	16.94	3.37	3.25	.14	2.28	6.19	3.94	.86	.24	0.00	0.00	0.00
66490134	57.60	.56	16.60	2.95	5.20	.13	3.85	7.70	2.95	.76	.14	.86	.74	0.00
66490147	69.10	.37	14.30	1.52	1.89	.08	1.05	3.60	3.95	1.54	.08	2.25	.16	0.00
66490151	52.78	.48	17.76	3.34	6.39	.16	5.69	10.55	2.23	.24	.17	0.00	0.00	0.00
66490152	54.93	.50	17.59	4.56	4.64	.17	4.34	8.96	2.67	.49	.17	0.00	0.00	0.00
66490153	66.99	.41	15.36	2.61	2.23	.13	1.41	4.83	4.06	1.05	.16	0.00	0.00	0.00
66490154	64.56	.47	16.00	2.64	3.37	.13	1.66	5.62	3.75	1.12	.16	0.00	0.00	0.00
66490159	63.31	.40	15.41	2.06	3.84	.12	3.66	6.75	3.23	1.05	.13	0.00	0.00	0.00
66490162	59.96	.44	16.20	3.06	4.56	.14	4.28	7.77	2.77	.86	.12	0.00	0.00	0.00
66490164	68.16	.40	15.20	2.99	1.37	.10	1.43	4.05	3.96	1.41	.15	0.00	0.00	0.00
66490171	54.74	.51	17.26	5.26	3.80	.12	3.75	8.66	2.66	.50	.15	0.00	0.00	0.00
66490174	57.26	.54	16.37	3.53	4.59	.14	3.65	8.55	2.95	.83	.17	0.00	0.00	0.00
51NG0225	56.40	.50	17.80	3.15	5.00	.14	4.35	8.25	2.80	.49	.09	.80	.16	.04
51NG0233	56.70	.53	15.80	3.40	4.10	.14	3.05	7.90	3.05	.63	.10	1.42	.06	.02
51NG0236	55.10	.56	18.40	3.25	4.95	.15	5.00	8.65	3.00	.43	.09	.20	.45	.10
51NG0239	52.50	.49	17.90	4.05	5.45	.16	5.60	10.20	2.15	.46	.06	.41	.16	0.00
51NG0241	52.20	.49	18.60	4.10	5.35	.17	5.55	9.85	2.20	.26	.06	.53	.36	0.00
51NG2686	57.20	.65	16.30	4.25	4.65	.13	3.90	8.15	2.65	.90	.16	.70	.30	.06
51NG3062	53.50	.66	16.90	4.30	4.95	.15	5.70	9.75	2.30	.35	.16	.61	.71	.06
51NG2682	62.60	.50	17.70	3.30	1.71	.08	1.81	5.90	3.45	1.10	.13	.62	.74	.07
51NG2683	63.40	.37	16.30	3.60	1.73	.10	2.40	6.00	3.05	1.15	.10	.7[illegible]	.71	.05
51NG2683	62.80	.38	16.30	2.65	2.15	.10	2.60	5.90	3.15	1.24	.10	1.02	1.27	.20
51NG2683	59.00	.45	19.90	1.46	3.35	.12	3.10	7.20	3.20	.80	.10	.41	.97	.18
51NG2683	57.20	.57	17.90	3.90	4.30	.14	3.75	7.45	2.75	.66	.10	.60	.60	.05
51NG2685	58.00	.55	15.70	3.10	3.25	.12	4.80	8.75	2.85	1.11	.10	.69	.75	.03
51NG2685	56.30	.46	15.90	3.65	3.75	.13	4.70	8.15	2.85	.86	.13	.45	.47	.04
51NG2699	57.50	.46	15.40	3.20	4.40	.14	5.25	8.40	2.50	.84	.09	.95	.67	.07
51NG2269	53.00	.51	16.60	4.20	5.25	.21	6.20	9.30	1.81	.43	.10	2.10	.10	0.00
51NG0270	53.50	.62	17.10	4.05	5.10	.15	5.45	10.40	2.10	.44	.11	.37	.33	.05
51NG0274	54.80	.43	17.60	3.85	5.40	.15	4.90	9.20	2.10	.41	.07	1.06	.20	.05
51NG0276	54.50	.36	18.40	3.15	5.40	.15	4.95	9.55	2.15	.42	.20	.73	.15	.03
51NG0277	53.70	.38	17.40	4.00	4.85	.15	6.65	10.40	1.85	.23	.07	.36	.42	.03
51NG0279	54.50	.45	16.50	3.85	4.70	.15	4.65	9.55	2.30	.41	.09	.47	.42	0.00
51NG0283	55.20	.44	13.30	2.60	5.60	.15	4.60	9.45	2.05	.34	.07	.46	.40	.13

ZONE G (SOUTHERN)

51NG0145	61.60	.50	15.70	3.15	3.55	.13	3.30	6.55	2.75	1.85	.13	.22	.16	.02
51NG0262	67.20	.55	14.90	2.92	1.35	.09	1.40	4.00	3.50	2.75	.10	.35	.37	0.00
51NG3063	61.50	.47	15.50	3.25	3.20	.12	3.45	6.70	2.80	1.91	.13	.34	.20	0.00
51NG3064	68.50	.54	14.60	1.62	2.15	.09	1.27	3.66	3.75	2.80	.16	.07	.19	0.00
51NG3065	62.70	.49	15.30	2.75	3.40	.12	3.20	6.20	2.90	1.90	.11	.03	.55	.05
51NG4704	59.60	.44	15.30	2.95	4.06	.13	4.15	7.40	2.65	1.62	.10	1.20	.30	.10
51NG2707	50.90	.52	15.60	5.20	4.85	.16	6.90	11.70	1.69	.62	.11	.82	.48	.05
51NG2707	62.00	.51	15.10	2.05	3.60	.11	2.95	6.15	2.85	2.10	.13	1.55	.26	.09
51NG2708	59.00	.51	16.90	3.15	3.90	.13	3.40	6.70	2.90	1.34	.14	1.07	.59	.05
51NG2709	60.60	.59	15.70	3.35	3.65	.13	3.25	6.80	3.00	1.90	.13	.09	.47	.05
51NG2713	61.80	.54	15.10	3.10	3.65	.12	3.40	6.55	2.95	2.05	.14	.29	.15	.06
51NG2713	61.70	.51	15.30	2.95	3.75	.13	3.40	6.60	2.90	1.77	.13	.20	.32	.05
51NG2714	62.40	.52	15.40	3.05	3.25	.11	2.65	6.10	3.00	2.05	.13	.91	.45	0.00
LOWDE279	72.19	.33	12.62	3.14	1.12	.05	.56	2.07	3.45	3.70	.02	.56	.24	0.00
LOWDE343	75.43	.27	12.56	1.56	.86	.07	.24	1.25	4.02	3.82	.02	.31	.09	0.00
51NG0255	57.10	.50	13.20	3.50	3.85	.14	7.35	9.05	2.35	1.26	.11	.45	.79	.10
51NG0271	75.60	.27	12.80	.33	.84	.07	.20	1.22	3.95	3.85	.03	.56	.02	0.00

	SiO_2	TiO_2	Al_2O_3	Fe_2O_3	FeO	MnO	MgO	CaO	Na_2O	K_2O	P_2O_5	H_2O^+	H_2O^-	CO_2
ZONE G (NORTHERN)														
LGNDE114	56.40	.89	15.30	2.25	6.71	.16	3.22	7.22	3.84	1.46	.25	.30	.07	0.00
LGNDE263	51.40	.75	15.07	3.30	7.74	.14	6.42	10.86	2.25	.70	.24	.54	.07	0.00
LGNDE296	52.40	.73	14.91	2.30	7.16	.16	7.42	10.84	2.36	.80	.17	.73	.14	0.00
LGNDE306	56.30	.71	14.63	1.53	3.77	.14	1.48	4.24	4.50	2.14	.21	.55	.12	0.00
LGNDE306	63.39	.74	15.15	2.12	4.46	.14	2.22	5.33	4.07	1.89	.21	.32	.06	0.00
LGNDE311	51.57	.80	15.91	2.72	7.04	.17	6.73	11.74	2.41	.44	.11	.35	.10	0.00
LGNDE319	66.91	.53	14.50	1.24	4.04	.14	1.29	3.76	4.65	2.22	.11	.56	.06	0.00
LGNDE339	53.83	1.01	15.46	5.00	6.74	.20	4.36	8.83	2.99	.92	.21	.44	.10	0.00
LGNDE341	58.93	.62	16.87	2.71	4.51	.16	2.92	6.67	3.66	1.63	.20	.86	.15	0.00
51NG0256	67.20	.66	14.40	1.45	3.55	.13	1.31	3.75	4.52	2.15	.24	.08	.18	.05
51NG0257	58.80	.86	15.50	2.35	6.50	.18	3.15	5.90	3.70	1.26	.25	0.00	.22	.05
51NG0258	66.70	.73	14.60	1.90	3.15	.14	1.46	3.25	4.40	2.00	.25	.75	.17	.14
51NG0259	53.50	.71	15.00	3.55	5.80	.16	6.05	10.80	2.40	.51	.14	.34	.17	.16
51NG0242	52.60	.76	16.50	3.60	5.75	.15	4.50	9.65	2.75	.40	.09	.21	.61	.10
51NG0245	66.10	.51	15.10	3.35	1.78	.11	1.79	4.75	4.05	1.03	.12	.55	.51	.26
51NG0246	49.20	.52	15.30	2.55	6.70	.18	10.10	13.00	1.51	.19	.06	.60	.23	0.00
51NG0248	51.10	.67	16.50	3.60	5.50	.16	5.75	10.60	2.25	.43	.07	.60	.34	.06
51NG0250	51.10	.69	16.50	3.60	6.10	.16	5.95	10.50	2.35	.42	.07	.27	.17	0.00
ZONE H														
48NG0006	50.50	.68	15.40	3.60	5.60	.17	8.55	12.00	2.25	.41	.09	.37	.17	0.00
48NG0013	53.70	1.07	16.10	5.30	5.30	.16	4.60	9.20	3.05	.93	.25	.15	.31	.07
48NG0020	57.50	1.14	15.60	5.15	4.25	.13	2.40	5.75	3.75	1.78	.42	.77	1.04	.03
48NG0022	52.40	.80	19.50	2.70	6.50	.16	4.45	11.20	2.65	.59	.15	.54	.16	.05
48NG0500	53.70	.58	15.30	2.35	6.00	.15	6.95	10.20	2.75	1.12	.17	.30	.22	0.00
48NG0505	58.20	.53	16.60	3.25	4.10	.18	4.00	7.35	3.65	1.72	.23	.03	.15	0.00
48NG0509	56.10	.90	16.60	4.15	4.60	.16	3.40	7.35	3.85	1.64	.20	.32	.28	.05
48NG0520	59.50	.80	15.40	3.70	4.25	.17	2.80	5.65	4.20	2.30	.28	.50	.52	.05
48NG0523	60.10	.36	16.40	3.15	3.30	.14	3.15	6.25	4.00	1.91	.25	.27	.27	.05
48NG0528	64.90	1.25	14.30	1.40	4.75	.20	1.51	4.05	5.50	1.21	.34	0.00	.19	0.00
48NG0533	52.50	1.42	15.70	2.10	8.10	.20	5.50	10.50	3.05	.41	.10	.07	.19	0.00
48NG0534	63.90	1.20	14.30	1.25	5.60	.19	1.69	4.50	5.15	1.21	.39	0.00	.19	0.00
48NG0536	52.60	1.43	16.30	1.80	8.45	.20	5.30	9.80	3.00	.41	.10	.04	.20	.05
48NG0526	64.50	1.20	14.60	1.50	4.80	.19	1.85	4.10	5.10	1.25	.27	0.00	.30	0.00
48NG0532	70.30	.66	13.40	.90	3.00	.15	.73	2.60	5.70	1.66	.14	.11	.25	0.00
48NG0547	53.70	1.54	15.10	3.95	7.95	.20	4.15	7.90	3.60	.45	.19	.43	.55	0.00
48NG0538	55.20	1.55	15.50	2.95	8.10	.21	3.45	7.30	4.10	.88	.24	.20	.20	.03
48NG0549	63.40	1.29	15.20	1.60	5.30	.17	1.79	4.40	4.95	1.29	.39	.13	.21	.02
48NG0556	54.90	1.75	15.00	4.90	6.70	.23	3.80	7.35	3.80	.51	.25	.03	.31	.05
48NG0559	55.40	1.30	16.40	3.90	6.10	.20	4.35	8.10	3.80	.53	.17	0.00	.16	.10
48NG0572	49.70	.85	16.50	1.55	7.65	.18	7.95	12.90	2.20	.20	.20	.01	.33	.05
48NG0038	49.20	1.15	14.40	1.90	8.10	.18	10.80	11.40	2.15	.19	.11	.20	.20	.05
48NG0042	48.60	1.91	15.90	2.40	8.85	.19	7.35	11.00	2.65	.16	.21	.52	.25	.30
48NG0044	49.60	1.11	15.90	2.30	6.85	.16	10.30	10.60	2.35	.24	.12	.16	.12	0.00
48NG0582	49.20	1.14	15.00	3.40	6.25	.16	11.30	10.60	2.20	.25	.11	0.00	.27	.05
48NG0592	49.90	1.01	16.60	2.30	6.30	.17	9.15	11.10	2.40	.21	.12	.17	.33	0.00
48NG0601	51.80	1.03	17.20	2.95	5.85	.18	5.95	10.60	2.55	.63	.19	.36	.16	0.00
48NG0605	51.70	.99	16.90	2.95	5.75	.16	6.45	10.90	2.50	.75	.18	.35	.15	.05
48NG0048	47.50	.95	18.40	6.20	3.80	.19	5.80	12.60	2.30	.72	.37	.37	.39	.05

APPENDIX 3

MULTI-ELEMENT TRENDS OF VARIATION OF THE SOUTH BISMARCK SEA ROCKS AS SHOWN BY THE NONLINEAR MAPPING ALGORITHM

by

R.J. HOWARTH* AND R.W. JOHNSON

Introduction

The major-element chemical analyses of rocks from each of the western and eastern arcs, discussed in the main part of this Report, can be considered as complex data sets consisting of a number of measurements (i.e., the weight percentages of eleven major oxides, excluding volatiles) for a larger number of samples. These data sets have been subdivided into classes on the basis of the geographic zones A to H (see p. 26 and Fig. 10), each of which has its own gross chemical characteristics.

To assess the overall chemical differences between the rocks in different zones, the percentages of all the major oxides, and their interrelations, should be evaluated. Multiple plots of pairs of oxides do not give a full picture of the overall data structure. What is required is a device which can produce a pictorial representation of the distribution of the samples in eleven dimensions (corresponding to the eleven major oxides), which is readily assimilated, and which contains as faithful as possible a representation of the multi-dimensional structure of the data; the magnitude of chemical differences between the zones, and by how much they differ from one another, can therefore be readily appreciated.

---

*Applied Geochemistry Research Group, Imperial College of Science and Technology, University of London

Samples defined by three measured variables can be represented by unique points in a three-dimensional model, or on a ternary diagram, and inspection of the model or diagram will determine if the sample points are grouped into 'clouds' of more closely packed points separated by empty or sparsely occupied volumes of 'measurement space'. In this way, points showing small interpoint distances would form 'clusters', and an inspection might reveal which one of the three measurements is best for distinguishing between the clusters. Sample points defined by more than three measurements cannot be seen; in other words, relationships cannot be visualized in higher-dimensional space.

To overcome this problem, Sammon (1969) introduced the nonlinear mapping algorithm (NLM) to produce a two-dimensional view of a set of points originally in multidimensional space. This view shows the 'structure' of a data set in a form which can be readily interpreted by eye (see also 'Q-mode factor analysis', page 63).

Theory

Suppose N points exist in L-dimensional space, and two of these points are i and j. The positions of i and j can be expressed as a number (L) of co-ordinates; thus, for i, the co-ordinates are: x_{i1}, x_{i2}, $x_{i3}\ldots x_{iL}$; and for j, the co-ordinates are; x_{j1}, x_{j2}, $x_{j3}\ldots x_{jL}$.

The distance between points i and j, d^*_{ij}, can be expressed by the following equation:

$$d^*_{ij} = \sqrt{\left\{ \sum_{l=1}^{L} (x_{il} - x_{jl})^2 \right\}}$$

For example, in two dimensions, the corresponding interpoint distance, d_{ij}, is:

$$d_{ij} = \sqrt{\left\{ (x_{i1} - x_{j1})^2 + (x_{i2} - x_{j2})^2 \right\}}$$

If the measurement $x_l (l=1,2,3,..L)$ is scaled to range between 0 and 1, the i-th and j-th samples will show maximum similarity when they occupy the same position in measurement space, i.e. $d^*_{ij} = 0$; when they are as far apart as possible, $d^*_{ij} = L$, and they show maximum dissimilarity. For example, in two dimensions the maximum dissimilarity will be:

$$d_{ij} = \sqrt{\left\{(1 - 0)^2 + (1 - 0)^2\right\}} = \sqrt{2}$$

Because some elements have larger values than others (e.g., SiO_2) and will outweigh the others in calculation of the interpoint distances, it is convenient to transform the variables so that they are given equal weighting. Although all the variables can be easily transformed by dividing through by the maximum, or range, for each variable, this procedure gives undue importance to the largest and smallest values. An alternative approach used in the NLM algorithm is to normalize by dividing through by the standard deviation (the root mean-square deviation of the values from the mean) of each variable. This has the effect of making the variance equal for each variable, rather than forcing the range into the interval 0 to 1.

Starting with a data set of N points in L-dimensional space, and an equal number of points scattered over a two-dimensional plane at random, the NLM algorithm proceeds in a cyclic fashion, adjusting the positions of the points individually in two dimensions in each iteration until the interpoint distances (d_{ij}) best match those in the original L dimensions (d^*_{ij}); that is, there is maximum similarity. At this time, the best possible representation of the original data structure is obtained. The adjustment process produces a non-linear transformation (as each point will be displaced by a different amount), and it operates by searching for the minimum of the 'mapping error', E, where:

$$E = \left[1/ \sum_{i<j}^{N} (d^*_{ij}) \right] \left[\sum_{i<j}^{N} (d^*_{ij} - d_{ij})^2 / d^*_{ij} \right]$$

Howarth (1973b) gave a detailed description of the method and its application to geological problems.

Application

The NLM computer program was developed by J.W. Sammon at the Rome Air Development Center, New York, and subsequently modified by the Applied Geochemistry Research Group, Imperial College, London, for use with geochemical data, so as to treat up to 500 samples at a time*. The data may be log-transformed (base 10), or left untransformed, and similar weighting may be given to each variable by dividing through by the variance before the NLM algorithm is executed. The program then prints out: (1) the initial two-dimensional co-ordinates (usually the measurements for the two variables showing the greatest variability are taken as the initial configuration rather than a completely random set of points); (2) the mapping error, E, on each iteration (50 cycles are usually more than sufficient for a stable solution to be reached); (3) a plot of the points using the final NLM two-dimensional co-ordinates. If required, points can be identified as belonging to particular classes, but this is done only to identify points on the final plots; it is not taken into account in calculating the mapping, which is based on the measurements alone.

The NLM algorithm has been used extensively on different sets of geochemical data since 1971 (Howarth, 1972, 1973a, b; Fanta, 1972; Castillo-Muñoz, 1973), in all of which it has proved a most effective method for the analysis of data structures.

---

*A copy of the NLM algorithm can be obtained by writing to the Programme Librarian, Imperial College Computer Centre, Exhibition Road, London SW7 2BX

The results of nonlinear mapping presented here for the western and eastern arcs show both the degree of overlap between classes defined by zones A to H, and also the variation within each zone. The algorithm was also found to be useful in clarifying interzone relations, as well as being a convenient method of portrayal for the eleven-dimensional system.

Rocks of the western and eastern arcs

Eleven NLM plots are presented for the south Bismarck Sea rocks in Figures I-XI. In each plot, variance has been normalized, but the data is not log-transformed. The samples used in the non-linear mapping are the same as those selected to estimate the relative abundances of rock types on pages 27-29 of this Report.

Plots for each of the western zones A to D are shown in Figures I-IV; Figure V is a composite diagram for all the western rocks; Figures VI-X are independent plots for rocks of the eastern zones E to H; and Figure XI is a composite plot for all the eastern zones. Each rock is represented by a single sample point, whose symbol corresponds to one of the zones A to H.

The position of every sample point in an NLM plot is defined by the dimensional co-ordinates, but, as the numerical values of these co-ordinates have no petrological significance, scales are eliminated from the x and y axes of each diagram. The most important aspect of NLM plots is the relative position of points within the borders of each diagram, and the pattern shown by points of one class in relation to those of another class, which reflects their position in the original eleven-dimensional space.

Points for the rocks of zone A are shown in Figure I. They fall in the bottom right-hand corner of the diagram; the upper left-hand part of the plot is noticeably free of points. In contrast, points representing the rocks of zone B occupy a broader

Figure I

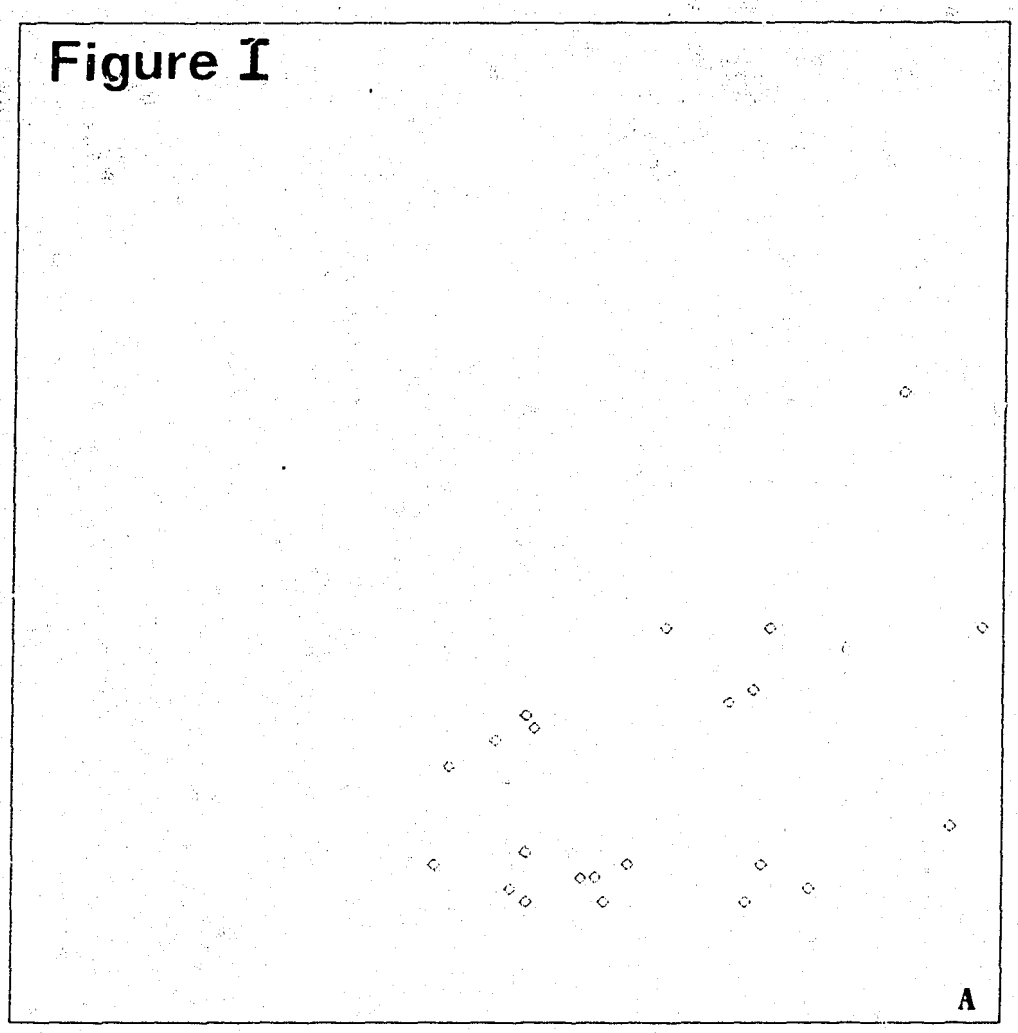

Figure II

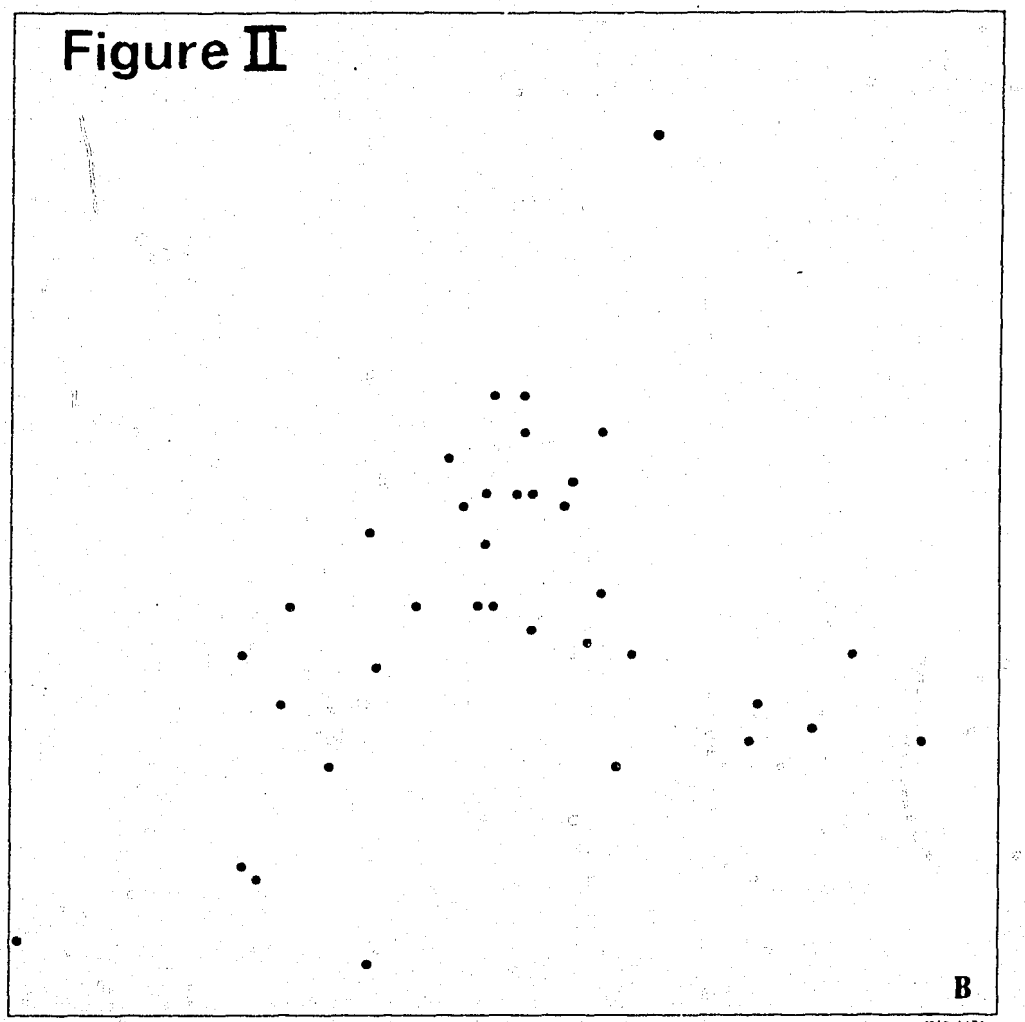

area of the NLM plot, as shown in Figure II. Although there is considerable overlap with the area covered by the rocks of zone A, many zone B rocks occupy an area up from, and to the left of, the zone A area, and fall in the lower central part of the diagram.

Points representing the rocks of zone C are plotted in Figure III, and indicate an even further migration away from the bottom left-hand corner of the diagram. These points form a group restricted almost entirely to the upper half of the diagram, and there is practically no overlap with the area of points representing rocks from zone A. Rocks from each of zones A and C are therefore seen to represent extreme compositions.

In the NLM diagram of Figure IV, the field occupied by zone D rocks is shown to be well separated from that of zone C. Most of the zone D points are restricted to the lower half of the diagram, and they cover an area whose extent is close to that defined by the rocks of zone B.

A regular progression of compositional change can therefore be demonstrated for each of the four western zones across the NLM diagram. This progression reflects the chemical changes using oxide-pairs (cf. Figs. 31 and 32) described in the main part of this Report, but here the changes are based on simultaneous considerations of all eleven oxides for rocks from the western end to the eastern end of the western arc. Compositions change in the same relative direction in both the NLM plot and along the arc, between zones A and B, and between B and C, but the direction is reversed between zones C and D, and the compositions of rocks from zones B and D are shown to be rather similar.

In Figure V, most of the points representing the western rocks cover the lower three-quarters of the NLM diagram, and constitute a coherent, single field of points. However, five rocks - four andesites from Long Island and a basalt from Crown Island - plot close to the top edge of the diagram, where they are separated

Figure III

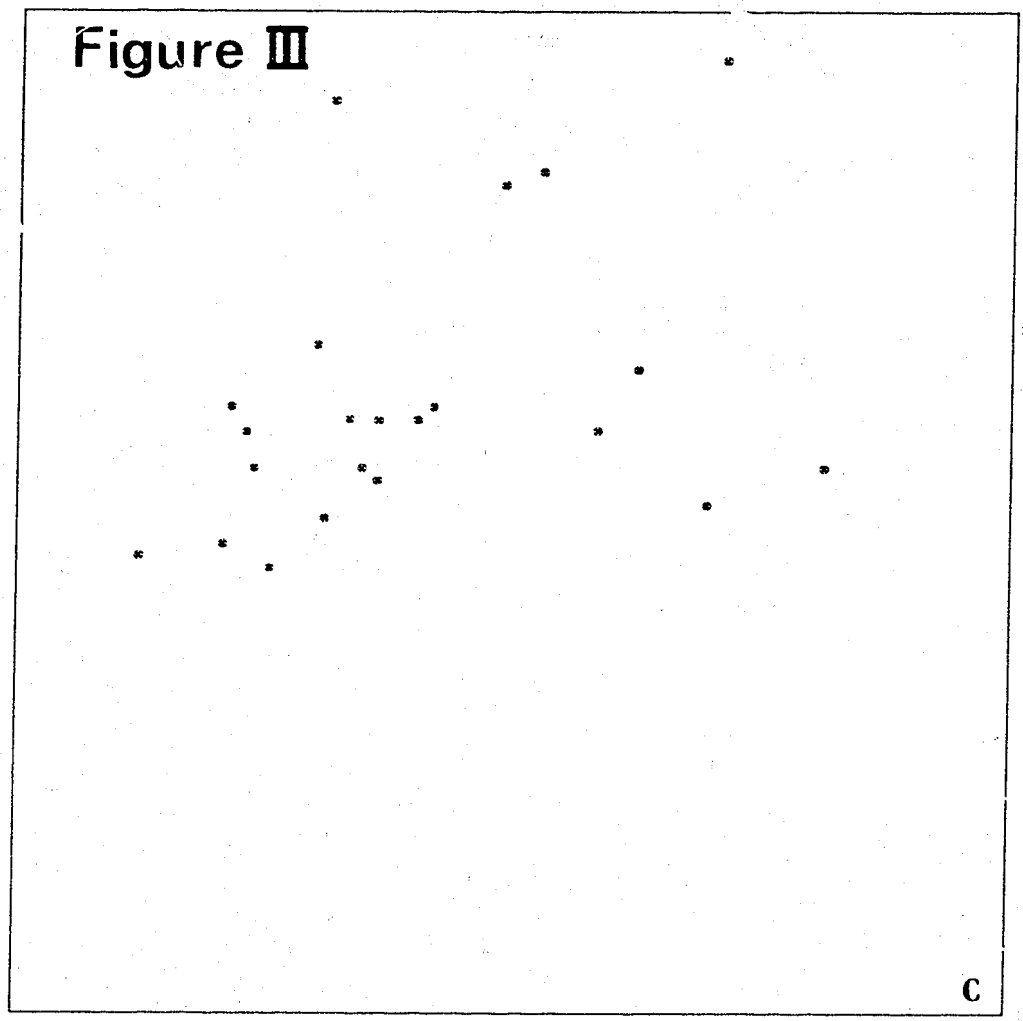

Figure IV

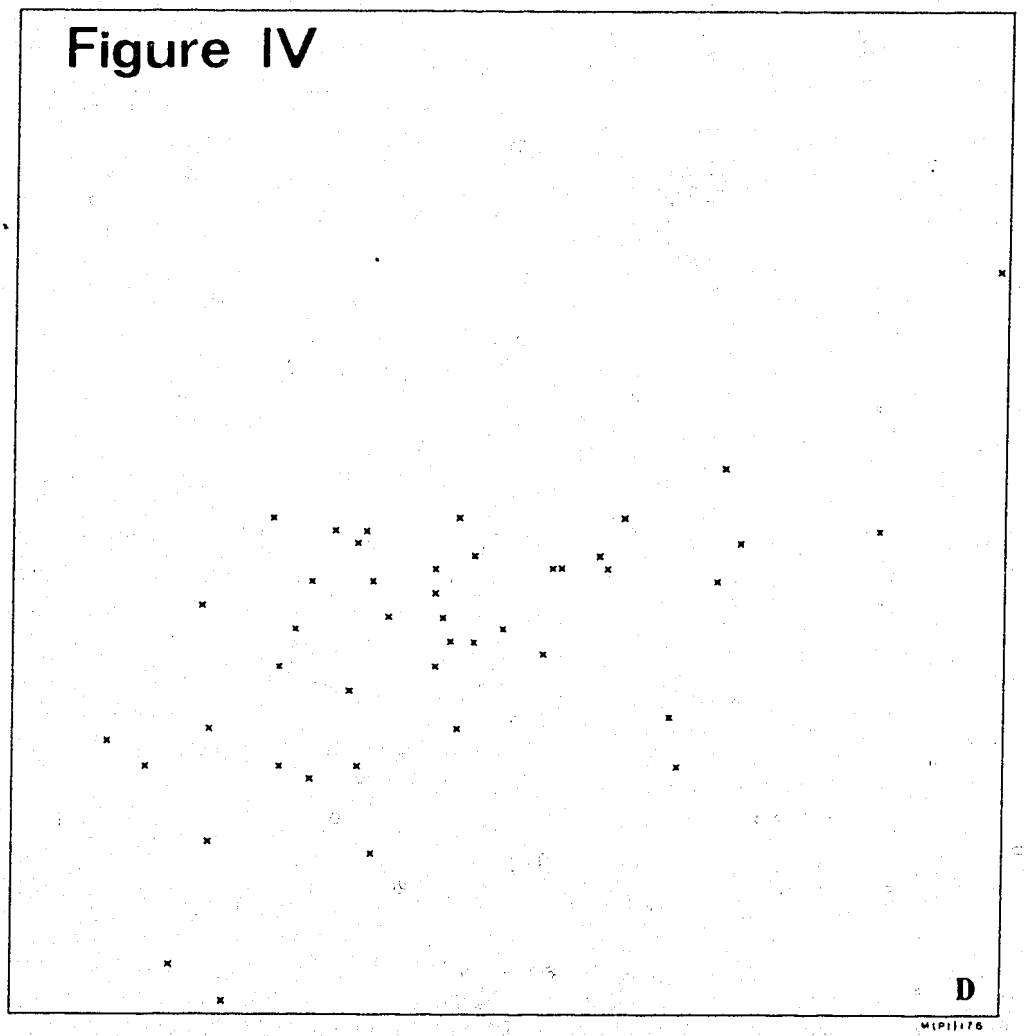

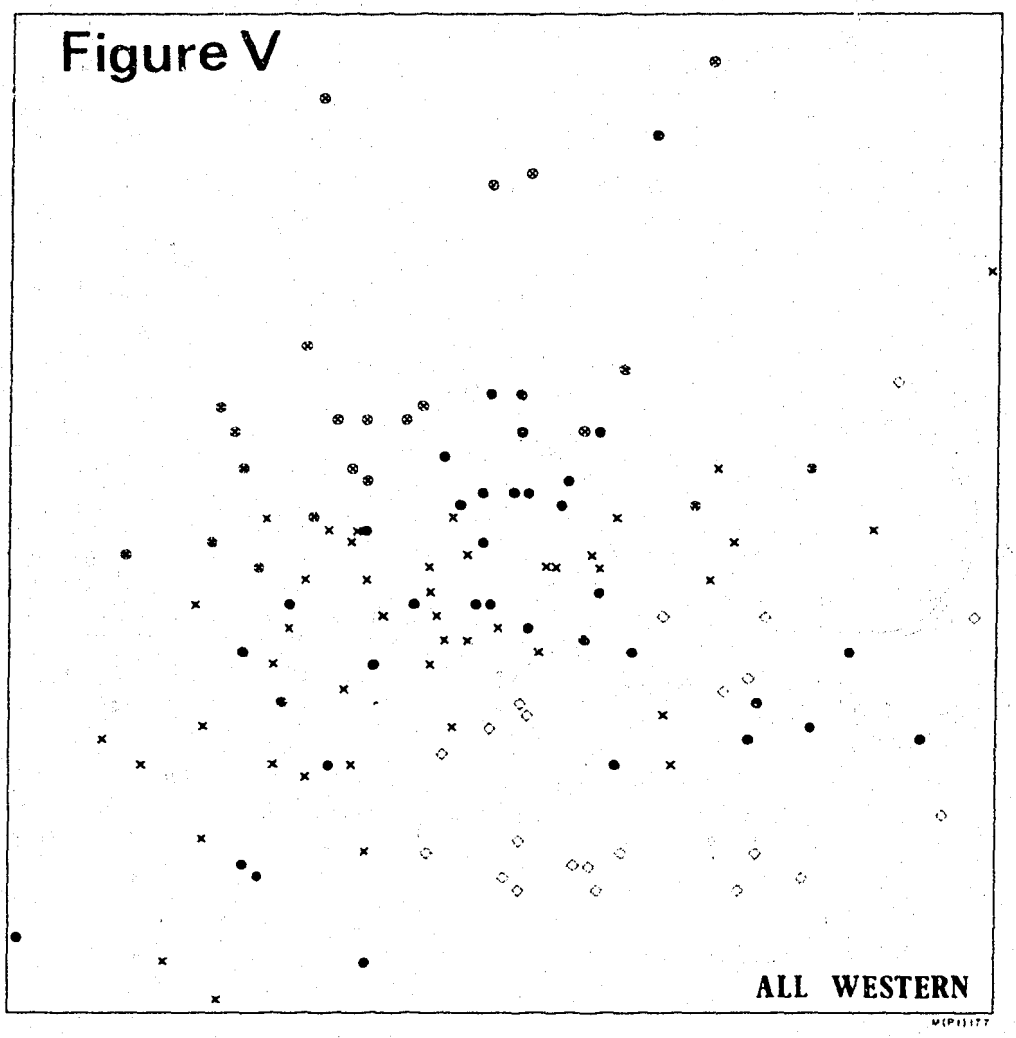
Figure V
ALL WESTERN

from the rest of the western rocks. This suggests that these five rocks have bulk compositions distinctly different from those of other western rocks; that is, they may not be part of the same 'series'. (As pointed out on page 75 of this Report, the rocks of Long Island have distinctive chemical properties, and the andesites in particular are unusually low in Al_2O_3.)

NLM plots for rocks from zones E and F, in the eastern arc, are similar to one another, as shown by a comparison of Figures VI and VII respectively and by Figure XI. The fields for both classes occupy the lower central parts of the diagrams, and concentrate towards the left-hand side, although here the points of zone E are displaced more towards the top edge of the diagram. Even though the oxide-pair diagrams presented in the main part of this Report demonstrate that chemical differences between the rocks of zones E and F are definitely present, the nonlinear mapping plot shows that these differences are smaller than those between other pairs of zones.

Only fifteen rocks from the southern part of zone G define the field shown in Figure VIII. The sample points are widely separated, but twelve of them (high-silica andesites and dacites) form a group consisting of a central cluster of ten points and two points to the right of them. Two other points, representing rhyolites, lie in the bottom right-hand corner, and the only basalt is represented by the point near the top left-hand corner; these three points are separated from the central group of andesites and dacites, reflecting their widely differing compositions. The points of Figure VIII cover more or less the same area as those for zones E and F, in Figures VI and VII, except that the points representing the basalt and two rhyolites are outside the areas of the zone E and F rocks.

Most sample points for the northern part of zone G plot in the upper half of Figure IX, and nearer the top edge of the square than points representing most rocks from zones E and F and the southern part of zone G. A further upward displacement of points is shown by the rocks of zone H, in Figure X, many of which plot

Figure VI

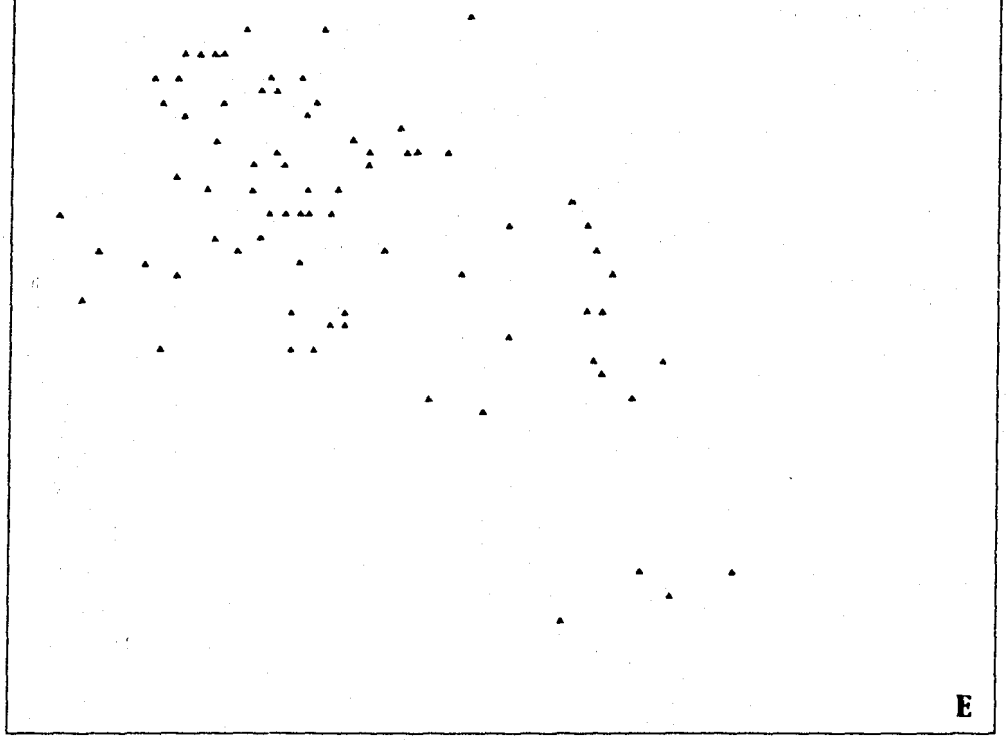

E

Figure VII

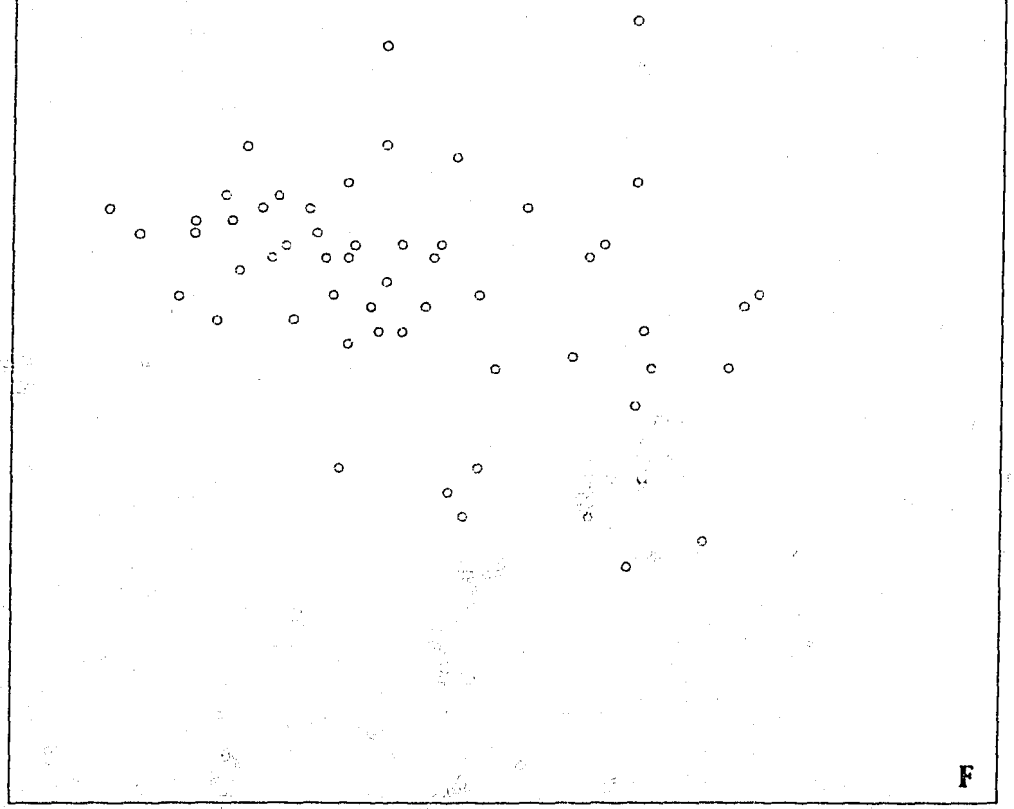

F

Figure VIII

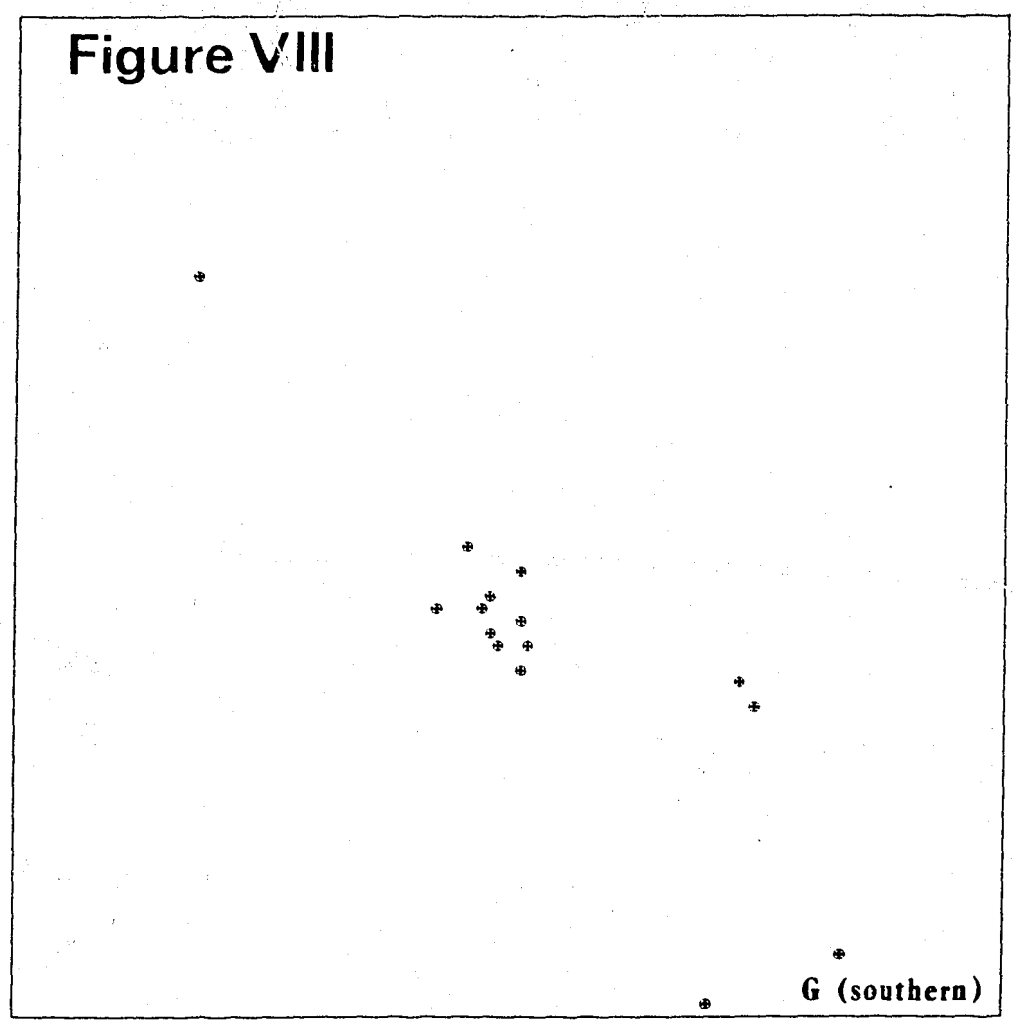

Figure IX

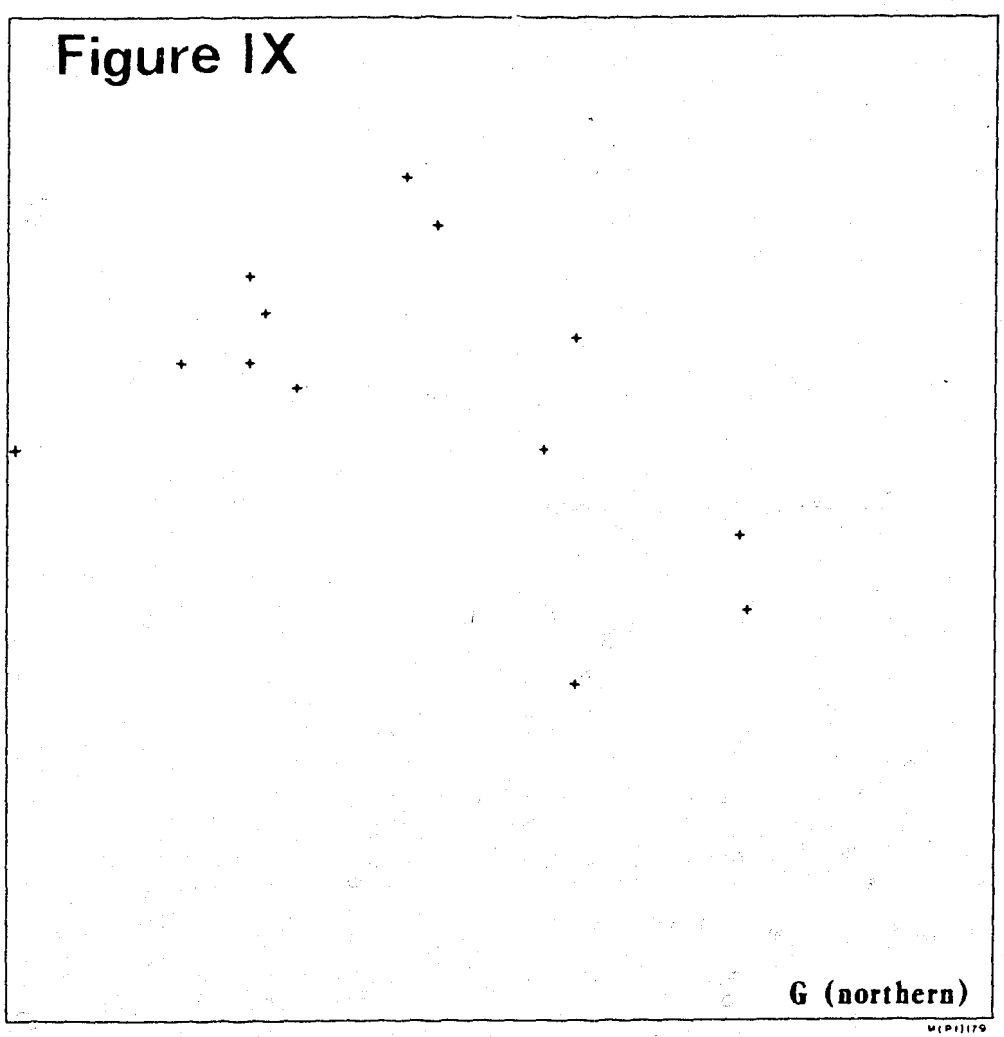

Figure X

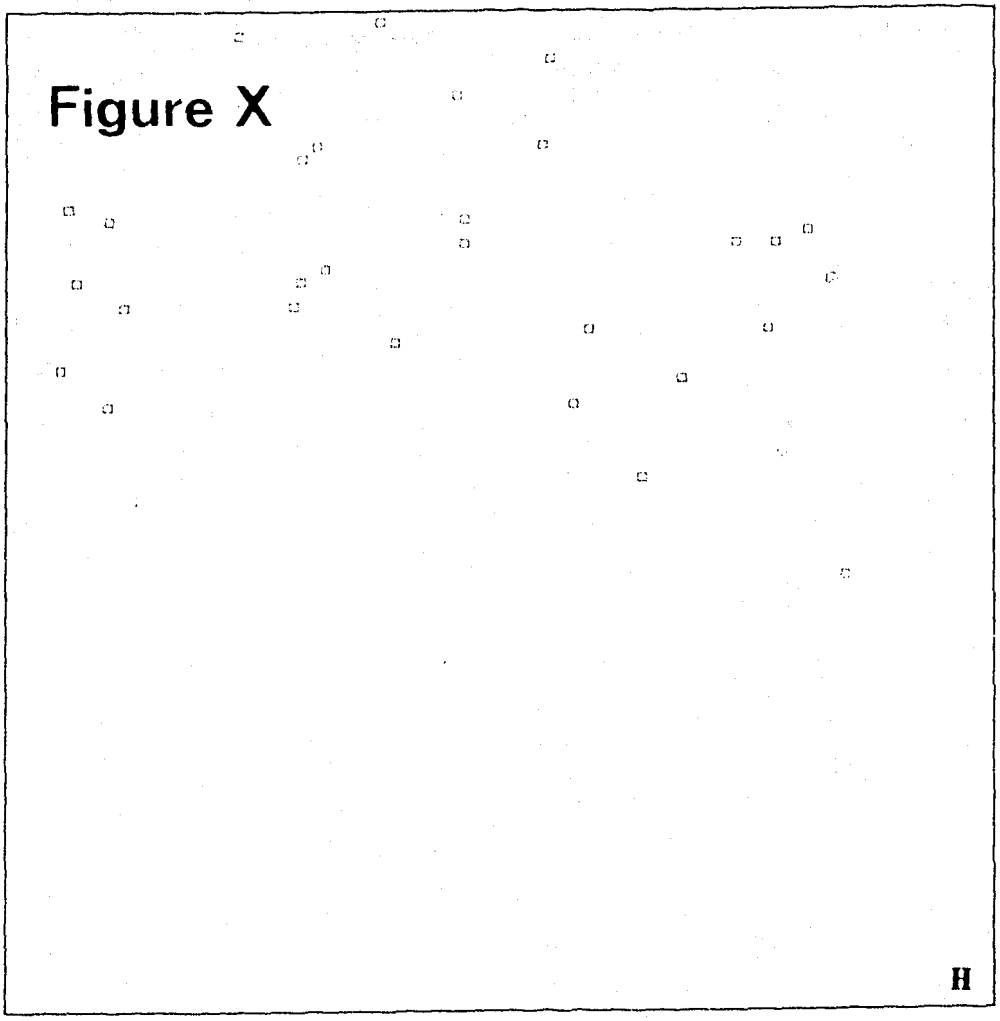

Figure XI

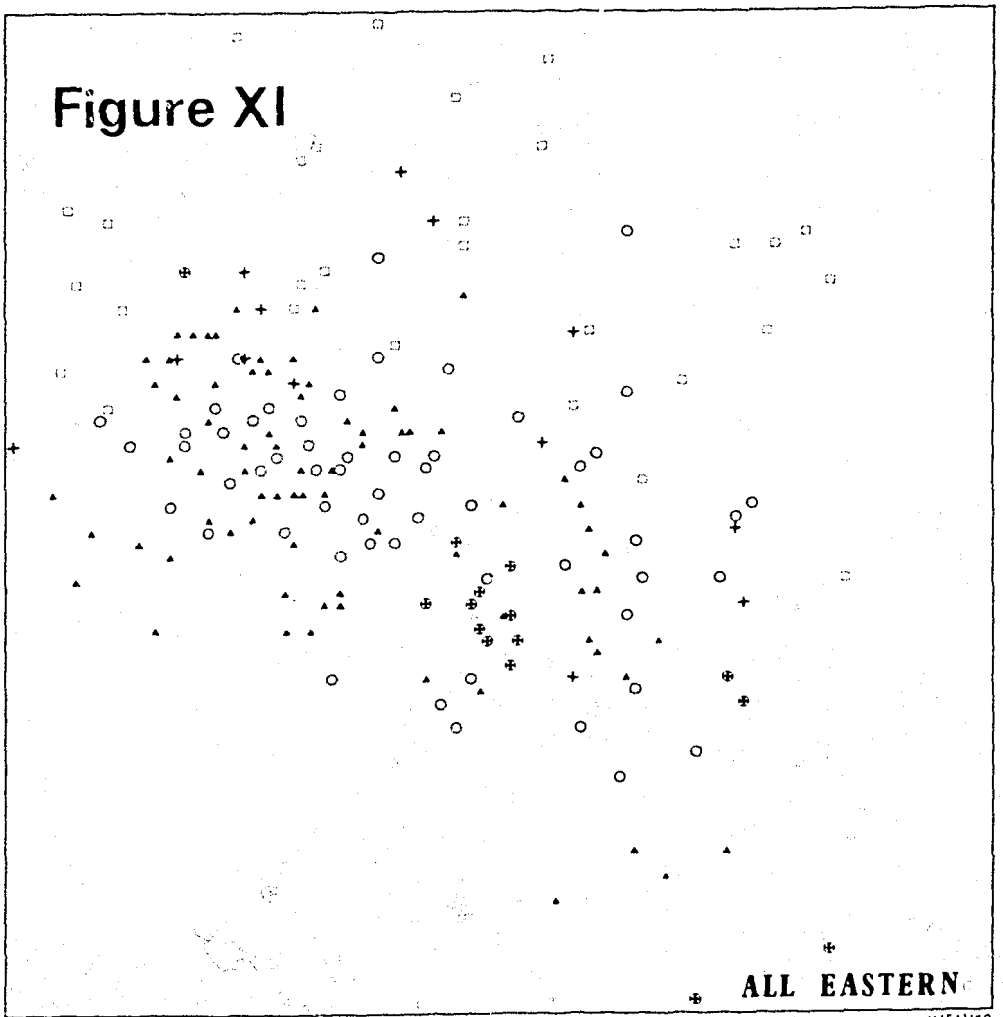

closer to the top edge of the diagram than do those from any of the other eastern zones, and all but one of which plot in the upper half of the diagram.

In Figures VI-X, therefore, an upward progression is demonstrated, from the fields defined by rocks from zones E and F, and the southern part of zone G, to the field of rocks from the northern part of zone G, to the zone H field. This progression, which is further illustrated in Figure XI, is analogous to the changes in composition observed in the eastern arc as distance to the underlying Benioff zone increases (cf. Figs. 31 and 32).

In Figure XI, many of the points representing zone H samples occupy fields which show no overlap with rocks from the other eastern zones. This indicates that the zone H rocks are less like other eastern rocks than are those from any other eastern zone.

Acknowledgements

The computations were carried out as the result of an investigation, supported by a grant from the Natural Environment Research Council under the direction of Professor J.S. Webb, into the applicability of statistical techniques to the interpretation of geochemical data. Computer time was provided by the Imperial College Computer Centre. The NLM algorithm was supplied by the Rome Air Development Center (New York), who have given their permission for its distribution.

References

CASTILLO-MUÑOZ, R., 1973 - Application of discriminant and cluster analysis to regional geochemical surveys. Ph.D. thesis, Univ. London (unpubl.).

FANTA, P., 1972 - Effects of seasonal variation on the iron, manganese, and associated metal contents of stream sediments and soils. M.Phil. thesis, Univ. London (unpubl.).

HOWARTH, R.J., 1972 - Discussion of 'Empirical discrimination classification of regional stream-sediment geochemistry in Devon and east Cornwall'. Trans. Inst. Min. Metall. Sec. B. 81, B116-9.

HOWARTH, R.J., 1973a - The pattern recognition problem in applied geochemistry; in JONES, M.J., (ed.) - GEOCHEMICAL EXPLORATION 1972. London, Inst. Min. Metall., 259-73.

HOWARTH, R.J., 1973b - Preliminary assessment of a nonlinear mapping algorithm in a geological context. Math. Geol., 5, 39-57.

SAMMON, J.W., Jr., 1969 - A nonlinear mapping for data structure analysis. IEEE Trans. Computers, C-18, 401-9.

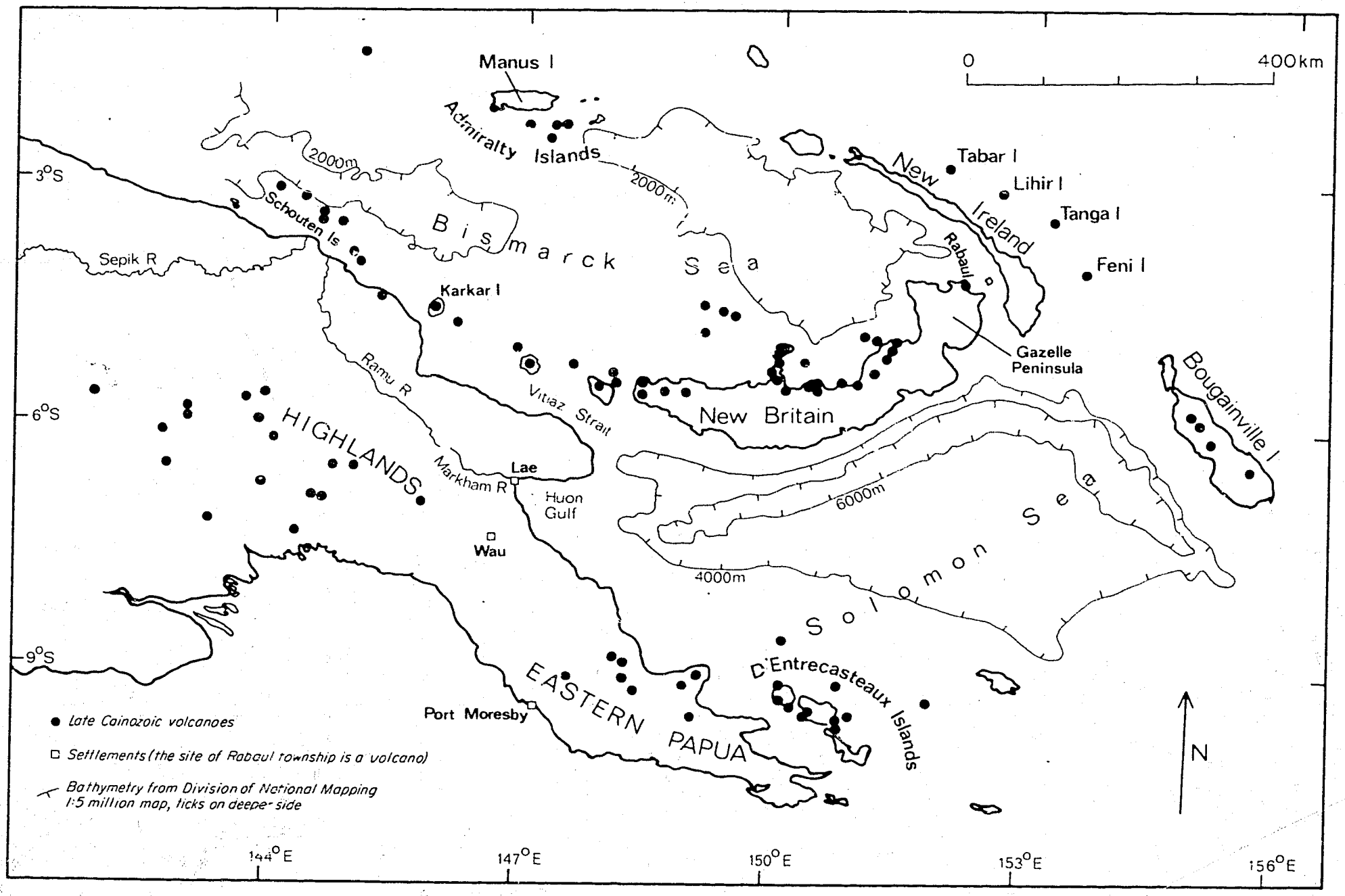

Fig. 1. Principal late Cainozoic volcanoes of Papua New Guinea.

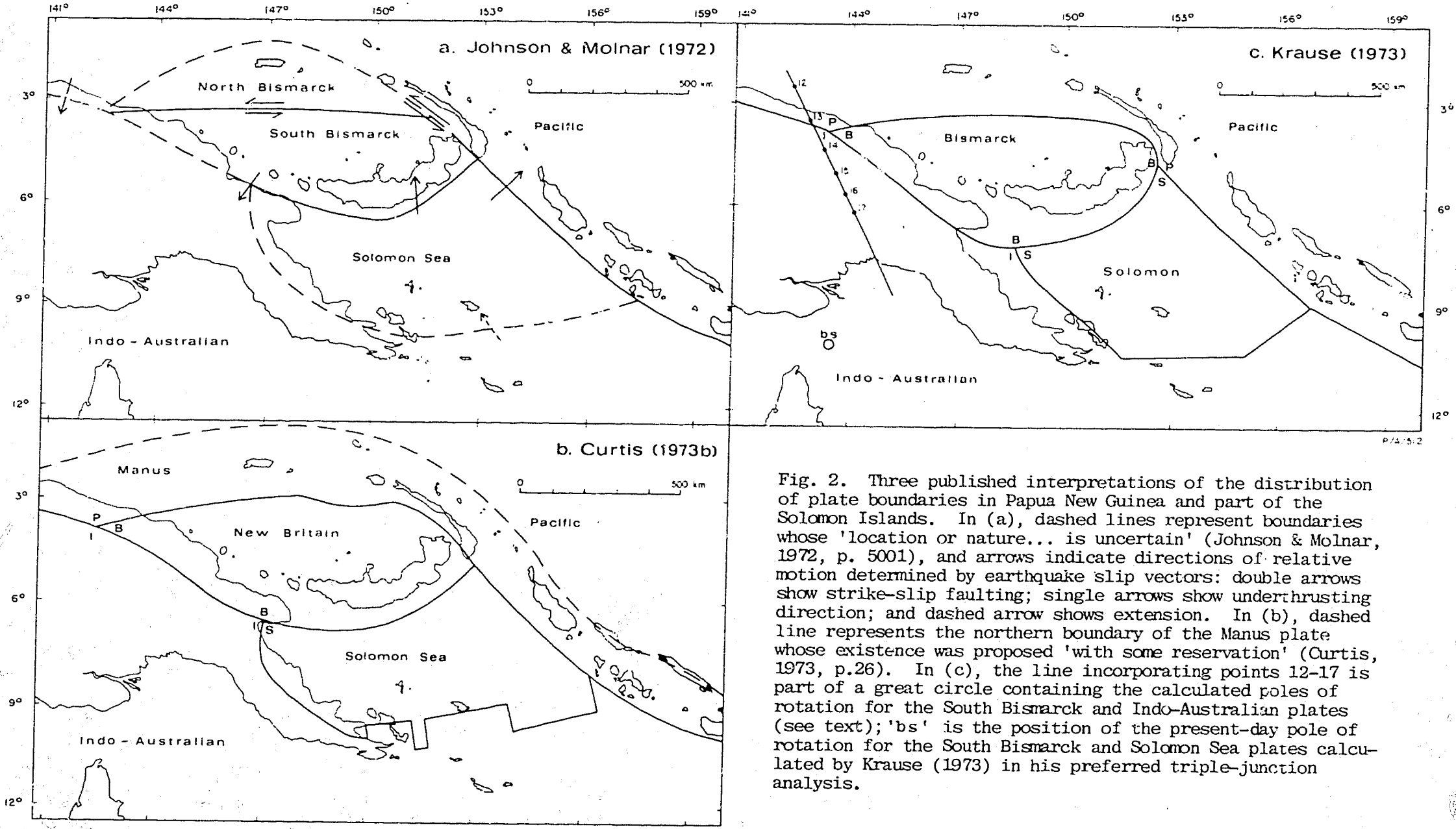

Fig. 2. Three published interpretations of the distribution of plate boundaries in Papua New Guinea and part of the Solomon Islands. In (a), dashed lines represent boundaries whose 'location or nature... is uncertain' (Johnson & Molnar, 1972, p. 5001), and arrows indicate directions of relative motion determined by earthquake slip vectors: double arrows show strike-slip faulting; single arrows show underthrusting direction; and dashed arrow shows extension. In (b), dashed line represents the northern boundary of the Manus plate whose existence was proposed 'with some reservation' (Curtis, 1973, p.26). In (c), the line incorporating points 12-17 is part of a great circle containing the calculated poles of rotation for the South Bismarck and Indo-Australian plates (see text); 'bs' is the position of the present-day pole of rotation for the South Bismarck and Solomon Sea plates calculated by Krause (1973) in his preferred triple-junction analysis.

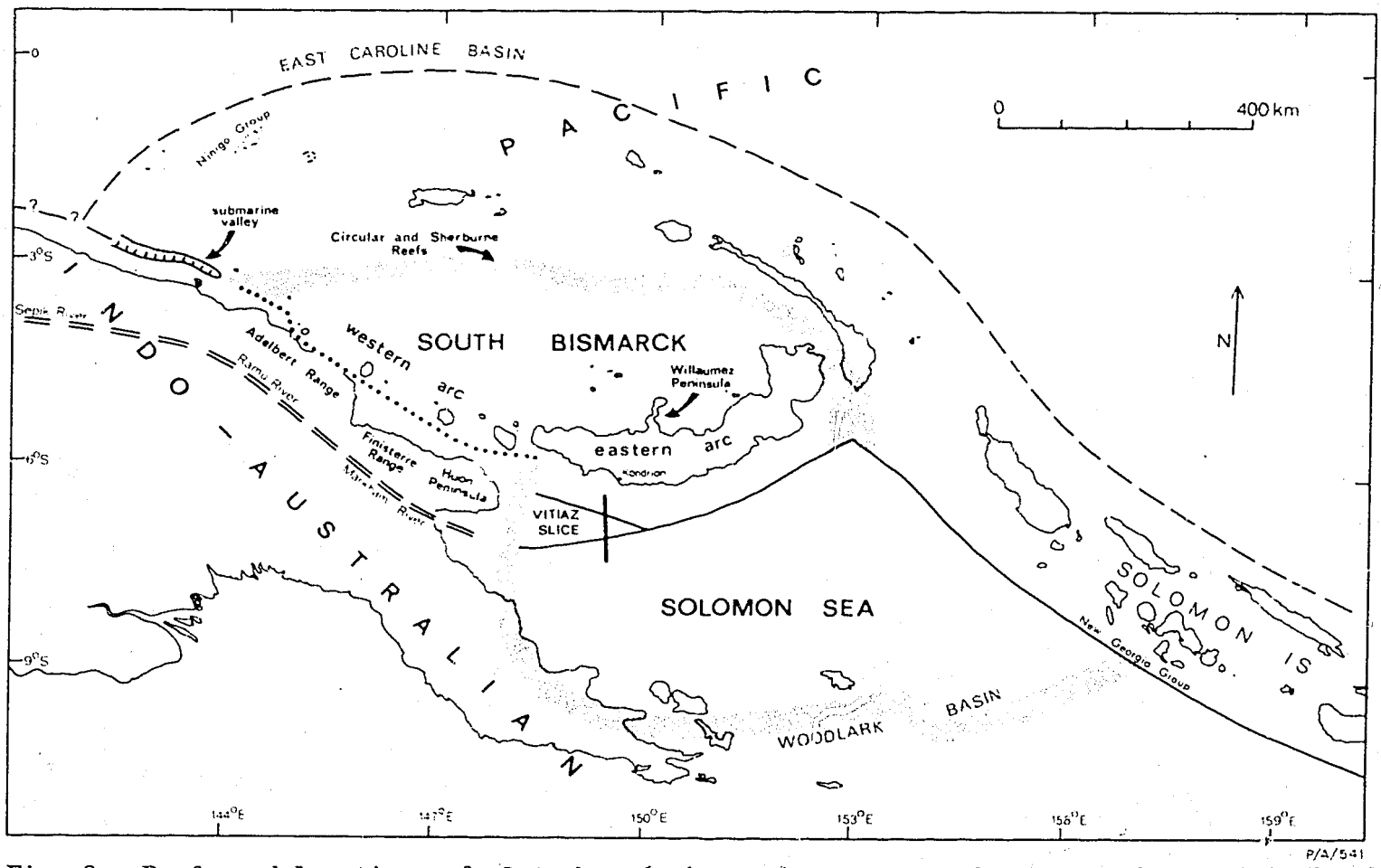

Fig. 3. Preferred locations of plate boundaries and some related tectonic features in Papua New Guinea and part of the Solomon Islands, in part adapted from Johnson & Molnar (1972), Curtis (1973b), Krause (1973), and Luyendyk et al. (1973). Solid lines are axes of submarine trenches. Stippling indicates currently active plate boundaries which are zones of seismicity that cannot be accurately portrayed by single lines. Single-dash line represents a boundary (or boundaries) which may have been more active during the earlier part of the late Cainozoic than at the present day; Johnson & Molnar (1972) and Curtis (1973) considered that this line, or part of it, represents the northern margin of a third minor plate - cf. Fig. 2. Double-dash line represents an old plate boundary that was destroyed by collision of the Australian continent (part of the Indo-Australian plate) with an Adelbert-Huon island arc (see text and Fig. 9 for details). Dotted line is a strike-line for the upper surface of the proposed lithospheric slab which dips steeply northwards beneath the western arc (see text and Fig. 39 for details). Thick line running southwards from near Kandrian is the ship's track of the seismic reflection profile given in Figure 8.

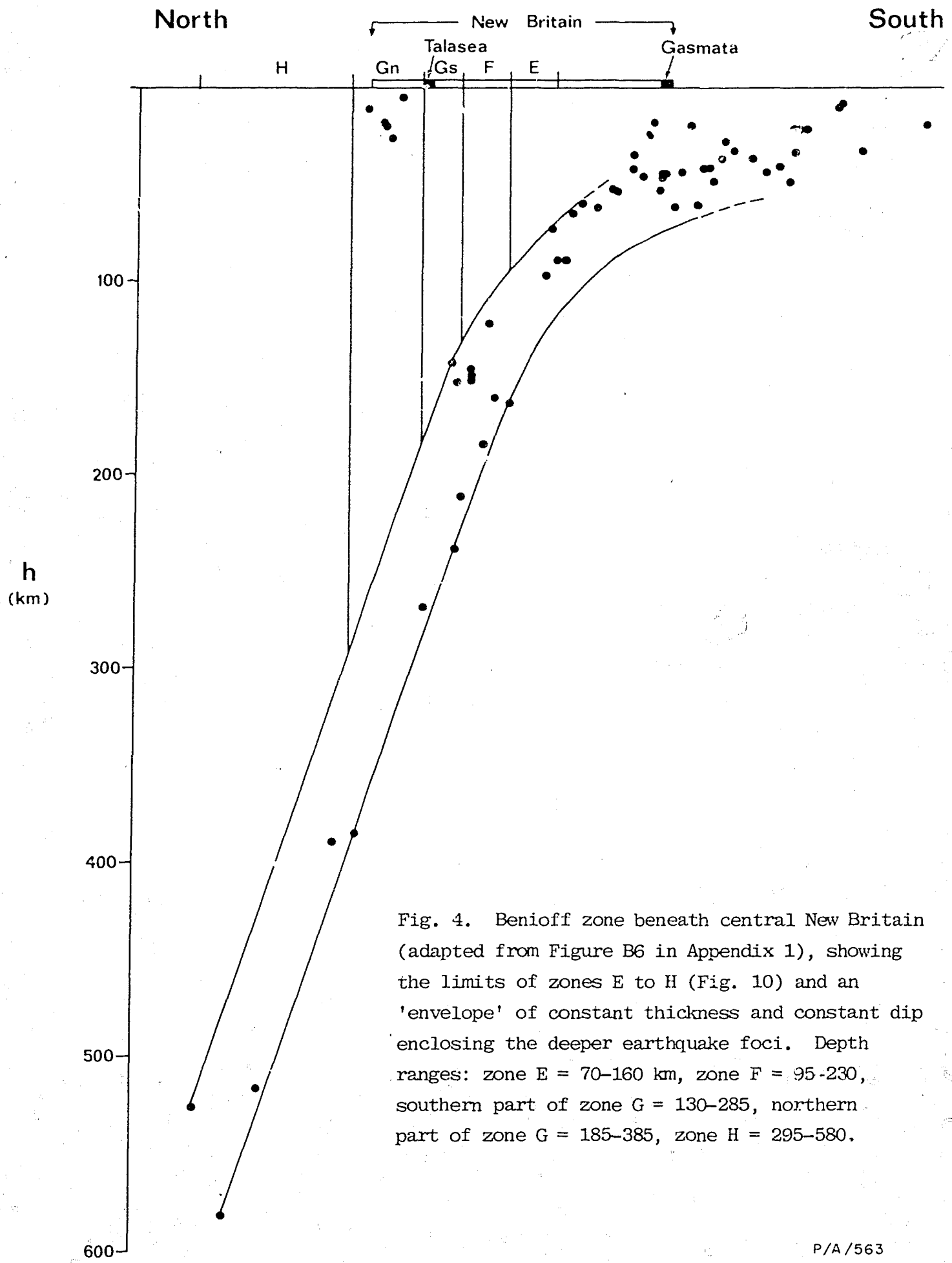

Fig. 4. Benioff zone beneath central New Britain (adapted from Figure B6 in Appendix 1), showing the limits of zones E to H (Fig. 10) and an 'envelope' of constant thickness and constant dip enclosing the deeper earthquake foci. Depth ranges: zone E = 70–160 km, zone F = 95-230, southern part of zone G = 130–285, northern part of zone G = 185–385, zone H = 295–580.

P/A/563

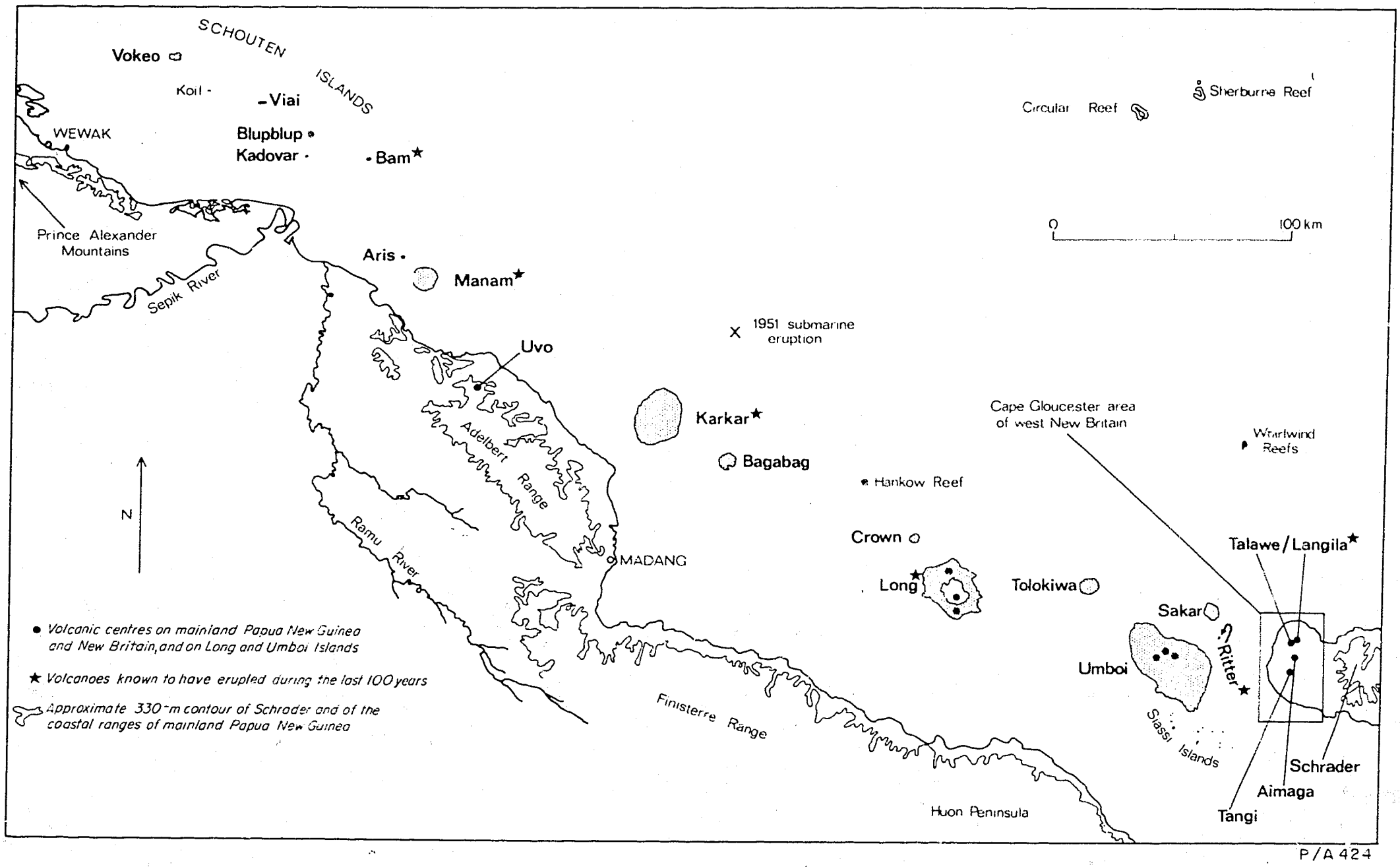

Fig. 5. Main volcanic centres of the western arc. Islands are shown stippled or solid, and volcanic islands are indicated by bold lettering. Langila is a cluster of satellite craters on the eastern flank of Talawe.

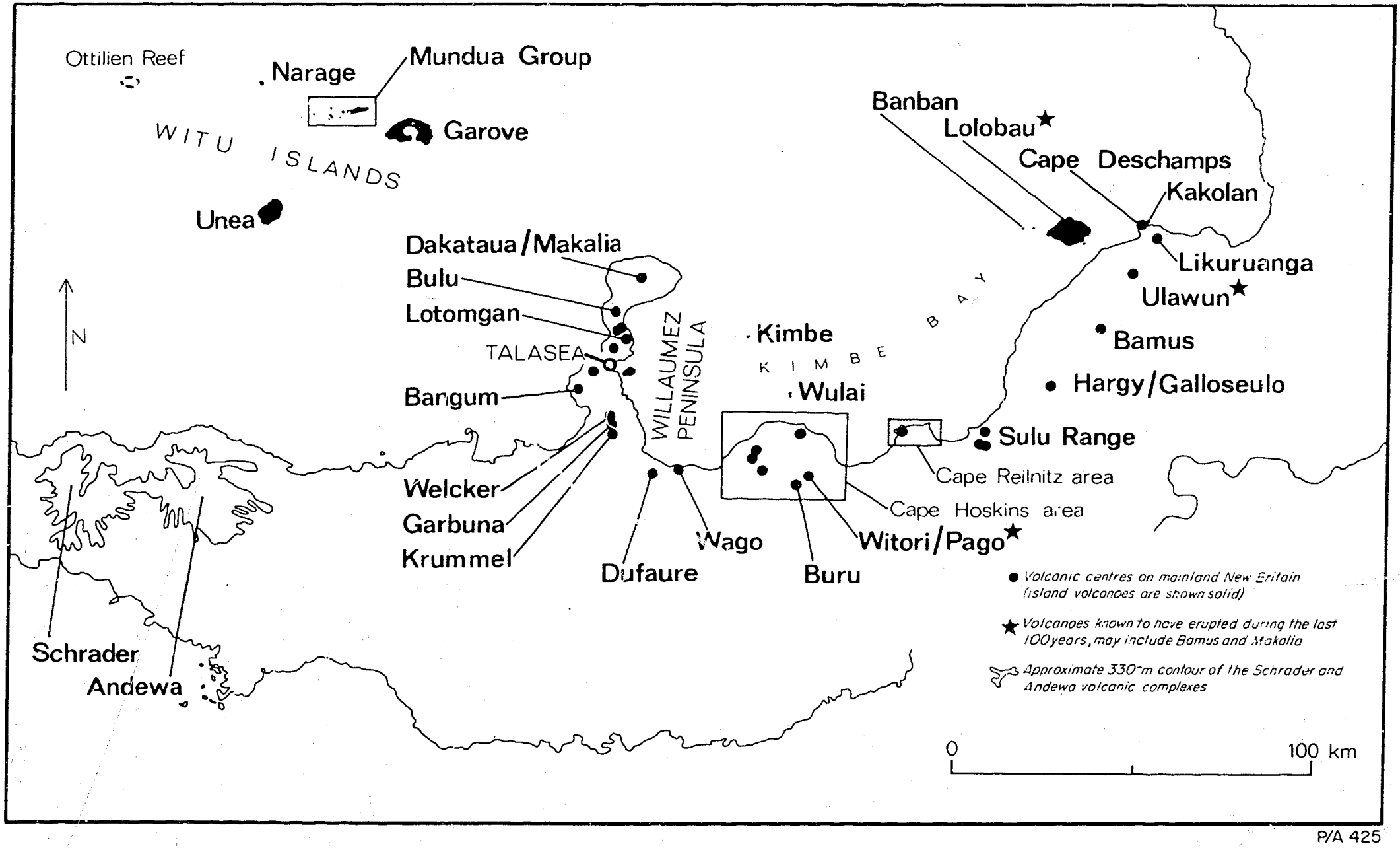

Fig. 6. Main volcanic centres of the eastern arc. Makalia, Pago, and Galloseulo are post-caldera volcanoes which respectively lie inside the older volcanoes of Dakataua, Witori, and Hargy.

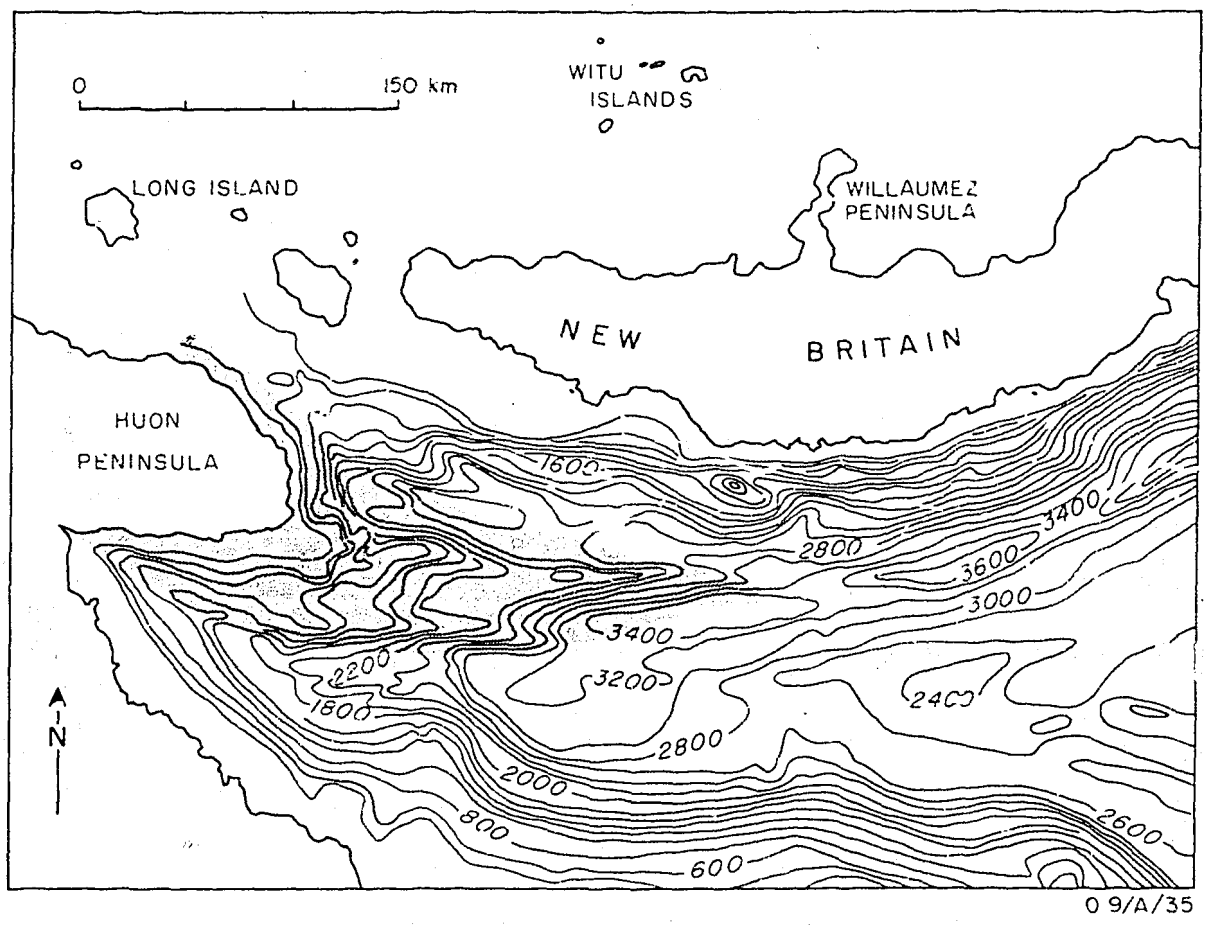

Fig. 7. Bathymetry of the northwestern corner of the Solomon Sea, showing 200-fathom isobaths (after Mammerickx et al., 1971). Submarine ridge (stippled) lies between the two branches of the western end of the New Britain trench.

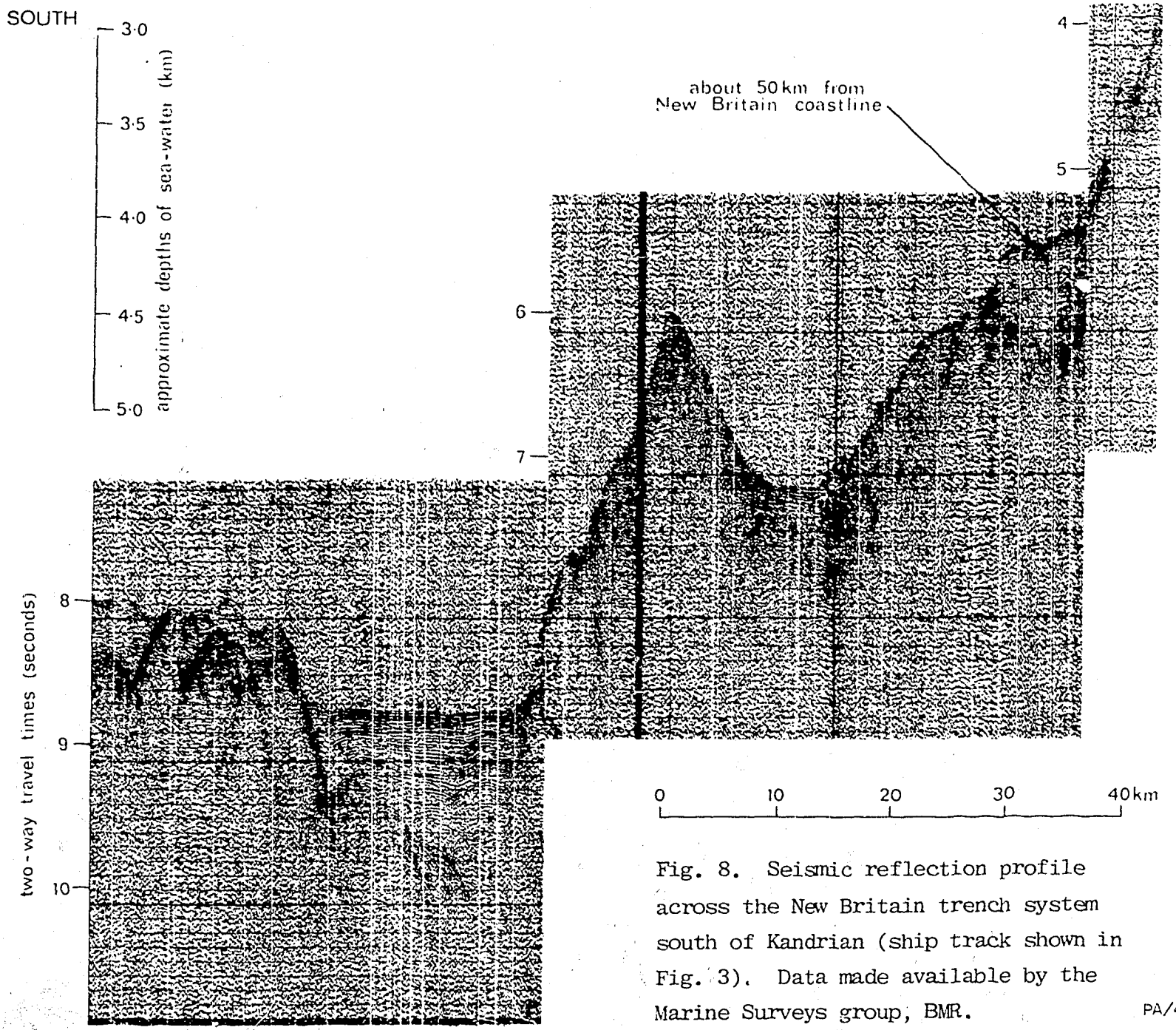

Fig. 8. Seismic reflection profile across the New Britain trench system south of Kandrian (ship track shown in Fig. 3). Data made available by the Marine Surveys group, BMR.

PA/480

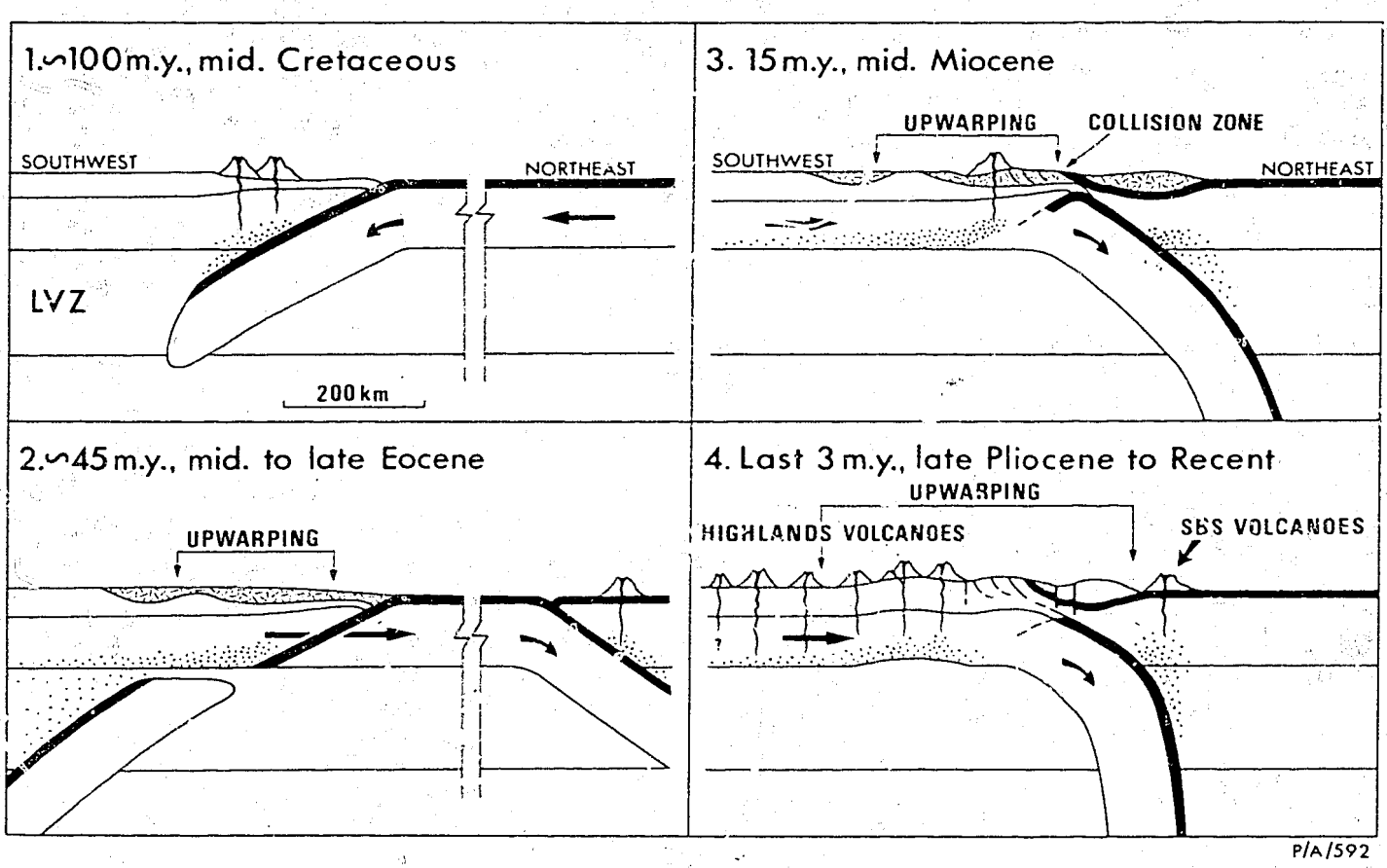

Fig. 9. Schematic representation of the tectonic evolution of mainland Papua New Guinea in a northeast-southwest section through the western arc, coastal ranges, and Highlands (see Figs. 1–3). Johnson, Mackenzie, & Smith (in prep. b) used these diagrams to illustrate the evolution of late Cainozoic volcanism in both the western arc and Highlands province (Fig. 1), but in the following description emphasis is given to those aspects of the interpretation that apply particularly to the development of the western arc. Black bands represent oceanic crust. Stippling represents chemical modification of mantle by slab-derived fluids. Short-line pattern in diagrams 2 and 3 represents post-Jurassic thickening of crust. The true thicknesses of the lithosphere and low-velocity zone (LVZ) throughout this region are unknown, and the assumed values are those determined by Brooks (1969) for the southern part of mainland Papua New Guinea.

1. Southward-dipping subduction in the mid-Cretaceous resulted in arc-trench-type volcanism, and chemically modified the mantle underlying the northern edge of the Australian continent.

2. In the Eocene the southward-dipping slab may have become detached. In the late Eocene, volcanism started in an island arc several hundreds of kilometres to the north as a result of northward subduction of the Indo-Australian plate, which carried the Australian continent northwards from Antarctica.

3. By the late Oligocene or early Miocene the continent had reached the island arc and, because it was too buoyant to descend into the subduction zone, began to collide with the arc. Subduction was arrested and island-arc volcanism ceased, but plate convergence continued, and the continental margin and arc were warped and raised. Middle Miocene magmatism south of the collision zone was initiated by partial melting of mantle which had been chemically modified during the Cretaceous subduction.

4. By the late Pliocene the slab beneath the Tertiary island arc had become steepened, and continuing subduction gave rise to the volcanoes of the western arc in the south Bismarck Sea (SBS volcanoes). Uplift and warping in the Highlands region led to partial melting in the chemically modified mantle.

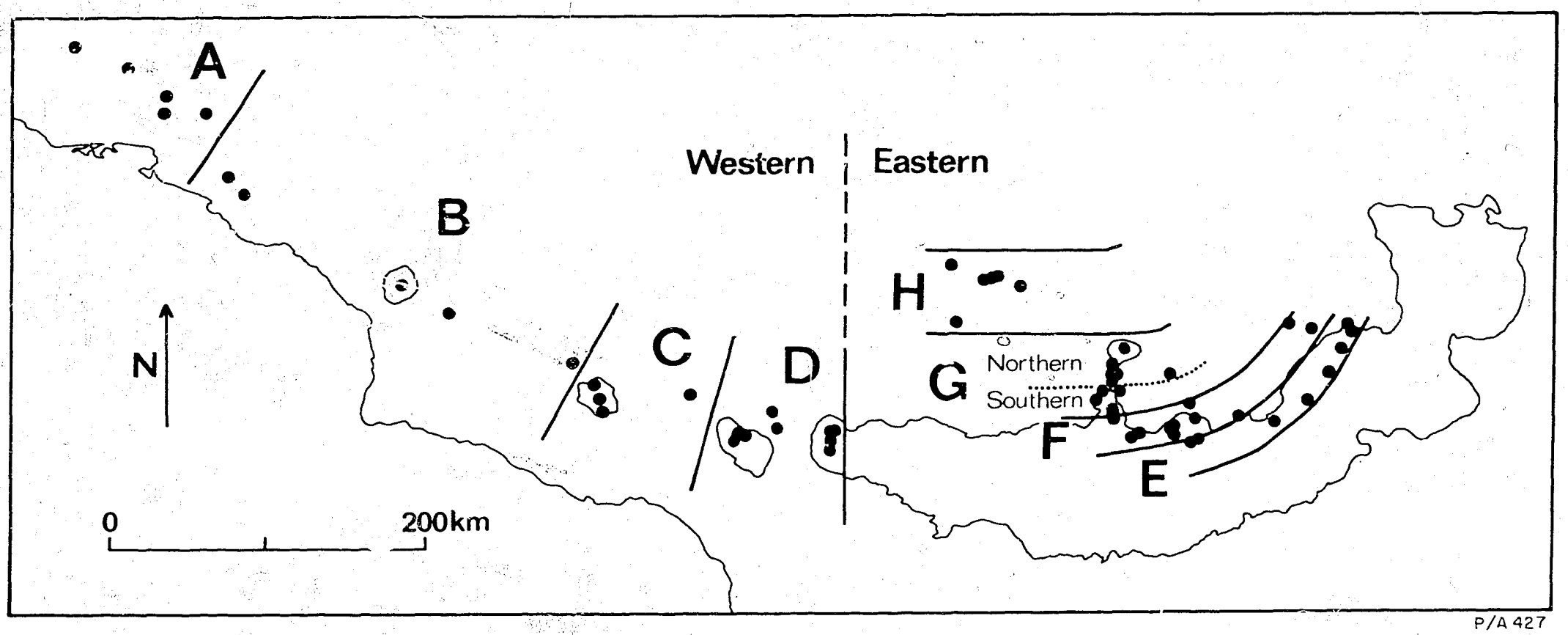

Fig. 10. South Bismarck Sea volcanoes (solid circles) grouped into western zones – A, B, C, D – and eastern zones – E, F, G, H. Zone A – Schouten Islands. Zone B – Aris to Crown. Zone C – Long and Tolokiwa. Zone D – Umboi to Cape Gloucester area. Zone E – Kakolan Island, Cape Deschamps, Likuruanga, Ulawun, Bamus, Hargy/Galloseulo, Sulu, Witori/Pago, and Buru. Zone F – Lolobau Island, Banban Island, Cape Reilnitz area, Cape Hoskins area (excluding Witori/Pago and Buru), Wulai Island, Dufaure, Wago, and Krummel. Zone G – Willaumez Peninsula (excluding Krummel) and Kimbe Island; the 'southern' volcanoes of zone G are Garbuna, Welcker, Bangum, and all those south of Lotomgan near Talasea Harbour. Zone H – the Witu Islands.

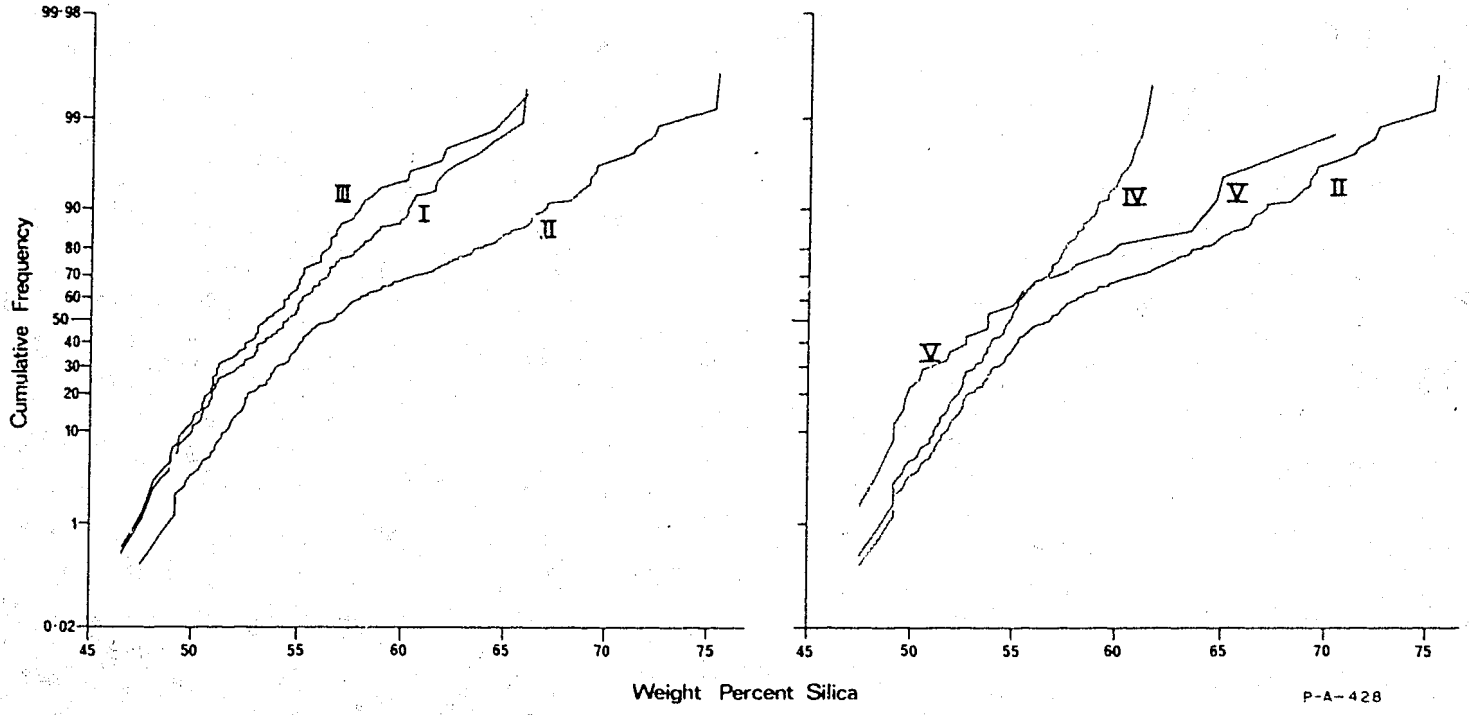

Fig. 11. Cumulative frequency curves for five suites of rocks from the south Bismarck Sea volcanoes. Silica values (% by weight) taken from original analyses. I = western rocks. II = eastern rocks. III = western rocks excluding those of zone A. IV = eastern rocks containing 61.5 percent by weight silica, or less. V = rocks of zone H.

Curve	Number of samples	Silica range	Median silica value
I	124	46.6 - 65.9	54.3
II	192	47.5 - 75.33	56.6
III	102	46.6 - 65.9	53.35
IV	138	47.5 - 61.5	54.77
V	29	47.5 - 70.3	53.7

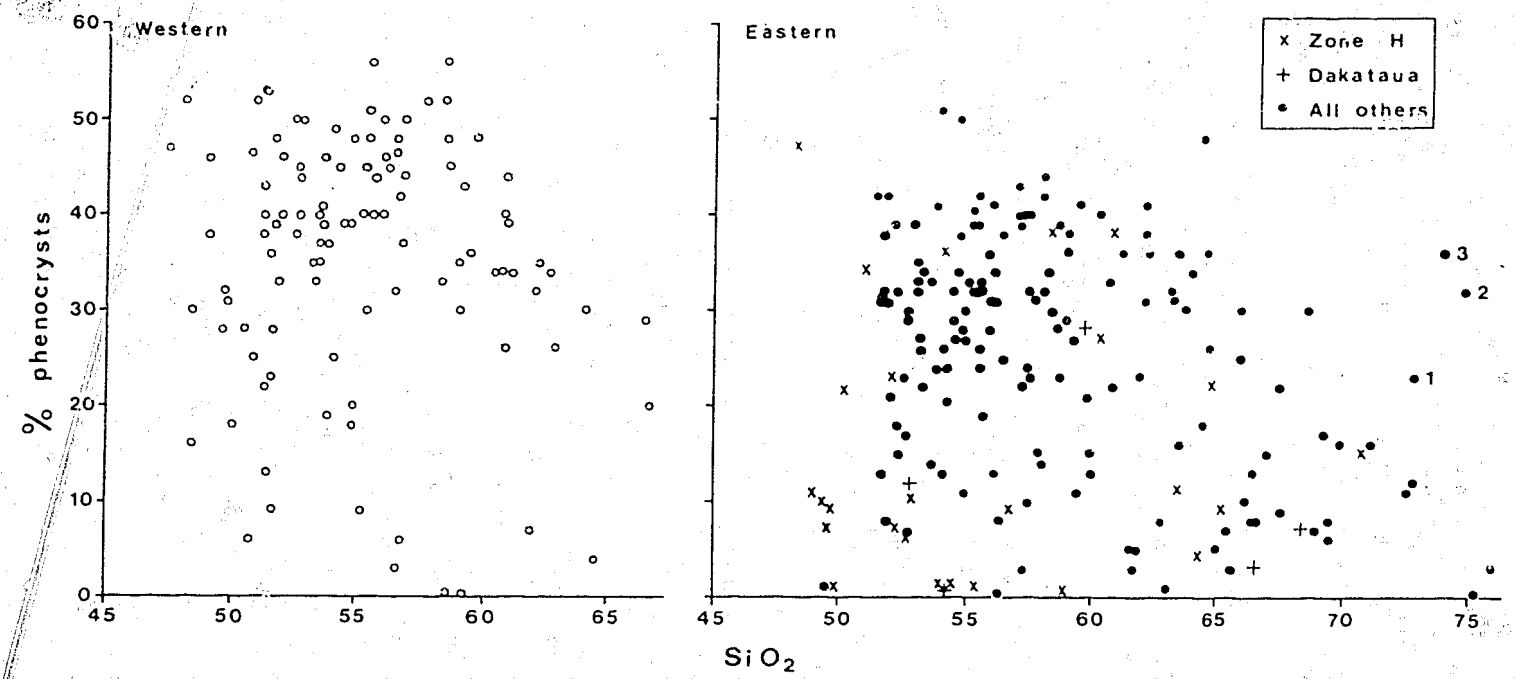

Fig. 12. Volume percent total phenocryst contents v. weight percent SiO_2 for 162 eastern and 106 western rocks (including data of Lowder & Carmichael, 1970, and Blake & Ewart, 1974). Samples 1, 2, and 3 are quartz-rich rhyolites from Sulu Range containing 4, 9, and 13 percent quartz phenocrysts respectively.

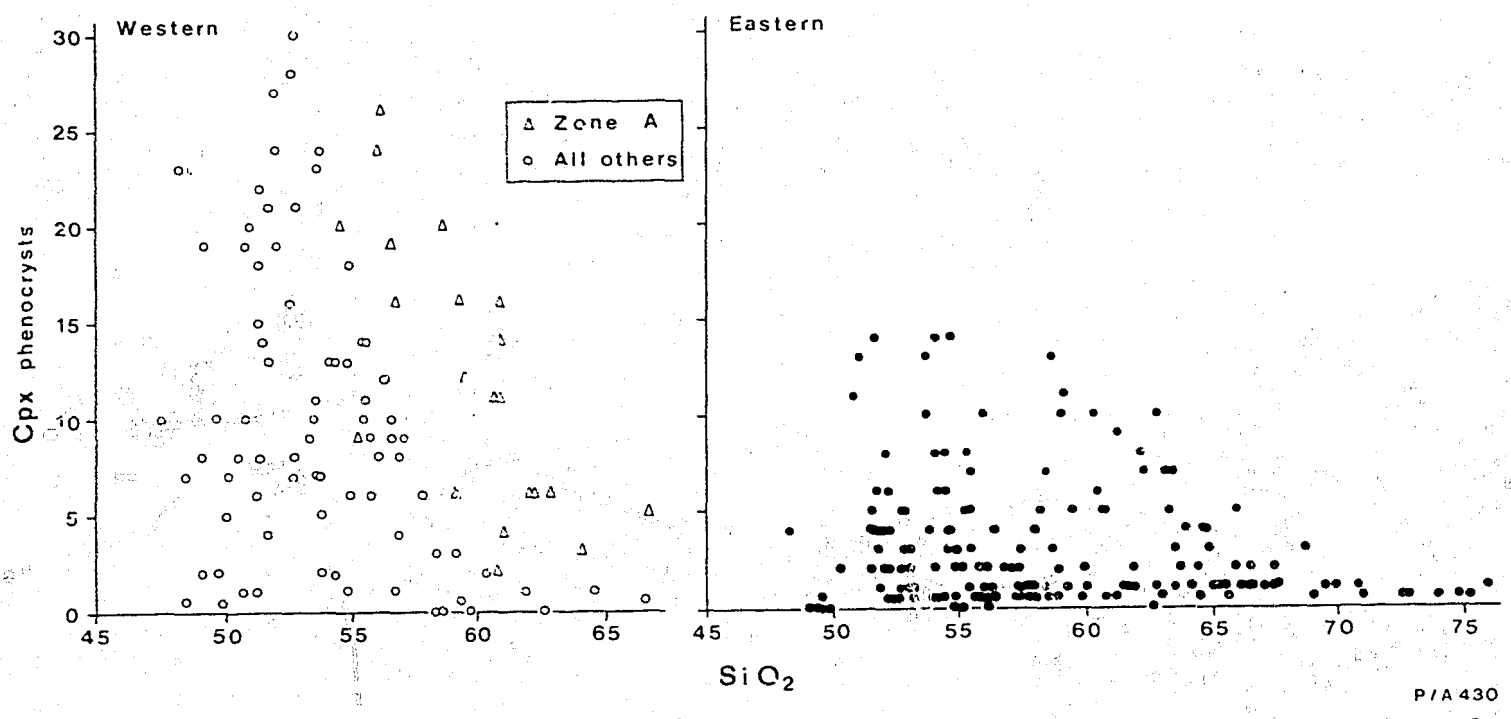

Fig. 13. Volume percent clinopyroxene (Cpx) phenocryst contents v. weight percent SiO_2 for rocks from the western and eastern arcs. Rare (about 2 percent, or less) low-2V clinopyroxene phenocrysts are present in a few rocks, and their abundances are included in the Cpx values.

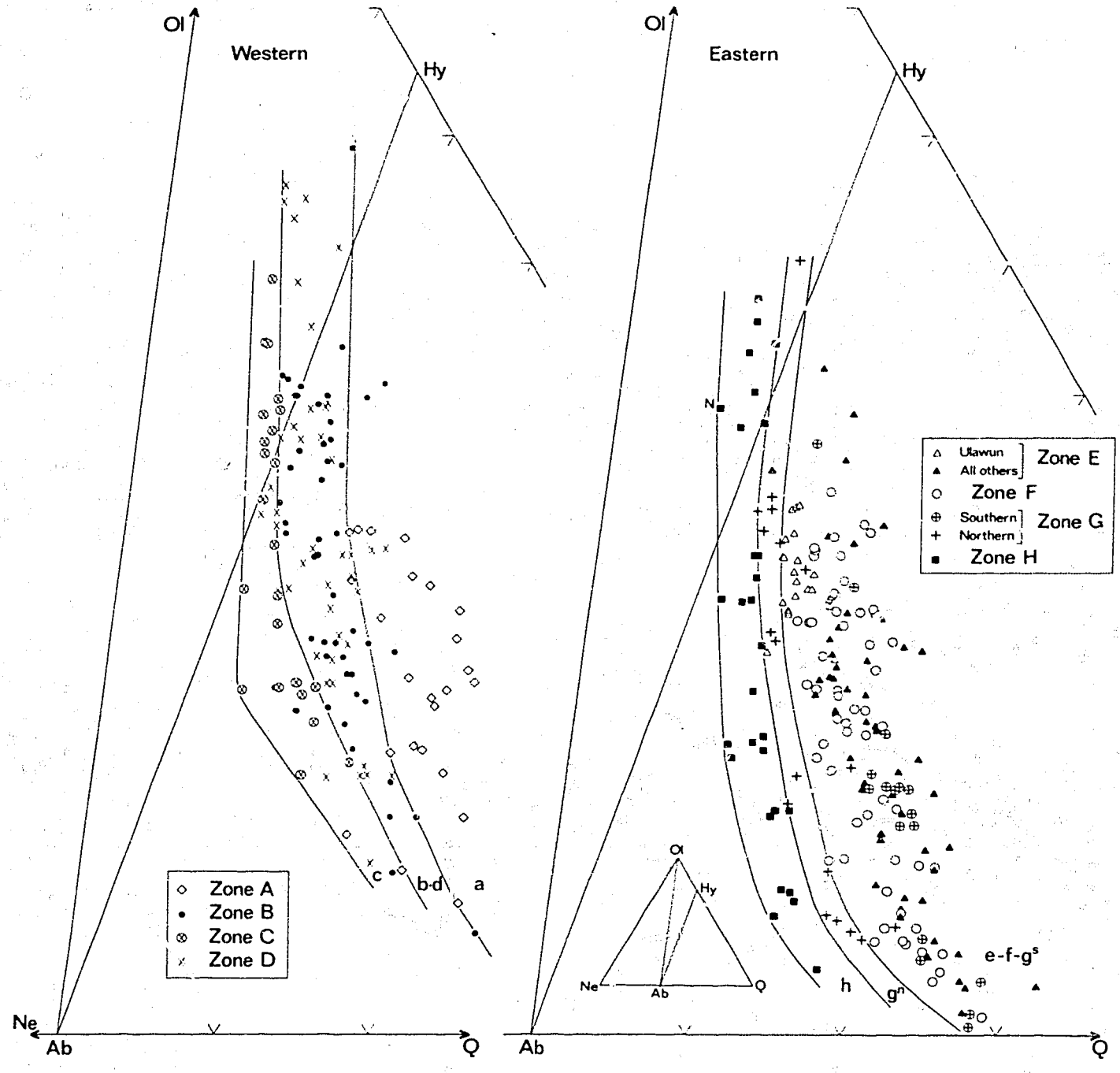

P/A 431

Fig. 14. Molecular percentages of rocks from the western and eastern arcs plotted in part of the normative pseudo-ternary system Ol-Ne-Q (see inset of right-hand diagram). 21 of 24 zone A rocks define field a. 83 of 96 rocks from zones B and D define field b-d. 22 of 23 zone C rocks define field c. 156 of 158 rocks from zones E and F, and from the southern part of zone G, define field e-f-g^S. 15 of 18 rocks from the northern part of zone G define field g^n. All 29 zone H rocks define field h. N is the one sample from Narage.

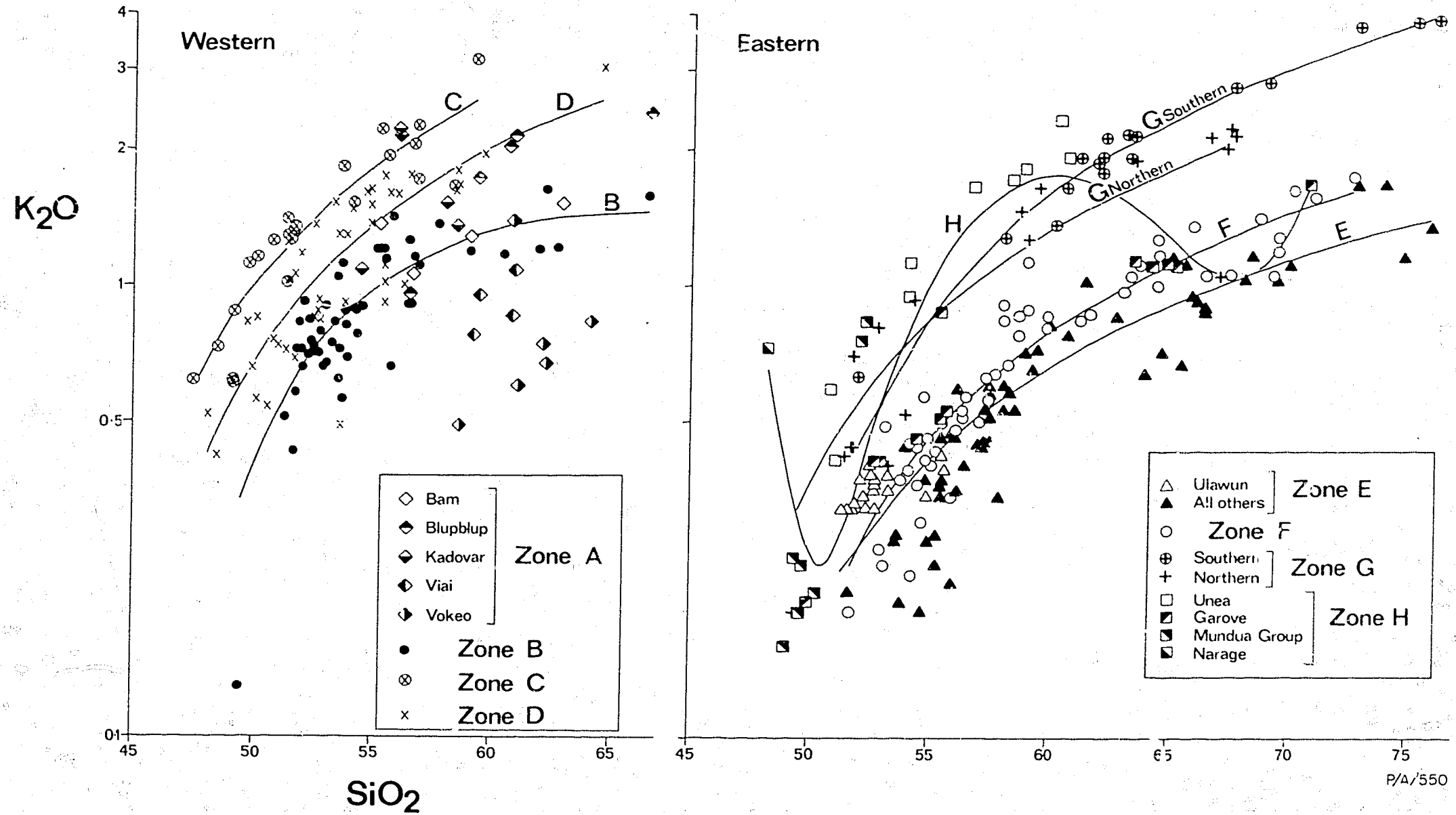

Fig. 15. Weight percent K_2O ($\log_{10}$ scale) v. SiO_2 for rocks from the western and eastern arcs. RSS values (x 10^3) for regression lines: B = 690, C = 817, D = 744, E = 859, F = 894, G southern = 978, G northern = 827, H = 788.

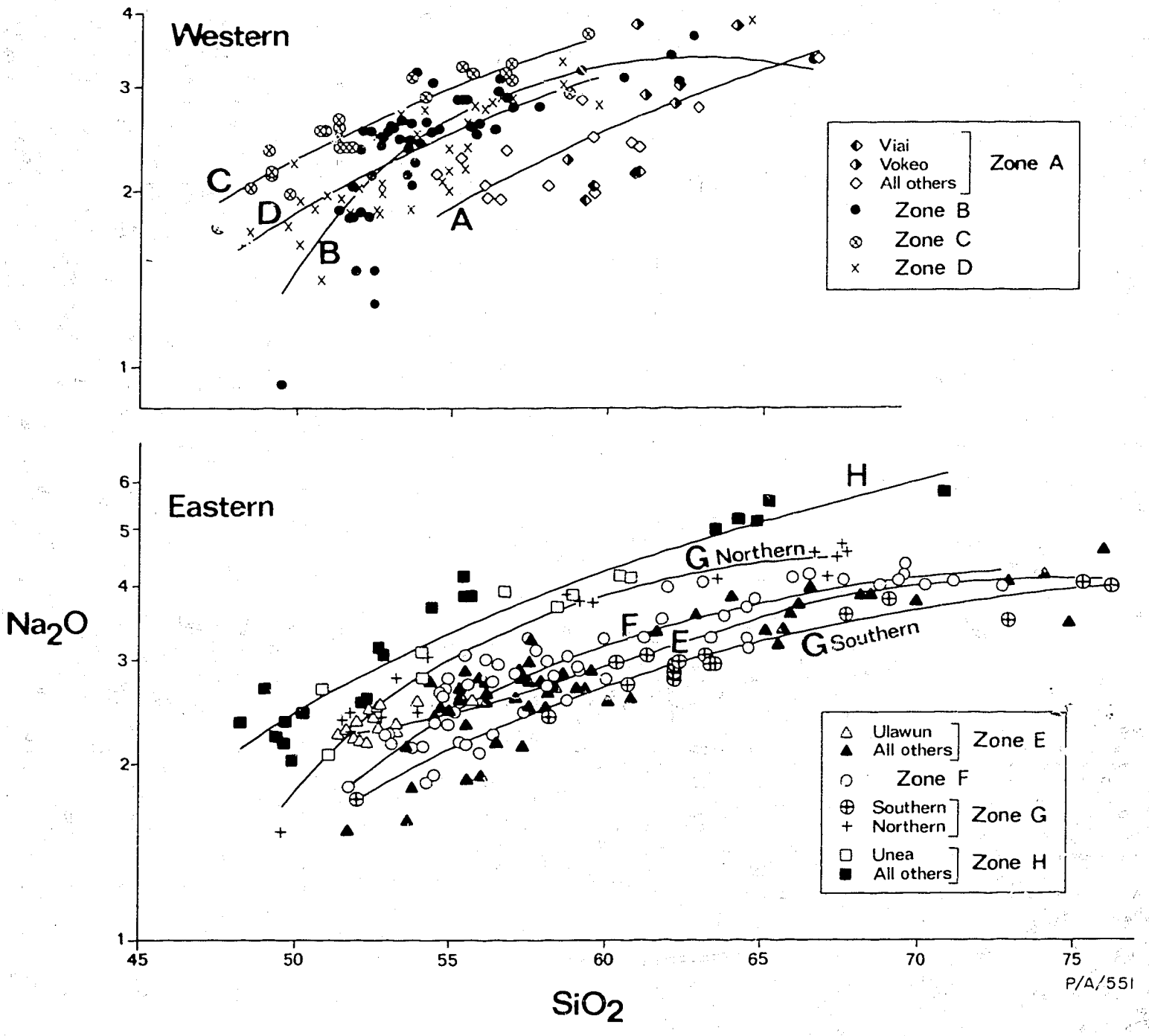

Fig. 16. Weight percent Na_2O (log_{10} scale) v. SiO_2 for rocks from the western and eastern arcs. RSS values (x 10^3) for regression lines: A = 473, B = 672, C = 886, D = 707, E = 819, F = 847, G southern = 933, G northern = 970, H = 918.

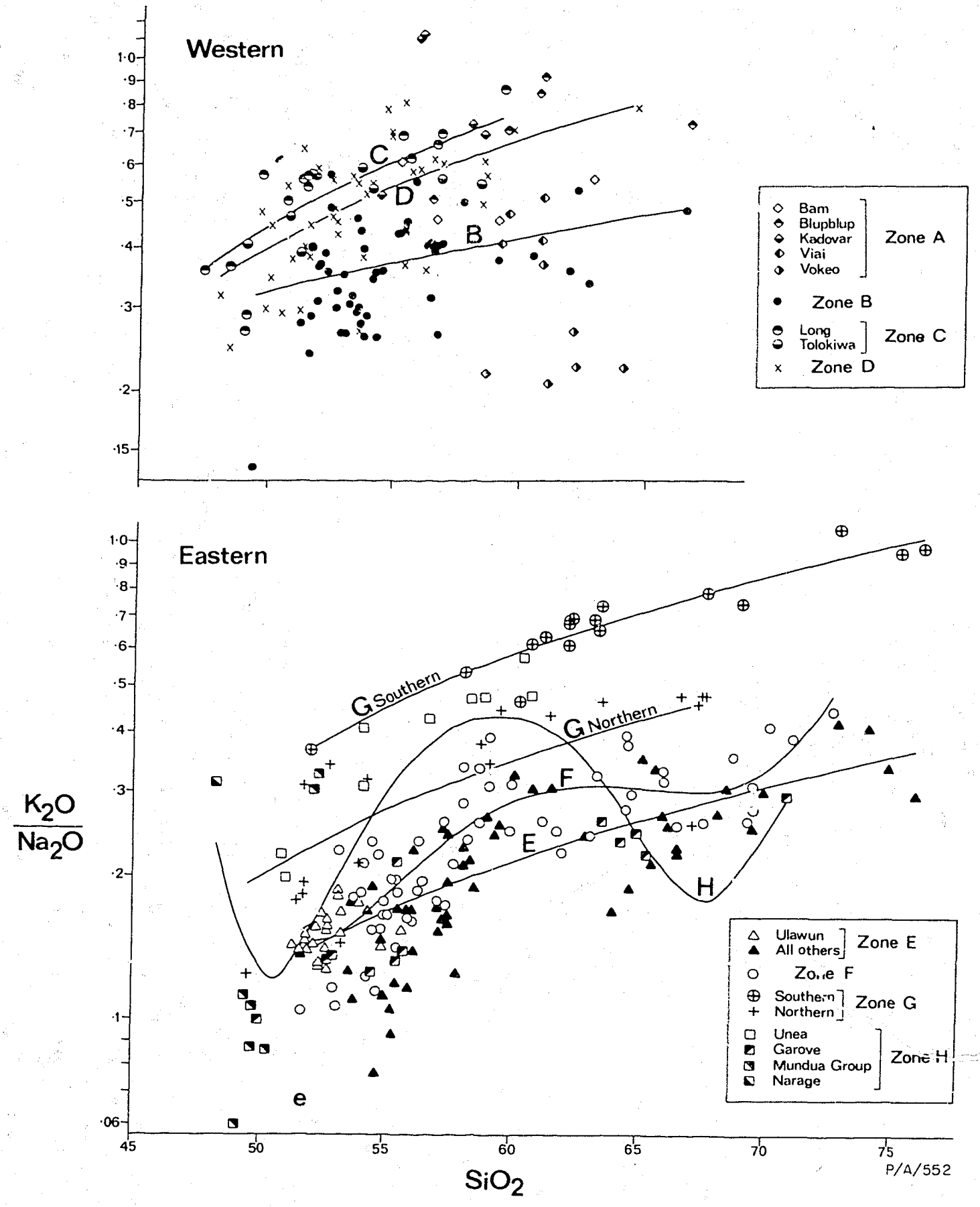

Fig. 17. Weight percent K_2O/Na_2O ($\log_{10}$ scale) v. SiO_2 for rocks from the western and eastern arcs. RSS values (x 10^3) for regression lines: E = 123, C = 644, D = 367, E = 646, F = 691, G southern = 886, G northern = 639, H = 527.

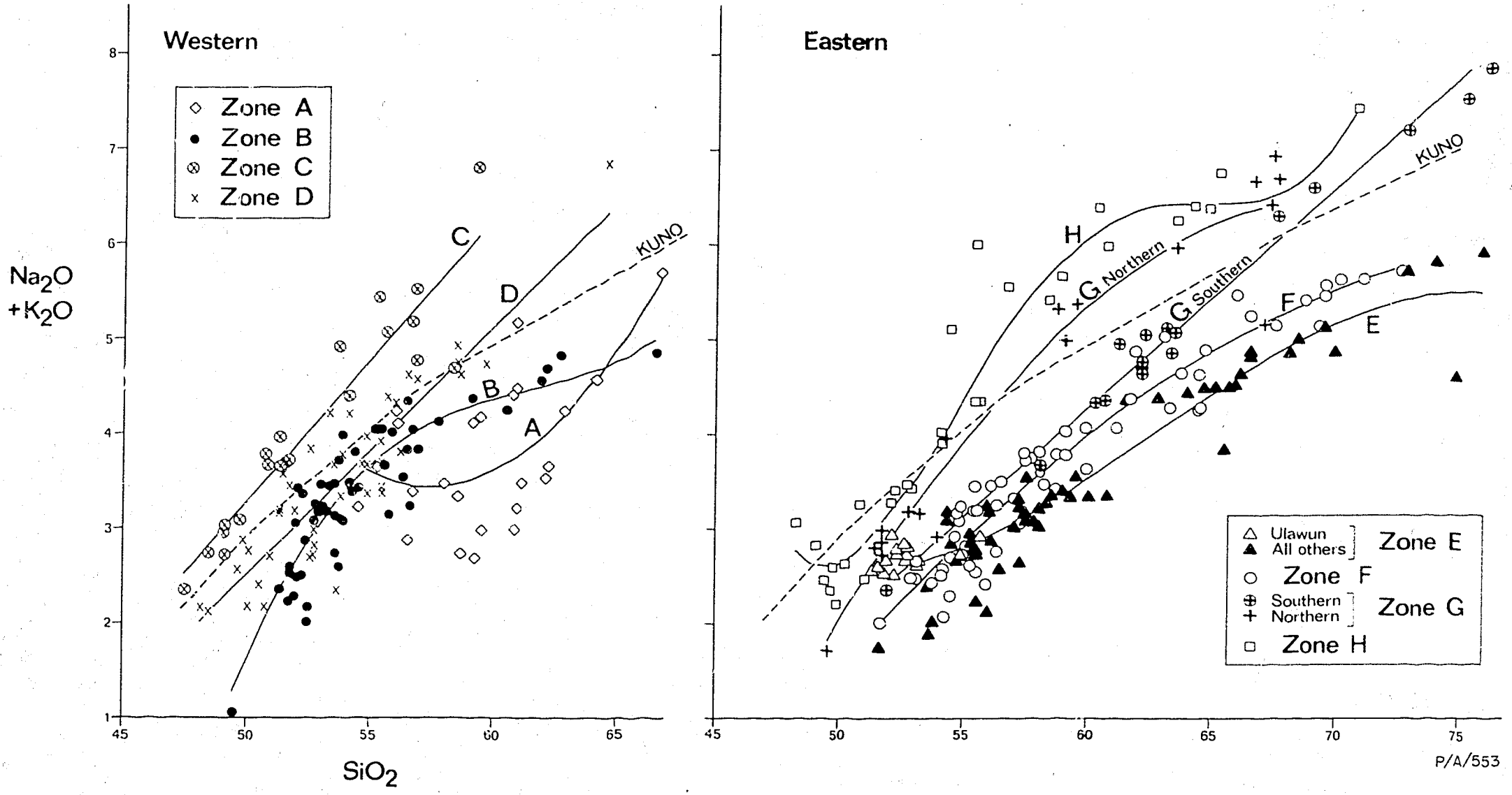

Fig. 18. Weight percent $Na_2O + K_2O$ v. SiO_2 for rocks from the western and eastern arcs. The dashed line separates Kuno's (1959) 'high-alumina basalt' (upper) and 'tholeiitic' fields. RSS values (x 10^3) for regression lines: A = 396, B = 791, C = 883, D = 811, E = 894, F = 931, G southern = 986, G northern = 946, H = 975.

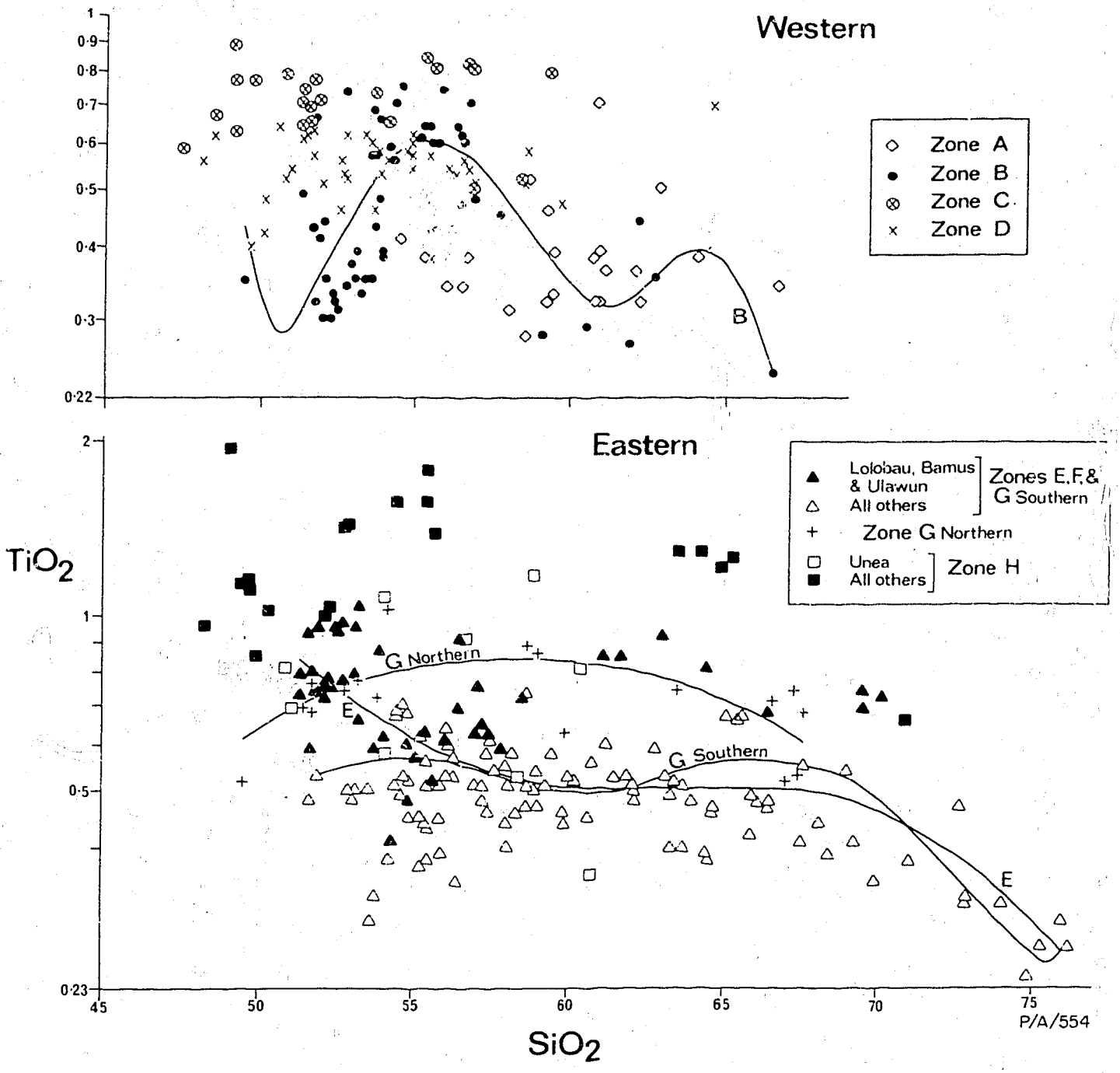

Fig. 19. Weight percent TiO_2 v. SiO_2 for rocks from the western and eastern arcs. RSS values (x 10^3) for regression lines: B = 455, E = 457, G southern = 892, G northern = 400.

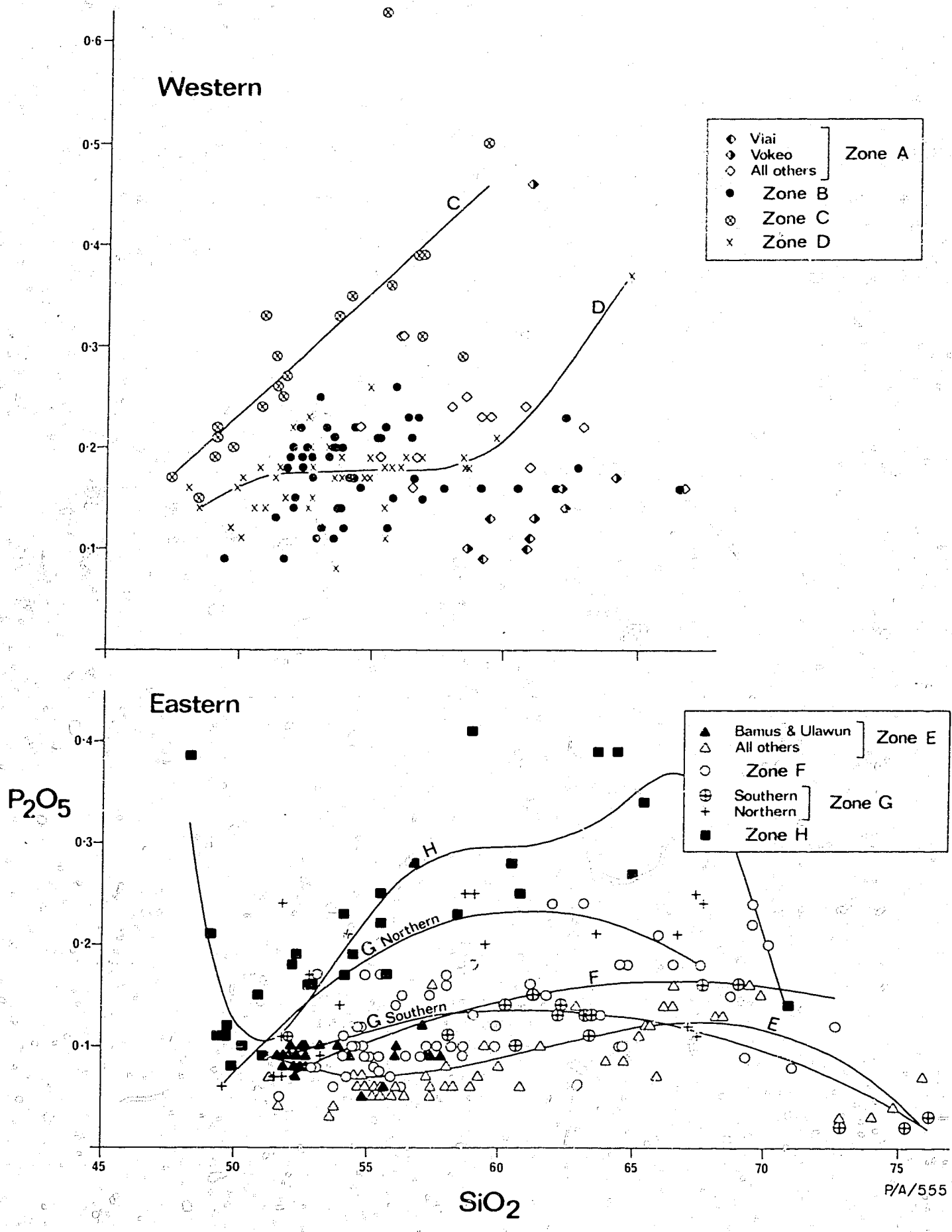

Fig. 20. Weight percent P_2O_5 v. SiO_2 for rocks from the western and eastern arcs. RSS values (x 10^3) for regression lines: C = 563, D = 447, E = 370, F = 318, G southern = 682, G northern = 452, H = 751.

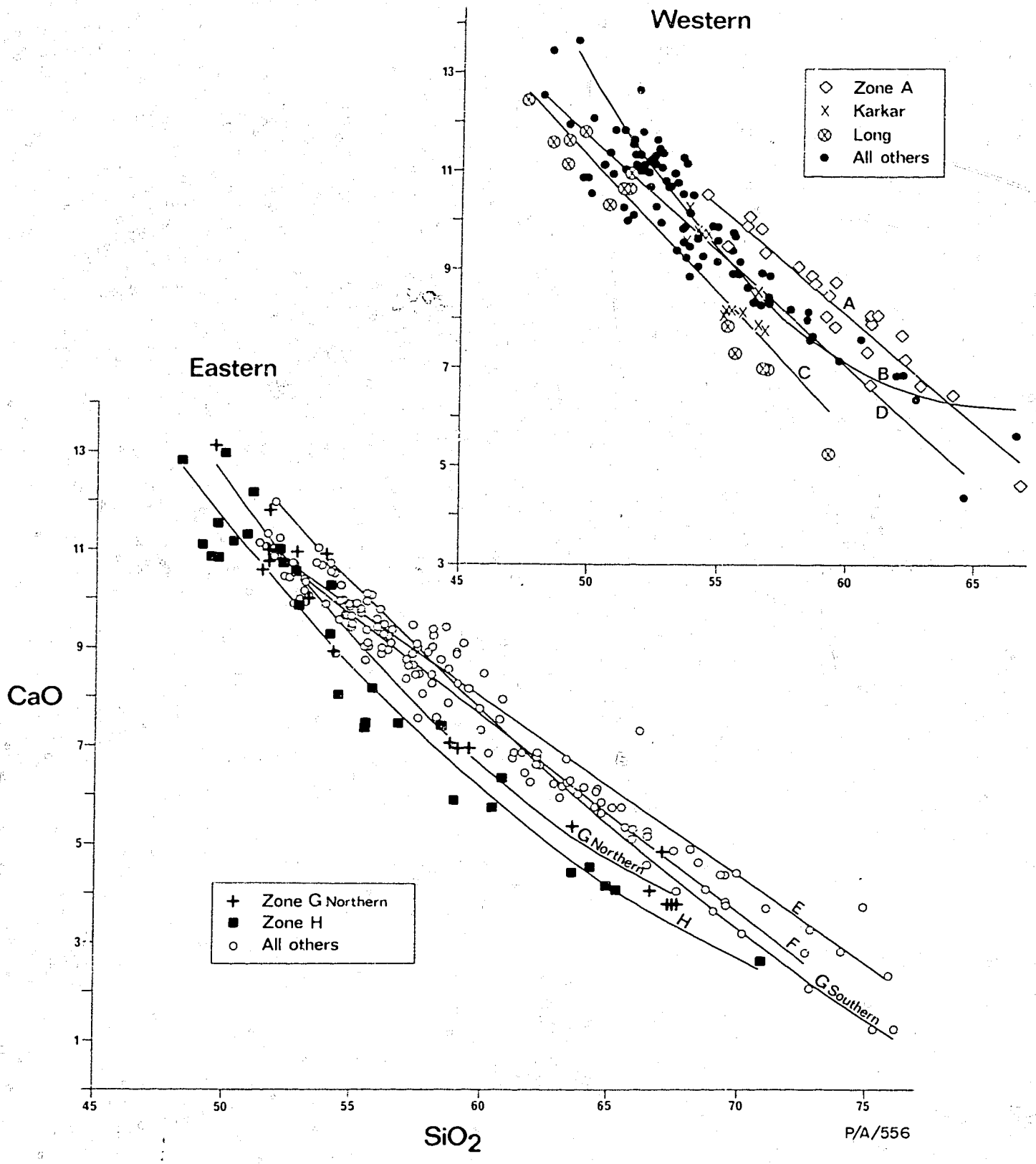

Fig. 21. Weight percent CaO v. SiO_2 for rocks from the western and eastern arcs. In order that the regression lines can be clearly seen, many low-silica rocks have not been plotted. RSS values (x 10^3) for regression lines: A = 913, B = 891, C = 917, D = 872, E = 957, F = 973, G southern = 990, G northern = 977, H = 944.

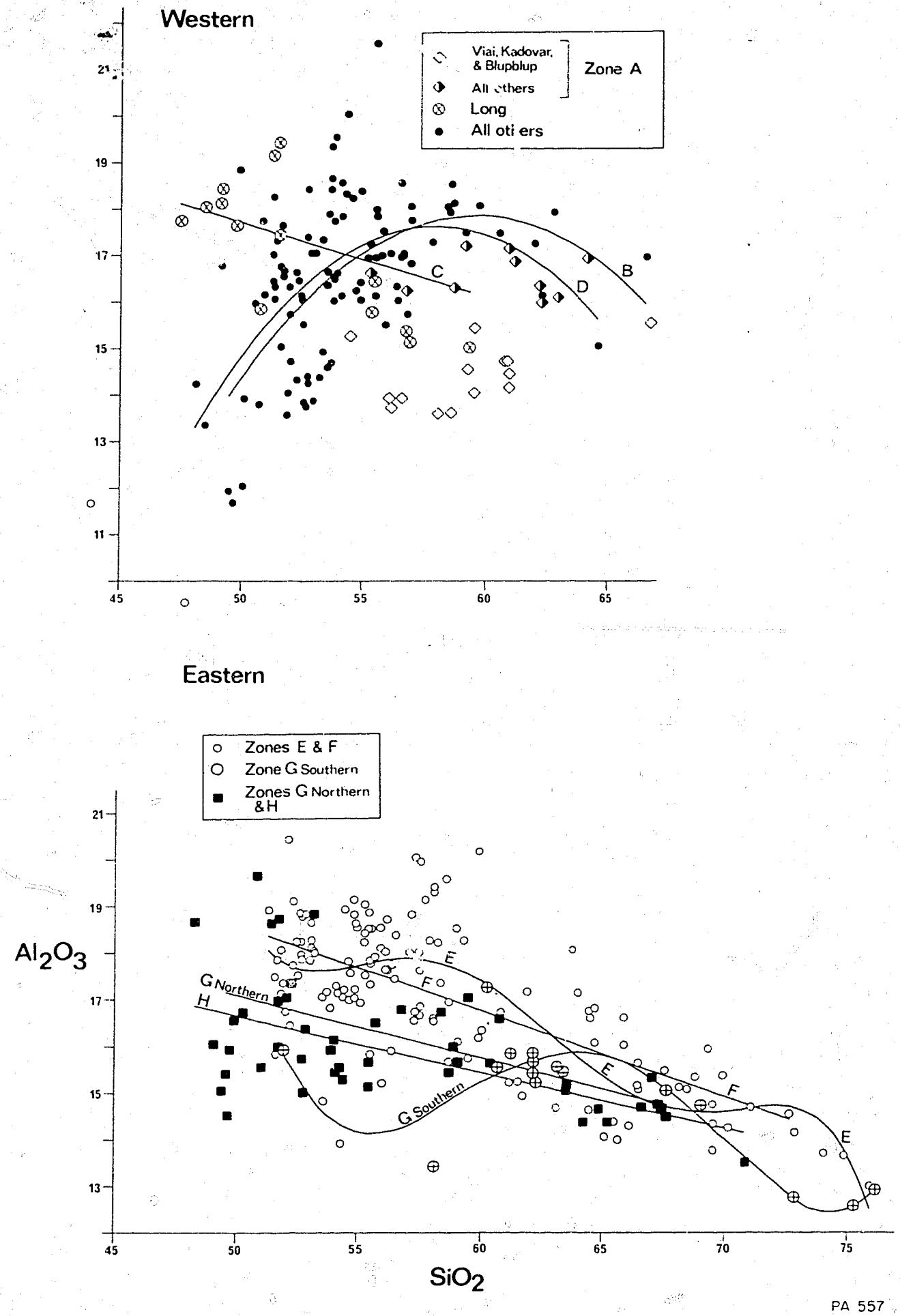

Fig. 22. Weight percent Al_2O_3 v. SiO_2 for rocks from the western and eastern arcs. RSS values (x 10^3) for regression lines: B = 274, C = 177, D = 320, E = 545, F = 519, G southern = 769, G northern = 387, H = 314.

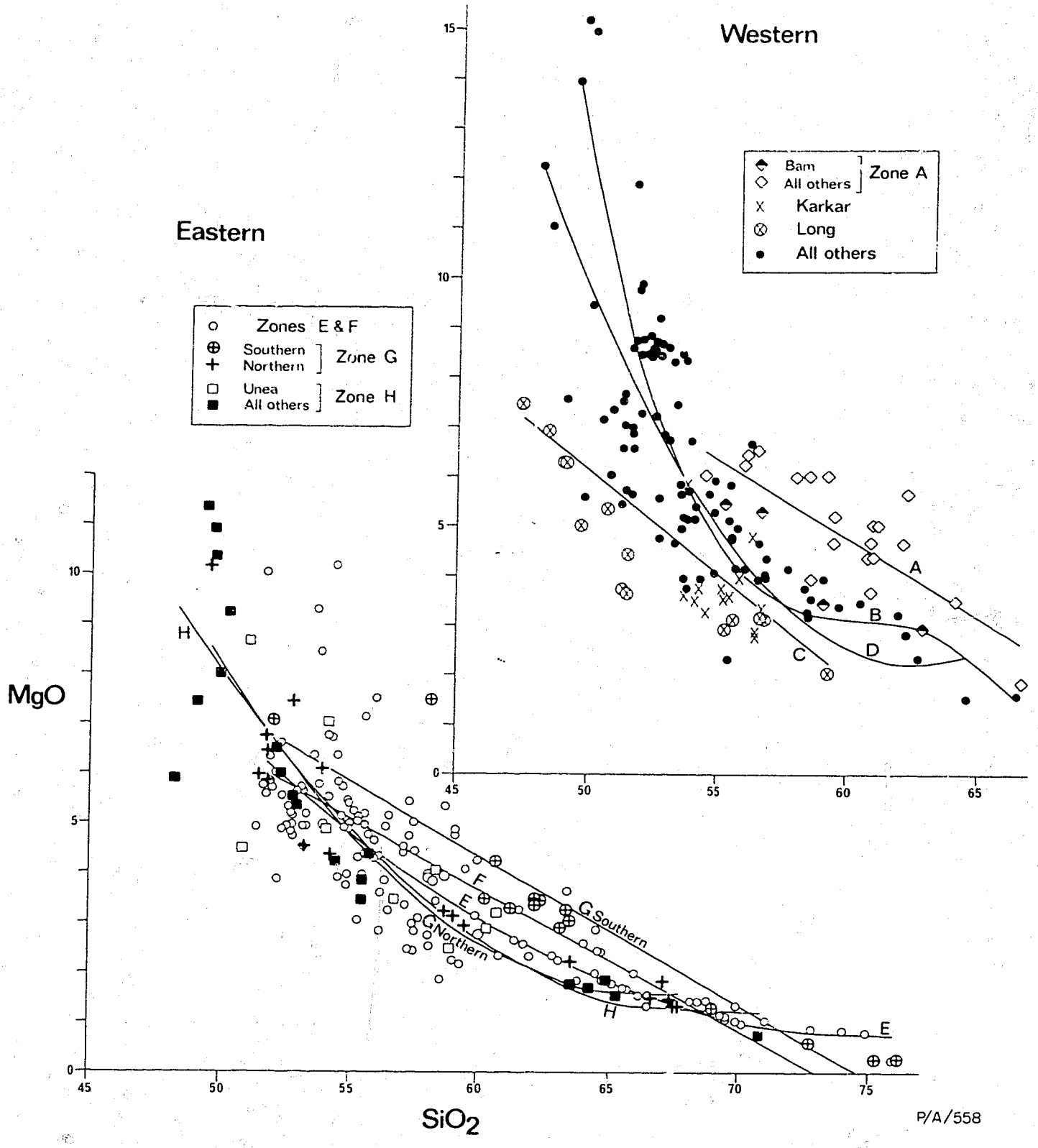

Fig. 23. Weight percent MgO v. SiO_2 for rocks from the western and eastern arcs. RSS values (x 10^3) for regression lines: A = 584, B = 767, C = 621, D = 629, E = 643, F = 847, G southern = 850, G northern = 909, H = 769.

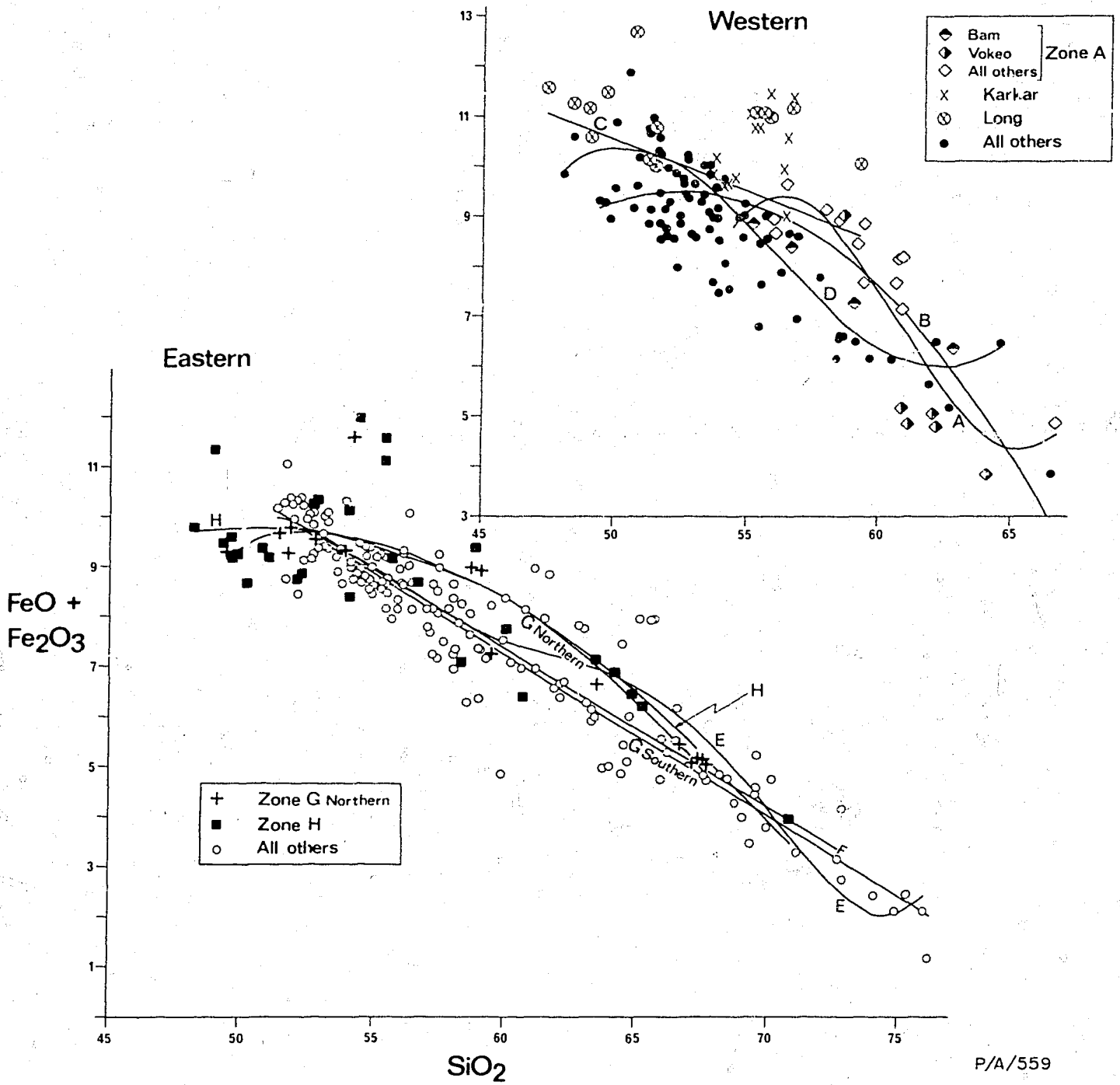

Fig. 24. Weight percent FeO + Fe_2O_3 v. SiO_2 for rocks from the western and eastern arcs. FeO and Fe_2O_3 proportions computed by the method of Irvine & Baragar (1971), and whole-rock analyses recalculated to 100 percent without volatiles. RSS values (x 10^3) for regression lines: A = 749, B = 579, C = 188, D = 772, E = 884, F = 841, G southern = 964, G northern = 912, H = 671.

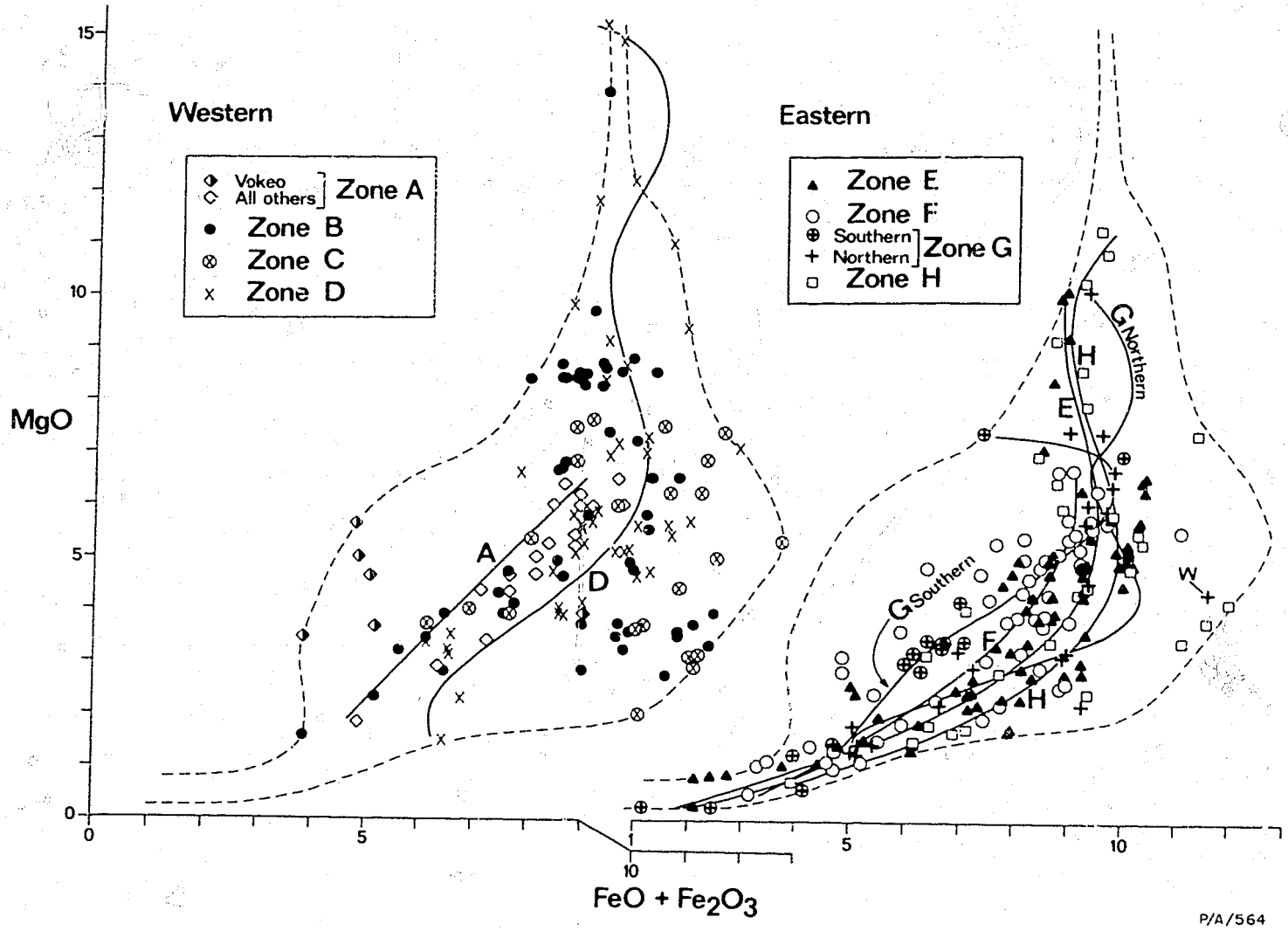

Fig. 25. Weight percent MgO v. FeO + Fe_2O_3 for rocks from the western and eastern arcs. FeO and Fe_2O_3 proportions computed by the method of Irvine & Baragar (1971), and whole-rock analyses recalculated to 100 percent without volatiles. The pairs of dashed lines in both diagrams define the compositional field covered by rocks from all the zones. W is sample 339 of Lowder & Carmichael (1970). RSS values (x 10^3) for regression lines: A = 392, D = 615, E = 814, F = 728, G southern = 939, G northern = 939, H = 592.

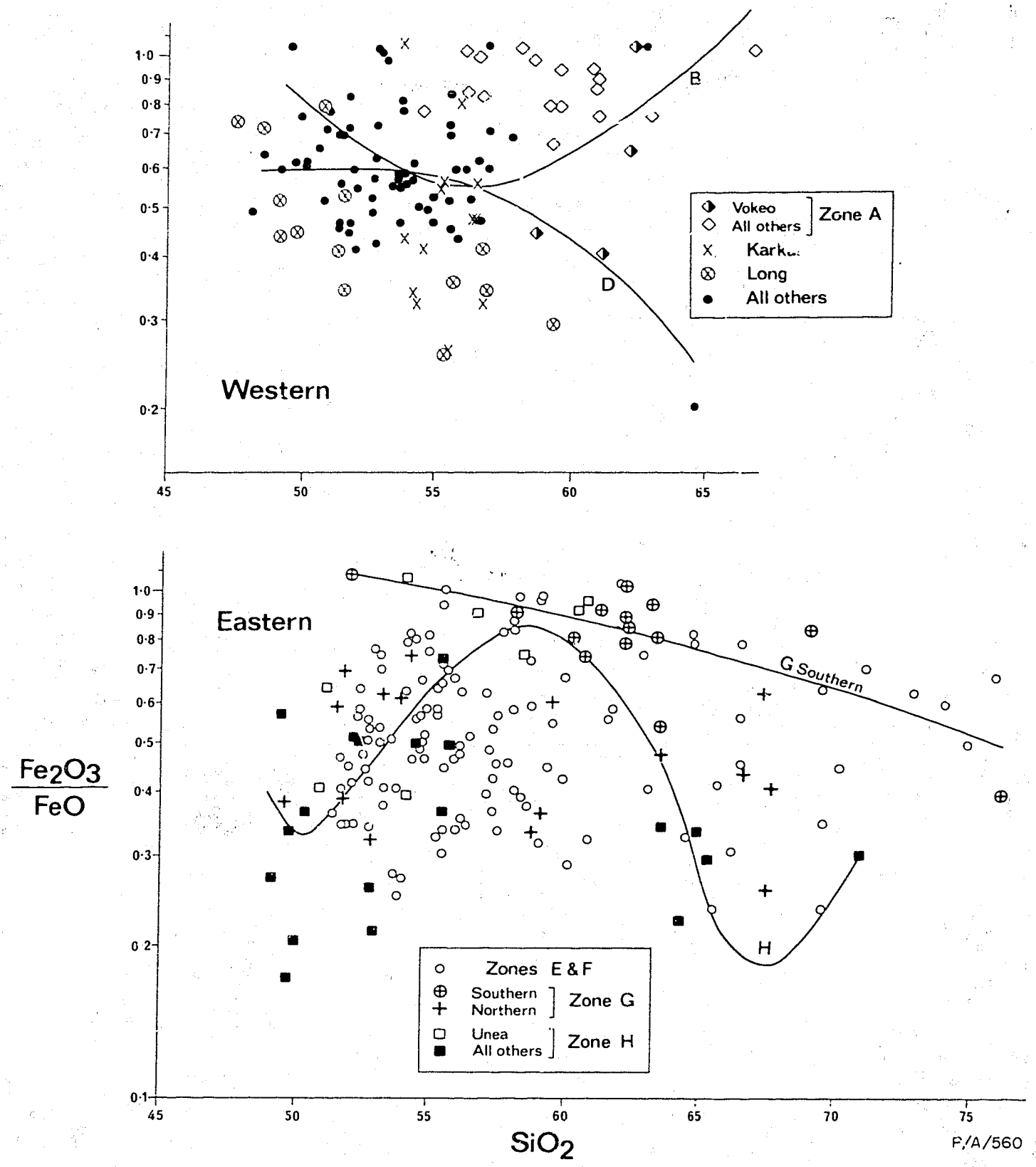

Fig. 26. Weight percent Fe_2O_3/FeO (log_{10} scale) v. SiO_2 for rocks from the western and eastern arcs. 27 western rocks and 24 eastern rocks showing Fe_2O_3/FeO values greater than 1.1 are excluded (see text). Fe_2O_3 and FeO values taken from original analyses. SiO_2 values are those used in Figures 11 to 27. RSS values (x 10^3) for regression lines: B = 281, D = 227, G southern = 538, H = 459.

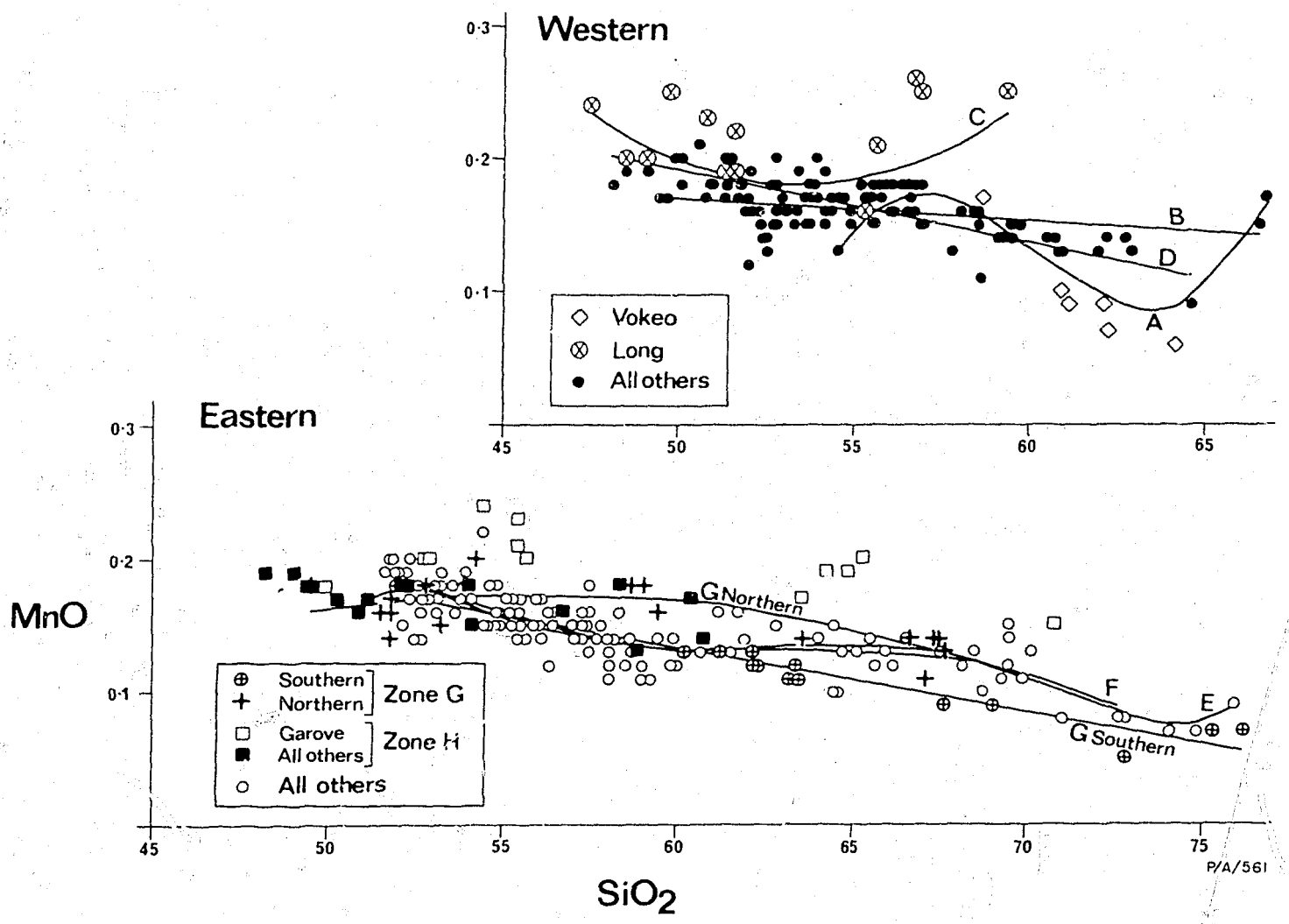

Fig. 27. Weight percent MnO v. SiO_2 for rocks from the western and eastern arcs. RSS values (x 10^3) for regression lines: A = 757, B = 118, C = 182, D = 426, E = 736, F = 549, G southern = 927, G northern = 582.

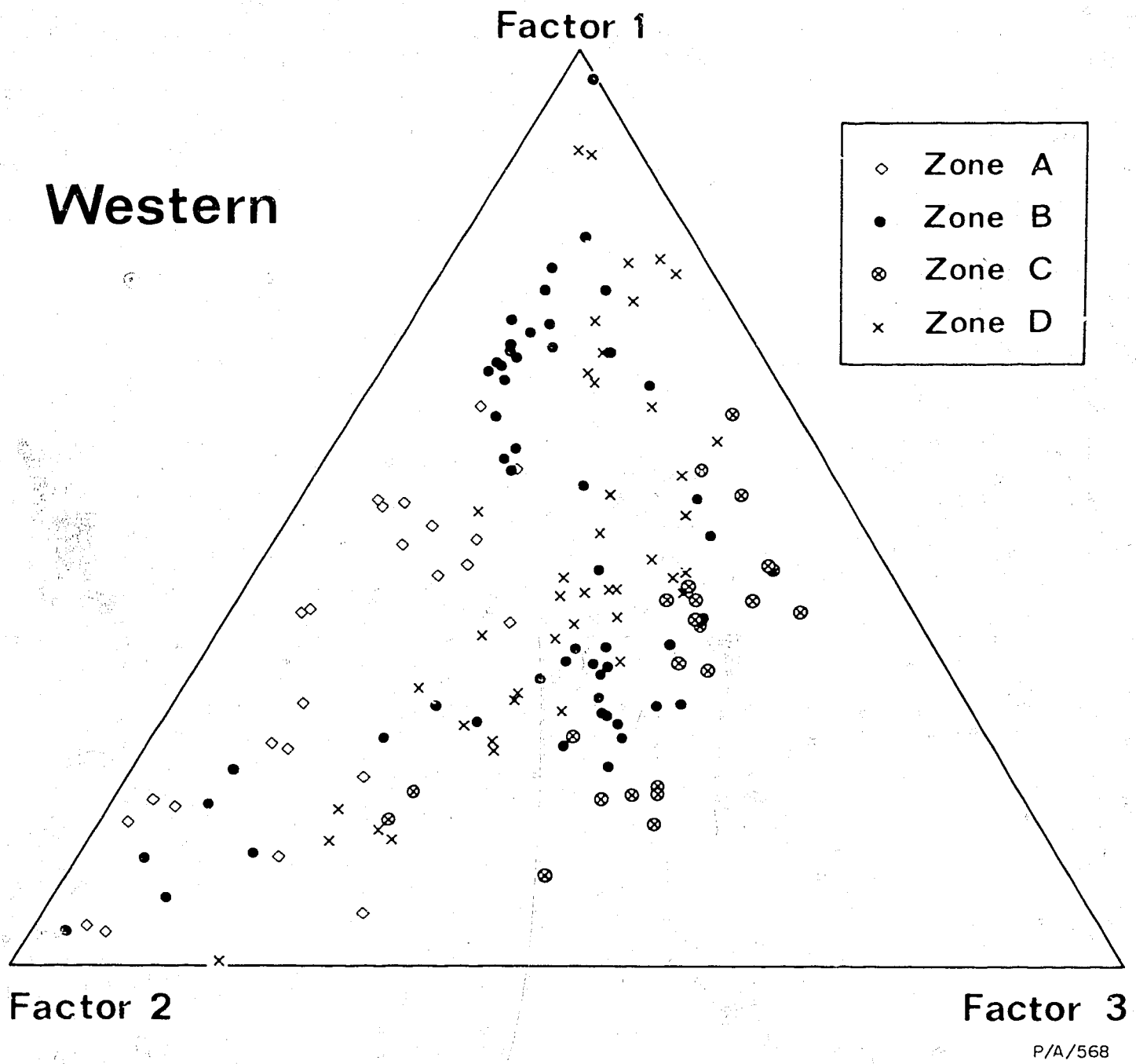

Fig. 28. Loadings for three Q-mode factors accounting for 96.93 percent of the variation among eleven oxides in analysed rocks from the western arc.

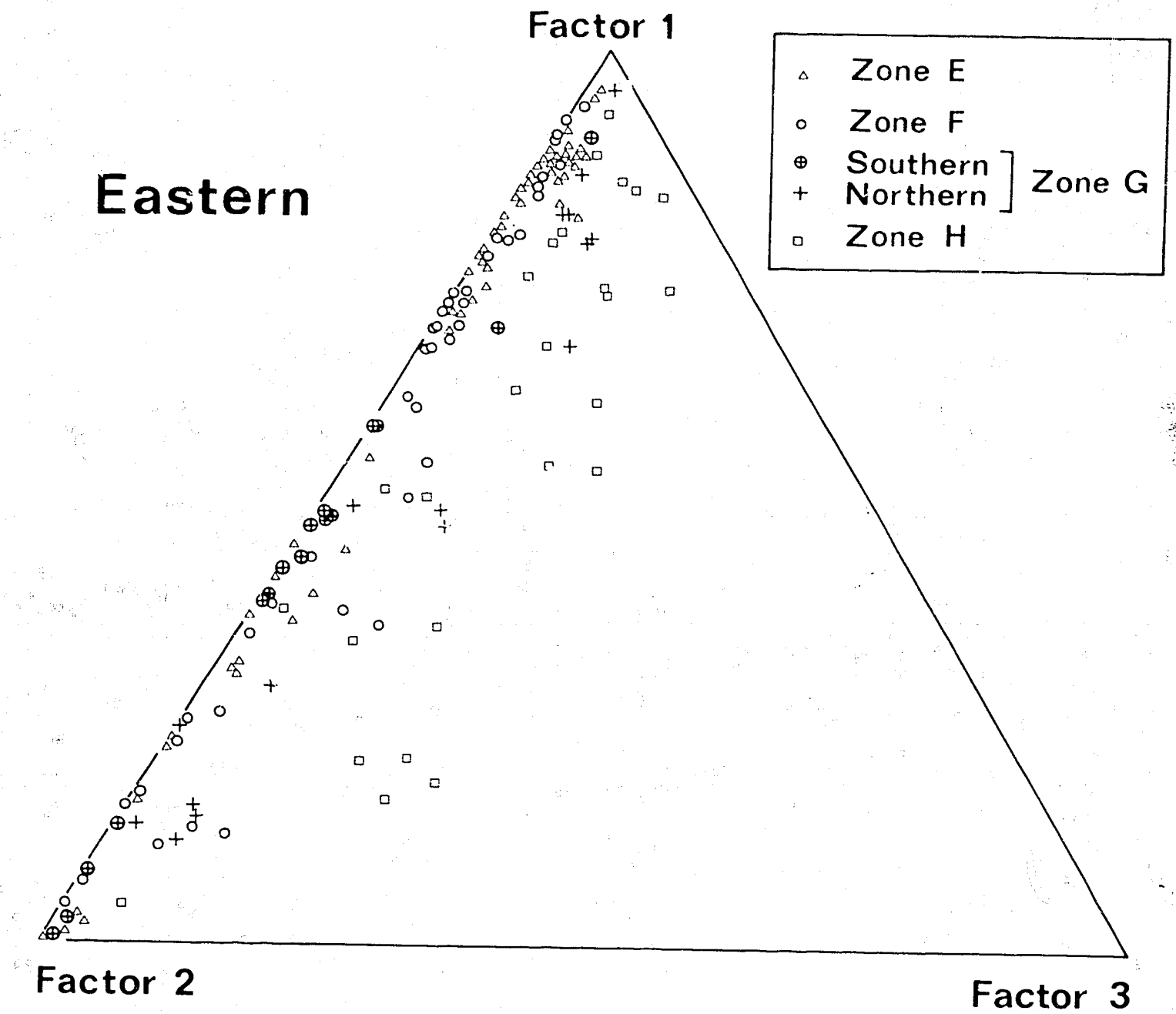

P/A/569

Fig. 29. Loadings for three Q-mode factors accounting for 96.93 percent of the variation among eleven oxides in analysed rocks from the eastern arc.

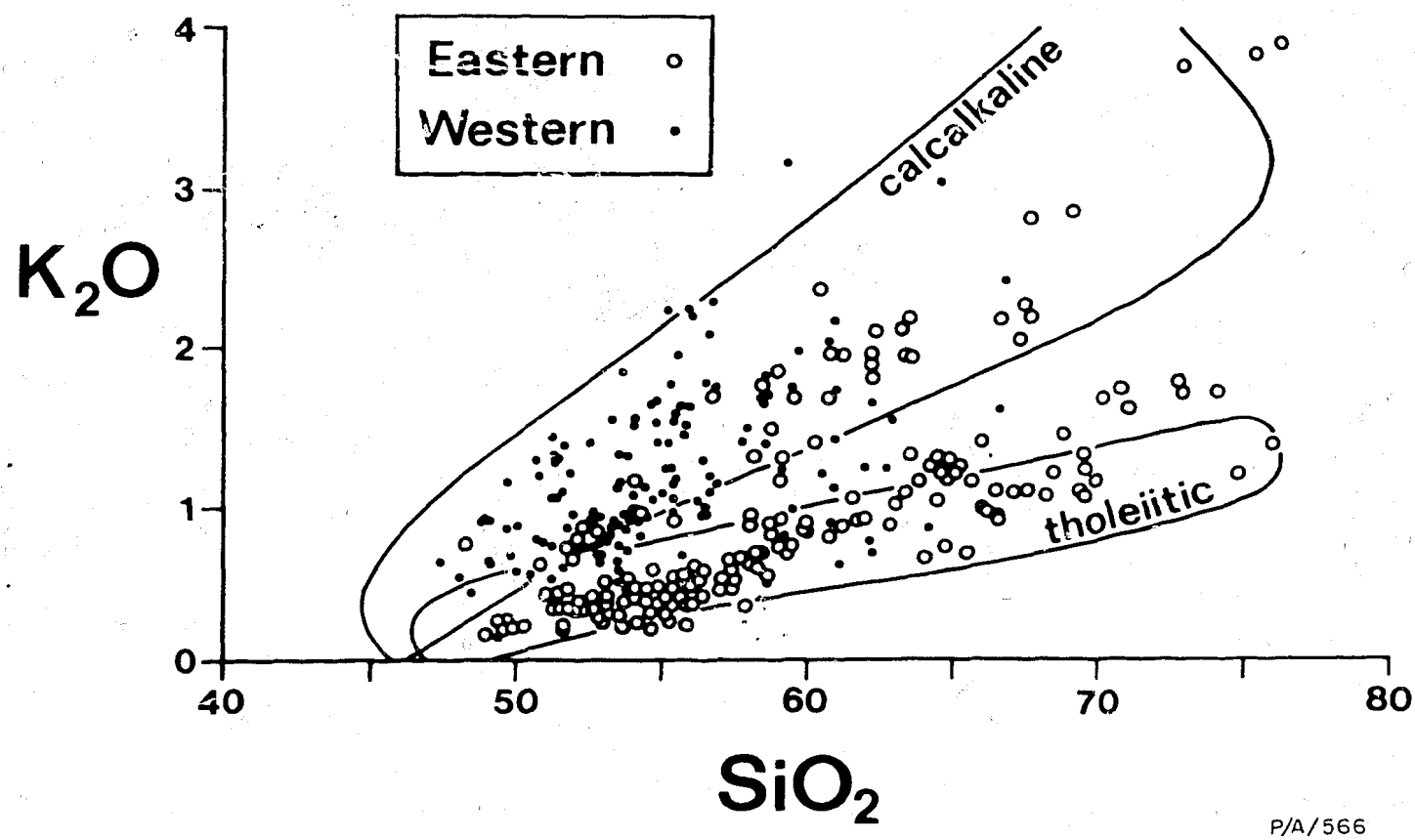

Fig. 30. K_2O:SiO_2 for rocks from the south Bismarck Sea volcanoes in relation to the generalized calcalkaline and tholeiitic field boundaries of Jakeš & Gill (1970).

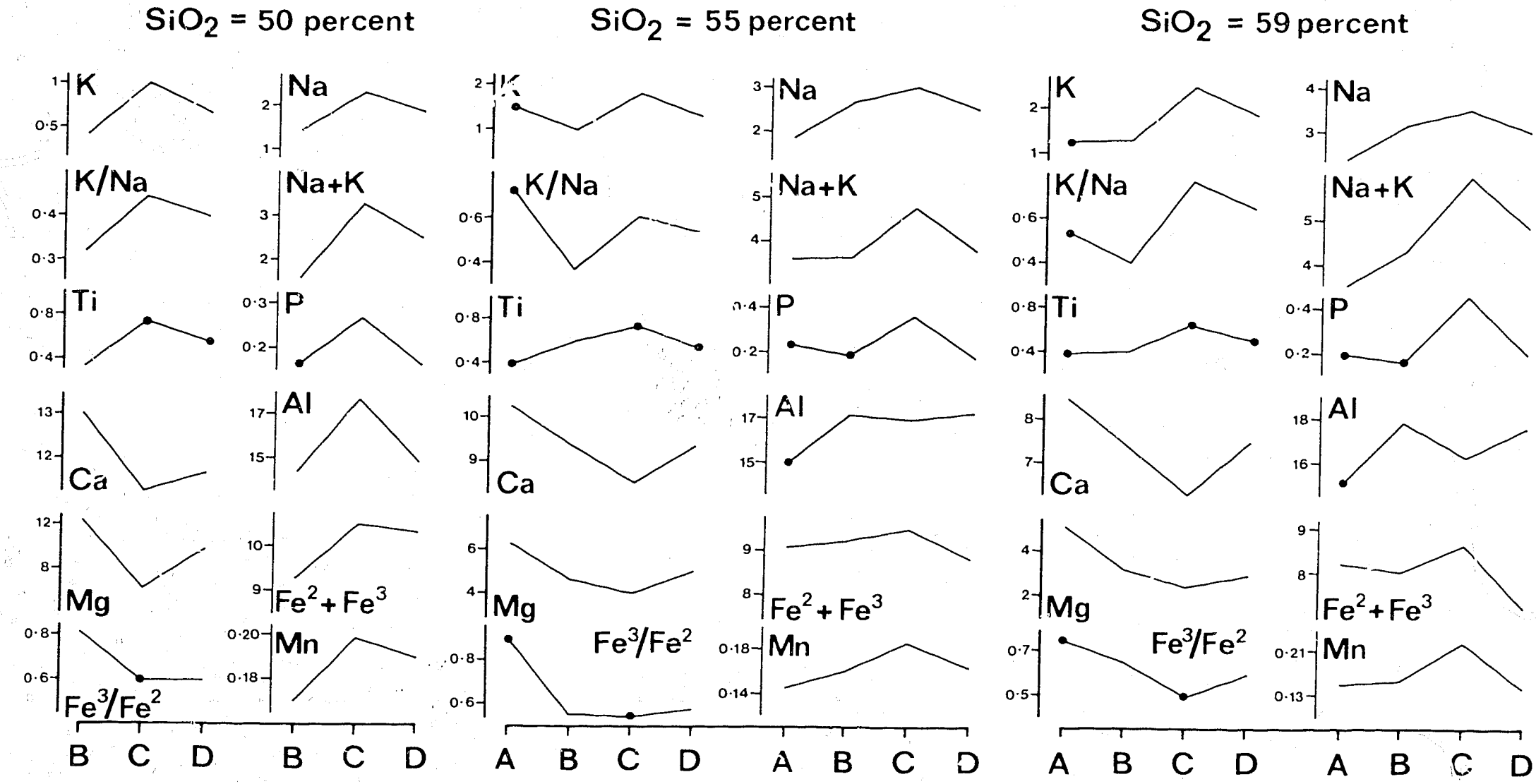

Fig. 31. Generalized oxide variations with different silica contents in rocks from the western arc. Individual oxide values for each zone are arithmetic means (dots) or were determined from the regression lines in Figures 15–24, 26, and 27 (see text for details).

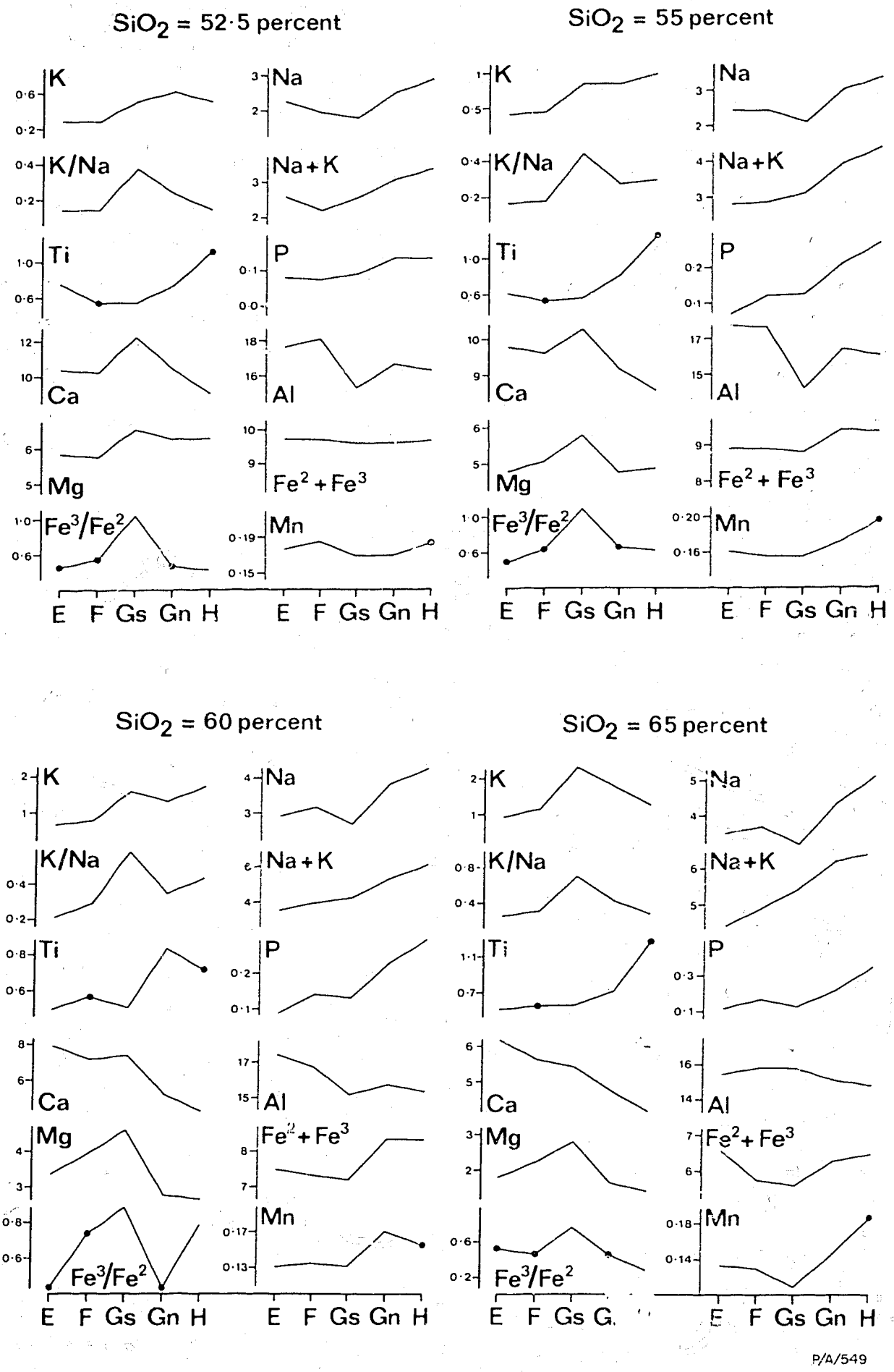

Fig. 32. Generalized oxide variations with different silica contents in rocks from the eastern arc. Individual oxide values for each zone are arithmetic means (dots) or were determined from the regression lines in Figures 15–24, 26, and 27 (see text for details).

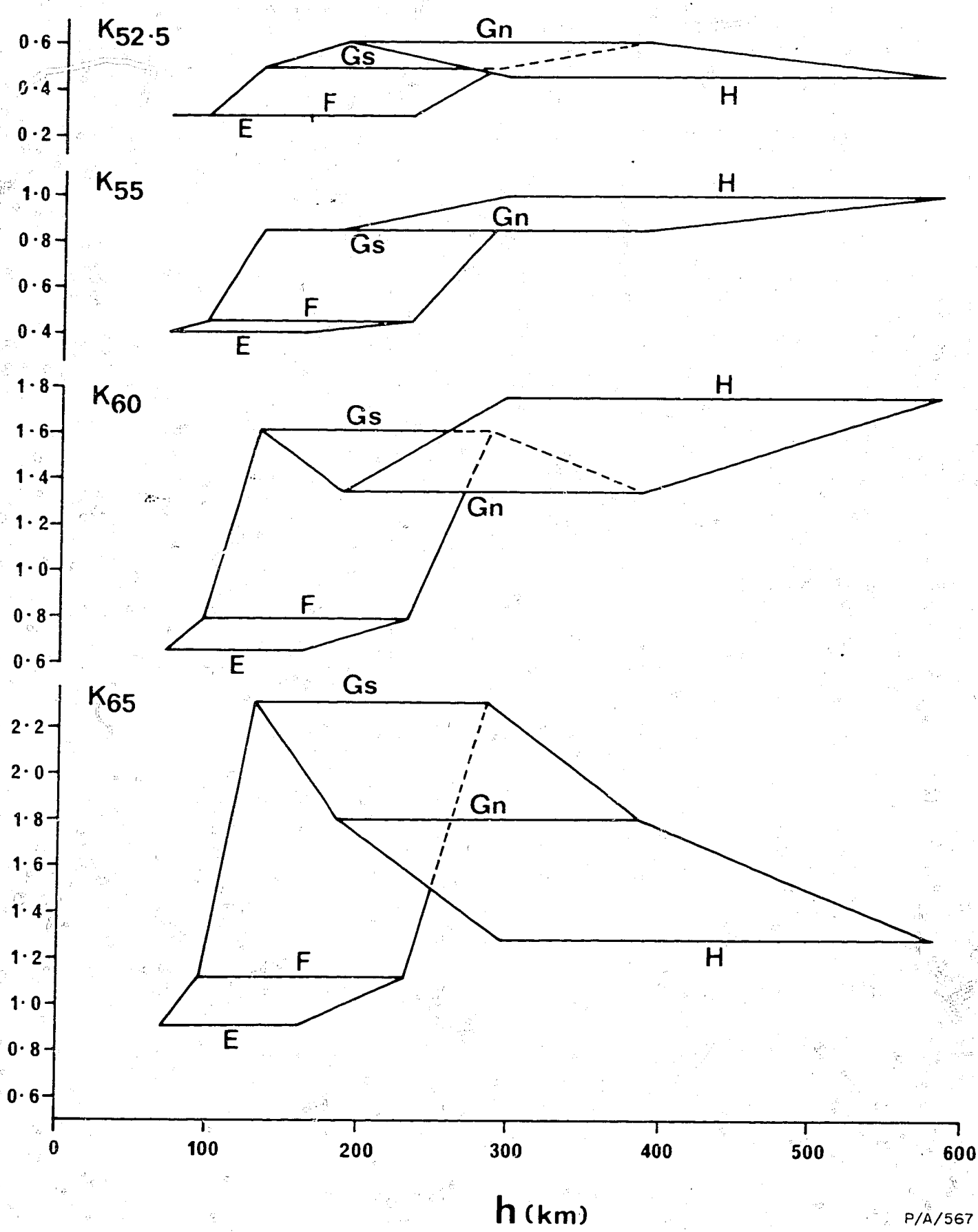

Fig. 33. K_2O contents - determined from the regression lines in Figure 15 at 52.5, 55, 60, and 65 percent silica levels - plotted against depth-ranges to the New Britain Benioff zone - determined from Figure 4, and for zone E also from Figure B7 in Appendix A. Letters corresponding to each zone are drawn opposite the midpoint of the lines representing each depth range.

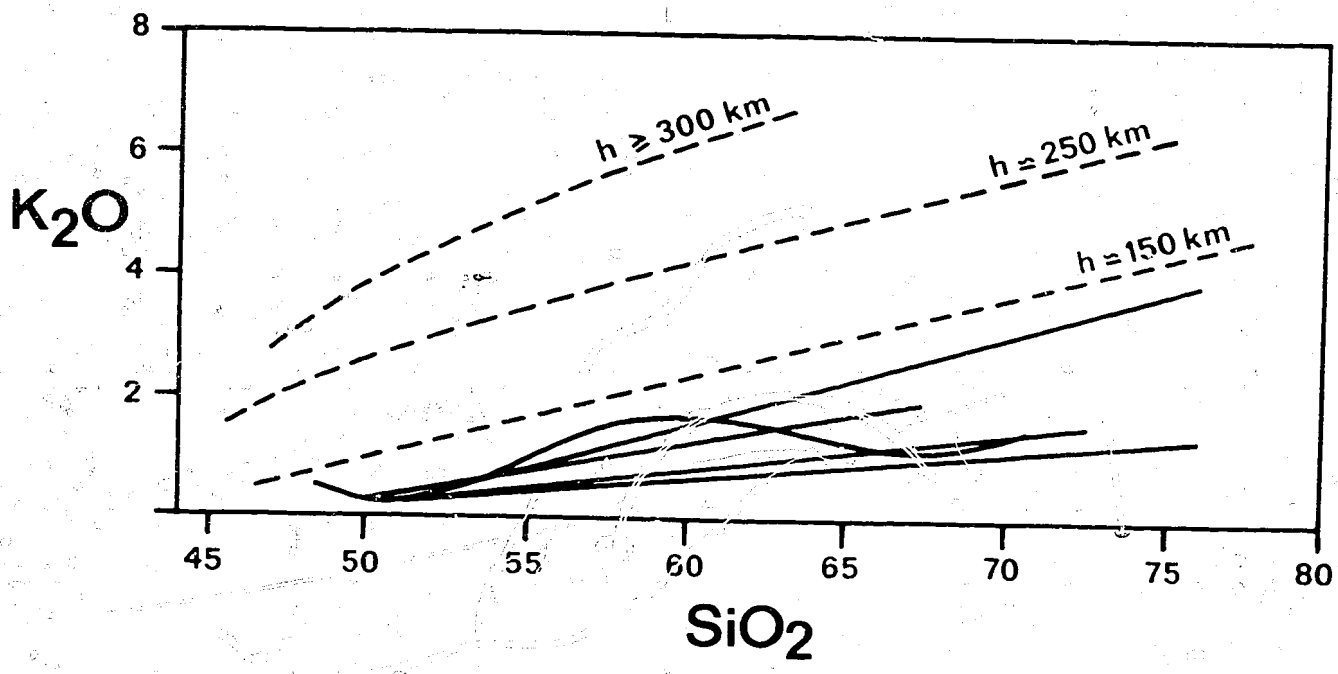

Fig. 34. Regression lines of Figure 15 plotted on the K-h grid of Ninkovich & Hays (1972); h values represent depths to Benioff zones.

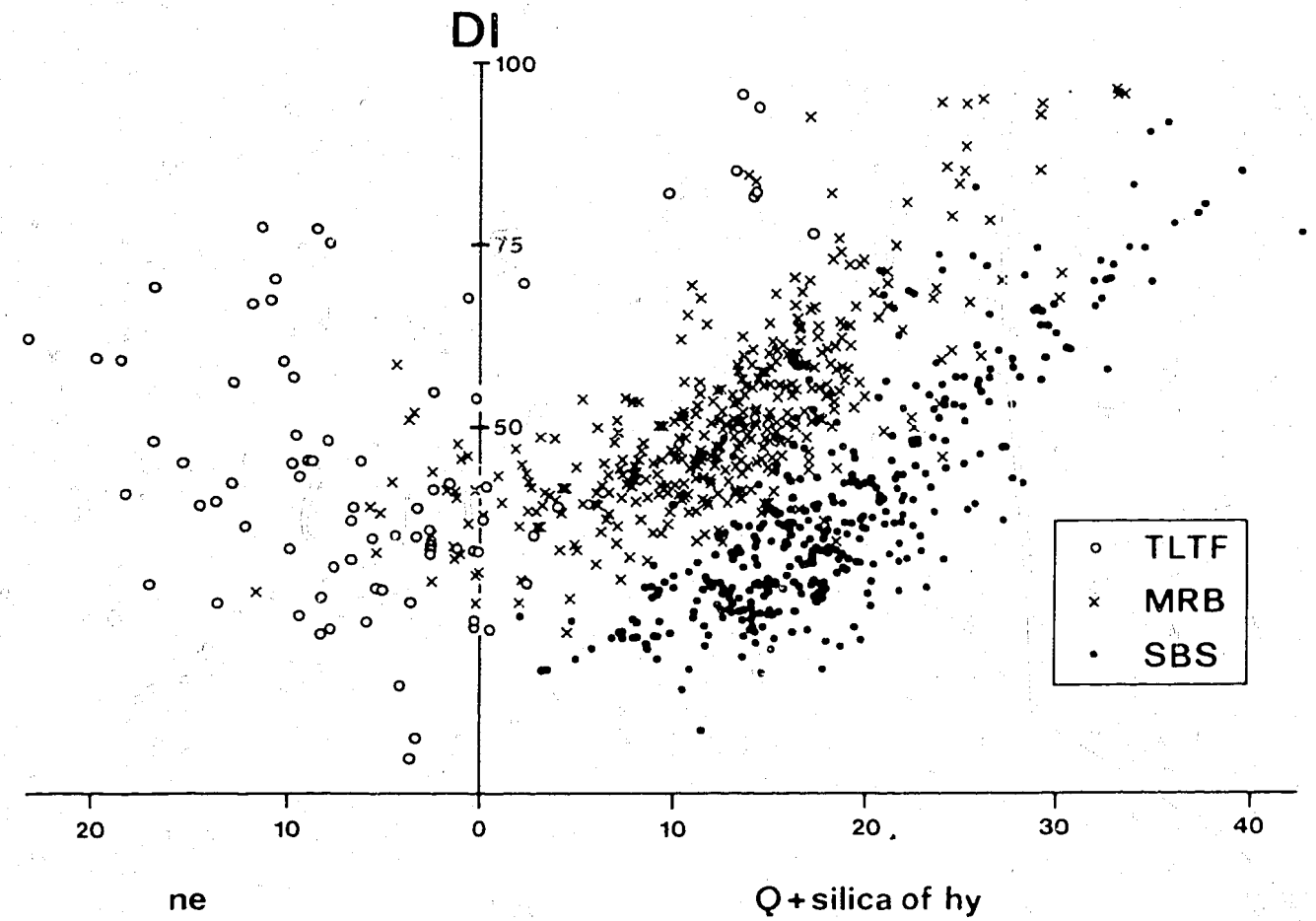

Fig. 35. Differentiation index (DI, Thornton & Tuttle, 1960) v. normative nepheline (ne) and normative quartz (Q) plus the silica of normative hypersthene (hy). See text for explanation of TLTF, MRB, and SBS rock groups. From Johnson et al. (in prep. a).

P/A/548

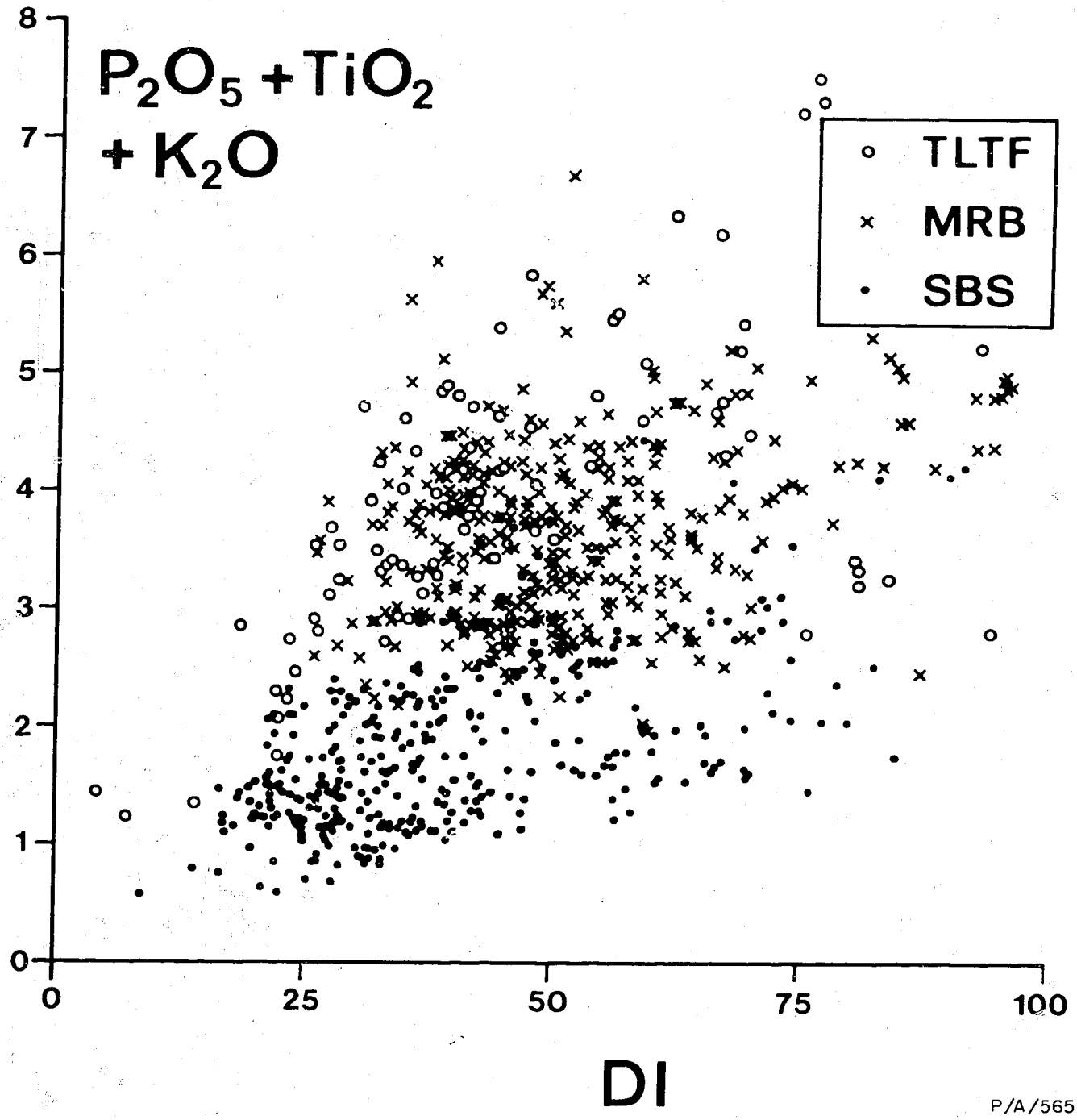

Fig. 36. $P_2O_5 + TiO_2 + K_2O$ v. differentiation index (DI). See text for explanation of TLTF, MRB, and SBS rock groups. From Johnson et al. (in prep.a).

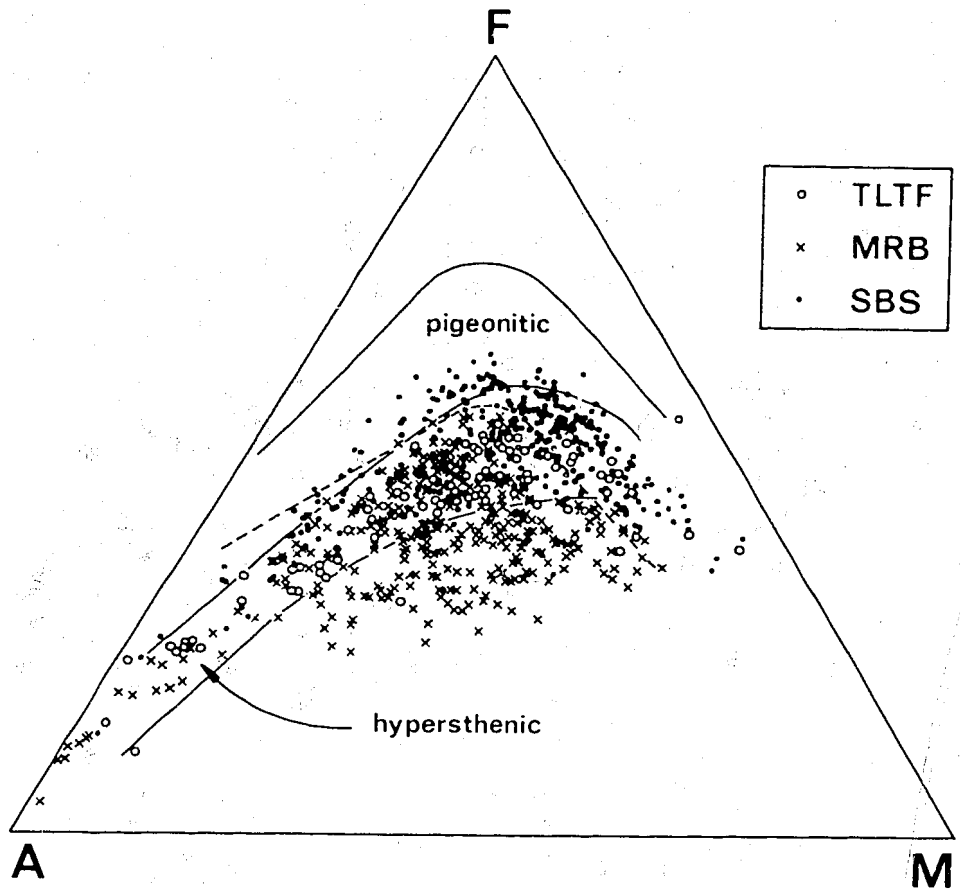

P/A/546

Fig. 37: Relations between F (FeO + Fe_2O_3), M (MgO), and A (Na_2O + K_2O), where the proportion of iron oxides is given by the formula Fe_2O_3/total Fe as Fe_2O_3 = 0.2 See text for explanation of TLTF, MRB, and SBS rock groups. From Johnson et al. (in prep.a).

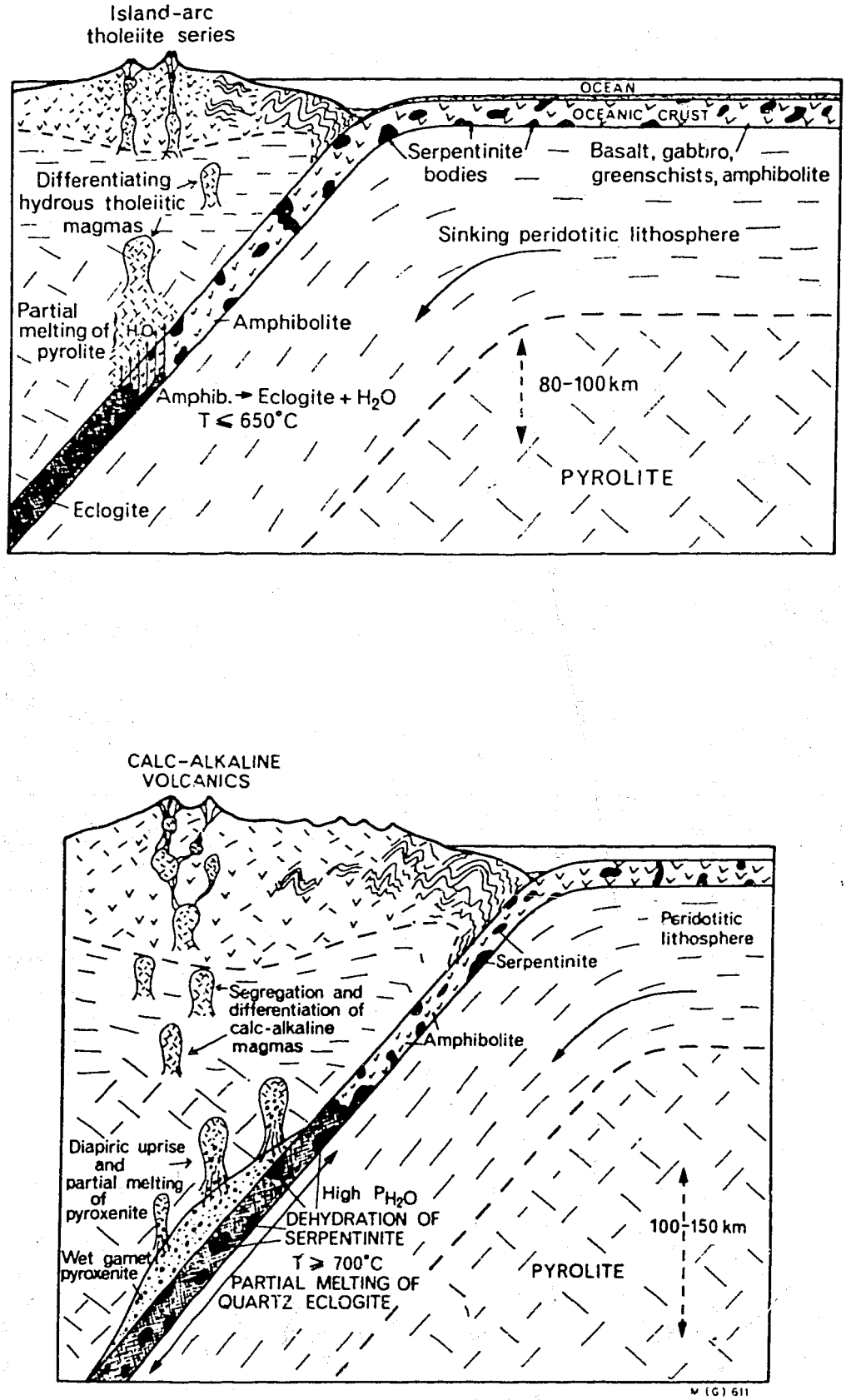

Fig. 38. Idealized cross-sections showing generation of island-arc-type magmas by the scheme of Nicholls & Ringwood (1972, 1973). From Ringwood (1974), and reproduced with the permission of the Geological Society of London. Upper: 'Early phase of development of an island arc involving dehydration of amphibolite in subducted oceanic crust, introduction of water into the overlying wedge, and generation of "island-arc tholeiite" igneous series'. Lower: 'Later phase of island-arc development involving partial melting of subducted oceanic crust, and reaction of liquids with mantle above Benioff zone, leading to diapiric uprise and formation of calcalkaline-type magmas'.

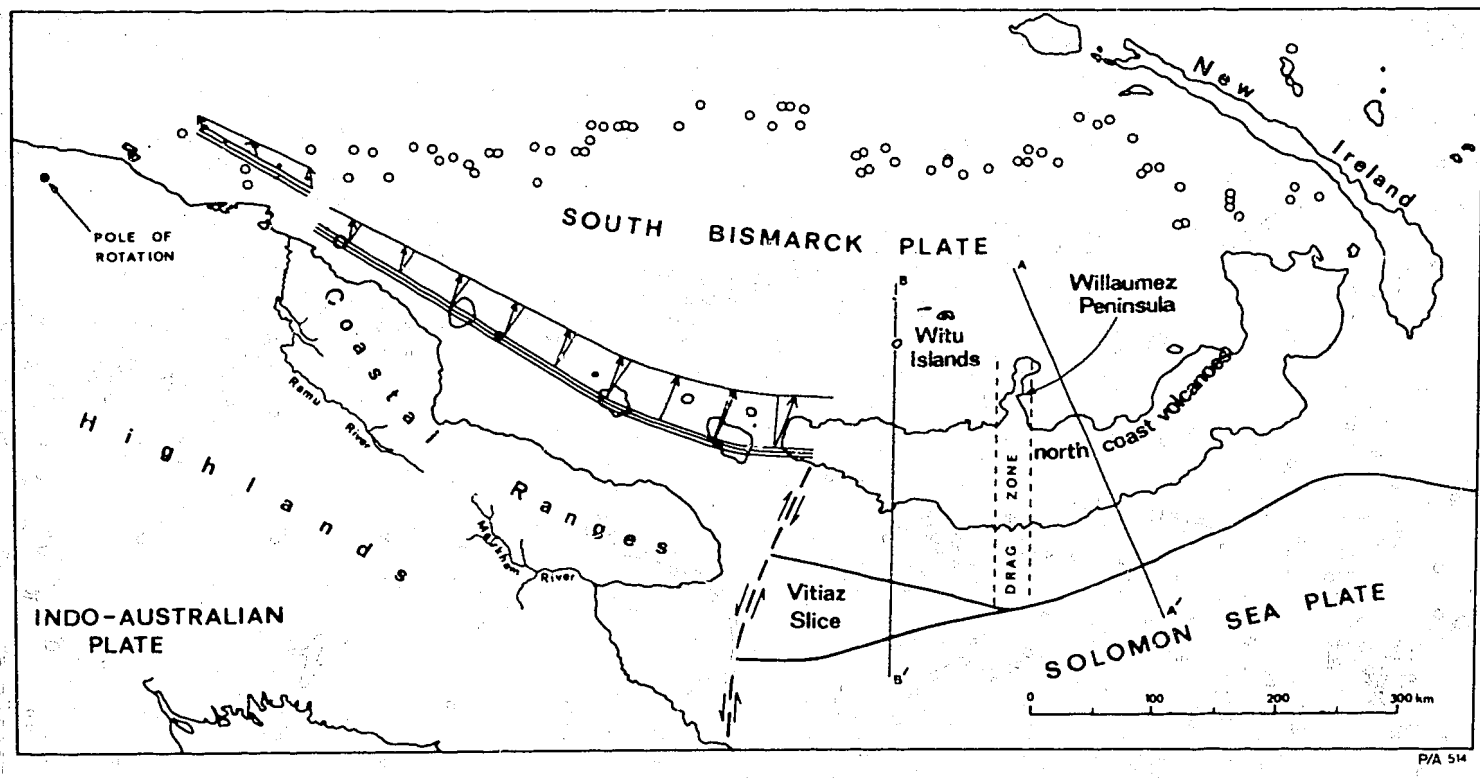

Fig. 39. Tectonic features at the southern margin of the Bismarck Sea. Open circles represent epicentres of earthquakes that define the northern margin of the South Bismarck plate (after Denham, 1973). This northern margin is thought to continue southeastwards and reach the Solomon Sea plate at a triple junction south of New Ireland (see Figs. 2 and 3). The three closely spaced lines north of the coastal ranges are hypothetical strike-lines for the upper surface of the postulated, northward-dipping slab beneath the western arc. The set of arrows illustrates the effect of plate convergence about a single position for a series of instantaneous poles of rotation (other positions in the northwest part of mainland Papua New Guinea have similar effects) - i.e., that those points at the upper surface of the downgoing slab further from the finite pole move greater distances for any rotation about the pole; in other words, rates of plate convergence increase away from the pole. The straight lines accompanying each arrow are normal to the strike-lines. Note that because of the differences in orientation of the strike-lines on either side of Long Island, the transcurrent components of movement for this particular pole position change from right-lateral west of the island to left-lateral east of it. A-A' and B-B' are lines of cross-sections in Figure 40A and B, respectively. See text for explanation of 'drag zone'.

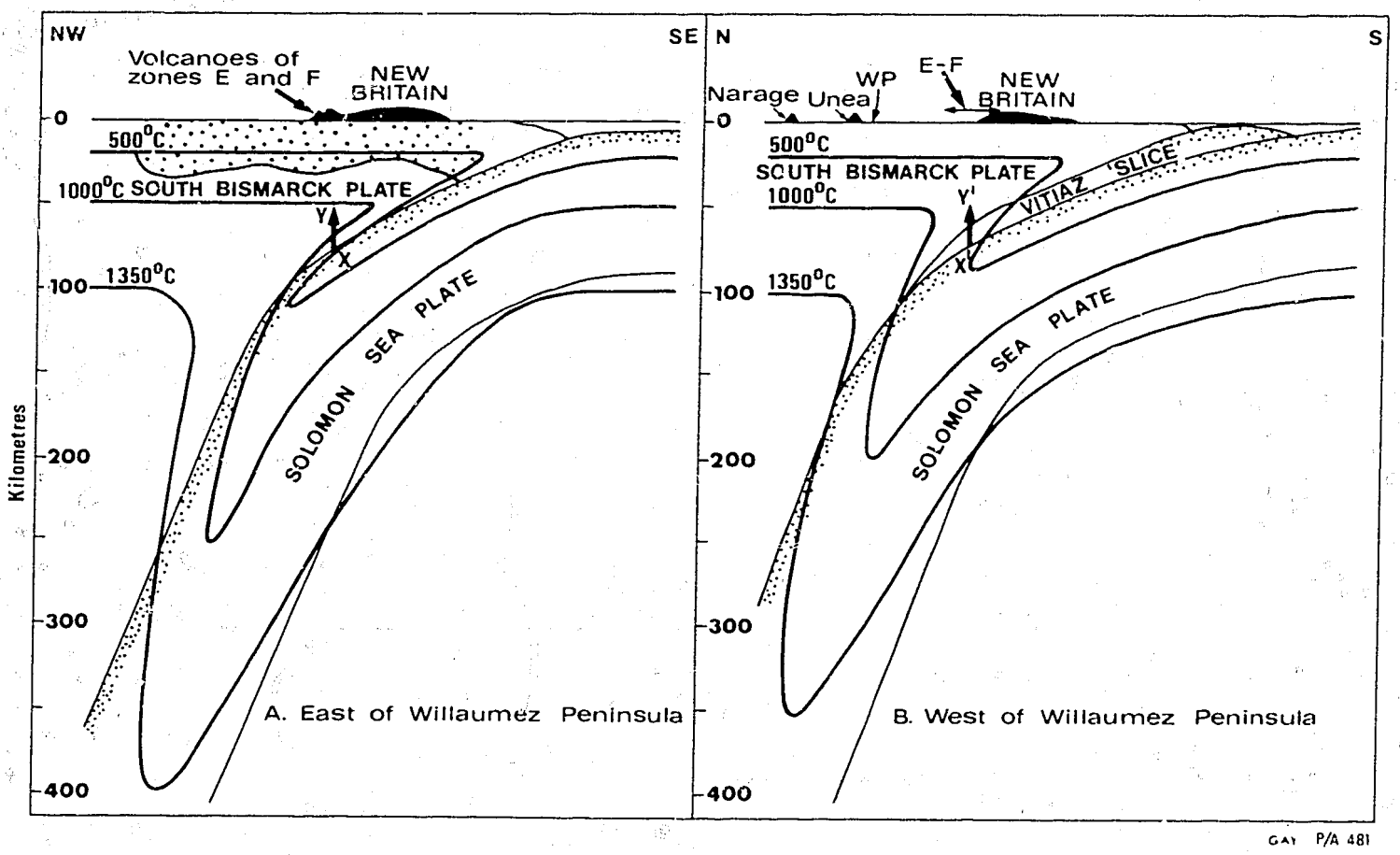

Fig. 40. Cross-sections showing schematic configurations of downgoing slabs and speculative thermal regimes east (A) and west (B) of Willaumez Peninsula. Lines of cross-sections are shown in Figure 39. Light stippling shows hydrated crustal rocks in the upper parts of the slabs. Coarse stippling indicates thickness of crust in cross-section A, which coincides with the crustal profile K-L given by Finlayson & Cull (1973, fig. 9b; crustal thicknesses beneath west New Britain are undetermined). WP and E-F represent the northern end of Willaumez Peninsula, and zones E and F (Fig. 10), respectively, projected from the east onto cross-section B. X-Y and X'-Y' are ascent paths of slab-derived water (see text for details). The flat parts of the isotherms are taken from the 'undisturbed' mantle geotherm of Griggs (1972).

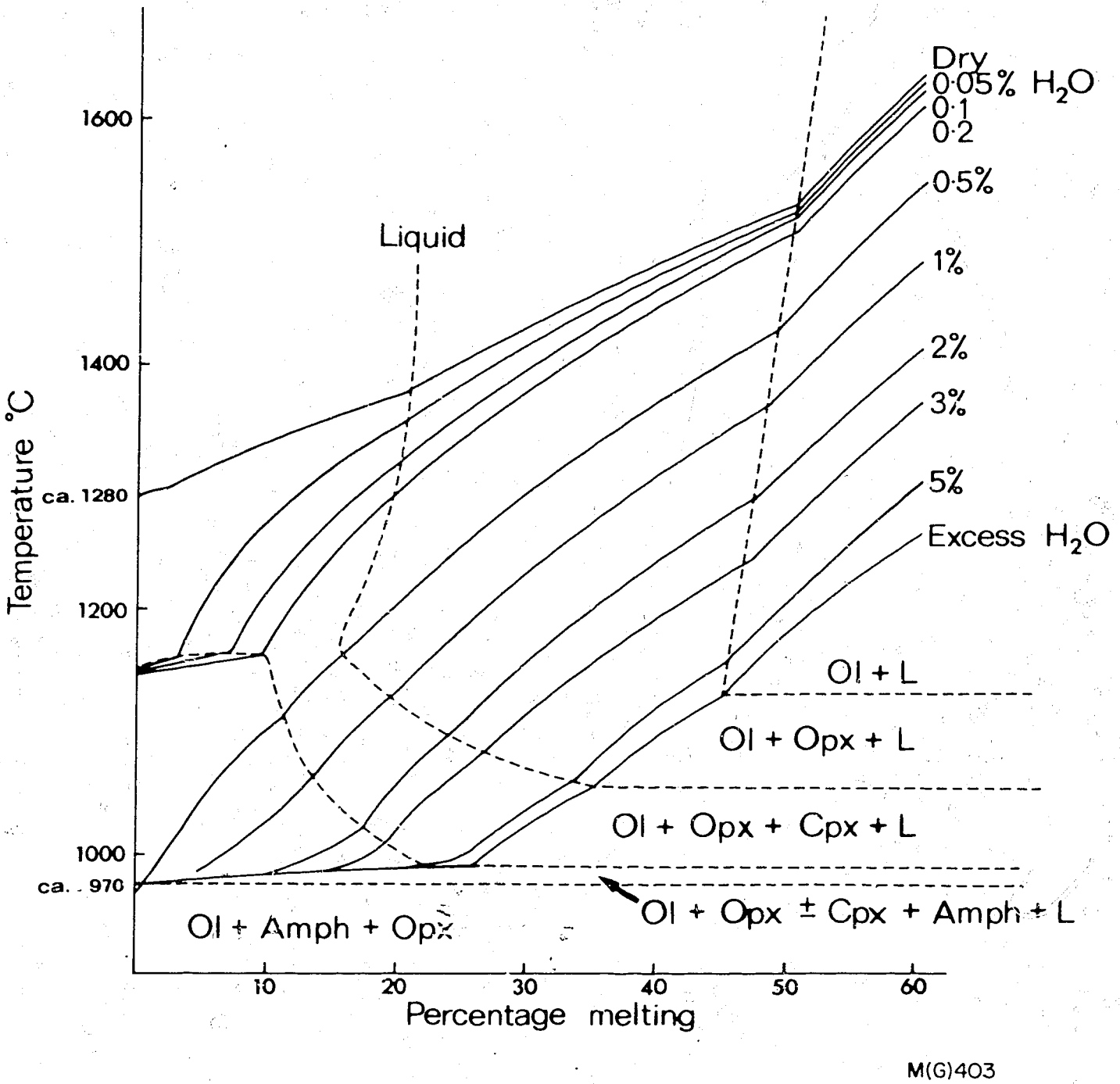

Fig. 41. Temperature v. percentage-melting diagram for a model peridotite composition at about 15 kilobars (after fig. 3 of D.H. Green, 1972). The solidus temperature of about 1280°C under water-free conditions decreases, as water content increases, to about 970°C under water-saturated conditions (excess water). For constant water contents, rises in temperature cause increasing degrees of melting along the stepped paths shown as solid curves. Different amounts of water introduced into peridotite at different temperatures will have different effects; for example, 0.5 percent water introduced into anhydrous mantle at 1200°C will cause about 20 percent melting, but at 1000°C only about 1 percent of melt will be produced. At temperatures of less than about 970°C, any amount of water will not cause melting; it will be used up in subsolidus reactions to form amphibole. (According to Green, up to about 30 percent amphibole could form from his model peridotite.) The dashed lines between the dry and excess water curves define four fields in which partial melts of different compositions are in equilibrium with different phase assemblages; Ol = olivine, Opx = orthopyroxene, Cpx = clinopyroxene, Amph = amphibole, L = liquid. Beneath the volcanoes of zones E and F (Fig. 10), water from the downgoing slab may have been introduced into the overlying upper mantle at a temperature above that of the water-saturated solidus, and so have caused melting. West of zones E and F, the mantle temperature may have been below the solidus temperature, and no melting may have taken place (see text and Fig. 40 for details).

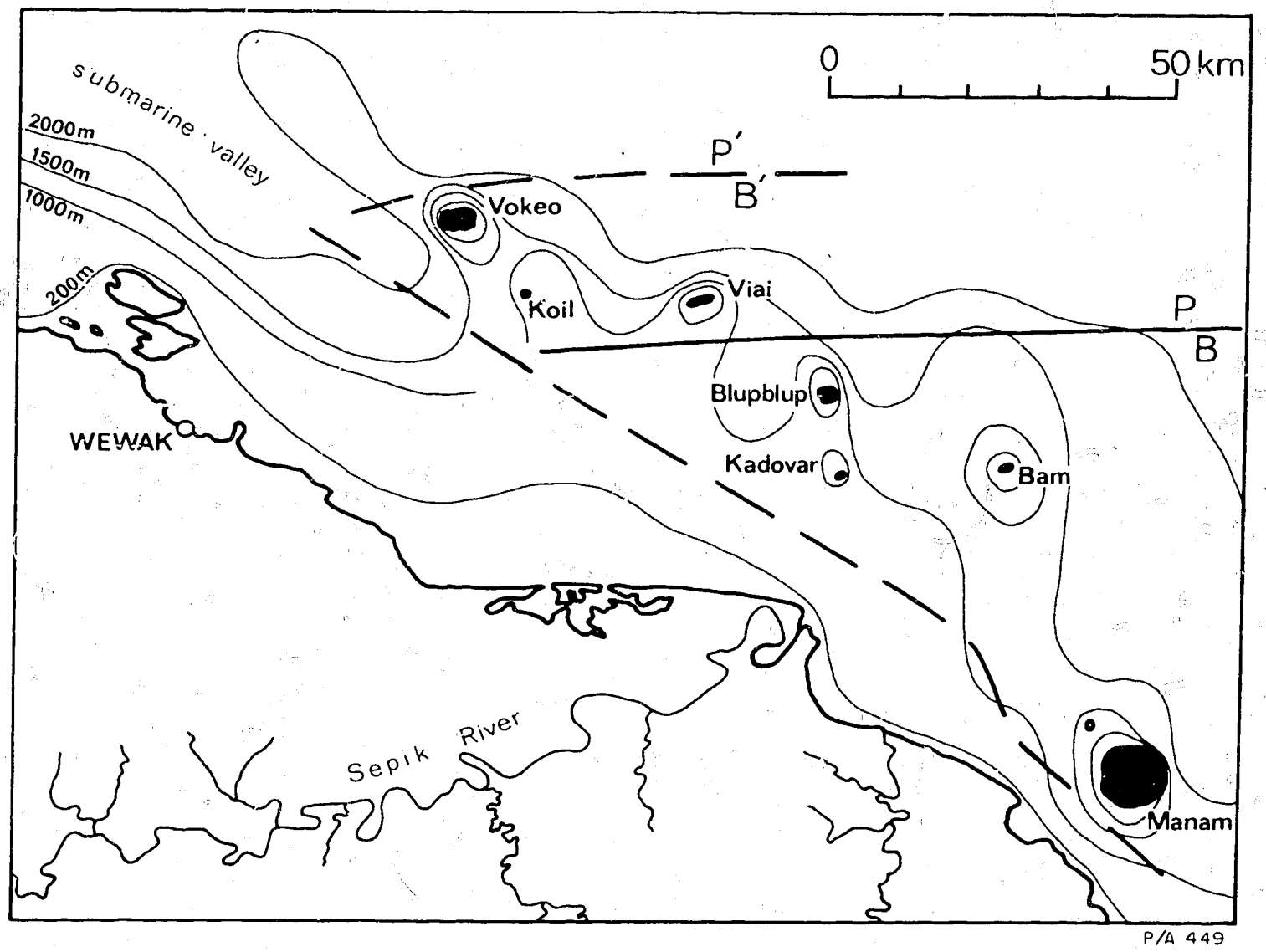

Fig. 42. Postulated relations between late Cainozoic plate boundaries at the western end of the western arc. Bathymetry adapted from 1:1 million geological map of Papua New Guinea (Bain et al., 1972). Assuming the Pacific(P)/South Bismarck(B) plate boundary (PB) is a single fault, the present-day position of PB is shown as a solid line between Viai and Blupblup: Vokeo and Viai are on the Pacific plate (Koil is a coral island), and Blupblup, Kadovar, and Bam are on the South Bismarck plate. A possible older position for the Pacific/South Bismarck plate boundary is shown by P'B', in which case all the volcanoes are on the South Bismarck plate (see text for an alternative interpretation). Longer dashed line represents speculative strike-lines for the upper surface of the downgoing slab.

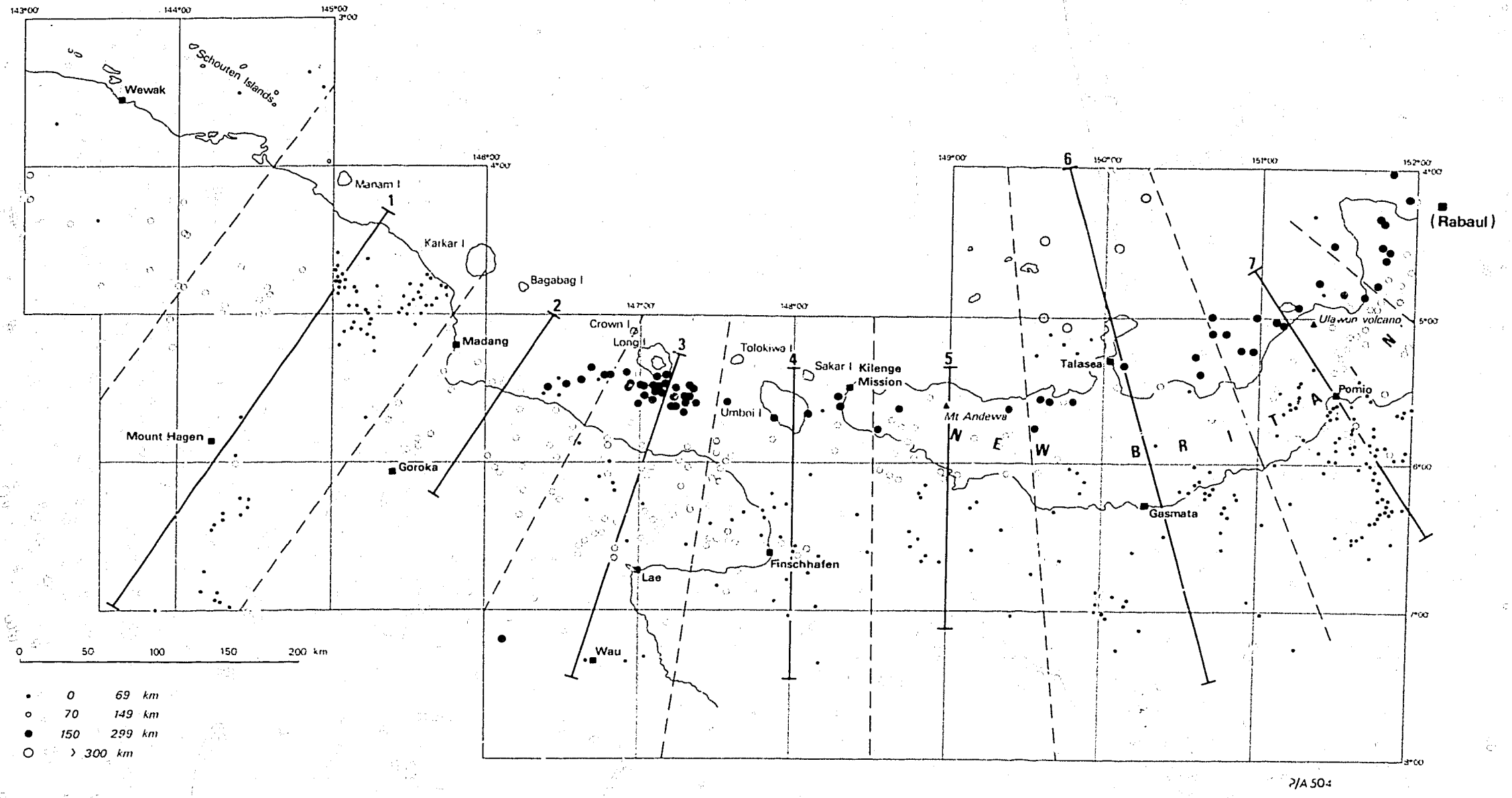

Fig. A. Distribution of epicentres.

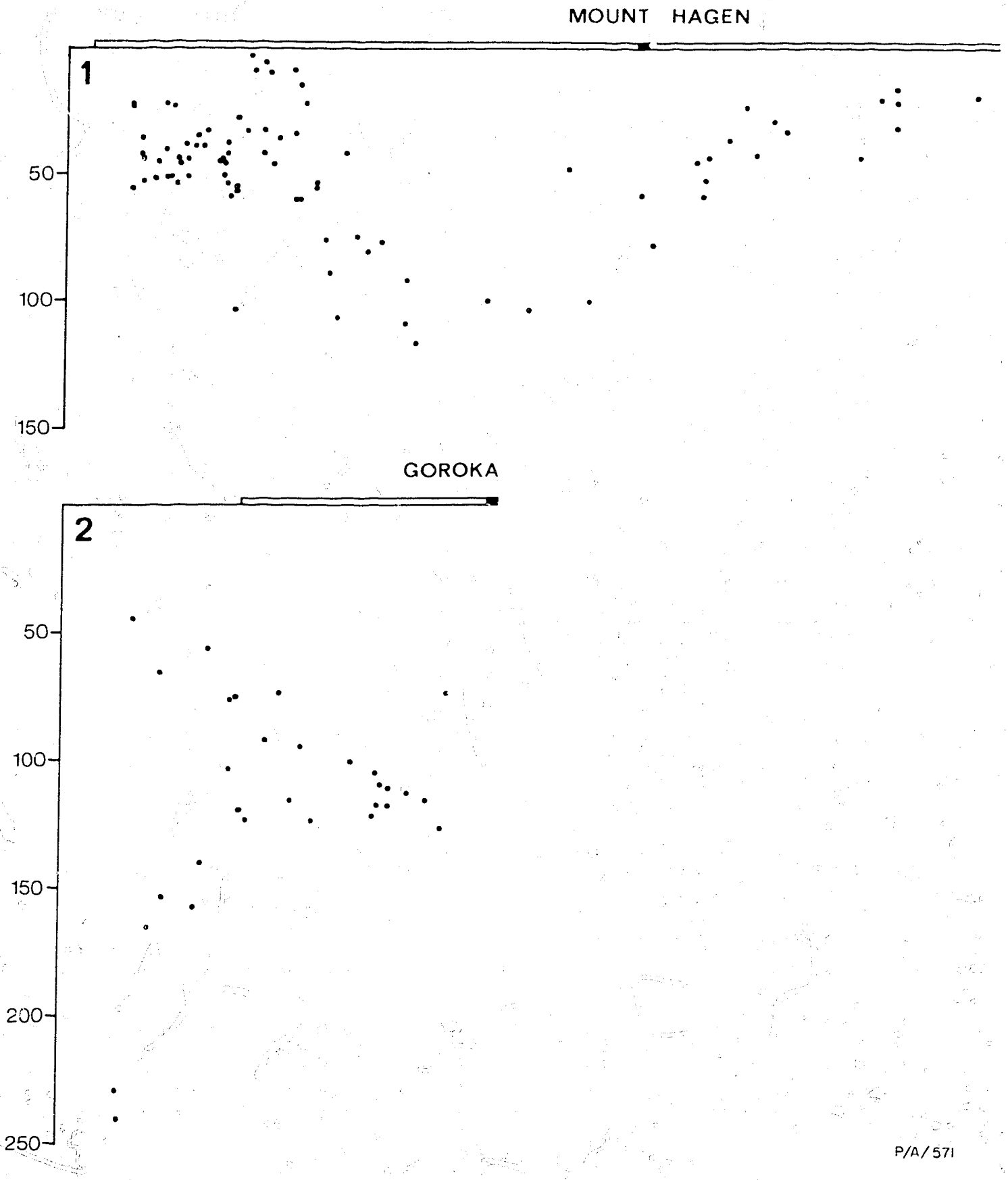

Fig. B, 1 to 7 (see also next four pages). Cross-sections through the western and eastern arcs (cf. Fig. A). Northern ends of the sections are on the left-hand side, and vertical and horizontal scales are equal.

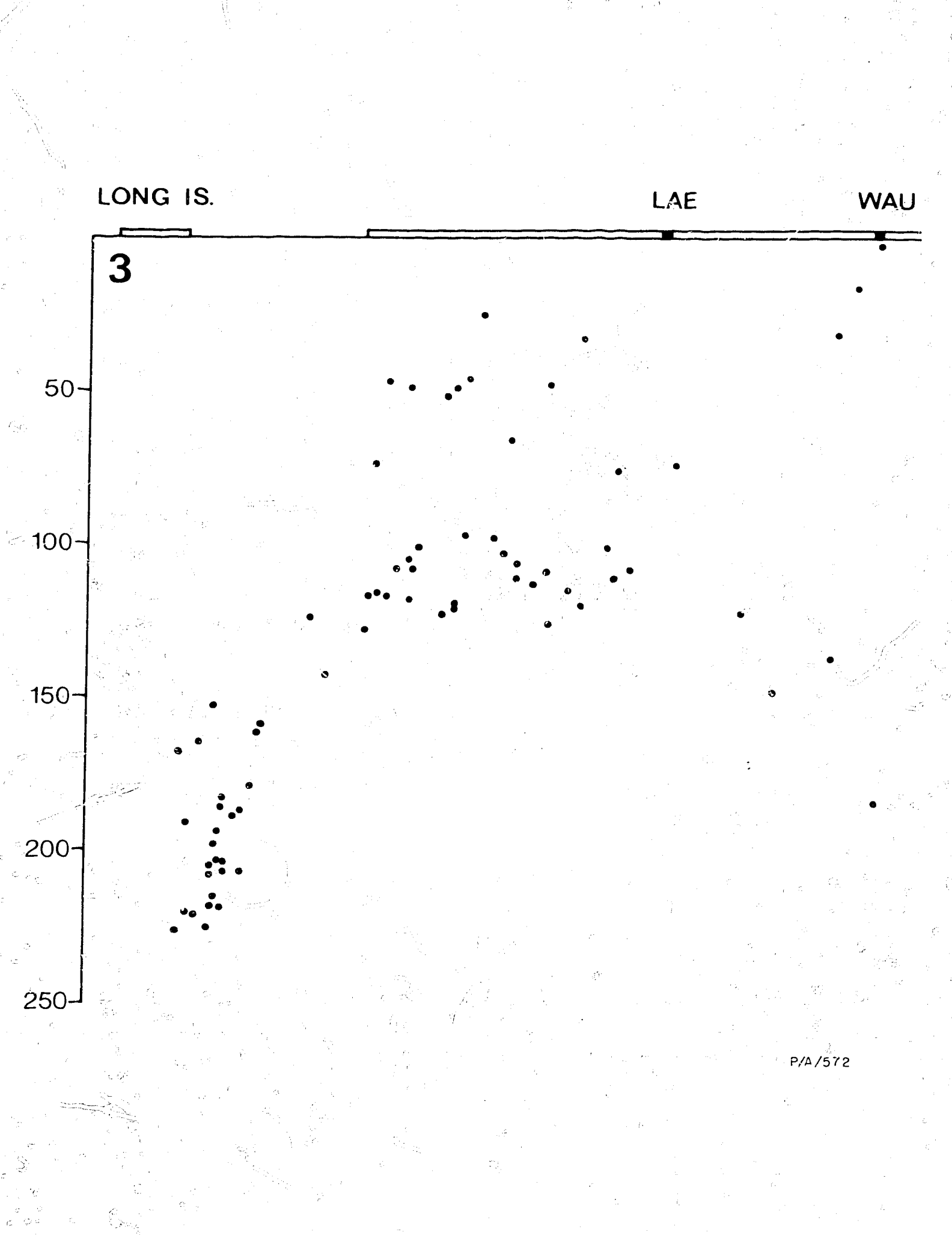
LONG IS.
LAE
WAU
3
50
100
150
200
250
P/A/572

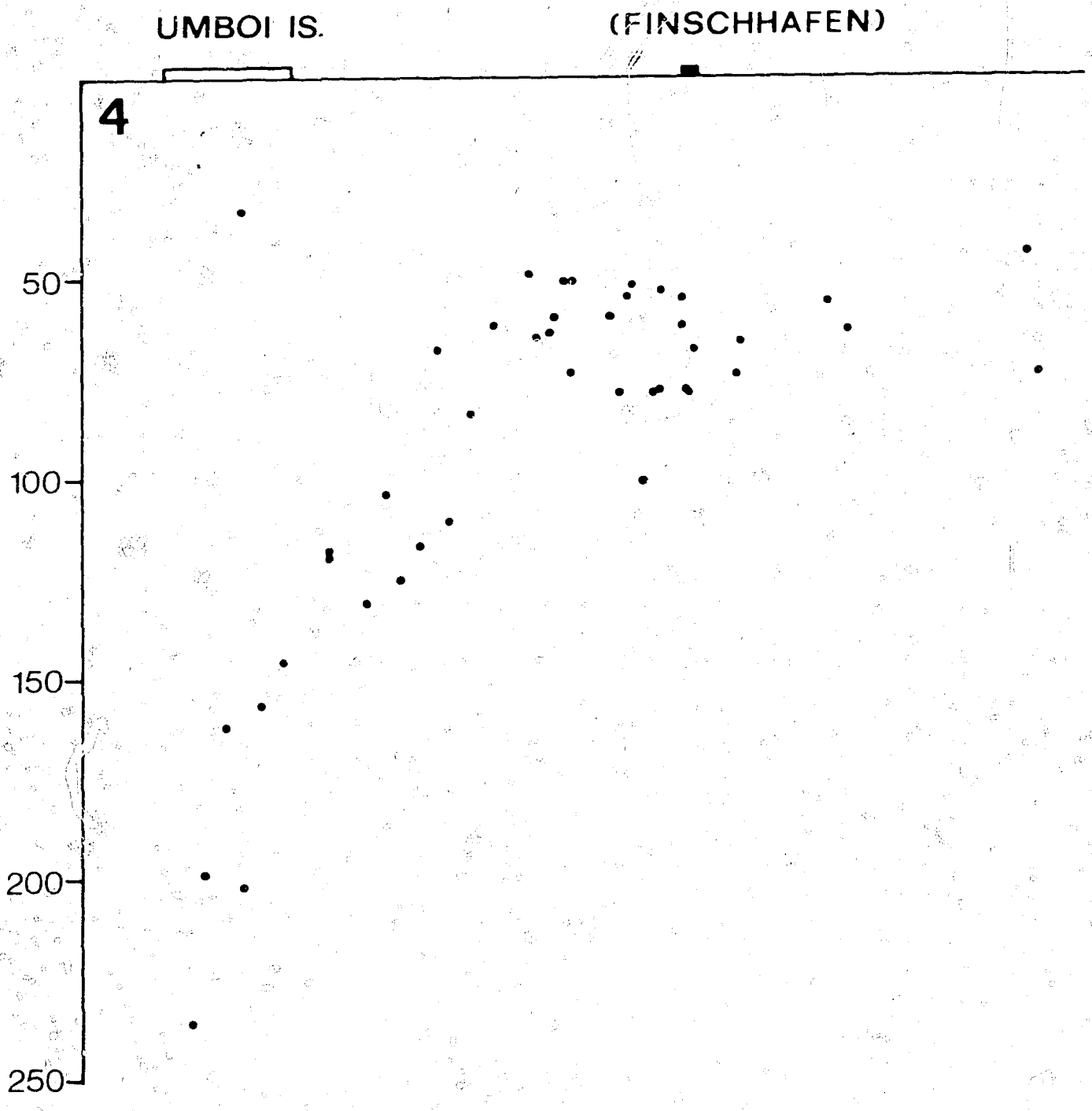

P/A/573

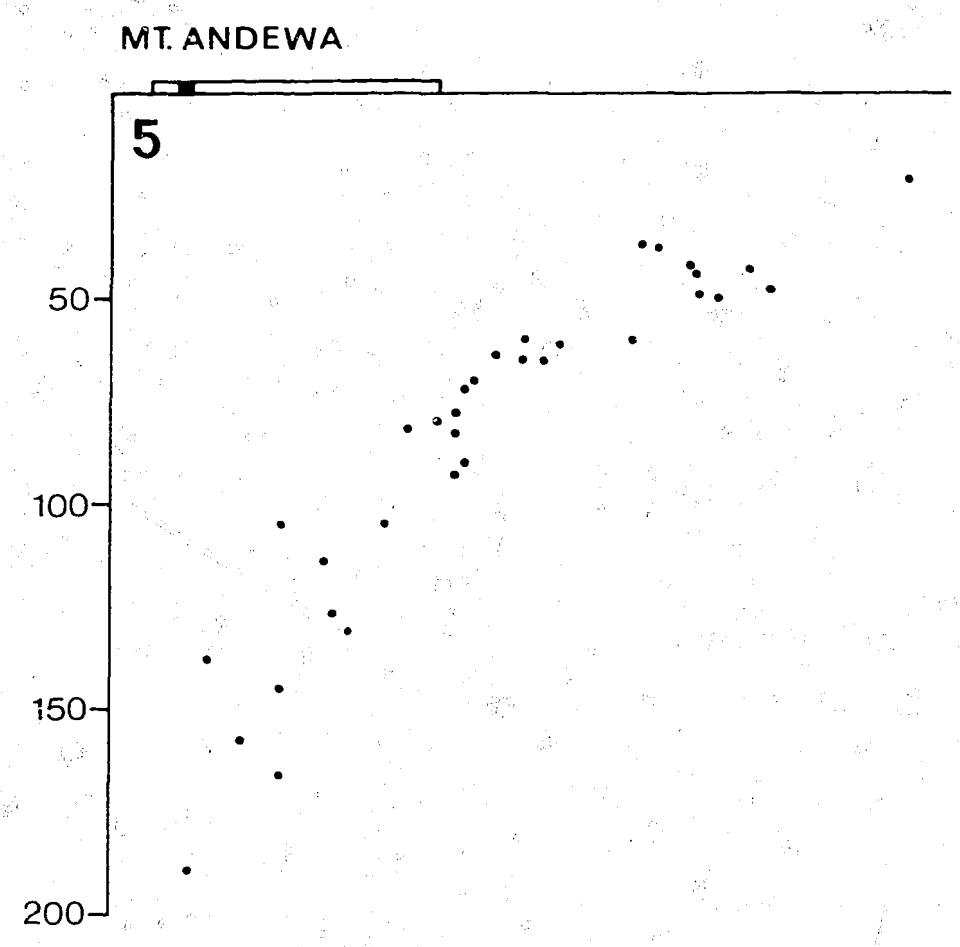

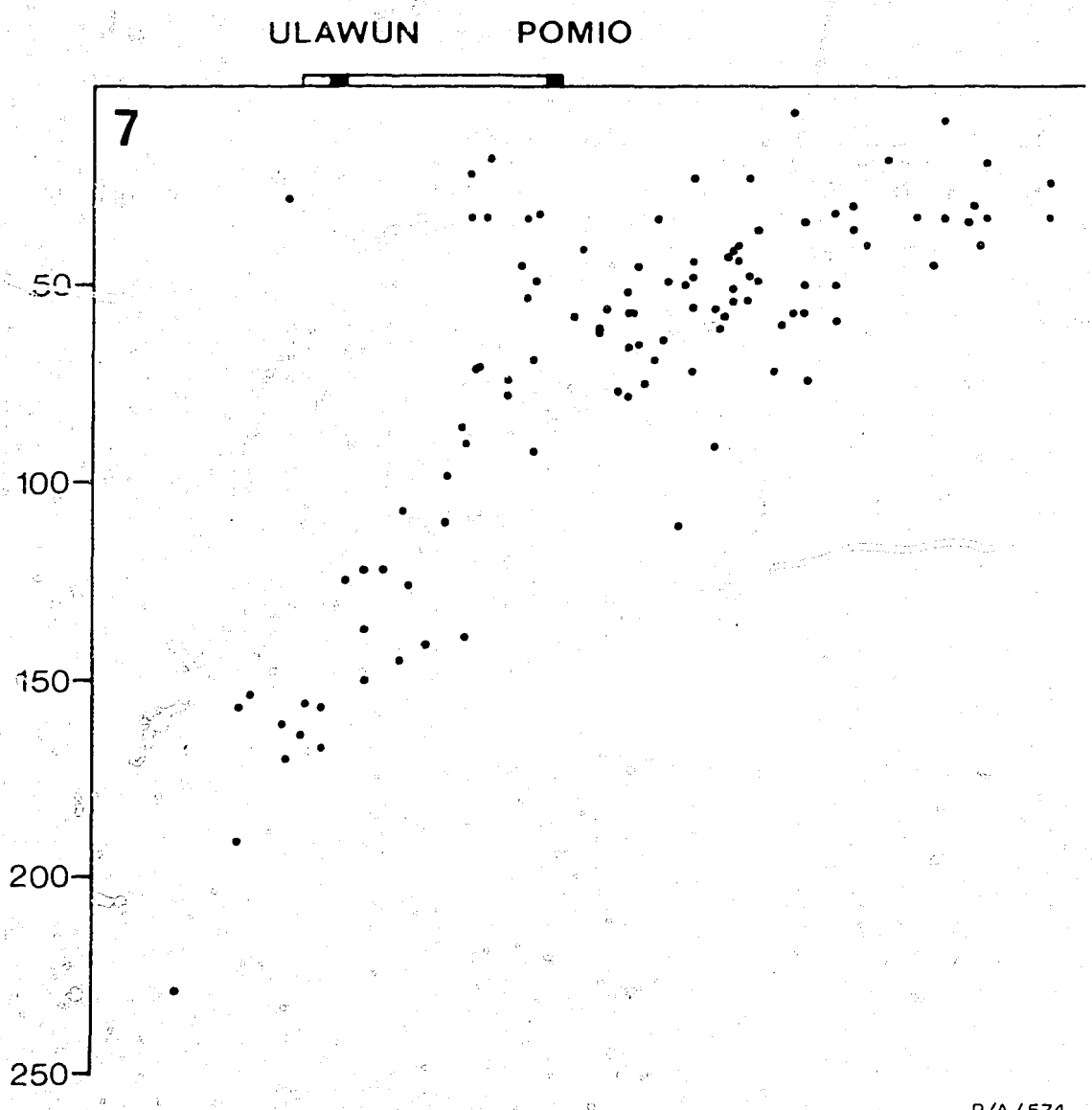

P/A/574

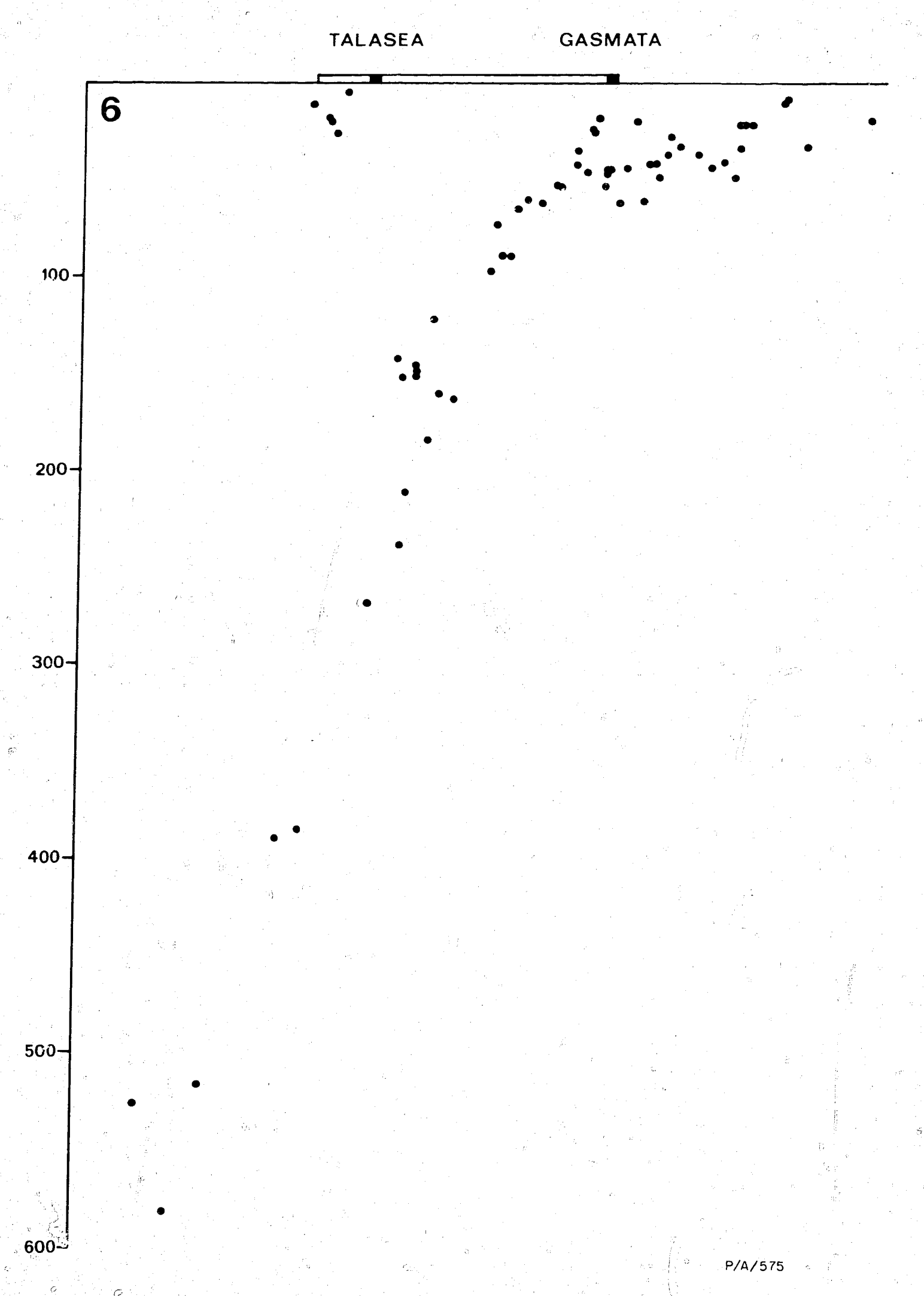
TALASEA
GASMATA
6
100
200
300
400
500
600
P/A/575

Figure I

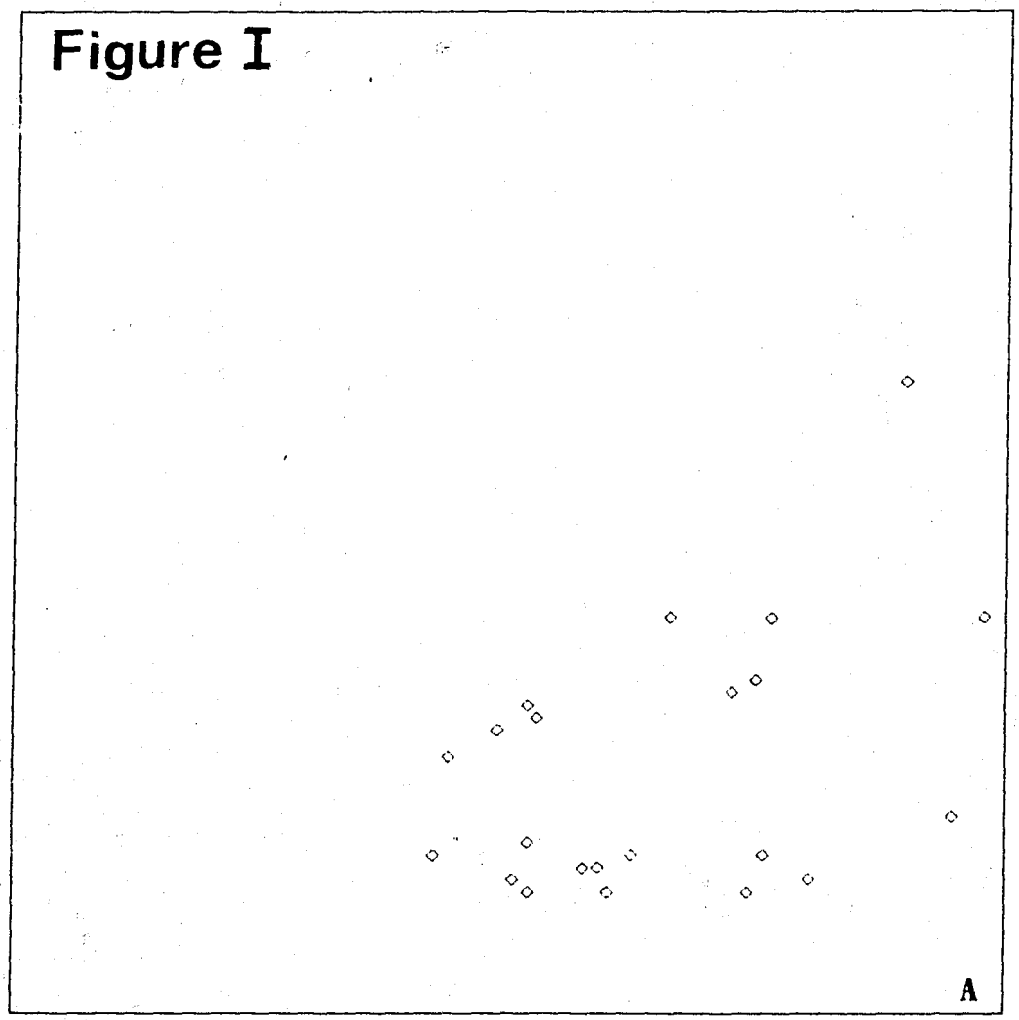

Figure II

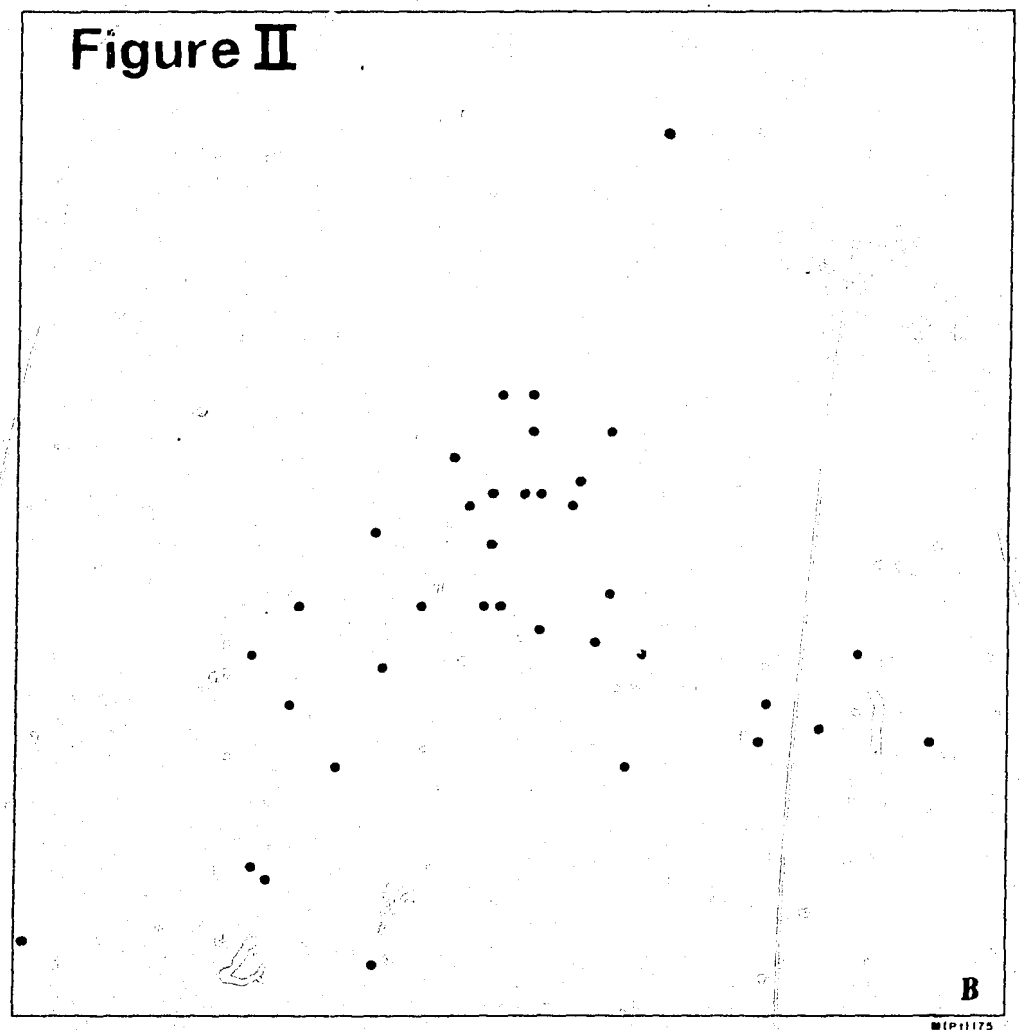

Figure III

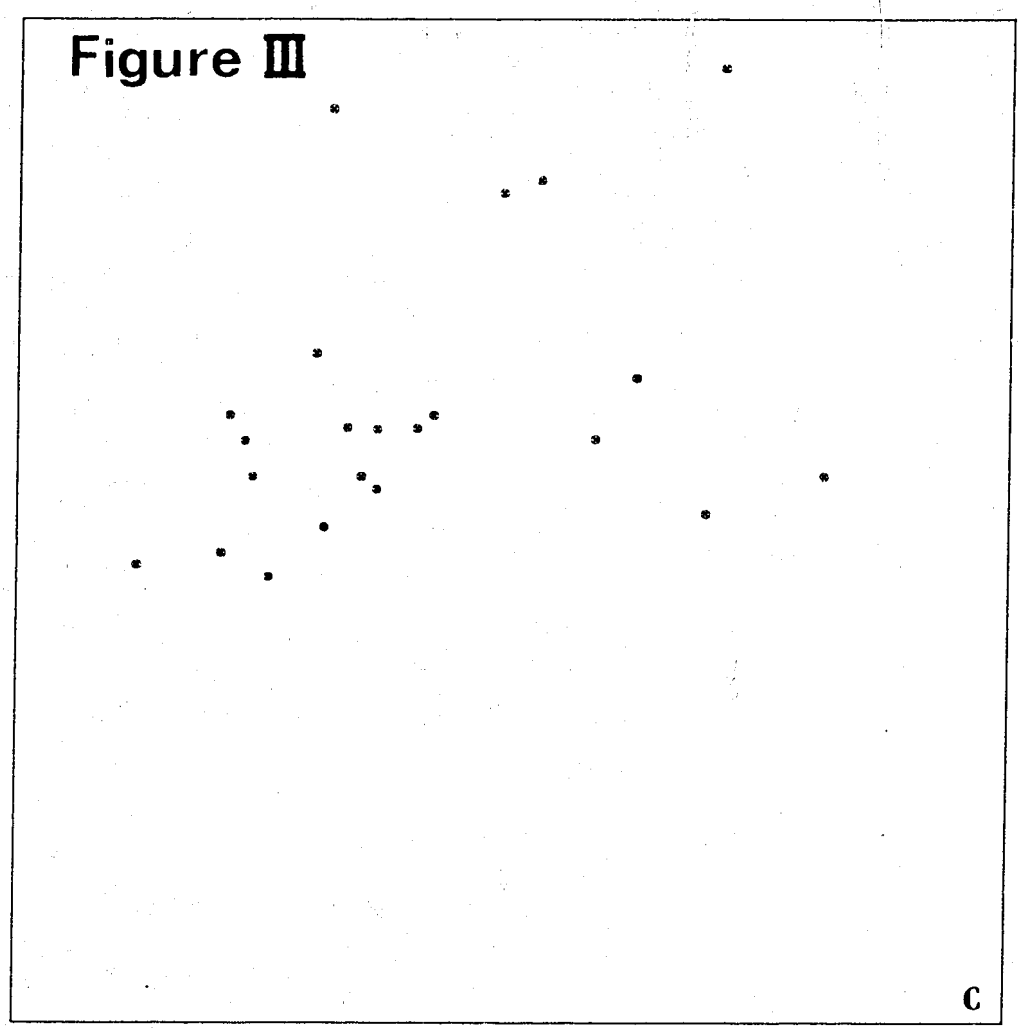

C

Figure IV

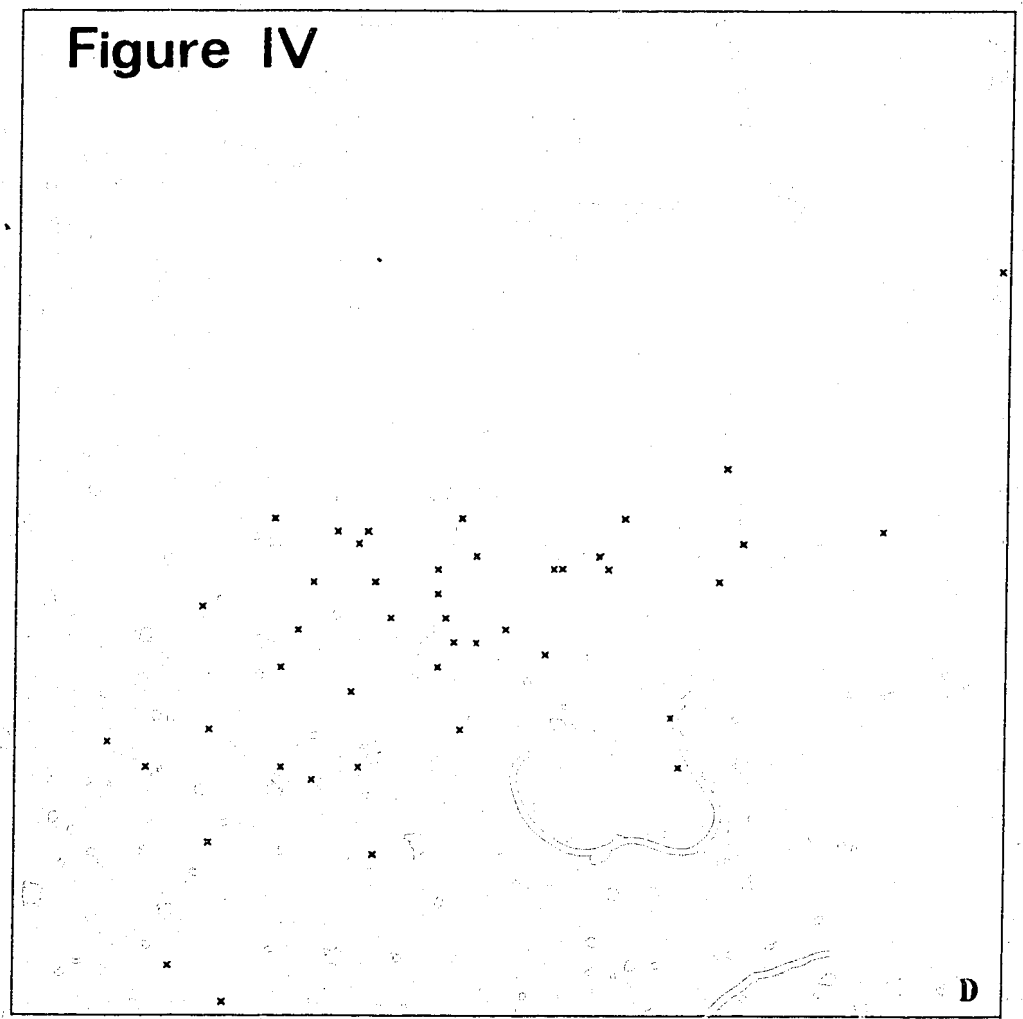

D

M(P1)176

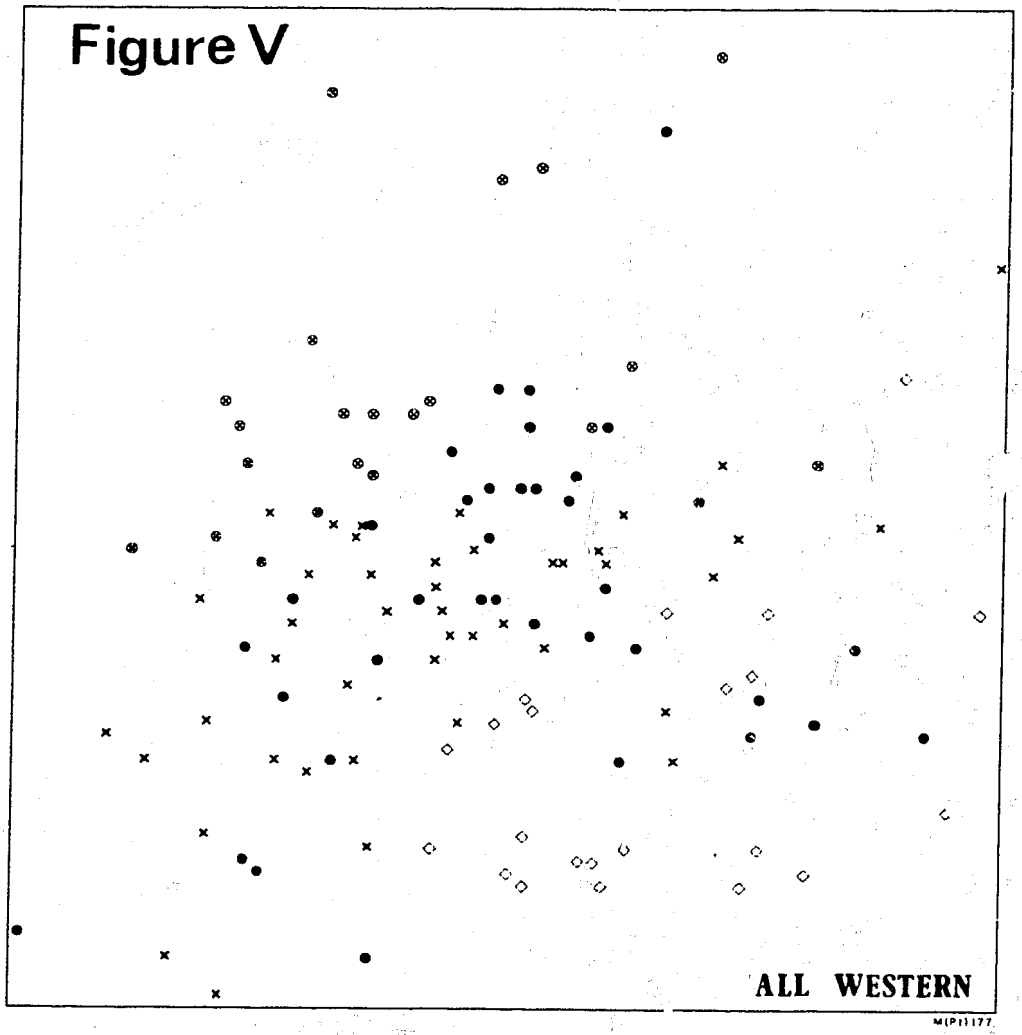
Figure V
ALL WESTERN
M(Pr)1177

Figure VI

E

Figure VII

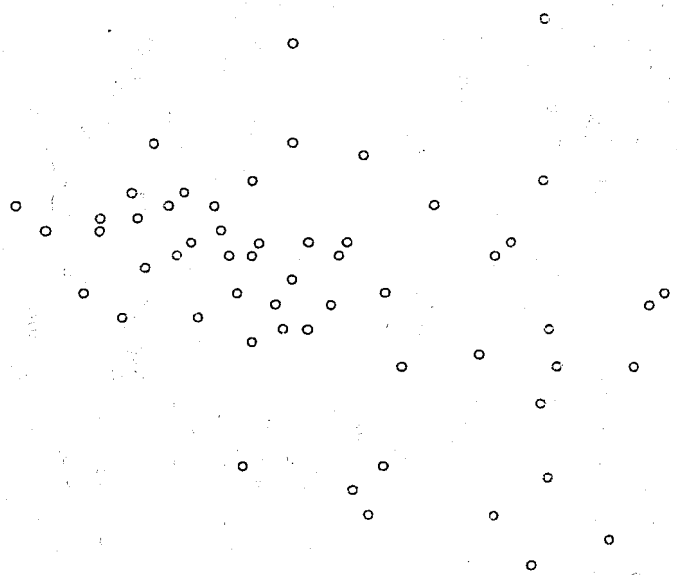

F

MEPI 1178

Figure VIII

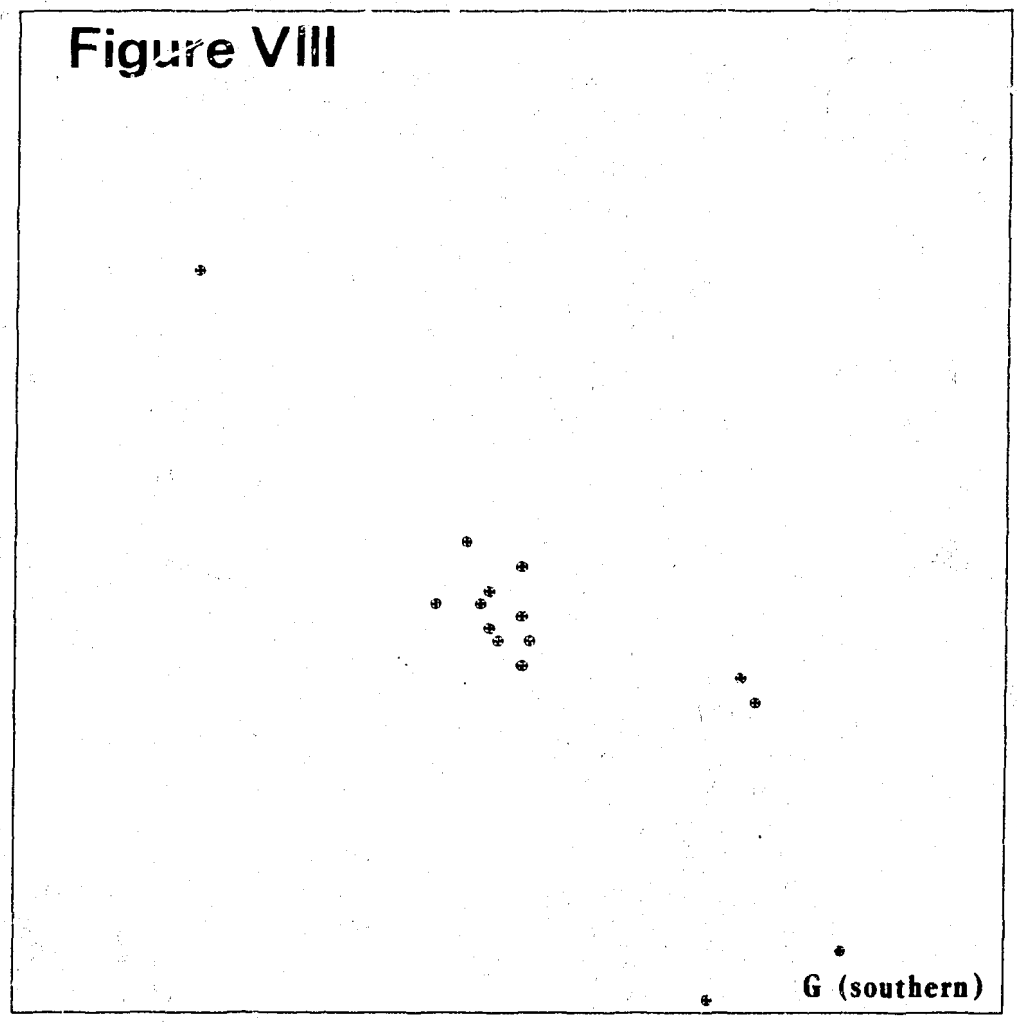

Figure IX

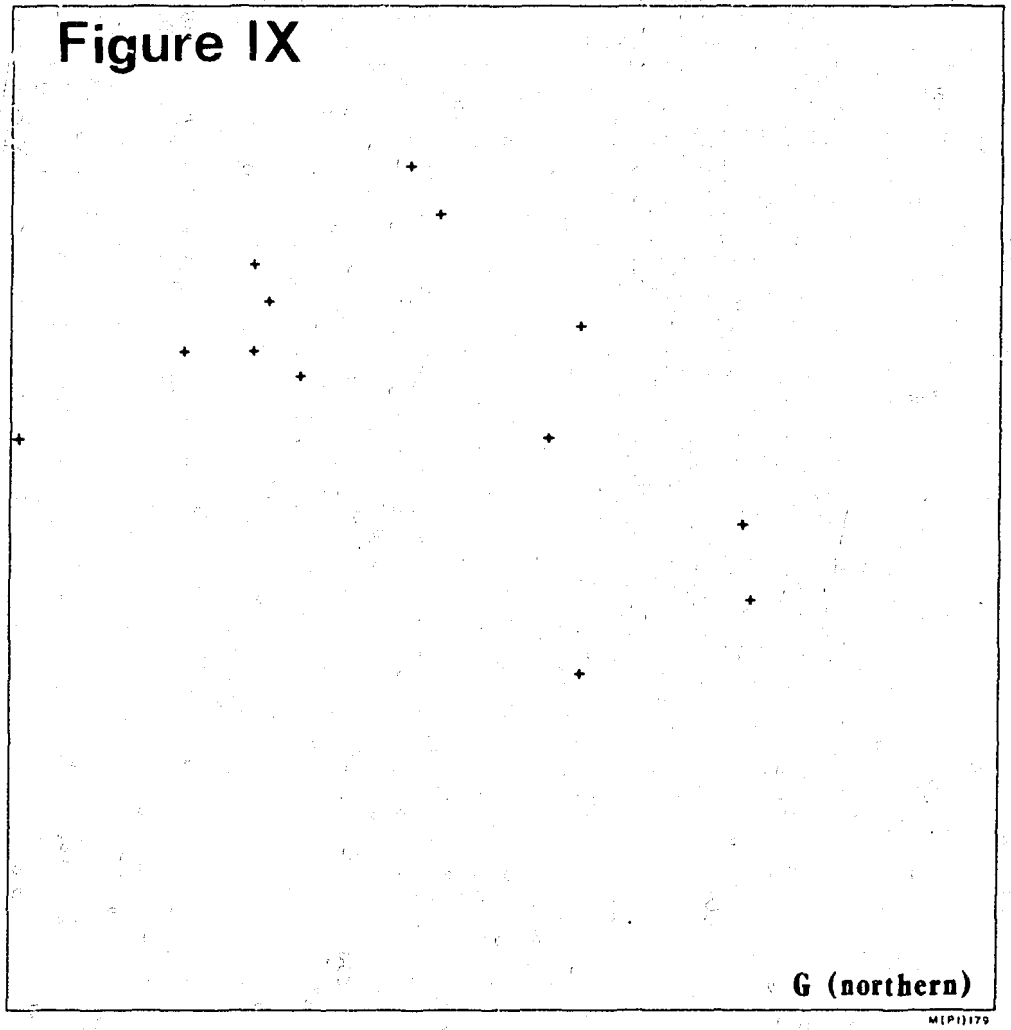

M(P)1179

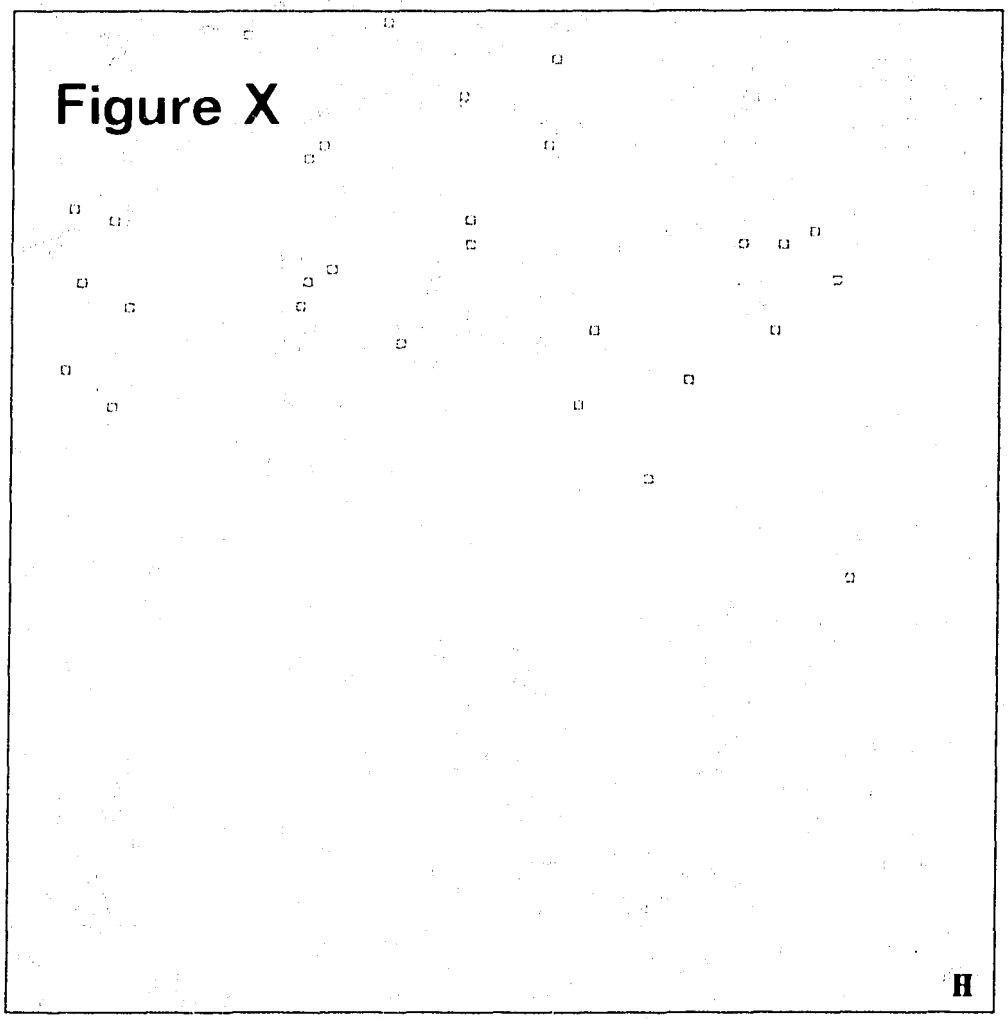
Figure X
H

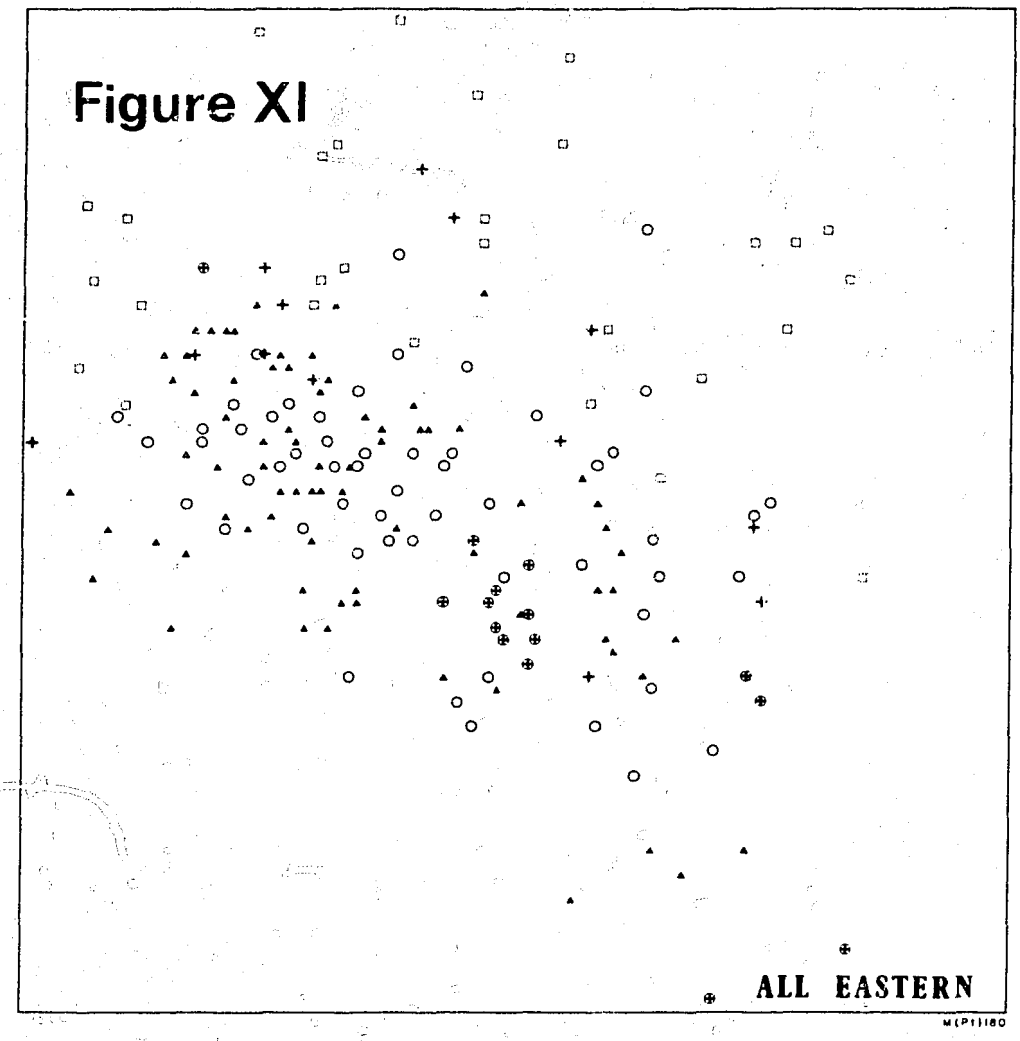
Figure XI
ALL EASTERN